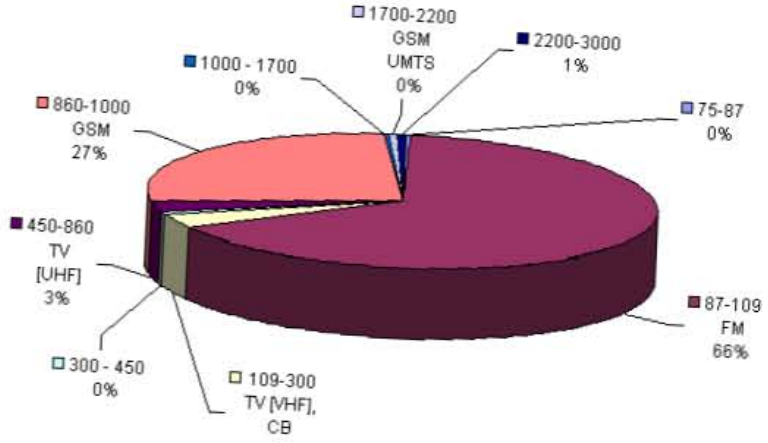


Figure 11: *Sample of Contribution of each band to the total electromagnetic radiation, calculated by SRM measurements (Narrow-Band)*

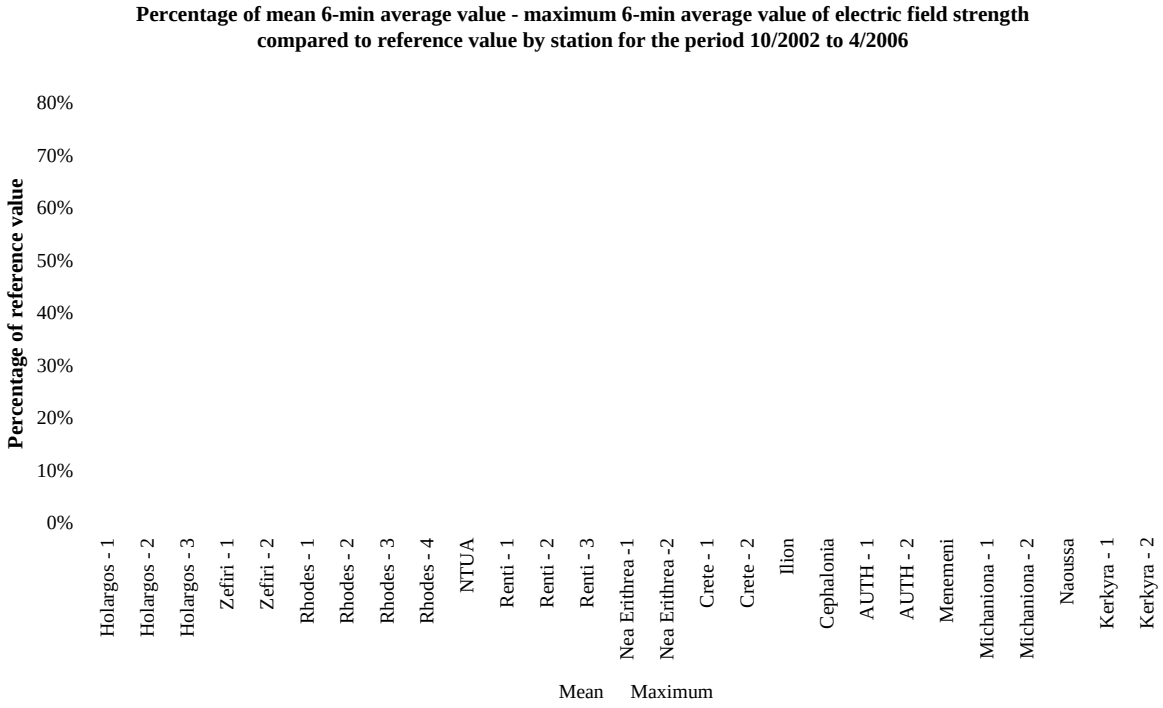


Figure 12 : *Percentages of electric field strength compared to reference value (overall)*

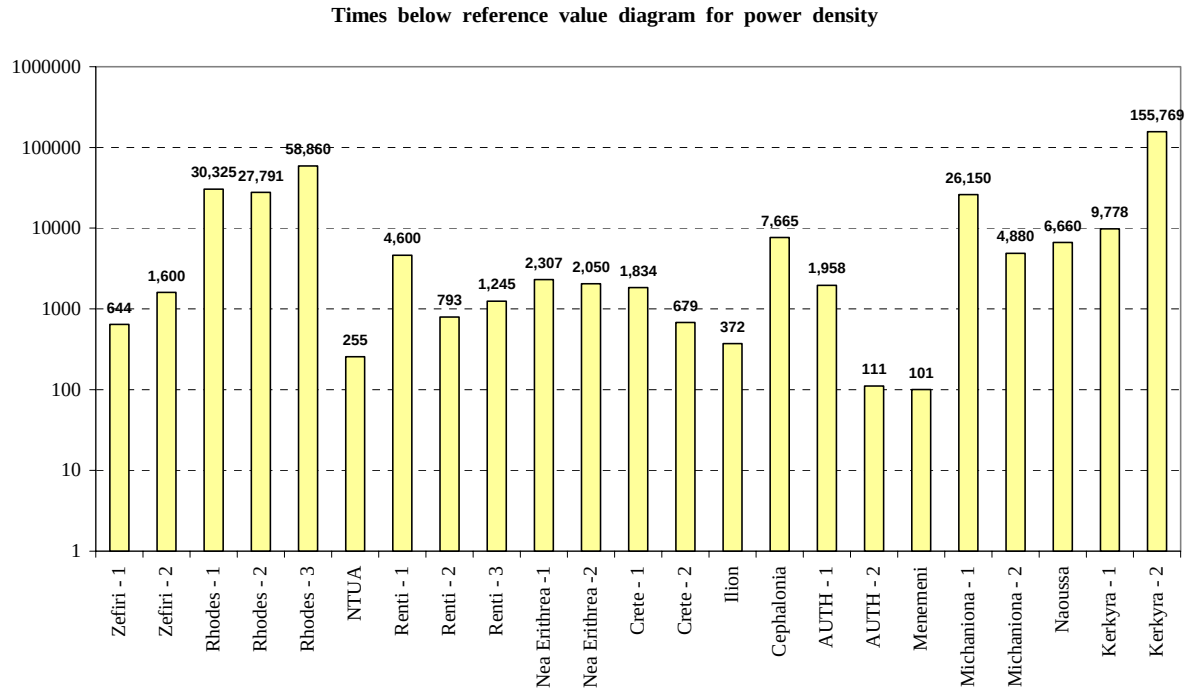


Figure 13: *Comparison of monitored power densities to reference value (overall)*

c. Comments on the Measurement results

Based on the above diagrams and the cumulative results from our measurement database, several general conclusions could be drawn:

- The electric field strength / power flux density values are several times lower than the safety reference levels, even on sites close to antennas (see Figure 4). As far as the mean E-field, the higher values have been recorded at the National Technical University of Athens (Table 1– Station ID 9) and at Aristotle University of Thessaloniki (Table 1– Station ID 21). The first is located near the Imittos Mountain hosting the Antenna Park of Attica (FM and TV broadcasting stations, Radars, etc.). The second measurement site is on the roof of the 9-floor Rectorate building, almost at the maximum of the main lobes of the antennas located at the Antenna Park of Hortiatis Mountain. Still, the mean values are respectively 2.9 V/m and 3.7 V/m, that is, 13% and 16.5% of the adopted reference level (22.4 V/m).
- The variation of the E-field on each site is negligible except for the two stations located in Heraklion, Crete. The standard deviation computed over the whole measurement period varies between 0.1 – 0.3 V/m for the majority of the sites.
- The measured E-field depends on the relative position between the site and the antennas, that is, the distance between them and the radiation pattern of the transmitting antenna(s).
- The recorded values to date indicate that in general higher E-fields are present on urban and dense urban sites in comparison with rural areas. Nevertheless, the contribution of mobile telephony cellular emissions to the total exposure is higher in rural areas.

IV. Summary - Future work

An automated nationwide monitoring network of the electric field strength in the RF spectrum was presented. The system uses reliable hardware based on electric field strength probes and the measured data is presented openly to the public using the Web. More than 4,000,000 E-field strength values have been recorded in our database and 63 “ad-hoc” measurements have been conducted in the context of “Hermes” Project. Since the commencement of operation the measured EM Radiation levels are significantly below the safety reference levels.

We are currently planning the installation of more remote stations in dense urban and rural environments. Our

intention is to extend the network of the monitoring stations. In the long-run and in conjunction with repetitive "ad-hoc" measurements using a Spectrum Analyser or a Selective Radiation Meter, a more detailed statistical analysis of the RF radiation levels in urban and rural areas is going to be performed. Our interest will be focused mainly in the proximity of cellular base stations.

References

[1] "monIT Project": Electromagnetic Radiation Monitoring in Mobile Communications http://www.lx.it.pt/monit/

[2] "Cassiopea Project": http://www.stroud.gov.uk/docs/cassiopea/cassiopea.asp

[3] "Progett Gardjola": http://gardjola.eng.um.edu.mt/emr

[4] "Project Horus": http://www.projecthorus.com/EMF/

[5] European Commission (EC), "Council Recommendation 1999/519/EC of 12 July 1999 on the limitation of exposure of the general public to electromagnetic fields (0 Hz to 300 GHz)", *Off. J. Eur. Comm.*, L 199, 59, 30 July 1999.

[6] Hellenic Republic Law No. 3431, About Electronic Communications and other Provisions, Government Gazette, FEK No. 13 A'/ 03.02.2006.

[7] "Hermes" Project: A Project for Systematic Measurements of the Electromagnetic Radiation, http://www.hermes-program.gr

[8] Narda Area Monitor System 2600, "Narda Safety Test Solutions": http://www.narda-sts.com/en/produkte/2600.htm

[9] PMM 8055S Electric and Magnetic Field Monitoring Station, "PMM Safety Products", http://www.pmm.it/main/safetyproducts.asp

[10] EE4070, EE4070S,MCE Monitoring System, "E.I.T. s.r.l", http://www.eitsrl.it/iMCE.htm

[11] A. Yalofas, A. Gotsis, C. Veranopoulos, P. Constantinou, G. Belesiotis, M. Petkaris, N. Babalis, *"A Fully Automated and Geographically Distributed Network for the Continuous Measurement of the RF Radiation – "Hermes" Project"*, TELSICS, IEEE 6th International Conference on Telecommunications in Modern Satellite, Cable and Broadcasting Services, Niš, Yugoslavia, October 2003.

[12] Electronic Communications Committee (ECC) within the European Conference of Postal and Telecommunications Administrations (CEPT) : ECC RECOMMENDATION (02)04 "MEASURING NON-IONISING ELECTROMAGNETIC RADIATION (9 kHz – 300 GHz)"

[13] Narda Selective Radiation Meter SRM-3000, "Narda Safety Test Solutions": http://www.narda-sts.com/en/produkte/srm.htm

THE NEW EMF PROTECTION FRAMEWORK REGARDING ANTENNA STATIONS IN GREECE

E. KARABETSOS G. FILIPPOPOULOS

NON IONIZING RADIATION OFFICE
GREEK ATOMIC ENERGY COMMISSION
P. O. BOX 60092, 15310 AGIA PARASKEVI, GREECE

Abstract
In February 2006, the Greek Parliament passed a Law setting new standards for siting antenna stations. According to this Law, the permissible general public exposure levels for EMF in the vicinity of all kinds of antenna stations are set in general to 70% of the EU Recommendation and ICNIRP's limits, and to 60% of them for stations located closer than 300 meters from the perimeter of schools, kindergartens, hospitals or eldercare facilities. Installation of mobile phone base stations at the premises of these facilities is now prohibited. Furthermore, it is not allowed to build a new antenna station before the approval by the Greek Atomic Energy Commission of a technical study showing that the EMF levels in the vicinity of the station will be lower than the aforementioned limits. The Greek Atomic Energy Commission will be monitoring EMF exposure levels by performing in situ measurements, ex officio or within 20 working days after request of any interested party. These measurements should, on an annual basis, concern at least 20% of all the antenna stations installed in urban areas and their results will be announced on the web site of the Greek Atomic Energy Commission. The provisions and ramifications of this new Law are presented in this paper.

Introduction

In 2000 Greece implemented legally binding measures for the protection of the public from exposure to electromagnetic fields by putting into force a national legislative act concerning all kinds of land-based antenna stations, [1]. In this legislative act, the basic restrictions and the reference levels set in the Council Recommendation, [2], and ICNIRP's guidelines, [3], for general public protection have been implemented. However, the Greek legislation applied additional safety parameters to the allowed EMF exposure levels. Hence, the safety limits for the exposure of the general public to all land based antenna installations were set to 80% of the EU values. Also, with this legislation the Greek Atomic Energy Commission is set as the national authority, responsible for the protection of the environment and the general public against man-made electromagnetic radiation.

In February 2006, the Greek Parliament passed a Law, [4], setting new standards for siting antenna stations. According to this Law, the permissible general public exposure levels for EMF in the vicinity of all kinds of antenna stations are now set, in general, to 70% of the EU Recommendation and ICNIRP's limits, and to 60% of them for stations located closer than 300 meters from the perimeter of schools, kindergartens, hospitals or eldercare facilities. It must also be noted that installation of mobile phone base stations at the premises of these facilities is now strictly prohibited. The Greek Atomic Energy Commission will be monitoring EMF exposure levels by performing in situ measurements, ex officio or within 20 working days after request of any interested party. These measurements should, on an annual basis, concern at least 20% of all the antenna stations installed in urban areas and their results will be announced on the web site of the Greek Atomic Energy Commission.

In the next paragraphs the EMF protection in Greece, after the introduction of the new Law is analysed.

Competent Authorities in Greece

The competent national authority for the protection of the general public and the environment against artificially produced non-ionising radiation is the Greek Atomic Energy Commission (EEAE, www.eeae.gr), which lies under the Ministry of Development. Specifically the EEAE:

- Publishes prototype technical studies-notes for all kinds of antennas (such technical notes have been

published for mobile phone base stations, earth satellite stations and microwave antennas, http://www.eeae.gr/el/services/templates/)
- Defines the measurements protocol based on international standards
- Organises educational programs for the personnel of all public sector and all interested groups concerning the protection of the general public to electromagnetic fields, informs and replies to requests from the public authorities and citizens about the possible health hazards induced by non- ionising radiation.
- Provides all details concerning the authorisation of teams that perform measurements in all non-ionising radiation installations and controls the measurements procedure.

Measurements in antenna stations according to the legislation, may also be performed by the Ministry for the Environment, Physical Planning and Public Works, the Ministry of Health and Welfare and the Ministry of Transport and Communications or other, authorised by the EEAE, laboratories (e.g. University laboratories).

Public Information

The EEAE is responsible for providing information to all interested public groups for matters concerning the health effects of electromagnetic fields. To this end, the EEAE published in 2001 a 16-page informative brochure entitled: “Non-ionising radiations: Mobile phones and base stations” (also available at www.eeae.gr), distributed freely to all interested parties. Recently (after the new Law) EEAE has published a new updated 36-page brochure entitled “Mobile telephony and health” that is also freely distributed (also available at www.eeae.gr).

The EEAE also organises or participates in lectures; courses and workshops open to the local authorities, the public and the media. Some major risk communication events have been the organisation of 5 one-day workshops, in the years 2001-2003, entitled: “Exposure of the general public from mobile phones base stations” open to the local authorities, the public and the media, organised by the Ministry of Transport and Communications, the National Committee of Post and Telecommunications, the EEAE and/or the municipal authorities (proceedings from some of these workshops have been published as booklets and are freely distributed from the National Telecommunications and Post Commission, EETT).

It must be also stated that the EEAE was recently financed by the General Secretariat of Research and Technology of the Ministry of Development in order to produce informative material in electronic and paper format (cd-roms and brochures) and to organise workshops for specially selected target groups (representatives of the ministries, the local authorities and the media) for matters concerning EMFs and Health. The scope of organising such workshops is to inform and train persons able to form a “critical mass” necessary for further dissemination of this information to the general public.

Exposure Limits

In 2000 legislative act [1], the basic restrictions and the reference levels set in the Council Recommendation, [2], and ICNIRP’s guidelines for general public protection, [3], have been implemented. However, this legislation applied additional safety parameters to the allowed EMF-exposure levels. Hence, the safety limits for the exposure of the general public to all land based antenna installations were set to 80% of the EU values.

In accordance with the new Greek Law, the limits for general public exposure to electromagnetic fields are set to 70% of EU Recommendation Values. In case that an antenna is sited at a distance lower than 300m from the perimeter of the premises of kindergartens, schools, hospitals or eldercare facilities the Greek limits are set to 60% of EU Values. Furthermore, it is not allowed to install mobile phone antenna stations at these premises. All existing installations at the above mentioned premises must be removed in 6 months from the publication of the new Law.

Technical Studies

According to the Greek Legislation, [1], before the construction and the operation of an antenna station a special license must be issued by the National Telecommunications and Post Commission, (EETT). The EEAE is involved in the license issuing process since a technical study of electromagnetic emissions is mandatory to be submitted to EEAE before the antenna station owner submits the application to the competent authority for issuing a license for an antenna station in a particular location. These studies include architectural blueprints and

topographical charts of the station as well as technical information about the operation of station's antenna system. The intensity of the incident electromagnetic radiation is calculated in places accessible to general public. The existence of any other antenna station at a distance lower than 50 meters from the examined antenna station is also taken into account.

Through these calculations it must be proven that the intensity of the electromagnetic radiation is lower than the established limits in the Greek Legislation at any place that is freely accessible to the public in the vicinity of the station. Of course, very close to the antenna systems (for example for mobile phones base stations usually till 4 to 8 meters), at the directions of maximum emission and at the height where the antennas are located it is possible that the radiation exceeds the established limits. If there is public access to these places the study foresees that it will be forbidden. The EEAE after the examination of the study sends its expert opinion (given that the study is not deficient or inadequate or mistaken) to the competent authority in order to issue license for installing the antenna.

It is noteworthy that these studies are composed on the basis of the very strict technical prototype studies that have been issued by the non ionizing radiation office of EEAE. These prototype studies adopt worst case considerations and assumptions, due to which the intensity of the electromagnetic radiation is overestimated in relation to the actual intensity in the vicinity of the station. This has been confirmed through the comparison of the calculated values in the studies with the results of measurements at areas close to antenna stations.

In accordance with the existing legislation [1], if the process of checking the technical study by EEAE took over 1 month the license by EETT for this installation could be issued without EEAE's positive expert opinion. However, with the new legislation [4], it is no longer allowed to build a new antenna station before the approval by the Greek Atomic Energy Commission of a technical study showing that the EMF levels in the vicinity of the station will be lower than the aforementioned limits. Also, due to the change of exposure limits the owners of all the installed antenna stations are obliged to submit new technical studies to EEAE showing that their stations adhere to the new limits.

Audits

In accordance with the existing legislation, the levels of the emitted electromagnetic fields from all kind of antenna stations are regularly monitored, in order to ensure compliance with the safety limits for the public or, if this is not the case, to ensure that all necessary protection measures around an antenna base station, are being taken in every case. To that end, the EEAE also carries out measurements in all kinds of antenna stations in order to monitor whether the general public exposure limits are being adhered to. It must be stated here that from the year 2000 until today, the non - ionising radiation office of the EEAE has performed over 1700 inspections and measurements at various sites in Greece, where all kinds of antenna stations are installed. Concerning cellular phone base stations, the EEAE has conducted measurements in the vicinity of 1200 such stations. The major part of this information is in the form of written measurement reports that have already been delivered to the authorities or persons who asked for these measurements, but are also available to everyone interested.

The non ionising radiation office of GAEC has expert personnel and suitable measuring equipment and is accredited in accordance with the requirements of the EN IS0/IEC 17025 standard by the Hellenic Accreditation Council (ESYD - the Greek National Accreditation Body) for performing measurements of low and high frequency fields, as it is determined in the accreditation certificate No. 117 (22-01-2003) for tests.

With the new legislation, [4], the audits of the electromagnetic fields in the vicinity of antenna stations are drastically intensified. To this end, the EEAE or other laboratories authorized by it, performs inspections and measurements in the vicinity of antenna stations either:

a) ex officio, through a sampling process and annually in the vicinity of 20% of all antennas installed in urban areas, or,
b) after the request of any interested party, in 20 working days

The results of these inspections are immediately published at EEAE's web site and collectively per year. Soon all this information about the already measured sites as long as the results for every new measured antenna station will be posted to the web page of EEAE

Penalties

In case EEAE finds trough measurements an excess of the limits, it informs the competent license-issuing authority, which then notifies the antenna owner in order to do the following:

• immediately cease the operation of the responsible equipment and then inform about this the competent license-issuing authority;

• clear the causes of malfunction before resuming operation

• inform the competent license-issuing authority about the operation resumption, providing explanations about the causes of the malfunction.

If, at any time after the initial notification, an irregular operation of the same equipment is found again, then the license is permanently recalled for this location.

Environmental aspects

According with the new Law, [4], the approval concerning all environmental aspects related to each antenna installation foreruns the license for the construction of this installation issued by EETT. Hence, a technical study examining the environmental impact of a new antenna station should be submitted to the General Secretariat of each District, which in 10 days sends it to EEAE asking its expert opinion. The General Secretariat of each District has to answer for each technical study, after a positive opinion by EEAE. However, the content and the process of these environmental studies are to be defined in a new decision by the Minister of Environment and Public Works. All the existing antenna stations that have not an environmental permission have to acquire one in 12 months from the publication of this ministerial decision.

Funding

According with the new Law, [4], the owners of all antenna stations are billed annually by EETT the sum of 200€ for each station and the total amount is transferred to EEAE. In this way, EEAE will have the necessary funds to achieve its duties.

Conclusions

The existing legislation in Greece imposed a strict framework for the protection of the general public from the electromagnetic fields emitted by antenna stations. It sets exposure limits based on the well-established limits of the EU recommendation and ICNIRP Guidelines. Furthermore, it established a mechanism for checking compliance with these limits before and after the installation of antenna stations. The new legislation reduced the exposure limits (towards the safe side) and made the control mechanisms stricter and intense.

References

[1] Greek legislation: Common Ministerial Decision, Protection measures for the exposure of the general public to all land based antenna stations, Act No.1105/Vol. B/6-9-2000.
[2] European Union Council Recommendation of 12th July 1999 on the limitation of exposure of the general public to electromagnetic fields (0Hz to 300 GHz) (1999/519/EC).
[3] International Commission on Non Ionizing Radiation Protection (ICNIRP), Guidelines for limiting exposure to time – varying electric, magnetic and electromagnetic fields (up to 300 GHz), Health Physics, Vol. 74, No 4, April 1998, pp 494 – 522.
[4] Greek legislation: Law No 3431 About electronic communications and other provisions, Act No. 13/A/03-02-2006.

NON-IONISING ELECTROMAGNETIC FIELD EXPOSURE MONITORING AND MEASUREMENT CAMPAIGNS IN MALTA

CHARLES V SAMMUT

DEPARTMENT OF PHYSICS, UNIVERSITY OF MALTA, MSIDA, MSD 06, MALTA

charles.v.sammut@um.edu.mt

ABSTRACT

This paper reports first on a completed three-year campaign to assess exposure of the public to electromagnetic fields from mobile phone base station antennas. The project was commissioned by the Malta Communications Authority (MCA) and consisted of information gathering and construction of a comprehensive database, field simulation at all sites in operation and detailed measurements at over half the base station sites installed on Malta.

The measurement results were analysed to supply useful information of a statistical nature. Measurement techniques are also described in the light of a recent preliminary standard (prEN 50413). Correlation exists between measured and calculated field intensities, although absolute values are not in good agreement. This occurs mainly on account of fluctuating power output from base stations, multiple reflections and diffraction effects due to surrounding structures. Field calculation is, however, useful for worst-case site assessment.

The paper proceeds by outlining the present non-ionising radiation monitoring and measurement campaign, which now includes all broadcast frequencies, and gives a brief account of a recent extensive survey conducted around the leading telecommunications tower situated in a village. Recent measurements show that, notwithstanding the proximity of some residences, radiation levels in publicly accessible areas rarely exceed much above 5% of ICNIRP reference levels for public exposure.

1. INTRODUCTION

The advent of mobile telephony and liberalisation of the telecommunications market in Malta brought about a proliferation of radio antenna sites. There are currently two companies operating mobile telephone networks in Malta, Vodafone-Malta (GSM900) and Mobisle Communications (GSM1800). Together they have about 300 base stations in operation and are developing UMTS networks, due to start operating later this year.

The country's high population density and restricted land area necessitate location of base station antennas predominantly within a densely built environment. An initial lack of public information and rapidity of base station deployment in response to increasing consumer demands have contributed to public concern that the perceived increase in exposure to radio frequency electromagnetic fields could be harmful to health. This concern was also fuelled by reports from various sources of possible exposure-related health effects. In this respect, the Stewart Report [1] has unwittingly contributed to this concern, as some of the recommendations made therein were based on the precautionary principle, which has often been misunderstood and misinterpreted by the media and the general public.

Public concern has led to some court cases instituted locally against the operators in order to prevent them from setting up new antenna sites. Some individuals living close to base station sites claimed they were suffering form adverse health effects and radio interference linked to radiation from these antennas. In some instances, adverse effects were reported soon after the installation of the base station hardware and even before its coming into operation.

In order to allay such fears and to ensure that the local mobile phone companies operate within the national guidelines [2], the MCA, which is the regulatory agency for electronic communications, post and e-Commerce, commissioned the Malta National Laboratory (MNL), as an independent provider of testing services, to conduct an extensive survey. Some preliminary results appeared in [3] and [4].

This project constituted the first phase and is followed by an ongoing programme of monitoring and measurement of emissions from all radiofrequency sources in use for telecommunications. This paper proceeds by outlining the elements of the first phase project and discussing the subsequent results. An outline of the present monitoring and field measurement activities then follows.

2. PHASE I: SURVEY OF MOBILE PHONE BASE STATION SITES

This project was spread over three years and consisted of three distinct tasks:

1. compilation of a detailed database of all base stations;
2. calculation/simulation of electromagnetic field exposure based on the transmission specifications contained in the database for each base station site;
3. measurement of electromagnetic fields at a sample of 150 of the transmission sites.

To the author's knowledge, the survey element of this project is relatively one of the most extensive yet reported in Europe, in that the measurement campaign involved over half of the licensed sites. This section describes each task, discusses calculations/simulations of electromagnetic field power density and the survey methodology, as well as analysing the measurement results.

2.1 Mobile phone base station database

The database was designed so as to enable easy record maintenance and update, as well as providing for easy access to site details, including antenna types, physical layout and transmission characteristics, as required for field calculations. The records are searchable through a number of fields and the user can retrieve associated information, such as polar plots of the antenna gain profiles in the vertical and horizontal planes and copies of field survey reports in the case of audited sites.

2.2 Field calculations and simulations

Field calculations are useful in cases where certification of site compliance is required as a precondition to granting of permits for transmission. Given maximum output power, field calculation and simulation results could generate worst case exposure scenarios. This is also useful in the case of operational transmitting stations, especially those, such as GSM, which are characterised by a fluctuating power output depending on network use. Field measurements will only reveal the prevailing emissions at the time of measurement and rarely result in registering maximum possible values.

Field simulation was an integral part of the project. Two-dimensional field intensity plots were generated for all the base station sites on the Maltese islands over planes containing publicly accessible areas. Both commercially available and in-house field calculation and simulation software were used. In both cases, far field strengths were calculated using manufacturer-supplied antenna gain profiles in the vertical and horizontal planes, and utilising height, vertical tilt, azimuth and power input information provided by the operators [3].

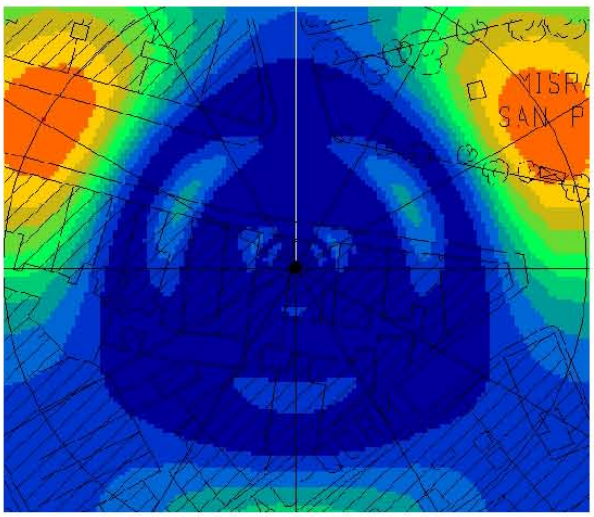


Figure 1: A typical two-dimensional field plot generated by MBSFIP™. A three-sector antenna is situated at the centre.

The commercial software used was Telstra's Mobile Base Station Field Intensity Plotter (MBSFIP™). This enabled two-dimensional colour mapping of field intensity which could be overlaid on the site plan (Figure 1). MBSFIP allows the user to select either a direct or a two-ray path model for the RF propagation loss calculations and if the two-ray model is selected, then calculations assume flat ground with ground constants (relative permittivity and conductivity) that have to be specified by the user. The program calculates reflection for vertical, horizontal or slant polarization. Information about the transmit antenna polarisation is obtained from an antenna pattern library. Thus, in the two-ray path model, the program combines the field intensity calculated along the direct path and combines this with the two ray path calculation.

Comparison between measured and calculated fields at some locations showed moderate agreement in absolute terms but high correlation [3, 10], suggesting

a systematic error, thought to be mostly due to fluctuating output power determined by network use. However, there are other factors, such as multiple reflections and diffraction effects due to surrounding structures.

2.2 Field measurement

The central and most publicly visible element of the project was the field measurement campaign which aimed to carry out audit measurements of electromagnetic field emissions at half the base station sites in operation. In fact, 151 base station sites were surveyed out of a total of 271. The sites can be classified as single operator GSM900 or GSM1800, shared (by the two GSM operators) and shared multiple technologies (GSM and other RF transmission technologies).

The aims of the base station emissions audit were to:

1. ascertain compliance of base station emissions with the ICNIRP guideline reference levels for exposure of the general public;
2. establish a baseline for typical emission scenarios which would help in deciding if and where to grant permission to operate base stations;
3. address public concerns in respect of perceived hazards of radiofrequency emissions from base stations;
4. inform and educate the public in matters concerning radiofrequency emissions.

At the beginning of the project, public concern about the possible hazard from mobile phone base station antennas was high. Selection of sites for audit was therefore a delicate task as we had to balance technical considerations with the need to allay public concerns. A broad representation of audit sites based on type and geographical location was sought. Sites were therefore selected roughly on the basis of the number of base stations installed per locality, which is indicative of population density and frequency of use. Within each locality, base station sites close to schools were audited and in all such cases the adjacent school premises were also surveyed carefully. The bulk of the base stations selected for the audit survey were sited over commercial buildings and private homes within or in the vicinity of densely built residential areas. In general, and wherever possible, measurements were taken over properties neighbouring the selected base station sites. Surveyed areas included accessible recreational open spaces situated in the vicinity of base station sites selected for audit. Table 1 lists the base station sites by type. Commercial buildings included hotels, shopping outlets of varying sizes, showrooms, stores and industrial units.

Table 1: Base station sites classified by type

SITE TYPE	Number of base stations	Number surveyed
Commercial buildings	105	61
Private residences	94	41
Social clubs	15	10
Churches	11	9
Public buildings	9	4
Transmission stations	6	1
Old people's homes	5	5
Hospitals	2	2
Schools	2	2
Other	22	16
TOTAL	271	151

Owing to expected higher power density levels and for reasons of greater public concern, 80% of shared sites were audited, compared to 62% and 45% respectively of single operator GSM900 and GSM1800 base stations. Broad representation on the basis of geographical location and population density was also achieved.

2.3 Field survey methodology

The project started when European measurement standards for non-ionising radiation safety assessment were still in a state of flux. The methods adopted were inspired by Canadian [5] and US [6] recommendations and developed by the author in the light of his own research and local experience. However, the methods subsequently described in the CENELEC preliminary standard prEN 50413 [7] and the ECC Recommendation [8] are similar and additional techniques were shown to generate useful data for assessing exposure realistically at most transmission sites [3, 4, 9, 10].

Measurement procedures and subsequent analysis were geared principally toward assessment of the extent of human exposure arising from operation of the sources present at the investigated sites. Each survey started with a visual inspection of the antenna site and all transmitting antennas were photographed for the records. The antenna locations were marked on the site plan and notes were taken describing the site, access restrictions and antenna configurations.

The field survey equipment used consisted of the Narda 8718B survey meter in conjunction with the models 8760D and the D8722D broadband, isotropic electric field probes. Summary specifications of these isotropic probes are listed in Table 2. The field survey started with a preliminary scan of the site conducted by meandering within areas where exposure was expected to be relatively higher, i.e. along the transmission directions facing the antenna panels. This procedure allowed the surveyor to establish a set of measurement points that included regions of maximum exposure. However, measurement points were also chosen on grounds of site use by the public or authorised personnel, in cases where the site was not accessible to the public.

Table 2: Broadband isotropic field probes used during the phase field surveys

Model No.	Frequency Range	Nominal Measurement Range		Frequency Response	Sensor Type
		Power Density	*E* [Vm^{-1}]		
8760D	300kHz – 3.0GHz	5.0×10^{-2} – 1.0 Wm^{-2}	0.5 – 19.4	Flat	Compensated Diode
D8722D	300kHz – 50GHz	0.3 – 300% of Standard*	–	Weighted	Compensated Diode and Thermocouple

* Referenced to ICNIRP guideline levels for occupational exposure

Three main measurement modes were used, depending on site-specific suitability:

Time averaging (TAV) – measurement of field intensity at a given point over a pre-defined time interval, the survey meter storing average and maximum field strengths during the process. About 1,500 such measurements were made during the course of the survey. The intervals varied between 10 and 120 seconds, depending on signal variability. At none of the sites investigated was it found necessary to take six-minute time averages because the power density levels recorded were below the ICNIRP reference levels for exposure of the public, as recommended in [7] and [8].

Spatial averaging over the human body area (BAV) – vertical scan with the probe moved at a slow, steady speed between points distant 10 and 200cm above ground level [3] while the survey meter stores the average and maximum field strengths. Over 1,500 such measurements were made during the course of the project. This allowed a more extensive exposure assessment than would have been possible with the more laborious procedures described in [5], [7] and [8].

Extended spatial averaging (ESA) over a defined three-dimensional region – a scan of a defined region with the probe raised and lowered at a steady speed while zigzagging systematically through the designated area, the survey meter storing average and maximum field strengths during the process. This technique was reported in [3] and further validated in [4]. In all, 277 ESA measurements were conducted at various sites throughout the project.

2.4 Field survey results

A total of about 3,300 field strength measurements were made during the course of the project at 151 sites. Summary values are represented in Figure 2. These values represent site average and maximum recorded field strengths. More than half the surveyed sites were found to have average exposure levels between 0.08 and 0.47% of the ICNIRP public exposure level (PEL), while the maximum exposure level at over half the sites ranged between 0.27 and 2.14%.

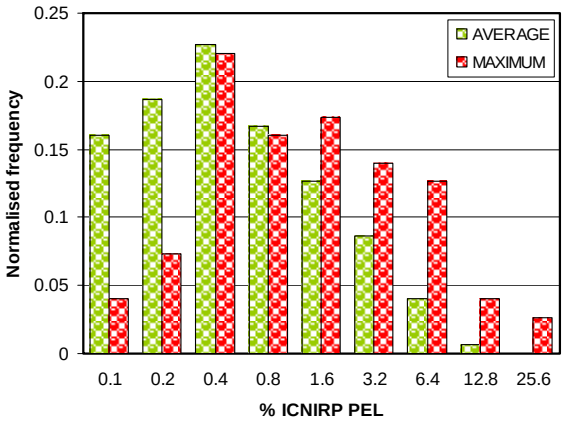


Figure 2: Normalised frequency distribution of measured site average and maximum field strengths.

At two sites the 25% ICNIRP PEL mark was exceeded but at locations that were not easily accessible to the general public. At one particular shared site, GSM900 and 1800 base stations were collocated on the roof of a hotel only accessible to authorised personnel for maintenance purposes. Broadcast radio and TV antennas were also in operation at that site. The maximum measured field strength recorded from the GSM base stations was 29.3%. A BAV of 61% and a maximum of 382% of ICNIRP PEL were also recorded at the same site with all sources operating together. It was possible to identify the GSM component by collaboration with the operators, who kindly switched off the relevant transmitting antennas during part of the

survey to allow measurement of the non-GSM component.

Figure 3 shows the normalised frequency distribution of time average field strengths (TAV), along with the maxima recorded during these measurements. The data included all measurements recorded during the project at all the sites investigated, except for the extreme values mentioned in the preceding paragraph. The distribution indicates predominantly low field strengths. Half the time average field strengths measured were between 0.04 and 0.42% of ICNIRP PEL (Table 3), while half the maxima were between 0.05 and 0.51%.

Table 3: Statistical summary of measured field intensity in % of ICNIRP PEL

	TAV-AV	TAV-MAX	BAV-AV	BAV-MAX	ESA-AV	ESA-MAX
Lower quartile	0.04	0.05	0.03	0.06	0.04	0.16
Median	0.14	0.17	0.08	0.19	0.09	0.34
Upper quartile	0.42	0.51	0.28	0.55	0.30	1.05

The measured BAV field strengths show similar overall characteristics, in that they are predominantly low, as can be seen from Figure 4, which shows the frequency distribution, along with maxima recorded during the averaging process. This analysis also included all the BAV measurements made throughout the course of the project at all the sites investigated, except for the mentioned extreme values. As indicated in Table 3, half the values obtained were between 0.03 and 0.28% of ICNIRP PEL, while half the recorded maxima were between 0.06 and 0.55%.

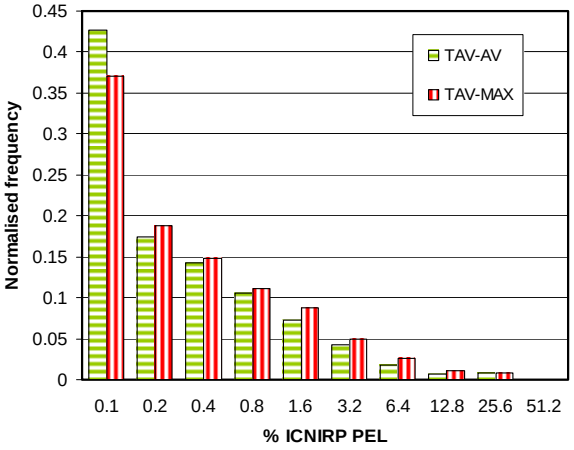


Figure 3: Normalised frequency distribution of measured time average (TAV-AV) and maximum (TAV-MAX) field strengths.

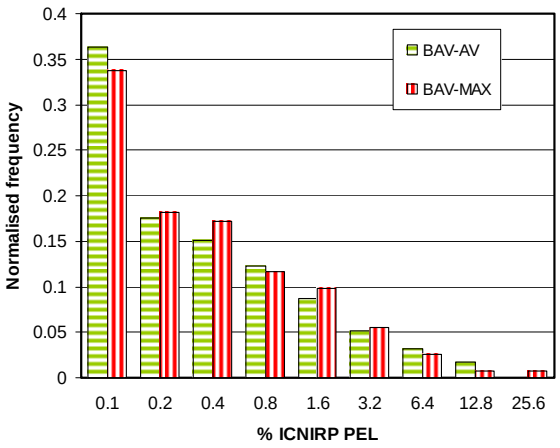


Figure 4: Normalised frequency distribution of measured body average (BAV-AV) and maximum (BAV-MAX) field strengths.

The ESA field strength values obtained are represented in Figure 5, which shows the frequency distribution of measured extended spatial average field strengths and maxima obtained during the averaging process. Some of these measurements were made in areas not accessible to the public and in close proximity to radiating antennas and this explains the relatively higher ESA-MAX median and quartiles given in Table 2. The TAV-MAX and BAV-MAX statistics are close. This is explained when considering that, during the BAV scans, the maximum field strength was recorded predominantly at about 2m above ground level, where most TAV measurements were made close to the same spot. Measurements at this level tend to be higher in the vicinity of a transmitting antenna, which would typically have its main beam directed well above accessible heights.

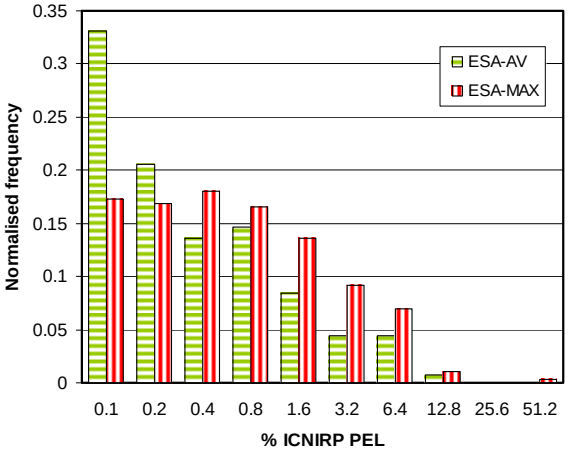


Figure 5: Normalised frequency distribution of measured extended spatial average (ESA-AV) and maximum (ESA-MAX) field strengths.

The BAV measurement records (about 1500) were analysed for possible variation with weekday and time of day. From Figures 6 and 7, it is not possible to draw suitable conclusions, when one considers the large standard deviation in the data, ranging from 0.4 to 1.3 %

ICNIRP over the week days Monday to Friday (Table 3). Such variation arises as a consequence of the fact that field measurements were conducted at many different locations and heights with respect to the transmitting antennas and were not intended to monitor diurnal fluctuations at specific locations.

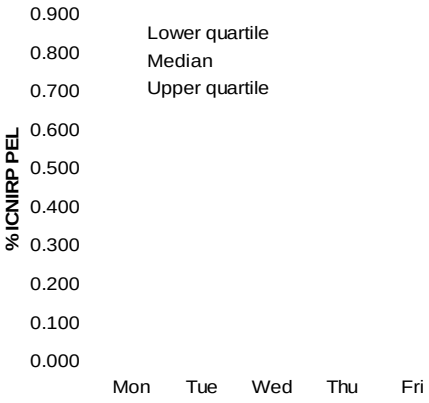


Figure 6: Variation of BAV-MAX by weekday.

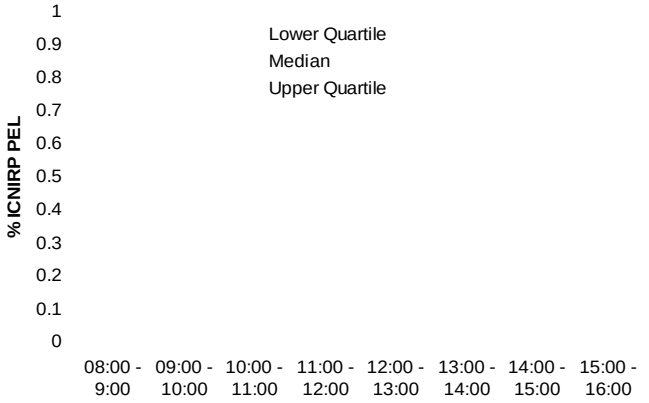


Figure 7: Diurnal variation of BAV-MAX (all weekdays).

3. PHASE II: ONGOING PROGRAMME OF AUDIT SURVEYS

At some shared radio sites, non GSM sources were present that had been set up before the present guidelines [2] came into force. It had been clear from the outset that at such transmission sites, field intensity apportionment and careful assessment of the antenna layout and transmission equipment were required. Having completed the first phase, the scope of the audit surveys was therefore widened in 2004 to include all telecommunications sources within the remit of the MCA. Monitoring compliance is now the major objective, since increased awareness of the general public, partly resulting from the phase I project, has somewhat succeeded in allaying public apprehension toward mobile phone base station emissions.

MCA now has an ongoing programme to verify compliance of radio transmission sites with ICNIRP reference levels for exposure of the general public. MCA technicians were trained by the author to conduct RF emissions using frequency selective and broadband techniques based on those outlined in [7] and [8]. Most transmission sites have by now been audited at least once.

The main instrument being used for the frequency selective measurements is the Narda SRM 3000 in conjunction with an isotropic electric field probe, covering the range 75MHz to 3GHz. Conventional spectrum analysers in conjunction with single axis antennas are also used for more accurate measurements when required.

One of the most sensitive sites investigated extensively during the second phase was the area surrounding the island's main telecommunications tower installed at the village of Gharghur. The tower, which for some years has been a source of concern to the residents, is situated about 400m from a primary school and close to private residences. It is host to the main broadcast TV and radio station repeaters, GSM and other communications antennas, as well as microwave links (Figure 8). Six-minute frequency selective time average field strength measurements were made at 15 carefully chosen locations in this village, including two inside the neighbouring school and several within private residences. Figure 9 represents the summary results including all emissions within the frequency range 75 MHz to 3 GHz. Again, the measured field intensities were relatively low, even within the tower precincts. The highest level recorded was 10% of ICNIRP PEL on a first floor terrace at a nearby residence.



Figure 8: The Gharghur telecoms tower.

Measurements conducted so far have rarely resulted in field strengths higher than about 5% of ICNIRP PEL. More accurate measurement techniques than those afforded by isotropic probes place an additional burden not required for the purpose of site compliance certification.

Field calculations will soon form part of the ongoing programme of radiation hazard assessment. The database will incorporate all licensed transmission sources and shall include technical details sufficient to permit field calculations. These will be used to generate worst-case

exposure scenarios in support of the measurement campaigns and should serve as an important tool in educating the general public, apart from helping to dispel misconceptions concerning emission levels.

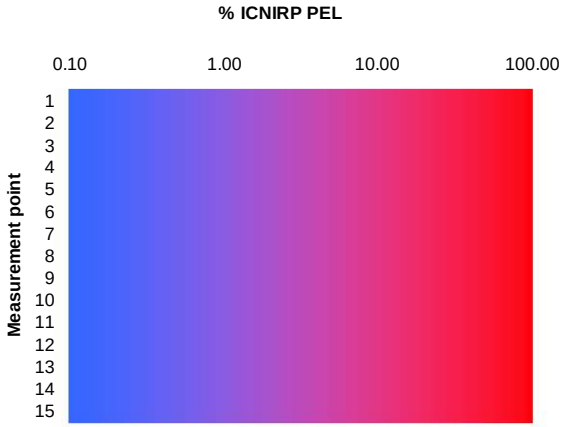


Figure 9: Summary of Gharghur survey results, indicating total field intensity from all sources obtained by taking six-minute time averages at 15 different locations in the village.

3. SUMMARY

A three-year national survey of emissions from GSM base stations in Malta started during 2002. This project was concluded and showed that the emissions in all areas accessible to the general public were well below the ICNIRP reference levels for exposure of the general population.

As part of this project, a detailed database containing relevant information on each operational base station was constructed and field simulations made on the basis of the data supplied by the operators. Although specific values of calculated and measured fields only concur moderately because of the variability of network use and clutter occurring within built environments, field calculation is a valuable tool that can be used to establish worst-case exposure to electromagnetic fields and is useful in cases where certification of site compliance is required as a precondition to granting of transmission permits.

Recently, MCA has updated measurement and survey techniques in line with the preliminary CENELEC standard prEN 50413 [7] and a Recommendation of the ECC [8]. All telecommunications sources are now being targeted in this second phase, which aims to survey fixed transmission sites periodically.

Finally, it is observed that broadband field measurement techniques used during the first phase resulted in many more measurements than were feasible with narrowband techniques, especially when conducting six-minute averaging. The case for narrowband measurements when conducting compliance-oriented field surveys can only really be justified at sites found close to the prevalent limit level as this would allow apportionment by source. Furthermore, although taking a six-minute time average is better than averaging over shorter time intervals, in the latter case more such measurements may be made with minimal additional effort. This could give a better picture of the prevailing exposure scenario at the site under investigation since, in the case of cellular networks, the power output fluctuates significantly over short time spans. Supporting such field surveys with reliable worst-case field calculations provides an economical and reliable means of examining site compliance.

ACKNOWLEDGMENTS

The author wishes to acknowledge the support of MNL, for providing the test equipment and logistics during phase I of the project and MCA for financing this phase and assisting in the often complicated logistical arrangements required during the measurement campaigns.

The author is indebted to John Bugeja (MNL) for assisting in the audit surveys conducted during phase I and acknowledges the support of Joanna Formosa Borg, Brian Sghendo and Kevin Aquilina from MCA, who have conducted most of the work during phase II.

REFERENCES

[1] S Steward, *Mobile Phones and Health*. A report from the Independent Expert Group on Mobile Phones. Independent Expert Group on Mobile Phones Secretariat.

[2] *Report on Recommendations for Limiting Human Exposure to Time Varying Electric, Magnetic and Electromagnetic Fields in the Frequency Range from 0 Hz to 300 GHz*, Ministry of Transport and Communications, Ministry of Health and Ministry for Social Policy, Malta.

[3] C V Sammut and A Micallef, *A An Extensive RF Emissions Survey at Cellular Mobile Phone Base Station Sites in Malta*, Proceedings of the 2nd International Workshop On Biological Effects of Electromagnetic Fields, 7-11 October 2002, Rhodes, Greece, 977-986.

[4] C V Sammut and A Micallef, *Analysis of a simple technique for measuring the average exposure to electromagnetic fields over an extended region of space*, 3rd International Workshop On Biological Effects of Electromagnetic Fields, 4-8 October 2004, Kos, Greece, 832-836.

[5] *Limits of Human Exposure to Radiofrequency Electromagnetic Fields in the Frequency Range from 3 kHz to 300 GHz*, Safety Code 6, Environmental Health Directorate, Minister of Public Works and Government Services, Canada 1999.

[6] *Evaluating Compliance with FCC Guidelines for Human Exposure to Radiofrequency Electromagnetic Fields*, OET Bulletin 65, Edition 97-01, Federal Communications Commission, Office of Engineering & Technology, August 1997.

[7] prEN 50413: *Basic Standard on measurement and calculation procedures for human exposure to electric, magnetic and electromagnetic fields (0 Hz – 300 GHz)*, CENELEC, 2006.

[8] ECC/REC/(02)04, *Measuring non-ionising electromagnetic radiation (9kHz – 300 GHz)*, Revised ECC Recommendation (02)04, Electronic Communications Committee within the European Conference of Postal and Telecommunications Administrations, October 2003.

[9] C V Sammut and A Camilleri, *An Extensive Survey of RF Emissions at Cellular Mobile Phone Base station sites in Malta and Gozo: First Year*, XII Annual Engineering Conference: Engineering the Environment, 21 May 2003, St. George's Bay, Malta.

[10] C V Sammut, *Exposure to electromagnetic fields from cellular phone base stations in Malta: Final report of the three-year national survey*, Malta Communications Authority, 2006.

THE ETIOLOGY OF MELANOMA

ÖRJAN HALLBERG

HALLBERG INDEPENDENT RESEARCH
POLKAVÄGEN 14B, 142 65 TRÅNGSUND, SWEDEN
http://hir.nu

Abstract
The main purpose of this project was to find a possible explanation for the steadily increasing incidence of melanoma in Western countries since the mid-20th century. A secondary purpose was to develop models with predictive value in order to estimate future melanoma trends. Results indicate that the immune defense system for cell repair and apoptosis was disrupted by body-resonant broadcasting radiation from FM towers, and that this disturbance can fully explain both local and temporal variations in melanoma incidence and mortality.

Introduction
In May 1998 the author became aware that at the end of the 1950's, there was a sudden increase in melanoma incidence in Sweden; this coincided with a time when the country was in the midst of the process of gradually becoming covered with FM and TV broadcasting towers. This realization led to a study comparing Nordic countries with the USA to see if there was any association between melanoma incidence and the appearance of large numbers of FM broadcasting towers. A second, later study investigated the geographical variation of melanoma incidence in Sweden and its possible correlation with the geographical variation of other cancers. In a third study, melanoma incidence over time was compared with the advent of FM broadcasting in Swedish counties and with increasing habits of taking charter travels to sunnier resorts. A fourth study investigated if melanoma incidence could successfully be modeled as a response to sudden changes in environmental stress. A theory and model to explain the increased incidence of melanoma were then developed, and the model was then refined to take into account the observation that UV radiation-induced cell damage is cumulative but normally compensated for by a cell repair process that was assumed to have become less efficient from a specific point in time.

Summary
An initial study showed that Nordic countries and the USA both appeared to have the same exposure-time-specific incidence of melanoma, despite the fact that the advent and subsequent spread of FM transmitter appearance differed among the different countries [1]. A second study showed that the incidence of some cancers correlated with variations in melanoma incidence across the Swedish counties, while others (e.g. leukemia) did not [2]. Melanoma also appeared to persist at a low and stable incidence in the counties as long as FM transmitters had not yet been substantially introduced. Mortality from existing cases of melanoma showed an immediate increase that correlated with the introduction of FM broadcasting towers, and the incidence of new cases started to increase a few years after the spread of FM towers [3]. Melanoma incidence appeared to be significantly correlated with the number of main FM towers simultaneously covering an area [4]. A model for melanoma incidence was developed based on a statistical distribution of the time from the introduction of FM broadcasting until the onset of melanoma [4, 5]. Finally, it was also shown that a model based on a precipitous decrease in the efficiency of the immune defense system (presumably caused by FM broadcasting towers) was able to accurately predict the reported age-standardized incidence and age-specific incidence of melanoma for all birth cohorts during the 20th century [6].

The project concluded that body-resonant radiation from FM broadcasting towers may disturb cell repair and apoptosis processes and that this may be one of the most important factors behind the observed increase in melanoma rates in the Nordic countries. Normal broadcasting radiation is not likely to be able to cause cellular damage *de novo*, but may be able to weaken defenses against cellular damage that may be caused by pervasive "natural" sources such as UV exposure etc. It would seem logical to extend this study to similarly review lung cancer and breast cancer to examine the possibility of a correlation between these cancers and FM broadcasting radiation.

Acknowledgements
The author thanks assoc. prof. Olle Johansson at the Experimental Dermatology Unit, Department of Neuroscience, the Karolinska Institute, Stockholm, Sweden, for co-operation in several papers related to this project.

References

1. Hallberg Ö, Johansson O. Melanoma incidence and frequency modulation (FM) broadcasting. Arch Environ Health 2002; 57: 32-40
2. Hallberg Ö, Johansson O. Cancer trends during the 20th century. ACNEM Journal 2002; 21: 3-8
3. Hallberg Ö. and Johansson O. Malignant Melanoma of Skin - Not a Sunshine Story!, Med Sci Monit, 2004; 10: CR336-340
4. Hallberg Ö, Johansson O. FM broadcasting exposure time and malignant melanoma incidence. Electromagnetic Biology and Medicine 2005; 24: 1-8
5. Hallberg Ö. Increasing incidence of malignant melanoma of the skin can be modeled as a response to suddenly imposed environmental stress. Med Sci Monit, 2005; 11: CR457-461
6. Hallberg Ö. A theory and model to explain the skin melanoma epidemic. Melanoma Research, 2006; 16: 115-118

FORCE CALIBRATION OF OPTICAL TRAP BY DIELECTROPHORESIS

T. SAVOPOL*, E. PAPAGIAKOUMOU**, M. CHIRILA*, M. MAKROPOULOU**, A. SERAFETINIDES**, M. RADU*, D. PIETREANU*, G. MARTÍNEZ-LOPEZ***, M. SANCHO RUIZ***, E. KOVÁCS*

**CAROL DAVILA MEDICAL UNIVERISTY, P.O.Box 35-43, BUCHAREST, ROMANIA*
***NATIONAL TECHNICAL UNIVERSITY OF ATHENS , GREECE*
****COMPLUTENSE UNIVERSITY OF MADRID, SPAIN*

Abstract
A calibration method for optical tweezers, based on equilibration with a dielectrophoretic force, is presented. The analytical method for the computation of the dielectrophoretic force is based on a mathematical model using Green's theorem. The dependence of the optical force profile on the particle position between the electrodes and on the vertical axis is rigorously analysed and the best operating conditions are determined.
In order to have an experimental validation of the model, we used a dielectrophoretic chamber with planar electrodes and a laser diode optical tweezers (800 nm). A suspension of red blood cells was placed between the electrodes of the dielectrophoretic chamber and the optical trapping force was measured under different conditions.
We show that by applying simultaneously dielectrophoretic and optical forces on a cell, the evaluation of intracellular dielectric parameters (i.e. cytoplasmic and membrane conductivity in normal and/or pathological states) at a single cell level is possible.

Introduction
Micromanipulation of cells has become in the last years an important tool for the fundamental research as well as for some clinical applications. There are different techniques to do this, including micropipettes, microelectrodes, optical and magnetic traps. When comparing these techniques, there are of course, for each of them, advantages and disadvantages, but, the most important and decisive advantage of optical and magnetic traps is the minimal mechanic contact with the cell, optical and magnetic trapping being nowadays considered to be the less invasive micromanipulation methods.
For research purposes, the method can be used to put cells into contact, to measure interaction forces between cells and / or molecules (e.g. ligand – receptor interaction forces). The main problem in pursuing such experiments is to calibrate the trapping force. In the following we will focus our attention only on optical trap force, but the rationale can be used as well for the magnetic trap.
We will show that one can use the dielectrophoretic force as a quite simple and reliable tool to calibrate the optical trap force, and, based on this, we'll show interesting possibilities to determine some physical properties of cells in relation with their physiological state.

Principles of the optical trap
Optical traps (or tweezers) were first described by Ashkin [1 – 3] and are based on the interaction of light with a particle. In this interaction different regimes of theoretical approach can be distinguished based on the ratio of the incident light wavelength λ to the diameter d of the irradiated particle: Rayleigh Regime ($\lambda/20 >> d$), Lorenz-Mie Regime ($\lambda \approx d$) and Ray Optics Regime ($\lambda/20 << d$).The net force is the result of a combination of two different components: scattering force and gradient force. In the Rayleigh Regime the particle is acting like an induced dipole in the electric field of the laser beam. The expressions of the forces are:

$$\vec{F}_{scatt}(\vec{r}) = \vec{z} n_m \frac{\sigma(S)_T}{c} \tag{1}$$

$$\vec{F}_{grad}(\vec{r}) = \frac{1}{2}\alpha\vec{\nabla}\vec{E}(\vec{r},t)^2 \tag{2}$$

where $(S)_T$ is the temporal average of the Poynting vector, which defines the intensity of the laser beam, $\sigma = \frac{8}{3}\pi(ka)^4 a^2\left(\frac{n^2-1}{n^2+2}\right)^2$ is the cross section of the particle, $\vec{z}$ is the laser beam direction, n_m is the relative refractive index, a is the radius of the particle, $k = 2\pi/\lambda$ is the wave number, c represents the light speed in vacuum, $\vec{E}$ is the electric field and n is the absolute refractive index of the particle.

For a spherical particle in Ray Optic Regime, Ashkin established formulae for these two forces as a function of the Fresnel coefficients [1]. The expressions can be deduced based on geometrical optics laws, their scalar form being:

$$F_{scat} = \frac{n_1 P}{c}\left\{1 + R\cos(2\theta) - \frac{T^2\left[\cos(2\theta - 2r) + R\cos(2\theta)\right]}{1 + R^2 + 2R\cos(2R)}\right\} \tag{3}$$

$$Fgrad = \frac{n_1 P}{c}\left\{R\sin(2\theta) - \frac{T^2\left[\sin(2\theta - 2r) + R\sin(2\theta)\right]}{1 + R^2 + 2R\cos(2R)}\right\} \tag{4}$$

where *P* is the power of the incident beam, n_1 is refractive index of the particle, R and T are the reflectance and transmittance coefficients, θ and r are the incident and refracted angles. The expressions (3) and (4) are true for a "normal" light ray. The laser beam, being a bundle of rays, has a specific profile which has a significant contribution to the gradient force.

Finally, the net force exerted on the particle is given by the expression

$$F_{optic} = Q\frac{n_{med} P}{c} \tag{5}$$

where Q is a scaling constant which depends on the size of the particle and the refractive index difference between the particle and the surrounding medium, P is the power of incident laser beam, n_{med} is the refractive index of the medium and c is the light speed in vacuum.

Summarizing, one can say that the optical force is proportional to the power of the laser beam, and depends on some physical properties of the particle. To calibrate the laser trap means to determine this scaling factor, Q.

Calibration methods

There are two main calibration methods which are presently used for optical traps:

- Brownian movement analysis: this method is based on the statistical analysis of the Brownian movement of a trapped particle, from which one can learn about the trapping force. The method implies an extremely rigorous temperature control of the microscope stage, which is not technically trivial considering that the laser beam itself provoke some local heating of the sample, and sophisticated mathematics for image analysis;
- Viscous drag of the trapped particle: the particle is placed in a capillary tube with a constant known diameter through which the suspension buffer flows with a constant speed. A particle is trapped, and the flowing speed is increased until the particle escapes. Assuming that the flow is Newtonian, one can calculate the viscous force, which, at that moment, equals the optical force. The major problem with this method is to ensure a real Newtonian flow through the capillary.

In this paper we describe a calibration method based on the dielectrophoretic force exerted on the trapped particle.

The dielectrophoretic force exerted on a particle depends on the induced dipole moment and is unaffected by the direction of the electric field, responding only to the field gradient. Accordint to Pohl [4], the dielectrophoretic force is given by the expression:

$$\vec{F}_{DEP} = \left(\vec{P}_{eff}\cdot\vec{\nabla}\right)\vec{E}_0 \tag{6}$$

For a spherical particle of radius r, the dielectrophoretic force is given by the expression:

$$\vec{F}(\omega) = 2\pi r^3 \varepsilon_m \,\mathrm{Re}\left[K(\omega)\right]\vec{\nabla}E^2 \tag{7}$$

with

$$K(\omega) = \frac{\left(\varepsilon_p^* - \varepsilon_m^*\right)}{\left(\varepsilon_p^* + 2\varepsilon_m^*\right)} \tag{8}$$

and

$$\varepsilon^* = \varepsilon - j\frac{\sigma}{\omega} \tag{9}$$

where ε_m^*, ε_p^* are the complex permitivities of the medium and the particle respectively and ω is the angular frequency of the applied field. For a particle with shell, the expression of the complex permitiviy becomes:

$$\varepsilon_p^* = \frac{\left[\frac{r}{r-d}\right]^3 + 2\left[\frac{\varepsilon_{\mathrm{int}}^* - \varepsilon_{mem}^*}{\varepsilon_{\mathrm{int}}^* + 2\varepsilon_{mem}^*}\right]}{\left[\frac{r}{r-d}\right]^3 - \left[\frac{\varepsilon_{\mathrm{int}}^* - \varepsilon_{mem}^*}{\varepsilon_{\mathrm{int}}^* + 2\varepsilon_{mem}^*}\right]} \tag{10}$$

The computation of the root mean square of the electric field at a specified point between and over the electrodes is made using the second Green's identity:

$$\int_V dV\left(\Phi\nabla^2\Psi - \Psi\nabla^2\Phi\right) = \oint_A dA\left(\Phi\frac{\partial\Psi}{\partial n} - \Psi\frac{\partial\Phi}{\partial n}\right) \tag{11}$$

One of the function (Φ) is choosen to be the potential between electrodes ($z = 0$), $\nabla^2\Phi = 0$ and the other (Ψ) is a Green function given by $\nabla^2\Psi\left(\vec{r},\vec{r}_0\right) = -4\pi\delta\left(\vec{r} - \vec{r}_0\right)$. Determination of the Green function is made using the mirror-image method.

$$\begin{aligned}\Psi &= \frac{1}{\left|\vec{r} - \vec{r}_0\right|} + \frac{-1}{\left|\vec{r} - \vec{r}_0'\right|} \\ &= \frac{1}{\sqrt{\left(x - x_0\right)^2 + \left(y - y_0\right)^2 + \left(z - z_0\right)^2}} \\ &+ \frac{-1}{\sqrt{\left(x - x_0\right)^2 + \left(y - y_0\right)^2 + \left(z - z_0\right)^2}}\end{aligned} \tag{12}$$

The first order approximation (assuming that the potential varies linearly between the two electrodes) is used, so that the boundary conditions are given by:

$$\Phi\left(x, y, z = 0\right) = \begin{cases} \frac{V}{2}\cos\left(\omega t\right), & -l_x - \Delta\langle x\langle -\Delta \\ -\frac{V}{2}\cos\left(\omega t\right)\frac{x}{\Delta}, & -\Delta \le x \le +\Delta \\ 0 & -\infty\langle x \le l_x - \Delta, l_x + \Delta\langle x\langle\infty \end{cases} \tag{13}$$

Where Δ is half distance between the electrodes.
The expression for the electrical field is then:

$$\Phi(x, y, z) = \frac{-V}{2\pi}\cos(\omega t)\left[\frac{z}{\Delta}\ln\sqrt{\frac{(x+\Delta)^2 + z^2}{(x-\Delta)^2 + z^2}} - \arctan\left(\frac{2xz}{z^2 + \Delta^2 - x^2}\right) + \frac{x}{\Delta}\arctan\left(\frac{2\Delta z}{z^2 - \Delta^2 + x^2}\right)\right] \tag{14}$$

After an algebric calculation, the root mean square of E^2 becomes, as it was shown by [5]:

$$E_{rms}^2 = \frac{V^2}{8\pi^2\Delta^2}\left[\frac{-8x^2z\Delta + \left[x^4 + 2x^2\left(z^2-\Delta^2\right) + \left(z^2+\Delta^2\right)^2\right]\arctan\left(\frac{2x\Delta}{x^2+z^2-\Delta^2}\right)}{\left[(x-\Delta)^2+z^2\right]\left[(x+\Delta)^2+z^2\right]}\right]^2 + \frac{V^2}{8\pi^2\Delta^2}\left[\frac{4x\Delta\left(x^2-z^2-\Delta^2\right) + \left[x^4 + 2x^2\left(z^2-\Delta^2\right) + \left(z^2+\Delta^2\right)^2\right]\ln\frac{(x+\Delta)^2+z^2}{(x-\Delta)^2+z^2}}{\left[(x-\Delta)^2+z^2\right]\left[(x+\Delta)^2+z^2\right]}\right]^2 \quad (15)$$

For the particular case of our dielectrophoretic cell, the root mean square of E^2 has the profile shown in Fig. 1.

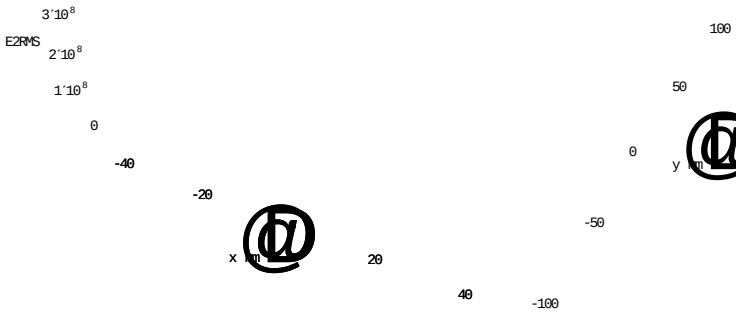


Figure 1: *Distribution of root mean square of E^2 between the electrodes of the dielectrophoretic chamber. The x axis is along a direction within the plane of the cell and perpendicular to the electrodes, while the y axis is perpendicular to the plane of the cell and along the optical axis of the microscope.*

The value of the dielectrophoretic force can thus be calculated by introducing this last equation in (7).
As an example, we give the profile of the horizontal (x) component of the force in the case of our experimental setup, at two different constant heights (5 μm and 35 μm) above the plane of the cell, as a function of the position of the particle between the electrodes (Fig. 2). In this case the distance between electrodes is 100 μm (Δ = 50 μm) , and the voltage is $V = \pm 1.5\,V$

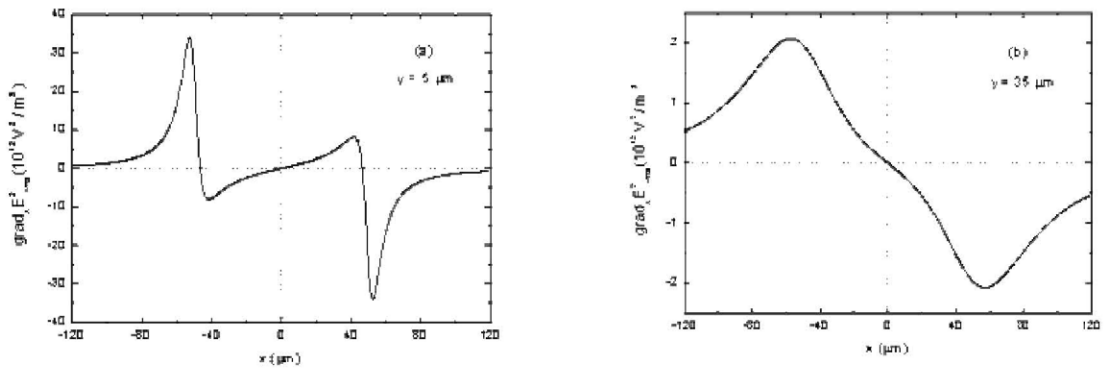


Figure 2: *The x-component force profile computed as a gradient of E_{rms}^2 at two different heights above the plane of the dielectrophoretic cell : (a) y = 5 5 μm and (b) y = 35 μm. The gap between the electrodes lays from*

-50 μm to 50 μm along the x axis.

The vertical component of the force can be also computed, but it is less important for our purposes.

Experimental protocol and results

The optical tweezers we used was built on a normal optical microscope (IOR MC9) on which a laser diode of 830 nm wavelegth and 40 mW maximum power was mounted. Maximum 27 mW power was getting out of the lens in the focal plane, as measured by a power-meter. The diode was connected to a variable power supply which allows adjustment of the laser beam output power.

The dielectrophoretic chamber consisted of two thin planar electrodes deposited on a microscope slide at a distance of $2\Delta = 100\mu m$. The electric field was applied by a computer controlled function generator (PC Generator PCG10/K8016 Welleman Instruments). For calibration, red blood cells with dielectric parameters, $\varepsilon_{\text{int}} = 50\varepsilon_0$ and $\sigma_{\text{int}} = 0.5\ S \cdot m^{-1}$, $\varepsilon_{mem} = 11.3\varepsilon_0$ and $\sigma_{\text{int}} = 10^{-7}\ S \cdot m^{-1}$ were used. The suspension buffer was a 0.3 M Mannitol solution at $pH = 7.4$ and dielectric parameters: $\varepsilon_{med} = 80\varepsilon_0$ and $\sigma_{med} = 235\ \mu S \cdot cm^{-1}$.

All measurements were performed using a 100X microscope lens with 1.25 numerical aperture.

The first step is to determine the output force of hte laser beam at the focal point as a function of the applied voltage on the diode. This is done by using an appropriate power-meter and measuring the emitted power at different voltages. The results can be seen in Fig. 3.

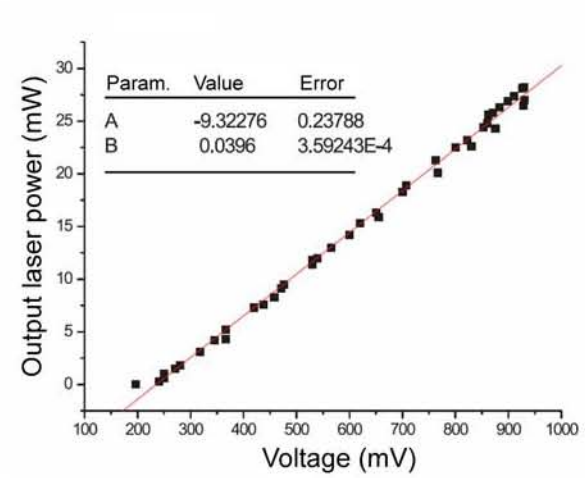


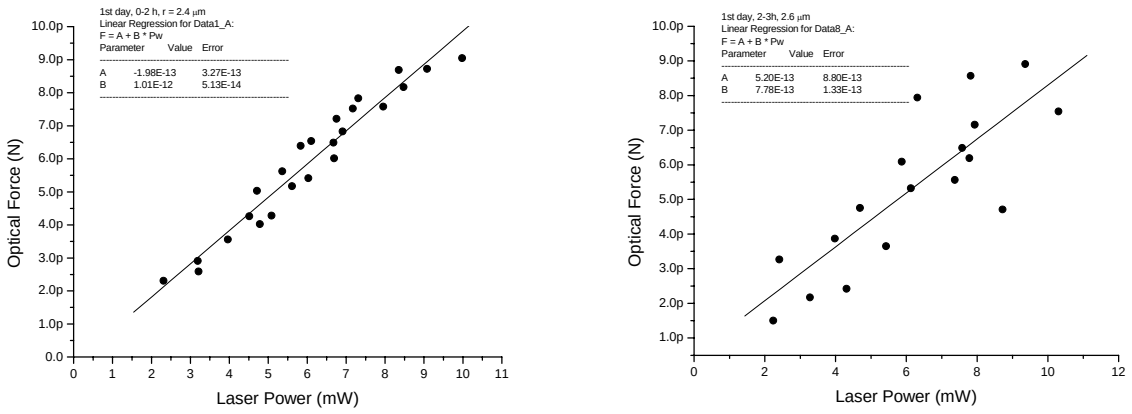
Figure 3: *Laser beam power calibration, as a function of the electric power applied to the laser diode.*

After this first step, we used a standard procedure which consists in the following:

- a cellular suspension is placed on the dielectrophoretic chamber and mounted on the microscope;
- a cell which lays between the electrodes, but closer to one of them is trapped in the laser beam using the maximum laser power;
- then an AC field of 1 MHz frequency and very low voltage amplitude is applied on the electrodes. As a result, a dielectrophoretic force will act on the trapped cell, which depends on the cell diameter and its position between the electrodes (the *x* position) and along the vertical (*y*) axis;
- the voltage is then increased until the cell escapes the trap (at this moment the dielectrophoretic force equals the optical force); introducing this last value of the voltage in equations (15) and (7), one can compute the optical force exerted by the laser on the cell.

We measured these forces for red blood cells at different intervals after the blood colllection and different times after withdrawal of the sample from the refrigerator.

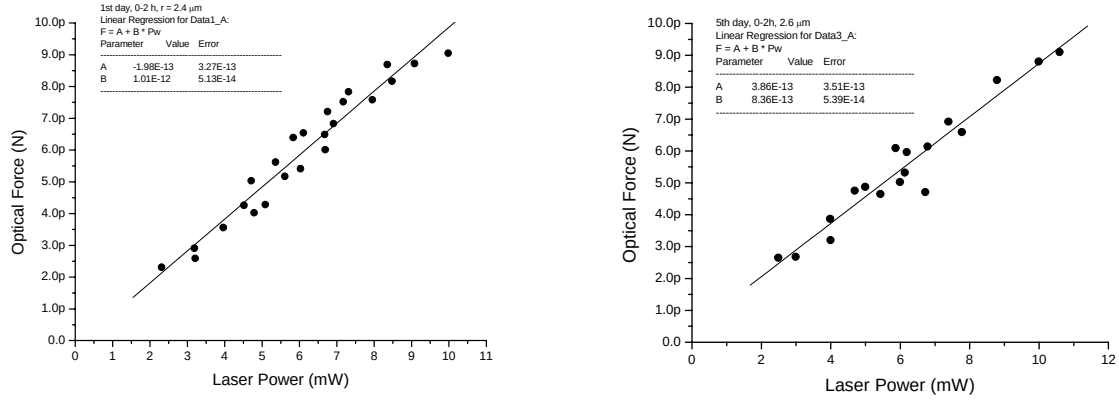
Some representative results can be seen in Figs. 4 and 5.



(a) (b)

Figure 4: *Optical trap force as a function of the applied laser power, measured soon after the sample was taken out of the refrigerator(a) and 2 h later (b) .*

Inspecting Fig. 4 it can be seen that the dependence is linear. It can also be seen that in similar conditions, cells which were kept for longer periods at the room temperature (Fig. 4b) present a much higher dispersion than samples measured immediately after they were taken out of the refrigerator.
In Fig. 5 we present results obtained on cells with the same diameter (2.6 μm), at different storage times (1st day after blood collection (a) and 5th day after (b)).



(a) (b)

Figure 5: *Optical trap force as a function of the applied laser power, measured at two different blood storage periods (a)- 1st day after blood collection and (b) – 5th day after blood collection .*

It can be seen that at the same laser power, the resulting optical force is lower as the sample becomes older, although the dispersion of the data remains almost unchanged (e.g. for 6 mW laser power, the optical force is 5.5 pN in Fig. 5a, and 6.5 pN in Fig. 5b).

Discussions

We have shown that dielectrophoretic force can be used to calibrate an optical trap force using an adequate model. On the other hand, analysing the behaviour of the cells in an optical trap combined with dielectrophoresis, we were able to detect significant differences in the cell's response, depending on their metabolic state.
Considering that the optical trap force depends essentially on the cell surface and the cytoplasmic refractive index, it is obvious that biochemical modifications associated with different states of the cell will influence its

behaviour in the optical trap.

References

1. Ashkin, J.M. Dziedzici, J.E.Bjorkholm and S. Chu, Observation of a single-beam gradient trap for dielectric particles, Opt. Lett., **11**, 288 – 290 (1986)
2. Ashkin, J.M. Dziedzici and T. and T. amane, Optical trapping and manipulation of single cells using infrared laser beams, Nature (London), **330**, 769 – 771 (1987)
3. Ashkin, K. Schultze, J.M. Dziedzici, U. Euteneuer and M. Schliwa, Force generation of organelle transport measured in vivo by an infrared laser trap, Nature (London), **348**, 346 – 348 (1990)
4. H.A. Pohl, Dielectrophoresis: the behaviour of neutral matter in nonuniform electric fields, Cambridge Univ. Press, London, 1978
5. E. Papagiakoumou, D. Pietreanu, M.I. Makropoulou, E. Kovacs, A.A. Serafetinides, Evaluation of trapping efficiency of optical tweezers by dielectrophoresis, J. Biomed. Opt., **11**, 1 – 8 (2006)

MULTIPLE ANTENNA SYSTEMS IN MOBILE PHONES AND THEIR PERFORMANCE IN TERMS OF EMF EXPOSURE

MICHAEL A. BALDAUF, CHRISTIANE KUHNERT, STEPHAN SCHULTEIS, AND WERNER WIESBECK

INSTITUT FÜR HÖCHSTFREQUENZTECHNIK UND ELEKTRONIK, UNIVERSITÄT KARLSRUHE (TH), KAISERSTR. 12, 76131 KARLSRUHE, GERMANY

Abstract

Communication systems with several antennas at the transmitting and receiving end are called multiple input multiple output (MIMO) systems. In a first approach it is shown that demanding a certain capacity expressed as information per bandwidth and time (in bit/Hz/s) MIMO systems permit a significant reduction of transmit power. Therefore, also the specific absorption rate (SAR) in the human head decreases. In a second approach the total transmit power is held constant. In this case the increased capacity of a MIMO system leads to a performance increase by which the time of the data transmission can be reduced. There exist different MIMO schemes: systems without channel state information available at the transmitter or systems having full channel knowledge at the transmitter. Comparing these schemes we show that MIMO systems show a better performance in terms of exposure than classical single antenna systems. The exposure efficiency of a system as quotient of capacity and SAR is suggested as a measure of the exposure.

Introduction

There are limit values concerning the human exposure to electromagnetic fields (EMF). A lot of countries refer to the ICNIRP Guidelines [1]. For the far field exposure due to base stations the exposure can be conveniently described by the electric field strength (E) or the power density (S). For the human head held close to a mobile phone there is a strongly varying near field over different tissue types. Therefore, a determination of the specific absorption rate (SAR) is necessary. The exposures which encounter in real life due to base and mobile stations are very different compared to the limit values. Safety distances to base stations based on the ICNIRP Guidelines [1] are typically just a few meters [2]. Thus, the exposures due to base stations are usually well below the limits. However, concerning the exposure to mobile phones some phones are quite close to the SAR limit [3].

Classical systems consist of one antenna at the transmitter and one antenna at the receiver. These are named Single Input Single Output (SISO) systems. Recently, wireless communication systems with multiple transmit and multiple receive antennas are subject to many research activities. In these Multiple Input Multiple Output (MIMO) systems, smart antenna techniques are exploited on both sides of the link. Simple MIMO systems have got no information about the propagation channel at the transmitter. In systems with channel knowledge the antenna arrays are adapted to the spatial properties of the propagation channel. The increased performance of MIMO systems in terms of capacity can be used to lower the transmit power leading to a lower exposure. The first approach to examine the exposure of MIMO systems presented in this paper is based on the decrease of the transmit power to achieve the same capacity as in SISO systems. On the other hand in a second approach presented in this paper the transmit power is held constant for SISO and MIMO. The increase in capacity is set into a relation with the SAR. Therefore, this approach shows that MIMO systems will result in lower doses.

Since the propagation channel is non-static the capacity is a random variable. In the investigations done here the term capacity refers to an outage capacity of 10 %. I.e. the calculated capacities are not reached in 10 % and exceeded in 90 % of the realizations.

Handy Model

The simulation model of the handheld device consists of a metallic block, representing the battery and the display of the device, and a PVC housing (cf. Fig. 1). The size of the housing is 55 x 115 x 27 mm^3. The metallic block is 40 x 80 x 10 mm^3 in size. A standard type of miniaturized antennas (Inverted-F) is built in the mobile phone. One, three or four Inverted-F antennas are mounted onto the metallic block spatially separated and with different orientations to exploit different diversity techniques, such as spatial, pattern and polarization diversity. Usually Inverted-F antennas require an infinite ground plane, which is not available in the small hand-held device. Thus the metallic block, representing the ground plane, acts as a part of the antennas and influences the shape of the patterns and the mutual coupling impedances. Detailed results on design and performance of these MIMO hand-held models can be found in [4].

An operating frequency of 2 GHz and a bandwidth of 3.84 MHz are considered for all the simulations performed. The maximum value of the localized SAR is averaged over any 10 g tissue SAR_{10g}. The calculation is done numerically with FEKO [5].

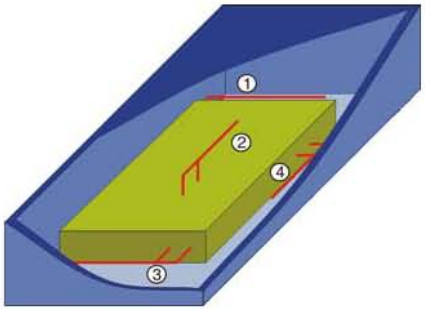


Fig. 1: Model of a hand-held device equipped with four Inverted-F antennas.

The hand-held device is attached to a phantom head, which has the size and the shape of an adult human head (density 1000 kg/m^3) and adequate dielectric properties ($\varepsilon_r = 40$, $\sigma = 1.4$ S/m) (cf. Fig. 2).

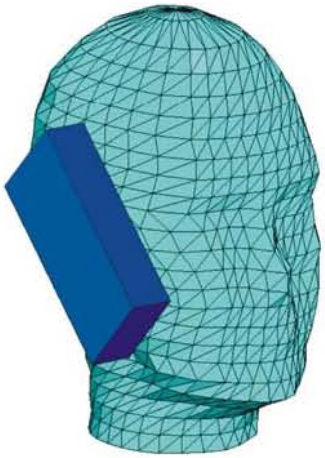


Fig. 2: Model of the user's head where the mobile phone is attached.

Model for the Propagation Channel

The campus of the University of Karlsruhe was modeled. Therefore, an outdoor scenario is considered for the wave propagation channel. The base station is mounted 3 m above the roof top of one of the highest buildings of the campus. The mobile phone is located at about 1000 randomly chosen positions on street level. By a ray-tracing technique the waves between the mobile and the base station are calculated [6].

Base Station Antennas

The base station is equipped with one antenna for the SISO case and three antennas with spacings of 1 m for the MIMO cases. The commercially available base station antenna Kathrein type 735147 is used and modeled [2]. The radiation pattern illuminates a 120° sector in the azimuth plane. The elevation pattern is tilted down by 5°, see Fig. 3.



(a) azimuth pattern (b) elevation pattern

Fig. 3: Radiation pattern of a base station antenna in azimuth and elevation.

MIMO schemes

MIMO systems can be classified by the transmission scheme applied. It is important to distinguish between MIMO systems with and without channel state information (CSI) at the transmitter. In other words, it has to be distinguished between transmitters that do know or do not know the channel. The channel can only be estimated by the receiver. To supply the transmitter with the channel knowledge, it has to be transmitted back to the transmitter. (For time division duplex systems reciprocity may be applied). This back transmission of the channel state information is difficult to realize and reduces the data rate available for the user of the link. Therefore, MIMO systems which do not need to know the channel at the transmitter are very attractive. On the other hand, the optimal capacity of a MIMO system is only reached with perfect channel knowledge at the transmitter. Thus, to reach very high data rates, the transmitter must be informed about the channel. To reduce the complexity of MIMO systems, systems that do only beamforming on both sides of the link, are an attractive option. Those systems do not (except for a very small signal to noise ratio) reach the capacity of normal MIMO systems, because only one data stream is transmitted at one time – in contrast to the spatial multiplexing systems described before.

The following three MIMO schemes are considered:

- MIMO without CSI at the transmitter
- MIMO with CSI at the transmitter
- Beamforming-based MIMO

The capacity and the SAR are calculated and compared for several antenna configurations.

Excitation of the Antennas at the Transmitter

In general, an excitation voltage excites an antenna. Hence, the electric field strength and therewith the SAR in the human head depend also on the excitation voltages of each antenna element. In a SISO system, this voltage is directly related to the transmit power. In a MIMO system the transmit power is distributed over all antennas. Each antenna in the mobile phone can be excited by an individual excitation voltage. The distribution of the transmit power is dependent on the MIMO scheme applied. In the case of MIMO without CSI the transmit power is distributed uniformly. In the case of MIMO with CSI or MIMO-based beamforming the excitation voltages are adjusted to obtain a high capacity. Therefore, the propagation channel has to be taken into account. The model given in [7] is applied. It describes the propagation channel for a MIMO system including the transmit and the receive antennas. It is based on a scattering parameter description.

Investigated Antenna Systems

The following antenna configurations are considered:

- SISO: the handheld with one antenna next to a human head, transmitting to a base station with one antenna
- SIMO 1x3: the single antenna handheld next to a human head, transmitting to a base station with three antennas
- MISO 3x1: the three-antenna handheld next to a human head, transmitting to a base station with one antenna
- MISO 4x1: the four-antenna handheld next to a human head, transmitting to a base station with one antenna
- MIMO 3x3: the three-antenna handheld next to a human head, transmitting to a base station with three antennas
- MIMO 4x3: the four-antenna handheld next to a head, transmitting to a base station with three antennas

For the case of MIMO without CSI it is assumed that via each antenna an independent subchannel is transmitted. At the receiving end the transmitted signal has to be reconstructed. For a system without CSI only configurations are possible were the number of transmit antennas is smaller or equal to the number of receiving antennas.

Approach 1: Constant Capacity

To show the performance of MIMO systems a constant capacity C = 0.25 bit/s/Hz is considered. For simplicity a MIMO scheme without CSI at the mobile phone is regarded. I.e. only systems were the number of transmit antennas is smaller or equal to the number of receiving antennas are taken into account.

A classical SISO system will need a transmit power P_T = 19.9 dBm to reach the demanded capacity, resulting in a SAR_{10g} = 0.46 W/kg (cf. Fig. 4). Increasing the number of antennas at the receiving base station will lower the required transmit power to P_T = 10.2 dBm. Since the transmit power can be decreased by almost 10 dB by just adding more antennas at the base station, while using the same antenna at the mobile phone, there is a decrease in the SAR by the same amount to 0.049 W/kg. Further on, adding two antennas to the mobile phone will allow a further decrease of the transmit power (P_T = 4.9 dBm) yielding a SAR_{10g} = 0.018 W/kg.

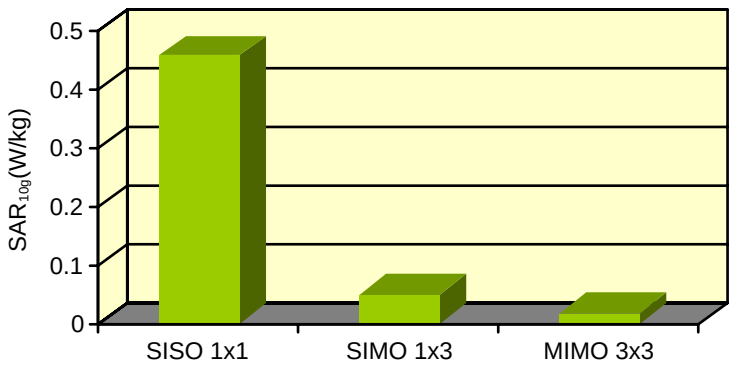


Fig. 4: SAR_{10g} for systems without CSI. Constant capacity C = 0.25 bit/s/Hz.

Approach 2: Constant Transmit Power

Since there is an increasing demand for higher capacities the transmit power of the mobile phone was fixed to P_T = 20 dBm, which is 1 dB below the maximum transmit power of a UMTS class 4 mobile phone [8]. As a rule of thumb: The more antennas there are the higher will be the achievable capacity. This capacity increase can be used to transmit the same information in a shorter time interval. The product of the SAR multiplied by the time of the exposure duration will give a dose.

Therefore, for different antenna configurations and the three mentioned MIMO schemes the SAR_{10g} (exposure) and capacities C are evaluated.

Systems without CSI

The cumulative distribution function (cdf) of the MIMO capacity is given in Fig. 5 for the case of MIMO without CSI at the transmitter. Shown is the probability P that the capacity is smaller than the value on the x-axis. The run of the curves demonstrates that adding further antennas tremendously increases the achievable capacity while keeping the total transmit power constant.

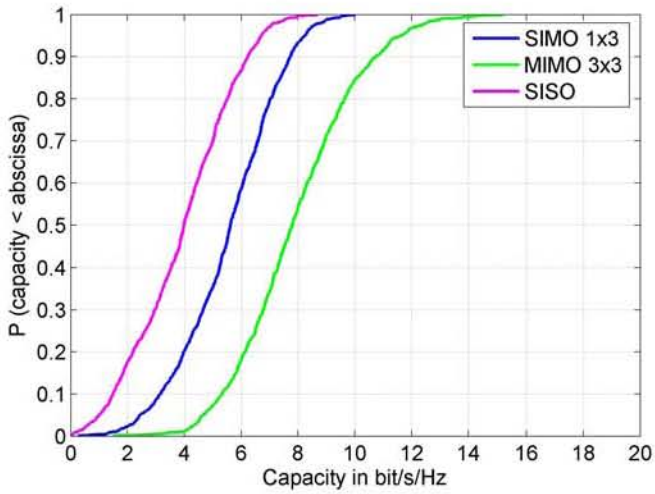


Fig. 5: Capacity for SISO and MIMO systems without CSI at the transmitter. Constant transmit power P_T = 20 dBm.

The calculation of the SAR is independent of the channel matrix in this case, because the excitation voltages are kept constant due to the lack of the channel knowledge at the transmitter. There is only one SAR_{10g} value for all channel realizations. This SAR_{10g} value is shown in Fig. 6 for different antenna configurations. SISO A1 and SISO A4 correspond to SISO systems were different transmit antennas are excited. Since the show very similar capacities there is just one line in Fig. 5.

The antenna configurations with only one antenna at the mobile station lead to the largest SAR_{10g}. Especially if the antenna is close to the head as in the case of SISO A4 the SAR_{10g} is close to 1.4 W/kg. The SAR_{10g} can be decreased by using an antenna position which is more optimized in terms of exposure. The configuration SISO A1 and SIMO 1x3 use the same transmit antenna at the mobile phone. For the MIMO case the SAR_{10g} is reduced to a value of 0.36 W/kg, although the transmit power is the same as in the single antenna cases and the capacity is remarkably higher.

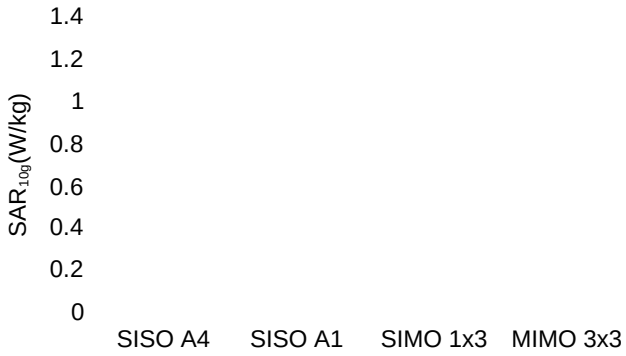


Fig. 6: SAR_{10g} for SISO and MIMO systems without CSI at the transmitter. Constant transmit power P_T = 20 dBm.

Systems with CSI

Figure 7 shows the cdf of the capacity for the optimum MIMO scheme with channel state information (CSI) at the transmitter. These MIMO systems by far exceed the other MIMO schemes in terms of capacity – keeping in mind that the total transmit power is kept constant for all systems.

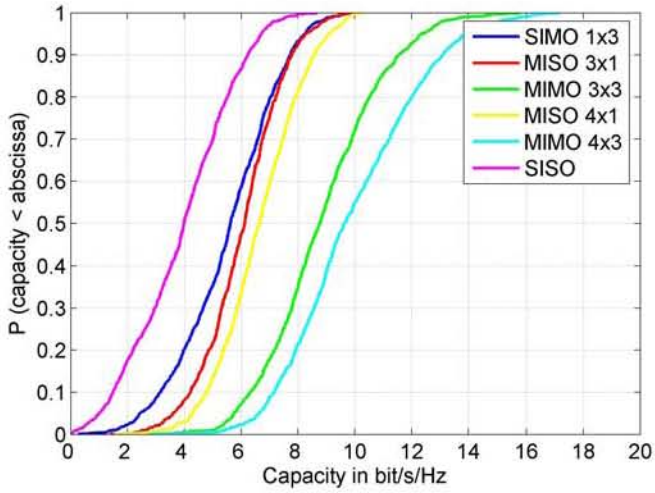


Fig. 7: Capacity for SISO and MIMO systems with CSI at the transmitter. Constant transmit power P_T = 20 dBm.

The localized SAR_{10g} are shown in Fig. 8. Since the channel changes with time the mean value of 100 SAR values is considered. For the MIMO cases, the scheme with CSI at the transmitter leads to larger SAR values than the scheme without CSI at the transmitter. For the SISO systems, the SAR values do not depend on the scheme applied, because the amplitude of the excitation voltage is held constant and its phase does not influence the SAR due to a lack of interfering signals.

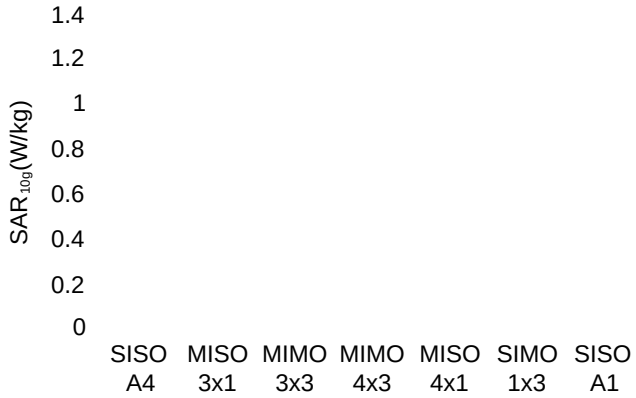


Fig. 8: SAR_{10g} for SISO and MIMO systems with CSI at the transmitter. Constant transmit power P_T = 20 dBm.

Systems with beamforming-based MIMO

Beamforming-based MIMO uses only the best subchannel, i.e. there is only one data stream transmitted. Fig. 9 shows that in this case the lowest capacities are obtained. Due to beamforming at both ends, the capacity is still enhanced by increasing the number of antennas.

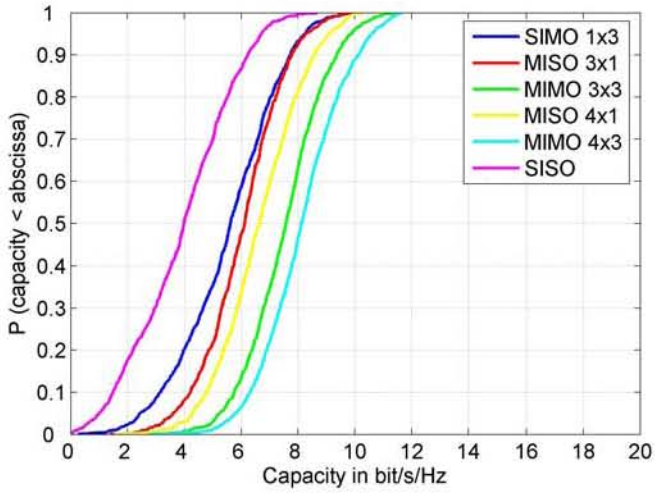


Fig. 9: Capacity for SISO and beamforming-based MIMO. Constant transmit power P_T = 20 dBm.

The results for the SAR_{10g} are given in Fig. 10. In systems where the minimum number of transmit and receive antennas equals one there exists only one subchannel. Therefore, there is no difference between MIMO with channel state information at the transmitter and beamforming-based MIMO in these cases and the SAR values are the same. For the MIMO 3x3 configuration the SAR values are quite similar, 0.88 W/kg with CSI and 0.86 W/kg for beamforming-based MIMO. For the MIMO 4x3 case, the SAR values are also similar.

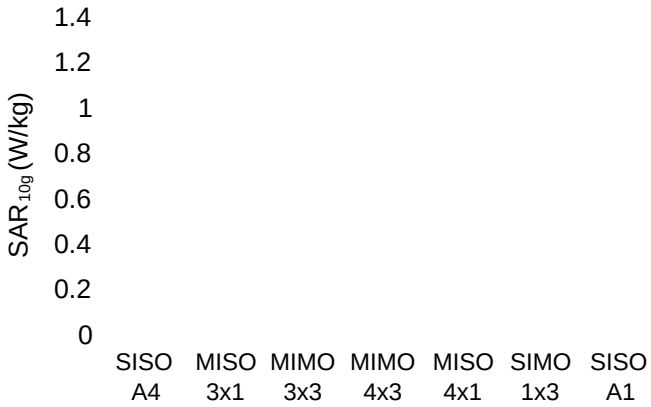


Fig. 10: SAR_{10g} for SISO and beamforming-based MIMO. Constant transmit power P_T = 20 dBm.

Exposure Efficiency

The total transmit power has been kept constant for all MIMO schemes and all antenna configurations in the second approach. But the capacity differs remarkably for the different cases.

For a further evaluation of the MIMO schemes and antenna configurations the quotient of 10% outage capacity *C* and the specific absorption rate SAR is computed. The result is given as exposure efficiency EE of the system:

$$\mathrm{EE} = \frac{10\%\ \text{outage capacity}}{\text{max. localized SAR averaged over 10g tissue}} = \frac{C}{\mathrm{SAR}_{10g}}$$

An exposure-optimized system exhibits a high capacity and low SAR_{10g}. I.e. for an exposure-optimized system the value of EP is larger compared to a system with poorer exposure efficiency. The higher the value of EE the smaller is the exposure integrated over time experienced by the operator of the mobile to transmit a certain amount of information.

Fig. 11 shows the exposure efficiency EE for all antenna configurations and MIMO transmission schemes. No results are shown for the case of a system without CSI at the transmitter if the number of transmit antennas is larger than the number of receiving antennas since the receiver can't reconstruct the transmitted data streams without a channel knowledge.

The exposure efficiency EE for configurations where there is only one transmit antenna is the same for all MIMO schemes since the fixed transmit power is radiated by the single antenna. Adding antennas at the receiving or transmitting end will yield a higher EE. The MIMO 3x3 system without channel knowledge shows the best EE. If channel knowledge is available for this configuration the antenna weightings are adjusted to increase the capacity. Howecer, this adjustment leads also to a higher SAR value. The increase in SAR is larger than the increase in capacity. The considered SISO systems show the worst exposure efficiency EE.

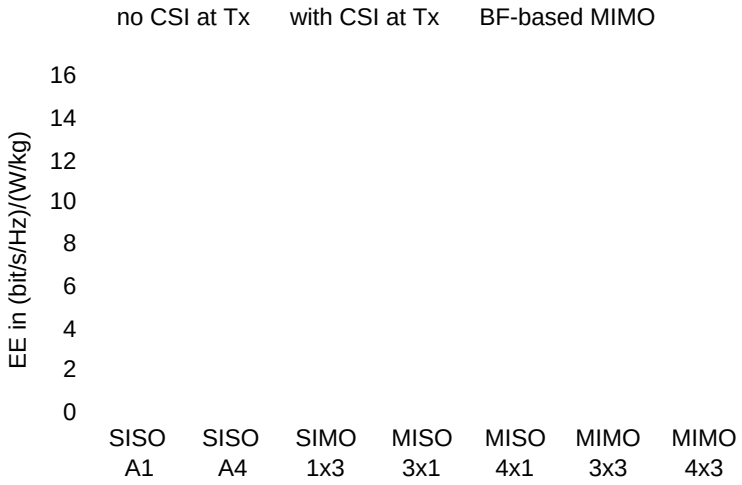


Fig. 12: Exposure efficiency for the investigated MIMO schemes.

Conclusion

It is shown that multiple antenna systems outperform classical single antenna systems by allowing higher capacities. To reach a demanded capacity the transmit power of a MIMO system can be clearly lowered compared to a SISO system. This leads to a tremendous decrease in exposure. Keeping the transmit power constant shows that MIMO systems with channel knowledge give the highest capacities. However, the exposure efficiency might be lower than in a system without channel knowledge. The MIMO scheme allowing the highest capacity is not necessarily optimized in terms of exposure.

References

[1] ICNIRP, "Guidelines for limiting exposure to time-varying electric, magnetic, and electromagnetic fields (up to 300 GHz)", *Health Physics*, vol. 74, no. 4, pp. 494-522, 1998

[2] M.A. Baldauf, A. Herschlein, W. Sörgel, W. Wiesbeck, "Safety Distances in Mobile Communications", *Proceedings of 2nd International Workshop on Biological Effects of Elektromagnetic Fields*, pp. 148-156, Rhodes, Greece, Oct. 2002

[3] http://www.mobile-phones-uk.org.uk/sar.htm

[4] C. Waldschmidt, C. Kuhnert, M. Pauli, W. Wiesbeck, "Integration of MIMO antenna arrays into hand-helds", *IEE Int. Conf. on 3G Mobile Communication Technologies*, London, UK, Sept. 2004

[5] FEKO. http://www.feko.info

[6] J. Maurer, C. Waldschmidt, T. Kayser, W. Wiesbeck, "Characterisation of the time-dependent urban MIMO channel in FDD communication systems", *Proc. IEEE Vehicular Technology Conference VTC-Spring*, April 2003, pp. 544-548

[7] C. Waldschmidt, S. Schulteis, W. Wiesbeck, "Complete RF system model for the analysis of compact MIMO arrays", *IEEE Transactions on Vehicular Technology*, vol. 53, pp. 579-586, May 2004

[8] *3rd Generation Partnership Project; Technical Specification Group Radio Access Networks; User Equipment (UE) radio transmission and reception (FDD) (Release 4)*, 3GPP TS 25.101, 2004

THE EFFECT OF 1800 MHZ ELECTROMAGNETIC RADIATION EXPOSURE ON CORTICAL AND HIPPOCAMPAL ELECTROGENY IN NEURODEFECTIVE AND HEALTHY BRAIN

JAN BARCAL[1], JAN VRBA[2], FRANTIŠEK VOŽEH[1]

[1]Charles University in Prague, Faculty of Medicine Pilsen, Department of Pathophysiology; Czech Republic
[2]Czech Technical University in Prague, Faculty of Electrical Engineering, Department of Electromagnetic Field; Czech Republic

Abstract

In this study a simultaneous registration of the brain cortical and hippocampal activity during a high-frequency electromagnetic field (HF EMF) exposure was performed. All procedures were done under urethane anaesthesia (20%, 2g/kg i.p.) in Lurcher mutant mice (LMM) which serve as an excellent model of neurodegeneration. Healthy wild type mice (WTM) were used as controls. The animals were exposed to 1800 MHz HF EMF corresponding with the mobile phone frequency. We used gel electrodes (silicon tubes or glass microcapillaries filled with agar) where the connection with metallic electrodes is located out of HF EMF space. The evaluation of electrocorticograms and spontaneous hippocampal rhythmicity showed a distinct shift in main components of frequency spectra but clear effect has been observed only in WTM. Mice with inborn neurodegeneration (LMM) exhibited only gentle differences. The comparison of cortical and hippocampal electrogeny suggest an opposite effect of HF EMF on the brain cortex and hippocampal neuronal circuits. These findings support ideas about possible influencing the central nervous system by HF EMF exposure and support also some recent results about hidden health risks resulting from the mobile phones use.

Introduction

Each electromagnetic source localized near the biological object produces electromagnetic field which may cause **both thermal and non-thermal biological effects.**

A basic principle of **thermal effects** is the rise of temperature produced by the energy absorbed from oscillating electric fields. The force produced by an electric field on charged objects, such as the mobile ions present in the body, causes them to move, resulting in electric currents, and the electrical resistance of the material in which the currents are flowing results in heating. This heat input causes the temperature to rise and it continues to do so until the heat input is balanced by the rate at which it is removed, mostly by blood flowing to and from other parts of the body. Theoretical studies are fosussed to the computation of specific absorption rate (SAR). The relationship between the SAR and the resulting temperature rise is complex, and significantly dependent on antenna configuration, location and frequency. The most problematic feature of a temperature calculation is modelling the effect of blood flow on heat transfer. Van Leeuwen et al. [1] published that heat deposition within the head was computed by coupling a finite difference time domain model for SAR with a new thermal model. T'he thermal model includes the convective effects of discrete blood vessels, whose anatomy was determined using magnetic resonance angiography of a healthy volunteer. For a 915 MHz dipole antenna with a time-averaged power output of 0.25 W (equivalent to a typical mobile phone), this study results in an SAR of about 1.6 W/kg and predicts a maximum brain temperature rise of 0.11 °C in the steady state.

An explanation of **non-thermal effects** seems to be more complicated and also controversial. The energy quanta of radiation at 0.9 and 1.8 GHz equal 4 and 7 μeV, respectively. Both these values are extremely small compared with the energy of around 1 eV needed to break the weakest chemical bonds in genetic molecules (DNA). Detectable changes can arise only if the effect of the electric field within the biological system exposed to RF fields is not masked by thermal noise. Thermal noise or random motion, also known as Brownian motion, is due to the thermal energy that all objects possess at temperatures above absolute zero. In solids, the atoms vibrate and in gases and liquids they move erratically to and fro following very frequent collisions with other atoms. So all components of biological tissue - ions, molecules and cells - are in

constant motion. Another mechanism involving cells concerns the attraction between them in the presence of an electric field [2], [3]. The electric field polarises the cell, that is to say charges in the cell move so that one side of it becomes positive with respect to the other. The cell is then an electric dipole (like a tiny torch battery) and attracts similarly polarised cells. For typical cells and frequencies below about 100 MHz, the energies involved are calculated to become comparable to thermal noise in electric fields of E=300 V/m. The energies are calculated to become appreciably less for RF fields, but Adair [3] suggests that, since these values would depend on the detailed structure of the biological elements involved, the possibility of biological effects for fields of this size cannot be excluded. Other possible biological effects are associated with cell membranes and the movement of currents through the membrane in either direction. Membranes are known to have strongly non-linear electric properties [4]. When a voltage is applied across the membrane, the current that flows is not always proportional to the voltage. Part of this non-linearity may, in fact, be due to the effect of the electric field on the proteins in the membrane or nearby, which assist the flow of the product currents through the membrane. The membrane also acts as a rectifier. If a voltage is connected across the ends of a wire, the size of the current that flows depends solely on the magnitude of the voltage: if the polarity of the voltage is reversed, the current changes direction but its size is unchanged. However, if the polarity of the voltage applied across a rectifier is reversed, the current changes direction but now its size also changes. So, if an oscillating voltage (electric field) is applied across a rectifier, the total current that flows when the field is in one direction is not balanced by the current when the field is in the other: an AC field produces a net DC current and hence a net flow of products through the membrane. However, the response times of the ion gates are very much slower than the period of microwave frequencies and, using data obtained from measurements on membranes [4], it has been shown that, for electric fields of 200 V/m, the relative change in the membrane potential is very small [3]. Another hypothesis is that the interaction with biological tissue depends on the coherence of the electromagnetic fields [5].

Possible effects on the brain and behaviour during acute exposure to RF fields are permanently discussed - mobile phones are conventionally held close to the head. Many results are about effects of RF fields on isolated nerve cells (neurons), on cultured nervous tissue, on living brain slices, on brain function in experimental animals, on the blood-brain barrier and on behavioural measures of brain function [6,7,8,9]. The behaviour of animals can be a very sensitive indicator of adverse health consequences. Early signs of potential insult are often behavioural rather than anatomical [10].

RF fields, continuous or pulsed, can affect membrane channels [11]. Experiments of Cleary [12,13] suggest that the flux of positively charged sodium and potassium ions across cell membranes can also be affected by RF exposure, over a wide range of frequencies (27 MHz to 10 GHz). Philippova [14] found that 900 MHz radiation, at SARs of 1 and 100 W/kg, specifically affects the binding of odorant molecules to receptor protein in the membranes of olfactory receptor neurons in the rat. Liburdy and Vanek [15] have also reported protein shedding from membranes as a result of RF exposure. A radiation at very low power can affect the ion channels associated with transmitter receptors: experiments of D'Inzeo et al. [16] suggest decrease in the frequency of opening of sodium channels associated with acetylcholine receptors in muscle membranes as a result of exposure to 9.75 GHz radiation at only 10-20 $\mu W/m^2$, which might cause a decrease in the excitability of the muscle. An increase in membrane conductance and a decrease in the spontaneous firing of impulses in neurons of the snail *Helix aspersa* when exposed for an hour to continuous and amplitude modulated 2.45 GHz radiation was described by Arber and Lin [17,18]. The effects were abolished by the application of ethylenediamine tetraacetic acid (EDTA), which chelates kalcium. Another studies also described a decrease in the electrical amplitude of impulses and a reduction in the excitability of the frog sciatic nerve when exposed to 2.45 GHz radiation [19], and a decrease in spontaneous activity of neurons isolated from the marine gastropod *Aplysia* at relatively high intensities [20, 21].

The main aim of the presented study was a electrophysiological investigation of an influence of high-frequency electromagnetic field (HF EMF) on brain functions in Lurcher mutant mice, which represent an excellent model of neurodegenerative disease, and healthy animals.

Animals and Methods

Lurcher mutant mice (Lurchers) represent a natural model of genetically determined olivocerebellar degeneration [22]. Heterozygote individuals (+/Lc) are characterized by the postnatal complete loss of cerebellar Purkinje cells (excitotoxic apoptosis) and by the decreased number of granule cells and inferior olivary neurons (secondary to the loss of Purkinje cells). Affected homozygots (Lc/Lc) are not viable. Unaffected homozygots, wild type mice (+/+) are completely healthy and serve as controls. Our previous results suggest that in Lurchers some cognitive functions are changed - in series of experiments studying the development of spatial learning in Lc/+ and +/+ during the first month of life using the standard Morris water maze [23, 24]. Some neurons of Lurchers are more sensitive to neurotoxic substances [25] and other experiments discovered a higher degree of the CNS excitability in Lc/+ when compared with +/+ using a metod of audiogennic epilepsy [26]. Similar

findings were obtained in experiments which measured brain cortical activity after previous electrical and drug stimulation [27, 28]. Also significant changes of hippocampal activity (LTP) were found in anesthetized Lc/+ in comparison with +/+ [29].

We expect that some brain structures in Lurchers would be more sensitive (i.e. with lower treshold) to different kind of stimulation and neuronal injury. It is possible to assume a higher effect of other types of stimulation on such neurons, including HF EMF. A direct registration of brain cortical and hippocampal activity during exposure to high-frequency electromagnetic field (HF EMF) and a depiction of possible changes in the hippocampal rhythmicity were performed. All experimental procedures were done under urethane anaesthesia (20%, 2g/kg i.p.) in adult (10-12 weeks) Lurcher mutant mice (n=20) and wild-type (healthy littermates) which served as controls (n=20). Experimental animals were exposed to HF EMF with frequency of 1800 MHz, similar to the range used by mobile phones. As a source of the HF EMF a high-frequency generátor was used; the power output was approximately 1 W. The radiation was directed by a waveguide to a space with the animals placed (modified stereotaxic frame in the Faraday's chamber). The area of the orifice was 150 cm^2.

An important problem in the use of classical EEG technology is the presence of conductive (contact) electrodes in brain tissue resulting to discontinuity of HF EMF and possible electrolytical processes caused by the nonhomogeneity on the boundary line of metal-tissue. Our original method [30] is based on the use of gel electrodes (silicon or glass capillary tubes filled with agar). The corresponding conductivity is achieved by supplementation of saline and final biophysical quality is adequate to the brain tissue. The connection with classical (wire) electrodes is performed out of HF EMF space. Spontaneous electrocorticogram (ECoG) was measured as 2 min segments from continously recorded activity either without HF EMF exposure or with it. Final calculation with Fourier analysis and averaging were performed off-line on DISYS-system (Software for data acquisition and analysis). Hippocampal activity was recorded by glass capillary filled with agar (used as a registration electrode), grounding electrode was a silicon tube filled with agar located on the neck. Stereotactic coordinates [31] - ref. point bregma: AP: 2.0; L: 1.5; V: 1.3 (CA1) – 2.0 (hilus DG). DISYS-system for a final averaging according to Fourier analysis with emphasis on a theta-oscillation especially was used.

Results

The experiments confirmed a possibility of direct EEG registration during exposure to HF EMF. Recording time for each experimental animal was aproximately 30 minutes and DISYS system was able to describe spontaneous activity either before influencing by the HF EMF or during it. Examples of five seconds recording in wild type mouse (Fig. 1, 2) and in Lurcher mutant mouse (Fig. 3, 4) are shown bellow.

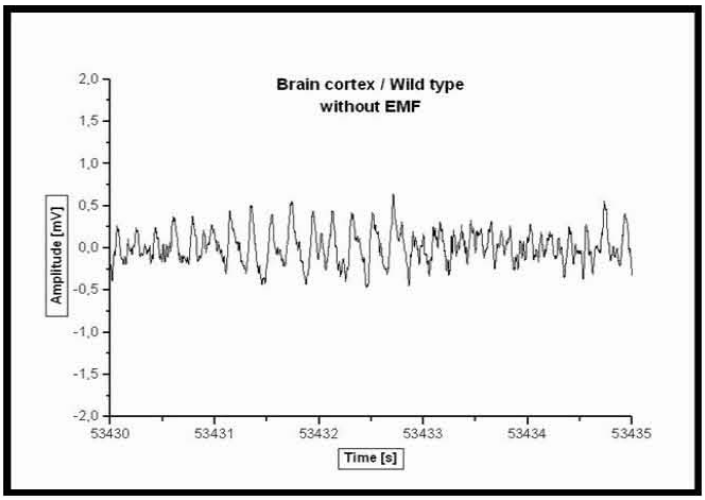


Fig. 1 – Spontaneous brain cortical activity (ECoG) in wild type mouse without HF EMF exposure

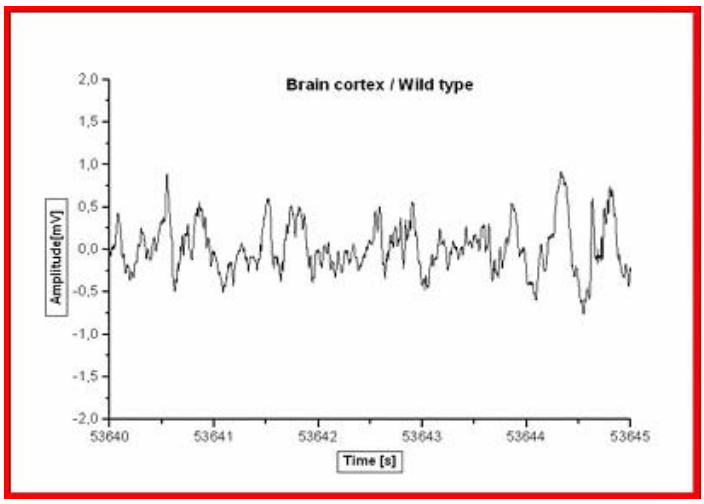


Fig. 2 – Spontaneous ECoG in wild type mouse during exposure to HF EMF

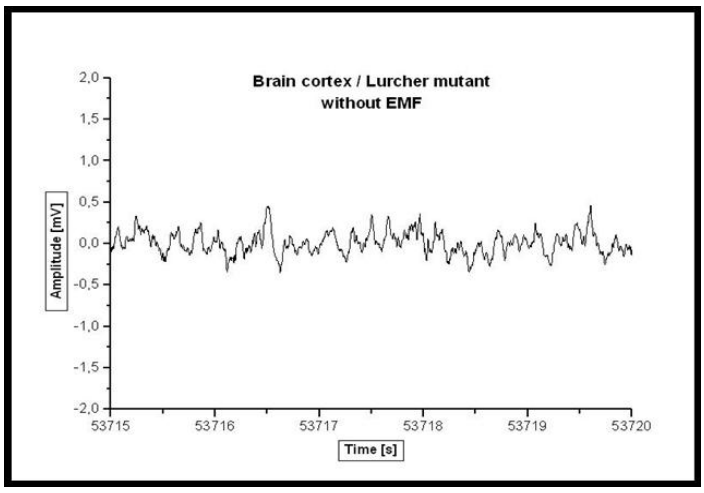


Fig. 3 – Spontaneous brain cortical activity (ECoG) in Lurcher mutant mouse without HF EMF exposure

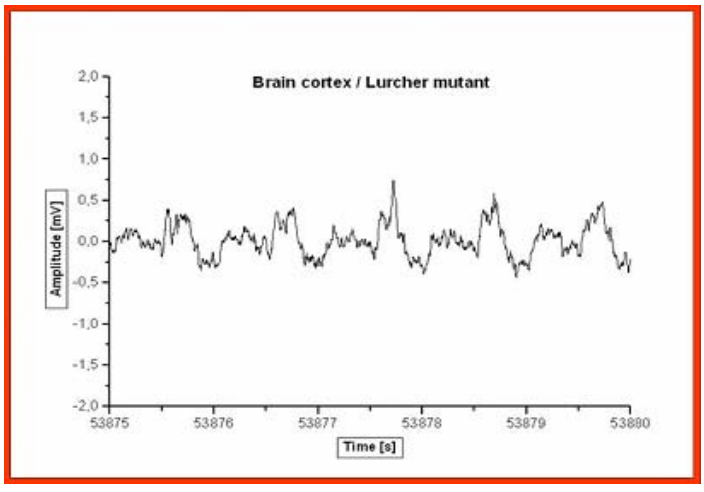


Fig. 4 – Spontaneous ECoG in Lurcher mutant mouse during exposure to HF EMF

The final evaluation and averaging of cortical activity showed a distinct shift to lower frequency components. These findings are in accordance with older and recent results but clear effect only in wild type

(healthy littermates) was observed (Fig. 5) whereas in Lurcher mutant mice only gentle differences between frequency spectra were found (Fig. 6).

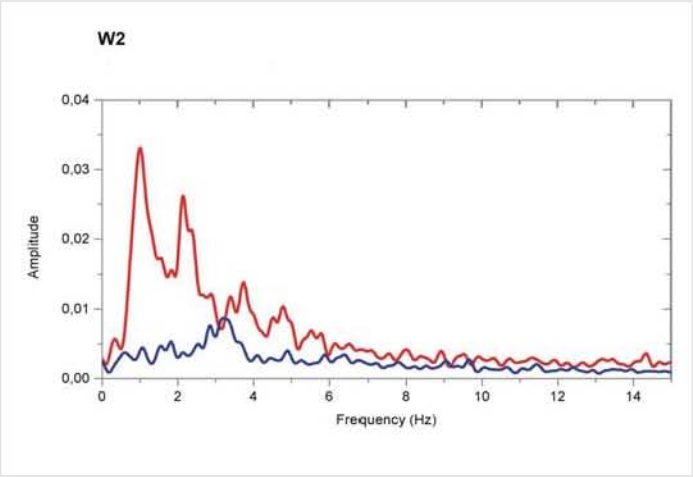


Fig. 5 – Fourier analysis of ECoG in wild type mice group before (blue line) and during (red line) exposure to HF EMF

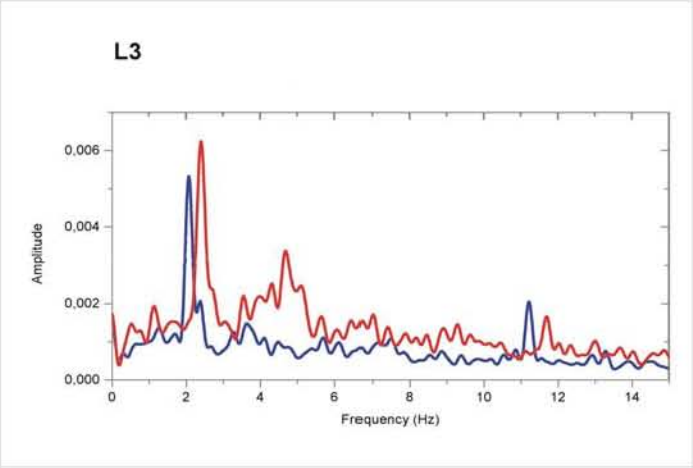


Fig. 6 – Fourier analysis of ECoG in Lurcher mutant mice group mice before (blue line) and during (red line) exposure to HF EMF

On the other hand, changes of hippocampal activity and shift towards higher frequencies in both types of animals (healthy and mutant) were observed (Fig. 7, 8).

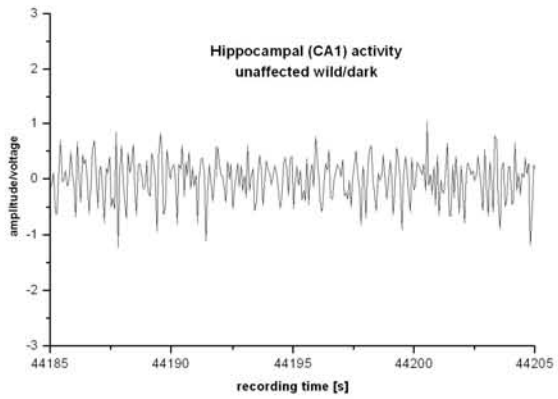


Fig. 7 – Hippocampal activity in wild type mouse before exposure to HF EMF

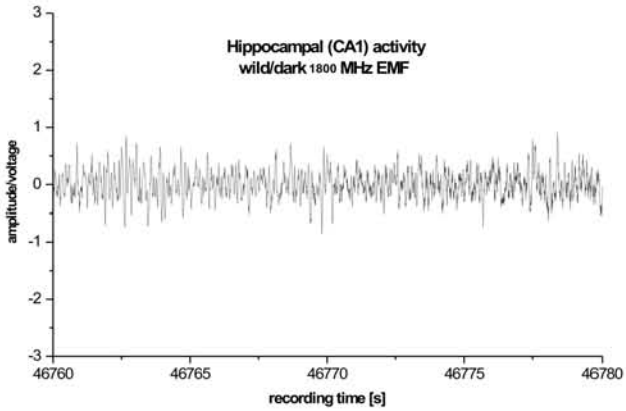
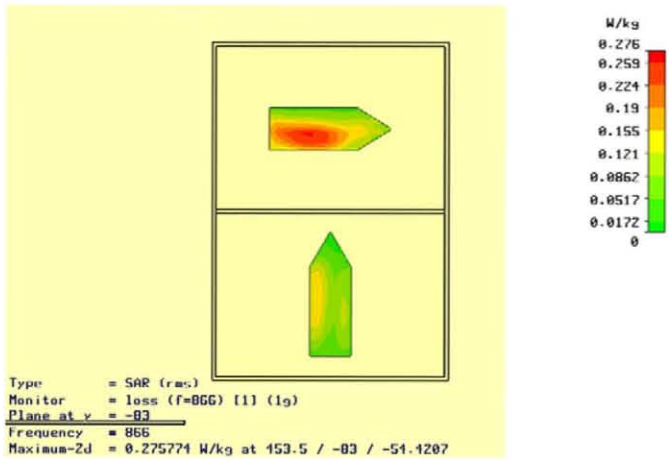
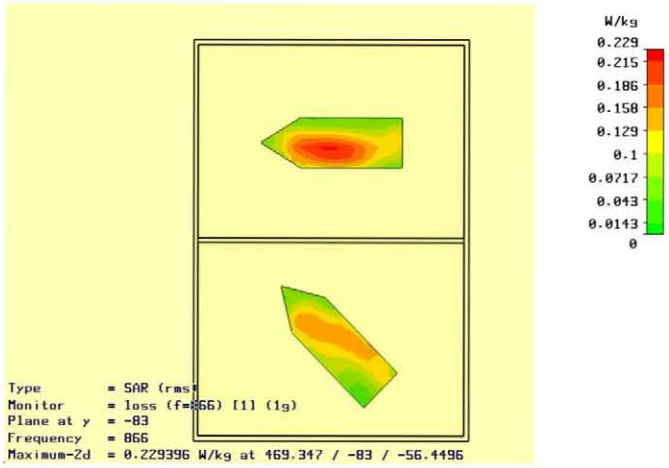


Fig. 8 - Hippocampal activity in wild type mouse during exposure to HF EMF

The serious problem is depiction of SAR which is generally accepted as a indicator of the energy absorption by different kinds of living tissue. In our experiments we used mathematical modelling of SAR calculation. In the figures 9 and 10 examples of SAR calculation were shown (both using 900 MHz HF generator, where power output was approximately 10 W). We expect a similar distribution of SAR corresponding to the lower power output at one side but higher concentration of HF EMF resulting from less area of waveguide orifice.





Figs 9 and 10 – mathematical model of SAR in two different mice position

Discussion

An arteficial source of HF EMF used in our experimental paradigm influenced spontaneous cortical activity. A shift towards lower frequencies was observed with gentle differences between Lurcher mutant mice and wild type mice. Our main working hypothesis was that some brain structures in Lurchers should be more sensitive (i.e. they have lower treshold) to different kind of stimulation and neuronal injury. We suppose that thermal gradient arising between lipo- and hydrophylic structures influences ion movement through membranes of neurons and/or glial cells. However, possible delicate changes were identified rather in the brain of healthy animals. These relatively ambiguous findings support our idea about a different vulnerability of the CNS in mice with neurodefective brain to some physical and chemical factors in comparison with controls. The higher CNS excitability in Lurcher mutant mice and its possible supression or masking effect on the HF EMF influence may be used as an explanation of unsignificant differences between healthy and mice with inborn neurodegeneration. Newertheless, our general findings are in accordance with previously published investigations of Bawin et al. [32, 33] that exposed cats, which had been previously conditioned to produce selected EEG rhythms in response to a light flash, to low level RF fields. The changes were reported in the performance of the conditioned EEG response task and in various other behavioural parameters. It was argued that the fields acted directly on brain tissue causing a minute release of calcium, resulting in changes in membrane excitability, which could possibly affect EEG rhythms. Takashima et al. [34] reported changes in EEG of rabbits following exposure to a modulated RF field of 1-10 MHz, a frequency range outside the main interest but Shandala et al.[35]; Thuroczy et al.[36] reported about subtle effects on the EEG in rats and rabbits exposed to RF fields within the frequency range of interest. McRee et al. [37] described experiments performed by Rosensteig of the US Environmental Protection Agency, who exposed rats to RF from late fetal life until adult. He saw no changes in either the spontaneous EEG or the electrical responses evoked by flashes of light (visual evoked responses). Mitchell et al. [38] reported the findings of a joint project on the same subject carried out in the USA and the former Soviet Union. Both groups exposed rats to fairly intense continuous-wave RF fields for seven hours. Interestingly, both

teams found small but statistically significant reduction of power in the EEG, but in different parts of the frequency spectrum.

Laboratory studies investigating the effects of mobile phone signals on the spontaneous EEG in awake subjects have produced somewhat mixed results. Reiser et al. [39] reported that exposure to GSM signals was associated with increases some 15 minutes later in the power of EEG frequencies of about 10 Hz and higher, Roschke and Mann [40] were unable to detect any differences in EEG spectra related to exposure to GSM signals. A similar inconsistency appears to hold for the study of sleep EEG. Mann and Roschke [41] reported that exposure to GSM-like signals reduced latency to sleep onset, and altered spectral characteristics of REM sleep, although a subsequent study by the same group [42] failed to replicate these findings. In other study [43], exposure to a "pseudo-GSM signal" (15 minute on/off cycles, 900 MHz, duty cycle of 87.5 % rather than the 12.5 % used in phone signals, and an estimated whole-body SAR of 1 W/kg) was associated with reduced waking after sleep onset and changes in EEG power spectra during the first of the night's episodes of non-REM sleep. In three studies „event-related potentials“ (ERPs) were investigated during exposure to GSM-like signals. In the first [44] visual sensory responses to checkerboard reversal were found to be unaffected during exposure. In two other studies [45, 46] positive effects were reported. In a recent study in Czech Recublic, Jech and colleagues [47] also found changes of visual event related potentials during exposure to HF EMF.

Taken together, main importance of this study was that neurodefective animals and their healthy littermates (as ideal controls) were used. Despite our experimental paradigm (i.e. whole-body HF EMF exposure characterised by lower amount of absorbed energy in comparison with human brain during cellular phone use), presented results suggest that some neuronal populations (cortical and subcortical) react on this type of radiation. Current WHO recommendation published by Repacholi [48] consists of basic principles of safety for individuals. The limiting of the lenght of calls or using „hands-free“ device has probably higher importance in children in which possible thermal effect on the developing brain may be connected with higher healthy risks.

References

1. Van Leeuwen G. M. J., Lagendijk J. J. W., Van Leersum B. J. A. M., Zwamborn A. P. M., Hornsleth S. N., Kotte A. N. T. J.: Calculation of brain temperatures due to exposure to a mobile phone. Phys. Med. Biol. 44: 2367-2379, 1999.
2. Schwan H. P.: EM-field induced force effects. In: Interactions between Electromagnetic Fields and Cells (A. Chiabrera, C. Nicolini and H. P. Schwan, Eds). New York, Plenum Press, 1985.
3. Adair R. K.: Effects of weak high-frequency electromagnetic fields on biological systems. In: Radiofrequency Radiation Standards (B. J. Klauenberg, M. Grandolfo and D. N. Erwin, Eds). New York, Plenum Press, p. 207-211, 1994.
4. Montaigne K., Pickard W. F.: Offset of the vacuolar potential of Characean cells in response to electromagnetic radiation over the range 250 Hz - 250 kHz. Bioelectromagnetics 5: 31–38, 1984.
5. Litovitz T. A., Penafiel L. M., Farrel J. M., Krause D., Meister R., Mullins J. M.: Bioeffects induced by exposure to microwaves are mitigated by superposition of ELF noise. Bioelectromagnetics 18: 422–430, 1997.
6. UNEP/WHO/IRPA: Electromagnetic Fields (300 Hz-300 GHz). Geneva, World Health Organization, Environmental Health Criteria 137, 1993.
7. Cleary S. F.: Effects of radiofrequency radiation on mammalian cells and biomolecules in vitro. In: Electromagnetic Fields: Biological Interactions and Mechanisms (M Blank, Ed). Washington, American Chemical Society, p 467, 1995.
8. Hermann D. M., Hossman K.-A.: Neurologic effects of microwave exposure related to mobile communication. J. Neurol. Sci. 152: 1, 1997.
9. Royal Society of Canada Expert Panel Report: A review of the potential health risks of radiofrequency fields from wireless telecommunication devices. An Expert Panel Report prepared at the request of the Royal Society of Canada for Health Canada. Ottawa, Royal Society of Canada, RSC.EPR 99-1, 1999.
10. Salzinger K.: Behavioral effects of electromagnetic fields in animals. In: Biological Effects of Electric and Magnetic Fields, Volume 1, Sources and Mechanisms (D. O. Carpenter and S. Ayrapetyan, Eds). New York, Academic Press, p 315, 1994.
11. Repacholi M. H.: Low level exposure to radiofrequency electromagnetic fields: health effects and research needs. Bioelectromagnetics 19: 1-19, 1998.
12. Cleary S. F.: Cellular effects of radiofrequency electromagnetic fields. In: Biological Effects and Medical Applicatians of Electromagnetic Energy (O. P. Gandhi, Ed.). Englewood Cliffs, New Jersey, Prentice-Hall, p 339, 1990.

13. Cleary S. F.: Effects of radiofrequency radiation on mammalian cells and biomolecules in vitro. In: Electromagnetic Fields: Biological Interactions and Mechanisms (M. Blank, Ed). Washington, American Chemical Society, p 467, 1995.
14. Philippova T. M., Novoselov V. I., Alekseev S. I.: Influence of microwaves on different types of receptors and the role of peroxidation of lipids on receptor-protein shedding. Bioelectromagnetics 15: 183-192, 1994.
15. Liburdy R. P., Vanek P. F., Jr.: Microwaves and the cell membrane. III. Protein shedding is oxygen and temperature dependent: evidence for cation bridge involvement. Radiat. Res. 109: 382-395, 1987.
16. D'Inzeo G., Bernardi P., Eusebi F., Grassi F., Tamburello C., Zani B.M. Microwave effects on acetylcholineinduced channels in cultured chick myotubes. Bioelectromagnetics 9: 363-372, 1988.
17. Arber S. L., Lin J. C. Microwave enhancement of membrane conductance: effects of EDTA, caffeine and tetracaine. Physiol. Chem. Phys. Med. NMR 16: 469-475, 1984.
18. Arber S. L., Lin J. C.: Microwave induced changes in nerve cells: effects of modulation and temperature. Bioelectromagnetics 6: 257-270, 1985.
19. McRee D. I., Wachtel H.: The effects of microwave radiation on the vitality of isolated frog sciatic nerves. Radiat. Res. 82: 536-546, 1980.
20. Wachtel H, Seaman R., Joines W: Effects of low-intensity microwaves on isolated neurons. Ann. N.Y. Acad. Sci. 247: 46-62, 1975.
21. Seaman R. L., Wachtel H.: Slow and rapid responses to CW and pulsed microwave radiation by individual Aplysia pacemakers. J. Microwave Power 13: 77-86, 1978.
22. Zuo J., Philip L., De Jager P. L., Takahashi K. A., Jiang,W., Linden D. J., Heintz N.: Neurodegeneration in Lurcher mice caused by mutation in δ-2 glutamate receptor gene. Nature 388: 769-773, 1997.
23. Vožeh F., Cendelín J., Motáňová A.: The development of different types of learning in cerebellar degeneration model. Homeostasis 39: 248-250, 1999.
24. Cendelín J., Barcal J., Korelusová I., Vožeh F.: The effect of various levels of dopaminergic transmission influencing the spatial learning process in healthy and neurodefective Lurcher mutant mice (C57B1/7). Homeostasis 42: 239-241, 2003.
25. Caddy K. W. T., Vožeh F.: The effect of 3-acetylpyridine on inferior olivary neuron degeneration in Lurcher mutant and wild type mice. Europ. J. Pharmacol. 330: 139-142, 1997.
26. Cendelín J., Vožeh F.: Assessment of CNS excitability in natural model of cerebellar degeneration. Homeostasis 39: 115-116, 1999.
27. Barcal J., Ježek K., Vožeh F., Žalud V.: Changes of excitability in the cerebellar degeneration model (Lurcher mutant mice). Physiol. Res. 49: 38P, 2000.
28. Sobotka P., Barcal J., Žalud V., Vožeh F.: The effect of caffeine on the heart activity of mice with inborn cerebellar degeneration. Homeostasis 40: 128-129, 2000.
29. Barcal J., Vožeh F., Štenglová V., Žalud V.: The effect of nitric oxide on hippocampal potentiation in the cerebellar degeneration model. Homeostasis 41: 67-69, 2001.
30. Žalud V., Barcal J., Cendelín J., Vožeh F.: EEG recording in mice during exposure to high-frequency electromagnetic field. Homeostasis 41: 203-206, 2001.
31. Franklin, K. B. J., Paxinos, G.: The mouse brain in stereotaxic coordinates. Academic Press, San Diego, 1997.
32. Bawin S. M., Gavalas-Medici R. J., Adey W. R.: Effects of modulated very high frequency fields on specific brain rhythms in cats. Brain Res. 58: 365–380, 1973.
33. Bawin S. M., Gavalas-Medici R. J. , Adey W. R.: Reinforcement of transient brain rhythms by amplitude-modulated VHF fields. In: Biological and Clinical Effects of Low Frequency Magnetic and Electric Fields (J. G. Llaurado, A. Sances and H. Battocletti, Eds). Springfield, Charles C. Thomas, p. 172–177, 1974.
34. Takashima S., Onaral B., Schwan H. P.: Effects of modulated RF energy on the EEG of mammalian brains. Radiat Environ. Biophys. 16: 15–27, 1979.
35. Shandala M. G., Dumanskii U. D., Rudnev M. I., Ershova L. K., Los I. P.: Study of nonionizing microwave radiation effects upon the central nervous system and behavior reactions. Environ. Health Perspect. 30: 115–121, 1979.
36. Thuroczy G., Kubinyi G., Bodo M., Bakos J., Szabo L. D.: Simultaneous response of brain electrical activity (EEG) and cerebral circulation (REG) to microwave exposure in rats. Rev. Environ. Health 10: 135–148, 1994.
37. McRee D. I., Elder J. A., Gage M. I., Reiter L. W., Rosenstein L. S., Shore M. L., Galloway W. D., Adey W. R., Guy A. W.: Effects of nonionizing radiation on the central nervous system, behavior and blood: a progress report. Environ. Health Perspect. 30: p. 123–131, 1979.
38. Mitchell C. L., McRee D. I., Peterson N. J., Tildin H. A., Shandala M.G., Rudnev M. V., Varetskii V.V., Navakatkyan M. I.: Results of a United States and Soviet Union point project on nervous system effects of microwave radiation. Environ. Health Perspect. 81: 201-209, 1989.
39. Reiser H , Dimpfel W., Schober F.: The influence of electromagnetic fields on human brain activity. Eur. J. Med. Res. 1: 27–32, 1995.

40. Roschke J., Mann K.: No short-term effects of digital mobile radio telephone on the awake human electroencephalogram. Bioelectromagnetics 18: 172–176, 1997.
41. Mann K., Roschke J.: Effects of pulsed high-frequency electromagnetic fields on human sleep. Neuropsychobiology 33: 41–47, 1996.
42. Wagner P., Roschke J., Mann K., Hiller W., Frank C.: Human sleep under the influence of pulsed radiofrequency electromagnetic fields: a polysomnographic study using standardized conditions. Bioelectromagnetics 19: 199–202, 1998.
43. Borbely A. A., Huber R., Graf T., Fuchs B., Gallmann E., Achermann P.: Pulsed high-frequency electromagnetic field affects human sleep and sleep electroencephalogram. Neurosci. Lett. 275: 207–210, 1999.
44. Urban P., Lukas E., Roth Z.: Does acute exposure to the electromagnetic field emitted by a mobile phone influence visual evoked potentials? A pilot study. Centr. Eur. J. Public Health 6: 288–290, 1998.
45. Eulitz C., Ullsperger P., Freude G., Elbert T.: Mobile phones modulate response patterns of human brain activity. NeuroReport 9: 3229–3232, 1998.
46. Freude G., Ullsperger P., Eggert S., Ruppe I.: Effects of microwaves emitted by cellular phones on human slow brain potentials. Bioelectromagnetics 19: 384–387, 1998.
47. Jech R., Šonka K., Růžička E., Nebuzelský A., Bohm J., Juklíčková M., Nevšímalová S: Electromagnetic field of mobile phones affects visual event related potential in patiens with narcolepsy. Bioelectromagnetics 22: 519–528, 2001.
48. Repacholi M. J.: Health risks from the use of mobile phones. Toxicol. Lett. 120: 323-331, 2001.

Acknowlledgments

This work was supported by the COST Action 281 „Electromagnetic fields and health emerging information and communication technologies“ and Research Program Project No. MSM ČR 021620816.

EEG BIOEFFECTS ON COCHLEAR DEAF FROM CELLULAR PHONES, (FIRST TESTS).

J.L. Bardasano
Department of Medical Specialities, University of Alcalá, Madrid, Spain
Corresponding author: E-mail: joseluis.bardasano@uah.es

J. Álvarez-Ude
Department of Physics, University of Alcalá, Madrid, Spain

I. Gutiérrez
Department of Medical Specialities, University of Alcalá, Madrid, Spain

M. Raposo
Department of Physics, University of Alcalá, Madrid, Spain

R. Goya
Department of Physics, University of Alcalá, Madrid, Spain

Abstract

- Objectives:

This work aims to provide evidence of an inductive electromagnetic bio-effect on the human brain, which is independent from sound waves and produced by mobile phones, in proximal field, through correlating the EEG data obtained from electrodes placed on both normal and cochlear deaf individuals.

- Methods

Two groups of four subjects are placed under controlled electromagnetic conditions inside a Faraday chamber, (two healthy and another two suffering from cochlear deafness). Each is sitting on a chair, fitted with additional support, and holding a cellular phone 2 cm away form the right auricular, in order to avoid a thermal effect as much as possible. All of them, relaxed and with their eyes closed, are EEG recorded in a basal state with their mobile phones off.

Then, each of them is again recorded under the same conditions but with the mobile on and listening to the same conversation. In order to assess the EEG changes so observed, a statistical analysis by means of the FFT (Fast Fourier Transform) was carried out.

- Results

For both, healthy and cochlear deaf, assimilation or integration of the mobile phone signal by some electrodes is to be found. This is due to the increase of amplitudes for alpha and theta waves, whereas the signal is not integrated in other electrodes. By correlating the spectra of frequencies of corresponding EEG records for the same brain areas, we have not observed significative differences for both groups.

- Conclusion

A possible electromagnetic direct inductive, non-thermal, bio-effect on the human brain is observed. This effect is produced by the use of mobile phones and it bears no relation to the sound waves.

Keywords: electromagnetic field, bio-effects, electroencephalogram, mobile phone, cochlear deaf.

Introduction

Recent technological advances in telecommunications have led to the use of electromagnetic fields (EMF) to man's own convenience, such as in Telemedicine, in the field of Medicine (Ramos and Monteagudo, 2006) or for diagnosis and treatment as well, within the field of medical specialities (Bardasano and Elorrieta, 2000, Rosch and Markov, 2004).

Nevertheless, electromagnetic fields from GSM mobile phones (Global System Mobile Communication) and from their base stations can have an effect on living beings and man, in particular, in different ways. More and more often we find proof from different fields of knowledge of this environmental electromagnetic pollution, which might involve the health of human and other living beings, (Navarro *et al*., 2003, Santini *et al*., 2003, Balmori, 2004, 2005, Hutter *et al*., 2006).

Neurons can respond to electromagnetic fields, (Beasond and Semm, 2002) and different degrees of neurological and other kinds of alterations, which may change the physiology of the brain, can also be found and are associated to mobile phone radiofrequencies, (Hossmann and Hermann, 2003, Westerman *et al*., 2004, Huber *et al*., 2005, Maby *et al*., 2005, Szyjkowska *et al*., 2005, Papageorgiou *et al*., 2006).

Evidence of alterations in the permeability of the hematoencephalic barrier in rats from mobile phones has been presented (Fritze *et al*., 1997) as well as histological changes due to neural damage in the cortex, hippocampus and basal ganglia in the brain of exposed rats (Salford *et al*., 2003) and changes in the EEG of the rabbit (Marino *et al*., 2003).

We also have evidence of alterations in the brain of rats not only at the biochemical level but also at that of the glial cells. There is evidence of molecular alterations in the rat's brain due to GSM mobile phones after an acute exposure to high power 900 MHz micro waves. (Mausset-Bonnefont *et al*., 2004).

Also, the effects of 900 MHz electromagnetic exposure on cochlear cell functionality in rats are evaluated as a distortion product due to otoacoustic emissions by Galloni *et al*., 2005. In this work, in order to evaluate the influence of mobile phones on the human brain, we give the EEG recording an essential role as a working tool, (Krause *et al*., 2004, Lin, 2004, Curcio *et al*., 2005, Loughran *et al*., 2006).

The EEG is a representative signal containing information about the condition of the brain. The shape of the wave may contain useful information, hence Croft *et al*., 2002, found that EMF exposure decreased 1 Hz – 4 Hz activity in right hemisphere sites, and was associated with increasing 8 Hz – 12 Hz activity as a function of exposure duration in the midline posterior sites.

Along the same lines, Kramarenko *et al*., 2003, used a telemetric EEG, and found that within 20 s – .40 s of exposure to a 900 MHz phone signal subjects showed slow-wave activity in the contralateral, frontal and temporal areas. They lasted for one second and were repeated every 15 s – 20 s. When the signal stopped the slow waves progressively disappeared in the next 10 minutes.

Furthermore, Cook *et al*., 2004, suggested that 30% of the variation in alpha activity seen in their study were due to the pulsed magnetic field exposure and also, Papageorgiou *et al*., 2004, found that baseline EEG energy was greater in males, while exposure to EMF decreased EEG energy of males and increased that of females. There were not statistically significant differences in memory performance between men and women, nor was there any difference between exposed and non-exposed states.

Additionally, in a small pilot study, Hamblin, *et al*., 2004, found some evidence of neural activity as a result of mobile phone exposure during an auditory task.

Moreover, the effects of EMF emitted by mobile phones on human EEG were studied during an auditory memory task. The energy was found concentrated at the four basic bands. The results show evidence of a strong gender radiation interaction effect on the EEG energy and on the peak amplitudes within each of the four rhythms (Nanou *et al*., 2005).

The EEG analysis performed with three different methods showed that statistically significant changes occur in the EEG rhythms, energy and dynamics between 12% and 30% of subjects. The results suggest that microwave exposure affects part of the population and can have an impact on health. (Hinrikus *et al*., 2006).

This research is aimed at providing evidence of electromagnetic induction from mobile phones, in proximal field, to the human brain by comparing the EEG of healthy normal individuals with that of cochlear deaf, regardless of sound stimulus (sound waves).

- **Materials and Methods**

We have followed the protocol (patterns), as in previous experiences in our laboratory, as to the subjects, procedures, materials (Faraday screen, mobile phones, electroencephalograph and recording), etc. For more details, see Bardasano *et al*., 2005.

Subjects

We have carried out this study on four individuals in two groups, (two healthy individuals and two suffering from cochlear deafness).

Procedure

Each subject is placed inside the Faraday chamber and comfortably seated on a plastic chair. The mobile phone is held over the right ear by an insulated device 2 cm from the auricular to avoid a thermal effect as much as possible. By means of the EEG, we tested the effects of the mobile phone on the subjects as follows: basal EEG activity, with eyes closed, for 5 min; each subject was recorded while listening to a five minute conversation with the phone placed on the right ear.

Materials

Mobile phone

Technical specifications: Global System Mobile Communication (GSM) class 4 (2 W), 880 MHz –960 MHz frequency band, which is a proximal field in relation to the subject. Specific Absorption Rate (SAR), highest value, 0.955 W/kg.

Electroencephalograph and recording

A digital EEG, with system plus software, model: SAM 32 FOFC I (latest version) by Micromed®, which incorporates amplitude and frequency maps, was employed. EEG signals were collected from 18 channels and filtered with a band filter.

Statistical Analysis

In order to assess our EEG results, we have applied the FFT (Fast Fourier Transform) mathematical analysis.

- **Results**

In healthy and cochlear deaf individuals, we find assimilation or integration of the mobile phone signal in some electrodes. This is due to the increase of the amplitudes of alpha and theta waves. By correlating the spectra of frequencies of corresponding EEG records for the same areas, significative differences for both groups are not observed (see Appendix, Fig. 1 and Fig. 2).

- **Discussion**

Our discussion focuses on physiological interpretation and on methodological observation.

Physiological interpretation

During transduction of external signals, FFT analysis shows that a healthy subject's brain behaves in two ways to the signal from the mobile phone. It rejects the incoming signal or integrates it by making it its own, and generates another signal as a response. This is done by increasing the spectral power density of the incoming signal which implies an increase of energy without altering the frequencies. This means that a larger number of neurons are being activated underneath than at the basal phase for the same activated frequencies.

In short, the brain responds by yielding signals which lead to the generation of alpha and theta rhythms. The EEG response of the cochlear deaf is similar to that of the healthy subject with the phones on. For both groups, the behaviour of the EEG towards the signal from the mobile shows that it can either be integrated in the brain or it appears in the spectrum of frequencies of the typical peaks of mobile phones which overwhelm the normal brain signal, on the same recording electrode and for the same subject at a given time.

Let us call *integration* the capacity for assimilating, processing an incoming signal, and for emitting another signal as a response. Given that, the sound waves do not seem to affect the integration of such a signal in the brain.

Methodological observation

Research on the harmful bioeffects of mobile phones on the brain faces one of its challenges; that is, to avoid suffering, lesion, and death of the neurons. Neuroprotection is a way of guarding neurons which, for different reasons, have their death scheduled. We find several programs in the central nervous system which schedule the death of mobiles, which are activated by internal alterations (genetic features of the patient) or external (biological, chemical, such as exposure to toxins, heavy metals in drinking water, pesticides, and others, and physical elements such as artificial and uncontrolled electromagnetic fields. (Bardasano *et al*., 2005)

The EEG shows the influence of mobile phones on man. In the field of Biomedical Engineering, research should contemplate at least the following aspects:

a. The General Adaptation Syndrome to changes in the state of mater and energy. Those changes take place in the environment of living beings, bearing in mind the threesome 'oppressor, depressor, stressor', adverse hypersensitive reactions and the microwave syndrome.

b. Electromagnetic Compatibility. In the field of the modern theory of the signal, the task is to observe machines or systems in good working condition and the human body, itself as a system, (the inductive influence of electromagnetism from a mobile phone and the bioelectromagnetism of the human brain).

c. The Physiology of Regulatory Systems and Chronobiology. To avoid alterations in the permeability of the hematoencephalic barrier or chronopathologies due to alteration of circadian rhythms, (waking and sleeping states), among others, due to this inductive influence.

Summary

By comparing the EEG data from mobile phones, independent from sound, through the electrodes glued onto normal and cochlear deaf subjects, we have tried to find evidence of an inductive electromagnetic bio-effect on the human brain.

We found that the signal is not integrated in some electrodes and we have not found significant differences for either group of healthy and cochlear deaf subjects, which, on the other hand, show assimilation or integration of the mobile phone in other electrodes because of the increase of amplitude of the alpha and theta waves. By comparing the spectrum of frequencies of the corresponding EEG for the same areas, we have not observed significant differences in both groups, either.

The effect, observed in the brain, is produced by the mobile phones.

Acknowledgements

This project was carried out thanks to the collaboration of Bioelectromagnetism European Foundation (BEF), BIOECODEFENSA 7, L.S. and sponsored by SIEMENS, AG.

References

Bardasano, J.L. and Elorrieta, J.L.: 2000, *Bioelectromagnetism, Science and Health*, McGraw-Hill, edit. Madrid, (In Spanish).

Bardasano, J.L., Álvarez-Ude, J., Gutiérrez, I. and Goya, R.: 2005, New Device against non-thermal Effects from Mobile Telephones, *The Environmentalist* **25**, 257-263.

Balmori, A.: 2004, Posibles Efectos de las Ondas Electromagnéticas utilizadas en la Telefonía Inalámbrica sobre los Seres vivos, *Ardeola* **51**(2), 477-490.

Balmori, A.: 2005, Possible Effects of Electromagnetic Fields from Phone Masts on a Population of white Storks, *Electromagn. Biol. Med.* **24**,109-119.

Beasond, R.C. and Semm, P.: 2002, Responses of Neurons to an Amplitude modulated Microwave Stimulus, *Neurosci. Lett.* **33**, 175-178.

Cook, C.M., Thomas, A.W. and Prato, F.S.: 2004, Resting EEG is affected by Exposure to a pulsed ELF Magnetic Field, *Bioelectromagn.* **25**, 196-203.

Croft, R., Chandler, J.L., Burgess, A.P., Barry, R.J. *et al*.: 2002, Acute Mobile Phone Operation affects Neural Function in Humans, *Clin. Neurophysiol.* **113**, 1623-1632.

Curcio, G., Ferrara, M., Moroni, F., D'Inzeo, G., Bertini, M. and De Gennaro, L.: 2005, Is the Brain influenced by a Phone Call? An EEG Study of Resting Wakefulness, *Neurosci. Res.* **53**(3), 265-70.

Fritze, K., Wiessner, C., Custer, N., Sommer, C., *et al*..:1997, Effect of global System for Mobile Communication (GSM) Microwave Exposure in Blood Brain Barrier Permeability in Rat, *Acta Neuropathol. (Berl)* **94**, 465-470.

Galloni, P, Lovisolo, G.A., Mancini, S., Parazzini, M. *et al*.: 2005, Effects of 900 MHz Electromagnetic Fields Exposure on Cochlear Cells' Functionality in Rats: Evaluation of Distortion Product Otoacoustic Emissions, *Bioelectromagn.* **26**(7), 536-47.

Hamblin, D.L., Wood, A.W., Croft, R.J. and Stough, C.: 2004. Examining the Effects of Electromagnetic Fields emitted by GSM Phones on Human Event-Related Potentials and Performance during an Auditory Task, *Clin. Neurophysiol.* **115**, 171-178.

Hinrikus, H., Bachmann, M., Lass, J., Tomson, R and Tuulik,V.: 2006, Changes caused by Microwave in Human EEG of Individuals. In Action COST-281, *Potential Health Effects of Mobile Communication Systems. Graz*, 20-21 april.

Hossmann, K.A. and Hermann, D.M.: 2003, Effects of Electromagnetic Radiation of Mobile Phones on the Central Nervous System, *Bioelectromagn.* **24**, 49-62.

Huber, R., Treyer,V., Borbely, A.A., Schuderer, J., Gottselig, J.M. *et al* : 2002, Electromagnetic Fields, such as those from Mobile Phones, alter regional Cerebral Blood Flow and Sleep and Waking EEG, *J. Sleep Res.***11**, 289-295.

Hutter, H.P., Moshammer, H., Wallner, P. and Kundi, M.: 2006, Subjetive Symptoms, sleeping Problems, and Cognitive Performance in Subjects living near Mobile Phone Base Stations, *Occup. Environ. Med*. **63**, 307-313.

Kramarenko, A.V. and Tan, U.: 2003, Effects of High-Frequency Electromagnetic Fields on Human EEG: A Brain Mapping Study, *Int. J. Nurosci.* **113**, 1007-1019.

Krause, C.M., Haarala, C., Sillanmaki, L., Koivisto, M. *et al*.: 2004, Effects of Electromagnetic Field emitted by Cellular Phones on the EEG during an auditory Memory Task: A Double Blind Replication Study, *Bioelectromagn.* **25**, 33-40.

Lin, J.C.: 2004, Human Electroencephalograms (EEG) and Mobile-Phone Radiation, *Radio Sci. Bull.* **308**, 52-54.

Loughran, S.P., Wood, A.W., Barton, J.M., Croft, R.J. *et al*.: 2005, The Effect of Electromagnetic Fields emitted by mobile Phones, *Neuroreport* **16**, 1973-1976.

Maby, E., Jaenés, R.L., Faucon, G., Liegeois-Chauvel, C. and De Seze, R.: 2005, Effects of GSM Signals on Auditory Evoked Responses, *Bioelectromagn.* **26**(5), 341-350.

Mausset-Bonnefont, A.L., Hirbec, H., Bonnefont, X., Privat, A. *et al*.: 2004, Acute Exposure to GSM-900 MHz Electromagnetic Fields induces Glial Reactivity and Biochemical Modifications in the Rat Brain, *Neurobiol. Dis.* **17**, 445-454.

Nanou, E., Tsiafakis, V., Kapareliotis, E., Papageorgiou, C., Rabavilas, A. and Capsalis, C.: 2005, Influence of the Interaction of a 900 MHz Signal with Gender on EEG Energy: Experimental Study on the Influence of 900 MHz Radiation on EEG, *The Environmentalist* **26**, 173-179.

Navarro, E.A., Segura, J., Portolés, M. and Gómez-Perretta, C.: 2003, The Microwave Syndrome: A preliminary Study in Spain, *Electromagn. in Biol. Med.* **22**, 181-171.

Papageorgiou, C.C., Nanou, E.D., Tsiafakis, V.G., Capsalis, C.N. and Rabavilas, A.D.: 2004, Gender related Differences on the EEG during a simulated Mobile Phone Signal, *Neuroreport*. **15**(16), 2557-2560.

Papageorgiou, C.C., Nanou, E.D., Tsiafakis, V.G., Kapareliotis, E *et al*.: 2006, Acute Mobile Phone Effects on Pre-attentive Operation, *Neurosci. Lett*. **397**(1-2), 99-103.

Ramos, V. and Monteagudo, J.L.: 2006, Assessment of EM Environment for Home Telemedicine. In International Conference and COST 281 *Workshop on Emerging EMF Technologies, Potential Sensitive Groups and Health*. *Graz*, April 20/21.

Rosch, P.J. and Markov, M.S.: 2004, *Bioelectromagnetic Medicine*, Marcel Dekker, Inc., edit. New York and Basel.

Salford, L.G., Brun, A.E., Eberhardt, J.L., Malmgren, L. and Person, B.R.: 2003, Nerve Cell Damage in Mammalian Brain after Exposure to Microwave from GSM Mobile Phones, *Environ. Health Perspect*. **111**, 881-883.

Santini, R., Santini, P., Danze, J.M., LeRuz , P. and Seigne, M.: 2003, Survey Study of People living in the Vecinity of Cellular Phone Base Stations, *Electromagn. Biol. Med*. **22**(1), 41.

Szyjkowska, A., Bortkiewicz, A., Szymczak, W. and Makowiec-Dabrowska, T.: 2005, Subjective Symptoms related to Mobile Phone Use, *Pol. Merkuriusz. Lek*. **19**(112), 529-532.

Westerman, R. and Hocking, B.: 2004, Diseases of Modern Living; Neurological Changes associated with Mobile Phones and Radiofrequency Radiation in Humans, *Neurosci. Lett.* **361**, 13-16.

Appendix

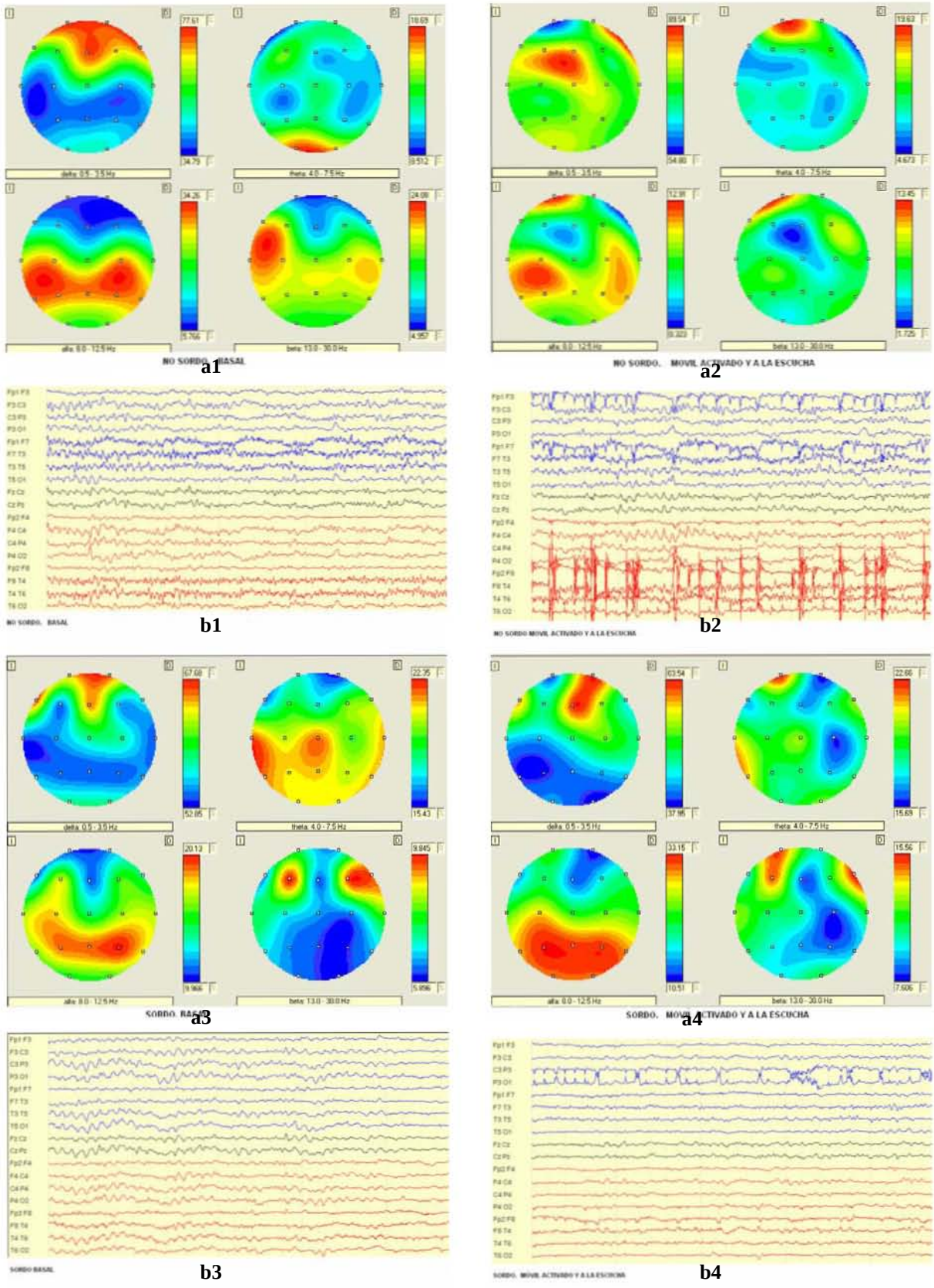
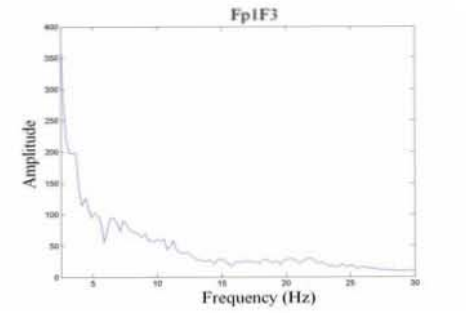
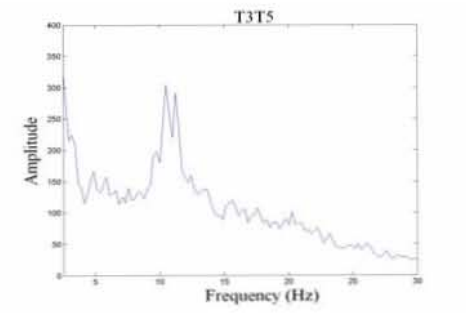


Fig. 1. Mapping of: **a1–** basal non-deaf, **a2–** non deaf with mobile on and listening, **a3–** basal deaf and **a4–** deaf with mobile on and listening.
EEG of: **b1–** basal non-deaf, **b2–** non deaf with mobile on and listening; **b3–** basal deaf and **b4–** deaf with mobile on and listening

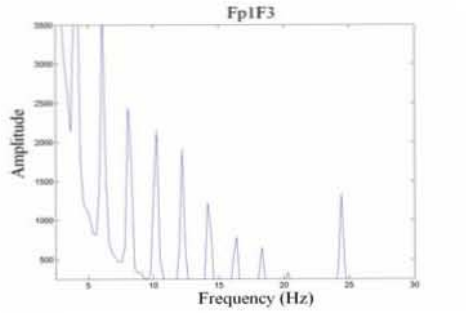
NON DEAF

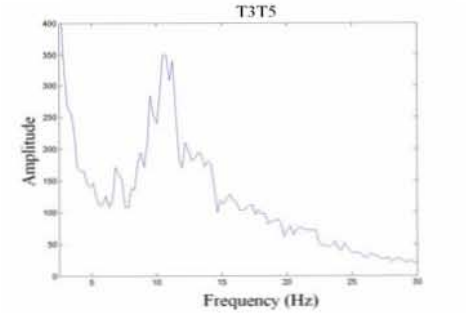
BASAL





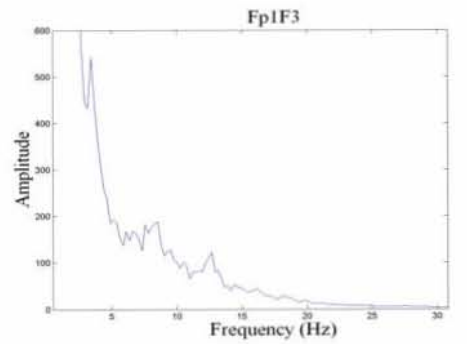
MOBILE

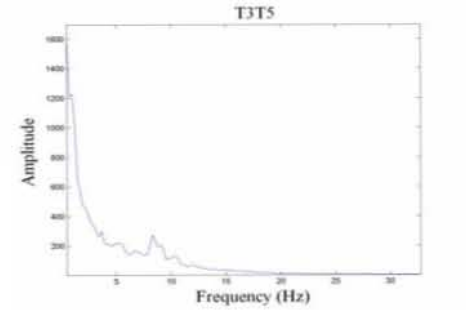




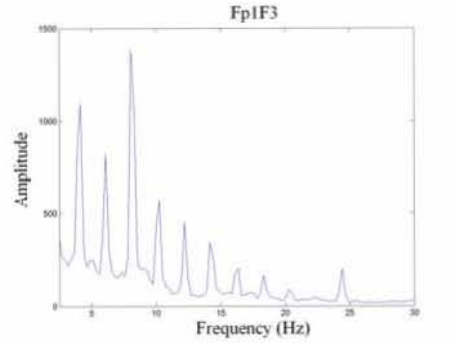
DEAF

BASAL





MOBILE



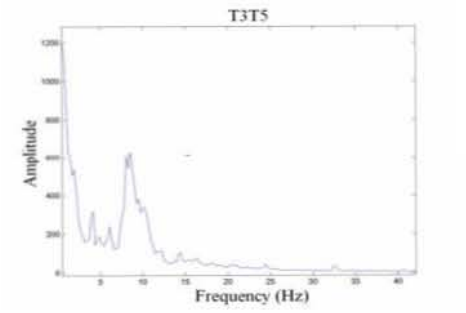


Fig 2: Spectrum of EEG frequencies obtained: **BASAL**– in basal position (electrodes Fp1F3 and T3T5) **MOBILE–**with the mobile on and listening (electrodes Fp1F3 y T3T5), for both, deaf and non-deaf.

EEG EFFECTS OF TRANSCRANIAL MAGNETIC STIMULATION AT pT RANGE

J.L. Bardasano
Department of Medical Specialities, University of Alcalá, Madrid, Spain
Corresponding author: E-mail: joseluis.bardasano@uah.es

J. Álvarez-Ude
Department of Physics, University of Alcalá, Madrid, Spain

I. Gutiérrez
Department of Medical Specialities, University of Alcalá, Madrid, Spain

M. Raposo
Department of Physics, University of Alcalá, Madrid, Spain

R. Goya
Department of Physics, University of Alcalá, Madrid, Spain

Abstract

- **Objectives**.

We aim to obtain a model or pattern among normal subjects. Thus, we are subsuming a diagnostic method (digital EEG) and a therapeutic one, which is the physiological TMS (Transcranial Magnetic Stimulation), into a new technique, pending validation. This new technique will be able to obtain an electroencephalographic response and to quantitatively evaluate the alteration of cerebral rhythms in healthy subjects, (pattern for normality), employing physiological TMS at 10 pT (picotesla) and 8 Hz, simulating the alpha rhythm. The study is single blind and the subjects do not know when they are being stimulated.

- **Material and Methods**

We have employed digital EEG, mod. SAM 32 FOFC 1, with System PLUS Software by Micromed, latest version, and spectral analysis by FFT (Fast Fourier Transform). The sample was made up of 16 healthy subjects with their eyes open, half males and half females. The recording cap, which is elastic has twenty Ag/AgCl electrodes (SIEMENS) placed bilaterally and is electrode-glued onto the scalp of the subject. The 10/20 IS (International System) of electrode placement is used. EEG signals are collected from 18 channels, filtered through a 0.5 Hz – 70.0 Hz band filter and sampled at 128 Hz. We have also used a TMS prototype stimulator, mod. MG28TR10, which incorporates a timer for the EEG recorder to control the stimulation periods and pauses (1.5 min followed by a 1 min pause). Twenty magnetic stimulation coils are placed on the EEG recording elastic cap at a distance of 2 cm between them and the recording electrodes. This way, stimulation and recording can be carried out without interference.

- **Results**

A global increase in the alpha and beta rhythms has been observed as well as a decrease in delta and theta. Alpha and delta register the highest increase and decrease, respectively. A 17.5% increase in alpha rhythm and a 4.5 % in beta are performed at the expense of a decrease in delta and theta rhythms.

The most relevant increase in alpha rhythm, as the stimulation was going on, was registered at the Fp1, Fp2, F3 and F4 frontal electrodes, as well as at the central Cz.

- **Conclusions**

By means of the TMS at 10 pT and 8 Hz, we obtain a mimetic global bioelectrical neuronal response, as the alpha rhythm magnetic field is simulated and the brain is timed to it. We also find an alpha rhythm displacement towards frontal and central areas of the brain.

Keywords: magnetic stimulation, EEG, brain rhythms.

Introduction

Research on 500 µT weak magnetic fields, extremely low frequencies (ELF) (between 0 Hz and 300 Hz), and their exposure to humans has yielded incomplete and contradictory evidence, (stemming mainly from clinical results) (Sandyk, 1992, Sandyk and Derpapas, 1993, Bardasano *et al*., 1997a, Ramírez *et al*., 1997, Anninos *et al*., 2003).

This may be due to the scarce number of studies conducted under EEG, MEG (Magnetoencephalography) examination conditions or evoked potentials and how they affect the perceptual and cognitive processes in human beings. It must also be added that most bioelectromagnetic results in the different studies have been inconsistent with one another. The most important explanations, which may account for those inconsistencies are those aimed to clarify how different the features of the applied field may be (different intensity and frequency, waveform, and duration of exposure). We also find differences among the disparate protocols employed, which can be more or less precise regarding the elimination of artefacts or elements that bring about confusion in the electrophysiological recording (Cook *et al*., 2002).

Most studies on low-power fields carried out inside Helmholtz coils generate a homogenous and continuous field, (Lyskov *et al*.,1993, Marino *et al*.,1996 and Heusser *et al*.,1997), in which the subject has electrodes placed on both his first and second fingers of his non-dominant hand and on his scalp. The former measures skin conductance and the latter cerebral electric activity. A computer controlled system allows us to change the type of field generated by the coils at desired intervals, in either a random or pre-determined pattern and to register the ongoing physiological changes.

Most EEG studies so far, which observe the effects after applying a weak magnetic field, have been using this magnetic fields generation model and have been comparing the differences so obtained.

As regards to physiological stimulation, the simultaneous registry between stimulator and EEG does not allow us to categorically state the effect it has on the brain because a signal under possible electromagnetic pollution leads to doubtful interpretations. To sort out that problem a new biomedical engineered prototype must be designed. That prototype will allow for evaluation of the electrical response of the brain, as a response to an electromagnetic stimulus, under the best conditions, free of pollution and interference.

We have studied and evaluated the physiological low field TMS (Transcranial Magnetic Stimulation) at pT (picotesla) with a new stimulation system whereas other authors used a high field TMS (Pascual-Leone *et al*. 1998, Iramina, *et al*. 2002). This technique also applies to the treatment of neurodegenerative diseases, (Parkinson's disease, Alzheimer's, multiple sclerosis), psychiatric, etc. (Bardasano *et al*., 1997a, b, Ramírez *et al*., 1997, Wassermann and Lisanby, 2001, Bardasano *et al*., 2005a, b, Bardasano *et al*., 2006).

Material and Methods

- **Subjects**

The sample is made up of sixteen healthy voluntary subjects, (an average of 35 years of age; 8 male and 8 female), properly and ethically informed, and the readings are registered inside a Faraday chamber (For details, see Bardasano *et al*., 2005c).

- **Electroencephalograph and recording**

We have employed digital EEG, mod. SAM 32 FOFC 1, with System PLUS Software by Micromed, latest version, and spectral analysis by FFT (Fast Fourier Transform). An elastic recording cap, glued to the scalp on both sides, holds twenty Ag /Ag Cl electrodes (SIEMENS) which are placed on both sides of the cap. The 10/20 IS (International System) of electrode placement is used and the actual placement has a common reference electrode placed at the frontotemporal intersection point and is grounded to the ear lobules. EEG signals are collected from 18 channels, filtered through a 0.5 Hz –70.0 Hz band filter and sampled at 128 Hz.

- **Stimulator**

Stimulating and recording can be carried out without interference using a TMS prototype mod. MG28TR10 at 10 pT and 8 Hz, which has a timer for the EEG recorder to control stimulation periods and pauses (1.5 min followed by a 1 min pause). Twenty magnetic stimulation coils are placed on the EEG recording elastic cap at a distance of 2 cm between them and the recording electrodes (Bardasano *et al*., 2006) (Fig.1).

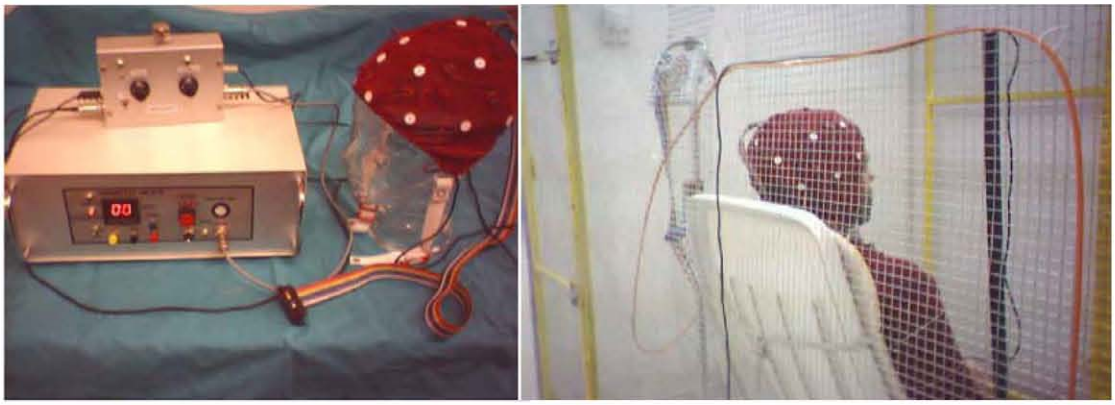


Fig. 1. TMS stimulator, mod. MG28TR10 (left). Subject sitting inside the Faraday chamber. Recording cap and amplifier are also shown here, (right).

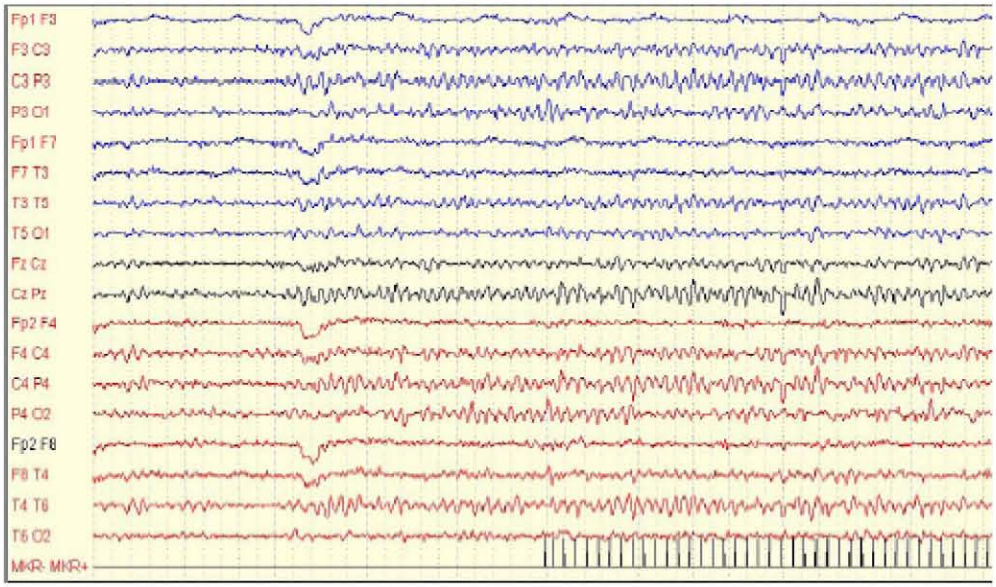


Fig 2. Beginning of the stimulation process. We can see a lower channel designed to observe the morphology and frequency of the stimulus. The stimulus-pause sequence allows for both he ulterior elimination of traces of stimulus and analysis of the pause tracks as though it had been done with a non-stop recording.

- **Procedure**

The subjects are comfortably seated (Fig 1) with their eyes open and without outside stimulation. A basal EEG is first done for 5 min and then a long 10 min sequence stimulation (Fig 2). The subjects are single blind, as they do not know when they are being stimulated.

- **Statistical analysis**

The data have been computed, analysed and interpreted by means of the statistical set SAS System Release 8.02 by SAS Institute Inc. Cary, N.C., USA.

In the frequency tables, (in ASCII format for the 19 electrodes applied), the comparison between groups was evaluated by differential pairing and contrast with the paired T-Student. The p-values are given for up to 4 decimal figures.

- **Results**

An important increase in the alpha and beta rhythms has been observed as well as a decrease in delta and theta. alpha and delta record the highest increase and decrease, respectively, (a 17.5% increase in alpha rhythm and a 4.5 % in beta rhythms, repeatedly, at the expense of a decrease in delta and theta (see Fig 3 and Appendix, Fig. 4).

The most significant increase in alpha rhythm, at the same time as the stimulation was being carried out, was registered at the Fp1, Fp2, F3 and F4 frontal electrodes and at the central Cz.

This leads us to believe that there is a displacement towards anterior brain areas of the physiological alpha rhythm, under stimulation.
Below, find bar graphs of mentioned electrodes where the basal state is the first bar, the second bar stands for stimulation and the third for the difference.

As soon as the recording was over, each subject was asked how he felt as a whole; 84% mentioned they experienced a pleasing and soothing sensation; the remaining did not mention any particular feeling, (indifference) and 3 cases felt their hands going numb.

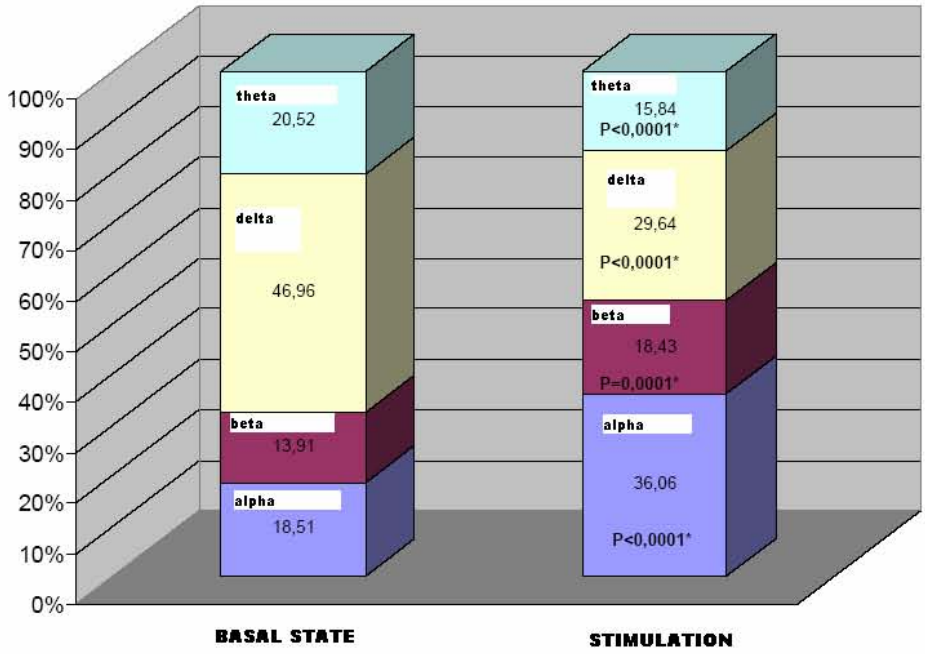


Fig 3. Comparison of frequency-percentage histogram. Redistribution of brain rhythms (alpha, beta, delta and theta), mean value of all the electrodes.

- **Discussion**

The systems usually employed for TMS have high intensity field-generating coils with a current peak of between 2 kA and 8 kA. This way, the different resulting potential, which is needed to induce functional stimulation or inhibition in the cortical area, can be achieved and it can be done with a 600 ms single-pulse field or with a 200 ms – 300 ms double-pulse field. These field intensities induce currents a lot higher than needed to obtain a selective effect. Furthermore, they expand over too large areas of the cortex to stimulate a target area round a few square millimetres. There is no reliable evidence found as yet to prove that the way to standardise the useful stimulation intensity may be based on the evoked muscular potentials obtained after stimulation. However, the fact that low intensity does not yield evoked muscular potentials does not imply there is not any effect. There are other effects, yet subclinical, that can be more relevant than the evoked motor responses.

Therefore, localization and selective stimulation objectives are not guaranteed with the high-power field systems which, additionally, provide undesirable thermal effects, preventing stimulation for long periods of time. The stimulated cerebral areas selected as objectives are not the only ones receiving this induced current. Besides the target area, there are stimulations in subcortical areas where their effect is yet unknown, or where undesirable effects are found, with hard to control collateral consequences.

Conversely, the intensity that flows through our coils is in µA, which allows for stimulations for as long a duration as desired without adverse effects on the patient. We should bear in mind that the intensity of the current is so high as it flows through the high-power field coils that there is a noise to be taken into consideration as we interpret the results (Nikouline *et al*., 1999). However, our subject can not hear a thing and, therefore, does not know whether the current is flowing; it is a single blind experiment.

High-power field stimulation is not physiological which is conceptually different from low-power field stimulation. The latter tries to simulate neuronal biophysics in that it works within the same ranks of frequency

and intensity, whereas a high-power field is quite a few ranks more intense than natural bioelectromagnetism and works with antiphysiological frequencies (Gutiérrez, 2004).

After a decade of experimentation, high-power field transcranial magnetic stimulation has not yet come up with a treatment for relief from any illnesses (Wassermann and Lisanby, 2001). However, studies on low-power field research have been fewer, isolated, inhomogenous, and contradictory. If we only focus on the physiological transcranial stimulation (at pT rank), the Sandyk, Anninos's team stands out alone in the world in the field of therapeutics as they aim to simulate the physiological cerebral magnetic field during stimulation (Sandyk *et al*., 1993, Anninos *et al*., 2003).

We must remark that all the studies we have analysed use the same methodology; firstly, they carry out a basal registry, then they stimulate a given field and, finally, they record EEG post-stimulation; the results are then compared and the "before-after" differences are observed. We, on the other hand, apply the stimulation and pause it serially. This allows us to see what goes on at consecutive moments, immediately after the moment of stimulation. This way, we do not need to observe a given effect much later. Furthermore, we use direct application coils on the skull, which generate small fields round it and does not require surrounding the subject with a large field.

By using pT magnetic field, the rank of physiological stimulation is never reached as opposed to those other studies which usually work at the μT rank.

Summary

We aim to obtain a model or pattern among normal subjects. We have used a new technique, the physiological TMS, (validation pending), which is a therapeutic method and a digital EEG, a diagnostic method. Thus, we are subsuming two methods. This new technique allows us to obtain an electroencephalographic response and also to measure changes in the rhythms of a healthy subject's brain, (pattern for normality). Physiological TMS at 10 pT and 8 Hz, simulating the alpha rhythm, were employed. The subject does not know when stimulation is taking place, so this study is single blind.

This way, we obtain a mimetic global bioelectrical neuronal response, as the alpha rhythm magnetic field is stimulated and the brain is timed to it. An alpha rhythm displacement towards frontal and central areas of the brain was also observed.

Acknowledgements

This project was carried out thanks to the collaboration of Bioelectromagnetism European Foundation (BEF) and sponsored by SIEMENS, A.G.

References

Anninos, P., Kotini, A., Adamopoulos, A. and Tsagas, N.: 2003, Magnetic Stimulation can modulate Seizures in Epileptic Patients, *Brain Topogr.* **16** (1), 57-64.

Bardasano, J.L., Ramos, J.L. and Picazo, M.L.: 1997a, Device for a non-invasive Treatment with ELF Electromagnetic Fields (pT Intensity). In *Bioelectromagnetismo y Salud Pública*, I.B.A.S.C., edit. Alcalá de Henares (University), 395-400, (In Spanish).

Bardasano, J.L., Ramírez, E., De la Hoz, J., Ramos, J.L. and Picazo, M.L.: 1997b, Extracranial Device for Noninvasive Neurological Treatments with pulsating ELF Magnetic Fields. Second World Congress for Electricity and Magnetism in Biology and Medicine, 8-13 June, Bologna.

Bardasano, J.L., Gutiérrez, I., Goya, R., Montiel, I., and Álvarez-Ude, J.: 2005a, Transcranial Magnetic Stimulation at pT and Synchronization of the alpha Rhythm, The First International Congress of applied Chronobiology and Chronomedicine, Antalya, June 1-5, Abstract Book, 43-44.

Bardasano, J.L., Carrillo, G.L., Gutiérrez, I., Goya, R. and Álvarez-Ude, J.: 2005b, Transcranial Magnetic Stimulation and EEG Changes in Multiple Sclerosis. Preliminary Results. First International Congress of Histology and Tissue Engineering. Alcalá de Henares, Sept.14-17. Item.: *Histol. Histopathol. Suppl.* **1**, 140-141.

Bardasano, J.L., Álvarez-Ude, J., Gutiérrez, I., Goya, R.: 2005c, New Device against non-thermal Effects from Mobile Telephones, *The Environmentalist* **25**, 257-263.

Bardasano *et al*.: 2006, Equipment for Magnetic Field Treatment for Neurodegenerative Illnesses. *Bol. Ofic. Prop. Industr*.1780, (In Spanish).

Cook, C.M., Thomas, A.W.and Prato, F.S.: 2002, Human Electrophysiological and Cognitive Effects of Exposure to ELF Magnetic and ELF modulated RF and Microwave Fields: A Review of recent Studies, *Bioelectromagnetics* **23**, 14-157.

Gutiérrez, I.: 2004, Electroencephalographic (EEG) Evaluation of Physiological Transcranial Magnetic

Stimulation Technique. New Application Device. Doctoral Thesis, Medical Specialities Department, School of Medicine, University of Alcalá, (In Spanish).

Heusser, K., Tellschaft, D. and Thoss, F.: 997, Influence of an Alternating 3 Hz Magnetic Field with an Induction of 0,1 Millitesla on Chosen Parameters on the Human Occipital EEG, *Neurosci. Lett.* **239**, 57-60.

Iramina, K., Maeno, T., Kowatari, Y. and Ueno, S.: 2002, Effects of Transcranial Magnetic Stimulation on EEG Activity, *IEEE Transactions on Magnetics* **38(**5), 3347–3349.

Lyskov, E.B., Juutilainen, J., Jousmäki,V., Hänninen, O., *et al*.: 1993, Influence of Short-term Exposure of Magnetic Field on the Bioelectrical Processes of the Brain and Performance, *Int. J. Psychophysiol*. **14**(3), 27-231.

Marino, A.A., Bell, G.B. and Chesson, A.: 1996, Low-level EMFs are traduced like other Stimuli, *J. Neurol. Sci.* **144**, 99-106.

Nikouline,V., Ruohonen, J. and Ilmoniemi, R.J.: 1999, The Role of the Coil Click in TMS assessed with simultaneous EEG, *Clinical Neurophysiol*. **110**, 1325-1328.

Pascual-Leone, A., Tormos, J.M., Keenan, J., Tarazona, F., Cañete, C. and Catalá, M.D.: 1998, Study and Modulation of Human Cortical Excitability with Transacranial Magnetic Stimulation, *J. Clin. Neurophysiol*. **15**, 333–343.

Ramírez, E., Bardasano, J.L., De la Hoz, J., Ramos, J. and Picazo, M.L.: 1997, Non invasive Treatment of some Neurodegenerative Illnesses with ELF (pT Intensity) Magnetic Fields. In *Bioelectromagnetismo y Salud Pública*, I.B.A.S.C., edit. Alcalá de Henares (University), 349-354, (In Spanish).

Sandyk, R.: 1992, Magnetic Fields in the Therapy of Parkinsonism, *Int. J. Neurosci*. **66,** 209-235.

Sandyk, R. and Derpapas, K.: 1993, The Effects of external Picoteslas Range Magnetic Fields on the EEG in Parkinson´s Disease, *Int. J. Neurosci*. **70**, 85-96.

Wassermann, E.M. and Lisanby, S.H.: 2001, Therapeutic Application of Repetitive Transcranial Magnetic Stimulation: a Review. *Clin. Neurophysiol.* **112**, 1367-1377.

Appendix

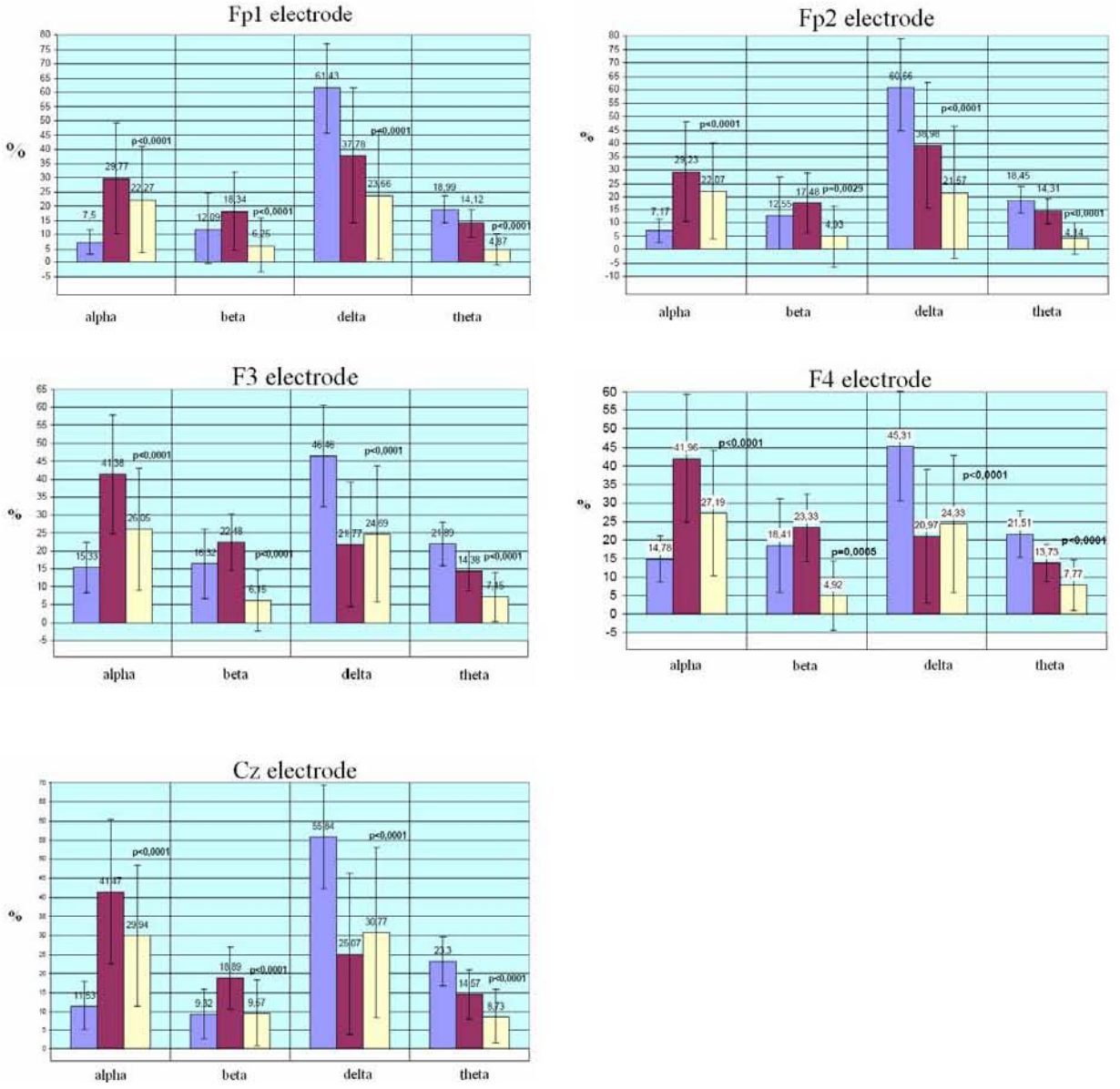


Fig 4. Diagrams of Fp1, Fp2, F3, F4 and Cz electrodes, where the four brain rhythms (alpha, beta, delta and theta) are analysed. For each rhythm, the left column stands for the basal state data; the central column, at 10 pT stimulation, and the right column stands for the difference between the other two.

TAMMEF (THERAPEUTIC APPLICATION OF MUSICALLY MODULATED ELECTROMAGNETIC FIELDS) THERAPY IN THE TREATMENT OF CHRONIC LOW BACK PAIN.

Battisti E.°, Albanese A.°, Bianciardi L.°, Piazza E.°, Rigato M.°, Vittoria A.*, Messa G.L.*, Giordano N.^.

°TAMMEF Centre - University of Siena, Italy.
*** Department of Clinical Medicine and Immunological Science - University of Siena, Italy.**
^ Department of Internal Medicine - University of Siena, Italy

Dr. Battisti Emilio
TAMMEF Centre – Ospedale S. Maria alle Scotte-
Strada delle Scotte,1
53100 Siena- ITALY
e-mail: battistie@unisi.it

ABSTRACT

Background: Numerous studies have demonstrated the utility of extremely low frequencies (ELF) electromagnetic fields in the treatment of pain. Moreover, the effects of these fields seems to depend on their respective codes (frequency, intensity, waveform).
Purpose of the study: In our study we want to value the effects of the TAMMEF (Therapeutic Application of a Musically Modulated Electromagnetic Field) system, which field is piloted by a musical signal and its parameters (frequency, intensity, waveform) are modified in time, randomly varying within the respective ranges, so that all possible codes can occur during a single application.
Ninety subjects, affected by chronic low back pain, were enrolled in the study and randomly divided into three groups of 30 patients each: A exposed to TAMMEF, B exposed to ELF, C exposed to a simulated field. All subjects underwent a cycle of 15 daily sessions of 30 minutes each and a clinical examination upon enrolment, after 7 days of therapy, at the end of the cycle and at a follow-up 30 days later.
Results: All the patients of groups A and B completed the therapy without the appearance of side effects: they presented a significant improvement of the subjective pain and the functional limitation, which remained stable at the follow-up examination. In group C, there was no improvement of the pain symptoms or articular functionality.
Conclusions: This study suggests that the TAMMEF system is efficacious in the control of pain symptoms and in the reduction of functional limitation in patients with chronic low back pain. Moreover, the effects of the TAMMEF system cover those produced by the ELF field.
Key words: electromagnetic fields, therapy, low back pain, TAMMEF.

INTRODUCTION

The effects of the various types of low frequency electromagnetic fields used in clinical practice depend on their codes (frequency, intensity, waveform, the number of impulses per train and the interval between one train and another). The electromotor forces induced at a given point of a biological system act on the electric charges present which respond, causing functional modifications in the cellular microenvironment (1-3).

The overall biophysical effect can be appreciated only by observation, since the level of complexity of the system does not allow one to predict what mechanisms of action will predominate. However, it is possible to

compare the effects of a certain field with those of an all-inclusive reference field whose parameters continually change in time so that all possible codes can occur in a single application.
Our group has already shown the efficacy and tolerability of the extremely low frequency (ELF) field in patients affected by osteoporosis (4), rheumatoid arthritis (5) and osteoarthritis (6,7). Recently to evaluate the utility of applying the widest possible magnetic field, we introduced the new TAMMEF (Therapeutic Application of a Musically Modulated Electromagnetic Field) system. The field is obtained from recorded musical passages; thus its parameters (frequency, intensity, waveform) are modified in time, randomly varying within the respective ranges, so that all possible codes can occur during a single application (6,7).
The aim of this study is to evaluate the efficacy of the TAMMEF system in the treatment of chronic low back pain. In particular, we wished to ascertain if the effects of the field piloted by a musical signal are comparable with those of field with frequency of 100 Hz and a sinusoidal waveform. Both fields are generated by an opposing pair of heteronomous polar expansions and thus present the characteristic spatial conformation.

METHODS AND PATIENTS

Methods
The instruments used to generate the ELF and TAMMEF fields are similar.
An audiotape player sends the relative monochannel-microphone signal to two low frequency amplifiers A and B, both with adjustable gain. The current from amplifier A, modulated according to the recorded signal, feeds two electromagnets with iron-silicon cores joined posteriorly by a ferromagnetic arc. The anatomical region to be treated is placed between the opposing faces (3x4 cm) of the polar expansions. The current from amplifier B feeds a loudspeaker that plays the pilot musical passage. The music can also be heard through headphones, with automatic exclusion of the loudspeaker. The gain of amplifier A is regulated so that when the audiotape contains a sinusoidal signal with frequency of 100 Hz, the electromagnetic field is equal to the ELF field used (about 3 gauss midway between the poles when this distance is 30 cm). This set-up is then left unchanged whatever the contents of the audiotape used subsequently. The patient is allowed to regulate the gain of amplifier B, with the volume preferred, whether the music is being transmitted over a loudspeaker or into a headset.

Patients
Ninety subjects (63 females and 27 males), between 59 and 76 years old, affected by chronic low back pain, were enrolled in the study (table 1a) and randomly divided into three groups: A = 30 patients subjected to TAMMEF, B = 30 patients subjected to ELF and C = 30 patients subjected to a simulated field**.** Group C was introduced because of the possibility that the TAMMEF effects would be indistinguishable from those of the ELF, and thus to test for the presence of a substantial placebo effect. All the patients including in group C listened to the music. Evaluation of the stage of the disease was based on the radiographic system of Kellegren and Lawrence (8). The clinical examination was based on the Million Instrument test (9), a validated questionnaire specific for back pain. On the basis of the point of the score of the test, the patients were divided into three subgroups, as shown in Table 1b.
All the subjects were out-patients and, correctly informed of the experimental plan, gave their written consent. All the patients underwent a cycle of 15 daily sessions of 30 minutes each, with application of the magnets in contact with the lumbar spine. In the past, all the patients had been treated occasionally or cyclically with analgesic (paracetamol) or non-steroidal anti-inflammatory drugs (diclofenac, or piroxicam, or celecoxib, or rofecoxib), but they had suspended any drug at least 15 days before the beginning of the cycle. The clinical examination was performed when the patients were enrolled in the study, after 7 days of therapy, at the end of the cycle and at a follow-up, 30 days later (10).
The evaluation of the possible therapeutic effects has been effectuated using the Million Instrument test as modified by the authors: we have divided the evaluation of pain from the evaluation of articular function because of the well-known subjectivity of pain to the placebo effect (11).

Statistical analysis
The differences between the means of the various parameters at 0, 15 and 45 days were tested by Student's t test or Mann-Whitney-U test as appropriate.

RESULTS

Above all, we specified that no significant differences were found between the three groups of patients, concerning private data and their degree of disease. All the patients of group A and B completed the therapeutic cycle, without side-effects that might have required suspension of the treatment. With regard to the efficacy of the therapy, it should be underlined that none of these patients had to take analgesic-

antiinflammatory drugs during the cycle and that all the patients presented a significant improvement of both subjective pain and regional functional limitation. In particular, in the TAMMEF group, the subjective pain progressively decreased in all subjects even after the first week and regressed completely at the end of treatment in 24 (80%) of the 30 patients. In the remaining 6 patients (20%), the pain symptoms, albeit not totally regressed, decreased significantly with respect to the basal values and to those recorded after the first week (Figure 1a). In the ELF group, the time course of subjective pain was equivalent to that of the TAMMEF group, with complete regression in 23 patients (76.6%) and a significant reduction in the remaining 7 patients (23.4%) (Figure 1b). With regard to the evaluation of articular functionality, there was a significant partial recovery of mobility in all patients, starting from the first week (thus concomitant with the improvement of subjective pain). At the end of the cycle, in the TAMMEF group, 21 patients (70%) manifested a total recovery of the partially compromised articular functionality, while 9 patients (30%) showed a significant further improvement with respect to the already positive trend recorded after the first week of therapy, although they did not achieve a total functional recovery (Figure 2a). In the ELF group, there was a total functional recovery in 19 patients (63.3%), while in 11 patients (36.7%) the change was similar to that of the TAMMEF group (Figure 2b). The clinical follow-up, one month after the end of the cycle, revealed that in 28 group A patients (93.3%), there was no appreciable variation in the regression or improvement of pain symptoms from what was recorded at the end of the magnetotherapy; in the other 2 subjects (6.7%), there was a clear relapse of pain. However, this was not accompanied by a concomitant worsening of articular functionality, which continued to show the same recovery as recorded at the end of the therapy one month previously. There was a very similar pattern in group B: in 27 patients (90%), there was no change from the situation at the end of therapy, whereas 3 subjects (10%) reported a relapse of the pain symptoms. The time course of the articular pathology was clearly different in the 30 subjects of group C. Only 3 of them (10%) presented a slight subjective improvement of the symptoms in the first 5 days of the cycle, while the other 27 patients (90%) reported no significant pain reduction. After the first week, application of the simulated magnetic field had to be suspended in 12 group C patients (40%) because of its ineffectiveness, while the remaining 18 patients (60%) completed the cycle. At the end of treatment and at the clinical follow-up one month later, all the patients who completed the cycle reported no improvement of pain symptoms or articular functionality; indeed, there was a slight worsening of pain (Figures 1c-2c).

DISCUSSION

All the patients treated with TAMMEF or ELF completed the therapeutic cycle and manifested a significant improvement of the clinical picture. The two electromagnetic fields had equivalent effects and produced a so-called “tail effect", continuing after the suspension of therapy, as if the biophysical action interfered with the pathogenetic mechanisms of the disease, probably by inhibition of the inflammatory process (4,5). The lack of efficacy in the group C patients confirms the therapeutic effects of the two fields. Indeed, considering the known relationship between the pain pathways and the psychic habitus of the patient (12-14), only the slight improvement of pain symptoms initially shown by the group C subjects could be attributed to the placebo effect. It should be mentioned that all the patients subjected to TAMMEF applications stated that they enjoyed listening to the music and they manifested a psychological attitude of trust and satisfaction. It also seems that these patients showed more evident and quicker responses, although this was not statistically significant and is reported only as an impression and a possible topic for future research.Our results confirm the efficacy and tolerability of low frequency magnetic fields as previously reported (4-7,10,15), also support the hypothesis that the effects of magnetic fields with parameters that change in time, like those produced by the music-piloted TAMMEF system, are equivalent to the effects of the ELF field (6,7).Moreover, in relation to current studies on interactions between the nervous, endocrine and immune systems (16,17), it may be possible to combine the electromagnetic stimulus with the corresponding acoustic stimulus, i.e. listening to the pilot musical passage. In fact, the two mechanisms, triggered in different sites and acting by different but simultaneous and coherent channels, might produce responses that reinforce one another (18).

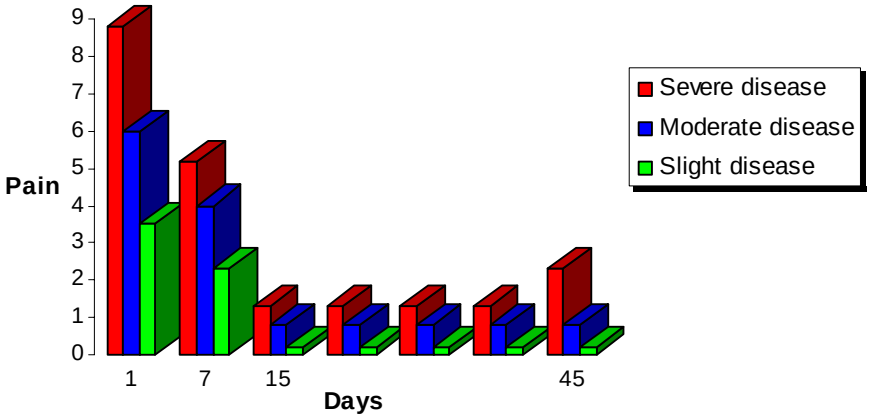
Acknowledgement: Work supported in part by a contribution of the “Fondazione del Monte dei Paschi di Siena”, Siena, Italy.

REFERENCES

1. KATSIR G, BARAM SC, PAROLA AH: Effect of sinusoidally varing magnetic fields on cell proliferation and adenosine deaminase specific activity. *Bioelectromagnetics* 1998;1:46-52.
2. MACRI MA, DI LUZIO S: Biological effects of electromagnetic fields. *Int J Immunopathol Pharmacol* 2002; 15: 95-105.
3. VOLPE P: Interaction of zero-frequency and oscillating magnetic field biostructures and biosystems. *Photochem Photobiol Sci* 2003; 2: 673-48.
4. GIORDANO N, BATTISTI E, GERACI S *et al.*: Effect of electromagnetic fields on bone density and biochemical markers of bone turnover in osteoporosis: a single blind, randomized pilot study. *Current Therapeutic Research* 2001; 62: 187-93.
5. GIORDANO N, BATTISTI E, GERACI S *et al.*: Analgesic-antiinflammatory effect of 100 Hz variable magnetic field in R.A. *Clin Exp Rheumatol* 2000; 18: 263.
6. RIGATO M, BATTISTI E, FORTUNATO M, GIORDANO N.: Comparison between the analgesic and therapeutic effects of a musically modulated electromagnetic field (TAMMEF) and those of a 100Hz electromagnetic field: blind experiment on patients suffering from cervical spondylosis or shoulder periarthritis. *Journal of Medical Engineering & Technology* 2002; 26: 253-8.
7. BATTISTI E, PIAZZA E, RIGATO M, NUTI R, BIANCIARDI L, SCRIBANO A, GIORDANO N: Efficacy and safety of a musically modulated field (TAMMEF) in patients affected by Knee osteoarthitis. *Clin Exp Rheumatol* 2004; in press.
8. KELLGREN JK, LAWRENCE JS: Radiological assessment of osteoarthritis. *Ann Rheum Dis* 1957; 16: 494-501.
9. MILLION R, HALL W, NILSEN KH, BAKER RD, JAYSON MI: Assessment of the progress of the back-pain patients. *Spinel* 1982; 7 : 204-12.
10. TROCK DH, BOLLET AJ, MARKOLL R : The effect of pulsed electromagnetic fields in the treatment of osteoarthritis of the knee and cervical spine. Report of randomized, double blind, placebo controlled trials. *J Rheumatol 1994*; 21: 1903-11.
11. WAGER TD, RILLING JK, SMITH EE *et al* : Placebo-induced changes in FMRI in the anticipation and experience of pain. *Science* 2004; 303:1162-7.
12. GRUBB BD: Peripheral and central mechanisms of pain. *Br J Anaesth* 1998; 81: 8-11.
13. SCHAFER M: Physiology and pathophysiology of pain. *Ther Umsch* 1999; 56: 426-30.
14. QUITTAN M, SCHUHFRIED O, WIESINGER GF, FIALKA-MOSER V: Clinical effectiveness of magnetic field therapy- a review of literature. *Acta Med Austriaca* 2000; 27: 61-8.
15. JACOBSON JI, GORMAN R, YAMANASHI WS *et al* : Low amplitude, extremely low frequency magnetic fields for the treatment of osteoarthritis knees: a double blind clinical study. *Altern Ther Health Med* 2001; 7: 54-64.
16. YANG EV, GLASER R: Stress-induced immunomodulation and the implications for health. *Int Immunopharmacol* 2002, 2: 315-24.
17. HARBUZ M: Neuroendocrinology of autoimmunity. *Int Rev Neurobiol* 2002; 52:133-61.
18. ESKANDARY F, STERNBERG EM: Neural-immune interactions in health and disease. *Ann N Y Acad Sci* 2002; 966: 20-7.

Figure 1 Evaluation of pain

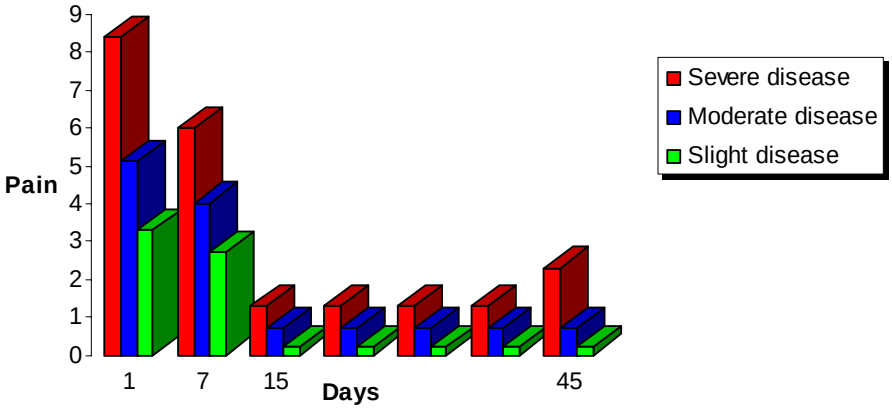
FIGURE 1A - Evaluation of pain at the start of the treatment, after 7, 15 (at the end of the treatment) and 45 days, in A group



Statistical significance between the start of the treatment and the end of the treatment (15 days):
- p < 0,05
- p < 0,001
- p < 0,001

Statistical significance between the start of the treatment and the final control (45 days):
- p < 0,01
- p < 0,001
- p < 0,001

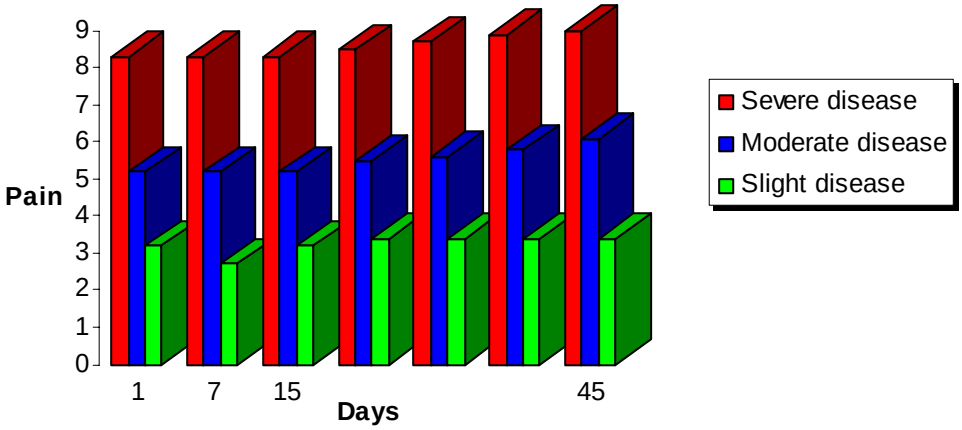
FIGURE 1B - Evaluation of pain at the start of the treatment, after 7, 15 (at the end of the treatment) and 45 days, in B group



Statistical significance between the start of the treatment and the end of the treatment (15 days):
- p < 0,05
- p < 0,001
- p < 0,001

Statistical significance between the start of the treatment and the final control (45 days):
- p < 0,01
- p < 0,001
- p < 0,001

FIGURE 1C - Evaluation of pain at the start of the treatment, after 7, 15 (at the end of the treatment) and 45 days, in C group

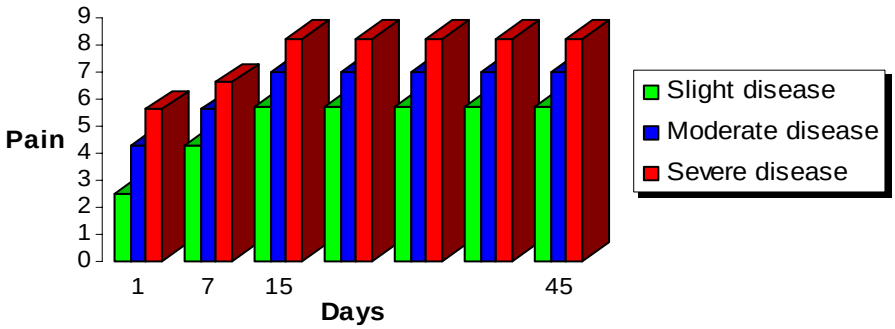


Statistical significance between the start of the treatment and the end of the treatment (15 days):
- no significant
- no significant
- no significant

Statistical significance between the start of the treatment and the final control (45 days):
- no significant
- no significant
- no significant

Figure 2 Evaluation of functionality

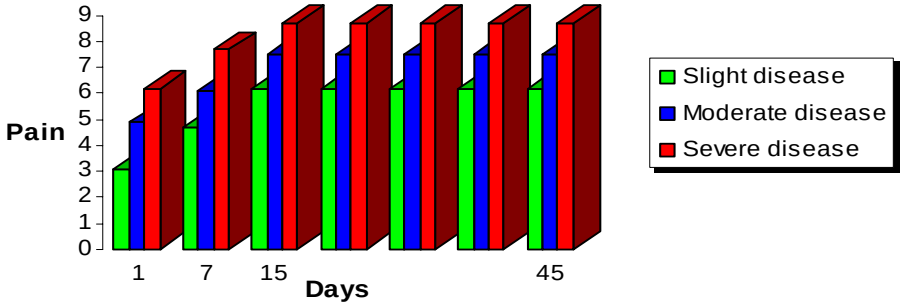
FIGURE 2A - Evaluation of functionality at the start of the treatment, after 7, 15 (at the end of the treatment) and 15 days, in A group



Statistical significance between the start of the treatment and the end of the treatment (15 days):
- $p < 0,05$
- $p < 0,01$
- $p < 0,01$

Statistical significance between the start of the treatment and the final control (45 days):
- $p < 0,01$
- $p < 0,01$
- $p < 0,01$

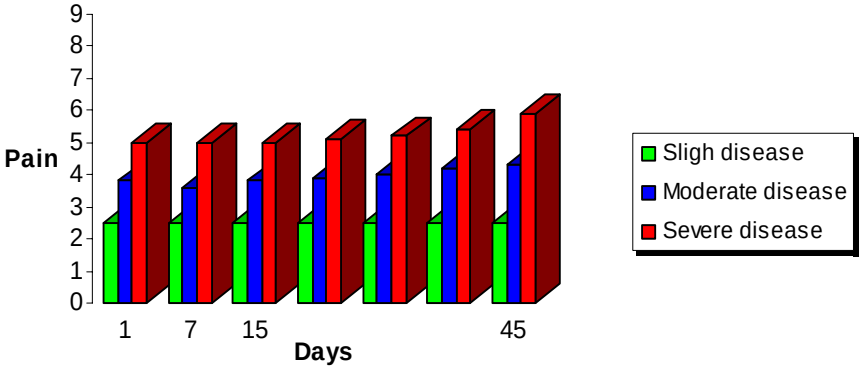
FIGURE 2B - Evaluation of functionality at the start of the treatment, after 7, 15 (at the end of the treatment) and 45 days, in B group



Statistical significance between the start of the treatment and the end of the treatment (15 days):
- $p < 0,05$
- $p < 0,01$
- $p < 0,01$

Statistical significance between the start of the treatment and the final control (45 days):
- $p < 0,01$
- $p < 0,01$
- $p < 0,01$

FIGURE 2C - Evaluation of functionality at the start of the treatment, after 7, 15 (at the end of the treatment) and 45 days, in C group



Statistical significance between the start of the treatment and the end of the treatment (15 days):
- no significant
- no significant
- no significant

Statistical significance between the start of the treatment and the final control (45 days):
- no significant
- no significant
- no significant

Table 1a Personal and clinical characteristics of the examined patiens (Pts)

Sex	Pts's number (%)	Mean age (years)	Duration of the disease (years)
M	27 (30 %)	54,3 ± 7,4	10,6 ± 2,2
F	63 (70 %)	58,6 ± 7,2	11 ± 3,3
Total	90 (100 %)	57,6 ± 7,3	10,9 ± 2,9

Table 1b Clinical characteristics of the examined patiens (Pts)

	Pts number (%) A B C	Slight disease (%) A B C	Moderate disease (%) A B C	Severe disease (%) A B C
Pts with low back pain (%)	30 30 30 100% 100% 100%	24 22 24 48% 44% 48%	20 22 20 40% 44% 40%	6 6 6 12% 12% 12%

EFFECTS OF VIDEO DISPLAY TERMINALS ELECTROMAGNETIC FIELDS INFLUENCE ON THE HEALTH OF THEIR USERS

Eleonora Bydianskaya
Kharkov Scientific Research Institute of Hygiene of Labour and Industrial Diseases
Trinklera st., 6, 61022, Kharkov, Ukraine

Eugeney Nikolenko
Kharkov Scientific Research Institute of Hygiene of Labour and Industrial Diseases
Trinklera st., 6, 61022, Kharkov, Ukraine

Abstract

A great experience of investigation of the EMF influence on the personal computers users' health has been accumulated. Carried out long-term observations of the health condition of the VDT users have shown that stress of their main life support systems: central nervous, cardiovascular, immune has been observed. Clinical-laboratory data have been obtained by the results of the profound medical examination of 1052 investigated users; from them 467 men and 585 women. The total number of factors, which have been put into database, is about 150000. Statistical processing of multivariate data was used for revealing early signs of negative influence of the factors of professional activity amongst VDT users. It is shown that reduction of the adaptation capacities of an organism is noted already in the first years of work at VDT. It causes breaches of the adaptation processes: decline of the functional activity of the antioxidant systems and activation of the processes free radicals oxidations, oppression of the immunological reactivity. Modification of the immunological and biochemical indices were considered and analysed with regard of the professional seniority and age. Such approach has allowed revealing the symptoms of fore-pathology of some part of working with VDT and referring them to the defined group of risk.

MODELING AND GIS SOFTWARE APPLICATIONS FOR EMF ENVIRONMENTAL MONITORING IN SICILY

S. CALDARA, P. COSTANZA, G. LISCIANDRELLO

REGIONAL AGENCY FOR ENVIRONMENTAL PROTECTION OF SICILY (ARPA SICILIA)

Via U. La Malfa, 169 90146 Palermo Italy

scaldara@arpa.sicilia.it, piero.costanza@gmail.it, glisciandrello@arpa.sicilia.it

Abstract

Regional Agency for Environmental Protection has been operating for 5 years in Sicily to ensure environment and consequently public health protection from EMF exposure.

This paper deals with EMF monitoring in all county territory.

In order to increase the knowledge of sources and their impact on environment, a register of telecommunication devices has been implemented; technical items have been used as inputs for modeling tools and simulation outcomes are compared with measurement results.

All these data are collected in GIS software.

In particular mobile phone networks and broadcasting systems have been studied. A complex site for TV and Radio broadcasting is reported as an example.

Moreover some comparison between two different simulation software has been developed.

GIS register show that whole Sicilian territory is covered by mobile phone base stations with high concentration in big cities (Palermo and Catania). Simulations have been used to determine measurements and monitoring policy according to particular needs related to special places like schools, hospital, etc.

Introduction

The development of new telecommunication systems, as mobile phone base stations and broadcasting antennas, as well as electric power plants and power delivery lines, even if has contributed to improve life quality, is also responsible of the increasing human exposure to electromagnetic fields (EMF) from manmade sources which are to be added to natural electromagnetic irradiation.

Italian national law n. 36 of 2001, separately regulates both extremely low-frequency (ELF) and radio-frequency (RF) electromagnetics fields and makes a difference between acute (thermal) and chronic (non thermal) adverse health consequences.

Acute exposures are associated with thermal hazards and are characterized by threshold exposures below which no health effects occur.

In case of long term exposure to low (non thermal) levels of EMF there are no threshold exposures significant for human health. In this case health risk is thought to be of probabilistic nature: if the time exposure increases not the magnitude of adverse health consequence but the probability to have consequences increases.

According to the A.L.A.R.A. caution principle of keeping the exposure to lower possible level, “attention values” and “quality aims” have been fixed; they are not safety threshold exposures but an operational reference for prevention and public health protection.

In particular, the Italian “DPCM July 8th 2003” law arranges “threshold exposures” (Tab. 1) and “attention values” (Tab. 2) to prevent short term and possible long term health effects due to exposure to EMF generated by RF fixed source in the range 100 kHZ up to 300 GHz; it also arranges “quality aims” to minimize, in a progressive way, people exposure to EMF and measurement standards.

The Regional Agency for Environmental Protection of Sicily has been operating for 5 years in Sicily to ensure environment and consequently public health protection from EMF exposure.

The Agency has an important role of technical support to local councils by giving preventive opinions about the installation of new TLC systems based on existing systems emission evaluation compared with threshold exposures and attention values.

Table 1 – Threshold exposures (DPCM July 8th 2003)

Frequency range (MHz)	RMS e. f. E (V/m)	RMS m. f. H (A/m)	Power density S (W/m^2)
0,1 - 3	60	0,20	-
>3 – 3.000	20	0,05	1
>3.000 – 300.000	40	0,10	4

Table 2 – Attention values (DPCM July 8th 2003)

Frequency range (MHz)	RMS e. f. E (V/m)	RMS m. f. H (A/m)	Power density S (W/m^2)
0,1 – 300.000	6	0,016	0,10

Register of TLC fixed EMF sources

Mobile phone base stations

In order to carriy out the register of TLC fixed EMF sources, which complies with the Italian law n. 36/2001, the Regional Agency for Environmental Protection of Sicily, in February 2003, has stipulated an agreement with the TLC Companies which periodically transfer data about their system.

All mobile phone base stations of the regional area have been then geo-mapped (Fig. 1 and 2). In particular, each point of the chart represents a site with several antennas of base stations. Of each site Gauss-Boaga co-ordinate, number and model of the antennas, the power (W), the gain (dB), the frequency and the eight of the electrical center are known.

As we can see from figures 1 and 2 and from table 3 the overall regional area is covered by mobile phone base stations. The highest concentrations are specially in big cities (Palermo and Catania) and near the coastline. Table 4 highlights the lower specific power of 3G (UMTS) systems compared with GSM technology based ones.

Table 3 – Base stations distribution

Town	n. of sites	n. of antennas	Total power (W)
Palermo	442	1960	46189
Catania	239	1044	22691
Messina	179	650	13696
Trapani	66	264	7735
Siracusa	72	268	6143
Ragusa	61	93	6226
Agrigento	25	86	2691
Caltanissetta	26	93	2183
Enna	12	36	835

Table 4 – Base stations characteristics

Frequency	n. of antennas	Power (W)	Specific power (W)
GSM - 900	4110	134925	32,82
GSM - 1800	2233	52482	23,50
UMTS	2878	55712	19,35

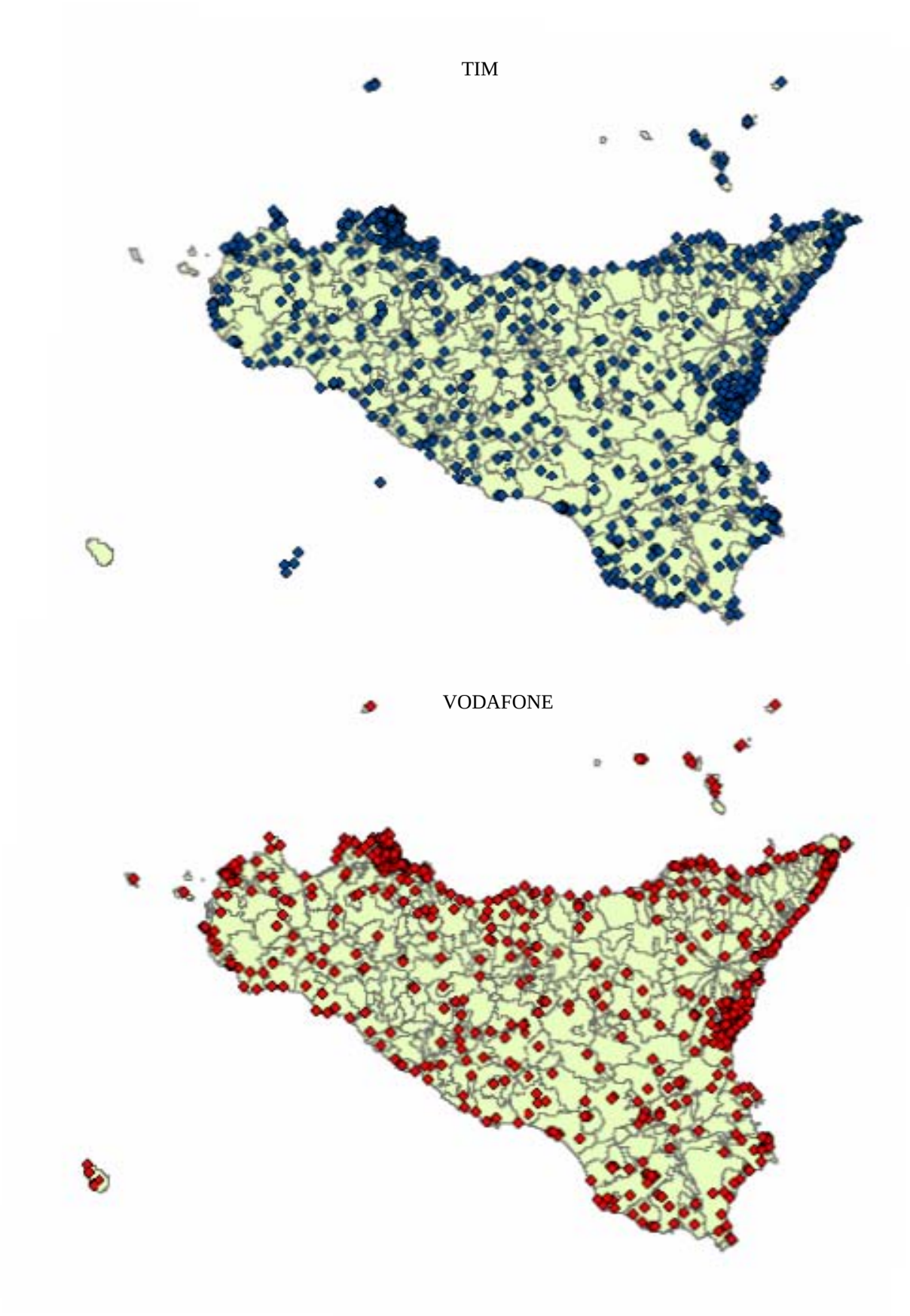


Figure 1 – GIS representation of mobile phone base stations distinguished per company

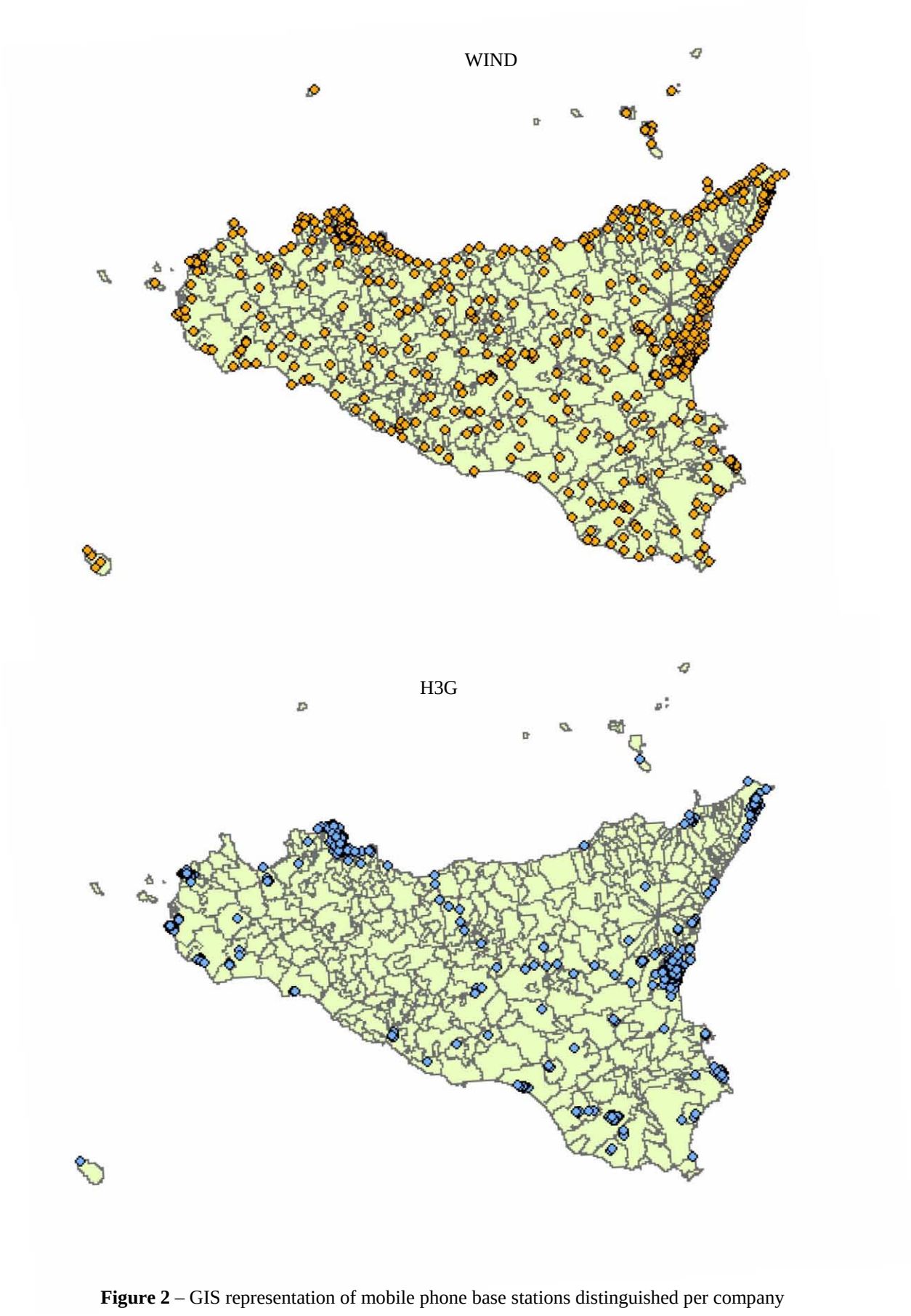


Figure 2 – GIS representation of mobile phone base stations distinguished per company

TV and Radio broadcasting

Data concerning Radio and TV supplied by the Telcomunication Regional Department were not complete so that all Radio and TV company in the regional area were directly asked to transfer information about broadcasting systems.

Such action brought to identify eleven crowded multiple antenna sites in the regional area (Fig. 3)



Figure 3 – RTV crowded multiple antenna sites

In particular, the features of broadcasting multiple antenna site of Caltanissetta are listed below:

Mount S. Anna

- Total power 20950 W
- Intersted Area 1,8 km^2
- Specific power 11 mW/m^2
- N. of antennas 9 RTV antennas (one of which with a power of 20000W)

Mount S. Giuliano

- Total power 6160 W
- Intersted Area 1,25 km^2
- Specific power 5 mW/m^2
- N. of antennas 19 RTV antennas (one of which with a power of 2000W)

Modeling and GIS software

The Geographical Information System (GIS) is based on a relational database containing all technical information of EMF sources, a cartography managing software and a model based software which, starting from geo-mapped and technical information, is able to simulate the EMF distribution in a given area.

The GIS returns the following informations:

1. number and positioning of geo-mapped sistems (Fig 1 e 2)
2. technical data-sheets
3. photographic documentation (Fig. 4)
4. EMF simulation based on “Radmap 8.0” 2D modelling software (Fig. 5).
5. EMF simulation based on “VICREM” 2D and 3D modelling software (Fig. 6).

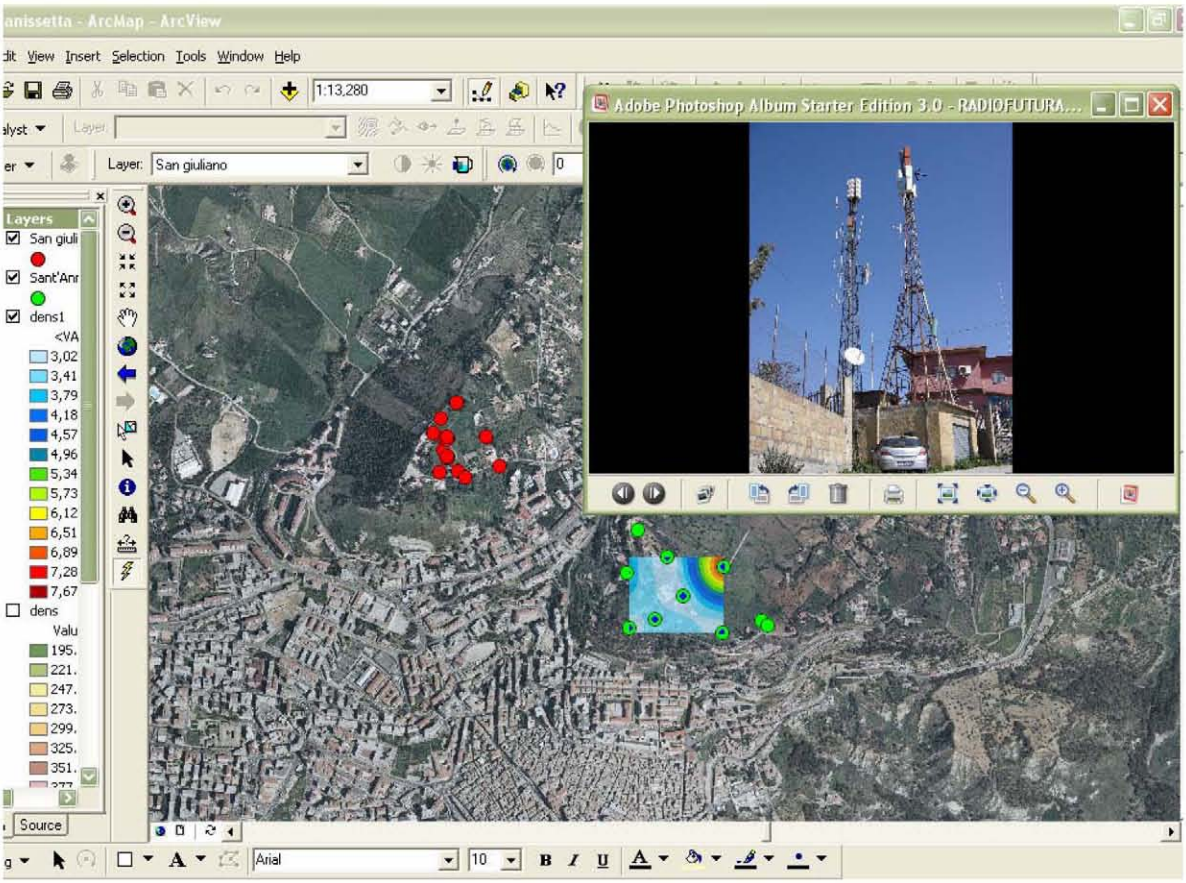


Figure 4 – Example of GIS informations (Caltanissetta)

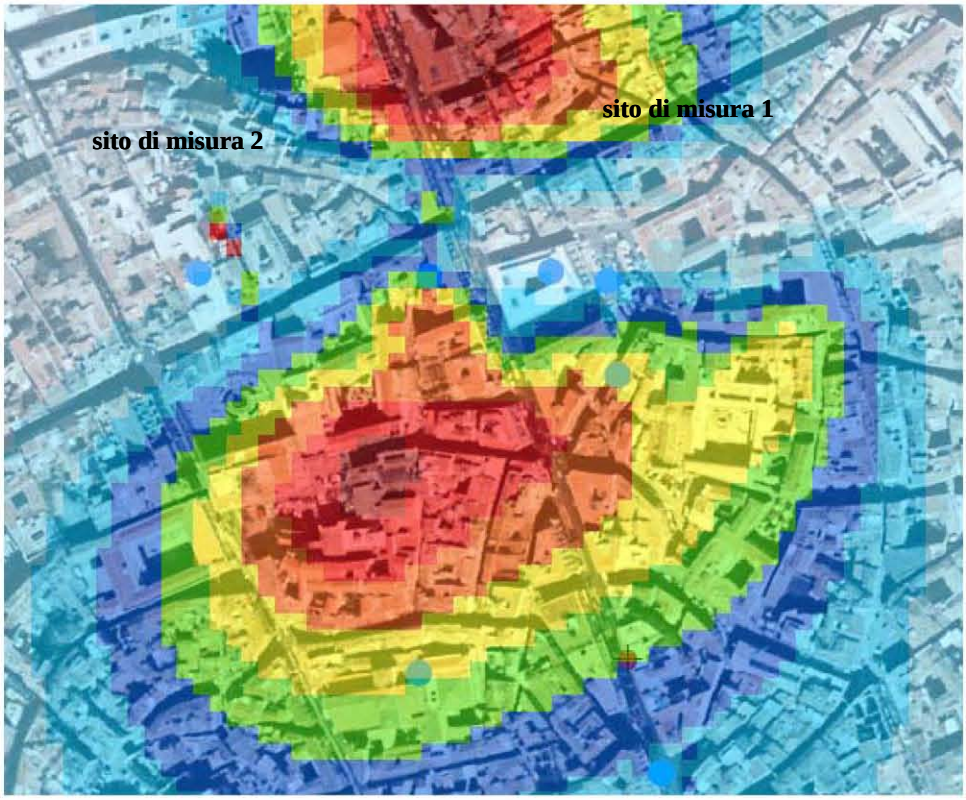
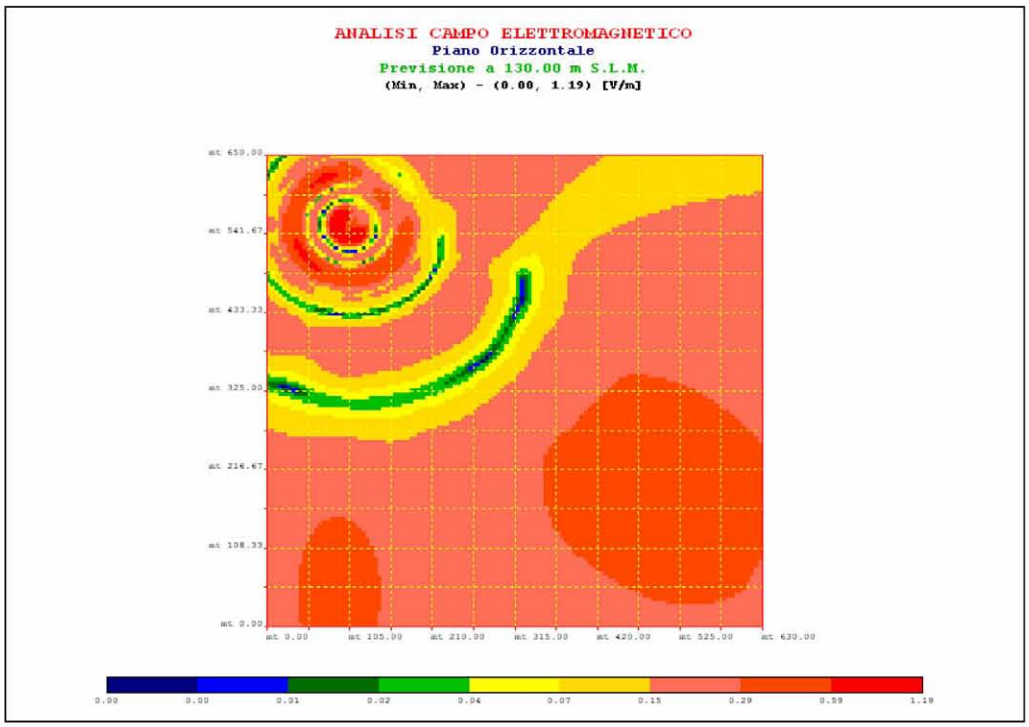


Figure 5 – Example of Radmap 2D simultation in Palermo



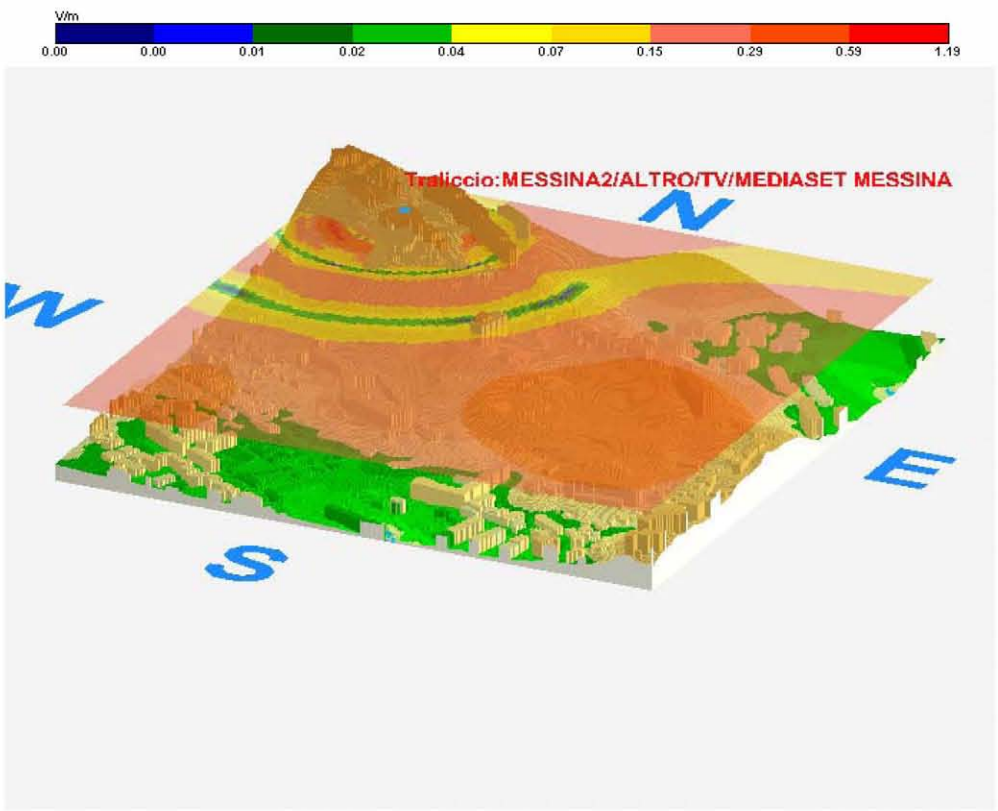


Figure 6 – Example of VICREM 2D and 3D simultation in Messina

Monitoring network

Continuous EMF monitoring is thought to be a suitable answer to the strong citizens' expectations of environmental controls which could give warranty threshold exposures respect 24 hours a day.

This measurement method is particularly significant because it takes into account the time history of the EMF level.

The ARPA Sicilia EMF monitoring network is based on 182 mobile monitoring devices, 102 of which have been supplied by the Ugo Bordoni Foundation for a national monitoring project.

The selection of monitoring sites has been based upon the following criterions:

- Analysis of already known sources generating EMF levels higher than threshold exposures;
- Analysis of particular sites in order to deal with the public concerns about potential health effects (schools, hospitals, etc.);
- Specific claims by local councils or citizens.

In Tab. 5 RF EMF (100 kHz – 3 GHz) monitoring results in Sicily in 2004 and 2005 are reported.

Table 5 – Continuous EMF monitoring results (2004-2005)

PROV.	N. town 2004	N. town 2005	N. town 04/05	N. sites 2004	N. sites 2005	N. sites 04/05	N. hours 2004	N. hours 2005	N. hours 2004 +2005
AG	4	5	7	15	11	26	12416	16962	29378
CL	1	5	5	2	30	32	839	11260	12099
CT	3	9	10	40	115	155	27182	81480	108662
EN	0	2	2	0	6	6	0	3856	3856
ME	5	2	7	13	15	28	6955	5891	12846
PA	6	18	19	34	157	191	14463	72049	86512
RG	1	3	3	1	13	14	186	7920	8106
SR	1	2	2	1	7	8	250	5769	6019
TP	5	1	5	8	1	9	8246	411	8657
TOTAL	**26**	**47**	**60**	**114**	**355**	**469**	**70537**	**205598**	**276135**

Monitoring results can be collected in the GIS. In Fig. 8 the GIS representation of monitoring activity in the city of Palermo is shown.

Monitoring results have been compared with the simulation software outcomes in order to setup the models and, at the same time, to check measurement procedures. The correlation between measurement results and simulations is good (Fig. 7 and Tab. 6) although simulations are lower than measurements.

Figure 7 – Simulations Vs Measurements correlation

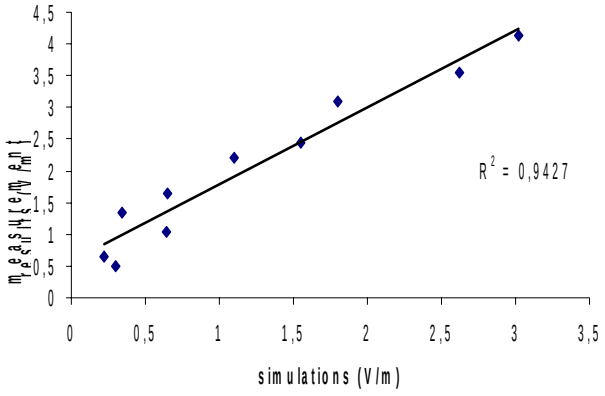
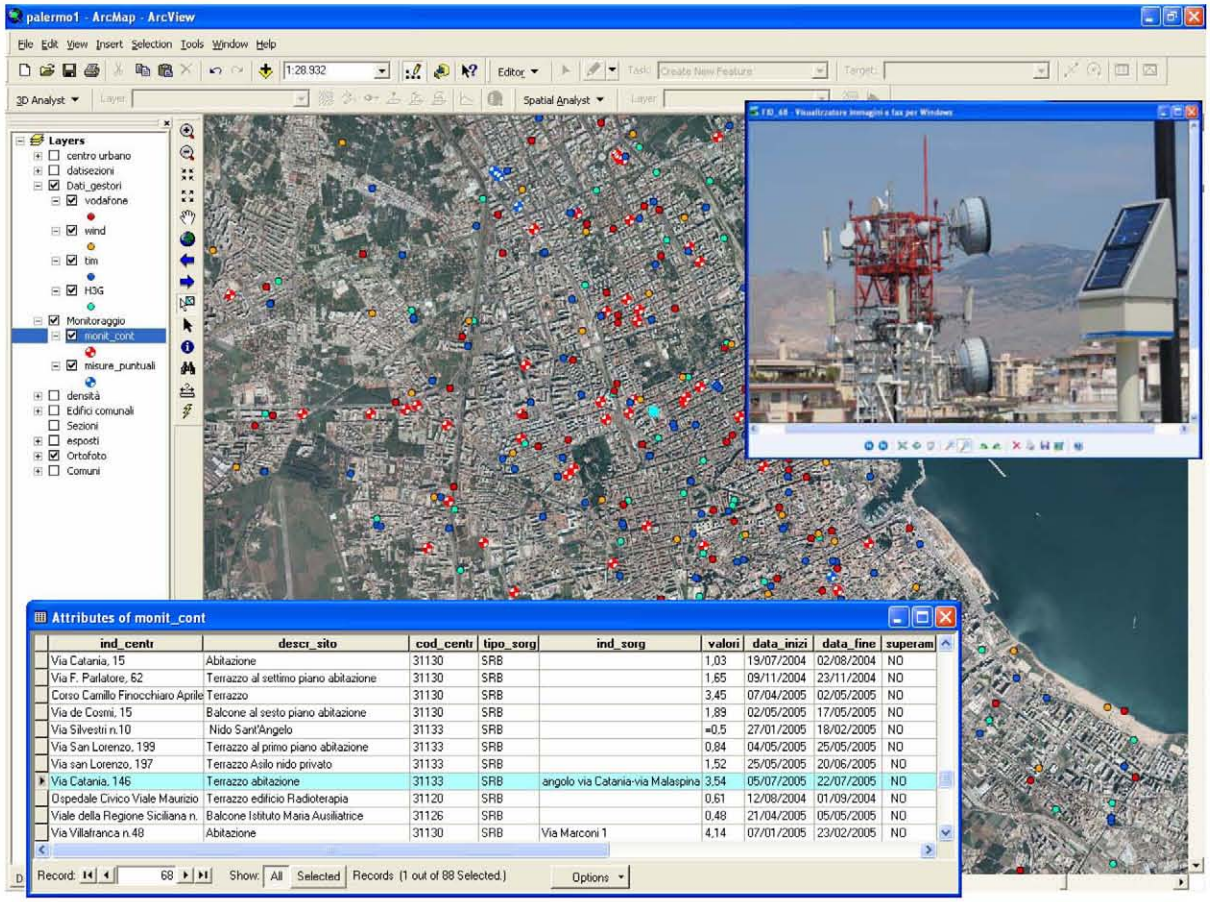


Table 6 – Difference between measurements and simulations (V/m)

simulations	measurements	difference
1.55	2.44	0.89
0.34	1.34	1
1.8	3.1	1.3
0.65	1.65	1
0.3	0.5	0.2
1.1	2.2	1.1
2.62	3.54	0.92
3.02	4.14	1.12
0.22	0.64	0.42
0.64	1.03	0.39
	average	**0.834**



ind_centr	descr_sito	cod_centr	tipo_sorg	ind_sorg	valori	data_inizi	data_fine	superam
Via Catania, 15	Abitazione	31130	SRB		1,03	19/07/2004	02/08/2004	NO
Via F. Parlatore, 62	Terrazzo al settimo piano abitazione	31130	SRB		1,65	09/11/2004	23/11/2004	NO
Corso Camillo Finocchiaro Aprile	Terrazzo	31130	SRB		3,45	07/04/2005	02/05/2005	NO
Via de Cosmi, 15	Balcone al sesto piano abitazione	31130	SRB		1,89	02/05/2005	17/05/2005	NO
Via Silvestri n.10	Nido Sant'Angelo	31133	SRB		=0,5	27/01/2005	18/02/2005	NO
Via San Lorenzo, 199	Terrazzo al primo piano abitazione	31133	SRB		0,84	04/05/2005	25/05/2005	NO
Via san Lorenzo, 197	Terrazzo Asilo nido privato	31133	SRB		1,52	25/05/2005	20/06/2005	NO
Via Catania, 146	Terrazzo abitazione	31133	SRB	angolo via Catania-via Malaspina	3,54	05/07/2005	22/07/2005	NO
Ospedale Civico Viale Maurizio	Terrazzo edificio Radioterapia	31120	SRB		0,61	12/08/2004	01/09/2004	NO
Viale della Regione Siciliana n.	Balcone Istituto Maria Ausiliatrice	31126	SRB		0,48	21/04/2005	05/05/2005	NO
Via Villafranca n.48	Abitazione	31130	SRB	Via Marconi 1	4,14	07/01/2005	23/02/2005	NO

Figure 8 – EMF Monitoring metadata in Palermo

Summary

In this paper ARPA Sicilia register of TLC fixed EMF sources is presented. The Geographical Information System (GIS) which all these data are collected in is presented as well. In particular mobile phone networks and broadcasting systems have been studied and a complex site for TV and Radio broadcasting is reported as an example.
Register data contain the technical items which have been used as inputs for modeling tools; simulation outcomes have been compared with measurement results showing an high correlation.
GIS register show that whole Sicilian territory is covered by mobile phone base stations with high concentration in big cities (Palermo and Catania).
Moreover the results of RF EMF continuous monitoring in Sicily and, in particular, graphical GIS data of Palermo have been reported.

Acknowledgments
The authors want to acknowledge the support from the “Ugo Bordoni Foundation” for the continuous monitoring devices availability.

References

[1] Guidelines on Limits of Exposure to Electromagnetic Fields in the Frequency Range from 1 Hz to 300 GHz, ICNIRP, 1998
[2] Non-Ionizing Radiation, Part 1: Static and extremely low frequency (ELF) electric and magnetic fields, WHO – IARC Press, Lyon, 2002

RESULTS OF EMF MODELLING AND GIS SOFTWARE APPLICATIONS FOR RISK COMMUNICATION AND MANAGEMENT IN SICILY

S. CALDARA, P. COSTANZA, G. LISCIANDRELLO

REGIONAL AGENCY FOR ENVIRONMENTAL PROTECTION OF SICILY (ARPA SICILIA)

Via U. La Malfa, 169 90146 Palermo Italy

scaldara@arpa.sicilia.it, piero.costanza@gmail.it, glisciandrello@arpa.sicilia.it

Abstract

Regional Agency for Environmental Protection has been operating for 5 years in Sicily to ensure environment and consequently public health protection from EMF exposure.

Another task of ARPA Sicilia is the correct EMF exposure risk communication to citizens.

ARPA Sicilia is already partner of a national monitoring program which gives information by web only for mobile phone b.s. generated emf.

This paper deals with the use of EMF modeling and GIS software results as possible tools for a clear risk communication.

In order to increase the knowledge of sources and their impact on environment, a register of telecommunication devices has been implemented; technical items have been used as inputs for modeling tools and simulation outcomes are compared with measurement results.

All these data are collected in GIS software and processed to generate charts which gives graphical information about base stations, TV and Radio broadcasting systems and power lines territorial distribution, simulations of EMF level, monitoring activity results and petitions. These charts, published in the Agency web site, can be a user-friendly instrument which allows people to get a correct perception of risk better than tables or numbers.

Introduction

In the societies with a high rate of industrialization Citizens' restlessness is increasing for the possible consequences of technological development. Such worries derive also from the changed image of science, than in general terms, it is not anylonger more perceived as caretaker of "sure knowledge", also because of the inability demonstrated by the scientific world in the last few decades to preview, to manage and to interpret some catastrophic events.

The risk is diffusely perceived and it invests multiple aspects of our life, the fear of unexpected events, of personal or collectives risks is so intense that it has made our society defined as "the society of risk". Particularly, regarding electromagnetic fields, the worries are magnified by the electromagnetic fields potential risks evaluation uncertainty.

The majority of the papers written on the topic have often been of dubious interpretation, moreover, some of them present methodological inaccuracies and it is quite difficult to make comparisons between different studies as the data seem to be strictly related to the various methodologies applied.

In ICNIRP's 1998 guidelines we read that: the results of epidemiological studies on exposure to electromagnetic fields and neoplastic pathologies do not allow the creation of a scientific base on which basing the guidelines for the exposure.

Even the definition of possible cancerogenous for the 50 - 60 Hz EMF, given from IARC, takes into consideration the fact that epidemiological tests so far carried out are limited and the tests on animals limited or inadequate. In this situation of uncertainty, mass media's tendency of emphasising such kind of news, surely contributes to instil worries to citiziten up to the point of transforming such worries in a real society issue

In the past, these worries were looked at as irrational and due to people's inability to understand scientific data

that, through probability theory, demonstrated how the risk related to a given technology (for example in terms of human life losses) was insignificant.
They have been later on analyzed, in a comprehensive way, the complex interactions between the factors that contribute to create in the citizen the perception of the risk and the consequent behaviours.
In particular, fears and worries on the risk deriving electromagnetic fields are inexplicable if the risk is only defined through statistical calculation.
The results of such studies have highlighted some persisting aspects which contribute to expand risks' perception from electromagnetic fields. Such aspects can be summarized as follows:

- Lack of confidence, the risk is more feared as it is caused by an immaterial and imperceptible physical agent;
- Uncontrollability, the subject exposed to the risk by not being able to control exposure feels incapable of dealing with the risk;
- Uncertainty, there are no realiable evidences about consequences, the apprehension is augmented by the fact that the risk could actuall be greater for children and that the possible effects could manifest themselves even after a long period;

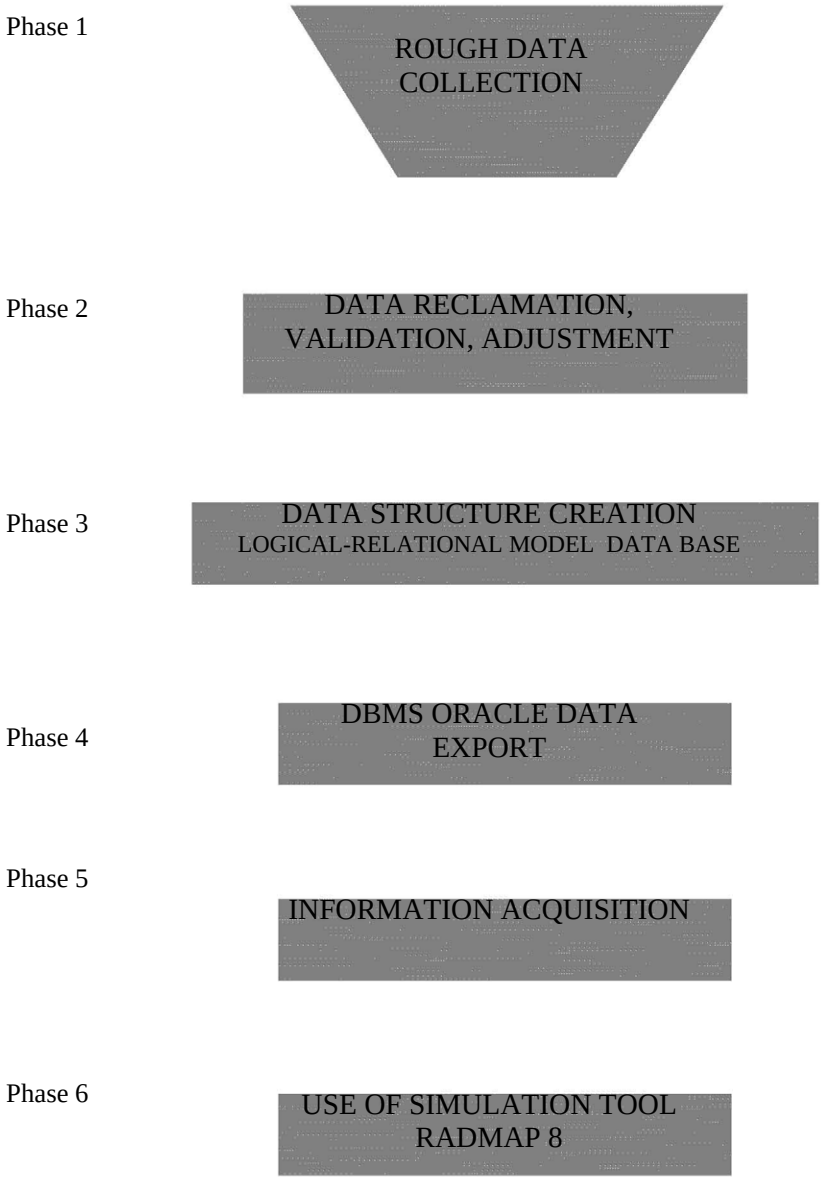
The World Health Organisation launched in 1996 an international programme on electromagnetic fields, suggesting the evalution of health and environment risks with the aim of defining research protocols to be carried out following standards compatible and comparable among them. This project will be ended by 2006.
In July 2003, when the first block of activities was over, ARPA Sicilia organised a conference on the topic which marked the beginning of a new path. All the stakeholders, which are involved, in the field , have been invited to participate from TLC companies to environmental association not forgetting the institutional stakeholders involved in the overall managing of the problem.
Such occasion has been useful in order to start a dialogue, an essential premise to establish a climate of mutual confidence needed to be able to manage the problem effectively.

Risk communication

ARPA Sicilia's plan for the communication of the risk due to electromagnetic fields exposure previews two articulations: on one hand, the essencial "usual" communication, even if accompanied by the use of the Internet, on the other hand, the new approach of communicating the results of monitoring activities aimed at encouraging and promoting citizens' involvement.
Taking into account these premise, a study on health implications deriving from the exposure to the electromagnetic fields has been commissioned the Department of Biotechnologies of the Medicine Faculty of the University of Palermo. The results of this research are avalaible on the Internet (www.arpa.sicilia.it).
Starting from a preliminary analysis of potential users' characteristics, the documents have been drawn up modelling the type of information to the different targets.
The preferred approach was based on divulgation, in fact, the adoption of a winning graphic and animated images, allowed not only to render basic concepts of physics easily comprehensible (an example could be the difference between an electric field, a magnetic field and electromagnetic field or between direct current and alternating current), but also epidemiology fundamental principles and base terminology.
The opportunity of getting deeper on the subject has also been guaranteed (links to specialized sites and a list of downloadable epidemiological studies)
Beside the communication of "usual" type, the plan currently being developed aims at the diminution of "uncontrollability of the risk" feeling and at responding adequately to the citizen steadily increasing need of involvement through the adoption of GIS.

The GIS software

The system, in ArcMap environment, allows the geo-mapping of electromagnetic fields sources of all types, from radio frequency (RF) and low frequency (ELF) collecting all the data in a database containing all the physical parameter that allow, by using ad-hoc models of calculation, to make forecasts about the distribution of a electric or magnetic field in a given area. Such simulations can be carried out on horizontal and vertical plans and to be overlapped to the cartography (orthophotographs and/or technical charts) for a correct understanding of the results in their context. It is also possible to relate the distribution of field with the buildings's height in order to characterize possible critical situation.
In order to obtain a structured and versatile communication a multi-steps and multi-phases procedural approach needs to be followed. The different phases are summarized in the following diagram:



Phase 1

In this phase the elementary information is received in the form of a electronic sheet in a classic tabular structure.

Phase 2

The rough data (radioelectric parameters, geographic coordinates, etc) are carefully examined, corrected if imprecise or incongruous, and once validated, manipulated in order to take the most suitable format for the successive elaborations (e.g. a file text information containing the attenuations in dB of the diagram of radiation of a given antenna , needs to be converted in a numerical format, or still it is necessary to execute the conversion of co-ordinates for a corrected geo-mapping). This often is the most laborious phase due to the various kinds of adjustments needed.

Phase 3

In this phase the data are organized, subdivided and correlated among them in order to reflect the logical relational model of the date base (already pre-existing) on which the tool of simulation is based. Congruency controls are carried out and the original electronic sheet format is abandoned in favour of a most suitable one such as MsAccess.

Phase 4

At this point, usually by means of specific queries, data are exported into DBMS Oracle as implied by the simulation tool and essential for its correct functioning.

Phase 5

To complete the supply of input data and to improbe the output data, it can be useful to collect additional information such as cartography, orthofotographies, raster images. Particular attention needs to be paid to cartographic data nearly always subordinate to procedures of adaptation (e.g poly-lines in polygons, creation of shapefiles, etc) and of conversion of coordinates.

Phase 6

The epilogue of this sequence of activities is the creation of a visual environment rich of details, able of producing visual and analytical reliable results for an immediate perception of the informative message derived from the analyses.

The informative system also allows to geo-map, by collecting the relevant information (meta data), not only the control activity carried out by ARPA's Provincial Laboratories but also the continuous monitoring activities and the state of claims and demands of the population resident on the territory.

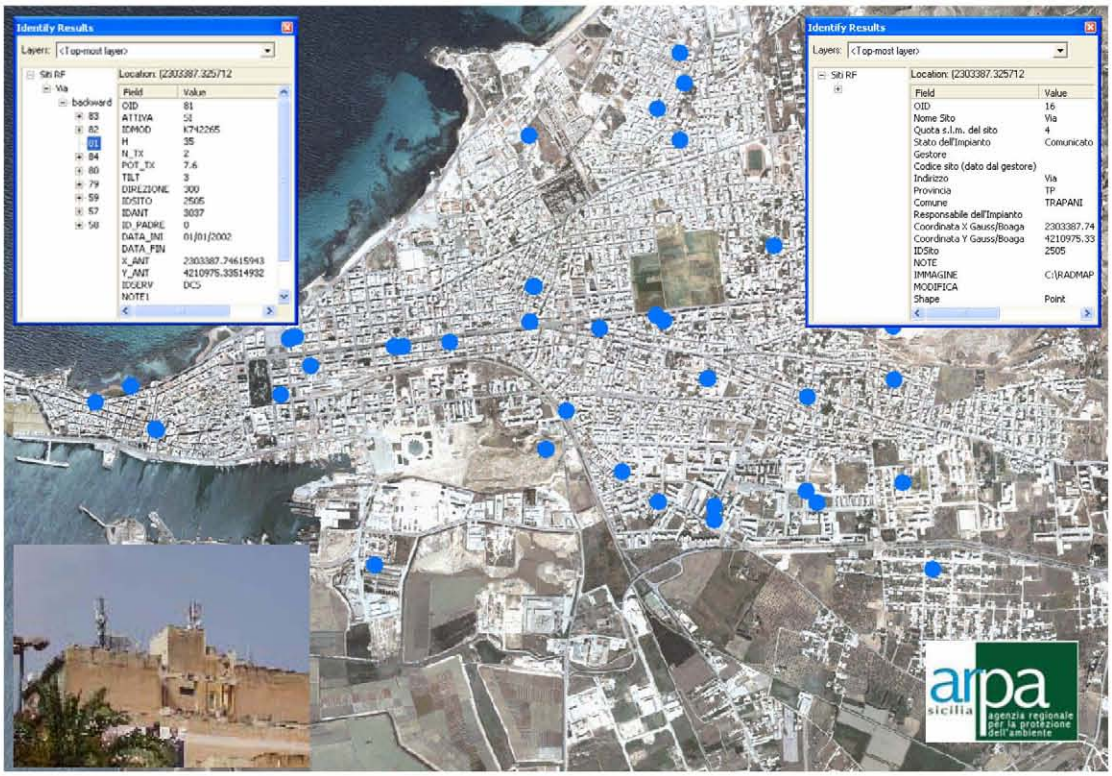


Fig. 1 GeoMapping of Mobile Phones Basic Radio Station in the City of Trapani



Fig. 2 Example of simulation of the distribution of electromagnetic field from RF source



Fig. 3 Example of simulation of the distribution of electromagnetic field from ELF source

In this way, the Agency monitoring activities will be available on the Internet.
The customer will be able to interact with the digital thematic chart obtained through the elaboration of the data already supplied by the companies; such elaborations, even with the approximations tied to the intrinsic simplifications of every model, will concur, intercrossed with the data of citizens' demands, to spot on the

territory the situations on which the worries of the population are mainly concentrated.
Following the identification of such areas, it will be possible to define "the sensitive" areas from the point of view of the emotional impact on the population, even if in such zones an overcoming of the limits of exposure or the values of attention (as defined in Italian law) is not found or expectable.

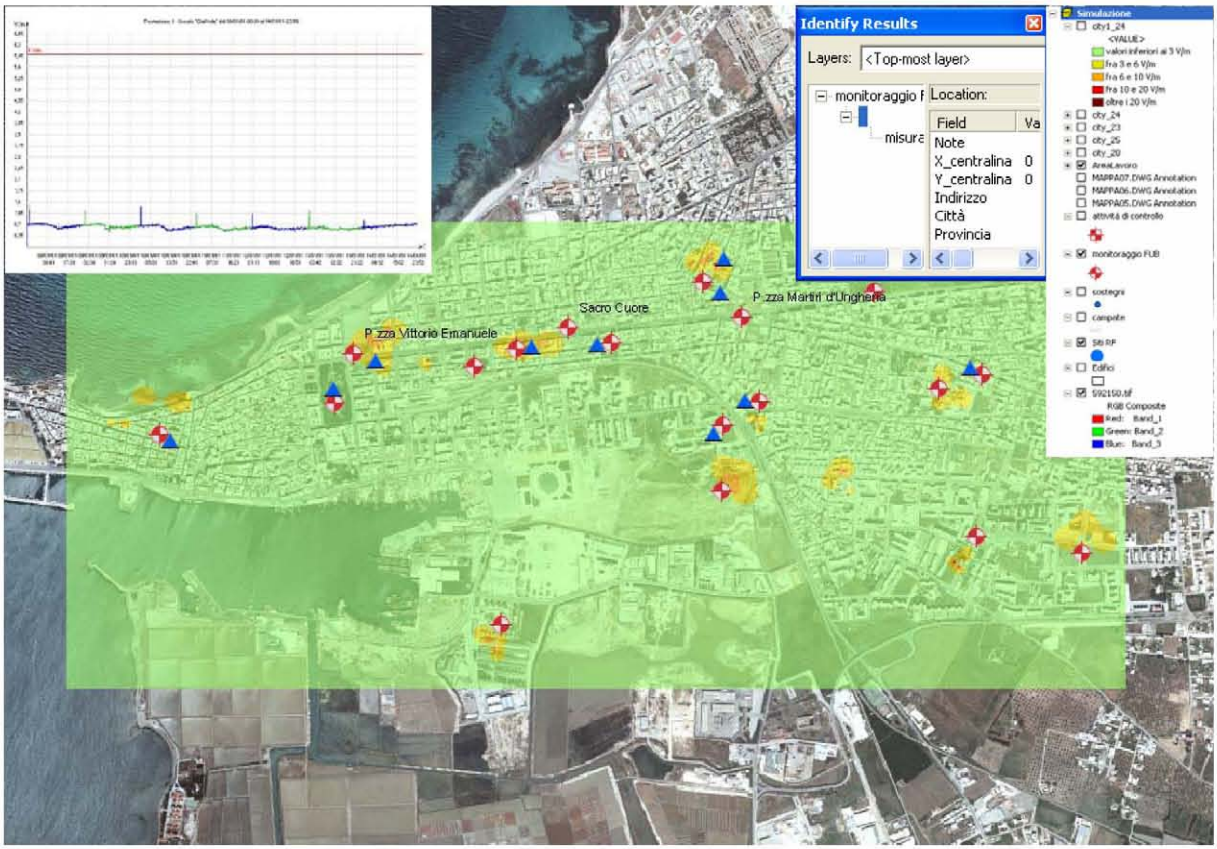


Fig. 3 Example of simulation chart, citizens' claims and demands theme and monitoring results.

The graphical reppresentetion, containing all the themes synthesizing all the informational elements used , will contribute to plan the monitoring activity let alone to communicate such programming by taking into account two elements: the quantitative data (the estimated value of the levels of electromagnetic field) and the population's perception level towards the problem manifested through claims, petitions, activity of civil society association etc.. In such identified areas, by applying a priority order determined trough the analysis of the quantitative element (outcomes of measures or provisional calculations) monitoring devices will be put in place and the collected data will be made available directly to the customer on the net.
The addressee of the information, will be able to interact with the thematic charts, on which they will be highlighted: the forecasted distribution of the levels of electromagnetic field, the claims, the monitoring-devices position. Connected to the theme of monitoring-devices, measure outcomes and graphs on the monitoring activity will also be displayed.

Conclusions
With such procedure that does not have a conclusion, but it is under continuous update, it will be possible for the citizen to follow the monitoring in all its phases, from the planning to the communication of the validated data.
It is believed that this way of transmitting the information, which supplies contextualized data on the territory which the customer can interact with, can be more effective as compared to a sterile communication of numbers or diagrams of difficult reading and comprehension and that it can contribute to clear the legitimate doubts of people and to supply to citizens the instruments needed to acquire an effective knowledge of the problem.

GENOMIC INSTABILITY IN BLOOD SAMPLES SUBMITTED TO CONTROLLED CELL PHONE RADIATION LEVELS

HEINRICH, JKR[1]; CAMPANHOL, CL[1]; RODRIGUES, RM[1]; FRANCO, VCO[1]; SANTOS, BP[1]; ALMEIDA, AM[2].

1. CYTOGENETICS LABORATORY – CAISM / UNICAMP – STATE UNIVERSITY OF CAMPINAS, BRAZIL 2. CPQD FOUNDATION, CAMPINAS, BRAZIL

Mailing Address: Dr. Juliana Heinrich
CAISM UNICAMP – Universidade Estadual de Campinas
Laboratórios Clínicos Especializados – Citogenética
Rua Alexandre Fleming, 101 Campinas – SP – CEP 13.083-881
Phone: +55 19 3788-9524 FAX: +55 19 3788-9395
Email: julianah@unicamp.br

ABSTRACT

Genomic instability is characterized by genetic alterations such as chromosomal rearrangements, aneuploidy, micronuclei frequency increase, microsatellite instability, mutations, gene amplification, gene transcription changes, transformation and cell death in the first and following generations of cells after the first insult. We have investigated the effect of AMPS and CDMA radiation in cultured blood samples from 10 donors in 200 replicates after 72hs exposure in a specially designed exposition set up (TEM CELL) at SAR levels from 0,8 to 10W/kg. The genome was investigated for structural chromosomal abnormalities, micronuclei frequency and aneuploidy of chromosomes 8 and 17 through both conventional and molecular cytogenetics (FISH) techniques. Genomic changes such as chromosomal breaks, translocations, marker chromosomes and aneuploidy, when compared to the controls, were detected in SAR levels above 5W/kg as well as the increase of micronuclei frequency above 10W/kg. As genomic instability and chromosome damage are frequently related to tumorigenesis, our findings support the hypothesis of a positive effect of RF radiation on the genome of cultured blood cells and also give further evidence to suggest continuous cytogenetic investigation of occupationally exposed individuals to SAR levels above the accepted international limits.

INTRODUCTION

In vitro studies are important to delineate possible damage mechanisms caused by non-ionizing radiation or radiofrequency (RF) fields and its interaction with biological systems such as cells, tissues and organisms. The main advantage of these studies are the possibility to control almost all variables and test conditions to discard interferences and also to delineate investigation targets to be explored through *in vivo* and clinical-epidemiological studies.

Genomic instability (GI) has been identified mostly in tumor cells and is characterized by the accumulation of multiple changes that converts the genome of a normal cell into an instable genome [1]. This instability is characterized by genetic alterations such as chromosomal rearrangements, aneuploidy, micronuclei frequency increase, microsatellite instability, mutations, gene amplification, gene transcription changes, transformation and cell death in the first and following generations of cells after the first insult [2].

In vitro investigations in different cell systems have shown both a positive and negative association of cell damage leading to GI after RF exposure although most of them were attributed to thermal effects. These groups suggested that RF is not mutagenic by itself and that the adverse effects of such exposition would be due to hyperthermia caused by cell exposition in high frequencies or high intensity fields [3,4,5,6].

By the other hand, aneuploidy of chromosome 17 was observed in a dose-dependent way along with alterations related to chromosome segregation suggesting that RF can interfere in the cell cycle and cause chromosome damage and genomic instability in temperature controlled exposition environments [7]. Other events were observed and associated with RF dose-dependent exposition such as transmembrane efflux of molecules, transcription errors, cell transformation, enzyme activity changes, fosforilation of hsp27 (heat shock protein 27) and increase of mRNA levels of the FOS gene [8,9,10,11,12].

Since there is a major concern regarding the association of RF exposition and tumorigenesis and as genomic instability is one of the first events for tumor onset we investigated the frequency of chromosome damage, micronuclei formation and aneuploidy in lymphocytes submitted to RF fields in a controlled and highly monitored exposition set-up.

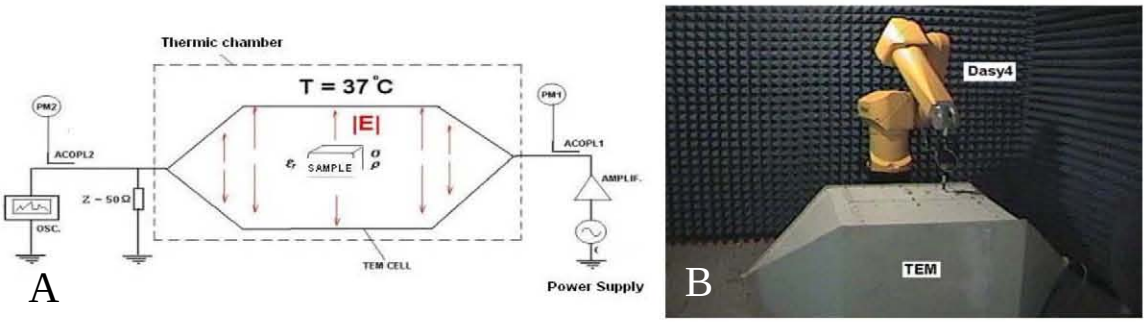
MATHERIALS AND METHODS

The study population consisted of 10 healthy, non-smokers male and female subjects that were not X-rayed in the last 12 months. The study was approved by the University's and by the National Ethical Committee (CONEP). Participants were informed of the study aims and asked to sign consent. Venous blood samples were collected in coded heparinized tubes and divided to be used in different assay as both test, sham-exposed and control samples.

1. Cytogenetics: short-term lymphocytes cultures were established using 0,5 ml of blood added to HAM F-10 medium (NUTRICELL) supplemented with phytohaemagglutinin (INVITROGEN) and 10% of fetal bovine serum (NUTRICELL). Cells were harvested after 72 hours of stimulation and colcemid (INVITROGEN) was added 1 hour before harvesting. Cultures were submitted to hypotonic shock for 10 min with 0,075 M KCl at 37o.C and then fixed in methanol-acetic acid (3:1) washes 3 times. For conventional cytogenetics analysis, after being air-dried and dropped onto glass slides in a humidified chamber, lymphocytes were stained with 5% Giemsa-Wright solution for 6 minutes. Structural aberrations such as chromatid and chromosome gaps and breaks, acentric and dicentric fragments, double minutes, satellite increase were evaluated. Each abnormality was scored as an event. Mean frequencies were obtained for each exposition type. For each donor, 200 cells were analyzed. For aneuploidy analysis, centromere probes for chromosomes 8 and 17 (QBIOGENE) were hybridized through mini-preps FISH assays according to the manufacturer's instructions. Mini-preps were obtained dropping 10 μl of cell suspension onto glass slides. For each probe, 200 cells were analyzed, per donor. Cells containing less and more than 2 hybridization signals were scored as aneuploidy. Mean frequencies were obtained for each exposition type.
2. Micronuclei: lymphocytes cultures were established as described previously for the cytogenetics assays but Cytochalasin B (SIGMA) was added after 44 h of estimulation. Cells were also submitted to hypotony but fixed only in methanol, 3 times. Cells were stained with 5% Giemsa-Wright solution for 6 minutes. For each donor, 1000 cells were analyzed and the mean frequencies for each exposition type were obtained. Micronuclei were evaluated only with SAR values of 0,8 and 10W/kg using AMPS technology.

The exposition set up was especially designed for this project. A transverse electromagnetic cell (TEM CELL) was used to irradiate the samples inside an incubator at 37oC (Figure 1A) for 72 hours that is the current standard time to obtain metaphases for cytogenetic analysis. Temperature was corrected by air insufflations, when necessary, especially in high SAR levels. All exposition parameters were controlled and the conditions to obtain the desired SAR levels were measured and established before the experiments through the robotic device DASY4 (Figure 1B). Cell cultures were submitted to 0,8; 2,0; 5,0 and 10,0 W/kg SAR levels in AMPS and CDMA technologies. Sham exposed (all transportation conditions and no exposition) and control samples (patient control, no transportation conditions, no exposition) were also analyzed.

Figure 1: Exposition set up. A. Diagram of the exposition system. B. DASY4 robotic device for set up characterization and calibration.



RESULTS

The results for chromosome abnormalities, aneuploidy of chromosomes 8 and 17 and micronuclei frequency are summarized in Table 1.

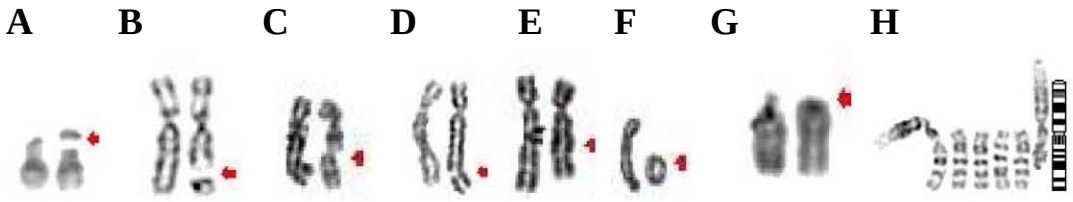
Table 1. Summarized results of the genomic imbalances

Type	*SAR*	Chromosome Ab.		Aneup 17		Aneup 8		Micronuclei Freq (%)	
		Mean	Range	Mean	Range	Mean	Range	Mean	Range
CDMA	**2**	0,019	0-0,058	0,48	0,96-1,92	0	0-0		
	5	0,021	0-0,070	0,13	0-0,95	2,15	1,96-6,14		
	10	0,039	0-0,079	2,91	0-5,56	4,44	4,0-9,84		
AMPS	**0,8**							8,93	(7,39-10,76)
	2	0,006	0-0,035	0,53	0,97-1,79	1,26	0,98-2,91		
	5	0,016	0-0,043	0,54	0,94-1,92	2,4	0,81-4,50		
	10	0,025	0-0,055	6,1	3,17-10,62	4,19	1,47-7,38	13,36	(6,06-19,44)
Control		0	0-0	1,04	0,65-2,80	0,375	0-1	4,07	(2,30-6,56)
SHAM		0,006	0-0,035	1,31	0,99-1,96	0,492	0-1,96	8,74	(7,50-11,24)

A dose dependent effect was clearly noted for all the evaluated patterns as the abnormalities were shown to be more frequent as higher were the SAR levels of exposition despite of CDMA and AMPS technologies.

The most frequent observed chromosome abnormalities were chromosome and chromatid breaks although other events such as fragment deletions and amplifications as well as ring chromosomes were also found as shown in Figure 2.

Figure 2: Chromosome Abnormalities A. Satellite length increase. B/C. Chromosome breaks. D. Chromatid gap. E. Deletion. F. Ring Chromosome G. Acentric Fragment. H. Amplification



The micronuclei frequency has increased with SAR levels of 10W/kg and the results obtained with a SAR level of 0,8 W/kg, which is close to what a person might be exposed realistically, was very similar to the frequency obtained in the sham-exposed samples. Aneuploidy of chromosome 17 was considered relevant only with SAR levels of 10W/kg, when compared to the mean frequencies of the control and sham exposed samples. Aneuploidy of chromosome 8 was considered relevant, when compared to the controls only with SAR levels of 5 and 10W/kg.

DISCUSSION

A general concern for people that are exposed to RF fields, especially with the increasing number of cell phone users, is the connection between radiation and cancer. Genomic instability is largely found in tumor cells and there is a strong evidence that high SAR levels, above the international regulation limits, may have a genotoxic effect and induce DNA damage at some level.

It is interesting to note that aneuploidy and chromosome damage have been considered two of the most notorious transformation-related events in tumorigenesis because it precedes malignant transformation in many tumors. Cancer aneuploidy and other imbalances affect gene dosage and a large number of proteins including those involved in the mitotic spindle apparatus resulting in a self-perpetuating chromosomal instability [13]. As we detect genomic imbalances in blood cells submitted to increasing SAR levels we remain to understand if these instable cells are still capable to escape to an apoptotic via in order to exterminate the imbalanced clones and preserve tissue integrity. We have observed much more translocations and marker chromosomes, yet to be identified through SKY (spectral karyotyping) than dicentrics, acentrics and rings which are considered much more unstable aberrations with fast disappearance *in vivo* [14,15].

In response to genotoxic such as RF, various chemicals and reactive cellular metabolites, cell cycle checkpoints that slow down or arrest cell cycle progression can be activated, allowing the cell to repair or prevent the transmission of damaged or incompletely replicated chromosomes. The balance between cell cycle arrest, damage repair and initiation of cell death could determine if cellular or DNA damage is compatible with cell survival or requires cell elimination by apoptosis. Defects in these processes may lead to hypersensitivity to cellular stress, and susceptibility to DNA damage, genomic defects, and resistance to apoptosis, which characterize cancer cells. This is the main issue to justify chromosomal studies in *in vitro* models [16]. Molecular chromosome techniques such as CGH – Comparative Genomic Hybridization [17] and SKY – Spectral Karyotyping [18] can add more information to conventional cytogenetics reports and indicate hot spots for chromosome structural abnormalities.

When individuals exposed to RF in a work environment were evaluated it was shown that other factors might potentiate the clastogenic effects of RF radiation such as light deprivation resulting in a disturbance of melatonin secretion [19]. Such observations may explain the fact that our sham-exposed samples have always shown higher mean frequencies of abnormalities when compared with the controls alone. It is necessary to consider that epigenetic and environmental factors may play an important role to potentiate the radiation effect on the DNA.

Our findings support other groups' results as we were able to demonstrate a dose-dependent effect against the genome particularly with SAR levels above 5W/kg [20].

The set up system used for the expositions was carefully designed to meet the needs described at the WHO´S EMF International Project. Parameters such as temperature, power input and output, TEM CELL characterization prior to the experiments and experimental dosimetry tests were developed and taken into account to achieve reliable results in isothermal conditions.

Our results have shown the importance of genomic analysis especially through conventional and molecular cytogenetics techniques and suggest the use of continuous cytogenetics analysis especially for occupationally exposed professionals who are the ones that might be exposed to higher SAR levels [15].

We are yet to describe the effect of RF in different systems and exposition parameters specially with regard to an intermittent mode of radiation exposure.

ACKNOWLEDGEMENTS

The authors would like to thank Mauro Lins, M.Sc for the initial technical support for the exposition set up. This research was supported by FUNTTEL.

REFERENCES

1. Smith, LE; Nagar,S; Kim,GJ; Morgan,WF. Radiation-induced genomic instability:radiation quality and dose response. Health Phys 2003. 85(1):23-9.
2. Huang, L; Snyder, AR; Morgan, WF. Radiation-induced genomic instability and its implications for radiation carcinogenesis. Oncogene, 2003; 22: 5848-5854.
3. Ivaschuk, OL; Jones, RA; Jones, TI; Haggren, W; Adey, WR; Phillips, JL. Exposure of nerve growth factor-treated PC12 rat pheochromacytoma cells to a modulated radiofrequency field at 836.55 MHz: effects on c-jun and c-fos expression. Bioelectromagnetics, 1997; 18:223-229.
4. Brusick, D; Chairman; Albertini, R; McRee, D; Peterson, D; Williams, G; Hanawalt, P; Preston, J. Genotoxicity of radiofrequency radiation. Environmental and Molecular Mutagenesis, 1998; 32: 1-16.
5. Moulder, JE; Erdreich, LS; Malyapa, RS; Merritt, J; Pickard, WE; Vijayalaxmi. Cell phones and cancer: what is the evidence for a connection?. Radiation Research, 1999; 151: 513-531.
6. Blettner, M; Berg, G. Are mobile phones harmful?. Acta Oncologica, 2000; 39(8): 927-930.
7. Mashevich, M; Folkman, D; Kesar, A; Barbul, A; Korenstein,R; Jerby, E; Avivi, L. Exposure of human peripheral blood lymphocytes to electromagnetic fields associated with cellular phones leads to chromosomal instability. Bioelectromagnetics, 2003; 24:82-90.
8. Goswani, PC; Albee, LD; Parsian, AJ; Baty, JD; Moros, EG; Pickard, WF; Roti, JLR; Hunt, CR. Proto-oncogene mRNA levels and activities of multiple transcription factors in C3H 10T1/2 murine embryonic fibroblasts exposed to 835.62 and 847.74 MHZ cellular phone communication frequency radiation. Radiation Research, 1999; 151:300-309.
9. Velizarov,S ; Raskmark,P; Kwee,S. The effects of radiofrequency fields on cell proliferation are non-thermal. Bioelectrochemistry and Bioenergetics 1999. 48:177-180.
10. French, PW; Penny, R; Laurence, JÁ; Mckenzie, DR. Mobile phones, heat shock proteins and cancer. Differentiation, 2000; 67:93-97.
11. Leszczynski, D; Joenväärä, S; Reivinen, J; Kuokka, R. Non-thermal activation of the hsp27/p38MAPK stress pathway by mobile phone radiation in human endothelial cells: molecular mechanism for cancer and blood-brain barrier-related effects. Differentiation, 2002; 70:120-129.
12. Di Carlo, A; White,N; Guo,F; Garrett, P; Litovitz,P. Chronic electromagnetic field exposure decreases HSP70 levels and lowers cytoprotection. J Cell Biochem 2002. 84(3): 447-54.
13. Bialy, H. Aneuploidy and cancer – the vintage wine revisited. Nature Biotechnology, 2001; 19: 22-23.
14. Johnson,KL; Tucker, JD; Nath, J. Frequency, distribution and clonality of chromosome damage in human lymphocytes by multi-color FISH. Mutagenesis, 1998; 13:217-227.
15. Lalic, H; Lekic, A; Radosevic-Stasic, B. Comparison of chromosome aberrations in peripheral blood lymphocytes from people occupationally exposed to ionizing and radiofrequency radiation. Acta Medica Okayama, 2001; 55 (2):117-127.
16. Ishikawa,K; Ishii,H; Saito,T. DNA damage-dependent cell cycle checkpoints and genomic stability. DNA Cell Biol 2006. 25(7):406-11.
17. Kallioniemi,A; Kallioniemi,OP;Sudar, D; Rutovitz,D; Gray, JW; Waldman,F; Pinkel,D. Comparative genomic hybridization for molecular cytogenetic analysis of solid tumors. Science, 1992. 258(5083):818-21.
18. Schrock E; Veldman, T; Padilla-Nash,H; Ning, Y; Spurbeck,J; Jalal,S; Shaffer,LG; Papenhausen,P; Kozma, C; Phelan, MC; Kjeldsen,E; Schonberg,AS; O´Brien,P; Biesecker,L; DuManoir,S; Ried,T. Spectral karyotyping refines cytogenetic diagnostics of constitutional chromosomal abnormalities. Hum Genet 1997. 101(3):255-62.
19. Cassone,VM; Warren,WS; Brooks,DS; Lu,J. Melatonin, the pineal gland and circadian rhythms. J Biol Rhythms, 1993. 8:S-73-S78.
20. Tice,RR; Hook,GG; Donner,M; McRee,DI; Guy,AW. Genotoxicity of radiofrequency signals. I. Investigation of DNA damage and micronuclei induction in cultured human blood cells. Bioelectromagnetics 2002. 23(2):113-26.

ANALYTICAL STUDY OF THE IRRADIATION OF A HUMAN HEAD MODEL BY AN ACTIVE IMPLANT

ANGELA P. MONEDA

ARISTOTLE UNIVERSITY OF THESSALONIKI
E-MAIL ADDRESS: apmoneda@egnatia.ee.auth.gr

DIMITRIOS P.CHRISSOULIDIS

ARISTOTLE UNIVERSITY OF THESSALONIKI
E-MAIL ADDRESS: dpchriss@auth.gr

P.O. BOX: 1562, ZIP CODE: 54124, THESSALONIKI, GREECE

Abstract
An exact, analytical solution has been used to calculate the electromagnetic (EM) radiation emitted by an active implant within an eccentric-spheres, human head model and variations thereof. The EM field is determined by use of Green's dyadic for a lossy, dielectric sphere containing any number of lossy, dielectric, spherical inclusions. The inclusions can be placed anywhere within the host sphere. The source is a point dipole encapsulated within a tiny, lossless, dielectric sphere. In theory, this implant can be placed anywhere within the head model; calculations have been made with the implant inside the scull, either at the side, near a temple, or at the side of the jaw. Numerical results have been obtained for frequencies ranging from 400 *MHz* to 4 *GHz*. The effect of the orientation of the dipole source has been investigated. The radiation absorbed by the head model has been studied by use of plots of the total absorbed power per tissue against the frequency as well as by use of maps of the Specific Absorption Rate (SAR) on cross sections of the head.

I. Introduction

The growing interest of the scientific community in the implantation of active antennas inside the human body has been related to communication and monitoring purposes. In this paper the operation of an active implant, which radiates in the RF or microwave band, from within the human head has been examined. Applications of this study may include (a) comparisons of SAR calculations with the guidelines of international standards, (b) controlled absorption, aimed at therapeutic interventions, and (c) diagnosis of anatomical abnormalities through measurements of near- or far-field radiation escaping from the head.

The analytical solutions that have been made available over the years treat the human head as a multilayered, lossy, dielectric sphere [1]-[3]. Herein, an eccentric-spheres model of the human head and two simplified versions thereof have been considered. The implanted antenna is an infinitesimal, electric dipole encapsulated within an acrylic sphere, which immunes the source dipole from the surrounding tissue, which may be conductive.

From the point of view of eventual health hazards of communication devices, the focus is on the power absorbed by the brain, the appearance of hot spots, and the peak SAR values. Furthermore, the characteristics of the implant are investigated by calculations of the delivered power, maps of the electric-field intensity around the head, and far-field radiation diagrams.

II. Head Model and Implant

All three head models, which are of interest in this paper, can be obtained from the geometry shown in Fig. 1. Model 1 comprises a spherical bone shell (host sphere), which represents the scull, and three inclusions; the latter are a major, spherical core, representing the brain and a pair of small eyeballs, all properly placed within the bone shell. The (outer) radius of the scull is $\alpha_0 = 9\,cm$, the radius of the brain is $\alpha_1 = 7\,cm$ and those of the eyes are $\alpha_2 = \alpha_3 = 1\,cm$. The center of the brain, O_1, is vertically displaced by $d_{01} = 1.5\,cm$ from the center of the scull, O_0. The eyes are centered at O_2, O_3, which are horizontally displaced by $d_{02} = d_{03} = 7.95\,cm$ from O_0; the left-hand eye is in the meridian plane $\varphi = 23^\circ$ (Fig. 1a), whereas the right-hand eye is in the meridian plane $\varphi = (360 - 23)^\circ = 337^\circ$. Thus, the eyes are symmetrically placed with respect to the coordinate plane

xO_0z . Model 2 is obtained from model 1 by omission of the eyeballs and model 3 is obtained from model 2 by the substitution $d_{01}=0$. The brain volume is $1436.75cm^3$, this value being in the range $[1400-1500cm^3]$ of normal, human brain volumes. The electrical properties assigned to bone, brain, and eye tissue as well as the corresponding density of each tissue, are shown in Table I for two frequencies which are of special interest [4].

The active implant is an infinitesimal, electric dipole, placed at the center of an acrylic sphere of radius $\alpha_4=0.5cm$ and refractive index $n_4=n_{acr}=1.61+j0$. The lossless capsule immunes the source from the conductive bony shell [5]. The implant is positioned at distance $d_{04}=8cm$ from O_0 , either on the *y*-axis (position 1) or on the yO_0z plane at $\theta=145°$ declination from the *z*-axis (position 2). The first position of the source is supposed to be inside the left auricular and the second in the mouth, where the lower left, 3rd molar (tooth #38) is found.

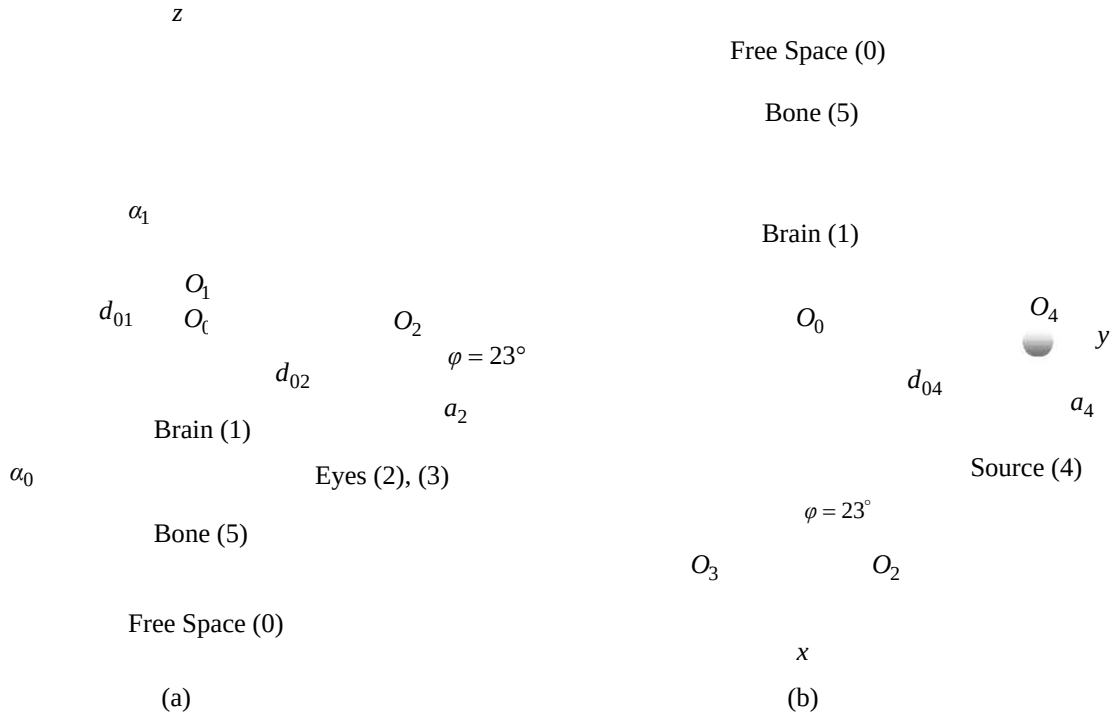


Figure 1. (a) Vertical ($\varphi=23°$) and (b) horizontal ($\theta=90°$) cross-sections of head model 1; the point source, encapsulated in an acrylic sphere of radius α_4 , is shown in position 1 (left auricular); position 2 is also in the meridian plane $\varphi=90°$, but below the xO_0y plane, at $\theta=145°$.

Table I. Relative, dielectric constant ε_r , conductivity $\sigma(mhos\ m)$, and density $\rho(kg\ m^3)$ of human head tissue layers

Frequency	**Bone**		**Brain**		**Eyes**	
(MHz)	$(1850\,kg\ m^3)$		$(1030\,kg\ m^3)$		$(1010\,kg\ m^3)$	
	ε_r	σ	ε_r	σ	ε_r	σ
1500	11.98	0.22	45.99	1.12	68.70	1.87
2400	11.41	0.38	44.33	1.62	68.24	2.44

III. Analytical Determination of the Electric-Field Intensity

The electric-field intensity anywhere within, as well as outside, the aforesaid head model is determined by use of the dyadic Green's function (dGf) $G_e(\vec{r},\vec{r}')$ of a dielectric sphere with several, eccentric, spherical, dielectric inclusions; all dielectrics may be lossy. The position vectors $\vec{r}$, $\vec{r}'$ correspond to the field and source points. The point source can be placed anywhere, but, in this study it has been placed in the bone shell, which is denoted as region 5 (Fig. 1); the generality of the analysis is not impaired otherwise. The analytical determination of $G_e(\vec{r},\vec{r}')$ is an intricate task which has been undertaken by the authors elsewhere [6]. Still, it

might be convenient to state that the analysis begins by consideration of the dGf of an unbounded space with electrical properties identical to those of the acrylic inclusion; that dGf is given by [7]

$$\bar{\bar{G}}_{e0}(\vec{r},\vec{r}') = -\frac{1}{k_4^2}\hat{r}\hat{r}\delta(\vec{r}-\vec{r}') + \\ + j\frac{k_4}{4\pi}\sum_{mn}(-1)^m\frac{2n+1}{n(n+1)}\begin{cases}\left[\vec{M}_{mn}^{(1)}(k_4\vec{r})\vec{M}_{-mn}^{(3)}(k_4\vec{r}')+\vec{N}_{mn}^{(1)}(k_4\vec{r})\vec{N}_{-mn}^{(3)}(k_4\vec{r}')\right] & r<r' \\ \left[\vec{M}_{mn}^{(3)}(k_4\vec{r})\vec{M}_{-mn}^{(1)}(k_4\vec{r}')+\vec{N}_{mn}^{(3)}(k_4\vec{r})\vec{N}_{-mn}^{(1)}(k_4\vec{r}')\right] & r>r'\end{cases} \quad (1)$$

where $k_4 = k_0\sqrt{\varepsilon_{r,4}}$ is the wavenumber within region 4 of the nonspherical body, which accommodates the source; $k_0 = \omega/c_0$ is the wavenumber of free-space, i.e. region 0, and $\varepsilon_{r,4}$ is the relative permittivity of the acrylic sphere; $\vec{M}_{mn}^{(1)}$, $\vec{N}_{mn}^{(1)}$ and $\vec{M}_{mn}^{(3)}$, $\vec{N}_{mn}^{(3)}$ are vector, spherical harmonics of an unbounded acrylic medium; the former pair comprises wavefunctions that remain bounded at the origin of coordinates, whereas the latter pair of wavefunctions are bounded at infinity. By application of the boundary conditions on every spherical interface of the nonspherical body, $\bar{\bar{G}}_e(\vec{r},\vec{r}')$ is ultimately obtained, but neither further details about that analytical formulation nor the resulting, cumbersome expression for $\bar{\bar{G}}_e(\vec{r},\vec{r}')$ are needed in this paper, which is focused on numerical results. The validity of the solution has been checked numerically through reciprocity and energy-conservation checks as well as analytically by simplifying the geometry and comparing the resulting solution to those of articles published before [8], [9].

The point source is represented by the current distribution

$$J(\vec{r}') = I_0 l\frac{\delta(r'-r_0)\delta(\theta'-\theta_0)\delta(\phi'-\phi_0)}{r'\sin\theta}\hat{e}, \quad (2)$$

wherein $I_0 l$ is the dipole moment and $\hat{e}$ is the orientation, i.e. polarization, vector. The electric-field intensity due to this dipole source can be determined anywhere in space by integration of the posterior scalar product of $\bar{\bar{G}}_e(\vec{r},\vec{r}')$ with the aforesaid current [10]:

$$\vec{E}(\vec{r}) = j\omega\mu_0\int_{\vec{r}'}\bar{\bar{G}}_e(\vec{r},\vec{r}')\cdot\vec{J}(\vec{r}')d^3\vec{r}' \quad (3)$$

IV. Numerical Results

The effect of the implant on the head has been investigated first by use of diagrams of the absorbed power versus the operating frequency of the implant, which is in the range $400MHz$ - $4GHz$, for both positions of the implant. The aforesaid frequency range is associated with ISM, TETRA, GSM, UMTS, WLAN, and Bluetooth devices. Moreover, these diagrams display lucidly which fraction of the radiated power is absorbed by each tissue at anyone of those frequencies. Absorption by the brain and the bone is shown in Figs. 2 and 3 as percentage of the total radiated power, respectively, for head models 1, 2 and 3. The dipole orientation is in every case along the *z*-axis.

The first remark yielding from the aforementioned diagrams is that the brain absorption is maximized at about $1500MHz$ when the dipole is placed in the ear and at $1700MHz$ when the implant is placed at the tooth. At the very same frequencies absorption by the bone shell is minimal.

When the eccentric-brain, head model, i.e. model 1 or 2, is under consideration it is obvious that there is strong dependence of the absorbed power on the dipole position. Absorption by the brain with the implant in the ear exceeds that with the implant in the tooth, and the opposite is true for absorption by the scull. This outcome can be justified by the different distance of the source from the brain in the aforesaid positions.

The remark made above does not apply to the concentric-brain, head model, i.e. model 3, because the source is equidistant from the brain for both the positions examined. In that model, the difference in the frequency, whereby absorption is maximized, can be justified by the different angle by which the dipole is aimed at the brain.

The overall absorption by the left eye, which in every case is closer to the implanted antenna, in model 1, is less than 0.05% and it is not shown. Finally, for all three models, a very small percentage of the radiated power escapes from the head into the free-space surrounding. That percentage is less than 3% for position 1 of the implant, with the maximum value occurring at $2700MHz$, and it does not exceed 1% of the radiated power for position 2, the maximum value being at $2200MHz$.

Next, the effect of the dipole orientation on the power absorbed by the brain, the bone and the eyes is investigated. In Figs. 4 and 5 the overall absorbed power by the brain and the bone, respectively, is plotted against the declination angle θ of the polarization vector of the point dipole; θ is measured from the *z*-axis. The operating frequency is $1500MHz$.

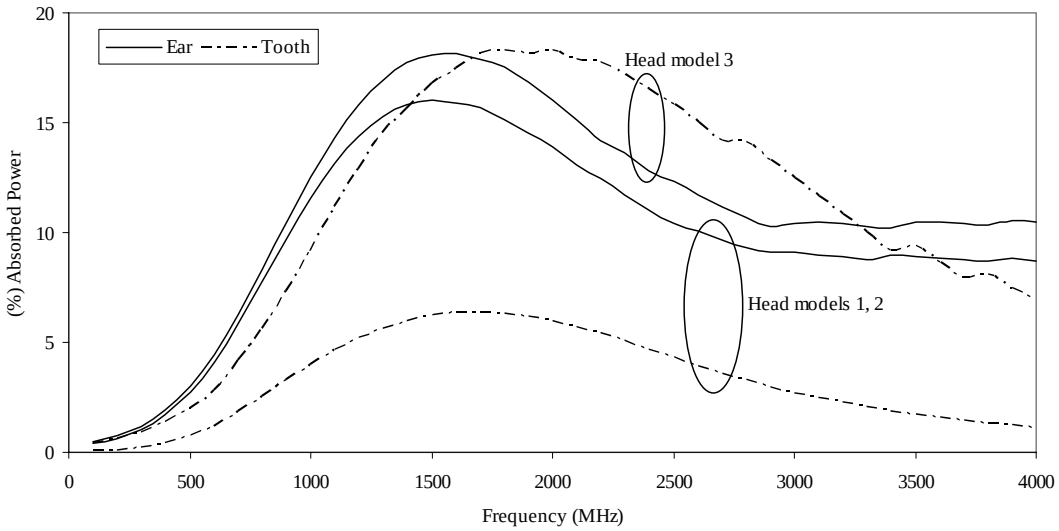


Figure 2. Absorption by the brain vs. frequency for head models 1, 2 and 3.

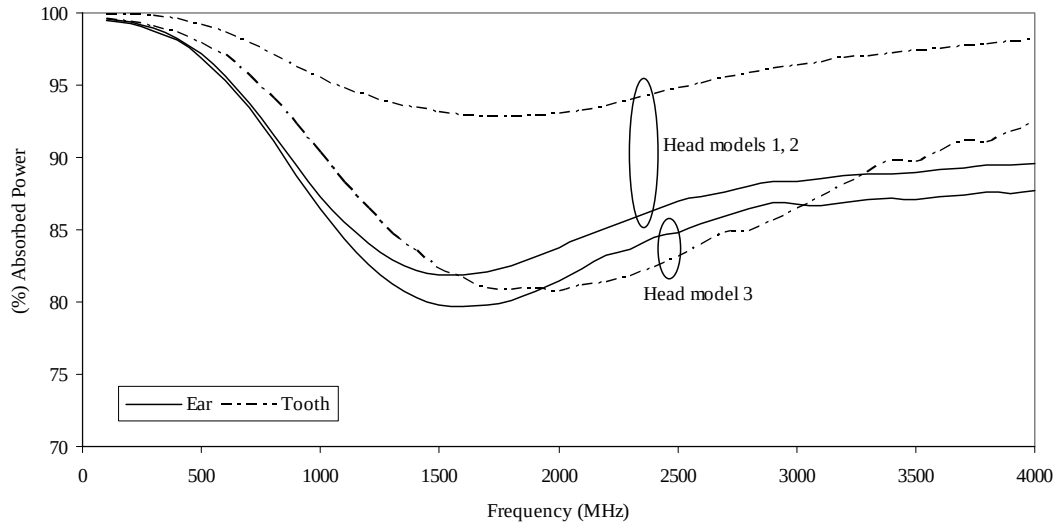


Figure 3. Absorption by the bone vs. frequency for head models 1, 2 and 3.

It is clear that absorption by the brain and the bone is practically unaffected by the orientation of the dipole when the latter is placed inside the ear. A slight increase in the absorption by the brain and a corresponding decrease in the absorption by the bone are observed when the dipole is placed at the tooth for all three head models.

The effect of dipole orientation on the absorption by the eyes is far more significant. As shown in Fig. 6, absorption by the left eye, which is closer to the radiating implant, increases as the main radiation lobe of the dipole rotates so as to include the eye, and decreases as that lobe points elsewhere. However, the overall power absorbed by the eyes remains a small percentage of the total radiated power

Subsequently, numerical results are shown for the SAR anywhere within the nonspherical head model; the SAR has been determined by use of the definition

$$SAR = \frac{\sigma |E|^2}{2\rho}, \tag{4}$$

wherein σ is the conductivity and ρ is the density of tissue.

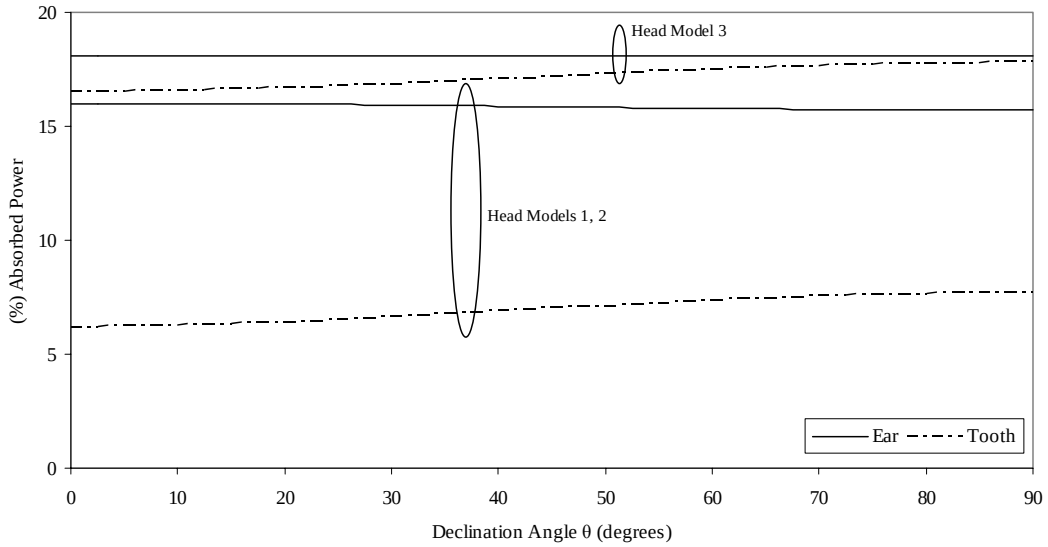


Figure 4. Absorption by the brain vs. dipole orientation (i.e. declination angle) for head models 1, 2 and 3

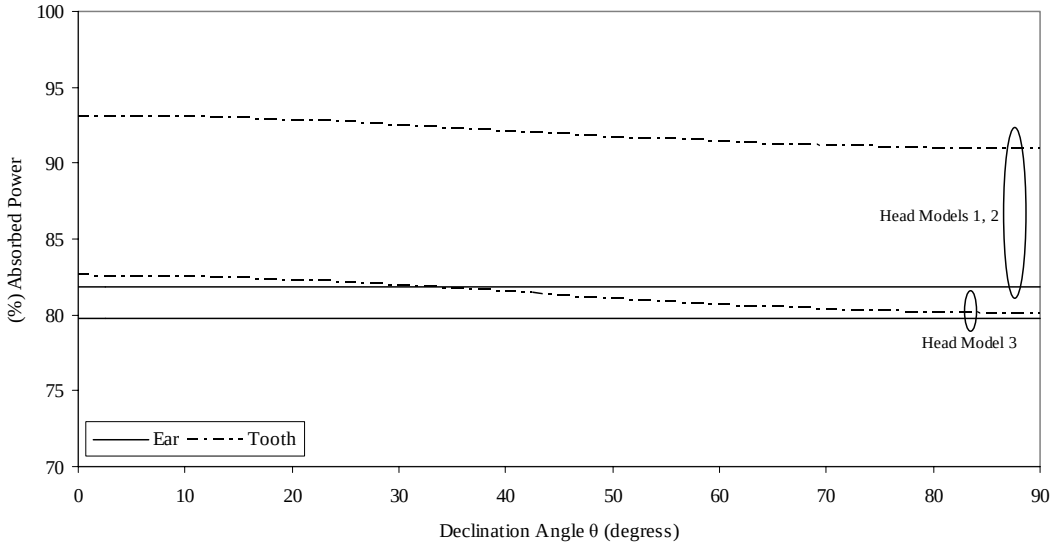


Figure 5. Absorption by the bone vs. dipole orientation (i.e. declination angle) for head models 1, 2 and 3

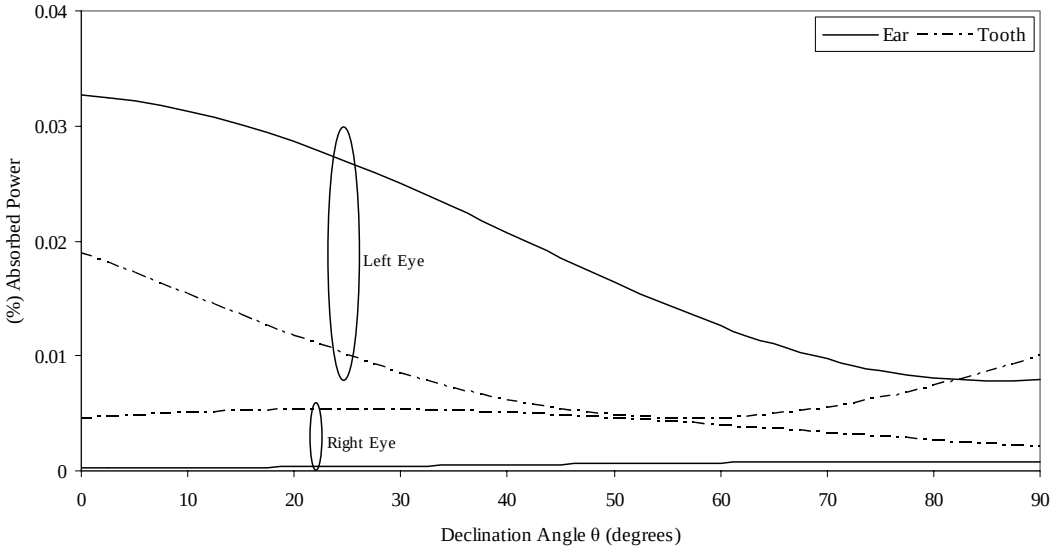
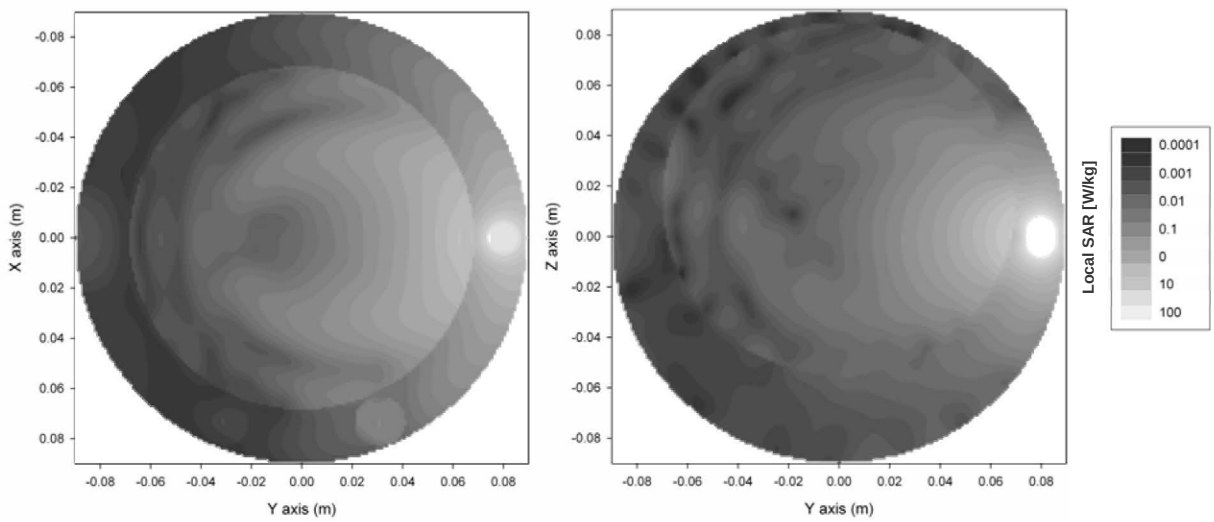


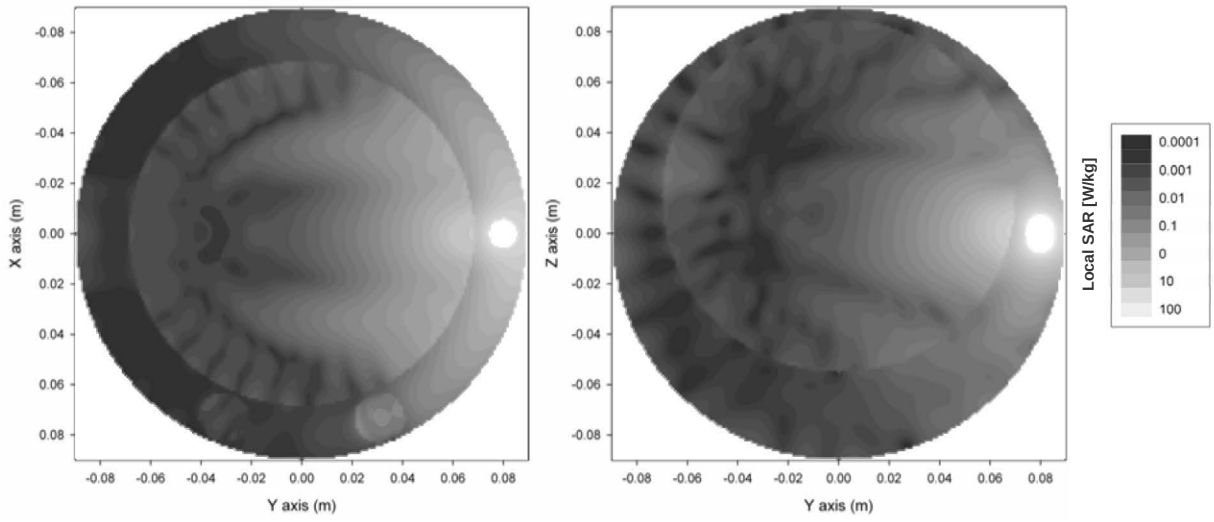
Figure 6. Absorption by the eyes vs. dipole orientation (i.e. declination angle) for head model 1

SAR maps are shown for characteristic cross-sections of the human head. The SAR maps of Figs. 7 and 8 correspond (a) to a horizontal cross section of the head through the centers of the scull and the eyes and (b) to a vertical cross section of the head through the centers of the scull, the brain and the acrylic capsule. The brain core in Figs. 7(a) and 8(a) seems smaller because it is somewhat raised above that cross section, i.e. the xO_0y plane. The active implant is inside the left ear and the operating frequency is $1500MHz$ in Fig. 7 and $2400MHz$ in Fig. 8. The radiated power is $1W$ for all the cases examined.



(a) (b)

Figure 7. SAR maps on (a) xO_0y and (b) yO_0z planes; the implant is inside the left ear and the frequency is 1500 *MHz*.

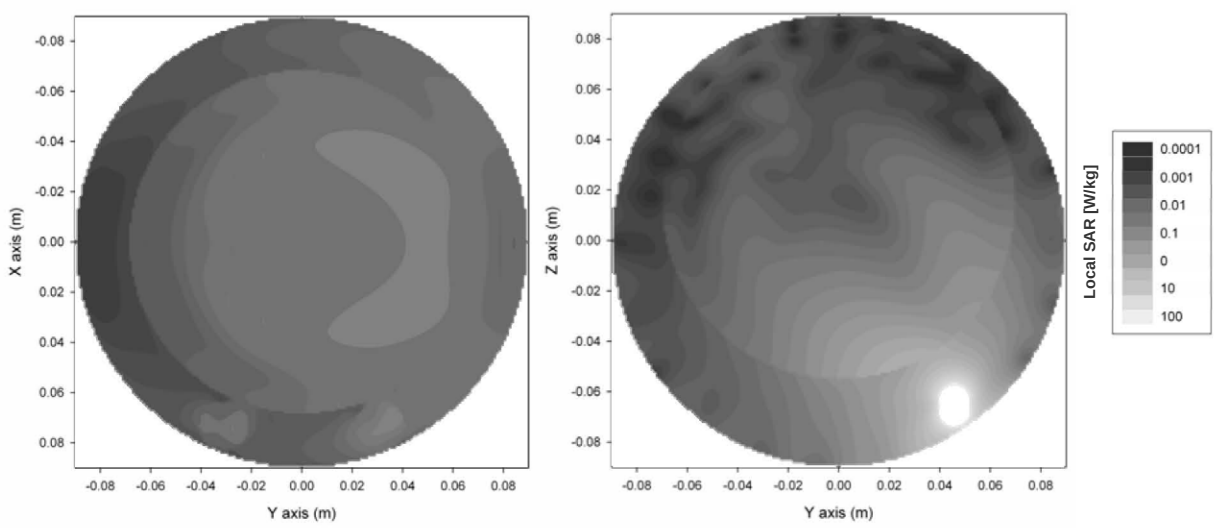


(a) (b)

Figure 8. As Fig. 7 at 2400 *MHz*.

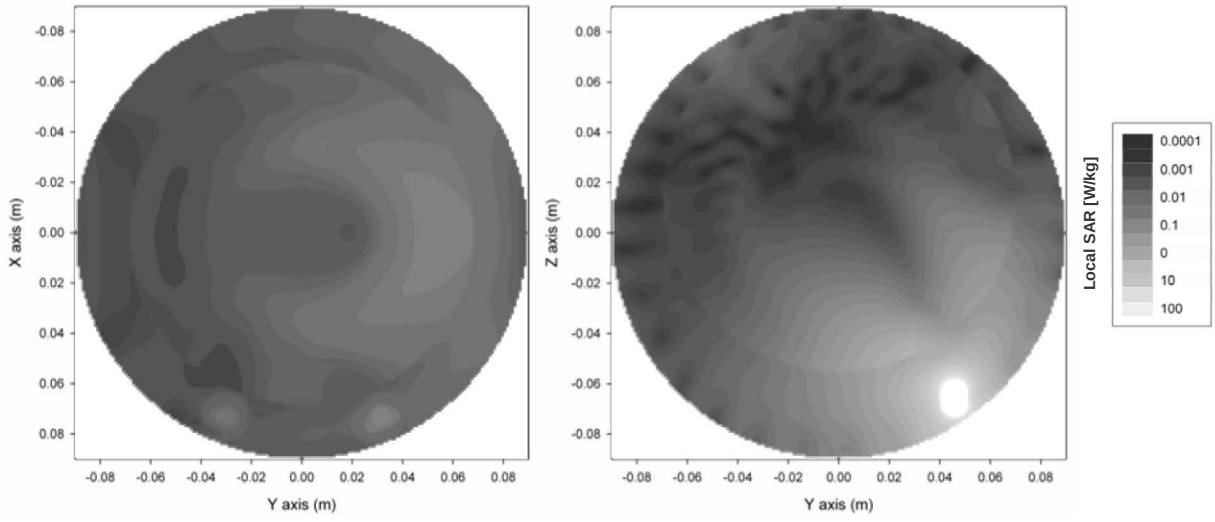
A cursory look at the above SAR maps suggests that the higher the frequency the more superficial is the penetration of the EM radiation inside the brain and the eyes. The maximum SAR in the brain is found at the cortex, directly in front of the implant, where the radiation is most intense. The maximum SAR in the brain is $10.8W\ kg$, when the frequency is $1500MHz$, and it reaches $21.0W\ kg$ at $2400MHz$.

Finally, local SAR evaluations have been made with the implant inside the tooth. Figs. 9 and 10 are SAR maps for the same cross-sections of the eccentric-brain head model as Figs. 7,8 and for the same frequencies. The aforesaid remark about the dependence of the penetration depth of the EM radiation on the operating frequency of the implant is reconfirmed. However, the importance of the distance of the implant from the brain on the power absorbed by the brain is now made evident, since the maximum local SAR in the brain in these cases is $1.6W\ kg$ at $1500MHz$ and $2.4W\ kg$ at $2400MHz$.



(a) (b)

Figure 9. SAR maps on (a) xO_0y and (b) yO_0z planes; the implant is inside a tooth and the frequency is 1500 *MHz*.

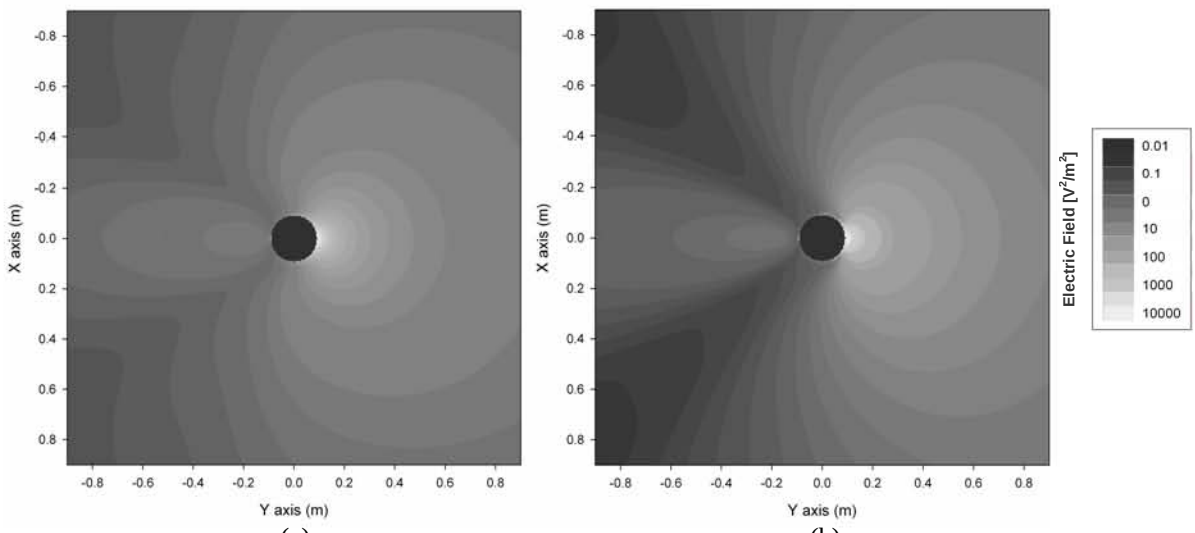


(a) (b)

Figure 10. As Fig. 9 at 2400 *MHz*.

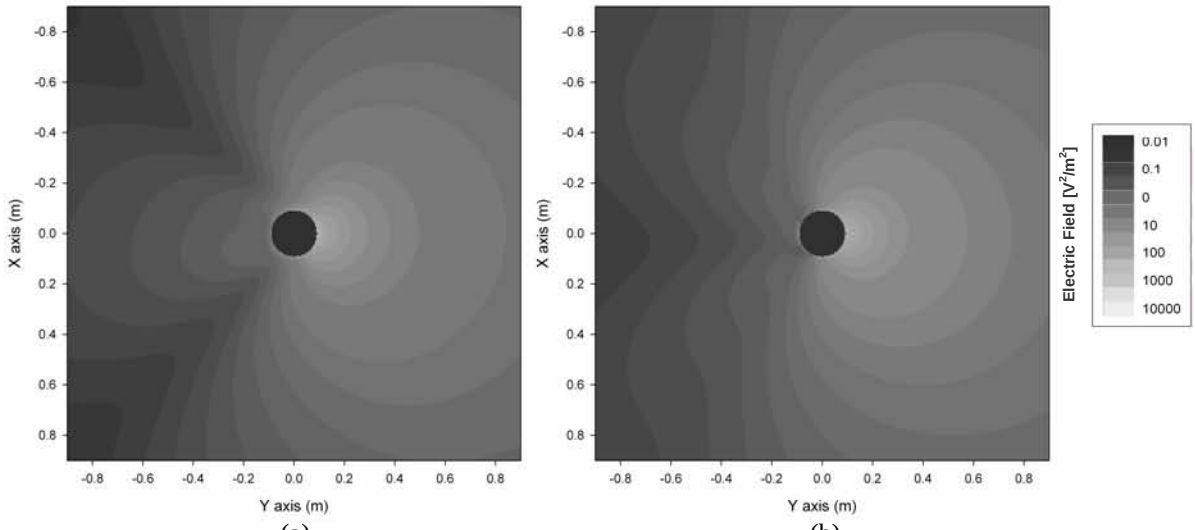
When the implant is intended for telecommunication or monitoring purposes the field outside the head is important for the appliance that receives the transmitted data. The EM field outside the head is shown in Figs. 11 and 12 as maps of the amplitude of the electric-field intensity up to distance $90\,cm$ from the center of the head. Those maps correspond to the coordinate plane xO_0y with the implant inside the ear or in a tooth. The operating frequency is either $1500MHz$ or $2400MHz$ and the power radiated by the implant power is $1W$. It is clear from those maps that the presence of the head orients the EM radiation in directions opposite to the head and this effect is stronger at the higher frequency, i.e. at $2400MHz$, for both positions of the implant examined. Finally, it is noted that, the average electric-field intensity on that plane is stronger with the implant in the ear than with the implant in the tooth. This, last remark holds even when the electric-field intensity is mapped on a horizontal plane through the tooth.

The study of the EM field outside the head model is completed by the radiation patterns shown in Figs. 13-16. Radiation patterns are plotted on all three coordinate planes, i.e. xO_0z (a), yO_0z (b), and xO_0y (c). The electric-field intensity in all those patterns has been normalized with respect to the maximum value of the electric-field intensity generated by the encapsulated dipole in free space. The comments incited by Figs. 11 and 12 about the re-orientation of the EM radiation due to the presence of the head and about the dependence of the electric-field intensity on the frequency and the position of the implant are compatible with Figs. 13-16.



(a) (b)

Figure 11. Field maps around head model 1; the implant is in the left ear and the frequency is (a) 1500 *MHz*, (b) 2400 *MHz*

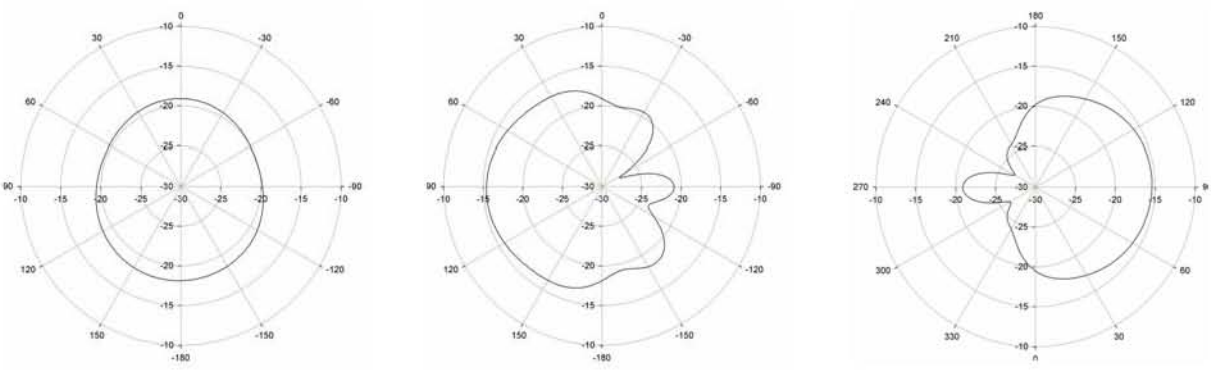


(a) (b)

Figure 12. As Fig. 11 with the implant in a tooth

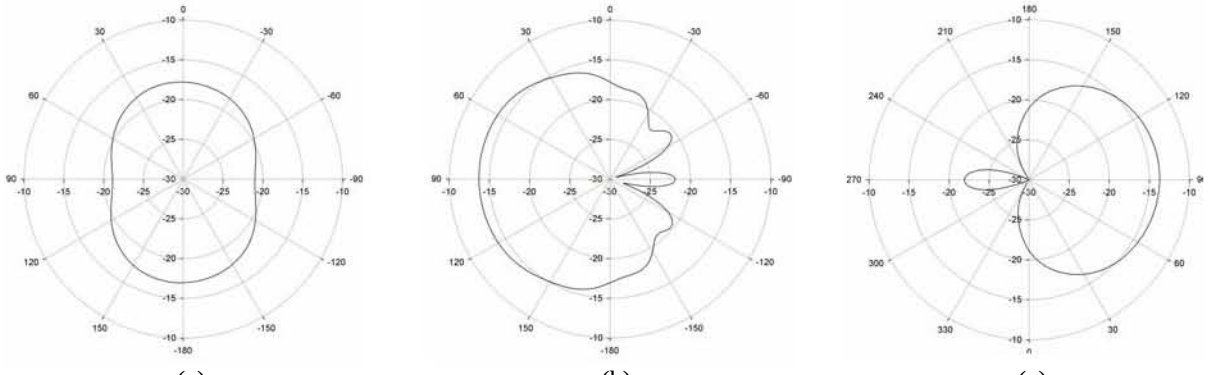
The radiation characteristics of the dipole itself are strongly affected by the electrical and geometrical features of the head model. Comparisons with radiation patterns corresponding to models 2 and 3 suggest that the position of the brain in the scull strongly affects the radiation patterns, whereas the effect of the eyes can hardly be noticed.

The final part of this investigation on the effect of the human head on the radiation characteristics of the implant, concerns the variation of the radiated power crossing the surface of the acrylic capsule with the operating frequency; that plot is shown in Fig. 17 across the frequency range $400MHz - 4GHz$. Since the acrylic medium has been considered lossless, the aforesaid radiated power is equal to power delivered by a tiny transmitter to the dipole, provided that matching between them is possible even though the current flowing along the dipole is modified by the presence of the head. The continuous line in Fig. 17 corresponds to power radiated by the dipole from within the acrylic sphere in free space; that power has been normalized with respect to the power radiated by the very same dipole in free space at every frequency; the dashed line corresponds to the power radiated by the implanted antenna and it has been normalized by the power radiated by the encapsulated dipole in free space. It can easily be seen from Fig. 17 that when the radius of the acrylic capsule is greater that 40 wavelengths, i.e. for frequencies above $1500MHz$, the power radiated by the implanted antenna varies periodically with the frequency and the effect of the head is minimal.



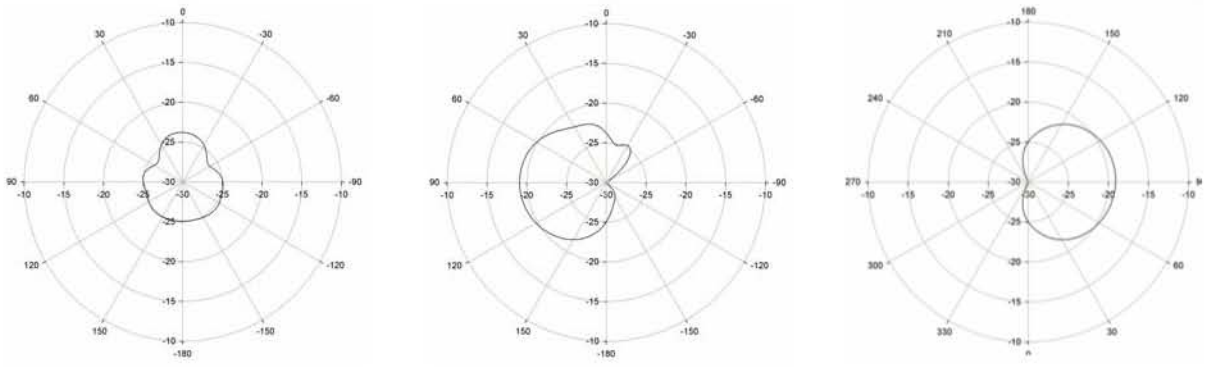
(a) (b) (c)

Figure 13. Radiation Patterns on xO_0z (a), yO_0z (b), and xO_0y (c) plane around head model 1; the implant is inside the left ear and the frequency is 1500 *MHz*



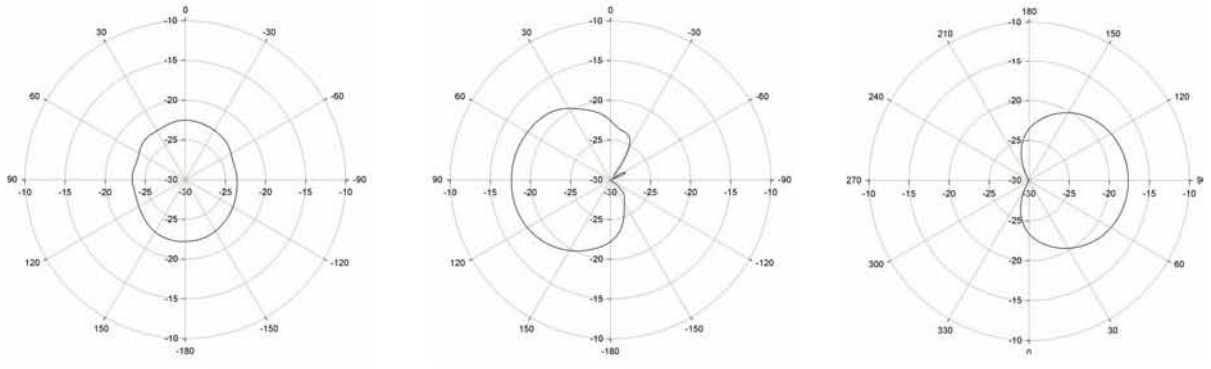
(a) (b) (c)

Figure 14. As Fig. 13 at 2400 *MHz*



(a) (b) (c)

Figure 15. As Fig. 13 with the implant in a tooth



(a) (b) (c)

Figure 16. As Fig. 14 with the implant in a tooth

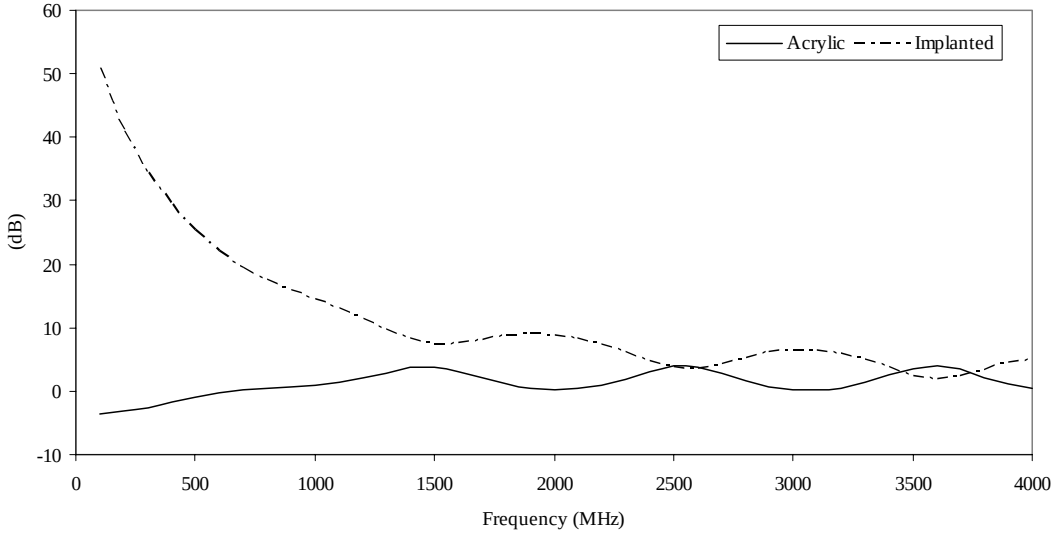


Figure 17. The power radiated by the encapsulated dipole against the frequency

V. Summary

The effects of an infinitesimal electric dipole placed at the centre of an acrylic sphere and implanted inside the human head have been studied by use of three head models. On the one hand, the absorbed power and the SAR in any part of the head models, have been evaluated and the importance of the operating frequency, the position and the orientation of the dipole have been established; the EM radiation escaping the head as well as the effects of the head on the characteristics of the implant have been examined. On the other hand, the importance of some anatomical details of the head models, within the framework of analytical methods, has been assessed, thus allowing for the appropriate head model to be used for the application at hand.

References

[1] S.M.S Reyhani and R.J. Glover, "Electromagnetic dyadic Green's function for a multilayered homogeneous lossy dielectric spherical head model for numerical EMC investigation," *Electromagnetics*, vol. 20, pp. 141-153, 2000.

[2] J. Kim and Y. Rahmat-Samii, "Implanted antennas inside a human body: Simulations, design, and characterizations," *IEEE Trans. Microwave Theory Tech.*, vol. 52, pp. 1934-1943, Aug. 2004.

[3] F. Liu and S. Crozier, "Electromagnetic fields inside a lossy, multilayered spherical head phantom excited by MRI coils: models and methods," *IOP Publishing, Phys. Med. Biol.*, vol. 49, pp. 1835-1851, 2004.

[4] C. Gabriel, "Compilation of the dielectric properties of body tissues at RF and microwave frequencies," Occupational and Environmental Health Directorate, RFR Division, Brooks AFB, TX, Final Tech. Rep. AL/OE-TR-1996-0037, 1996.

[5] C.T. Tai and R.E. Collin, "Radiation of a Hertzian dipole immersed in a dissipative medium," *IEEE Trans. Ant. Prop.*, vol. 48, no. 10, pp. 1501-1506, Oct. 2000.

[6] A.P. Moneda and D.P. Chrissoulidis, "Dyadic Green's function of a dielectric sphere with an eccentric inclusion," submitted to *J. Opt. Soc. Am. A.*

[7] K.S. Nikitia, G.S. Stamatakos, N.K. Uzunoglu, and A. Karafotias, "Analysis of the interaction between a layered spherical human head model and a finite-length dipole," *IEEE Trans. Microwave Theory Tech.*, vol. 48, no. 11, pp. 2003-2013, Nov. 2000.

[8] L.W. Li, P.S. Kooi, M.S. Leong, and T.S Yeo, "Electromagnetic dyadic Green's function in spherically multilayered media," *IEEE Trans. Microwave Theory Tech.*, vol. 42, no. 12, pp. 2302-2310, Dec. 1994.

[9] A.P. Moneda, M.P. Ioannidou, and D.P. Chrissoulidis, "Radio-wave exposure of the human head: analytical study based on a versatile eccentric spheres model including a brain core and a pair of eyeballs," *IEEE Trans. Biomed. Eng.*, vol. 50, no. 6, pp. 667-676, June 2003.

[10] C.T. Tai, *Dyadic Green Functions in Electromagnetic Theory*, 2nd Edition, New York, IEEE Press, 1993.

EFFECTS OF MELATONIN AND 50 Hz MAGNETIC FIELDS ON GAP JUNCTIONAL INTERCELLULAR COMMUNICATION IN HEPG2

M.A.CID, M.L. HERNÁNDEZ-BULE, M.A. MARTÍNEZ, A. ÚBEDA, J. LEAL AND M.A. TRILLO

DEPT. INVESTIGACIÓN-BEM, HOSPITAL RAMÓN Y CAJAL, 28034 MADRID, SPAIN
mariancid@yahoo.es; angeles.trillo@hrc.es

ABSTRACT

Experimental evidence exists suggesting that Extremely Low Frequency Magnetic Fields (ELF-MF) and Melatonin (MEL) can exert antagonistic effects on different cellular responses. However, the nature of such an interaction remains unknown. Our previous studies have shown that MEL significantly reduces proliferation and stimulates cytodifferentiation in HepG2 human hepatocarcinoma cells, these effects being antagonized by the exposure to 50 Hz, 10 µT MF. Conversely, the MF increases the growth rate of HepG2 when administered alone, but not in the presence of MEL. The present work investigates whether gap junctional intercellular communication (GJIC) could be involved in the described MF/MEL responses. Connexin32 (Cx32) expression (Immunocytochemistry - Image analysis) and functional GJIC (Parachute technique) have been analyzed in cultures exposed to the following conditions: Control, MEL (10 nM), MF (50 Hz, 10 µT) and MEL + MF. The results show that MEL stimulates dye transfer and induces expression of Cx32. Both effects are inhibited by the simultaneous exposure to MF. Therefore, the results suggest that previously reported antagonistic effects of MEL/MF in the proliferation and/or differentiation of HepG2 could be mediated by modulation of Cx32 expression and functional GJIC.

INTRODUCTION

There is mounting evidence that the pineal gland's hormone melatonin (MEL) intervenes in the control of neoplastic processes in cells, animals and humans (Blask *et al.*, 1993; Stevens, 2005). Melatonin has been reported to inhibit cell proliferation in different tumor types, such as hepatoma and colon cancer from rodents (She *et al.*, 2004; Dakshayani *et al.*, 2005; Mei *et al.*, 2005) and to reduce the incidence and growth of chemically induced mammary tumors (Melancon *et al.*, 2005; Cos *et al.*, 2006a). Also, several studies addressing oncostatic effects of MEL in the human breast cancer cell line MCF-7 have shown that MEL can inhibit proliferation and the metastatic behavior in these cells (Cos *et al.*, 2006b). Although different mechanisms have been proposed to explain the potential ability of MEL to suppress tumor promotion and progression, the actual mechanisms responsible for the oncostatic capacities of this hormone remain unidentified. Recent experimental evidence suggests that MEL could also influence proliferative processes due to its oxidative function and free radical scavenging properties (reviewed by Vijayalaxmi *et al.*, 2004). In addition, MEL has been reported to affect processes involved in cell differentiation (Radio *et al.*, 2006), including the establishment of cell adhesion and cell contacts, (Cos and Fernández 2000). In previous works we have reported that MEL enhances junctional transfer in normal C3H/10t1/2 cells and in primary cultures of mouse hepatocytes (Úbeda *et al.*, 1995a; Blackman *et al.*, 2001a). These results suggest that melatonin could exert its antitumoral action, at least in part, by modulating the levels of gap junctional intercellular communication (GJIC).

On the other hand, a number of *in vivo* studies have shown that extremely low frequency (ELF) magnetic fields (MF) can influence the development of tumor-promoting processes (reviewed by Loscher and Mevissen, 1994; Fedrowitz *et al.*, 2004) and alter MEL secretion by the pineal gland (reviewed by Reiter, 1994; Henshaw and Reiter 2005). The results of different studies suggest that ELF MF-induced reduction of MEL levels in the circulating blood could be determinant to the tumor promoting action of these fields. In vitro, 60/50 Hz MF have been reported to block Melatonin-induced inhibition of cell proliferation in human breast cancer MCF-7 cells (Liburdy 1993; Blackman *et al.*, 2001b; Ishido *et al.*, 2001). The HepG2 cell line has been extensively used for studying the mechanisms of action of a wide spectrum of potential carcinogens including ELF MF, which have been shown to promote proliferation in these cells (Trillo *et al.*, 2001). Moreover, previous studies by our group have shown that MEL significantly reduces proliferation and stimulates cytodifferentiation in HepG2 cells, these effects being antagonized by the exposure to 50 Hz, 10 µT MF. Conversely, when administered alone, the MF increased the growth rate in HepG2, whereas the presence of

MEL in the medium blocked such a cellular response (Cid *et al.,* 2004; Cid *et al.,* 2005). The present work investigates whether gap junctional intercellular communication could be involved in the previously described MF/MEL antagonistic responses on the proliferation or differentiation of HepG2. For that purpose the functionality of GJIC and the expression of connexin32 (Cx32) were analyzed on samples exposed to 50 Hz, 10 µT MF and/or treated with 10 nM MEL.

MATERIAL AND METHODS

Cell culture

HepG2 human hepatocarcinoma cells (ECACC, TDI S. A., Madrid) were cultured in Dulbecco's-Eagle modified medium (DMEM; Bio-Whittaker) supplemented with 5% heat-inactivated Fetal Bovine Serum (FBS, GIBCO), 10% Glutamine, and 10% penicillin/streptomycin (GIBCO), in water-jacket incubators (Forma Scientific) at 5% CO_2, 37 ºC and 100% RH atmosphere.

MF exposure

The exposure set-up used in these experiments was reproduced from that described by Blackman *et al.,* (1993). Each exposure system consisted of two identical sets of two 1000-turn, 20-cm-diameter coils of enameled wire, aligned coaxially 10 cm apart, in a Helmholtz configuration, and oriented to produce vertically polarized magnetic fields. Each set of coils was kept inside a magnetically shielded chamber (co-netic metal; Amuneal Corp., Philadelphia, PA) placed inside a CO_2 incubator (Forma Scientific). The generating (Newtronic Model 200MSTPC, Madrid, Spain) and monitoring (Hewlet Packard, 974A, Loveland CO) equipment was connected to the coils. The flux density and electromagnetic background in the exposure area were measured and recorded before and after the experiment with a fluxgate magnetometer (EFA-3, Wandel & Golterman GMW & Co. Germany). The background MF inside the shielded chambers was AC: 0.04 ± 0.03 µT, DC: 0.05 ± 0.04. In each experimental run only one of the two sets of coils was energized. The samples in the unenergized set were considered sham-exposed controls. Both incubators were used, in a random sequence, alternatively for MF exposure and sham-exposure. The MF exposure parameters were chosen on the basis of our previous observations (Trillo *et al.,* 2001; Trillo *et al.,* 2003; Martínez et al., 2006), which revealed that a 42-h exposure to a sinus wave 50 Hz intermittent (3-h On/3-h Off) MF at 10 µT significantly stimulates cell growth in both, the HepG2 human hepatocarcinoma cell line and the NB69 human neuroblastoma cell line.

GJIC assay: Parachute and Flow cytometry techniques

The GJIC was examined through a two-dye method based on the parachute technique, previously described by Goldberg *et al.* (1995). This technique is currently used to detect and quantify GJIC functionality in different cellular systems (Czyz *et al.,* 2000; reviewed by Fonseca *et al.,* 2006). The high sensitivity of this method allows for detection of small changes in functionality of GJIC by examining a large number of cells in a single experimental run. In our experiments, the samples were seeded at a density of 10 x 10^4 cells/ml. After allowing for cell attachment (4 hours post-plating) the dishes were distributed in two groups and an initial dose of Melatonin (N-acetyl-5-methoxy-tryptamine, Sigma) was added to one of the two groups. At the end of day 3 postplating the medium was renewed and a second dose of MEL was administered to the previously treated group. At this time both groups, with or without MEL, were divided in sham-exposed and MF-exposed samples. The cells were subjected to: a) no treatment: controls, b) treatment with MEL, c) exposure to MF, and d) MF exposure imposed upon MEL treatment. The MF-exposed samples were treated intermittently, 3h On/3h Off, with a 50 Hz, 10 µT MF for 24 h. At the end of day 4, when cells were close to confluence, all the samples were distributed into two groups: the recipient and the donor group. The group of recipient cells was pre-stained with a permanent, non-toxic lipophilic dye that binds to membranes irreversibly, DiI (1-1´dioctadecyl-3,3,3´,3´-tetramethylindocarbocyanine perchlorate; Molecular Probes). The donor population was treated with a gap junction-permeable dye Calcein, a derivative of Calcein acetoxymethyl ester (Calcein-AM, Molecular Probes). After seeding the donor cells on the corresponding recipient samples under conditions promoting gap junction (GJ) formation, the four experimental groups were exposed and/or incubated for an additional 18 h lapse. At the end of this period the samples, two per experimental condition: Control, MEL, MF and MEL + MF, were analyzed by flow cytometry (Cell Quest software) and the percent of cells showing both dyes (Cal+ / DiI+ events) vs. the total Cal+ events, were determined. A total of 20,000 events per sample were recorded. Two additional samples were used to establish the basal level of fluorescence.

Cx32 expression assay

The Cx32 expression was estimated as the percent of Cx32 positive cells by immunochemistry and Computer-Assisted Image-Analysis. The methodology used for treatments with MEL and/or MF has been described previously by Cid *et al.* (2004). In short, cells were seeded at a density of 9.5 x 10^4 cells/ml on 12 mm ∅

coverslips sited into the Petri dishes. Additional Petri dishes were used to test viability and cell proliferation. A total of 12 or 20 dishes, to obtain 3 or 5 plates, per experimental condition: Control, Melatonin, MF and Melatonin + MF, were assayed. After allowing for cell attachment to the coverslips (4 hours post-plating) the dishes were distributed in two groups and an initial dose of Melatonin was added to one of the two groups. At day 3 post-plating the medium was renewed, and a second treatment with MEL was administered in the previously treated group. Each of the two groups, treated with MEL or untreated, was distributed in sham-exposed and MF-exposed samples. The MF-exposed samples were treated intermittently, 3h On/3h Off, with a 50 Hz, 10 μT MF for 42 h. At the end of this period the cells were tested for appropriate viability and cell proliferation before being processed for analysis of connexin32. Cells on coverslips were fixed with periodate-lysine-paraformaldehyde (PLP). After washing with PBS, cells were permeabilized, (acetone 50%) and the endogen peroxidase was inactivated (H_2O_2 3%.) The non-reactive sites were blocked (FCSi 10%, Triton X-100 0.05% in PBS) for 1 h at room temperature. Then, the samples were incubated for 24 h at 4 ºC with a monoclonal antibody against the central cytoplasmic loop of human Cx32 (IgG clone M12.13; Chemicon Int.), dilution 1:200, in FCSi 5% / Triton X-100, 0.15% / PBS. Immunostaining was enhanced through the ABC method (Vectastain ABC Elite kit, Vector Laboratory, Burlingame CA), and revealed with the peroxidase substrate, diaminobenzidine tetrahydrochloride (DAB). The nuclei were counterstained with Hematoxiline. Background controls without the primary antibody were also included in the study. The samples were visualized and evaluated through a photomicroscope. Two coverslips per experimental condition were randomly chosen and a total of 20 microscope fields per coverslip were analyzed. The quantification of the immunolabeling was carried out through Computer Assisted Image-Analysis (IPWin and AnalySIS software). The ratio of Cx32 positive cells vs. total cells per microscope field was determined. Additional analysis taking into account the total immunostaining area of Cx32 vs. total cells per microscope field was carried out.

RESULTS

GJIC functionality in samples exposed to MF in the presence or the absence of MEL

Previous studies by our group showed that a dose of 10 nM MEL was effective inducing decreases in cell proliferation and in the promotion of differentiation in HepG2. These effects were antagonized by the exposure to 50 Hz, 10 μT MF (Cid *et al.*, 2004; Cid *et al*., 2005). On that basis, in the present study the concentration 10 nM MEL was assayed to study the functional GJIC in cells exposed to 50 Hz 10 μT MF in the presence or absence of MEL. The parachute technique revealed that untreated HepG2 cells (control condition) exhibit a low degree of junctional activity. However, the presence of 10 nM MEL in the medium increases significantly the coupling rate (17.7 ± 0.4 % over controls $p<0.01$) in these cells (Fig. 1). In contrast, the coupling response to the MF exposure did not differ significantly from that in controls, both in the presence and in the absence of MEL; which reveals that the 10 μT MF, per se, does not change the functional GJIC in HepG2, but can block the MEL-induced coupling in these cells.

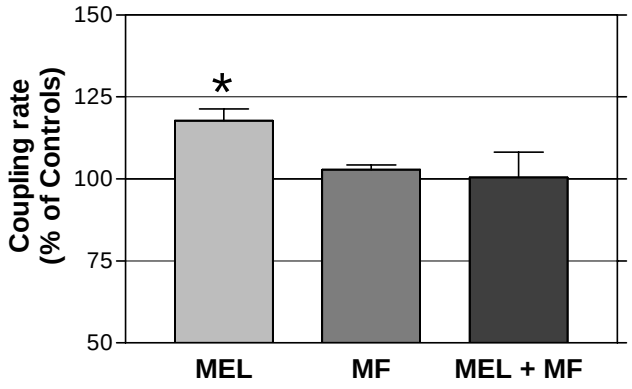


Fig. 1. The functional GJIC was measured as the percent of cells showing both dyes (Cal+ / DiI+ events) over the total Cal+ events. Coupling rate in the different conditions tested, Control, MEL, MF and the combined treatment, MEL + MF. The MEL-induced coupling was antagonized by the exposure to MF. Data normalized over controls N = 4 experiments. Mean ± SEM *, $p< 0.05$ (ANOVA followed by Student's T test).

Cx 32 expression in samples exposed to MF in the presence or the absence of MEL

The effect of the treatments with MEL and/or MF on the Cx32 expression and on its subcellular distribution was determined through Computer Assisted Image-Analysis. The analysis was focused on the expression of Cx32 because changes in both, the amount and distribution of this connexin have been suggested to be implicated in human hepatocarcinogenesis (Nakashima *et al.,* 2004), and increases in Cx32 expression induce phenotypic normalization in HepG2 (Yang *et al.,* 2003), whereas decreases in Cx32 seem to be linked to cell proliferation and progression in rodent hepatocarcinomas (Temme *et al.,* 1997). In the untreated cells the Cx32 expression presents an abnormal localization and distribution when compared to normal hepatocytes (data not shown). This abnormal pattern of expression consists on an increased cytoplasmic accumulation, either distributed in vesicular structures or presenting a diffuse appearance located generally in the perinuclear zone. The cytoplasmic membrane presents little expression of Cx32, with no immunoreactive gap junctional plaques. This aberrant pattern of Cx32 expression in HepG2 cells was not modified by the exposure to MF or by the MEL treatment. However, in MEL treated samples a significant increase (32.9 ± 0.9 % over controls, $p< 005$) in the percent of cells expressing cytoplasmic Cx32 immunostaining was observed at day 5 of treatment (Fig 2). In contrast, the response to MF alone or to the combined treatment (Mel + MF) was similar to that observed in controls. These data reveal that, when applied alone, the MF did not exert significant effects on Cx32 expression or on functional GJIC. However, when applied on MEL treated samples, the MF exposure antagonized the MEL-induced responses. Preliminary data (not shown) on immunoblot for Cx32 confirm these results.

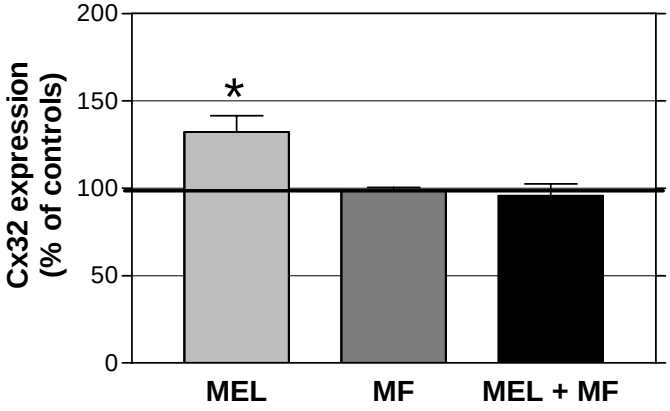


Fig. 2. Percent of Cx32 positive cells, quantified by the Image Analysis software IPWin, in the different experimental conditions tested. The treatment with 10 nM MEL increased significantly the percent of cells expressing Cx32. This response was counteracted by the exposure to 50 Hz, 10 µT MF. Data normalized over controls, Mean ± SEM of 4 experimental replicates; *, $p< 0.05$ (ANOVA followed by Student's T test.)

DISCUSSION

Previously reported results by our group have shown that MEL significantly reduces proliferation and stimulates cytodifferentiation in HepG2 human hepatocarcinoma cells; these effects being antagonized by the exposure to sinusoidal 50 Hz, 10 µT MF. Conversely, the MF increases the growth rate of HepG2 when administered alone, but not when in the presence of MEL (Cid *et al.,* 2004; Cid *et al*., 2005). It is currently believed that a tight regulation of gap junctional intercellular communication mediated by connexins may contribute to cell growth and differentiation by keeping important signals, such as those involved in growth control, at equilibrium among gap junction-connected cells. The present work investigates whether gap junctional intercellular communication could be involved in the MF/MEL responses described before. The results of the present work show that untreated, control HepG2 cells have a low degree of junctional activity and an aberrant expression of Cx32. However, the treatment with MEL increases the functional GJIC and the percent of cells that express the gap-junctional protein Cx32 in HepG2. On the other hand, although the exposure to MF alone does not exert any significant influence on these junctional processes, when applied on MEL-treated cells the MEL-induced responses on the functionality of GJIC and on Cx32 expression were abolished.

The stimulating effect of MEL on GJIC functionality has been well described in a variety of cell lines. Úbeda *et al.* (1995a) reported that physiological concentrations of MEL between 0.01 and 0.1 nM, induce significant increases in the junctional transfer of mouse normal fibroblast C3H/10T1/2. Blackman *et al.* (2001a)

found similar results in primary cultures of mouse hepatocytes treated with MEL at the physiological doses of 0.2 and 0.4 nM. In the present study, the HepG2 human hepatocarcinoma line also responded with significant increases of the coupling rate (parachute technique) when treated with a concentration (10 nM) higher than the above described as effective in normal, non-cancer cells. Even higher, pharmacological concentrations of MEL (10 µM) have been reported to efficiently increase GJIC functionality in the breast cancer cell line MCF-7 (Cos and Fernandez 2000). Taken together, these results are consistent with the hypothesis that cancer lines are, in general terms, less sensitive to MEL than normal cells.

It has been well established that the restoration of connexin expression in tumor cells often leads to a partial reversion of the tumoral phenotypes and to increased growth control (King and Lampe 2004). Like reported by other authors working with poorly differentiated hepatocarcinomas (Krutovskikh *et al.*, 1994), an aberrant pattern of Cx32, mainly cytoplasmic and diffuse, was observed in the present study in the HepG2 line. This may represent a general pattern in hepatocarcinoma cells, potentially due to the presence of abnormalities in the intracellular transport of Cx32, in the exportation of this connexin to the cell membrane, in the process of formation of GJIC plaques or in the recycling of the connexons. All these alterations would provoke the retention of the Cx32 in compartments of the endoplasmic reticulum, Golgy or lysosomes (Segretain and Falk 2004). In the present study, the MEL treatment stimulated the Cx32 expression. However, the connexin remained in the cytoplasm and did not stimulate the formation of GJ plaques in cell membranes. Moreover, growing experimental evidence supports the hypothesis that connexins can exert by themselves anti-proliferative effects that are independent of their functionality in intercellular communication. Such effects have been observed in a number cellular types including, glioma C6 (Bond *et al.*, 1994), bladder carcinoma BC31, (Krutovskikh *et al*., 2000) and the breast cancer line MDA-MB-231 (Qin *et al*., 2002). Although the mechanism responsible for the described effect remains unknown, some authors have suggested that interactions with transcription factors and regulation of gene expression of specific proteins, like the cell cycle regulator p27 could be involved in the effect (review, Jiang and Gu 2005). Consequently, the effects of MEL in the GJIC functionality and in the expression of Cx32 observed in the present work could be responsible, at least in part, for the antiproliferative and differentiating actions exerted by MEL in the same, HepG2 cell line (Cid *et al.*, 2004; Cid *et al*., 2005.)

Although a number of in vivo and in vitro studies have described MEL/MF interactions on the growth and/or differentiation, the mechanisms responsible for the these interactions remain unknown. In the present study, the exposure to a 50 Hz, 10 µT MF did not influence significantly the functionality of the GJIC or the Cx32 expression in the absence of MEL. However, in MEL-treated samples, the exposure to the MF abolished the stimulating effect of MEL on the gap junctional activity and on the expression of Cx32. These results are consistent with those previously reported by our group (Úbeda *et al.*, 1995b) showing that a 30-minute exposure to a 50 Hz, 1.6 mT MF blocks MEL-induced increase in GJIC in C3H/10T1/2 cells. Úbeda and coworkers proposed that the MF could influence the regulation of the permeability of the GJ channels and/or the channels' renovation. Other authors have suggested that the MF could exert an influence on signal transduction pathways that regulate the cell cycle, through modifications in the functionality of cell membrane receptors, including the MEL receptors (Ishido *et al.*, 2001). Thus, in the present study, the antagonistic effects exerted by MF on the cellular responses to MEL could be due to a blocking of the MEL's stimulatory actions at different levels including GJIC regulation and signal transduction pathways that regulate the cell cycle.

SUMMARY

In the present work we studied the effects of a 50 Hz 10 µT magnetic field on melatonin-induced responses on GJIC. The HepG2 human hepatocarcinoma cell line has been previously shown by our group to be responsive to a 50 Hz, 10 µT MF, which acts on these cells as a promoter of proliferation when administered alone, but not in the presence of MEL. Conversely, MEL reduces the growth rate of HepG2 and the field antagonizes such a response. The present results show that at a 10 nM concentration the neurohormon melatonin stimulates GJIC and Cx32 expression in HepG2, a cell line that exhibit a low degree of functional GJIC and an aberrant expression of Cx32. On the other hand, the exposure to MF alone does not influence the GJIC parameters, but blocks the MEL-induced responses on GJIC. Consequently, the herein reported effects of MEL in the GJIC functionality and in the expression of Cx32 could be responsible, at least in part, for the antiproliferative and differentiating actions exerted by MEL in the same HepG2 cell line (Cid *et al*., 2004*; Cid et al*., 2005). Besides, the antagonistic effects exerted by MF on the cellular responses to MEL could be due to a blocking of the MEL's stimulatory actions at different levels including GJIC regulation and signal transduction pathways that regulate the cell cycle.

Supported by FISS-03/0806 and Project I+T under agreement MOU EUROPA, ERG 101.013.

REFERENCES

Blackman C.F., Benane S.G., House D.E. and Pollock M.M. 1993. Action of 50 Hz magnetic fields on neurite outgrowth in pheochromocytoma cells. Bioelectromagnetics 14(3): 273-86.

Blackman C.F., Andrews P.W., Úbeda A., Wang X., Trillo M.A. and Pimentel M.E. 2001a. Physiological levels of melatonin enhance gap junction communication in primary cultures of mouse hepatocytes. Cell Biology and Toxicology. 17: 1-9.

Blackman C.F., Benane S.G. and House D.E. 2001b. The influence of 1.2 microT, 60 Hz magnetic fields on melatonin- and tamoxifen-induced inhibition of MCF-7 cell growth. Bioelectromagnetics. 22(2): 122-8.

Blask, D.E. 1993. Melatonin in oncology. In Yu, H.-S. and Reiter, R.J. (eds.) Melatonin, Biosynthesis, Physiological Effects and Clinical Applications. CRC Press, Boca Raton, pp. 448-475.

Bond S.L., Bechberger J.F., Khoo N.K. and Naus C.C. 1994. Transfection of C6 glioma cells with connexin 32. The effects of a non endogenous gap junction protein. Cell Growth Differ 5: 179-186.

Cid M.A., Martínez M.A., Úbeda A., Chacón L., Leal J. and Trillo M.A. 2004. Melatonin at a physiological concentration inhibits power frequency magnetic field-induced growth in human hepatocarcinoma cells. 11th International Congress of the International Radiation Protection Association (IRPA), 23-28 May Madrid, Spain. Abstract Book: 310.

Cid M.A., Úbeda A., Henández-Bule M.L., Martínez M.A., Díaz-Enriquez M., Leal, J. and Trillo M.A. 2005. Power frequency magnetic fields block melatonin-induced changes in alpha-fetoprotein and albumin in human hepatocarcinoma cells. Meeting of The Bioelectromagnetics Society and The European BioElectromagnetics Association. June 19 – 24; University College. Dublin, Ireland. Abstract Book: 316.

Cos S. and Fernandez R. 2000. Melatonin effects on intercellular junctional communication in MCF-7 human breast cancer cells. J Pineal Res 29: 166-171.

Cos S., González A., Guezmes A., Mediavilla M.D., Martínez-Campa C., Alonso-González C. and Sánchez-Barceló E.J. 2006a. Melatonin inhibits the growth of DMBA-induced mammary tumors by decreasing the local biosynthesis of estrogens through the modulation of aromatase activity. Int J Cancer 118(2): 274-8.

Cos S., González A., Martines-Campa C., Mediavilla M.D., Alonso-González C. and Sánchez-Barceló E.J. 2006b. Estrogen-signaling pathway: A link between breast cancer and melatonin oncostatic actions. Cancer Detect Prev 30(2): 118-28.

Czyz J., Irmer U., Schulz G., Mindermann A. and Hulser D.F. 2000. Gap-junctional coupling measured by flow cytometry. Exp Cell Res 255(1): 40-6.

Dakshayani K.B., Subramanian P., Manivasagam T., Essa M.M. and Manoharan S. 2005. Melatonin modulates the oxidant-antioxidant imbalance during N-nitrosodiethylamine induced hepatocarcinogenesis in rats. J Pharm Pharm Sci 8(2): 316-21.

Fedrowitz M., Kamino K. and Loscher W. 2004. Significant differences in the effects of magnetic field exposure on 7,12-dimethylbenz(a)anthracene-induced mammary carcinogenesis in two substrains of Sprague-Dawley rats. Cancer Res 64(1): 243-51.

Fonseca P.C., Nihei O.K., Savino W., Spray D.C. and Alves L.A. 2006. Flow cytometry analysis of gap junction-mediated cell-cell communication: advantages and pitfalls. Cytometry A 69(6): 487-93.

Goldberg G.S., Bechberger J.F. and. Naus C.C. 1995. A pre-loading method of evaluating gap junctional communication by fluorescent dye transfer. Biotechniques 18: 490-497.

Henshaw D.L. and Reiter R.J. 2005. Do magnetic fields cause increased risk of childhood leukemia via melatonin disruption? Bioelectromagnetics (Suppl 7): S86-97.

Ishido M. Nitta H, and Kabuto M. 2001. Magnetic fields (MF) of 50 Hz at 1.2 μT as well as 100 μT cause uncoupling of inhibitory pathways of adenylyl cyclase mediated by melatonin 1a receptor in MF-sensitive MCF-7 cells. Carcinogenesis 22: 1043-1048.

Jiang J.X. and Gu S. 2005. Gap junction- and hemichanel-independent actions of connexins. Biochim Biophys Acta 1711: 208-214.

King T.J. and Lampe P.D. 2004. Mice deficient for the gap junction protein Connexin32 exhibit increased radiation-induced tumorigenesis associated with elevated mitogen-activated protein kinase (p44/Erk1, p42/Erk2) activation. Carcinogenesis 25(5):669-80.

Krutovskikh V., Mazzoleni G., Mironov N., Omori Y., Aguelon A-M., Mesnil M., Berger F., Partensky C. and Yamasaki H. 1994. Altered Homologous And Heterologous Gap-Junctional Intercellular Communication In Primary Human Liver Tumors Associated With Aberrant Protein Localization But Not Gene Mutation Of Connexin 32. Int. J. Cancer 56: 87-94.

Krutovskikh V.A., Troyanovsky S.M.,Piccoli C., Tsuda H., Asamoto M. and Yamasaki H.. 2000. Differential effect of subcellular localization of communication impairing gap junction protein connexin43 on tumor cell growth in vivo. Oncogene 19: 505-513.

Liburdy,R.P. (1993) ELF magnetic fields, breast cancer and melatonin: 60 Hz fields block melatonin's

oncostatic action on ER+ breast cancer cell proliferation. J Pineal Res 14, 89–97.
Loscher W. and Mevissen M. 1994. Animal studies on the role of 50/60-Hertz magnetic fields in carcinogenesis. Life Sci 54(21): 1531-43.
Martínez M.A., Cid M. A., Úbeda A.,. García V. J., Leal J., and Trillo M.A. 2006. A role of ERK signaling in the proliferative effects of 50 Hz magnetic fields on human neuroblastoma cells. The 4th International Workshop on Biological Effects of Electromagnetic Fields. 16-20 October, Crete, Greece.
Mei Q., Xu J.M., Xiang L., Hu Y.M., Hu X.P. and Xu Z.W. 2005. Change of nitric oxide in experimental colitis and its inhibition by melatonin in vivo and in vitro. Postgrad Med J 81(960): 667-72.
Melancon K., Cheng Q., Kiefer T.L., Dai J., Lai L., Dong C., Yuan L., Collins A., Thiyagarajah A., Long S., and Hill S.M. 2005. Regression of NMU-induced mammary tumors with the combination of melatonin and 9-cis-retinoic acid. Cancer Lett 227(1): 39-48.
Nakashima Y., Ono T., Yamanoi A., El-Assal O.N., Kohno H. and Nagasue N. 2004. Expression of gap junction protein connexin32 in chronic hepatitis, liver cirrhosis, and hepatocellular carcinoma. J Gastroenterol 39(8): 763-8.
Qin H., Shao Q., Curtis H., Galipeau J., Delliveau D.J., Wang T., Alaoui-Jamali M.A. and Laird D.W. 2002 Retroviral delivery of connexin genes t human breast tumor cells inhibits in vivo tumor growth by a mechanism that is independent of significant gap junctional intercellular communication. J. Biol Chem 277: 29132-29138.
Radio N.M., Doctor J.S. and Witt-Enderby P.A. 2006. Melatonin enhances alkaline phosphatase activity in differentiating human adult mesenchymal stem cells grown in osteogenic medium via MT2 melatonin receptors and the MEK/ERK (1/2) signaling cascade. J Pineal Res 40(4): 332-42.
Reiter R.J. 1994. Melatonin suppression by static and extremely low frequency electromagnetic fields: relationship to the reported increased incidence of cancer. Rev Environ Health 10(3-4): 171-86.
Segretain D. and Falk M.N. 2004. Regulation of connexin biosynthesis, assembly, gap junction formation and removal. Biochim Biophys Acta 1662: 3-21.
She M.H., Chen B.B., Wang X.M. and He S.S. 2004. p53-dependent antiproliferation and apoptosis of H22 cell induced by melatonin. Ai Zheng 23(7): 803-7.
Stevens R.G. 2005. Circadian disruption and breast cancer: from melatonin to clock genes. Epidemiology 16(2): 254-8.
Temme A., Buchmann A., Gabriel H.D., Nelles E., Schwarz M. and Willecke K. 1997. High incidence of spontaneous and chemically induced liver tumors in mice deficient for connexin32. Curr Biol 7(9): 713-6.
Trillo M.A., Martínez M.A., Cid M.A., Úbeda A., García V.J., Chacón L. and Leal J. 2001. Influence of 50 Hz magnetic fields on the proliferation of human hepatocarcinoma cells in vitro. BEMS, Twenty-Third Annual Meeting, St. Paul, Minnesota, June 10-14, Abstract Book: 211.
Trillo M.A., Martínez M.A., Cid M.A., García V.J., Ubeda, A. and Leal, J. 2003. Action of 50 Hz magnetic fields on the growth of human neuroblastoma cells. 25th BEMS Meeting, Maui, Hawaii, Abstract Book: 287.
Úbeda A., Trillo M.A., House D.E., and Blackman C.F. 1995a. Melatonin enhances junctional transfer in normal C3H/10T1/2 cells. Cancer Lett 91: 241-245.
Úbeda A., Trillo M.A., House D.E., and Blackman C.F. 1995b. A 50 Hz magnetic field blocks melatonin-induced enhancement of junctional transfer in normal C3H/10T1/2 cells. Carcinogenesis 16: 2945-2949.
Vijayalaxmi, Reiter R.J., Tan D.X., Herman T.S. and Thomas C.R. Jr. 2004. Melatonin as a radioprotective agent: a review. Int J Radiat Oncol Biol Phys 59(3): 639-53.
Yang J., Ichikawa A., and Tsuchiya T. 2003. A novel function of connexin 32: marked enhancement of liver function in a hepatoma cell line. Biochem Biophys Res Commun 307: 80-85.

A DETAILED ANALYSIS OF THE ELECTRICAL DYNAMICS OF THE HODGKIN-HUXLEY CELLULAR MODEL INCLUDING ELECTROPORATION

N. CITRO[*], V. TUCCI [**]

[*] DEPT. OF ELECTRICAL AND INFORMATION ENGINEERING, UNIVERSITY OF SALERNO NCITRO@UNISA.IT

[**] DEPT. OF ELECTRICAL AND INFORMATION ENGINEERING, UNIVERSITY OF SALERNO VTUCCI@UNISA.IT

Abstract

Electro-permeabilization of biological cells has been proposed as a very efficient method in medicine for gene therapy, cancer chemotherapy, and drug delivery. Although the molecular processes involved in the permeabilization mechanisms are very complex, the formation of "pores" in the plasma membrane, under the influence of an electric field, is deemed responsible of the cellular responses. The model accuracy is crucial to understanding the behaviour of the cell. It must include the majority physical phenomena in order to obtain realistic results from the numerical scheme approximating the theoretical model (circuital or field based). In this work an improved electrical model of the cellular membrane is presented taking into account the electro-permeabilization phenomena occurring under the action of electrical impulses. In particular, the presented model consists of a modified Hodgkin-Huxley–type non linear equivalent circuit for the cell membrane. The electroporation phenomena are considered by introducing a controlled current source in the basic model. The global cellular dynamics is examined for different characteristics (amplitudes, duration, rise and fall time) of the applied electrical pulses. The trans-membrane voltage and the conduction dynamics of the ionic channels are evaluated through an efficient simulation procedure.

Introduction

Since its introduction the conceptually simple model of the cell membrane behaviour, firstly proposed by Hodgkin and Huxley (HH) [1], has been widely studied in order to describe a wide class of biological phenomena associated to the transmission of information in excitable cells systems (see for example [2-3]. The HH approach has been employed to model electrical activation in a range of cell types including neurons [4], [5], ventricular myocytes [6], smooth muscles [7], etc. Although several studies have put in evidence that the HH model needs some improvements, its simplicity and efficiency in describing significant properties of the biological processes still motivate its use in medicine, biology, bioengineering etc.

The physical mechanisms allowing the development of excitable cell signal dynamics are based on the mutual interactions among ionic currents flowing through the membrane. The flux of the different ionic species taking place through channels across the cellular membrane is considered as a time continuous, deterministic and voltage-dependent phenomenon driven by the potential difference across the membrane (Trans-Membrane Voltage, TMV).

From an electrical point of view the cell membrane can be effectively modelled as a lumped parameter circuit, as shown in fig. 1. The membrane is represented by a capacitance, the ionic channels as linear or nonlinear conductances and the voltage generators are linked to the so called Nernst equilibrium potential, determined by the ratio of the specific ionic concentrations inside and outside the cell.

The TMV dynamics in response to electrical stimuli has been extensively analyzed in the literature on the basis of such a circuit model, thus allowing to infer or verify many interesting properties of the cell behaviour. In some cases the applied

electrical pulses are such that the number and dimensions of the pores on the membrane may be affected giving rise to the so called phenomenon electroporation [8-10]. The increased pore density on the cell surface determines an additional current path which has been traditionally modelled by a current generator characterised by a constant value. However, since the modification of the pores number and dimensions is dependent on the instantaneous value of the TMV, a more accurate model can be envisaged in which the current injection associated to electroporation is taken into account by considering a voltage dependent instead of a constant current generator.
Therefore, in this paper an accurate analysis of the electrical dynamics of the Hodgkin-Huxley cellular model is performed. The modifications induced by the voltage dependent electroporation generator is studied for different values of the amplitude, duration, rise and fall time of the applied electrical stimulus applied to a cell. The dynamics of trans-membrane voltage and conduction currents associated to the ionic channels are evaluated through an efficient simulation procedure. It is worth remarking that the aim of this first work is exclusively oriented to the numerical analysis of the modified HH circuit. The biological implications on the cell behaviour due to the obtained numerical results, which require complex and multidisciplinary research efforts, will be developed in future works.

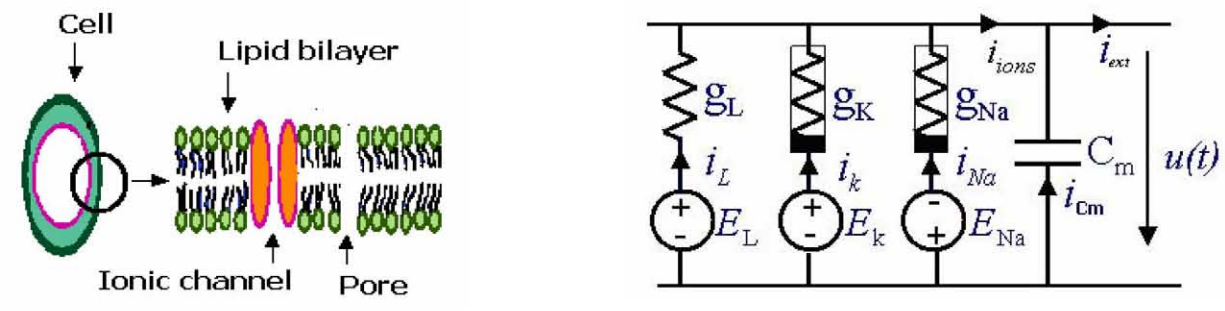


Fig. 1 Cell membrane and associated Hodgkin-Huxley circuit model.

Proposed circuit model including electroporation

In the electric circuit of Fig. 1, the total ionic currents $i_{ions}(u,t)$ can be expressed as:

$$i_{ions}(u,t) = i_{Na}(u,t) + i_K(u,t) + i_L(u,t) = \\ [g_{Na}^{\max} \cdot m^3(u,t) \cdot h(u,t) \cdot (u - E_{Na})] + [g_K^{\max} \cdot n^4(u,t) \cdot (u - E_K)] + [g_L^{\max} \cdot (u - E_L)] \quad (1)$$

where $g_c^{\max}$ (c=K, Na, L) is the maximum value of the conductance corresponding to the largest aperture of the channel, m (or n) and h are two nonlinear variables describing the activation or inactivation of the channel and p and q are suitable exponents depending on the ion type, E_c is the Nernst voltage and $u(t)$ is the trans-membrane voltage. The Nernst voltage is linked to the ratio of the external and internal ionic concentrations [C]: $E_c \propto \ln \frac{[C]_{ext}}{[C]_{int}}$. In Tab. 1 the values of the typical parameters are reported.
It has to be noted that all voltages are referred to the value E_R assumed at rest across the membrane.

Tab. 1

C_m [µF/cm^2]	E_R [mV]	E_{Na} [mV]	E_K [mV]	E_L [mV]	g_{Na}^{max} [mS/cm^2]	g_K^{max} [mS/cm^2]	g_L [mS/cm^2]
1.0	-75.0	E_R+15.0	E_R- 2.0	E_R+0.613	120.0	36.0	0.3

In order to describe the electroporation phenomenon, a voltage controlled current generator is introduced through a branch in parallel as shown in Fig. 2. It accounts for the ions exchange between an external cleft space around the cell where charge build-up and depletion occurs, and the cell interior.
Its influence in the charge dynamics across the cell can be particularly remarkable when the TMV assumes high values and for quasi static variation.

The charge flow, governed by the ions concentration gradient, can be modelled by a current I_{ep} given by:

$$I_{ep}=N\cdot i_{ep}= \quad N\cdot\left\{\frac{\pi\cdot r_m^2\cdot\sigma\cdot\upsilon_m\cdot R\cdot T}{F\cdot h}\cdot\frac{e^{\upsilon_m-1}}{w_0\cdot e^{w_0-n\upsilon_m}-n\cdot\upsilon_m\; e^{\upsilon_m}-\; w_0\cdot e^{w_0+n\upsilon_m}+n\cdot\upsilon_m}\right\}\qquad w_0-n\cdot\upsilon_m \qquad\qquad w_0+n\cdot\upsilon_m \tag{2}$$

where N is the pore density, r_m is the radius of the pore, σ is the conductivity of the fluid solution, F is the Faraday constant, R is the gas universal constant, T is the absolute temperature, h is the thickness of the cell membrane, w_0 and n are the energy gap and the length of the pore. $\upsilon_m = u(t)\left(\frac{F}{RT}\right)$ is the adimensional TMV. The pore density $N(t)$ is governed by a firs order differential equation:

$$\frac{dN(t)}{dt} = \alpha e^{\left(u(t)\ V_{ep}\right)^2}\left(1-\frac{N(t)}{N_0}e^{-q\left(u(t)\ V_{ep}\right)^2}\right) \tag{3}$$

where N_0 is the pore density for $u(t)$=0 and α, V_{ep} and q are suitable constants. In Tab. 2 the values adopted for the different quantities appearing in (2) and (3) are reported together with the initial condition considered for the integration of eq. (3).

Tab. 2

r_m [nm]	**h** [nm]	**s** [mS/cm]	**R** [mJ/molK]	**T** [°K]	**n**	**w_o**	**q**	**a** [$cm^{-2}s^{-1}$]	**V_{ep}** [mV]	**N_0** [cm^{-2}]	**N(t=0)** [cm^{-2}]	**F** [Coulomb/mol]
0.76	50.	13.0	8314.0	279.3	0.15	2.65	2.46	100.0	258.0	$1.5\text{x}10^5$	$1.7\text{x}10^5$	$9.6487\text{x}10^4$

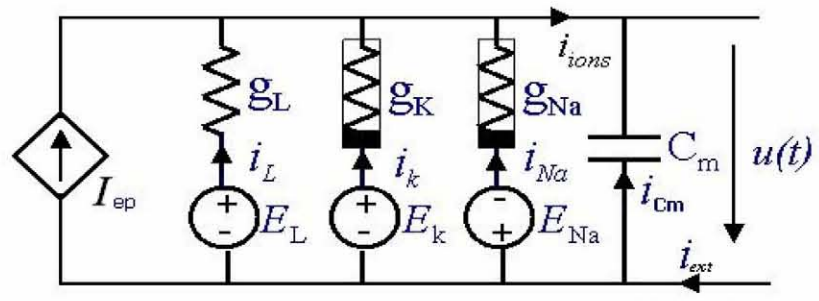


Fig. 2 Proposed circuit model including the electroporation generator

Numerical experiments and results

Kirchhoff current law applied to the circuit of Fig. 2 gives:

$$C_m\frac{du(t)}{dt} = i_{ext}-[I_{ep}+i_L+i_{Na}+i_k]$$

The dynamic evolution of the TMV and the different current can be determined by evaluating at each time step the unknowns the 5 unknowns *u, m, n, h, N:*

$$\mathbf{Y} = [m(u,t),\, h(u,t),\, n(u,t),\, u(t),\, N(t)]^{\mathrm{T}}$$

$$\begin{cases} \dfrac{d\,\mathbf{Y}}{dt} = \mathbf{f}(t, m, n, h, u, N) = \mathbf{f}(t, \mathbf{Y}) \\ \mathbf{Y}\big|_{t=0} = \mathbf{Y}_0 \end{cases} \tag{4}$$

$$\mathbf{Y}|_{\mathrm{t=0}} = \begin{bmatrix} m(u,0) \\ h(u,0) \\ n(u,0) \\ u(0) \\ N(0) \end{bmatrix} \qquad \mathbf{Y}_0 = \begin{bmatrix} m_\infty(E_r) \\ h_\infty(E_r) \\ n_\infty(E_r) \\ E_r \\ N(t=0) \end{bmatrix}$$

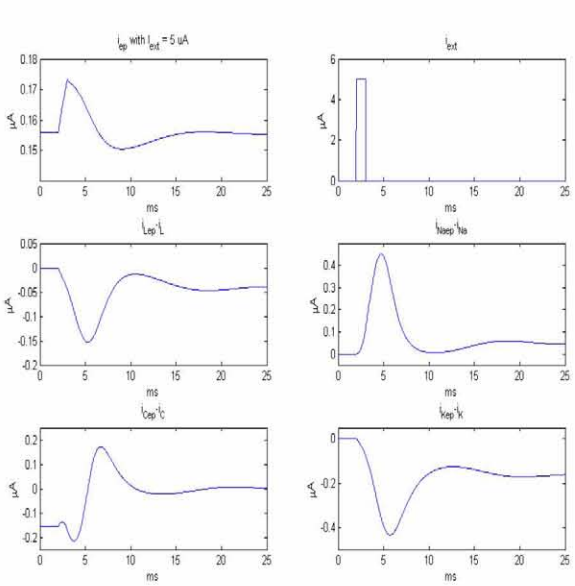
In order to solve the nonlinear equation system (4) a Runga-Kutta scheme has been implemented in a suitable numerical procedure written in C language. The effectiveness of such a numerical scheme has been proven in a previous work concerning a range analysis on a simpler circuit based on the HH model [11]

In order to envisage the influence of the electroporation generator on the TMV and different current components dynamics, the most relevant quantities appearing in the model have been calculated either with the classic HH model (i.e. the circuit of fig. 1) or with the modified one (i.e. the circuit of fig. 2). In particular, the different current components have been evaluated as a response to an applied external rectangular pulse i_{ext} characterised by a duration Δt=1ms and by variable amplitudes (I= 5, 7.5, 10, 15,20, 25, 30, 40 e 50μA).

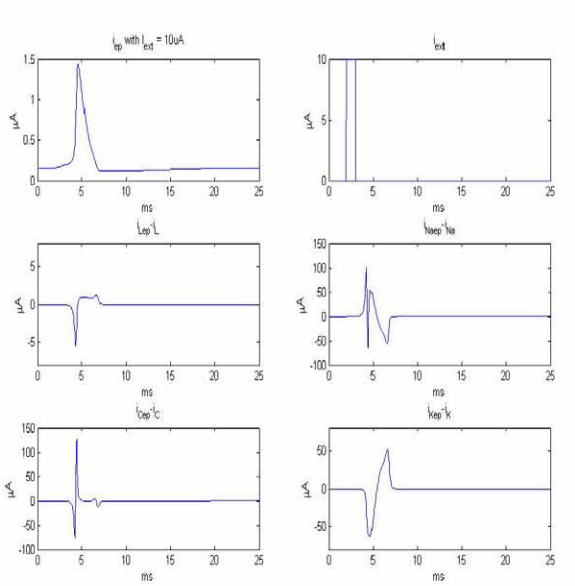
The effects of the electroporation generator is described by the plots of Figs 4, where the difference between the time evolution of the current components obtained in presence of such a generator (characterised by the suffix *ep*) or with the classic HH model are reported for the different values of the external current pulse.

As can be noted by the analysis of the presented simulation results, the greater influence of the electroporation generator is obtained for an applied pulse of 10μA where a very strong variation appears for ionic currents, especially those associated to Na and K channels, and for the displacement current i_{Cm} through the membrane. For greater values of the external pulse amplitude the presence electroporation current becomes weaker as it concerns all the considered variables. In fact the pulse of about 100 μA for i_{Cm} and i_{Na} corresponding to an external pulse of 10μA reduces of about one tenth for an applied current of 50μA. This findings are also summarised in Fig. 5, where the absolute value of the max discrepancies between the currents values obtained with or without the electroporation generator are presented.

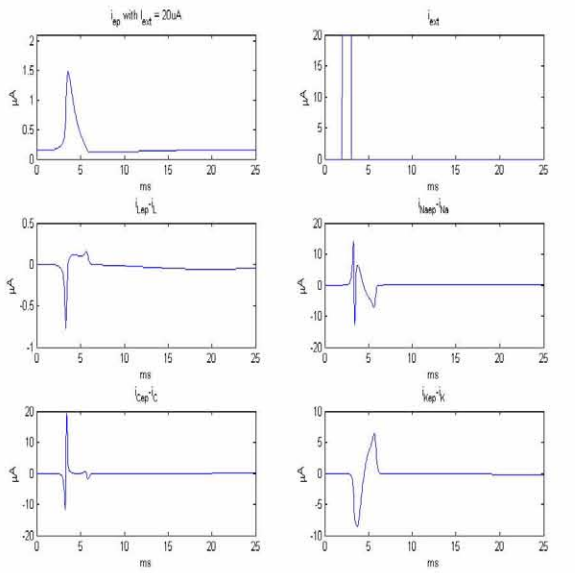
A similar influence can also be noted for the TMV, as can be evinced from the results shown in Fig. 6. Even for this variable the more sensible effect of the presence of the electroporation in limited to applied current pulses of about 10-15μA.



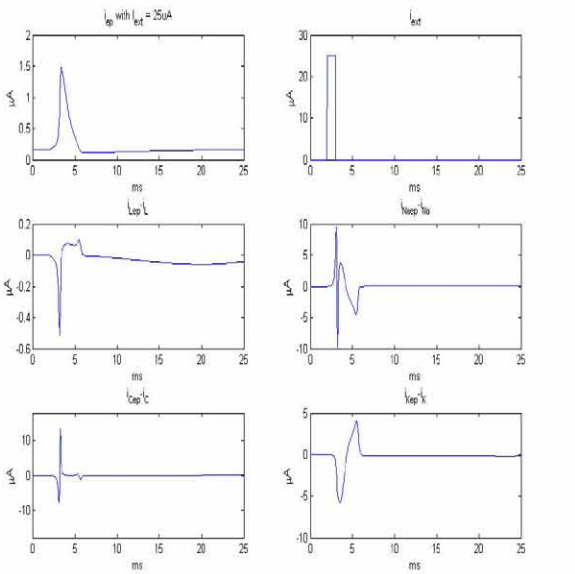
i_{ext}^{max} =5μA



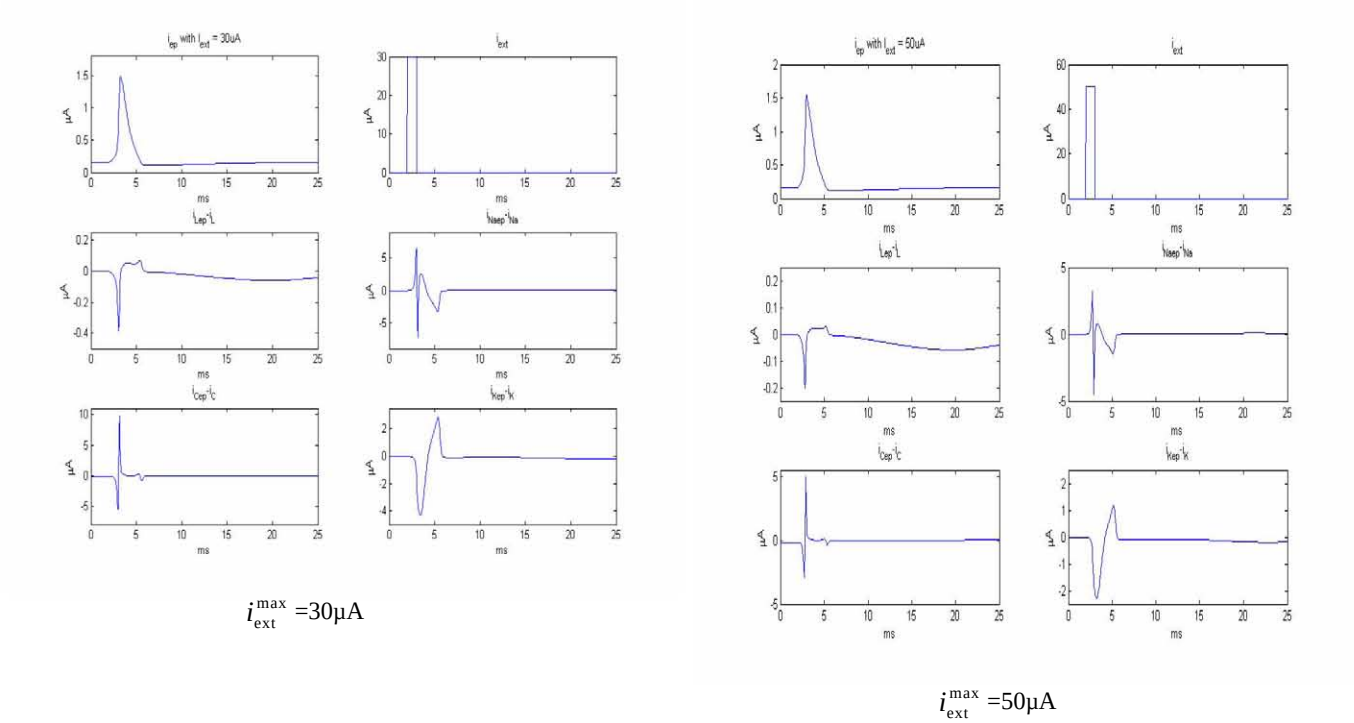
i_{ext}^{max} =10μA



i_{ext}^{max} =20μA



i_{ext}^{max} =25μA



i_{ext}^{max} =30μA

i_{ext}^{max} =50μA

Fig. 4: Difference between the time evolution of the ecurrent components induced by the presence of the electroporation generator for the different values of the external current pulse.

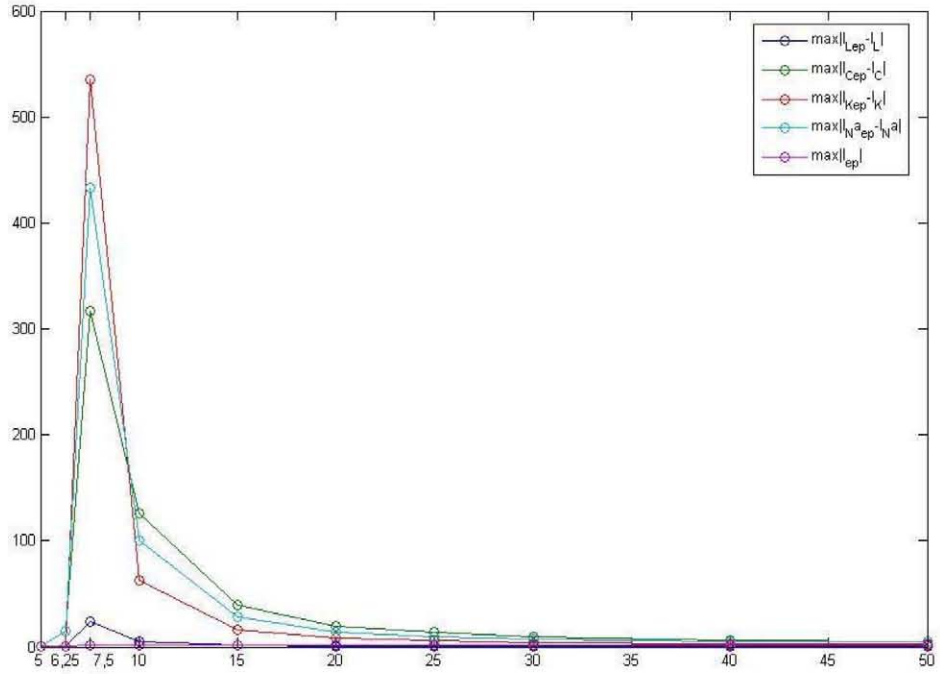


Fig. 5 Max discrepancies between the absolute values of the different currents obtained with and without the electroporation generator

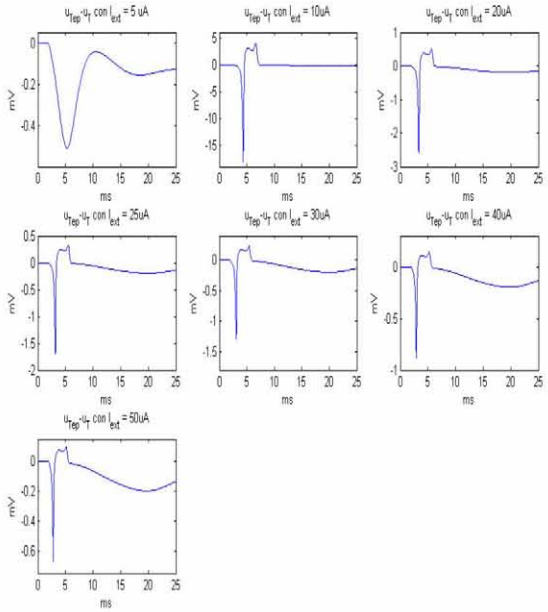


Fig. 6 Differences between the time evolution of the TMV induced by the presence of the electroporation generator for the different values of the external current pulse.

Conclusions

In this paper an analysis of the electrical dynamics of a modified Hodgkin-Huxley cellular model which takes into account the electroporation phenomenon has been performed. The modifications induced by a voltage dependent current generator emulating the electroporation has been studied for different values of the amplitude, of the applied electrical stimulus applied to a cell.

The dynamics of trans-membrane voltage and conduction currents associated to the ionic channels obtained by adopting an efficient simulation procedure put in evidence that the electroporation phenomenon is effective for moderate values of the applied current stimulus. The peak effect is obtained for an external pulse of about 10-15 μA. Greater values of the applied pulse induce a masking effect on the electroporation phenomenon: the dynamics of either the trans membrane voltage and the ionic currents become increasingly governed by the external pulse rather than the electroporation generator.

References

[1] A. L. Hodgkin, A. F. Huxley: "A quantitative description of ion currents and its applications to conduction and excitation in nerve membranes", J. Physiol., (1952), 117, pp. 500-544.

[2] B. Hille, "Ion channels of excitable membranes", Sinauer Associates Inc., Sunderland, (MA) 2001.

[3] Gerstner and Kistler: "Spiking Neuron Models. Single Neurons, Populations, Plasticity", Cambridge University Press, 2002.

[4] R. E. Plant, M. Kim: "Mathematical description of a bursting pacemaker neuron by a modification of the Hodgkin-Huxley equations", Biophys J. 1976 March; 16(3): 227–244.

[5] P. R. Shorten, D.J.N. Wall: "A Hodgkin–Huxley model exhibiting bursting oscillations" Bull. Math. Biol., 2000, 62, pp. 695–715.

[6] G. W. Beeler, H. Reuter: “Reconstruction of the action potential of ventricular myocardial fibers”. J Physiol, 1977; 268, pp. 177-210.
[7] R. J. Lang, C. A. Rattray-Wood: “A simple mathematical model of the spontaneous electrical activity in a single smooth muscle myocyte”, in Smooth Muscle Excitation, eds. T. B. Bolton, T. Tomita, London, Academic, pp. 391– 402.
[8] K. A. DeBruin, W. Krassowska, “Modeling Electroporation in a Single Cell. I. Effects of Field Strength and Rest Potential”, Biophysical Journal Volume 77 September 1999, pp. 1213-1224
[9] Y. A. Chizmadzhev, J. C. Weaver, “Theory of electroporation: A review” Bioelectrochemistry and Bioenergetics, Volume 41, No. 2, Dec. 1996, pp. 135-160 (26).
[10] R. P. Joshi, Q. Hu, H. P. Hjalmarson, K. H. Schoenbach: “Improved energy model for membrane electroporation in biological cells subjected to electrical pulses”, Phys. Rev. E 65, 041920 1-8 (2002).
[11] N. Citro, B. De Vivo, G. Spagnolo, V. Tucci: ““Range Analysis of Biological Cells Subjected to Pulsed Electric Fields” Proc. Of the Conference on Electrical Insulation and Dielectric Phenomena. October 2005, pp. 511-514.

IMMUNE STIMULATION EFFECTS IN CHICKEN BROILERS WITH COCCIDIA INFECTION THROUGH WEAK LOW FREQUENCY ELECTROMAGNETIC FIELDS

J.J.M. Cuppen[1], M.A. Elmusharaf[2], A.C. Beynen[2], H.N.A. Grooten[3], W. Smink[3]

1: Immunent BV, 2: Utrecht University, 3: FIS BV, The Netherlands

Abstract

A series of experiments was designed to determine the potential of EMF exposure to stimulate the immune system of chicken against infections that are common in farm practice.

In a first experiment 32 groups of six one-week old chicken were either (8) or not exposed (8) to *campylobacter* infection and exposed (16) to both infection and EMF treatment with an LF alternating field (Immunent BV, 30 minutes per day, 6,5 µT). Fresh excrement samples were taken on 6 different time points during the trial and were analyzed for the quantitative presence of *Campylobacter jejuni*. No difference in the course of this infection was observed between the non-treated and EMF treated groups.

Birds were weighed individually on day of arrival and subsequently on days 7, 14, 21, 28, 35 and 42. Feed intake is measured per cage on a weekly basis. A large and significant difference ($p<0.0005$) in feed conversion (feed intake divided by growth) was observed between the EMF group (1.61) and the non treated group (1.75).

In a second and third experiment 32 groups of eight chickens were either (8+8) or not (8+8) exposed to infections with *Eimeria* parasite (coccidiosis) and either (8+8) or not (8+8) given the same EMF treatment as above. Thus all combinations of treatment and/or infection were given to 8 groups of eight chickens.

Feed conversion was determined as above. Infection course was determined by counting oocysts in excrement as above. Moreover intestinal lesions were scored (blind) as caused by the different *Eimeria* after the chickens were slaughtered after the growth period.

Feed conversion was equally good between the negative control and both EMF groups. For the EMF treated infected chicken feed conversion was better (1.52) than the non-treated infected chicken (1.62).

In both experiments a significant reduction ($p<0.01$) in intestinal lesions caused by the different subspecies of the parasite was observed in the EMF treated group.

Introduction

For chicken farmers infectious disease poses the biggest problem both for animal welfare as economically.

Preventive antibiotics have been used as a growth promoter in animal production. These could eliminate infectious disease early, before the animals had to spend energy on the disease. In general up to 5% increase of growth could be achieved with preventive antibiotics. However, preventive antibiotics have been banned in Europe from animal feed since 2006, because of development of microbial resistance in humans.

In chicken farming, hygiene and waiting periods between production cycles are measures that help against infectious disease for pathogens that cannot survive outside the host. However in particular Coccidia parasites with their long surviving spores are an infection that cannot in practice be avoided. Chemical/pharmaceutical agents against coccidia infection will be banned in the EU from 2012 onwards. This has led to a cessation of development of such agents. The farming community has the impression that the existing agents already increasingly lose their effectiveness due to development of resistance in the coccidia parasites.

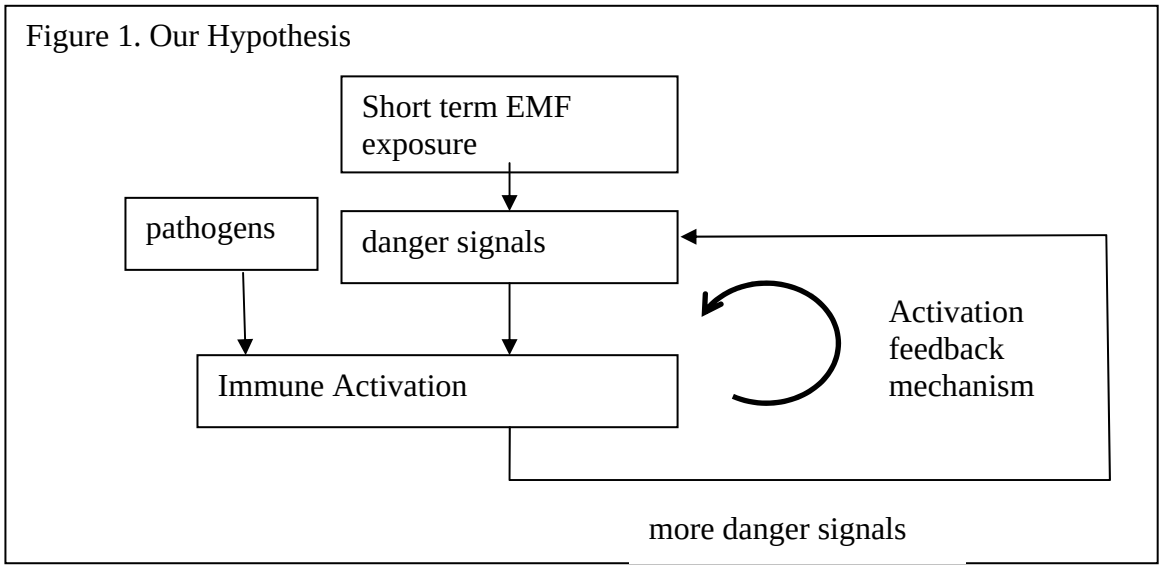
Coccidiosis is a common infectious disease in poultry, causing major economic losses. The protozoan parasite of the genus *Eimeria* explosively multiplies in the intestinal tract of poultry and produces tissue damage, resulting in interruption of feeding and digestive process or nutrient absorption, reduced body-weight gain, dehydration and blood loss, and increase susceptibility to other diseases agents (McDougald, 2003) such as *Clostridium perfringens*, leading to necrotic enteritis (Helmond and Bryant, 1971; Maxy and Page, 1977; Shane et al., 1985).

Economically the damage due to coccidia infection is estimated at 10 points feed conversion (100 grammes more feed necessary for 1 kg weight growth), which translates into a result loss of 5 euro cts per chicken.

Immunent has designed a technology in which low field strength (around 5 micro Tesla) LF EMF is applied for the treatment of chicken. In (Cuppen et al. 2006a) , it is proposed that the working mechanism of this treatment is that LF EMF induces positive stress at cell level, which causes an increased production of cytokines (called

danger signals) that put the immune system in a higher state of alertness and activity.

Figure 1. Our Hypothesis



This reduces the time that it takes for a self sustained immune reaction to pathogens to be established. Therefore pathogens have less time to multiply and damage is reduced.
Many studies have suggested that the immune response to *Eimeria* infection in part is mediated through the release of cytokines. Breed et al. (1997) reported that chicken peripheral blood leucocytes of *E. tenella* infected chickens produce interferon-γ after in vitro re-stimulation. Moreover, it has been shown that treatment of chickens with interferon-γ preceding infection with *E. acervulina* decrease the negative effect of infection on weight gain (Lowenthal et al., 1997).

The aim of this study is to determine the potential of the treatment with the Immunent LF EMF signal as a weapon against infections in chicken that are common in practice.

Experiment design
Three experiments have been done, with 1) campylobacter infection, 2) coccidia infection with high infection pressure and 3) coccidia infection with lower, more practical infection pressure.
For the three subsequent experiments 192, 288 and 272 one-day old female broilers (Ross 308) are purchased from the hatchery. On day of arrival, they are wing-banded, weighed and randomly housed in wire-floor, suspended cages. Each cage is provided with thick foil and litter. Each test cage was provided with a 16 loop coil under the floor through which LF EMF treatment was administered for 30 minutes per day. No attempt was made to create a uniform field since in another experiment it was determined that effective field strengths lie between 0.1 and 50 micro Tesla. Moreover the practical application that is our goal will also not allow uniform field strengths. The field strength (rms) in the middle of the cage was set at 6,5 micro Tesla, measured with a F.W.Bell 5180 Tesla meter with sensitive probe. Dosimetry control during the experiment was ensured by constantly monitoring the (rms) current through the coil. The applied signal was designed by Immunent, which contains several LF components with frequencies between 100 and 10.000 Hz.
Continuous lighting is provided throughout the experiment. The temperature in the cage at arrival is 32°C as required by one day chicken and is gradually decreased to ambient temperatures during the experiment.
Two different basal diets are produced for this experiment by Research Diet Services BV in Wijk bij Duurstede, The Netherlands: a starter diet (week 1 – 2) and a grower/finisher diet (week 3 – 6).
Feed and water were available ad libitum.

Treatment and control groups for the three experiments are indicated in Table 1.

Table 1. Test groups in 3 experiments.
-/+camp indicates without/with campylobacter infection; -/+cocc indicates without/with coccidia infection.

A	B	C	D
Experiment 1, 42 days, each replicate starts with 6 chicken, of which 2 are removed at random and analyzed on day 12. Infection pressure at day 6 with *Campylobacter jejuni* (indicated as +camp)			
Negative control, -camp 8 replicates	Positive control, +camp 8 replicates		EMF, +camp 16 replicates
Experiment 2, 35 days, each replicate starts with 8 chicken, 2 are removed and analyzed at day 21, 2 at day 28, 2 at day 36. Infection pressure (high) at day 15 with Coccidia (+cocc)			
Negative control, -cocc 8 replicates	Positive control, +cocc 8 replicates	EMF, -cocc 8 replicates	EMF, +cocc 8 replicates
Experiment 3, 35 days, each replicate starts with 8 chicken, 2 are removed and analyzed at day 21, 2 at day 28 and 2 at day 36. Infection pressure (low) at day 15 with Coccidia (+cocc)			
Negative control, -cocc 8 replicates	Positive control, +cocc 8 replicates	EMF, -cocc 8 replicates	EMF, +cocc 8 replicates

Measurements

Chickens are weighed individually on day of arrival and subsequently on days 7, 14, 21, 28, 35 and 42 in experiment 1, on day 13 in experiment 2 and day 8 in experiment 3, and on days 21, 29 and 36 in experiment 2 and 3. Feed intake is measured per cage on a weekly basis. Feed intake per broiler is calculated as feed intake per cage divided by number of broiler days. Mortality is registered on a daily basis, but rates are only calculated for the total period.

Statistical analysis

The oocyst values were logarithmically transformed (log10 (X + 1)) to create a normal distribution before being analyzed, and lesion scores were transformed using multinomial transformation.
All performance data for each variable are subjected to an analysis of variance, in which the treatment (control vs. EMF) and infection (positive or negative) were the independent factors with the statistical program SAS.
The level of statistical significance is set at $P< 0.05$.

Infection with *Campylobacter jejuni* in experiment 1

On day 7, after collection of control excrement samples, water infected with *Campylobacter jejuni* C356 (ASG-Lelystad) (~$1*10^5$ per ml) is offered to the broilers in a separate drinking cup. For infection, broilers need to drink only 1 ml of this infected water. The birds had access to drinking water for 1 hour.

Collection of excrements in experiment 1

On days 7, 12, 19, 26, 33 and 40 plastic foil is placed on top of the litter in each cage in order to collect fresh excrements. After 2 hours, plastic is removed, fresh excrements are scraped of the foil and stored in plastic jars. Samples are sent to the laboratory the same day. Analysis of the excrements starts within 24 hours after collection according to the method of Jacobs-Reitsema et al. (1995).

Inocula and contamination procedure experiment 2

Sporulated oocysts of *E. acervulina* (W119, Weybridge), *E. maxima* (Weybridge), and *E. tenella* (Houghton) laboratory strains were obtained from the Animal Health Service, Poultry Health Centre (Deventer, The Netherlands). The number of oocysts per milliliter of suspension was counted with a hemocytometer (Fuchs-Rosenthal counting chamber). A volume containing sporulated oocysts ($1.76x10^4$ E. acervulina, $1.25x10^4$ E. maxima, and $7.5x10^3$ E. tenella) in K2Cr2O7 was transferred into a scaled plastic tube and the K2Cr2O7 was washed out by centrifugation. On day 15 of the experiment birds in 18 cages (144 birds) were individually infected. The sporulated oocysts were administered with 1 ml of tap water via a scaled 1-ml syringe directly into the crop.

Inocula and contamination procedure experiment 3

In this experiment a natural simulation of a coccidial infection within the broilers' test facility was developed. This was accomplished by seeding a portion of the litter with coccidial oocysts prior to broiler placement on new litter on day 15 of the trial. A similar dose of *Eimeria* species was used as in experiment 2, e.g. E. acervulina, E. maxima and E. tenella. Equal amounts of each species was mixed into the wood shaving and spread evenly across the back half of each contaminated group pens. The broilers picked up the oocysts from the seeded litter, mimicking a natural infection, as all birds do not pick up oocysts at the same time, which led to a progression of the infection as in the field. The non-infected broiler groups were reared in clean litter.

Infection measurements experiments 2 and 3

Oocyst Count (OPG)

The oocyst per gram faeces (OPG) counting were performed on fresh faeces collected on days 15, 29, and 36 (days 6, 14, and 21 post infection). Oocyst shedding was assessed on one sample of homogenized faeces material collected from each cage. Modified MacMaster counting chamber techniques of Hodgson (1970) was used to determine the OPG in the homogenized faeces. A 10% (w/v) faeces suspension in a salt solution (1.1%) was made. After shaking vigorously, 1 ml of the suspension was pipetted into 9 ml-saturated sodium chloride (1.2%). After mixing again, a portion of the later suspension was run into the MacMaster chamber and the oocysts per gram faeces were counted.

Caecal lesions

Intestinal lesion scorings were performed blindly to the treatment modality on days 15, 29, and 36 (days 6, 14, and 21 PI). Two birds per cage (36 cages) were euthanized by cervical dislocation, dissected and different coccidial lesions were scored. The 0-4 scoring system described by Johnson and Reid (1970) was used. The scores for the individual birds of the same treatment group were summed up to arrive at a treatment value.

Results and discussion

Feed intake and feed conversion

Daily feed intake per broiler is calculated as weekly feed intake per cage divided by so-called 'broiler days', which is the number of broilers per cage times the number of days corrected for drop outs. Data show that the feed intake of broilers of the EM group was significantly lower than the negative control group for all three experiments.

Feed conversion is calculated as the growth [g] divided by the feed intake [g] over the total period. The results of the feed conversion are shown in Table 2. Feed conversion of the broilers of the EM group with infection (as in practice) was significantly lower than controls for all three experiments.

Table 2: Feed conversion of broilers

Total period	Negative control	Positive control	EMF no infection	EMF w infection
Experiment 1	1.78 ± 0.02	1.73 ± 0.04		1.61± 0.03*
Experiment 2	1.58 ± 0.04	1.63 ± 0.04	1.57 ± 0.05	1.52 ± 0.06 *
Experiment 3	1.83 ± 0.03	1.84 ± 0.05	1.73 ± 0.03*	1.72 ± 0.03*

∗ significant ($p<0.05$)

Comparing negative control with EMF no infection, and positive control with EMF with infection results it turns out that in 4 out of 5 cases a significant and economically highly relevant improvement in feed conversion is achieved by EMF treatment. In chickens, one explanation for less feed uptake indicates could be less energy spent on developing infections. Given a certain amount of meat consumption this also translates in the corresponding 8% decrease in resource usage for meat production. Assuming that manure production is proportional to feed conversion minus 1 (the amount of feed *not* transformed into live weight) and assuming that digestion of phosphates in feed is 60%, this corresponds to a reduction in phosphate load, for equal end weight of the animals, to the environment of about 16%.

The calculation is as follows: Feed contains X per kg. The animal takes up Y = X * 60% * 1.84. Excretion is (X * 40% * 1,84) without EMF and (X * 1.72 – Y) in the second case. Reduction is ((X * 0.4 * 1.84 – (X * 1.72 – X * 0.6 * 1.84))/ (X * 0.4 * 1.84) = 16%.

Moreover it should be noted that the reduction in feed conversion achieved rivals the best results achieved in comparable trials with preventive antibiotics (now illegal in animal feed in the EU). This indicates that EM treatment is as effective in suppressing infections and the resulting productive loss in chicken as preventive antibiotics were.

Microbiological analysis of excrements

Fresh excrement samples were taken on different time points during the trial and were analyzed for the quantitative presence of *Campylobacter jejuni* in experiment 1 and OPG count (oocyst shedding – parasite spores) in experiments 2 and 3.. The results are presented in Table 3.

Despite proper hygienic conditions the negative control group and negative EMF groups were also infected during the course of the experiment. Thus they became also infected groups, though there is no control of the level of infection.

Table 3:

	Negative control	Positive control	EM not infected	EM infected
Experiment 1, Amounts of colony forming units (cfu) of *Campylobacter jejuni* in excrements of broilers (expressed as 10 log CFU per g of excrement)				
Day 6	negative	negative		negative
Day 12	3.24 ± 0.61*	6.05 ± 0.15		5.78 ± 0.14
Day 19	5.71 ± 0.24	6.55 ± 0.08		6.37 ± 0.15
Day 26	5.25 ± 0.65	6.16 ± 0.23		6.60 ± 0.21
Day 33	4.58 ± 0.54	5.66 ± 0.24		5.88 ± 0.21
Day 40	6.20 ± 0.26	5.98 ± 0.17		5.53 ± 0.19
Experiment 2, OPG counts (oocysts per gram faeces, expressed as log10 (X+1))				
Day 21	0.00 ± 0.00	5.70 ± 0.35	0.00 ± 0.00	5.96 ± 0.06
Day 29	2.10 ± 0.69	4.02 ± 0.34	2.89 ± 0.66	3.86 ± 0.17
Day 36	4.10 ± 0.20	2.24 ± 0.52	3.87 ± 0.58	1.93 ± 0.59
Experiment 3, OPG counts (oocysts per gram faeces, expressed as log10 (X+1))				
Day 21	1.72 ± 0.87	4.03 ± 0.12	2.17 ± 0.83	4.11 ± 0.10
Day 29	3.26 ± 0.71	4.58 ± 0.18	2.05 ± 0.78	4.35 ± 0.27
Day 36	4.04 ± 0.27	3.82 ± 0.13	2.36 ± 0.71*	3.66 ± 0.23*

Results show that the infection with *Campylobacter* was significantly lower in the negative control group than in the other two groups on day 12. One week later, on day 19, infection with *Campylobacter jejuni* was similar for all three groups. Applying the EM field under the cages of the broilers had no effect on the infection rate of *Campylobacter* throughout the experiment in terms of bacteria excretion.

Also during experiments 2 and 3 cross-contamination occurred again in both uninfected groups despite proper hygienic conditions, which indicates that *Campylobacter* and *Coccidiosis* are both very infectious in practical circumstances.

OPG counts on day 29 and day 36 are numerically lower for infected EMF group compared to the infected control group and only in experiment 3 on day 36 this difference is statistically significant. More investigations are required to determine whether the EMF treatment can contribute to a diminished outbreak of a coccidiosis contamination.

Coccidial lesion scores in experiment 2 of intestines due to E. acervulina and E. maxima were significantly lower in the positive EMF group compared to the positive control group on day 21 (Table 4a). On day 14 of the experiment cross contamination was detected, but still lesion due to E. maxima of the EMF positive group was significantly lower than that of the positive control group. This might suggest that the EMF treatment counteracts the onset of a coccidiosis infection.

Table 4a: Mean lesion scores of intestines for experiment 2

	Control		EMF	
	- cocc	+ cocc	- cocc	+ cocc
E. acervulina				
Day 21	0.00 ± 0.00	1.95 ± 0.15	0.00 ± 0.00	1.19 ± 0.10*
Day 29	0.30 ± 0.11	0.90 ± 0.10	0.50 ± 0.13	0.63 ± 0.13*
E. maxima				
Day 21	0.00 ± 0.00	2.30 ± 0.15	0.00 ± 0.00	1.50 ± 0.13*
Day 29	0.45 ± 0.17	1.55 ± 0.20	0.63 ± 0.18	0.81 ± 0.19*
E. tenella				
Day 21	0.00 ± 0.00	2.65 ± 0.13	0.00 ± 0.00	2.00 ± 0.20*
Day 29	0.30 ± 0.12	1.00 ± 0.16	0.56 ± 0.18	0.69 ± 0.15*

During experiment 3lesions scores of intestines were also determined (see Table 4b) due to the same *Eimeria spp*. These results show that the EMF treatment caused significantly lower lesions scores for all species investigated during the whole trial for both infected as well as uninfected groups, except for E. acervulina and E. tenella on day 21 (numerically lower).

Lesions scores of both infected groups in experiment 1 started at a similar level compared to the individual contamination of experiment 2, although lesions due E. acervulina were higher and lesions due to E. tenella were lower. Results further show that lesions scores decreased during the trial for both infected groups, which showed that the contamination by seeded litter is a good contamination method in order to study immunity against coccidiosis during natural contamination. Lesion scoring of both uninfected (control and EMF) groups increased during the trial, which shows that these broilers did not yet reach immunity against coccidiosis.

Table 4b: Mean lesion scores of intestines for experiment 3

	Control		EMF	
	- cocc	+ cocc	- cocc	+ cocc
E. acervulina				
Day 21	0.44 ± 0.22	2.44 ± 0.15	0.44 ± 0.18	2.00 ± 0.16*
Day 29	1.06 ± 0.27	1.69 ± 0.09	0.31 ± 0.13*	1.50 ± 0.15*
Day 36	1.38 ± 0.26	1.75 ± 0.19	0.94 ± 0.24*	1.22 ± 0.10*
E. maxima				
Day 21	0.13 ± 0.08	2.25 ± 0.19	0.06 ± 0.06*	1.67 ± 0.13*
Day 29	0.56 ± 0.20	1.63 ± 0.08	0.00 ± 0.00*	1.33 ± 0.21*
Day 36	1.50 ± 0.38	2.10 ± 0.12	0.50 ± 0.25*	1.22 ± 0.21*
E. tenella				
Day 21	0.13 ± 0.08	1.50 ± 0.09	0.06 ± 0.06	1.42 ± 0.11
Day 29	0.19 ± 0.09	1.31 ± 0.13	0.06 ± 0.06*	1.00 ± 0.11*
Day 36	0.56 ± 0.15	1.42 ± 0.15	0.13 ± 0.08*	1.17 ± 0.11*

It is unlikely that there is a direct effect of EMF on the *Eimeria* parasites. In literature there are no indications that organisms are directly and seriously damaged by EMF without an extremely high energy content. In our experiments, the energy levels are extremely low. On the other hand, cytokine production has been reported, as well as oxygen burst, both of which are instrumental in immune activation. It is therefore not unlikely that the reduction in pathology found is caused by a more effective immune reaction in the animal.
Mortality was almost equal between EMF and corresponding control groups in all experiments (11 vs. 12%, 7 vs. 7% and 16 vs. 14% total mortality respectively for experiments 1, 2 and 3).

Conclusions

The study indicates that

- LF EMF treatment does not seem to reduce a *Campylobacter* infection in broilers, which is in agreement with our hypothesis since this bacteria is a commensal for chicken and an enhanced immune system cannot be expected to fight it.
- LF EMF treatment reduces the damage, in terms of intestinal lesions of Coccidiosis infection in broilers. This supports the hypothesis that LF EMF can enhance the immune response.
- LF EMF treatment was shown in 4 out of 5 measurements to improve feed conversion up to 12 points. This is highly interesting to farmers economically, but also to society as a whole since it represents a decrease in resource usage of 8% and a decrease in phosphate load on the environment of 16%.
- Since feed conversion improvement is not restricted to the experiments where the chickens were actually suffering from (for them) relevant infections it seems that LF EMF improves the immune competence of the animals, independent of one particular infection.

References

Breed D.G., Dorrestein J., Schetters T. P., Waart L. V., Rijke E., and Vermeulen A. N.. (1997). Peripheral blood lymphocytes from Eimeria infected chicken produce gamma-interferon after stimulation in vitro. Parasite Immunol. 19:127-135.

Cuppen J.J.M., Parmentier H.K. and Savelkoul H.F.J. (2006a): Immune Stimulation In Fish And Farm Animals Through Weak Low Frequency Electromagnetic Fields, A. Hypothesis, this proceedings.

Helmboldt, C.F., and E.S. Bryant. 1971. The pathology of necrotic enteritis in domestic fowl. Avian Dis. 15:775-780.

Hodgson J.N. (1970) Anticoccidial drugs: lesion scoring techniques in battery and floor-pen experiments with chickens. Exp. Parasitol. 28: 30-36.

Jacobs-Reitsma W.F., Giessen A.W. van de, Bolder N.M. and Mulder R.W. (1995) Epidemiology of Camplyobacter spp. at two Dutch broiler farms. Epidemiology and Infection 114(3): 413-421.

Johnson, J. and Reid W.M. (1970). Anticoccidial drugs: Lesion scoring techniques in battery and floor-pen experiments with chickens. Exp. Parasitol., 28:30-36.

Lowenthal J.W., York J.J.,. O'Neill T.E, Rhodes S., Prowse S. J., Strom D.G., and Digby M.R.. (1997). In vivo effects of chicken interferon-gamma during infection with Eimeria. J. Interferon Cytokine Res. 17:551-558.

Maxey B.W and Page R.K. (1977) Efficacy of lincomycin feed medication for the control of necrotic enteritis in broiler-type chickens. Poult Sci., 56: 1909-13.

McDougald L.R. (2003) Coccidiosis. In: Saif et al. (Eds.), Poultry Diseases. Iowa State Press, Iowa, pp: 947-991.

Shane S.M., Gyimah J.E., Harrington K. S. and Snider III T.G. (1985). Etiology and pathogenesis of necrotic enteritis. Vet. Res. Commun. 9: 269-287.

Acknowledgements

Messrs Van Kraaij, Brock, Berghs, and Bloo provided indispensible services in creating the hardware and software that supported these experiments.

IMMUNE STIMULATION EFFECTS IN FISH AND FISH IMMUNE CELLS THROUGH WEAK LOW FREQUENCY ELECTROMAGNETIC FIELDS WITH VARIABLE FIELD STRENGTH

J.J.M. Cuppen[1], G.F. Wiegertjes[2], M. Molenaar[2], J. Geervliet[3], W. Smink[3]

1: Immunent BV, 2: Wageningen University, 3: FIS BV, The Netherlands

Abstract

A series of experiments (n=14) was designed to determine the potential of LF EMF exposure to stimulate the immune system of fish.

Common carp head kidney-derived phagocytes were used to determine respiratory burst activity as a measure for immune activation. Exposure to the Immunent LF EMF signal at 5 µT or 1,5 mT led to 42% or 33% increase in immune activity, respectively, compared to negative control values. EMF could also additionally stimulate chemically pre-stimulated samples up to 18% (5 µT) or 22% (1,5 mT). Statistical analysis was carried out with SAS via a meta-analysis of the 14 datasets. A significant ($p<0.0001$) increase on the response of the EMF exposed cells was found.

Subsequently, a series of experiments were performed using live goldfish. During transport from the grower commercial goldfish suffer from heavy parasitic and microbial infections to such an extent that without treatment high mortality will be observed over a period of a few weeks.

Groups of fish were housed under equal conditions in at least 4 control tanks and 8 to 16 EMF-exposed tanks. Exposure was done at field strengths between 0,15 and 50 µT by coils positioned around the outside of the fish tanks, creating a predominantly vertical field.

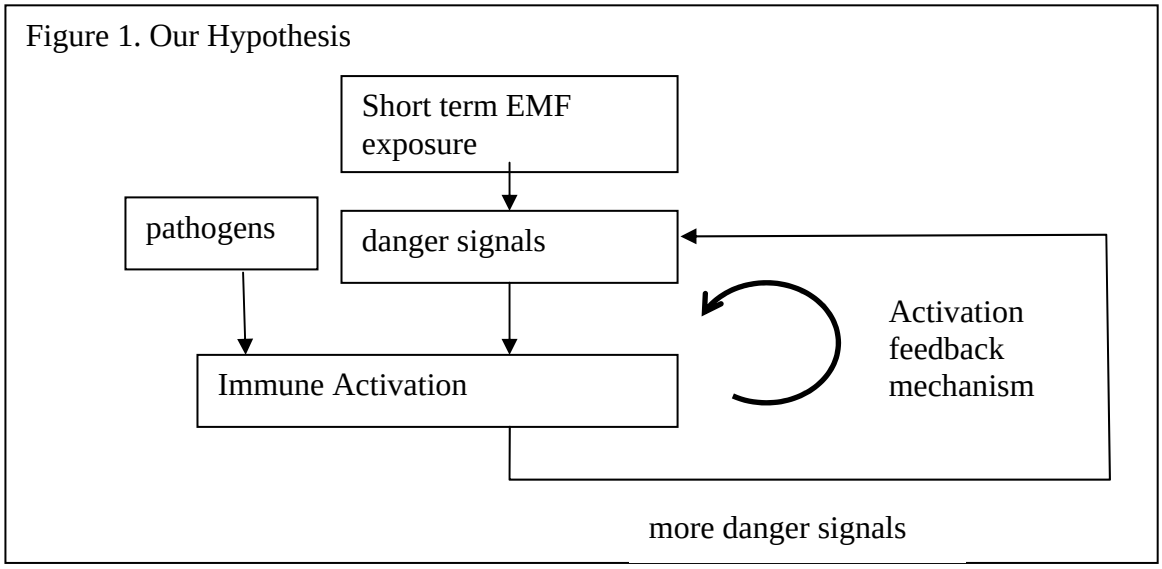
In the experiments without treatment mortality was about 50% after 18 days, while the treatment at 5 µT reduced it to 20%.

In a third experiment the treatment field strength was varied between 0,05 µT and 50 µT in 6 steps. The decrease in mortality after EMF exposure was equally strong between 0,15 and 50 µT and only slightly less strong at 0,05 µT. In a fourth experiment the field strength was further reduced to 0,01 and 0,003 µT. The effect is gone at 0,001 µT and below, while the situation between 0,003 and 0,06 µT an increasing dose response is visible.

Introduction

Immunent has designed a proprietary low field strength (around 5 micro Tesla) LF EMF treatment, aimed at stimulating the immune system. In another paper in this proceedings (Cuppen et al. 2006a), it is proposed (see Fig. 1.) that the working mechanism of this treatment is that LF EMF induces stress at cell level, which causes an increased production of cytokines (called danger signals) that put the immune system in a higher state of alertness and activity. This reduces the time that it takes for a self sustained immune reaction to pathogens to be established. Therefore pathogens have less time to multiply and damage is reduced.

In aquaculture and farming, infectious disease is one of the biggest, if not the biggest problem and challenge, economically as well as in terms of animal welfare and environmental pressure. "Disease is the biggest single impediment to aquaculture development," said Rohana Subasinghe, Senior Fisheries Research Officer at the United Nations' Food and Agriculture Organization (FAO). Total damage in aquaculture of infectious disease is estimated at 9 billion $ yearly. In Equador in 1999 70% of the crop of farmed shrimp was lost due to a single virus infection, that led to a national crisis and a loss of 150.000 jobs. Environmentally, infectious disease causes a lot of pressure: by the chemicals and pharmaceuticals used, by the pathogens that multiply in farms and increase disease pressure on the surrounding wildlife, and by the pressure on farmers to abandon farms with disease and start new farms in nature areas.



Fish and other aquatic animals such as shrimps are particularly vulnerable to infectious disease because they have no, or much less adaptive immune system and have no transferred immunity from the mother.

Simkó, Droste, Kriehuber and Weiss (2001) and Lupke, Rollwitz and Simkó (2004), have demonstrated that human and murine macrophages can be stimulated to higher activity through LF EMF. In this research we will likewise determine the effect of the Immunent signal at cell level by measuring oxygen burst, and then proceed to in vivo experiments aimed at demonstrating, and then optimizing the effectiveness of Immunent treatment on fish.

Materials and methods

In vitro experiments

Common carp head kidney-derived phagocytes were used to measure oxygen burst activity as a measure for immune activation.

Oxygen burst causes a marked increase in oxygen uptake, which is mainly channeled to a pathway initiated by the reduction of oxygen to super oxide anion (O2-), using NADPH or NADH as the electron donor. The O2- is subsequently converted to hydrogen peroxide (H2O2) with the aid of the enzyme super oxide dismutase (SOD).

$$202 + NADPH \xrightarrow{\quad} 202^- + NADP^+ + H^+$$

$$202^- + 2H^+ \xrightarrow{\text{SOD}} H_2O_2 + O_2$$

The objective of this test is to measure the modulation of the oxygen burst activity in macrophages and neutrophilic granulocytes of the carp pronephros, or head-kidney.

The measurement is based on the reduction of a salt: Nitro Blue Tetrazolium NBT by O2-. This results in a blue color, which is measured spectrophotometrically.

Biochemical Materials

Phorbol 12-myristate 13-acetate (PMA), 0.01 µg/µl, a standard chemical stimulant of Oxygen burst in leukocytes known to give a high response as a positive control

RPMI without phenol red: washing and culture media (the red indicator dye disturbs the final reading on the spectrophotometer)

Nitro Blue Tetrazolium in RPMI without phenol red. (NBT; grade III) 1 mg/ml final concentration

2N KOH (Potassiumhydroxid)

100% and 70% methanol

Dimethylsulfoxide (DMSO)

flat bottomed 96-well microtiterplate (sterile) coated with adherent cells

spectrophotometer with filter at 690 nm

Biochemical Methods

Leukocytes are collected from the head kidney and placed at 4 degrees Celcius overnight. Next, they are plated

out in 96 well trays with 100 µl in each well. The cells are allowed to adhere for 30 mins at 27 oC (5 % CO2, humidity 100 %). After inspection, non-adherent cells are washed away by rinsing twice with 100 µl of RPMI-phenol red culture medium (one row at a time).
The NBT assay is started by removing the supernatant and by adding 150 µl of NBT and subsequently the stimulators (10 µl of PMA and/or 30 mins EMF), followed by or, in case of EMF, in parallel to incubation of the cells for 90-120 minutes at 27 oC (5 % CO2, humidity 100 %).
After the incubation, the NBT solutions are removed and the cells are washed once by rinsing with RPMI medium without phenol red. The remaining cells are fixated for 5 minutes with 100 µl 100 % methanol, then washed twice with 100 µl 70 % methanol to remove possible NBT-rests. The plate is left to dry.
The blue formazan inside the cells is solubilized in 100 µl 2N KOH to which 100 µl DMSO is added. The content of the well is mixed thoroughly.
The optical density is measured at 690 nm (ref. filter at 414 nm) in a spectrophotometer.

EMF materials
An exposure magnet was designed for exposing one or two rows of a 96 well plate simultaneously. Since earlier experience indicated cross talk to controls at enormously low field strengths we aimed for the lowest fringe fields possible. Based on experience from MRI magnets, eight Ferrite C arm units were built (six used), each for exposing one or two rows of a 96 well plate to a uniform AC magnetic field. The “C” of the magnet was built of 16 mm2 Ferrite 3C90, the pole shoes were 99x30x8 mm. above and below the pole shoes, coils with 600 turns each were placed around the C arm. Saturation in the ferrite occurs above 170 mT, therefore this setup allowed a field strength of 5 mT to be achieved in the exposure gap without saturation effects in the C. A uniformity of 10% or better was achieved at the well positions.
Side ways, the fringe field was measured to decrease by at least a factor 2 every 2 cm. Thus at a distance of 5 meters (which was kept for the controls) one may safely assume the fringe field to be below 1 pT. It was no longer measurable with our equipment at 1 m distance.
Signals were generated by an Immunent signal generator, capable of generating field strengths between 0,15 µT and 1.5 mT in the exposure area, with a proprietary signal consisting of several LF components with frequencies between 100 and 10.000 Hz.
The signal generator monitored currents through the coils during the experiment, which were calibrated to correspond to the desired field strength using an F.W.Bell 7000 Tesla Meter with sensitive probe.

Experiment design
Each run measured 48 samples, in six groups of 8 samples. Half of the groups were not chemically pre-stimulated (negative) and half were pre-stimulated with PMA (positive). Two groups were taken as controls, while EMF stimulation was done on four groups, two at 5 µT field strength and two at 1,5 mT field strength.
Exactly those runs were included in the results where the positive control average exceeded the negative control average by at least 50%, independent of the measurements for the EMF exposed cells. If that is not the case it must be assumed that the cell isolation was not properly done. This led to the exclusion of 6 runs out of a total of 20 runs executed.

In vivo experiments
Subsequently, a series of experiments were performed using fantail goldfish (*Carrassius auratus spp*.), heavily infected with ecto parasites (gill parasites) such as *dactylogyrus/ gyrodactylus, trichodina, chilodinella* and *costia*. Infection with those parasites occurs consistently at the grower and increases during storage, packing and international transport due to crowding. This and subsequent secondary bacterial infections cause high mortality if not treated. The progress of the diseases can be measured by daily counting and removing dead fish over a period of a few weeks. Fish were randomly allotted over the tanks. Individual fish weight was 2.5 (± 0.5 g)
Daily, the fish were checked for health. Dead fish were counted, removed and discarded.
The number of fish per replicate tank varied between the experiments, 12 in the first and second experiment, 21 in the third, and 30 in the fourth.
Fish were housed in PVC tanks with a content of 30 liter. Aeration of water and daily change of 20 % of the water maintained water quality. |Fish were fed commercial feed ad libitum.

Groups of fish were housed under equal conditions in at least 4 control tanks and 8 to 16 EMF-exposed tanks. Exposure was done at field strengths between 0,15 and 50 µT by coils positioned around the outside of the fish tanks, creating a predominantly vertical field. Lower field strength exposures were achieved by placing additional tanks in the stray field of a tank with a coil, calibrating that stray field to the current in the coil, and then controlling the current.

The tanks were standard PVC tubs of 50 cm height, 30 cm diameter, around which standard isolated 1.5 mm2 electricity wire was tightly wound in 160 turns. At the lower end a spiral end cap of 12 turns over the outer half of the diameter and at the top flange 20 additional turns were wound to optimize uniformity in the tub. Thus inside the tubs a practical, but close approximation was achieved of the field of a long solenoid coil. The deviation of the theoretically uniform field of the solenoid was calculated using Vector Fields software by dr. Johan Overweg of Philips Research, MRI section, and is better than 5% in the water volume further than 4 cm from the lower outside circumference of the tub, and better than 20% further than 2 cm from that outside circle. The signal generator was as described above for the in vitro experiments.

Results and discussion

In vitro experiments

Oxygen burst measurements were averaged over the 8 samples available in each group. Averages of the measurements without pre-stimulation and of the positive control group (with pre-stimulation) were divided by the negative control average in the corresponding run. The averages of pre stimulated measurements were divided by the corresponding positive control average. The resulting data, with standard deviation estimates derived from the data in each group, are given in Table 1.

Table 1. Oxygen burst results of 14 runs with 6 times 8 samples each

			% average normalized to negative control average						% average normalized to positive control average			
	neg contr		neg, 5 µT		neg, 1,5 mT		pos contr		pos, 5 µT		pos,1,5 mT	
	gem	stdev	gem	stdev	gem	stdev	gem	stdev	gem	stdev	gem	stdev
v50131	100%	8%	109%	6%	95%	7%	223%	41%	99%	13%	87%	10%
v50202	100%	6%	131%	23%	108%	8%	162%	30%	117%	19%	103%	30%
v50209	100%	24%	138%	36%	142%	23%	418%	73%	115%	9%	190%	17%
v50215	100%	54%	278%	120%	176%	131%	788%	118%	98%	17%	113%	46%
v50222	100%	24%	118%	41%	115%	50%	319%	59%	130%	25%	144%	32%
v50223	100%	50%	75%	17%	151%	32%	235%	90%	136%	22%	104%	24%
v50315	100%	10%	120%	25%	62%	18%	166%	28%	131%	34%	106%	21%
v50405	100%	15%	128%	29%	112%	31%	162%	23%	141%	42%	141%	31%
v50406a	100%	17%	142%	25%	152%	23%	179%	37%	143%	26%	126%	16%
v50406b	100%	31%	206%	119%	322%	70%	230%	33%	143%	54%	175%	26%
v50419a	100%	28%	93%	27%	66%	11%	201%	48%	92%	20%	101%	14%
v50419b	100%	10%	212%	50%	138%	40%	259%	54%	133%	26%	110%	17%
v50420	100%	15%	112%	27%	118%	21%	205%	38%	86%	17%	122%	14%
v50426	100%	55%	126%	89%	112%	67%	323%	86%	82%	13%	92%	19%
average	100%		142%		133%		276%		118%		122%	

Oxygen burst was increased in 12 out of 14 cases after 5 µT treatment, in 11 out of 14 cases after 1,5 mT treatment. With pre stimulation, oxygen burst was further increased in 9 out of 14 cases at 5 µT, and in 12 out of 14 cases at 1,5 mT.

On average, exposure to 5 µT or 1,5 mT led to 42% or 33% increase in immune activity, respectively, compared to negative control values. EMF could also additionally stimulate PMA-stimulated samples up to 18% (5 µT) or 22% (1,5 mT). Statistical analysis was carried out with SAS via a meta-analysis of the 14 datasets. A significant ($p<0.0001$) increase on the response of the EMF exposed cells was found.

These data are in line with those reported for 50 Hz, sinusoidal, 1 mT fields in murine and human macrophages in Simkó et al. 2001 and Lupke et al. 2004.

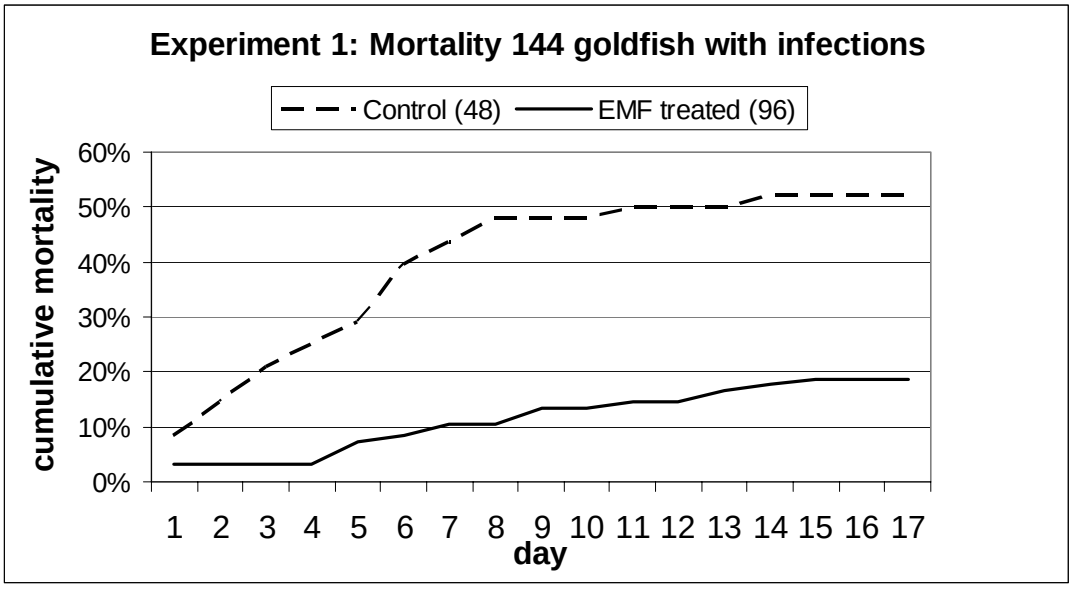
In vivo experiments

The subsequent series of experiments with diseased goldfish returned the following results. In each graph mortality is indicated in % of the total number of fish in each test group, as it develops over the course of the experiment. As can be seen the horizontal mortality lines after day 20 in experiment 3 (no further mortality), after 18 to 20 days usually the surviving fish had recovered from the diseases both in the control and the test groups, as was confirmed by visual inspection. Most test groups consisted of at least 4 replicates, in which the number of fish initially was gradually increased after more experience was gained. For some experiments

however with gradually varying parameters 2 replicates were taken.
Please note that in each experiment a new batch of fish was procured from the importer of the fish. Fish from groups heavily infected with parasites were selected. However the initial disease/health level of the fish varies between experiments. The absolute levels of survival between experiments are therefore not comparable. Within one experiment the fish had comparable health so the comparisons within one experiments are valid.

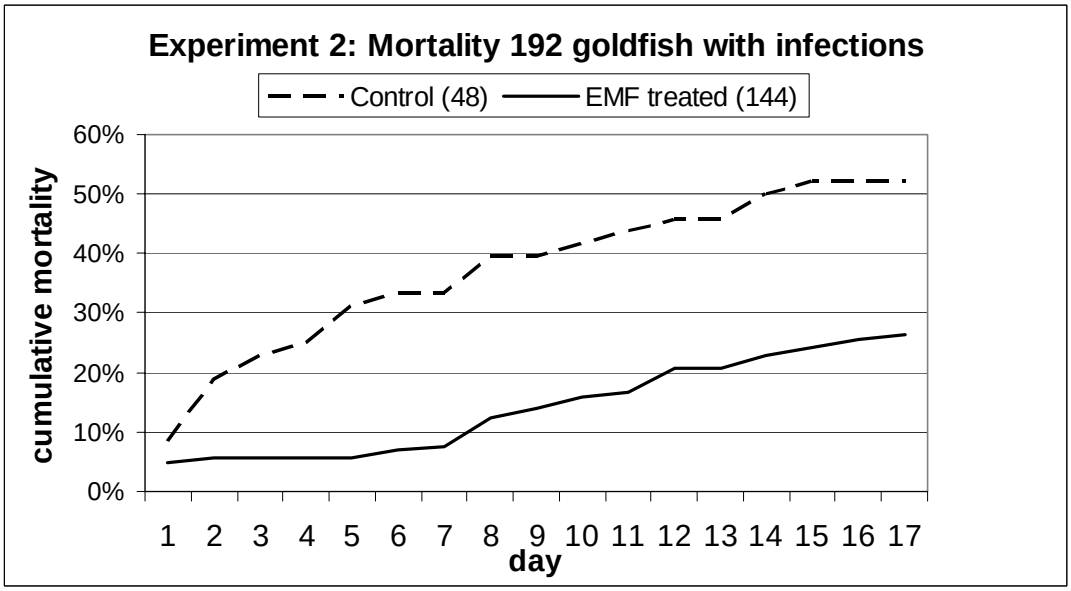
The first experiment compared survival in 4 control groups with 8 groups treated at 5 µT. Each group contained 12 fish.

Figure 2. Experiment 1.



As can be seen there is a large difference in the survival, which was consistently more than 80 % better in the treated group over the course of the experiment. The end values were 52% ± 14% untreated and 19% ± 10% treated. The experiment was repeated, this time with 12 treatment groups of 12 fish each.

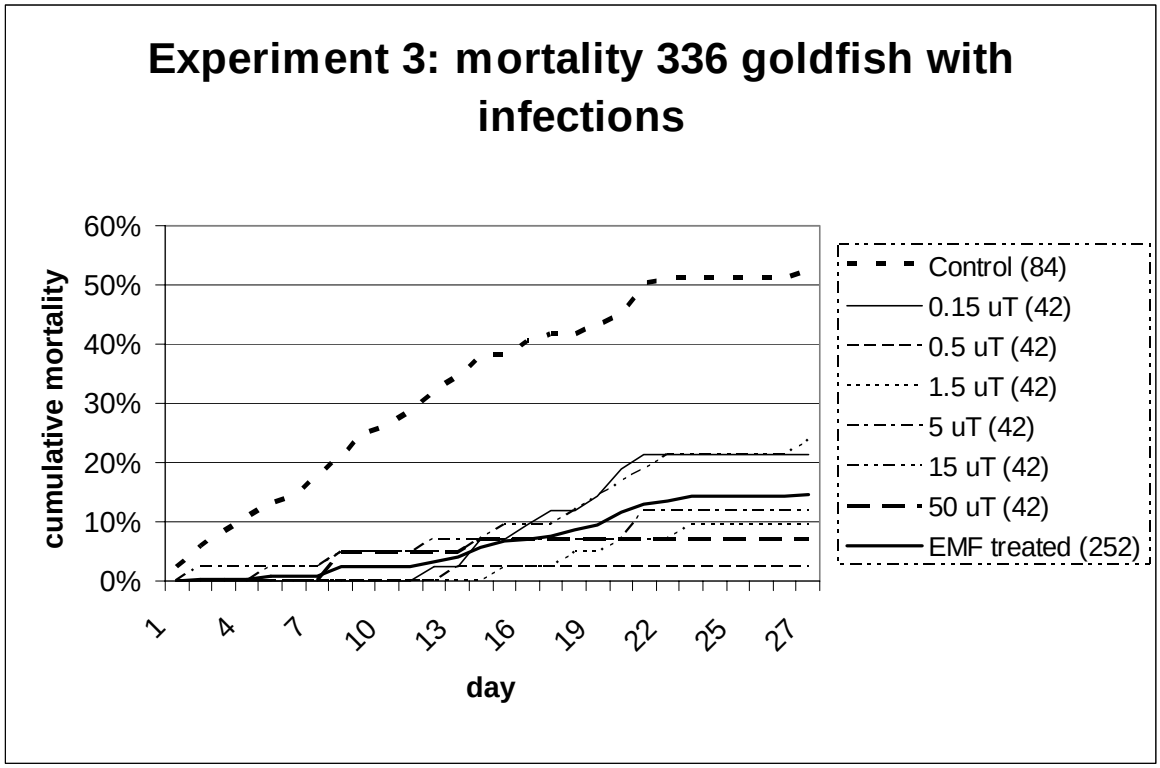
Figure 3.



This time the improvement was again a factor 2. The end values were 52% ± 8% untreated and 26% ± 19% treated.
In order to find out more about the field strength dependency of the effect and to determine the required distance between tubs for parameter variation experiments, a next experiment was done with varying field strength. There

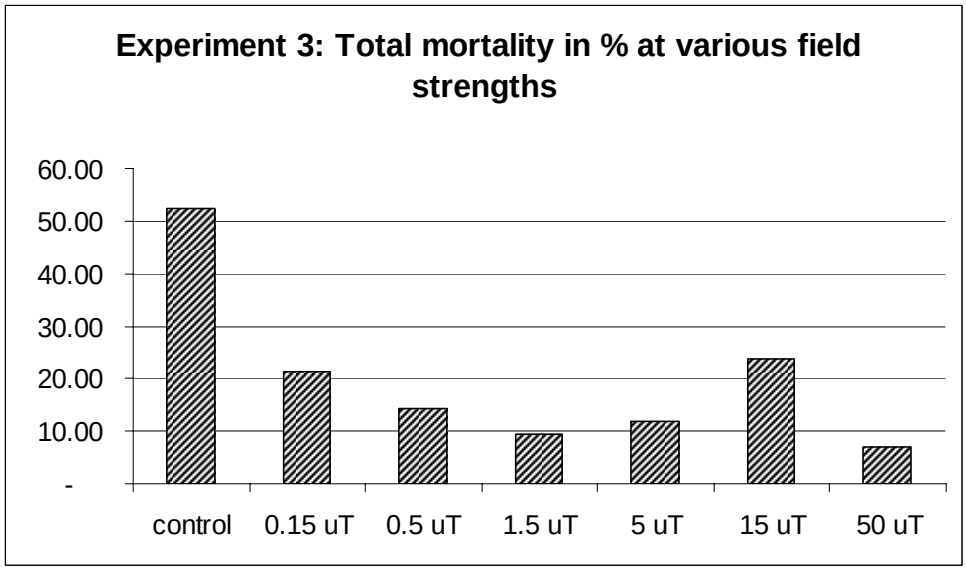
were 4 control groups and 2 test groups for 6 different field strengths varying from 0.15 to 50 µT. Each group contained 21 fish initially.

Figure 4.



In this figure for 6 different field strength, ranging from 0.15 µT (thin solid line) to 50 µT (thick, long dashed line) the mortality development is given as before. Again, the control groups suffered mortality increasing to 52% on day 28 (upper, thick short dashed line). The average of all treatment groups is also given (thick solid line), this increases to 15% at day 28. The end values were 52% ± 29% untreated and 15% ± 11% treated (all together). Again, the treatment resulted in a strong decrease in mortality at all field strength levels. The final percentages at day 28 are given for clarity also in Figure 5.

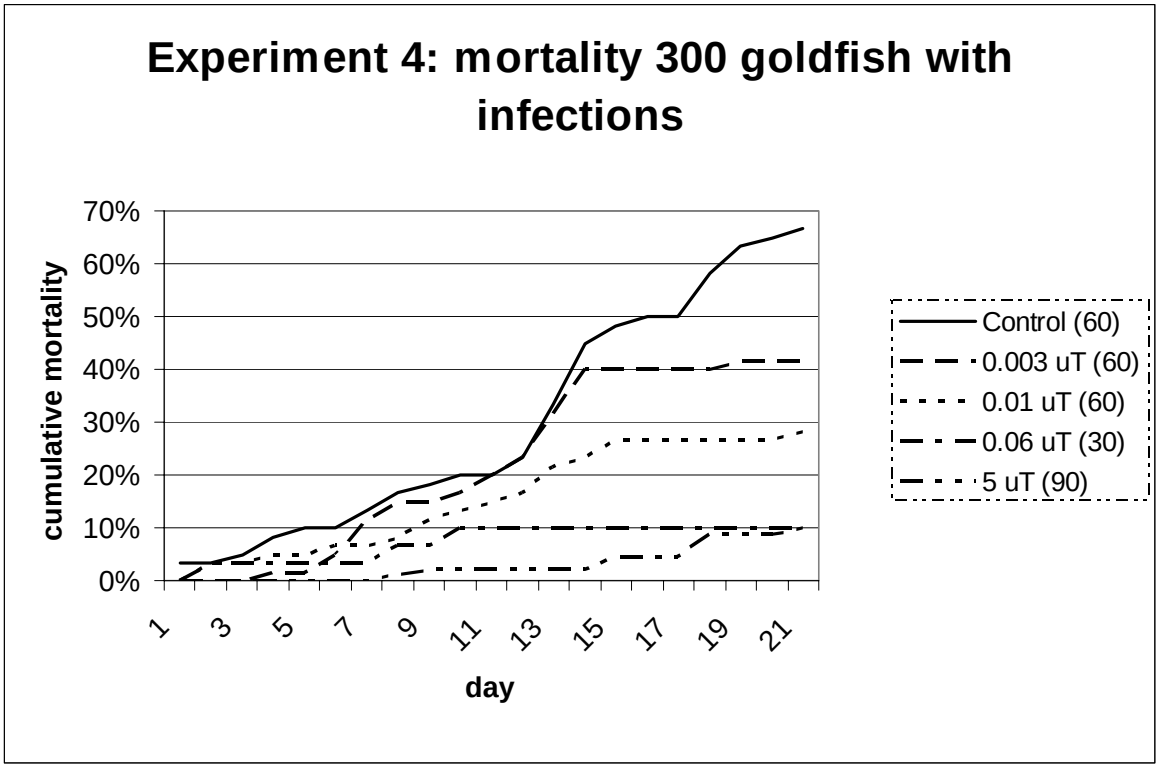
Figure 5.



The result indicated that the decrease in mortality after EMF exposure was equally strong between 0,15 and 50 µT, except at 15 µT. There seems to be a decease in effectiveness from 0,05 µT downwards which becomes noticeable at 0,015 µT.

Since for our application especially the lowest field strength range is important a follow up experiment was performed that simulated lower field strength than 0,15 µT by placing test tubs in the stray field of a 5 µT tub. This was done because the voltages and currents needed to create such small fields are so low that electronic noise became too high. The 5 µT tub is built as a solenoid coil along the complete height of the tub. Such a solenoid coil has a small but rather uniform stray field that is suitable for the analysis that we wished to perform. The result is given in Figure 6.

Figure 6.



From the .06 µT group in Fig. 6 one replicate was lost due to a technical problem.
It can be observed that over the whole period mortality is highest in the control group and lowest in the group treated at 5 µT. From day 7 onwards mortality is strictly increasing with decreasing field strength.
Even at 0.003 µT (3 nT) these results indicate that there still is an effect of the treatment.
These results indicate that in order to be reasonably confident that there is no influence of EMF on control groups one must go to field strength levels of 1 nT or lower.

Conclusions

This research shows that the ELF EMF treatment as used by Immunent is capable of stimulating the immune system. On a cell level phagocyting cells have been shown to become more active after treatment. This result was obtained at 1,5 mT as well as at 5 µT.

On the level of the whole organism it was shown that at and around 5 µT the survival of diseased fish could be greatly improved by the treatment. In the light of the cell experiments also reported on, it is likely that this is based on an increased immune activity of the fish. The effect is present in a large window of field strengths around 5 µT, and one must go to the level of 1 nT or lower to be confident that the effect is no longer present. Proper distances between controls and test tubs are therefore important.

Because of the low field strengths required, and the surprisingly large effects on animal health, the results indicate that practical application with important economic advantages for farmers is possible. Moreover, the new experimental model used in this study can be important for bioeffects studies for EMF in general.

References

Simkó M., Droste S., Kriehuber R. and Weiss D.G. (2001): Stimulation of phagocytosis in murine macrophages by 50 Hz electromagnetic fields. Eur. J. Cell Biol. 80, 562-566

Lupke M., Rollwitz J. and Simkó M. (2004) 50 Hz magnetic fields induce reactive oxigen intermediates in human monocytes and in Mono Mac 6 cells. Free Radic. Res. 38, 985-993

Matzinger P. (2002): The danger model: a renewed sense of self. Science 2002;296:301-5.

Cuppen J.J.M., Parmentier H.K. and Savelkoul H.F.J. (2006a): Immune Stimulation In Fish And Farm Animals Through Weak Low Frequency Electromagnetic Fields, A. Hypothesis, this proceedings.

Acknowledgements

Messrs Van Kraaij, Brock, Berghs, and Bloo provided indispensible services in creating the hardware and software that supported these experiments.

ENVIRONMENTAL ANALYSIS OF THE ELECTRIC FIELD DUE TO MV OVERHEAD LINES SUPPORTED BY CONCRETE POLES

D. DESIDERI, A. MASCHIO, E. POLI

UNIVERSITY OF PADOVA, DEPARTMENT OF ELECTRICAL ENGINEERING
VIA GRADENIGO 6/A, I-35131 PADOVA (ITALY)

Abstract
This paper presents an environmental analysis of the electric field due to MV overhead lines supported by concrete poles with a pole-top-pin construction. A three-phase system of voltages has been applied to an electric model of the configuration and a three-dimensional numerical analysis has been done by using the charge simulation method. The time variation of the electric fields at the frequency of 50 Hz has been numerically computed and the obtained results have been experimentally validated by means of an extensive campaign of measurements. The preliminary set-up checks in order to minimize the perturbation error due to the measurement instrument are described. The rms values of the three components of the electric field have been measured and the data obtained around a MV line, at different heights (up to 2 m from the ground), far and near a supporting concrete pole are reported. A significant result is that the electric field at the pole surface at the height of 2 m is greater than the one at the same level under the line in the midpoint of the span.

Introduction
A three-phase MV overhead power line is relevant to an environmental analysis of the electromagnetic field in the ELF range. Poles made in reinforced concrete are extensively used as line supporting structure [1, 2], but their inclusion in the electric field evaluation is not easy. In fact, the electric field analysis far from the concrete poles, e.g. in the midpoint of the span, is a well-known case, and a bi-dimensional (2-D) model can be used obtaining good results [3, 4]. On the contrary, the inclusion of a supporting conductive structure is complicated, requiring the use of a three-dimensional (3-D) model [5].
In the following the results of an analysis on a pole-top-pin configuration used in MV overhead lines are referred. The paper is split in three sections; the first section reports the numerical analysis of the configuration, starting from an electric model, and then describing the numerical method and the obtained results. The second section reports the extensive campaign of measurements performed, whose data have been used for the validation of the numerical results. The third section presents a discussion of the results. The conclusive remarks have been reported in a final short summary.

Numerical analysis

a) Electric model of the pole-top-pin construction
The simplified structure of the analyzed MV overhead line supported by concrete poles with a pole-top-pin construction is shown in fig. 1. The three wires are represented by three straight cylindrical conductors; each one of them will be referred to in the remainder as "overhead conductor"; the axes of the conductors are parallel to each other and to the ground. The diameters of the overhead conductors (*Ø*) are the same. A three-phase system of voltages is applied to the overhead conductors.
The supporting concrete pole (referred to in the remainder as "pole") is assumed to be a cylindrical conductor, with vertical axis and radius *R* of the cross-section. The pole is assumed equipotential with the ground.
A Cartesian coordinate system has been adopted, where z is the vertical pole axis and x is the direction of the central overhead conductor (fig. 1).
The height of the pole is *a*. The axis of the central top overhead conductor (marked with 2 in fig. 1) is high *b* over the top of the pole, while the axes of the two lateral overhead conductors (marked with 1 and 3 in fig. 1) are high *a* over the ground and distant *c* from the pole axis.
In MV overhead lines with a pole-top-pin construction different values are used for the geometry, i.e. for the pole height, the pole diameter, the spacing of the overhead conductors, or the wire diameter. Among all the cases, for the numerical analysis an average value for *a* and typical values for the other parameters have been

chosen. The following values have been taken: a = 10.5 m, b = 0.8 m, c = 0.76 m, R = 0.1 m, and $Ø$ = 0.01 m [1, 2].

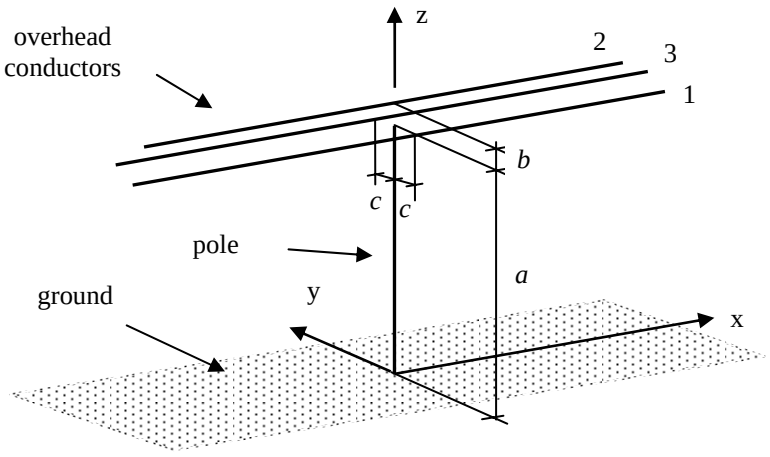


Fig. 1 Three-phase MV power line: overhead conductors, pole and ground.

b) The charge simulation method

The electric field around the MV power line was computed by using the charge simulation method (CSM). In this method conductors and their surface charges are replaced by simulating charges placed inside the equipotential contours of the conductors [6-9]. The presence of the ground plane is taken into account by a corresponding set of image charges. The charge density is initially unknown but is readily calculated when potentials are set on a number of points of the contours. Then potentials and electric field can be computed everywhere. The accuracy of the method is tested, by determining potentials and fields on control points of the conductors different from those at fixed potential.

In this study, uniformly charged segments have been used. A section of the MV line, extending 30 m apart from the pole on both sides, was considered: the equipotential contour of each overhead conductor was simulated by means of 60 couples of segments, symmetrically placed close to the axis and parallel to it, one twentieth of the radius apart from the axis. Other 70 couples of segment charges were arranged in the same way to simulate the pole equipotential contour. These 70 couples were placed on two axes, parallel to the pole axis and at opposite sides to it along y.

The accuracy was tested following two different, widely used, criteria, on potentials and on fields [7]. With 1 kV applied on one phase and 0 V on the other two, an electric potential difference generally lower than 0.2 V was found on control points. Furthermore, the ratio between tangential and normal components of the electric field on control points on the surface of the conductors was calculated, and resulted to be generally lower than 0.01 (i.e. a deviation of less than one degree of the direction of the computed field from the normal to the surface of conductors).

It is worth noting that the charge simulation method was chosen in this study because it allows to compute the electric field with a very small number of simulating charges: for the calculation, a matrix of only 500x500 elements shall be solved. Consequently, each computation run requires about 5 seconds on a PC with 256 MB RAM, 1.8 GHz Pentium IV.

c) Electric field computations

It is well known [1, 2] that the electric field around a three-phase transmission line is generally a vector rotating in a plane, where it draws an ellipsis. In order to get the complete description of the ellipsis, in this research the field was computed by means of the CSM at different times along the whole cycle: the direction and magnitude of the electric field at its maximum and minimum were recorded, giving the major and minor axes of the ellipsis and the plane where it lies.

In order to achieve this result, the three contributions to the electric field due to each conductor at unit potential, while the two others are at zero potential (with the pole always at zero potential), were computed.

Indicated with $\mathbf{E}(x, y, z, V_1, V_2, V_3)$ the vector of the electric field in a point x, y, z due to the potentials V_1, V_2, V_3 applied to the three overhead conductors 1, 2 and 3, the contributions are:

$$\begin{aligned}\mathbf{E}_1(x, y, z) &= \mathbf{E}(x, y, z, 1, 0, 0)\\ \mathbf{E}_2(x, y, z) &= \mathbf{E}(x, y, z, 0, 1, 0)\\ \mathbf{E}_3(x, y, z) &= \mathbf{E}(x, y, z, 0, 0, 1)\end{aligned} \quad (1)$$

and the total electric field is:

$$\mathbf{E}(x, y, z, V_1, V_2, V_3) = \mathbf{E}_1(x, y, z)\, V_1 + \mathbf{E}_2(x, y, z)\, V_2 + \mathbf{E}_3(x, y, z)\, V_3 \quad (2)$$

The potentials V_1, V_2, V_3 have been set with reference to a three-phase line voltage of 20 kV rms: 3600 values have been computed with an iteration process, by increasing the phase of 0.1° each step, in order to cover the whole cycle of 360°.
Recording the maximum of E_x, E_y and E_z, their rms value can be computed simply dividing the maximum by $\sqrt{2}$. Moreover the rms value of the intensity of the total electric field results as the root sum square of the three rms values of E_x, E_y and E_z.
Finally, the major and minor axes of the ellipsis are found by recording the maximum and minimum of the magnitude of $\mathbf{E}(x, y, z, V_1, V_2, V_3)$, while the values of the three components E_x, E_y and E_z at the maximum and the minimum give the direction of the axes.

d) Numerical results

As a first analysis, the rms values of E_x, E_y and E_z on the plane y = 0 have been considered up to z = 2 m. The numerical results of E_x, E_y and E_z at z = 1 m and at z = 2 m are reported in fig. 2, respectively on the left, at the centre and on the right. The data are reported up to 10 m from the pole.

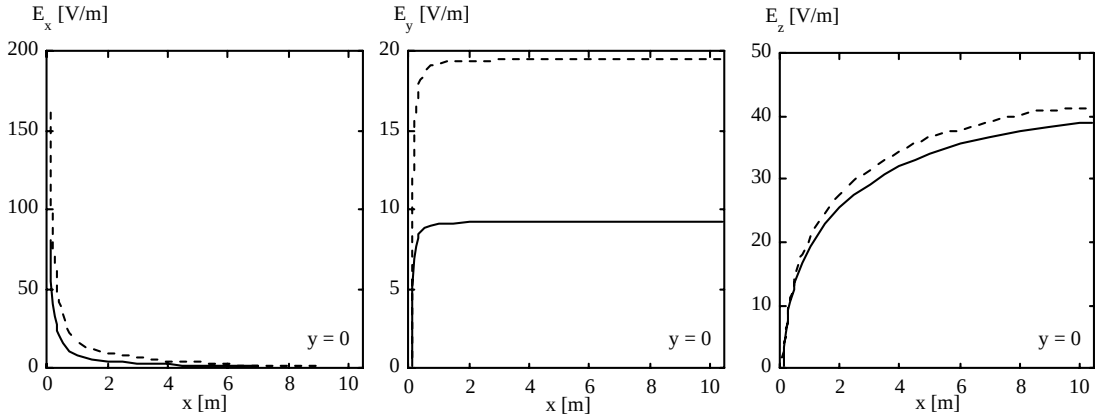


Fig. 2 Numerical results of E_x (left), E_y (centre), E_z (right) at y = 0, z = 1 m (continuous lines) and at y = 0, z = 2 m (dashed lines).

The effect of the pole is clear. At the pole, the electric field is normal to the pole surface. E_x is large, while E_y and E_z are null.
Moving from the pole in the x direction, from fig. 2 it can be seen that E_y quickly reaches the same value that is found far from the pole, i.e. at the midpoint of the span at y = 0. In particular the effect of the pole for E_y is extremely localized. E_x and E_z reach the same value found far from the pole approximately after a few meters. Increasing x, at y = 0, E_x tends to zero, while E_z increases its value at the one expected at the midpoint of the span.
It can be noticed that the reinforced concrete pole makes E_x at the pole even higher than the values of E_y and E_z evaluated at the midpoint of the span.
A second analysis has been performed at x = 0 and at x = 5 m and the rms values of E_x, E_y and E_z have been considered again up to z = 2 m. The values at x = 5 m are assumed not affected by the pole, as indicated by the data reported in fig. 2. On the other hand, the data at x = 0 are reported to analyze the effect of the pole in the y direction.
The numerical results of E_y and E_z at z = 1 m and at z = 2 m are reported in fig. 3 and fig. 4 respectively, showing on the left the value at x = 0 and on the right the value at x = 5 m. The data are reported up to y = 10 m.
Again, at the pole, the electric field is normal to the pole surface. At x = 0, on the pole surface, E_y is large, while

E_x and E_z are null. It is worth noting that the value of E_y at the pole surface is equal to E_x, at the pole at y = 0, as shown in fig. 2.
At a few meters from the pole E_y has the same value at x = 0 and at x = 5 m, and E_z behaves in the same way. It is again confirmed that at this distance the pole effect is negligible.
From the numerical analysis it results that E_x is null at x = 0, as expected from the symmetry of the configuration, and quite small (only few volts per meter) at x = 5 m and z not greater than 2 m.

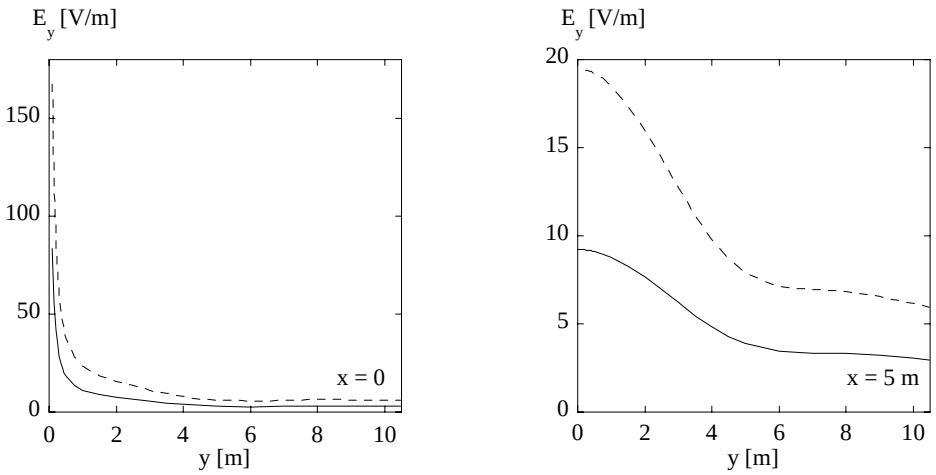


Fig. 3 Numerical results of E_y on the left at x = 0, z = 1 m (continuous line) and at x = 0, z = 2 m (dashed line); on the right at x = 5 m, z = 1 m (continuous line) and at x = 5 m, z = 2 m (dashed line).

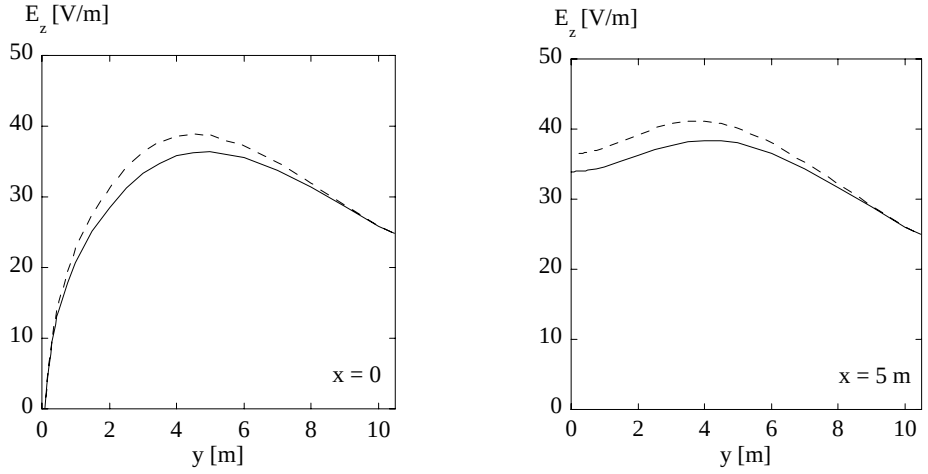


Fig. 4 Numerical results of E_z on the left at x = 0, z = 1 m (continuous line) and at x = 0, z = 2 m (dashed line); on the right at x = 5 m, z = 1 m (continuous line) and at x = 5 m, z = 2 m (dashed line).

A third analysis was done on the magnitude and on the direction of **E** at its maximum and minimum, thus identifying the axes of the ellipsis drawn by the field. The direction can be indicated by means of the angles of the vector of the field with the three coordinate axes. As an example, in the plane z = 2 m and on x = 0, 0.5, 1 and 5 m, the magnitude of the field vector and its minor angle (0 ÷ 90°) with the vertical axis z, as a function of y up to 10 m, are reported in fig. 5, on the left and on the right respectively.
About the angle with the z direction, at x = 0, it is noticed that on the pole surface only a field at 90° with z is allowed, while, increasing the distance from the pole, the angle is reduced to 20° at y = 2 m, is almost null at y = 5 m, and is about only 10° for greater distances. Near y = 0, at x = 0.5 m the influence of the pole gives still a deviation of about 70° from the perpendicular, while at x = 1 m the angle is reduced to 40°. Finally, for x = 5 m the angle with the z direction is generally equal or less than 10° for any y up to 10 m.
It is interesting to note that also the data reported in fig. 5 show that the influence of the pole tends to vanish at a distance of a few meters, in agreement with the observations done on the electric field components.

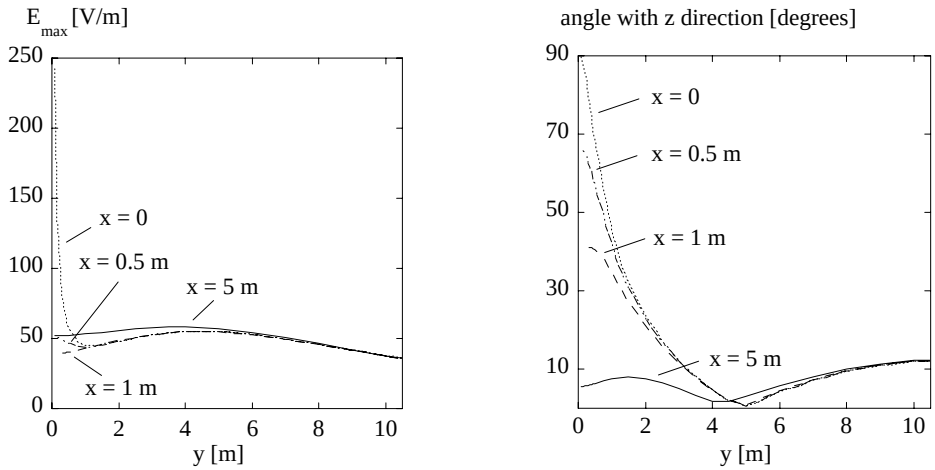


Fig. 5 Numerical results of E_{max} and the angle with the z direction versus y at different values of x.

Experimental results

a) Instrumentation and perturbation error

The instrumentation used for the electric field measurement consisted in a PMM EHP-50C probe, connected via an optical fibre to a PMM 8053 portable field meter.

The probe is approximately a cube with 8 cm side. The experimental data are referred to the barycentre of the probe: therefore with the probe placed on the ground, the z quote is 0.04 m.

The probe was taken at a distance of at least five meters from the PMM 8053 and the operator. The PMM 8053 unit was set to measure electric fields in the frequency range 6 ÷ 500 Hz; the display showed the rms value of the total electric field, together with the rms values of the three field components along the probe axes. The system allows the analysis resolved in frequency of the measured signal and the measure of the rms value of the electric field at a specific frequency (among those allowed).

For the measurements at different heights, the probe is installed on an insulating rod and then connected to a supporting structure, mainly a wooden tripod with a limited metallic parts, e.g. at the connection between the insulated rod and the wooden tripod.

The effect of these metallic parts on the measurements was investigated. It was considered that if a local variation was due to these metallic parts and the probe was near to them, the probe should have measured a distorted electric field, so affecting the data. In this respect a few measurements have been taken with different distances *d* between the EHP-50C probe and the metallic parts of the tripod. The data have been taken under a MV power line, with the two configurations planned for the experimental campaign. The most critical was the configuration for the measurements at z = 1 m, where *d* might be taken very small. At z = 1 m, a clear variation on the measurements have been obtained with *d* set at a few centimetres, while the effect became negligible when *d* was kept greater than about 0.3 m. For the experimental campaign it has been decided to keep *d* greater than 0.4 m, for the measurements taken at z = 1 m. For the measurements at z = 2 m, *d* was always about 0.7 m.

b) System description

Fig. 6 shows the place where the measurement campaign has been performed. No objects of any kind (trees, fences, etc,) are present at a distance less than 20 m from the pole.

Measurements of the geometry have been done by a laser meter (Bosch, mod. DLE 150). The height *a* of the pole was about 10.5 m; the spacing of the overhead wires at the pole were in good agreement with the *b* and *c* values used for the numerical analysis. The pole radius was about 0.15 m at the ground level, and was reducing its value of about 0.075 m per meter of increase along the pole height.

Small ground irregularities and few centimetres of grass and brushwood, evenly distributed, have given local perturbations to the electric field at ground level.

On the side where the measurements have been done, the increase of the ground level was of about 0.1 m at a distance of 10 m from the pole under the overhead wires. By using a rough estimate of the sag in the midpoint of the span, combined with the catenary curve, at 10 m from the pole the overhead wires lowering was estimated to be about 0.3 m.

A Cartesian system was used, the same indicated in fig. 1.



Fig. 6 The MV power line.

During the experimental campaign, the measurements were performed with the PMM EHP-50C probe at three different distances from the ground: 0.04 m, 1 m and 2 m respectively. Preliminary measurements have been done to check the contribution of harmonics to the electric field. As they have shown to be negligible, the data have been obtained with the range 6 ÷ 500 Hz and assumed to be due only to the main component, at 50 Hz.
The measurements have been performed in three days of fine and dry weather, with a temperature between 18°C and 24°C. About the measurement uncertainties, from the certificate of calibration of the instrument, the expanded uncertainty [10] at 50 Hz is 3% on the magnitude of the electric field at 23±3°C. Moreover a temperature effect of 0.05 dB/°C, obtained from the probe technical data sheets, has also been considered. With a temperature between 18°C and 24°C, a maximum value of 0.4 dB has been considered due to the temperature effect. Without considering further components of uncertainties, with a normal distribution for the uncertainty reported on the certificate of calibration, and a rectangular distribution for the temperature, a combined standard uncertainty has been calculated and a coverage factor of two has been used for obtaining the expanded uncertainty [10]. In this way the uncertainty results 6% of the total electric field value.
The rms value of the line voltage was 20 kV.

c) Experimental results and validation of the numerical analysis
A first set of experimental results is reported in fig. 7. The data are taken at y = 0.

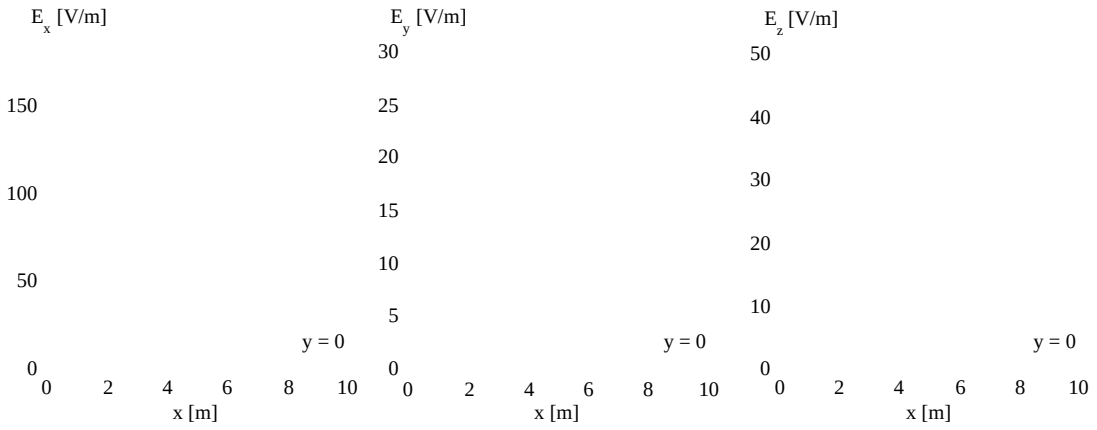


Fig. 7 Comparison between numerical and experimental data. Numerical results of E_x (left), E_y (centre), E_z (right) at y = 0, z = 1 m (continuous lines) and at y = 0, z = 2 m (dashed lines). Experimental data of E_x (left), E_y (centre), E_z (right) at y = 0, z = 1 m (full squares) and at y = 0, z =2 m (full diamonds).

The rms values of E_x, E_y and E_z at z = 1 m and at z = 2 m are reported respectively on the left, the centre and the right of fig. 7: full squares show the experimental data at z = 1 m, and full diamonds show the experimental data at z = 2 m. For comparison, also the numerical data at y = 0 are reported: continuous lines show the numerical results at z = 1 m, dashed lines show the numerical results at z = 2 m. The numerical data are those already reported in fig. 2, which are repeated here for a simpler comparison between numerical and experimental data.
It can be noticed a good agreement between the results obtained from the CSM and the experimental data. Moreover the lowering of the overhead wires, combined with the variation of the ground level, agrees with the increase in the experimental data of E_y and E_z at distances greater than about 4 m from the pole.

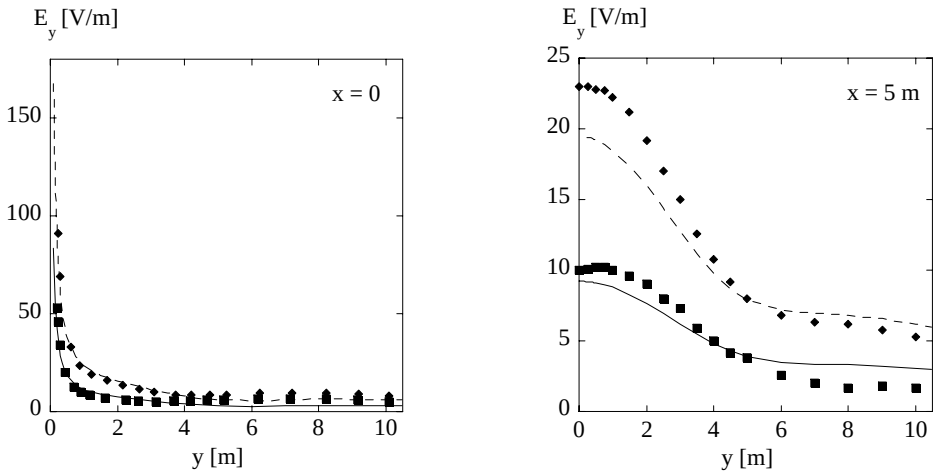


Fig. 8 Comparison between numerical and experimental data. Numerical results of E_y on the left at x = 0, z = 1 m (continuous line) and at x = 0, z = 2 m (dashed line), on the right at x = 5 m, z = 1 m (continuous line) and at x = 5 m, z = 2 m (dashed line). Experimental data of E_y on the left at x = 0, z = 1 m (full squares) and at x = 0, z = 2 m (full diamonds), on the right at x = 5 m, z = 1 m (full squares) and at x = 5 m, z = 2 m (full diamonds).

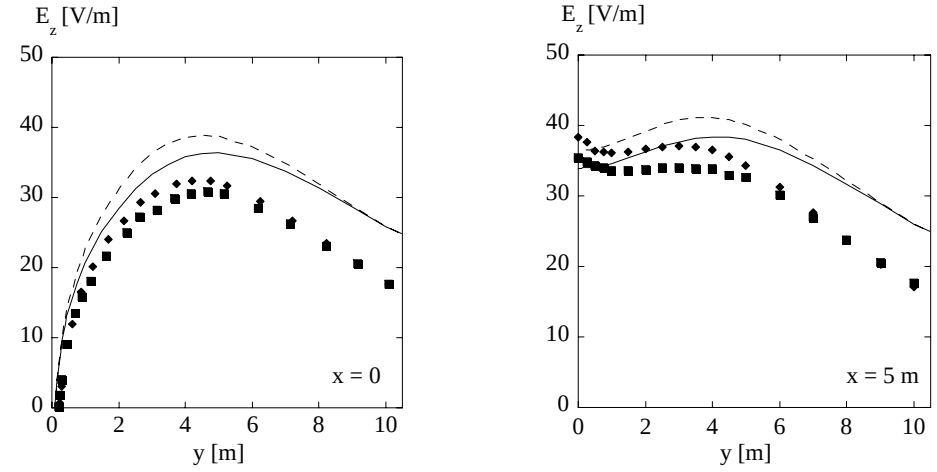


Fig. 9 Comparison between numerical and experimental data. Numerical results of E_z on the left at x = 0, z = 1 m (continuous line) and at x = 0, z = 2 m (dashed line), on the right at x = 5 m, z = 1 m (continuous line) and at x = 5 m, z = 2 m (dashed line). Experimental data of E_z on the left at x = 0, z = 1 m (full squares) and at x = 0, z = 2 m (full diamonds), on the right at x = 5 m, z = 1 m (full squares) and at x = 5 m, z = 2 m (full diamonds).

A second analysis has been performed at x = 0 and at x = 5 m. The rms values of E_y and E_z at z = 1 m and at z = 2 m are reported in fig. 8 and fig. 9 respectively, showing on the left the values at x = 0 and on the right the values at x = 5 m. In both figures numerical and experimental data are reported: continuous lines show numerical results at z = 1 m, dashed lines show numerical results at z = 2 m, full squares show experimental data at z = 1 m, and finally full diamonds show experimental data at z = 2 m. The numerical data are those already

reported in fig. 3 and fig. 4.
Numerical and experimental data are in good agreement, with in general a difference of about 20% for E_z and a lower difference for E_y. Therefore the validation of the numerical analysis previously reported has been obtained.

Discussion

The analysis performed up to z = 2 m, has shown that a reinforced concrete pole used in a MV power line, with a pole-top-pin construction, and with a height of 10.5 m, extends its effects in the electric field configuration around the pole up to a few meters.
At the pole, at the quote z = 2 m, the value of the electric field normal to the pole equipotential surface is higher than the value of its main component at the midpoint of the span. This result appears from the values of E_x, E_y and E_z under the line (y = 0) reported in fig. 7, and the values at x = 0 and at x = 5 m reported in fig. 8 and fig. 9.
Therefore, the usual analysis performed at the midpoint of the span is not able to give an evaluation of the maximum exposure to the electric field with a MV power line supported by reinforced concrete poles, at least with reference to a maximum quote of z = 2 m.

Summary

The electric field due to a MV power line with a pole-top-pin construction has been analyzed in this paper.
A numerical analysis has been performed, based on an electric model equivalent to the configuration. The numerical results have been validated by an extensive experimental campaign of measurements, performed after checks on the measurement equipment, in order to minimize the perturbation errors.
At z = 2 m, at the pole surface, the maximum rms value of the electric field has been obtained: this value is greater than the one calculated far from the pole at the midpoint of the span.

References

[1] *Standard Handbook for Electrical engineers*, 10th ed., D. G. Fink and J. M. Carroll, Eds. McGraw-Hill, 1968
[2] V. Cataliotti, *Impianti elettrici*, vol. I, Italy: Flaccovio Editore, 2005.
[3] CEI 211-4, Guide to calculation methods of electric and magnetic fields generated by power-lines, Comitato Elettrotecnico Italiano, Milano 1996.
[4] CIGRE WG 36-01, Electric and magnetic fields produced by transmission systems. Description of phenomena - practical guide for calculation, Paris 1980.
[5] D. Desideri, M. Guarnieri, and E. Poli, "MV line electric field evaluation near a concrete pole," *IEEE Trans. Magn.*, vol. 40, pp. 718-721, Mar. 2004.
[6] H. Singer, H. Steinbigler, and P. Weiss, "A charge simulation method for the calculation of high voltage fields, " *IEEE Trans. Power App. Syst*., vol. 93, pp. 1660-1668, Sept. 1974.
[7] N. H. Malik, "A review of the charge simulation method and its applications," *IEEE Trans. Electr. Insulation*, vol. 24, pp. 3-20, Feb. 1989.
[8] E. Poli, "The use of image charges in the charge simulation method: a parallel-plane dielectric plate covering a conductor," *IEEE Trans. Magn.*, vol. 28, pp. 1076-1079, Mar. 1992.
[9] P. N. Nikolopoulos, "On the accurate evaluation of the electric field and of the field-lines of three-phase overhead lines with smooth or stranded conductors," 4th Int. Symp. on High Voltage Engineering, paper 12.10, Athens 1983.
[10] *NIS 3003 - The expression of uncertainty and confidence in measurement for calibrations*, NAMAS, England, edition 8, May 1995.

DEVELOPMENT OF A SIMPLE AND LOW COST MAGNETIC FIELD MEASUREMENT EQUIPMENT UP TO 400 kHZ

D. DESIDERI, A. MASCHIO

UNIVERSITY OF PADOVA, DEPARTMENT OF ELECTRICAL ENGINEERING
VIA GRADENIGO 6/A, I-35131 PADOVA (ITALY)

Abstract

In this paper the design, realization and operative ratings of a new simple and low cost magnetic field measurement equipment in the frequency range from 10 Hz to 400 kHz are reported. The design specifications of this device have been chosen following the indications given for the magnetic field reference sensor in Standard EN 50366, concerning emissions of household and similar electrical appliances with reference to human exposure to electromagnetic fields. The developed equipment consists of three mutually perpendicular concentric coils, each one of two turns, for magnetic field analysis up to 400 kHz. By using operational amplifiers, an electronic elaboration of the coil signals has been done and is described. The characterization of the equipment has been performed by using a laboratory set-up, where the test magnetic field configuration has been obtained with a single layer solenoid in house developed.

Introduction

Quantitative determinations of the magnetic field emissions from equipments in the Extremely Low Frequency (ELF) range have been performed and reported [1, 2]. The analysis of electric appliances, relevant to the evaluation of the human exposure to electromagnetic fields, is in particular required by Standard EN 50366, that in general considers for the magnetic fields a frequency range from 10 Hz to 400 kHz [3].

Purpose of this work is to develop a new simple and low cost instrument able to measure the magnetic field in the above mentioned frequency range.

The paper is divided in two main sections. In the first part, the design and realization of the measurement equipment are reported. In the second section, the laboratory set-up used for the characterization of the system is depicted, and the obtained operative ratings of the developed device are reported.

Finally, in the summary, the conclusive remarks are given.

Design and realization of the measurement equipment

a) *Coils*

For the measurement of the magnetic flux density, Standard EN 50366 indicates a reference sensor that consists of three mutually perpendicular concentric coils, with a total measuring area for each coil of 100 ± 5 cm^2. The outside diameter of the reference sensor must be lower than 13 cm.

Following the specifications given in Standard EN 50366 for the magnetic field reference sensor, a simple and low cost probe has been developed.

It consists of three mutually perpendicular concentric coils. Three two turns coils have been built by using a transformer wire with a cross-section area of 0.3 mm^2. Two of the three coils are almost rectangular in shape, with dimensions for each turn of 65 mm x 76 mm and 64 mm x 78 mm respectively; the third coil has a circular cross section, with diameter of each turn of 79 mm. In such a way a measuring area of about 100 cm^2 is obtained for each coil.

For supporting the three mutually perpendicular coils a PVC cylindrical structure has been built, 68 mm height and 80 mm diameter, on which three grooves have been drawn for placing the coils. Each coil ends with a twisted pair 0.6 m long.

The cylindrical PVC structure is mounted on a PVC base.

For the wires a fixing structure has been set, in order to make the system stable during operation.

In fig. 1 a picture of the three coils probe is shown.

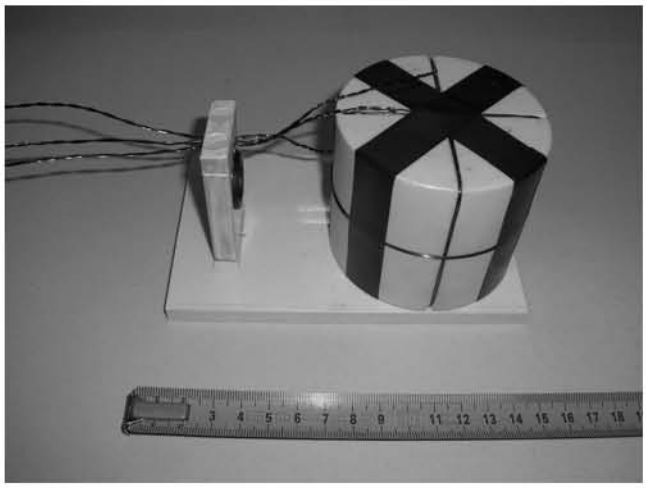


Fig.1 Picture of the three-coils probe

b) *Equivalent electrical parameters for a coil*

The frequency range of interest for the system is the one indicated in the Standard EN 50366, i.e. from 10 Hz to 400 kHz. Related to it, an electrical analysis of each coil has been performed.

The length of the wires of the three coils is almost equal for all of them; so their electric resistance R can be considered the same, and it is about 0.12 Ω in DC. When the frequency f increases, the resistance increases due to the skin effect. The parameter involved is the penetration depth δ that is:

$$\delta = \frac{1}{\pi f \mu_0 \sigma} \tag{1}$$

with the permeability of free space $\mu_0 = 4\ \pi\ 10^{-7}$ H/m and the conductivity of the copper $\sigma = 5.8\ 10^7$ S/m. At 400 kHz, δ is about 0.1 mm, and assuming a current evenly distributed near the surface on a depth equal to δ, it results an estimated value for R of 0.22 Ω, in agreement with the value obtained by an LCR meter (Agilent 4285A) that has been of about 0.25 Ω at 400 kHz.

As far as the calculation of the inductance L is concerned, being the coils made up of only two turns, the concept of total inductance L_{tot} of a circuit split in two parts has been used:

$$L_{tot} = L_1 + L_2 + 2M \tag{2}$$

where $L_1 = L_2 = L$ is the self inductance of one turn and M is the mutual inductance between the two turns. For the evaluation of L and M, the two rectangular coils have been approximated with a square one (side length 71 mm); according to [4], the corresponding value of L_{tot} is 1 μH when the current is evenly distributed inside the coil conductor. Increasing the frequency, a correction due to the skin effect could be introduced as the current tends to concentrate on the outer part of the conductor, but is quite small and can be neglected: in fact, with the current concentrated on the conductor surface, the inductance decreases down to 0.97 μH. In a similar way, for the circular coil, a value of 0.92 μH for the current evenly distributed and 0.90 μH for the current concentrated in the outer part of the conductor have been estimated. Finally, an additional term of about 0.15 μH, due to the length of the twisted pair connection, must be added to the previous values. By using an LCR meter (Agilent 4285A) a value of about 1.2 μH for L was measured for the three coils (with their connections) up to a few MHz, in good agreement with the estimation above reported.

A coil, without load, has an output voltage $v_0(t)$ equal to:

$$v_0(t) = -\frac{d\Phi(t)}{dt} = -\frac{d}{dt}\int_{A_p} \mathbf{B}(t) \bullet \mathbf{n} dA = -A_p \frac{d}{dt} B_{\perp av}(t) \tag{3}$$

where A_p is the coil area and $B_{\perp av}$ is the average value on A_p of the component of **B** perpendicular to the coil area.

In the frequency range from 10 Hz to 400 kHz, an equivalent electrical scheme of the probe, shown in fig. 2, is

therefore given by an ideal voltage source in series with a resistance *R* and an inductance *L*, with *R* and *L* above reported; with $v_1(t)$ it has been indicated the coil output voltage.

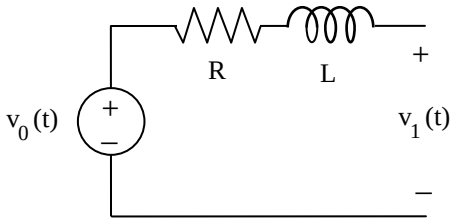


Fig.2 Equivalent electrical parameter for a coil.

Finally, in the frequency domain, by using phasors, (3) becomes:

$$\overline{V}_0 = -j\omega A_p \overline{B}_{\perp av} \tag{4}$$

where $\omega = 2\pi f$; j is the imaginary unit, and $\overline{V}_0$ and $\overline{B}_{\perp av}$ are the phasors of $v_0(t)$ and $B_{\perp av}(t)$ respectively.

c) *Electronics*

An integration of the coil output signal is required in order to obtain the value of $B_{\perp av}$, as derives from (3). Therefore the electronic circuit is basically an integrator, combined with a low pass filter, as schematically indicated in fig. 3.

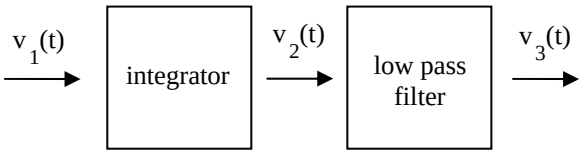


Fig.3 Schematic of the electronic circuit.

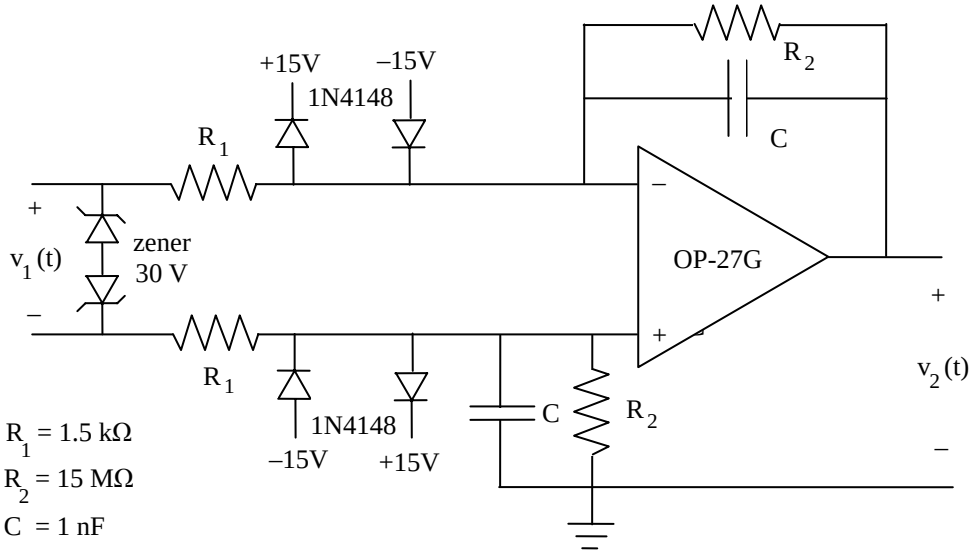


Fig.4 The integrator.

For the integrator, the basic circuit is the one commonly used for magnetic field coil, depicted in [5]. The detailed circuit is reported in fig. 4. An OP-27G has been used as operational amplifier. In the input, zener diodes and 1N4148 diodes are placed for protection. The input of the integrator has two resistances (R_1) each one of

1.5 kΩ: when the coil is connected to the integrator, it results that the resistance *R* and the inductance *L*, equivalent of the coil, are in series with R_1, and, on considering their values and the frequency range of interest, *R* and *L* can be neglected in the analysis. Therefore, in the frequency domain and using (4) it results that:

$$\overline{V}_1 = \overline{V}_0 = -j\omega A_p \overline{B}_{\perp av} \tag{5}$$

In the frequency domain, with $\overline{V}_2$ phasor of the integrator output voltage, the transfer function $A_1(j\omega)$ of the integrator is:

$$A_1(j\omega) = \frac{\overline{V}_2}{\overline{V}_1} = -\frac{R_2}{R_1}\frac{1}{1+j\omega C R_2} \tag{6}$$

with R_1, R_2, and *C* indicated in fig. 4. The DC gain of the integrator is 80dB (i.e. 10000), and a pole is set at 10 Hz.
An active filter has been placed after the integrator: it is a second order Butterworth low-pass filter [6]. In the frequency domain, with $\overline{V}_3$ phasor of the low-pass filter output voltage, the transfer function $A_2(j\omega)$ of this filter is:

$$A_2(j\omega) = \frac{\overline{V}_3}{\overline{V}_2} = K_1 \frac{1}{1+j\omega R_3 C_3 (3-K_1) - (\omega R_3 C_3)^2} \tag{7}$$

C_3 has been set at 1 nF, R_3 at 390 Ω, and therefore the cutoff frequency has been set at 400 kHz, in order to filter the noise at frequencies higher than those of interest. The DC gain K_1 is equal to 4dB, i.e. 1.586.

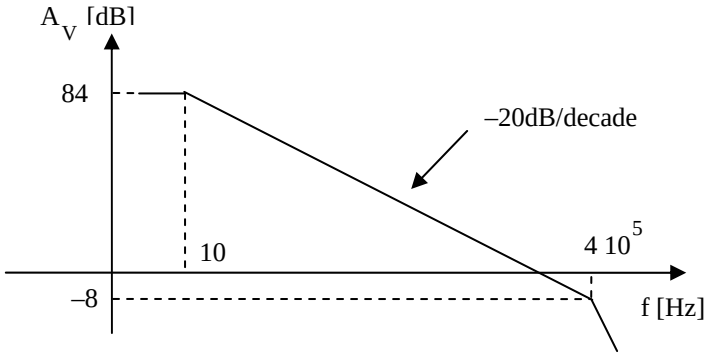


Fig.5 Bode diagram of the amplitude of $A_V(j\omega)$.

Combining the two electronic stages, a voltage transfer function in the frequency domain $A_V(j\omega)$ results, that is given by the product of (6), and (7):

$$A_V(j\omega) = A_1(j\omega)\, A_2(j\omega) = \frac{\overline{V}_3}{\overline{V}_1} \tag{8}$$

The Bode diagram of the amplitude of $A_V(j\omega)$ is reported in fig. 5.
In the frequency range from 10 Hz to 400 kHz, the amplitude of the voltage transfer function of the electronics has a slope of –20dB/decade, from 84dB at 10 Hz down to –8dB at 400 kHz.

d) *Coil function transfer*
Considering the coil, from (5) and (8), the function transfer $H(j\omega)$ of the system results:

$$H(j\omega) = \frac{\overline{V}_3}{\overline{B}_{\perp av}} = \frac{\overline{V}_1}{\overline{B}_{\perp av}}\frac{\overline{V}_3}{\overline{V}_1} = -j\omega A_p\ A_V(j\omega) \tag{9}$$

The coil therefore adds a zero to the transfer function $A_V(j\omega)$, resulting a Bode diagram of the amplitude of

H(jω) that has been reported in fig. 6.

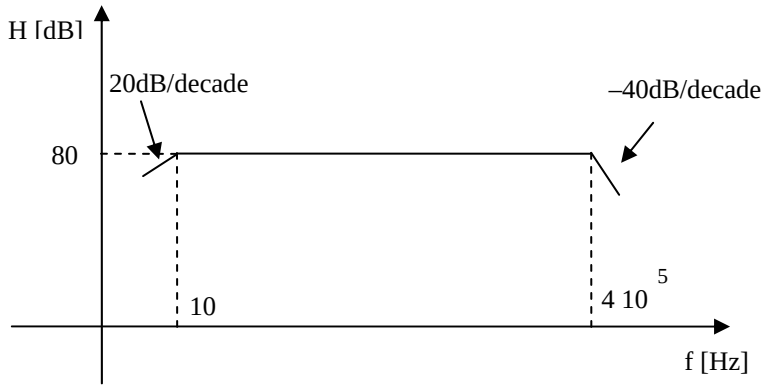


Fig.6 Bode diagram of the amplitude of the function transfer of the system H(jω).

Therefore, in the frequency range from 10 Hz to 400 kHz, the integrator stage and the coil (that makes the derivative of $B_{\perp av}$) give an output voltage proportional to $B_{\perp av}$; a constant gain of 80dB (i.e. 10000) results, i.e. at 100 μT of average perpendicular magnetic flux density corresponds an output voltage of 1 V. Frequency components out of the considered frequency range are filtered.
As the output voltage can vary from ± 10 V, a maximum rating of 1 mT results. It must be noticed that, due to the slew rate (typically of 2.8 V/μs) of the OP-27G that has been used in all the electronic stages [7], a distortion of the signal occurs with the maximum output signal at the highest frequencies of the considered frequency range.

Characterization of the measurement equipment
An experimental laboratory set-up has been performed for the characterization of the measurement equipment. It consisted of a large solenoid, inside which the three coils have been placed during the tests.

a) *Test solenoid*
A single layer cylindrical solenoid, with the characteristics given in Table I, has been realized. The solenoid ends with a twisted pair 4.5 m long. The solenoid has been built on a polypropylene tube, 5 mm thick and with nominal minor diameter of 305 mm. The turns have been realized by using a conductor with a section of 2.5 mm^2.

Table I. Construction data of the test solenoid.

Number of turns	N	187
Internal diameter	Φ	0.305 m
Length	a	0.67 m
Section of the conductor	S_{cond}	2.5 mm^2
Diameter of the conductor (including insulation)	Φ_{cond}	3.6 mm

Two LCR meters (a Metrix IX 3131 at 120 Hz and 1 kHz, and an Agilent 4285A from 75 kHz up to 30 MHz) were used for evaluating the parameters of the solenoid. The equivalent circuit consisted of a capacitance *C* in parallel to the series of a resistance *R* and an inductance *L*.

Table II. Electrical parameters of the test solenoid.

Inductance	L	4.3 mH
Capacitance	C	220 pF
Resistance (DC)	R	1.6 Ω

The parameters found for the solenoid are reported in Table II; L and C values hold up to a few MHz. With reference to the measured inductance value, it is well in agreement with the one estimated from the geometry: in fact, the short solenoid approximation gives for *L* an estimated value of 4.1 mH. From the short solenoid

approximation also results that the calculated magnetic flux density in the centre of the solenoid is 316 μT (directed along the axis of the cylinder) for 1 A of current in the solenoid turns.
A check of this value has been performed by measuring the current in the solenoid turns with a LEM PR50 (DC-50 MHz bandwidth) current probe and the magnetic flux density with a PMM EHP-50C (DC-100kHz bandwidth) probe connected via an optical fibre to a PMM 8053 portable field meter. Tests have been performed at 50 Hz, 100 Hz, 1 kHz, and 10 kHz, and the magnetic flux density directed along the axis of the cylinder was between 330 and 340 μT for 1 A of current in the solenoid turns. This values are in good agreement with the estimated one.

b) *Test circuit*
Two power supplies have been used for the solenoid: a Kepco BOP-100-4D and an Agilent 33120A function generator. The output signal from the electronic circuit has been acquired by a Yogokawa DL1540L digital oscilloscope. The block scheme of the test circuit is shown in fig. 7.

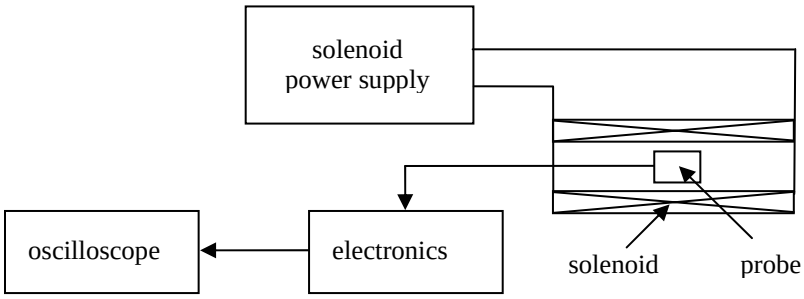


Fig.7 Block scheme of the test circuit for the probe characterization

The probe has been placed in the centre of the solenoid, with the coil under test with the area perpendicular to the solenoid axis. The solenoid has been connected to the Kepco BOP-100-4D power supply, driven by the Agilent 33120A function generator.

c) *System ratings*
An offset was present at the output of the electronics, and was eliminated by selecting the AC signal input coupling of the oscilloscope: a less than 10 Hz cutoff frequency is introduced in this way.
An output voltage noise of about ± 2 mV has been measured, that is 0.02% of the output maximum voltage.

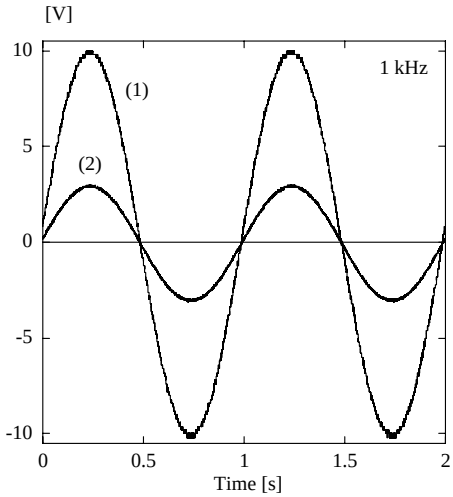


Fig.8 Test at 1 kHz: (1) electronics output voltage $v_3(t)$ and (2) solenoid turns current (1 V corresponds to 1 A).

By using the test circuit previously described, tests have been performed at 10 Hz, 1 kHz, 10 kHz and 100 kHz.
At 10 Hz and 1 kHz, the maximum of the magnetic flux density was 1 mT (i.e. 707 μT rms value), obtained with a maximum current in the solenoid turns of 3 A (i.e. 2.12 A rms value); the electronics output voltage $v_3(t)$ was

measured and the rms value is reported in Table III. As an example, at 1 kHz, in fig. 8, the electronics output voltage $v_3(t)$ and the solenoid turns current (1 V corresponds to 1 A) are reported, indicated with (1) and (2) respectively.
The test circuit could not test the system at the maximum ratings at 10 kHz and 100 kHz, and therefore at these frequencies the tests have been performed at the reduced ratings shown in Table III. The solenoid turns current has been measured directly at the output of the solenoid, in order to avoid the capacitance effect of the connections.
The results are in good agreement with the design ratings.

Table III. System ratings

Frequency [kHz]	B [μT] rms	I [A] rms	V_3 [V] rms
0.01	707	2.12	5.00
1	707	2.12	7.07
10	70.7	0.212	0.723
100	1.5	0.0045	0.015

c) *Analysis at 400 kHz*
At 400 kHz the analysis has been performed by using a simple equivalent model of the system.
The power supply has been modelled with an ideal voltage source, and the solenoid has been considered an ideal inductor (with L = 4.3 mH), magnetically coupled with the coil. The ratio between the ideal voltage source and the coil output voltage results of about 1300.
For the test, the Agilent 33120A function generator has been used as solenoid power supply. Its 50 Ω equivalent output resistance is in effect negligible compared with the equivalent impedance of the test solenoid at 400 kHz. With a 7 V rms value of power supply voltage and the test circuit of fig. 7, the electronics output voltage was about 2 mV rms value. This value is in agreement with the value expected from the system, even if it is close to the noise of the electronics output voltage.

Summary
A new simple and low cost magnetic field measurement equipment in the frequency range from 10 Hz to 400 kHz has been developed.
The design and realization of the equipment has been reported. The function transfer of the system has a constant 80dB gain in the above mentioned frequency range.
The characterization of the system has been performed at maximum ratings from 10 Hz up to a few kHz. At the higher frequencies, the characterization has been performed only at small signals.
The results are all well in agreement with the design ratings.

References
[1] M. Addari, F. Bessi, O. Bottauscio, G. Crotti, G. D'Amore, I. Gallimberti, G. Molinari, M. Repetto, S. Tofani, and U. Tromboni, “Household ELF environment assessment,” in *Proc. EMC '94 International Symposium on Electromagnetic Compatibility*, Roma, 1994, pp. 21-26.
[2] *CEI 211-6 - Guide for the measurement and the evaluation of electric and magnetic fields in the frequency range 0 Hz - 10 kHz, with reference to the human exposure*, Comitato Elettrotecnico Italiano, Milano 2001.
[3] *Household and similar electrical appliances - Electromagnetic fields - Methods for evaluation and measurement*, European Standard EN 50366: 2003-05.
[4] F. Glover, *Inductances calculations – Working formulas and tables*, Instruments Society of America, Research Triangle Park, NC, 1973.
[5] I. Hutchinson, *Principles of Plasma Diagnostics*, Cambridge University Press, Cambridge, 1987.
[6] P. Horowitz, and W. Hill, *The art of electronics*, Cambridge University Press, 2nd ed., 1989.
[7] *Analog Devices data sheets.* Available: http://www.analog.com

EFFECT OF MOBILE PHONE (GSM-900) FIELD ON KINDLED SEIZURES (AS AN INDEX OF NEURAL EXCITABILITY) IN RATS

A. BAYAT

DEPARTMENT OF MEDICAL PHYSICS, TARBIAT MODARES UNIVERSITY, TEHRAN, IRAN

agbayat@gmail.com

S. M. P. FIROOZABADI

DEPARTMENT OF MEDICAL PHYSICS, TARBIAT MODARES UNIVERSITY, TEHRAN, IRAN

Pourmir@Modares.ac.ir

J. MIRNAJAFI-ZADEH

DEPARTMENT OF PHYSIOLOGY, TARBIAT MODARES UNIVERSITY, TEHRAN, IRAN

mirnajafi@yahoo.com

M.E. REZVANI

DEPARTMENT OF PHYSIOLOGY, TARBIAT MODARES UNIVERSITY, TEHRAN, IRAN

Abstract

The rapid expansion of mobile communication has generated intense interest, but has also fuelled ongoing concerns. Radiofrequency radiations are suspected to affect cognitive functions in both humans and animals. Previous studies have suggested that biological parameters of central nervous system can be impaired by "Global System for Mobile Communication" (GSM) exposure in animals.

In this study, the effect of GSM radiation on kindled seizures (as an index of neural excitability) was investigated. All the animals were implanted with a tripolar (stimulating and recording) electrode in the amygdala and were kindled by daily electrical stimulating of amygdala. Different groups of full kindled rats exposed by radiofrequency fields emitted from GSM (950 MHz, Band with: 200 kHz, pulsed at 217 Hz) mobile phone simulator (output power of antenna: 3 and 5 W, power density: 1.8 mW/cm^2) for 2 and/or 4 hours and at different times after the last kindling seizure (24, 48 and 72 h) and their seizure parameters (afterdischarge duration, latency to stage 4 seizure, stage 5 seizure duration and seizure stage) were measured immediately after radiation. The exposed rats were compared to those of sham-exposed and cage-control rats. There was no difference between exposed, sham, and cage-control rats. Therefore, the data indicates that GSM radiation with the mentioned parameters had no effect on seizure severity in kindling model of epilepsy.

Keywords: GSM, mobile phone, neural excitability, seizure, kindling

Introduction

The increasing use of mobile communication has raised serious concerns among people and governments about possible health hazard effects. Radiofrequency waves emitted by GSM mobile phones have a frequency band between 890 MHz and 960 MHz. Mobile phones in operation emit a pulsed radiofrequency electromagnetic field (EMF), a large part of which is absorbed into the user's head [1]. Some EEG and ECG studies have reported that GSM-EMF affects brain electrical activity [2, 3, 4, 5, 6, 7, 8], specially during cognitive performance [9, 10]. Also other investigators that have worked on this issue believe that mobile phones exposure modifies biological parameters of excitable tissues and disturbs performance of neural systems [11, 12, 13, 14, 15, 16, 17]. In a recent study it has been suggested that the EMF emitted by a commercial GSM mobile phone affects regional cerebral blood flow (rCBF) in human [18].

On the contrary, some of the studies have revealed that mobile phones EMF have no significant effects on human health (19, 20, 21, 22, 23). These results have remained controversial yet. In this study we tried to investigate the effect of GSM EMF on neural excitability. Using kindling model of epilepsy, we created seizure conditions in rats. In this situation the excitability of the CNS was high enough to study if the GSM field had any effects on this excitability. Chronic exposure of kindled rats by magnetic field (50 Hz, 100 micro tesla) exerts weak inhibitory effects on some seizure parameters [24]. However there is no report concerning effect of mobile phone (GSM-900) field on neural excitability in kindling model of epilepsy.

Materials and Methods

Surgical and kindling procedure

Male Sprague–Dawley rats weighing 330–360 g, under ketamin and rampoune anaesthesia (50 mg/kg) were stereotaxically implanted with bipolar stimulating and monopolar recording electrodes (twisted into a tripolar configuration) terminating in the basolateral amygdala of the right hemisphere (coordinates: A, 2.5 mm; L, 4.8 mm and 7.5 mm below dura). Electrodes (stainless steel, Teflon coated, A-M Systems, Inc., USA) were insulated except at their tips. Two other electrodes were connected to skull screws, placed above the left cortical surface, as earth and differential electrodes. One week after surgery, afterdischarge (AD) threshold was determined in the amygdala by a 2 s., 60 Hz monophasic square wave stimulus of 1 ms per wave. The stimulations were initially delivered at $10\,\mu A$ and then at 5 min intervals increasing stimulus intensity in increments of $10\,\mu A$ until at least 5s of AD were recorded as previously described [25]. Then, animals were stimulated daily at the AD threshold intensity until five consecutive stage 5 seizures (according to Racine, 1972) were elicited [26]. The recorded parameters were: a) seizure stage (SS) which was measured by observing the behaviour of the animal; b) AD duration (ADD) which was measured from starting of stimulation to the end of AD recording; c) the latency to the onset of bilateral forelimb clonus (S4L) which was measured from starting of stimulation to starting of stage 4 seizure; d) the duration of stage 5 seizure (S5D) which was started with loss of balance and stopped after acquisition of balance; and e) seizure duration (SD) which was measured from starting of stimulation to the end of seizure behaviours.

Radiation procedure

The EMF was provided by a GSM simulator in two level 3 and 5 mean power. When the GSM system was on, the antenna emitted a 950 MHz EMF with mean field strength 1.8 mW/cm^2 pulsed at a frequency of 217 Hz with a pulse width of 0.577 ms. According to the measurements that achieved by Iranian atomic energy organization experts, field strength was 1.78 m mW/cm^2 and 1.82 mW/cm^2 for 3 w and 5 w mean power of antenna, respectively. Thus mean field strength of this EMF is double of workers permissible limits [27].

Exposure chamber that we employed for radiation procedure was a cylindrical shape with 30 cm height and 30 cm diameter of base circle. It was made of special hard transparent PVC. The Simulator antenna with 15 cm height was placed in the centre of base circle (Fig. 1).

Exposure chamber was placed in a greater space (we call it radiation box) with dimensions of 1.1 m×1.1m×1.1m. For protection intentions the external sidewalls of the box covered with aluminium sheets. Long time EMF radiation generates hot and cavity spots throughout the radiation space. Hot spot have high density of field lines and energy and cavity spots have no field lines or energy. Avoiding to this phenomena and creation a uniform RF field around the chamber, we used conical shape absorbers that were made of graphite dyed spongy matters in internal sidewall of the radiation box. Fig. 2 shows these electromagnetic absorbers dimensions. Reflection Coefficient for these electromagnetic absorbers in 950 MHz is -40 dB approximately [28]. Obviously, in this condition we would have a uniform field throughout the exposure chamber. Fig. 3 shows a rat in near field of the antenna within the exposure chamber and radiation box, respectively. During radiation, for eliminating the external stress, animal was released in the chamber. So average distance from antenna was 10 cm that is equal with near field of GSM antenna [29]. Mean field strength was measured in this distance.

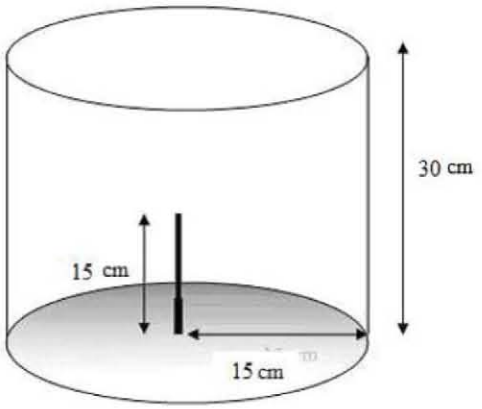


Fig. 1. The exposure chamber and the position of the antenna.

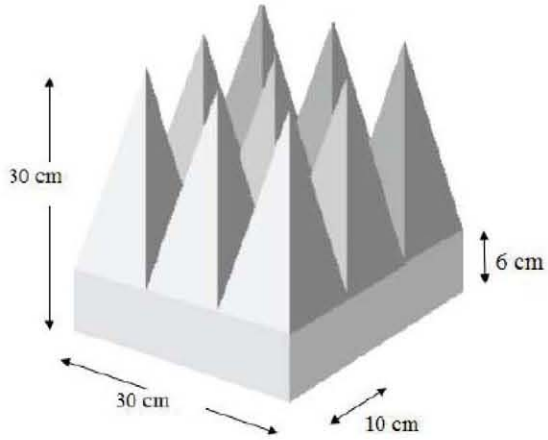


Fig. 2. Electromagnetic absorbers



Fig. 3. A rat is released in near field of the antenna within the exposure chamber. The black shapes are electromagnetic absorbers in internal sidewall of the radiation box.

We only considered non-permanently effects of GSM exposure on kindling parameters. In this way, we used four radiation paradigm and a different group of full-kindled animals (n=6) were employed in each experiment. The results were expressed as the mean ± S.E.M. for each test groups. The comparison between last fully kindling (control) values and sham exposure or GSM radiation values was done by paired t-test. A P-value of less than 0.05 was considered to represent a significant difference.

Results

The assessment of probable effect of radiation chamber and its dark environment on seizure severity was an essential note for research accuracy. Therefore, 24 h after the last kindling seizure, rats were affected by muted GSM generator (sham exposure) for 2 hours. This work was repeated at 48 and 72 h after full kindling creation for each subject, similarly. Immediately after each radiation animals were stimulated and their seizure parameters were measured and were compared with the last kindling or control values. Obtained results showed no significant differences between data (Table 1).

The above method was performed similarly, except that GSM exposure had a mean power of 3 watt and field strength of 1.78 mW/cm^2 (experiment 2) or a mean power of 5 watt and field strength of 1.82 mW/cm^2 (experiment 3). Statistical analysis showed no significant affect of GSM on seizure parameters (Tables 2, 3). In experiment 4, at 24 h after the last kindling seizure animals affected by GSM generator with a mean power of 5 watt and field strength of 1.82 mW/cm^2 for 4 hours and seizure parameters were measured immediately after radiation. Again, no significant difference was observed in compared to pre-exposure data (Table 4).

Discussion and Conclusion

In this study we found that, a GSM simulator with field strength of 1.8 mW/cm^2 and mean power of 3 and 5 watt doesn't create any considerable effect on amygdala kindled seizure parameters and there is no evidence for predicting reduction or increasing in neural excitability. Radiation time for 2 and 4 hours had no sensible or measurable effects too. Therefore these results confirm that radiation time and mean power of GSM antenna have no essential effects on seizure parameters in kindling model of epilepsy. This conclusion is in adjusted with several studies that have indicated mobile phone and radiofrequency fields have no effect on neural excitability [21, 22, 30, 31]. It is specially in adjusted with a coincident study that has showed a 900 MHz exposure with SAR of 0.25, 1, 2, 4 W/kg, has no effect on hippocampus parameters of free rats in cage [32].

However, this study doesn't confirm EMF field effects on epileptiform activity induced by amino pyridine in hippocampal slices [33, 34]. Additionally, according to this study, GSM EMF field, hadn't any inhibitory effects on seizure parameters in kindling model of epilepsy such as low frequency magnetic field [24, 35].

Also these results are differing with another research that has investigated effects of GSM-900 field (SAR less than 2 W/kg) on neural lesion possibility in rats [36].

Compatibility, some studies have suggested that GSM field couldn't change EEG parameters (that shows normal function of neural activity) in volunteers. Therefore GSM mobile phones exposure (according to this study conditions) couldn't modify seizure parameters in an excited neural system and have no significant effects on seizure biological parameters in kindling model of epilepsy. Obviously, this conclusion is exceptionally fastened to above conditions, experimental setup and methodologies.

Acknowledgement

We thank the Iran Telecommunication Research Center (ITRC) for its financial support in this project (grant No. 500/6639).

Table 1. Effect of sham exposure of animals in radiation box on seizure parameters

	Control	24 h	48 h	72 h
S4L	24.68 ±2.86	25.36±2.57	23.50±1.80	24.55±2.35
S5D	45.57±3.20	43.74±4.80	46.25±3.64	44.63±5.43
ADD	86.29±9.16	89.82±6.86	83.52±8.52	88.40±6.65
SD	103.00±7.78	100.5±2.57	104.0±7.60	99.60±8.46

Animals were exposed at 24, 48 and 72 h after the last kindling seizure and their parameters were compared with pre-exposure (control) values. Mean power and sham radiation time were 0 watt and 2 hours, respectively. Values (s) are mean±SEM. No significant difference was observed with compared to control data.

Table 2. Effect of GSM (3 watt, 2 h) exposure of animals on seizure parameters

	Control	24 h	48 h	72 h
S4L	16.66± 3.46	15.90±3.05	16.10±3.33	14.53±3.93
S5D	33.41±3.15	34.02±3.55	30.58±3.63	35.70±5.63
ADD	89.53±11.2	83.20±9.73	87.18±10.2	84.74±12.4
SD	93.50±7.55	92.50±7.73	93.00±6.06	99.00±2.20

Animals were exposed at 24, 48 and 72 h after the last kindling seizure and their parameters were compared with pre-exposure (control) values. Values (s) are mean±SEM. No significant difference was observed with compared to control data.

Table 3. Effect of GSM (5 watt, 2 h) exposure of animals on seizure parameters

	Control	24 h	48 h	72 h
S4L	22.93±1.91	22.18±1.85	20.40±1.49	19.98±1.05
S5D	42.37±2.00	41.63±1.62	43.37±2.7	43.10±3.07
ADD	96.71±9.16	91.82±7.66	92.52±7.22	90.96±6.44
SD	113.0±7.78	105.0±3.96	109.0±7.98	102.0±3.66

Animals were exposed at 24, 48 and 72 h after the last kindling seizure and their parameters were compared with pre-exposure (control) values. Values (s) are mean±SEM. No significant difference was observed with compared to control data.

Table 4. Effect of GSM (5 watt, 4 h) exposure of animals on seizure parameters

	Control	24 h
S4L	19.50±1.48	17.88±1.24
S5D	39.86±3.20	42.53±2.93
ADD	85.40±6.80	83.30±5.40
SD	89.25±5.60	92.50±4.54

Animals were exposed at 24 h after the last kindling seizure and their parameters were compared with pre-exposure (control) values. Values (s) are mean±SEM. No significant difference was observed with compared to control data.

References

1- Schonborn F, Burkhardt M, Kuster N. Differences in energy absorption between heads of adults and children in the near field of sources. Health Phys 1998; 74:160–8

2- Röschke J, Mann K. The Effects of Digital Mobile Radio Telephones on the Electroencephalogram of Humans. In Proceeding of the International workshop on electromagnetic fields and non-specific health symptoms; 1998 Sep 19 – 20; Graz, Austria. p. 69-79.

3- Borbely AA, Huber R, Graf T, Fuchs B, Gallmann E, Achermann P. Pulsed high-frequency electromagnetic field affects human sleep and sleep electroencephalogram. Neuroscience Letters 1999; 275:207-210.

4- Freude G, Ullsperger P, Eggert S, Ruppe I, Effects of microwaves emitted by cellular phones on slow brain potentials. Bioelectromagnetics 1998; 19:384-7.

5- Fritze K, Wiessner C, Kuster N, Sommer C, Gass P, Hermann DM, Kiessling M, Hossmann KA. Effect of global system for mobile communication microwave exposure on the genomic response of the rat brain. Neurosience 1997; 81(3): 627-39.

6- Mausset AL, de Seze R, Montpeyroux F, Privat A. Effects of radiofrequency exposure on the GABAergic system in the rat cerebellum. Brain Res 2001; 912(1):33-46.

7- Reiser HP, Dimpfel W, Schrober F. The influence of electromagnetic fields on human brain activity. Eur J Med Res 1995; 1:27–32.

8- Croft RJ, Chandler JS, Burgess AP, Barry RJ, Williams JD, Clarke AR. Acute mobile phone operation affects neural function in humans. Clin Neurophysiol 2002; 113:1623–32.

9- Eulitz C, Ullsperger P, Freude G, Elbert T. Mobile phones modulate response patterns of human brain activity. Neuro Report 1998; 9:3229–32.

10- Freude G, Ullsperger P, Eggert S, Ruppe I. Microwaves emitted by cellular telephones affect human slow brain potentials. Eur J Appl Physiol 2000; 81:18–27.

11- Kavaliers M, Eckel L A, Ossenkopp K P. Brief exposure to 60 Hz magnetic fields improves sexually dimorphic spatial learning in the meadow vole, Microtus pennsylvanicus. J Comp Physiol 1993; 173: 241–48.

12- Lovely RH, Creim JA, Bushbom RL, Miller DL, Anderson LE. Changes in rat's error rates in a radial arm maze during exposure to magnetic fields may have a chronological basis. Sixteenth Annual Meeting of the Bioelectromagnetics Society; 1994; p.62.

13- Lai H, Carino MA, Ushijima I. Acute exposure to a 60 Hz magnetic field affects rats water-maze performance. Bioelectromagnetics 1998; 19: 117–22.
14- Lai H, Singh NP, Melatonin and a spin-trap compound block radiofrequency electromagnetic radiation-induced DNA strand breaks in rat brain cells. Bioelectromagnetics 1997;18(6): 446-5.
15- Koivisto M, Krause CM, Revonsuo A, Laine M, Hamalainen H,The effects of electromagnetic field emitted by GSM phones on working memory. Neuro report 2000;11: 1641–3.
16- Tattersall JEH, Scott IR, The effects of radiofrequency radiation on hippocampal long potentiation in vitro. In Proc. Of International conference and exhibition on Electromagnetic compability; (EMC York 99)1999; p. 26-9.
17- Hamblin DL, Wood AW, Croft RJ, Stough C. Examining the effects of electromagnetic fields emitted by GSM mobile phones on human event-related potentials and performance during an auditory task. Clinical Neurophysiology 2004; 115:171–8.
18- Sargo Aalto, Christian Haarala, Anna Bruck, Hannu Sipila, Heikki Ha¨ma¨la¨inen and Juha O Rinne, Mobile phone affects cerebral blood flow in humans, Journal of Cerebral Blood Flow & Metabolism 2006; Pp: 1–6.
19- Hietanen M, et al. Human brain activity during exposure to radio frequency fields by cellular phones. Scandinan journal of work, Enviroment and health 2000; 26(2):87-92.
20- Wagner P, Röschke J, Mann K, Hiller W, Frank C. Human sleep under the influence of pulsed radiofrequency electromagnetic fields: A polysomnographic study using standarized conditions. Bioelectromagnetics 1998; 18:199-202.
21- Johansen C, Olsen JH. Cellular telephones, magnetic field exposure, risk of brain tumors and cancer at other sites: a cohort study. Radiate Prot Dosim 1999; 83: 155.
22- Morrissey JJ, Elder J, Swicord ML, Joyner KH. A Review of Completed and Ongoing RF Bioeffects Research Relevant To Cancer Risk Assessment. In Proceedings of the International Conference on Non-Ionizing Radiation at UNITEN: Electromagnetic Fields and Our Health (ICNIR 2003); 2003 Oct. p.20- 22.
23- Wagner P, Roschke J, Mann K, Fell J, Hiller W, Frank C, Grozinger M, Human sleep EEG influenced of pulsed radiofrequency electromagnetic fields. Neuropsychobiology 2000; 42:207-212.
24- Potschka H, Thun-Battersby S, Wolfgang Loscher. Effect of low-intensity 50-Hz magnetic fields on kindling acquisition and fully kindled seizures in rats. Brain Research 1998; 809:269–276.
25- Pourgholami MH, Mirnajafi-Zadeh J, Behzadi J. Effect of intraperitoneal and intrahippocampal 2-chloroadenosine in amygdaloid kindled rats. Brain Res. 1997; 751: 259–264.
26- Racine RJ. Modification of seizure activity by electrical stimulation: 2. Motor seizure. Electroencephalogr. Clin. Neurophysiol. 1972; 32: 281–294.
27- Trzaska H. SAR? In the proceedings of 3rd International workshop on biological effects of electromagnetic fields; 2004 Oct 4-8; Greece.
28- www.emctest.com
29- Zervos T, Alexandridis AA, Petrovic VV, Dangakis K, Kolundzija BM, Dordevic AR, Soras C.Comparison between helical and monopole antennas regarding mobile handset and human head interaction.In proceedings of the 3rd International workshop on biological effects of electromagnetic fields; 2004 Oct 4-8; Greece.
30- Dubreuil D, Jay T, Edeline JM. Head-only exposure to GSM 900-MHz electromagnetic fields does not alter rat's memory in spatial and non-spatial tasks. Behav Brain Res 2003; 145:51–61.
31- Dubreuil D, Jay T, Edeline JM, Dose head only exposure to GSM 900-MHz electromagnetic fields affect the performance of rats in spatial learning task?. Behav Brain Res 2002; 129:203-210.
32- Finnie J, Gebski V. Neuronal changes produced in mouse brain after short and long term exposure to global system for mobile communication (GSM)- link radiofrequency fields. In proceedings of the 3rd International workshop on biological effects of electromagnetic fields; 2004 Oct 4-8; Greece.
33- Tattersall JE, Scott IR, Wood SJ, Nettell JJ, Bevir MK, Wang Z, Somasiri NP, Chen X. Effects of low intensity radiofrequency electromagnetic fields on electrical activity in rat hippocampal slices. Brain Res 2001; 904:43–53.
34- Bawin SM, Satmary WM, Jones RA, Adey WR, Zimmerman G. Extremely-low-frequency magnetic fields disrupt rhythmic slow activity in rat hippocampal slices. Bioelectromagnetics 1996; 17:388–395.
35- Ossenkopp KP, Cain DP. Inhibitory effects of acute exposure to low- intensity 60- Hz magnetic fields on electrically kindled seizures in rats. Brain Res 1988; 442: 255-260.
36- Eberhardt J. L., Persson B., Brun A., Salford L. G., Effect of microwaves from GSM mobile phones on the rat brain, in proceedings of 3rd International workshop on biological effects of electromagnetic fields; 2004 Oct 4-8; Greece.

50 HZ MAGNETIC FIELD EFFECT ON THE MORPHOLOGY OF BACTERIA

LUKÁŠ FOJT[1,2], PETR KLAPETEK[3], LUDĚK STRAŠÁK [1,2], VLADIMÍR VETTERL[1,2]

1 INSTITUTE OF BIOPHYSICS, CZECH ACADEMY OF SCIENCES, KRÁLOVOPOLSKÁ 135, 612 65 BRNO, CZECH REPUBLIC
2 DENTAL RESEARCH CENTRE, MASARYK UNIVERSITY, VINAŘSKÁ 6, 603 00 BRNO, CZECH REPUBLIC
3 CZECH METROLOGICAL INSTITUTE, OKRUŽNÍ 31, 638 00 BRNO, CZECH REPUBLIC

Abstract

In our previous works we found that different strains of bacteria are affected by the magnetic field exposure. The decrease of CFU number (colony forming units) was observed in cultures of different bacterial strains after 12 minutes exposure to 10 mT 50 Hz magnetic field. This effect was strain dependent and the relative decrease was from 30% (*Escherichia coli*) to 12% (*Staphylococcus aureus*). We observed that rod-like bacteria (*Escherichia, Leclercia*) are more affected than spherical ones (*Staphylococcus, Paracoccus*). We carried out AFM study to determinate surface changes of bacteria after 60 minutes of 50 Hz 10mT magnetic field exposure of *Escherichia coli* and *Paracoccus denitrificans*. We have not observed any change in bacterial morphology of both used bacterial strains. Magnetic field did not influence the surface and shape of bacteria.

Introduction

Investigation of effects of electromagnetic fields on living organisms is needed in our community. It is important to know, how biological objects react to exposure of external electromagnetic field. According to this knowledge, we will be able to estimate health and economical aspects of using of many electrical and magnetic devices. Recently, there have been a lot of studies concerning these problems. We can found many studies of magnetic and microwave effects on DNA (1-3), enzymatic activity (4,5), proliferation control (6,7) and many others (8,9).

In our previous studies we have found, that effect of 50 Hz magnetic fields on different types of bacteria is strain-dependent (10-13). This effect was even shape dependent. We used CFU – colony forming units – method to determinate proliferation of bacteria after magnetic field exposure. Rod-like bacteria (*Escherichia coli* and *Leclercia adecarboxylata* - decrease of CFU number after 12 minute exposure to 10 mT 50 Hz magnetic field was about 40%, respectively 30% - survived in lower number than spherical ones (*Paracoccus denitrificans* and *Staphylococcus aureus* - decrease of CFU number after 12 minute in 10 mT 50 Hz magnetic field was about 14%, respectively 21%). Thus, we decided to measure surface characteristics of *Escherichia coli* and *Paracoccus denitrificans* with AFM technique to estimate possible morphological change after magnetic field exposure.

Material and Methods

Bacteria *Escherichia coli* was obtained from Biological department of Masaryk university Brno (strain K12, Row, genotype 58–161 *metB1rpsL* 1+ F^{def}P.Fredericq), *Paracoccus denitrificans* CCM 982 (NCIB 8944) was obtained from the Czech Collection of Microorganisms. For AFM measurements was used Explorer AFM (Veeco). Cylindrical coil parameters are given in our previous papers (10-12).

For morphological changes determination we used this procedure: bacteria were placed on thin glass surface. After evaporating, we take control samples measurements. Than were the bacteria placed to center of the coil and kept here for 60 minutes in 10 mT 50 Hz magnetic field. After this exposition we took another AFM pictures. Thus, we were able to detect the same bacteria before and after exposure.

Results and Discussion

On Fig.1 an Fig. 2 we can see the AFM pictures of control and exposed samples of bacteria. We have done some correlation data processing (for x,y and z position of every pixel on AFM picture). We have found, that the bacteria had not changed their morphology. There were only small changes on edges of samples, but these could be satisfactory explained by AFM head drift. Every experiment was at last 3 times repeated in high-resolution scans (area around 5x5μm) and 3 times in low resolution (area around 50x50 μm).

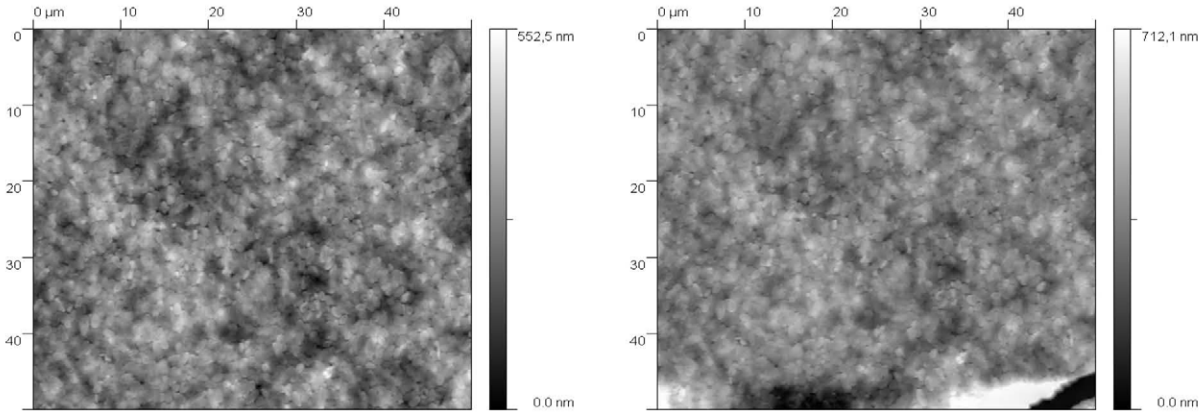


Fig. 1 Escherichia coli, sample before exposure (left), and exposed sample (1 hour 10 mT, 50 Hz) – (right)

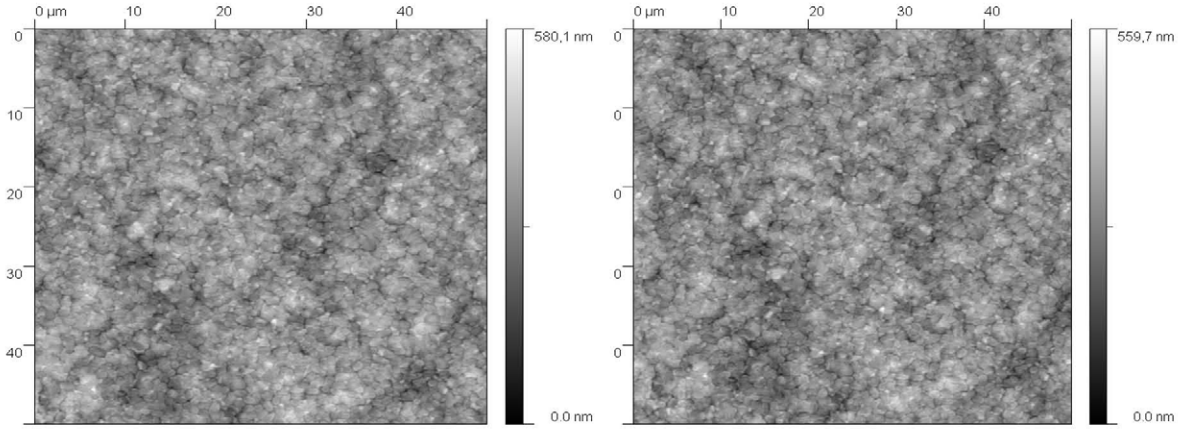


Fig. 2 Paracoccus denitrificans, sample before exposure (left), and exposed sample (1 hour 10 mT, 50 Hz) – (right)

We have found, that both types of used bacteria - *Escherichia coli* and *Paracoccus denitrificans* did not change their shapes after 1 hour exposure to 50 Hz magnetic field, B_m=10 mT. We used AFM method for bacterial surface monitoring.

Reference

1. Federica I. Wolf , Angela Torsello, Beatrice Tedesco, Silvia Fasanella, Alma Boninsegna, Marcello D'Ascenzo, Claudio Grassi, Gian Battista Azzena, Achille Cittadini. 50-Hz extremely low frequency electromagnetic fields enhance cell proliferation and DNA damage: Possible involvement of a redox mechanism, Biochimica et Biophysica Acta 1743 (2005) 120– 129

2. Maciej Lopucki, Ivo Schmerold, Agnes Dadak, Henryk Wiktor, Hans Niedermüller, Marta Kankofer. Low dose magnetic fields do not cause oxidative DNA damane in human placental cotyledons in vitro, Virchows Arch 446 (2005) 634–639

3. C. Schmitz, E. Keller, T. Freuding, J. Silny, H. Korr. 50-Hz magnetic field exposure influences DNA repair and mitochondrial DNA synthesis of distinct cell types in brain and kidney of adult mice, Acta Neuropathol 107 (2004) 257–264

4. Tomonori Sakurai, Shin Koyama, Yoshiki Komatsubara, Wang Jin, Junji Miyakoshi. Decrease in glucose-stimulated insulin secretion following exposure to magnetic fields, Biochemical and Biophysical Research Communications 332 (2005) 28–32

5. Maria Piera Piacentini, Elena Piatti, Daniele Fraternale, Donata Ricci, Maria Cristina Albertini, Augusto Accorsi. Phospholipase C-dependent phosphoinositide breakdown induced by ELF-EMF in *Peganum harmala* calli, Biochimie 86 (2004) 343–349

6. Masakazu Iwasaka, Masateru Ikehata, Junji Miyakoshi, Shoogo Ueno. Strong static magnetic field effects on yeast proliferation and distribution, Bioelectrochemistry 65 (2004) 59– 68

7. Strašák L, Vetterl V, Fojt L., Effects of 50 Hz magnetic fields on the viability of different bacterial strains,ELECTROMAGNETIC BIOLOGY AND MEDICINE,24, 293-300, 2005

8. H. Berg. Possibilities and problems of low frequency weak electromagnetic fields in cell biology, Bioelectrochem. and Bioenerg. 38 (1995) 153-159

9. C Polk.Physical mechanism for biological effects of low field intensity ELF magnetic fields, Biological Effects of Magnetic and ElectromagneticFields, Plenum Press, New York, 1996, 63-83.

10. L. Strašák, V. Vetterl, J. Šmarda. Effects of low-frequency magnetic fields on the bacteria Escherichia coli, Bioelectrochem. Bioenerg. 55 (2002) 161– 164.

11. L. Fojt, L. Strašák, V. Vetterl, J. Šmarda. Comparison of the low-frequency magnetic field effects on bakteria Escherichia coli, Leclercia adecarboxylata and Staphylococcus aureus, Bioelectrochemistry 63 (2004) 337– 341.

12. L. Fojt, L. Strašák, V. Vetterl,Effect of electromagnetic fields on the denitrification activity of *Paracoccus denitrificans*, Bioelectrochemistry, in press

13.L.Strašák, V.Vetterl, L.Fojt, Effects of 50 Hz magnetic fields on the viability of different bacterial strains, Electromagnetic Biology and Medicine, 24(2005) 293-300

SUBJECTIVE SYMPTOMS IN GSM NETWORK WORKERS

GADZICKA E., BORTKIEWICZ A., SZYJKOWSKA A., SZYMCZAK W., SIŃCZUK-WALCZAK H.

NOFER INSTITUTE OF OCCUPATIONAL MEDICINE, 91-348 LODZ, 8 TERESY ST., POLAND, E-MAIL: ela@imp.lodz.pl

Abstract

The aim of the study was to investigate the effect of EMF from mobile phones and stress perception on general health condition. The subjects were 208 GSM communication workers who responded to a 53-item questionnaire. Most of them (57%) assessed their health condition as good, 14.% as very good and 18% as fair. The level of stress was assessed in 89 workers (mean age 30.3±7.7, employment duration 4.1±1.7 years) using the Perceived Stress Scale (PSS) by Cohen and the Subjective Assessment of Work Characteristics Questionnaire (SAWCQ). EMF exposure was calculated as daily call duration (CT). The study population was divided into two groups (similar in age and employment duration): I with CT below 60 min., mean 23 min., II with CT above 60 min., mean 158 min. Group II more frequently reported headache (58% vs. 78.4%, p=0.045), dizziness (10% vs. 32.4%; p.=0.009), impaired concentration (2% vs. 13.5% p.=0.05), and heat sensation in the auricular area (30% vs. 51.4%, p.=0.044). The score on SAWCQ was higher in group II (p=0.05). The risk of a headache was significantly dependent both on CT (OR=3, p=0.0044) and PSS (OR=1.12, p=0.043). EMF exposure and stress significantly contributed to an increased rate of subjective symptoms reported by GSM workers.

Introduction

The professional group of mobile communication workers who can experience simultaneous exposure to EMF and work-related stress has developed as a result of the dynamically growing mobile communication systems and the increasing demand for mobile phone services. Mobile communication workers are exposed at work to stress related to a high pace of work performance (time pressure), high responsibility and continuous contact with customers; the level of stress depending on a given workpost. When evaluating the impact of work environment on the workers' health, one should take into account the factors related to job characteristics. Relevant literature reports on the significance of psychosocial factors such as work-related stress, effort-reward imbalance, shift work, sedentary work and other work-related stressors [1]. It seems then, that apart from the 'hard' parameters of work environment, such as EMF, one should also consider the potential influence of the psychosocial factors. Therefore, our study focused on the assessment of the level of stress related to work and everyday activities. Stress at work is associated not only with some objective factors but depends on the subjective assessment of working conditions and job requirements. This assessment evokes emotions that in turn trigger different physiological processes and mechanisms that can lead to adverse health effects if such activity is long-term or too intensive [2,3,4]. The health impact of prolonged experience of stress combined with EMF exposure may concern large communities because most of the executive staff and administration, whose duties can be perceived as highly stressful, can also be subjected to EMF exposure, as a result of a common use of mobile communication both at work and at home.

The aim of the study was to investigate the combined effect of EMF from mobile phones and stress perception on the health condition of GSM workers.

Material and Methods

Study population

The study was performed on a population of Polish workers of GSM network who are occupationally exposed to EMF from mobile phones. For this population it was possible to precisely determine the level of EMF exposure through analysis of billing and work history documentation to elicit call duration and time of EMF exposure. Some of the workers performed their duties using a stationary telephone (Call Centre operators), while others (sale dept. workers and individual and company service workers) used mobile phones. We could thus ensure study groups with

varying type and level of exposure for our investigation. In total, 208 workers were qualified for the survey. Of this number, 89 persons responded to the psychological questionnaire.

Exposure to EMF evaluation
Since most of the workers used the same type of mobile phone in their job, exposure assessment could be limited to analyzing the parameters regarding the intensity of phone use. The level of occupational exposure to EMF was calculated based on the time and frequency of mobile phone calls, SAR, and an output for a given phone used.

Each worker had the following parameters calculated:
- total period of mobile phone use
- mean daily number of calls
- mean duration of a single call
- mean daily exposure (call) duration (mean call time x daily number of calls)

Questionnaire on subjective symptoms related to mobile phone use
The questionnaire was designed specifically for this study and focused on general health condition and health complaints as well as the frequency of mobile phone use. It was tested on a group of 600 individuals using mobile communication. When developing the questionnaire, the authors consulted Scandinavian and Australian researchers about similar surveys conducted in their countries. Finally, some items from a Swedish and an Australian questionnaire were included to facilitate comparison with their findings [5,6].

The questionnaire comprises 53 items regarding (a) personal data: age, gender, education, history of work under EMF exposure; (b) self-assessment of health condition, and specific symptoms: headache, dizziness, tinnitus, visual impairments, skin symptoms of the head and neck area, sleep disturbances, and present or past diseases; (c) mobile phone use: type of phone (handsets, hands-free kits), and (d) habits related to phone use: frequency and duration of calls; (d) subjective symptoms related to mobile phone use.

Stress evaluation:
- Subjective Assessment of Work Characteristics Questionnaire (SAWCQ). The questionnaire has been developed and validated at the Nofer Institute of Occupational Medicine, Lodz, Poland. It consists of 50 items inquiring about different psychosocial stressors (factors) related to work [7]. Each subject is asked to assess whether a given factor occurs at his/her workpost and if so, to what extent it accounts for his/her irritation, fatigue, anger, stress, etc. A five-point scale is used to assess the impact of every potential stressor. The individual index of job stressfulness is calculated as a total score on all questionnaire items indicated by the subject. SAWCQ proved to be a reliable measuring instrument: r_{tt}= 0.87 an Cronbach α= 0.84. Raw scores can be transformed into normalized scores on a 10-point scale. The questionnaire was positively validated on a large sample (N = 2570) of Polish working population
  - low level of stress - score 65-80 points
  - medium level of stress - score 81-101 points
  - high level of stress - score about 102 points

- Perceived Stress Scale (PSS) developed by Cohen [1983]. The Scale is used for measuring the perceived stress, both related to everyday life situations and work performance [8]. The Scale consists of 14 questions on the frequency of recent stressful conditions that the person could or could not cope with. The recipients answer the questions using a five-point scale, with '0' denoting the absence of such a situation and '4' a high frequency of stressful events. The higher the total score, the more a given individual perceives his life course as unpredictable and beyond his/her control.

Statistical analysis
The following methods were used for the statistical analysis: Student's t-Test or F-Snedecor test to compare mean values of parameters in the study groups; chi^2 test or Fisher exact test for comparing frequency of the analysed parameters in the study groups; uni- and multivariate logistic regression for quantitative risk assessment of symptoms in relation to exposure level, after adjusting for confounders.

Results
The study population was homogenous with regard to the occupation, educational level, lifestyle, health status etc., while it differed with respect to the level of EMF exposure and work-related stress.

Mean age of the examined workers was 30.3 ± 7.7 years (21-62 years). The study group included 41 female workers aged 23-45 years (mean 27.8±4.5) and 48 male workers aged 21-62 years (mean 32.4±9.2). The mean age of female workers was significantly lower (p=0.0089).

Mean employment duration was 4.1 ± 1.7 years (2 month-8 years) and did not differ significantly in relation to gender: 3.5±1.7 years (from 2 months to 6.5 years) for female workers and 4.6±1.7 years (from 2 months to 8 years) for male workers.

The mean daily duration of phone calls was 80.4±105.1 min. (2 min.- 600 min.) and was similar in both groups: 75.8±97.5 min. (2 min.-400 min) for females and 84.1±111.8 min (2 min.- 600 min) for males (table 1).

Most of the subjects (75.4%) had university education and 24.6% of workers presented secondary/college level education.

Table 1. Exposure characteristics for the total study population

Exposure parameters	Mean value ±SD
period of mobile phone use (years)	4.1±1.8
mean daily call duration [min]	80.4±105.1

Self-assessment of general health condition and subjective symptoms
Most of the examined people (57%) assessed their health condition as good, 14% as very good and 18% as fair. Nobody reported bad or very bad condition of health and no significant differences in the health status could be found between male and female workers.

67,5% subjects complained of headache; this symptom was significantly (p=0.05) more frequent in female workers (78% vs. 58%) but only 10% of female workers related this symptom to using a mobile phone. 19% of the total subjects reported dizziness; it was more prevalent among females (27% vs. 12.5%) but the difference was statistically insignificant. Other symptoms, like tinnitus, visual impairments etc., were reported by 12.5% of the subjects, with roughly similar prevalence in the groups of female and male workers (17.1 % vs. 10.4%) Impaired concentration occurred in 37.1% of respondents, prevailing among females (41.5% vs. 33.3%). Sleep disturbances occurred in 30.3% of the subjects; they were more frequent among males (33.3% vs. 26.8%) but the difference was statistically non-significant. Facial dermatitis was reported by 12.6% of the subjects. The most prevalent symptom related to mobile phone use was the thermal sensation within the auricle and behind/around the ear. This was reported by more women than men (43.9% vs. 33.3%). 15.7% of the subjects reported fatigue after the call, even if the conversation was a pleasant one, and 6.7% impaired concentration. 11.2% reported difficulties in recalling what they had been doing before they answered the phone call (short-term memory impairments). This symptom was significantly more prevalent among male workers (18.8% vs. 2.4%).

Stress assessment
In the study population, the level of general stress was estimated at 22.1±6.9 and was significantly (p=0.0089) higher among female workers (24.2±6.6 vs. 20.3±6.7). The work-related stress was assessed at 95.3±19.1 and a higher level was found among male workers (96.8±20.2 vs. 93.5±17.8) but the difference was not statistically significant. Although in the study group, the level of stress, according to the classification adopted in earlier studies, assumed medium values (81-101), some individual workers presented very high values (134-145).

Analysis of relationship between reported symptoms and occupational factors (EMF from mobile phone, and stress)
The study population was divided into two groups according to EMF exposure calculated as daily call duration (CT):

- Group I (50 subjects): CT below 60 min., mean 23 min (2-50 min).
- Group II (39 subjects): CT above 60 min., mean 158 min (60-600 min).

These groups were similar with respect to age and employment duration.

The prevalence of the symptoms depended on the total daily duration of calls: the subjects with CT of more than 60 min. more frequently reported symptoms than the subjects with shorter CT (Table 2).

Table 2. Prevalence of symptoms in relation to call duration

Symptoms	Group 1	Group 2	p
Headache	58%	78.4%	0.045
Dizziness	10%	32.4%	0.009
Headache related to mobile phone use	4%	16%	0.05
Impaired concentration	2%	13.5%	0.05
Impaired short-term memory	4%	21.6%	0.01
Thermal sensation in the auricular area	30%	51.4%	0.044
Thermal sensation in the auricle	26%	51.4%	0.015

The level of stress was assessed in the study group with different exposure levels (table 3)

Table 3. General and work-related stress in relation to exposure level

Study groups	General stress (Cohen)	Work-related stress
(I)	21.2±7.3	92.0±18.2
(II)	23.1±6.5	100.2±19.9
(p)	ns	0.05

Analysis by exposure and stress parameters
The analysis was made using logistic regression model including EMF exposure parameters and level of stress.

After adjusting for stress, in group I (with CT of more than 60 min), the risk for headache related to mobile phone use was four times as high as in group II with CT of up to 60 min (Table 4).

Table 4. The risk for headache related to mobile phone use

Parameters	Regression coefficient (B)	Standard error (SE)	p	Odds ratio (OR)
Stress after Cohen	011	0.062	0.059	1.1
CT	1.44	0.87	0.075	4.2

The risk for headache as a symptom that was not associated with mobile phone use was also significantly higher in group II than in group I (OR=3).

Apart from the duration of the call, also stress perception significantly contributed to an increased risk for headache (Table 5).

Table 5. The risk for headache not related to mobile phone use

Parameters	Regression coefficient (B)	Standard error (SE)	p	Odds ratio (OR)
Stress (Cohen)	0.11	0.04	0.0044	1.12
CT	1.10	0.54	0.043	2.97

The risk for dizziness unrelated to mobile phone use was significantly higher (OR =6.8) in group II in comparison with group I (Table 6).

Table 6. The risk for dizziness unrelated to mobile phone use

Parameters	Regression coefficient (B)	Standard error (SE)	p	Odds ratio (OR)
Stress (Cohen)	0.17	0.07	0.0084	1.19
CT	1.91	0.70	0.0058	6.81

As regards concentration impairments, both related and unrelated to mobile phone use, the risk for this symptom was higher among the workers with a high level of work-related stress but was not dependent on the intensity of the calls (tables 7, 8).

Table 7. Risk for concentration impairments related to mobile phone use

Parameters	Regression coefficient (B)	Standard error (SE)	p	Odds ratio (OR)
Work-related stress	0.15	0.05	0.0044	1.17

Table 8. The risk for concentration impairments unrelated to mobile phone use

Parameters	Regression coefficient (B)	Standard error (SE)	p	Odds ratio (OR)
Work-related stress	0.04	0.014	0.0026	1.049

At the next stage of the analysis, we investigated whether including the duration of daily calls in the model describing stress and exposure parameters had influence on the risk for a given symptom. The daily call duration did significantly increase the risk for headache related and unrelated to mobile phone use ($p=0.0063$ and $p=0.02$, respectively), after adjusting for other parameters. Likewise, the risk for dizziness significantly increased with an increasing duration of daily calls ($p=0.0041$). No relationship was found between sleep disturbances and the level of stress.

Summary

The findings of the present study revealed that EMF exposure from mobile phone combined with parallel stress perception significantly increased the prevalence of symptoms reported by GSM workers. This referred to headache, dizziness and sleep disturbances that were much more frequent among workers who reported intensive use of mobile communication (frequent and long calls) and had a high level of stress perception. Concentration impairments were significantly related to the level of occupational stress. It seems that the best parameter to assess EMF exposure was the daily call duration, for it significantly correlated with the prevalence of the reported symptoms.

The study demonstrated that parallel activity of these factors: EMF from mobile phone and a high level of stress, both of the general and work-related stress, produce negative health consequences and increase the prevalence of subjective symptoms among workers. No research has been performed that could explain whether this effect is additive, duplicate or potentiating.

The results of our previous studies indicated that exposure to EMF from mobile phone might increase arterial blood pressure, have influence on melatonin level resulting in sleep disturbances, produce concentration and short-term memory impairments [9,10]. Similar physiological reactions (increased blood pressure, heart rate, headache, sleep disturbances) have been associated with stress.

Surveys on subjective symptoms from mobile phone use conducted in Sweden, Norway, UK, US, New Zealand and Australia revealed headache as the most frequently reported symptom [6,11,12,13]. The Australian study demonstrated that headache (including cluster headache and migraine) appeared during or shortly after the phone call and often turned more intense during the day. About 50% of the subjects reported that they had receded within one hour after the call was over and the rest of the subjects complained they could persist throughout the whole day and recede no earlier than in the evening or even on the day after [6]. The first reports on headache following exposure to microwave and radiofrequency EMF were published about 30 years ago but at that time EMF exposure at these frequencies was not common and the findings had little if any response [14]. Apart from headache, the persons using mobile phone reported malaise and fatigue, muscle pain, nausea, and thermoregulation impairments [15].

Seeking explanation to the concomitant activity of electromagnetic fields emitted by mobile phones and stress needs further studies.

References

1. Kristensen T.S., Kronitzer M., Alfedsson L.: Social factors, work, stress, and cardiovascular disease prevention. Brussels, The European Heart Network, 1998

2. Hanke W., Dudek B.: The effect of stress in the workplace on the risk of ischemic heart diseases--the role of epidemiologic studies. Med. Pr., XLVIII, 6, 1997.
3. Hammar N., Alfredsson L., Johnson J.V.: Job strain, social support at work, and incidence of myocardiel infarction. Occupational and Environmental Medicine 55 (8), 548-553, 1998.
4. Schnall PL., Landsbergis PA, Schwartz J, et al.: A longitudinal study of job strain and ambulatory blood pressure: Results from 3-year follow-up. Psychosom Med. 60, 697-706, 1998.
5. Oftedal G., Wilen J., Sandstrom M., Mild K.H.: Symptoms experienced in connection with mobile phone: Occup. Med. 50 (4), 237-245, 2000.
6. Hocking B. Preliminary report: Symptoms associated with mobile phone use. Occup. Med. 48, 357-360, 1998.
7. Dudek B., Waszkowska M., Hanke W.:. Workers protection against health effects of work-related stress IMP, Łódź 1999.
8. Cohen S., Kamarck T., Mermelstein R.A.: A global measure of perceived stress. Journal of Health and Social Behavior 24, 385-396, 1983.
9. Bortkiewicz A., Jarupat S., Kawabata A., Tokura H., Szymczak W., Gadzicka E.: Heart rate and blood pressure during exposure to cellular phone-an experimental study in: Environmental Ergonomics IX. Eds. J. Werner & M. Hexamer, 227-230, Aachen, 2000.
10. Bortkiewicz A., Piłacik B., Gadzicka E., Szymczak W.: The excretion of 6-hydroxymelatonin sulfate in healthy young men exposed to electromagnetic fields emitted by cellular phone-an experimental study. Neuroendocrinol. Lett 23 (suppl. 1), 88-91, 2002.
11. Sandstrom M., Wilen J., Oftedal G., Hansson Mild K.: Mobile phone use and subjective symptoms. Comparison of symptoms experienced by users of analogue and digital mobile phones. Occup. Med. 51 (1), 25 – 35, 2001.
12. Lundgren K.: GSM phones-no more symptoms than NMT. Working Life, Research and Development News, Newsletter 3, 1998.
13. Royal Society of Canada: A review of the potential health risks of radiofrequency fields from wireless telecommunication devices. Royal Society of Canada, Ottawa, Ont, 1999.
14. Frey A.: Headaches from cellular Telephones: Are they real and what are the implications. Environ Health Perspect 106, 101-103, 1998.
15. Repacholi M.H.: Low level exposure to radiofrequency electromagnetic fields. Health effects and research needs. Bioelectromagnetics 19, 1-19, 1998

EFFECT OF ELF-EMF ON APOPTOSIS OF K562 CELL LINE INDUCED WITH QUERCETIN AND OXIDATIVE STRESS

AKAN ZAFER,[1] TULUNAY AYSIN,[2] İNHAN GARIP AYŞE[1]

[1] Marmara University, School of Medicine, Biophysics Dept. İstanbul
[2] Marmara University, School of Medicine, Immunology Dept. İstanbul

Correspondence to : Ayşe İnhan Garip, e-mail: aysein9@yahoo.com

Abstract

This work aimed to determine the effect of ELF-EMF (50Hz,1mT) on 1-apoptosis of cells induced with the hydrogen peroxide and 2- quercetin on K562 cells. Quercetin is a flavonoid, a group of polyphenolic phytochemicals known for their beneficial effects. Quercetin has been shown to induce apoptosis. Oxidative stress is well known for its apoptosis or necrosis inducing effect. Recent work has shown that ELF-EMF affects the free radical levels probably by increasing their life-time. K562 cells were induced with quercetin or H_2O_2 and ELF-EMF (1mT,50 Hz) was applied for three hours. ELF-EMF decreased the number of viable cells in H_2O_2 induced cells. ROS levels were increased with ELF-EMF application implying the free radical stabilizing effect of ELF-EMF on free radicals and were well correlated with the viability of cells. When quercetin was used to induce cells to apoptosis it was observed that ELF-EMF abolished the apoptotic effect, increasing viability to control levels suggesting that ELF-EMF interfered with apoptotic pathway. In conclusion we showed that ELF-EMF affected the viability of cells induced with quercetin or oxidative stress and that a free radical stabilizing effect of ELF-EMF may be involved.

INTRODUCTION

The extremely low electromagnetic fields have been found to produce a variety of biological effects. It has been shown that ELF-EMF can cause changes in cell proliferation, cell differentiation, cell cycle, apoptosis, DNA replication and expression [1,2].

Flavonoids are a large group (5000 flavonoids described) of low molecular weight naturally occurring polyphenolic compounds distributed in vascular plants and are important constituents of human diet. They have a broad range of biological functions in plants and also in animal cells since they have co-existed for over a billion years [3]. They regulate the activity of many enzymes and cell cycle progression they can alter gene expression and have anti-oxidative properties. Quercetin (3,3',4',5,7-pentahydroxyflavone) is a plant flavonoid that occurs naturally in a wide range of fruits and vegetables. It is the most studied flavonoid. It has been observed that Quercetin interferes with regulatory pathway of apoptosis [4] and causes cell cycle arrest [5].

ROS including H_2O_2, O_2 .- and OH-, are endogenously generated inside cells by a variety of enzymes and through the mitochondrial respiratory chain. ROS levels are balanced by the intracellular

antioxidative defense which consists of enzymatic (superoxide dismutase which reduces O_2 .- to H_2O_2, catalase, and glutathione peroxidase which reduce H_2O_2 to H_2O) and nonenzymatic components (the vitamins C, A, E, lipoate, thiols, urate, ubiquinone, glutathione (GSH), thioredoxin, and glutaredoxin) [6]. However exogenous H_2O_2 can cause cellular injury by both apoptosis and necrosis.[7]

Extremely low frequency electromagnetic fields are considered to be weak stressors and it is thought that they may act as costressors in the presence of a stress factor [8]. And since membrane poses a barrier to these weak fields the interaction must involve a physicochemical change in the membrane leading to changes in the signal transduction system of the cell [2] and/or as Myrtill proposed cause deleterious effects by stabilizing the metabolically formed free radical [9]

Taking these facts into consideration we aimed to determine the effect of ELF-EMF on viability of K562 induced with the two above mentioned stressors. The results were correlated with ROS levels.

1. Materials and Methods

a. Cell Culture

K562 cells were cultured at 37°C in suspension in RPMI 1640 (Sigma-Aldrich Chemie GmbH, Taufkirchen, Germany) containing 10% FCS (Gibco-Invitrogen Ltd. , Paisley, Scotland) in a humidified 5% CO_2 atmosphere. Cell count was made with trypan blue. Viability was 85-90%. Quercetin (Sigma-Aldrich QO125) was added by the indicated concentrations. K562 cells were induced to apoptosis with 150, 300 µM H_2O_2 (Riedel Dehaen D3016)

b. Exposure System

Electromagnetic field was generated with two solenoids (25 cm diameter and 10 cm height) serially connected each having 400 turns of copper wire. During exposure the cells (control and ELF-EMF applied) were kept in a water bath (37° ± 0.5°C) . The magnetic field, obtained with 20V 1 mA was measured to be 1mT. Field intensity varied for ± 0.1mT during exposure. For the measurement a Hall Effect Teslameter of Leybold Heraous 54 050 model was used.
1mT, 50Hz ELF EMF was applied for three hours.

c. Apoptosis detection and Annexin V Staining Protocol

After induction with quercetin or H_2O_2 and /or application of ELF-EMF cells were washed twice with PBS and suspended in 1x binding buffer at a concentration of approx. 1 x 10^6 cells/ml. 5 µl of Annexin V-FITC and 10 µl of propidium iodide was added to each cell suspension (control and induced). After incubation at room temperature for 10 minutes the fluorescence of the cells was determined immediately with a flow cytometer (Becton-Dickinson FACSCalibur).

d. ROS determination

After washing with PBS, cells were plated in 96-well plates (10^4cells/well). Cells were incubated for 45 min with PBS supplemented with 1 mM p-nitro blue tetrazolium (NBT, Molecular Probes),1 mM $CaCl_2$. Measurements were made in the absence or presence of EMF exposure. $O2^-$ generation reduces NBT to blue formazan within the cells, which was measured using a microplate reader (Thermo Multiscan EX) at 550 nm. Intracellular formazan crystals were solubilized in 100 ml DMSO prior to reading.

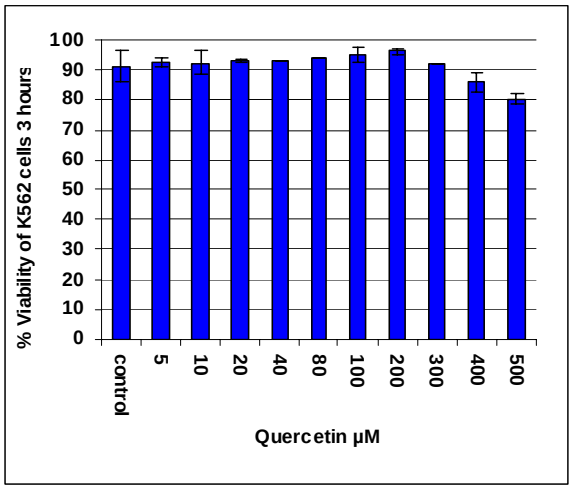
SUMMARY

1. Results

a. Viability of cells induced with different concentrations of quercetin.

The viability of K562 cells were determined starting from 5µM quercetin to 500µM quercetin to be able to obtain a concentration response. Indicated concentrations of quercetin were added for three hours and viability measured with flow-cytometer using Annexin V Flow kit taking into consideration apoptotic

and necrotic cells. As can be seen from Figure 1(A.B) viability decreased starting from 200μM quercetin. After having determined the breaking point, several concentrations were chosen and viability measured after 24 hours of quercetin induction (Figure 1.).



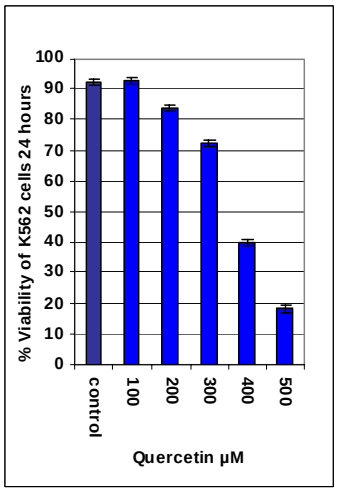


Fig.1 (A) Viability of K562 cells induced with quercetin. Quercetin concentrations from 50μM to 500μM were applied for three hours and viability was determined using Annexin V Flow kit. Concentrations greater than 200μM started to decrease viability.

(B) Several concentrations were chosen and viability measurements were made after 24 hours. It was observed that the decrease in viability was concentration dependent as expected. Results are mean ± S.E.M .n= 4.

b. Effect of ELF-EMF on quercetin induced apoptosis of K562 cell line.

300μM quercetin was chosen to determine the effect of ELF-EMF on quercetin induced apoptosis of K562 cells. Cells were induced with quercetin for three hours and ELF-EMF (1mT, 50Hz) applied at the onset of induction for the same duration. Measurements of viability were made at the end of ELF-EMF application and 24 hours later with Annexin as indicated in Methods. (Fig.2)

Quercetin decreased the number of viable cells (about 12% decreases in 24 hours) as expected. ELF-EMF alone did not change the viability of K562 cells although a slight increase which did not seem to be significant, in the number of cells was observed. When ELF-EMF was applied together with quercetin it was seen that ELF-EMF increased % of viable cells indicating that it blocked the apoptotic pathway induced by quercetin.

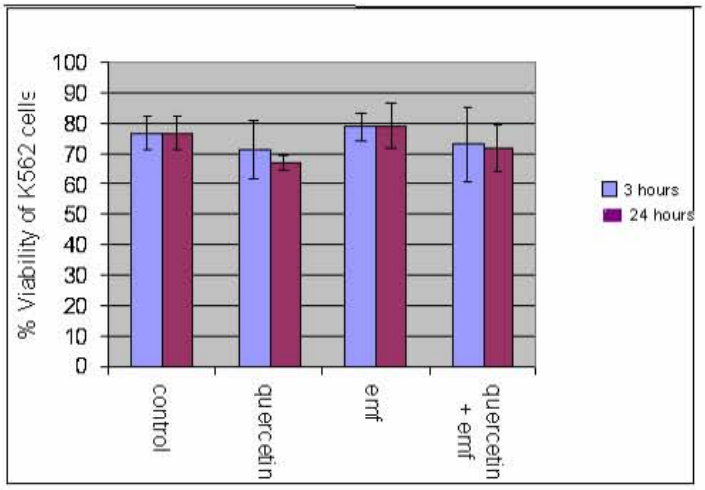


Fig.2 Effect of ELF-EMF on viability of K562 cells induced with quercetin.

Measurements were made at the end of incubation and ELF-EMF application period (3 hours) and 24 hours later. Quercetin decreased the viability as expected. ELF-EMF alone had no significant effect on the viability of K562 cells. However when ELF-EMF (1mT, 50Hz) was applied the viability of quercetin induced cells increased when measured 24 hours later. Results are mean ± S.E.M .n= 4.

c. Effect of ELF-EMF on viability of K562 cells induced with H2O2

Two H_2O_2 concentrations (150µM and 300µM) were used to determine the effect of ELF-EMF on the viability of K562 cells. Cells were induced with H_2O_2 for three hours and ELF-EMF applied during induction. Viability was determined at the end of three hours using Annexin. As expected H_2O_2 decreased viability. Application of ELF-EMF decreased viability which was seen to be more pronounced for 150µM H_2O_2 . (Fig.3).

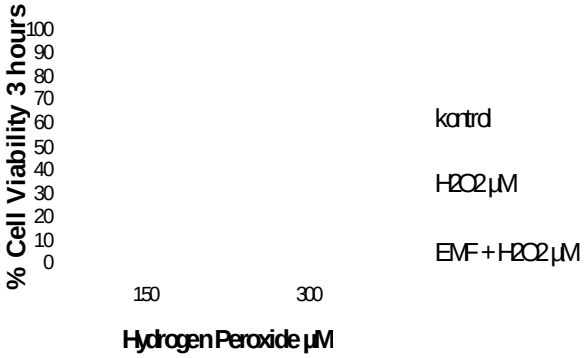


Fig.3. Effect of ELF-EMF on viability of K562 cells induced with H_2O_2.
Cells were incubated with the indicated concentrations of H_2O_2 and ELF-EMF applied for three hours during the incubation period. Measurements were made at the end of incubation and ELF-EMF application period and 24 hours later with flow cytometer. ELF-EMF decreased the viability indicating it's stabilizing effect on free radicals. Results are mean ± S.E.M .n= 4.

d. Effect of ELF-EMF on ROS levels in K562 cells with or without H2O2 induction.

Cells were kept for three hours under ELF-EMF (1mT, 50Hz). In case of H_2O_2 induction, ELF-EMF was applied immediately after induction. As can be seen from Fig.4 ELF-EMF increased ROS levels either with or without H_2O_2 induction. When cells were induced with H_2O_2 the increase was more pronounced with 150µM H_2O_2. The results indicate the stabilizing effect of ELF-EMF on free radicals.

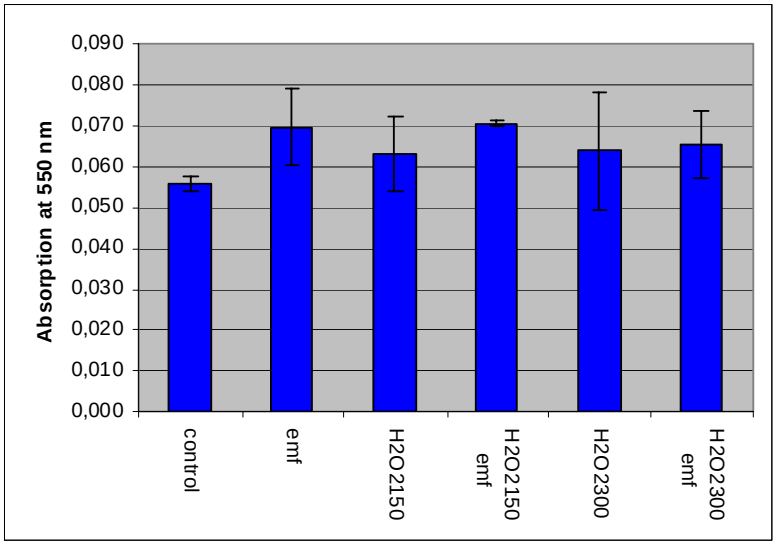


Fig.4 Effect of ELF-EMF on ROS levels in K562 cells with or without H2O2 induction.

Cells were induced with or without H_2O_2 for three hours and ROS levels were determined with NBT assay. ELF-EMF increased ROS levels in both cases. Results are mean ±S.E.M, n=4

2. Discussion

We observed that the concentration of quercetin that caused a decrease in viability, through apoptotic pathways, was 200μM to 300μM (Fig1). This is in contrast with the observation of Kothan et al [10]. They found that much lower concentrations of quercetin caused early apoptosis. On the contrary we found that low concentrations of quercetin protected the cell from oxidative stress (data not shown). As expected viability decreased with increasing concentrations of quercetin.

300μM quercetin, which was the concentration that initiated a decrease in viability, was chosen to determine the effect of ELF-EMF. The reason for this choice was that since ELF-EMF is weak stressor [8] higher concentrations of quercetin would suppress the effect of ELF-EMF. ELF-EMF caused a small increase in the viability of cells in 24 hours indicating that it interfered in the apoptotic pathway of quercetin (Fig2). There may be two reasons for this. It has been shown that quercetin modifies the membrane via reaction with lipids and proteins and thus may cause alterations in lipid transduction pathway [11]. ELF-EMF might have interfered with this modification by altering the electrical properties of the membrane. Or the reason may be a change in the expression of heat-shock proteins. It has also been observed that Quercetin and other flavonoids inhibited the induction of heat shock proteins [12]. However Goodman et al has shown that ELF-EMF increases heat shock protein levels that were exposed to short term 60 Hz. magnetic field [13] ELF-EMF may have increased hsp levels thus protecting the cell from quercetin induced apoptosis.

Reactive oxygen species are known to cause apoptosis and necrosis in many cell types [14]. This cytotoxicity is mediated by an oxidative event that produces the hydroxy radical. We first measured the concentration dependence of the viability of K562 cells induced with 150μM, 300μM and 600μM H_2O_2 which as expected decreased with increasing concentration (data not shown).

To be able to detect the effect of ELF-EMF two H_2O_2 concentrations (150μM, 300μM) were chosen. As can be seen from Fig.3. ELF-EMF caused a small but significant decrease in viability. These results were correlated with ROS measurements. It was observed that when ELF-EMF was applied to H_2O_2 induced K562 cells ROS levels increased for both of the concentrations used. This correlated very well with the decreased viability of these cells under the same conditions (Fig.4). Application of ELF-EMF alone without any H_2O_2 induction was also seen to increase ROS level which is another indication of the free radical stabilizing effect of ELF-EMF.

References

[1] Nie, K., Micic-Vasovic, A., Henderson, A.S. Molecular and cellular response to EMF exposure; a review of studies of EMF and the relationship to signal transduction. In *Biological Effects of Electromagnetic Fields* ; Stavroulakis P.,Ed; Springer-Verlag,2003.

[2] Lacy-Hulbert, A., Metcalfe, J.C., Hesketh, R. Biological responses to electromagnetic fields. FASEB J. 12, 395-42, 1998

{3] Middleton, JR E., Chithan , K., Theoharides C.T. The Effects of Plant Flavonoids on Mammalian Cells:Implications for Inflammation, Heart Disease, and Cancer Pharmacological Reviews Vol. 52, 4, 673-751. 2000

[4] Xianming Zhang, Qiang Xu and Ikuo Saiki. Quercetin Inhibits the Invasion and Mobility of Murine Melanoma B16-BL6 Cells through Inducing Apoptosis via Decreasing Bcl-2 Expression. Clin Exp. Metastasis.; 18(5): 415-421. 2001

[5] Choi, J.A., KimJ.Y., Lee,J.Y.,Kang,C.M., Kwon,H.J., Yoo,Y.D.,Kim,T.W., Lee,Y.S.Induction of cell cycle arrest and apoptosis in human breast cancer cells by quercetin. Int J Oncol. Oct;19(4):837-44.2001

[6] Heinrich Sauer, Maria Wartenberg and Jórgen Hescheler. Reactive Oxygen Species as Intracellular Messengers During Cell Growth and Differentiation. Cell Physiol Biochem 2001;11:173-186 Accepted: June 13, 2001

[7] Bladier C, Wolvetang EJ, Hutchinson P, deHaan JB, Kola I: Response of a primary human fibroblast cell line to H_2O_2: senescence- like growth arrest or apoptosis? Cell Growth Differ;8:589-598. 1997

[8] Gutzeit, H.O. Interaction of stressors and the limits of cellular homeostasis.Biochem Biophys Res Commun., 283(4), 721-5. 2001

[9] Myrtill S. Induction of cell activation processes by low frequency electromagnetic fields. The Scientific World Journal, 4(S2), 4-22. 2004

[10] Kothan, S., Dechsupa, S., Leger,G., Moretti, J.L., Vergote,J., Mankhetkorn,S. Spontaneous mitochondrial membrane potential change during apoptotic induction by quercetin in K562 and K562/adr cells. Ca. J. Physiol. Pharmacol. 82;1084-1090. 2004

[11] Pawlikowska-Pawlega,B., Gruszecki,W.I., Misiak, L.E., Gawron, A. The study of the quercetin action on human erythrocyte membranes. Biochem Pharmacol. 15;66:605-12. 2003

[12] Rusak,G., Gutzeit,H.O., Ludwig-Móller,J. Effects of strycturaly related flavonoids on hsp gene expression in human promyeloid leukemia cells. Food Technol. Biotechnol.,40,4, 267-73. 2002.

[13] Goodman, R., Lin, H., Blank, M. The mechanism of magnetic field stimulation of the stress response is similar to other environmental stresses. In *Electricity and Magnetism in Biology* ; Bersani F.,Ed.; Kluwer Academic/Plenum Publishers: New York, 1999.179-182.

[14] Lennon, S V; Martin, S J; Cotter, T G. Dose-dependent induction of apoptosis in human tumor cell lines by widely diverging stimuli. Cell Proliferation Volume 24, Issue 2 , pp.203-214.1991

EFFECT OF MAGNETIC FIELD ON SOME PHYSIOLOGICAL AND BIOCHEMICAL ASPECTS OF GROWTH OF PEA (CICER ARIENTINUM)

FAEZEH GHANATI, PARVIZ ABDOLMALEKI, MOHAMMAD YAZDANI
DEPT. BIOL. FAC. SCI. TARBIAT MODARES UNIV (TMU), POB: 14115-175, TEHRAN -IRAN

Abstract
Magnetic fields (MF) are widely distributed in the environment and their effects are increasing by the development of electrical machines. Moreover, many investigators are studying the effect of MF on the various functions or living organisms. In the present study, we tested the influence of exposure to 30 mT static magnetic field (SMF) on seed germination, growth and some physiological and biochemical aspects in roots and shoots of intact pea plants (*Cicer arientinum*). The results showed that under SMF with 30 mT intensity, seed germination was increased. The root growth was inhibited but shoot length partially increased. Furthermore, a significant increase was observed in the activity of amylase and peroxidase enzymes probably due to the oxidative stress in both roots and shoots. In addition, lignin content was increased in both roots and shoots but the level of increase of lignin in shoots was not significant.

Introduction
With the increased extent of urbanization application of electrical appliances are increasing and living organisms are inevitably subjected to the frequent exposure to low electric and magnetic fields (Patterson, 1992; Breysse et al., 1994; Frey, 1994; Merchant et al., 1994). The magnetic fields (MF) generated by electrical equipment are many times higher than those occurring naturally, and their prevalence is a consequence of technological developments in the second half of the 20th century (Jackson, 1992). However, the role of MF and its influence on organisms' functioning are still insufficiently investigated (Belyavskaya 2001). There have been several studies on the effects of MF on plants (Kato et al., 1989; Phirke et al., 1996; Ruzic & Jerman, 2002). Smith et al. (1993) found that using different field combinations, one could separately alter the root mass, leaf size and stems thickness. Roots seem much more susceptible to the magnetic than shoots (Kato, 1988; Kato et al., 1989). The 15-min treatment of wheat seeds by MF (30 mT) followed by 17-h imbibitions, when they initiated root growth, increased the root formation (Aksyonov et al., 2001). Singh et al. (1994) found that MF with a magnetic flux density of 3000 gauss applied from a permanent magnet for l-6 h inhibited the growth of *Anabaena doliolum*. Takahashi et al. (1985) investigated the effect of MF on the growth of *Chlorella* using MF with magnetic flux densities of 60-580 gauss, and have identified facilitation of growth below 400 gauss and inhibition of growth at 580 gauss. The mechanisms of facilitation or inhibition of the growth of microorganisms by MF still remain to be elucidated. It has also been found that such fields cause an increase in the free radicals activity in living organisms (Savitz, 1995; Kula et al., 2002) which results in the formation of excessive amounts of reactive oxygen species (ROS). In the present study, in order to obtain more insights into the effects of a MF on plants, we investigated the influence of 30 mT SMF on the growth and certain physiological and biochemical aspects of the growth of pea plant (*Cicer arientinum*).
Seeds of uniform size were selected and surface sterilized with 0.1% sodium hypochlorite solution for 10 min and then germinated between wet filter paper at 25˚C in the dark for 4 days, with or without exposure to magnetic field. The seedlings of uniform size were then transferred to sand culture in plastic pots in growth chamber providing white fluorescent light with an irradiance of 150 µ mol m^{-2} s^{-1}, 25±3 ˚C and 60 (± 5) % relative humidity, for 20 days.
Exposure to SMF was performed by a locally designed SMF generator. The electrical power was provided using a 220 V AC power supply equipped with variable transformer as well as a single-phase full-wave rectifier. The maximum power and passing current were 1 KW and 50 A DC, respectively. This system designed to generate SMF in range of 0.5 µT – 30 mT with stable conditions. It consisted of two coil (each 3000 turns of 3 mm copper wire) equipped with a U-shaped laminated iron core (to prevent eddy current losses). Using two vertical connectors, the arms of the U-shaped iron core were terminated to four circular iron plates covered with thin layer of Nickel (each 23 mm thickness, 260 cm in diameter). An electronic board was used to stabilize the system so that we always got a uniform SMF. A water circulation system around the coils was employed to avoid the increase of the temperature.

The temperature between the circular iron plates (where the samples were located), was measured by a thermometer and was almost the same as other parts of the room (e.g., the location site of the control cells) ±1°C. Since no other electric appliance was working, the control samples were only exposed to the extremely low MF of the earth, as the treatment group was too. Moreover, the control cells were kept far enough from the EMF producing apparatus, to avoid any potential exposure to the magnetic field.Calibration of the system as well as tests for the accuracy and uniformity of the magnetic fields were performed by a Teslameter (PHYWE, Germany) with a probe type of Hall Sound. The accuracy of the system was ±0.1% for static field and the range of measurements was 3 μT – 30 mT 20-day old pea plants were treated with 30 mT, discontinuously for 5 days, each 5 h. After treatments, the roots and shoots of pea were harvested and frozen in liquid N_2 and kept at – 80 °C until used for biochemical measurements.

Iodometric method was used to determine the endo-amylase activities (Lecker & Khan, 1996). The starch solution (1.5 g/L) was made by dissolving starch in 2 M NaOH solution at room temperature, followed by the addition of an equal volume of 2 M HCl. The resulting solution was then heated to a clear solution before its pH was adjusted to desired value by addition of 2 M NaOH. Final solutions were made by dilution with buffer at the desired pH. A solution (126.9 mg/L), containing the same volume of 0.1 M iodine and 5 g/100 mL potassium iodide, was diluted with cold distilled water to obtain a cold iodine solution (around 2 °C). Activity values were determined at 25 °C by allowing the enzyme solution in buffer (0.5 mL) to react with the starch solution (5 mL) for 2 min. The reaction was then stopped by adding 2.5 mL of cold iodine solution, which converts the nonhydrolyzed starch to starch-iodine blue complex. The resulting solution was afterwards placed in a thermostatic bath at 25 °C for 10 min and its absorbance was measured at 615 nm.

Peroxidase (PO) was extracted and determine in three fractions; the soluble-(SPO), ionically-(IPO) and covalently-(CPO) bound fractions, using guaiacol as an electron donor, as described previously (Ghanati et al. 2004). The activity of SPO and IPO was expressed as the increase in absorbance per min per mg protein and of CPO was expressed as the increase in absorbance against cell wall dry weight The protein content was determined by the method of Bradford (1976) using bovine serum albumin (BSA) as a standard.

Total sugar content was measured by the anthrone-sulfuric acid method (Dubois et al., 1956).

Lignin content was measured via a modified acetyl bromide procedure (Iiyama & Wallis, 1990). In brief, 6 mg of fine-powdered wall preparation was treated with a mixture (total of 2.5 ml) of 25% (w/w) AcBr in HOAc and 0.1 ml of 70% $HClO_4$ at 70 °C for 30 min with shaking at 10 min intervals. After cooling with ice, the digestion mixture was transferred to a 25 ml volumetric flask containing 5 ml of 2 M NaOH and 6 ml HOAc and made up to 25 ml. The lignin content was determined by measuring the absorbance at 280 nm using a specific absorption of 20.0 g^{-1} L cm^{-1}. All of the experiments were carried out with at least three independent repetitions in triplicate. All values are shown as the mean ± SD. Statistical analysis was performed using Student t.Test and the differences at level of p <0.05 were considered significant.

Exposure to 30 mT SMF had a positive effect on germination of pea seeds but it inhibited elongation of those seedlings that had not been treated with MF during their germination (data not shown).

The sugar content of roots and shoots of pea was affected greatly by SMF and a significant increase was observed at 30 mT (Fig. 1).

The starch content of roots and shoots was considered as the activity of amylase enzyme. Compared to the controls, we found that the starch content of roots and shoots of pea plant reduced significantly after exposure to 30 mT SMF (Fig. 2).

Our experiments showed that the activity of SPO in roots of pea plant was significantly increased by exposing to 30 mT SMF (Fig.3 A,D). Moreover, the activity of IPO and CPO increased substantially compared to those in control plants (Fig.3 B,C,E,F).

The lignin content of roots of pea plant treated with 30 mT SMF was significantly higher than non-treated roots (Fig. 4). Compared to the control, an increasing in the lignin content was also observed in shoots of pea plant treated with 30 mT SMF, although it was not statistically significant (Fig.4).

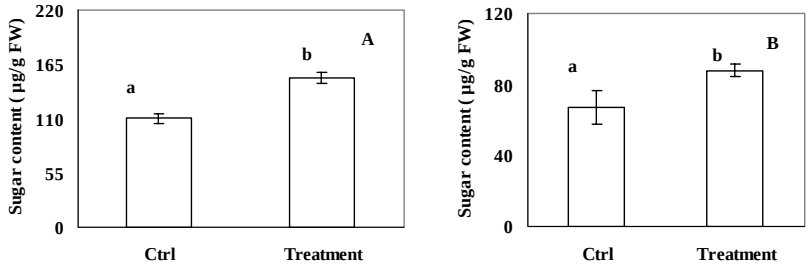


Fig.1 Effect of SMF on sugar content of shoot (A) and roots (B) of pea. Data are means of at least three different experiments in triplicate ±SD. Signs with different letters indicate significant differences at $P < 0.05$ according to Student's t-Test.

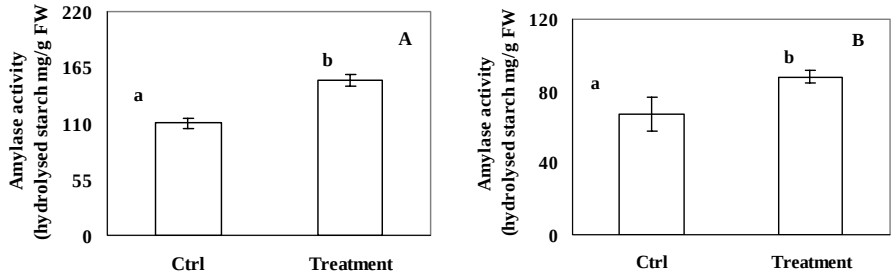


Fig.2 Effect of SMF on the activity of amylase in pea shoots (A) and roots (B). Data are means obtained from at least three different experiments in triplicate ±SD. Signs with different letters indicate significant differences at $P < 0.05$ according to Student's t-Test.

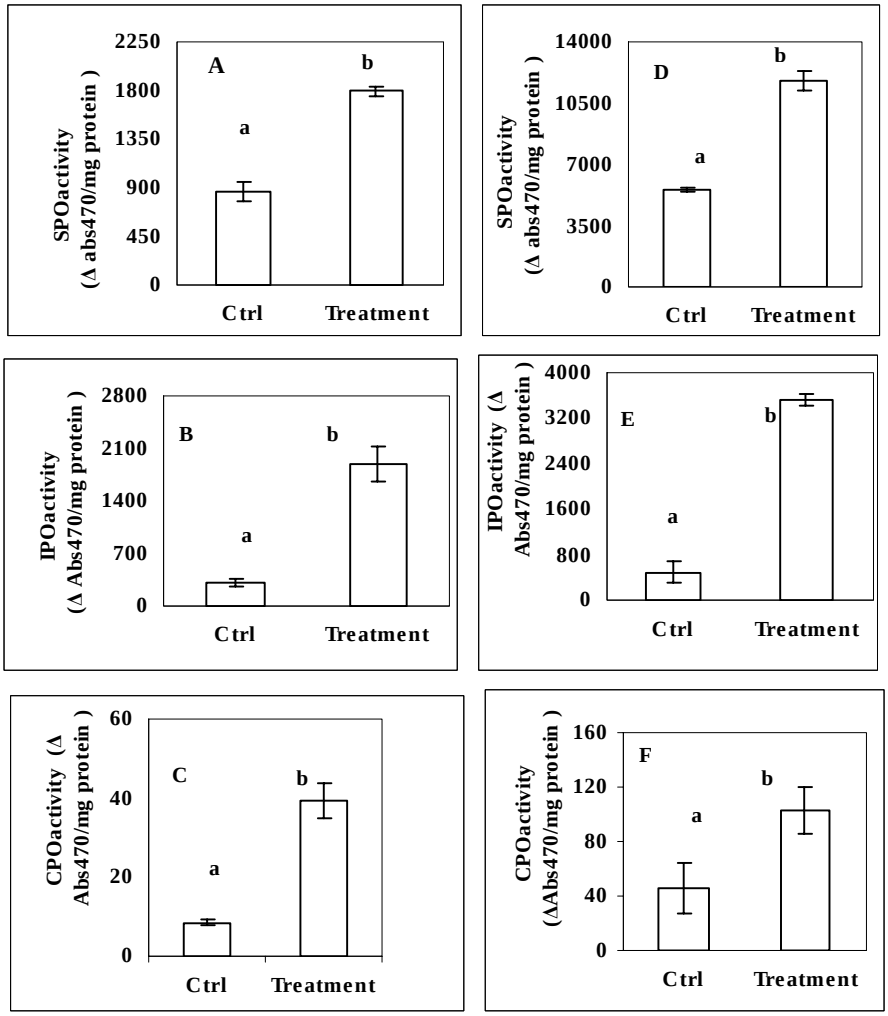


Fig 3. Effect of SMF on different fractions of PO in pea shoots (A-C) and roots (D-F). Data are means of at least three different experiments in triplicate ±SD. Signs with different letters indicate significant differences at $P < 0.05$ according to Student's t-Test.

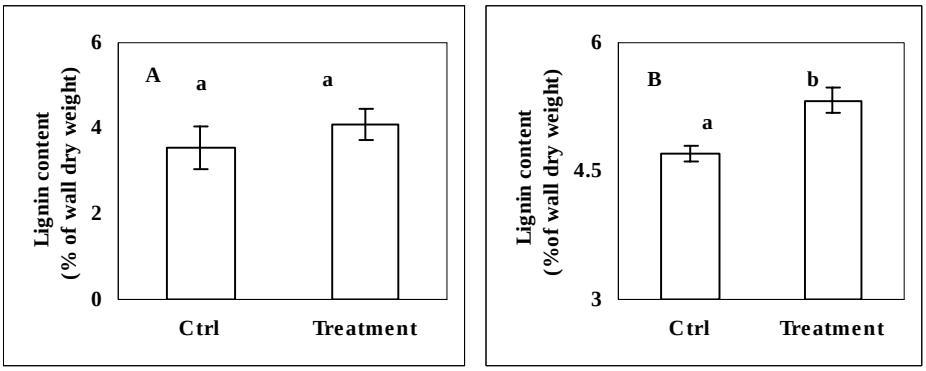


Fig.4 Effect of SMF on lignin content of pea shoots (A) and roots (B). Data are means obtained from at least three different experiments in triplicate ±SD. Signs with different letters indicate significant differences at $P < 0.05$ according to Student's t-Test.

Summary

Investigations of many authors showed that treatment of plants seed by MF increases their germination. In our study, germination of pea seeds increased by 30 mT SMF. Similar results were obtained by the effect of MF on rice, wheat, barley and soybean seeds (Cho et al., 1992). The studies show that this increasing in germination is probably due to the alteration of water relations in seeds by MF (Reina et al., 2001). Root growth reduction may be related to a reduced extensibility of the cell wall. Such effect could result from the stiffening of the wall, partly regulated by PO responsible for the polymerization of monolignins (Fry, 1986). In shoots, we have seen a slight increasing on the length of two latest internodes. This increasing was probably due to the lower synthesis of lignin in shoots than roots under 30 mT SMF, resulted in enhancement of cellular turgor and cell enlargement. Negishi et al. (1999) were observed the epicotyle elongation in pea seedlings exposed to MF. They suggested that the promotion of cell elongation under MF may relate to an increase of osmotic pressure in the cells. The effects of MF on photosynthesis in plants have not been studied in detail. In our study, the sugar content in roots and shoots of pea plant increased at 30 mT SMF. These results suggest that MF probably promote the photosynthetic processes. The similar results were obtained at the study of the effect of MF (100 gauss) on photosynthesis of the *Spirulina platensis* (Hirano et al., 1998). The authors suggested that MF accelerate the light excitation of chlorophyll, reactions of electron transfer and the conversion of light energy to chemical energy.

It has been proposed that α-amylase may be a regulatory enzyme of starch breakdown since this enzyme, unlike β- amylase, can attack and degrade intact starch granules (Dunn, 1974; Manners, 1985), while β-amylase is thought to hydrolyse oligosaccharide products of α-amylase activity and play a secondary role in the regulation of starch hydrolysis (Gallagher et al., 1997). In this research, increased soluble sugar content and also decreased starch in MF-exposed roots and shoots suggest that the hydrolysis of starch under 30 mT SMF is mainly attributed to the enhanced amylase activity. This enhancement was probably due to the increasing of ROS production under MF stress. Similar to our observations, enhanced amylase activity have been reported under water stress in barley leaves (Jacobsen et al., 1986) and cucumber cotyledons (Todaka et al., 2000). Furthermore, Mishra et al. (2005) reported significant increase in activity of amylase by increase in the level of ROS in *Bacillus subtilis*. These authors showed that the increase in enzyme activity was result of adaptive responses induced under oxidative stress.

POs are heme containing proteins that utilize H_2O_2 in the oxidation of various organic and inorganic substrates (Asada, 1994). These enzymes participate in developmental processes, ethylene biosynthesis, defense, wound healing, etc. (Asada, 1992). POs are widely accepted as stress enzymes (Asada, 1992). Induction in PO activity has been documented under a variety of stressful conditions such as water stress (Zhang & Kirkham, 1994), salinity (Mittal & Dubey, 1991), chilling (Prasad et al., 1995) and γ-radiation (Wada et al., 1998). In plants, POs have been mainly detected in cell walls, endoplasmic reticulum, Golgi apparatus and vacuoles, and this distribution is presumably related to different physiological functions (Pandolfini et al., 1992). It has also an important role in the lignification (Asada, 1992; Castillo et al., 1984) and the formation of cross-links between extension and feruloylated polysaccharides, resulting in the

increase of wall stiffening and reduction of cell expansion (Castillo et al., 1984). Our results indicated an enhancement in the activity of SPO in both roots and shoots of pea plants when compared to controls.
It is demonstrated that the activity of SPO is related to the stress conditions (Pandolfini et al., 1992). Furthermore, in the present study an increased activity was seen in IPO and CPO in both roots and shoots. In some cases, the increased activity is mainly due to the extracellular POs (cell-wall-bound) which are known to play an important role in the lignification and the formation of cross-links between extension and feruloylated polysaccharides (Castillo & Greppin, 1986; Fry, 1986). The enhanced PO activity in the intercellular spaces, involved in cell wall lignification might represent a mechanical defense under biotic and abiotic stress conditions (Gaspar et al., 1985; Castillo, 1986).

References

Aksyonov S I, Bulychev A A, Grunina T Yu, Goryachev S N, Turovetsky V B. 2001. Effects of ELF–EMF treatment on wheat seeds at different stages of germination and possible mechanisms of their origin. *Electromagnetic Biology and Medicine* 20:231–253.
Asada K. 1994. Production and action of active oxygen species in photosynthetic tissues, in: C.H. Foyer, P. Mullineaux (Eds.), Causes of photo-oxidative stress and amelioration of defense systems in plants. CRC Press, Boca Raton, FL. pp. 77 - 104.
Asada K. 1992. Ascorbate peroxidase- a hydrogen peroxide scavenging enzyme in plants. *Plant Physiology* 85:235-241.
Belyavskaya N A. 2001. Ultrastructure and calcium balance in meristem cells of pea roots exposed to extremely low magnetic fields. *Advances in Space Research* 28:645-650.
Bradford M M. 1976. A rapid and sensitive method for the quantitation of microgram quantities of protein utilizing the principle of protein-dye binding. *Analytical Biochemistry* 72:248-254.
Breysse P, Less P S, Mc Diamid M A, Curbow B. 1994. ELF magnetic field exposures in an office environment. *American Journal of Indastrial Medicine* 25:177-185.
Castillo F J, Greppin H. 1986. Balance between anionic and cationic extracellular peroxidase activities of *Sedum album* leaves after ozone exposure. Analysis by high-performance liquid chromatography. *Physiologia Plantarum* 68:201-208.
Castillo F J, Penel C, Greppin H. 1984. Peroxidase release induced by ozone in *Sedum album* leaves: involvement of Ca^{+2}. *Plant Physiology* 74:846-851.
Cho E G, Kweon S J, Suh D Y, Suh S H, Lee S K, Sohn J K, Oh J F. 1992. Studies of utilization of magnetic force in agricultural genetic engineering. *Research Reports of the Rural Development Administration Biotechnology* (Korea Republic), 34: 10-14.
Dubois M, Gilles K A, Hamilton J K, Rebers P A, Smith F. 1956. Colorimetric method for determination of sugars and related substances. *Analytical chemistry* 28:350-356.
Dunn G. 1974. A model for starch breakdown in higher plants. *Phytochemistry* 13:1341-1346.
Frey A H (Ed.). 1994. On the nature of electromagnetic field interactions with biological systems. R. G. Landes, Austin TX.
Fry S C. 1986. Polymer-bound phenols as natural substrates of peroxidases. In Molecular and Physiological Aspects of Plant Peroxidases (eds H Greppin, C Penel & Th Gaspar), University of Geneva, Geneva, pp.169-182.
Gallagher J A, Volence J J, Turner L B, Pollock C J. 1997. Starch hydrolytic enzyme activities following defoliation of white clover. *Crop Science* 37:1812-1818.
Gaspar T, Penel C, Castillo F J, Greppin H. 1985. A two step control of basic and acidic peroxidases and its significance for growth and development. *Physiologia Plantarum* 64:418-423.
Ghanati F, Morita A, Yokota H. 2004. Deposition of Suberin in roots of soybean by Excess Boron Plant Sci., 168: 397-405.
Hirano M, Ohta A, Abe K. 1998. Magnetic field effects on photosynthesis and growth of the cyanobacterium *Spirulina platensis*. *Journal of Fermentation and Bioengineering* 86: 313-316.
Iiyama K, Wallis A F A. 1990. Determination of lignin in herbaceous plants by an improved acetyl bromide procedure. *Journal of the Science of Food and Agriculture* 51: 145-161.

Jacobsen J V, Hanson A D, Chandler P C. 1986. Water stress enhances expression of an α–amylase gene in barley leaves. *Plant Physiology* 80:350-359.
Jackson J D. 1992. Are the stray 60 Hz electromagnetic fields associated with the distribution and use of electric power a significant cause of cancer? *Proceedings of the National Academy of Sciences*.USA. 89:3508-3510.
Kato R. 1988. Effects of magnetic fields on the growth of primary roots of *Zea mays*. *Plant and Cell Physiology* 29:1215–1219.
Kato R, Kamada H, Asashma M. 1989. Effects of high and very low magnetic fields on the growth of hairy roots of *Daucus carotta* and *Atropa belladonna*. *Plant and Cell Physiology* 30:605–608.
Kula B, Sobczak A, Kuska R A. 2002. study of the effects of static and extremely low frequency magnetic fields on lipid peroxidation products in subcellular fibroblasts fractions. *Electromagnetic Biology and Medicine* 21:173-180.
Lecker D N, Khan A. 1996. Theoretical and Experimental Studies of the Effects of Heat, EDTA, and Enzyme Concentration on the Inactivation Rate of α-Amylase from *Bacillus* sp. *Biotechnology Progress* 12:713–717.
Manners D J. 1985. Starch. In: Dey P M, Dixon R A, eds. Biochemistry of storage carbohydrates in green plants. London: Academic Press, pp. 149-203.
Merchant C J, Renew D C, Swanson J. 1994. Exposure to power-frequency magnetic fields in the home. J. Radiol. Protect. 14:77-87.
Mishra S, Noronha S B, Suraishkumar G K. 2005. Increase in enzyme productivity by induced oxidative stress in *Bacillus subtilis* cultures and analysis of its mechanism using microarray data. *Process Biochemistry* 40:1863–1870.
Mittal R, Dubey R S. 1991. Behaviour of peroxidases in rice: changes in enzyme activity and isoforms in relation to salt tolerance. *Plant Physiology and Biochemistry* 29: 31- 40.
Moore R L. 1979. Biological effects of magnetic fields: studies with microorganisms. *Canadian Journal of Microbiology* 25:1145-1151.
Negishi Y, Hashimoto A, Tsushima M, Dobrota C, Yamashita M, Nakamura T. 1999. Growth of pea epicotyl in low magnetic field: implication for space research. *Advances in Space Research* 23:2029–2032.
Pandolfini T, Gabbrielli R, Comparini C. 1992. Nickel toxicity and peroxidase activity in seedlings of Triticum aestivum L. *Plant, Cell and Environment* 15:719-725.
Patterson R M. 1992. Exposure assessment for electric and magnetic fields. *Journal of Exposure Analysis and Environmental Epidemiology* **2**:159-176.
Phirke P S, Kubde A B, Umbarkar S P. 1996. The influence of magnetic field on plant growth. *Seed Science and Technology* 24:375–392.
Prasad T K, Anderson M D, Stewart C R. 1995. Localization and characterization of peroxidases in the mitochondria of chilling acclimated maize seedlings. *Plant Physiology* 108:1597-1605.
Reina F G, Pascual L A, Fundora I A. 2001. Influence of a stationary magnetic field on water relations in lettuce seeds. Part II: experimental results. *Bioelectromagnetics* 22:596–602.
Ruzic R, Jerman I. 2002. Weak magnetic field decreases heat stress in cress seedlings. *Electromagnetic Biology and Medicine* 21:69–80.
Savitz D A. 1995. Overview of occupational exposure to electric and magnetic fields and cancer: Advancements in exposure assessment. *Environmental Health Perspectives* 69:103-108.
Singh S S, Tiwari S P, Abraham J, Rai S, Rai A K. 1994. Magnetobiological effects on a cyanobacterium, *Anabena doliolum. Electro and Magnetobiology* 13:227-235.
Smith S D, McLeod B R, Liboff A R. 1993. Effects of CR-tuned 60-Hz magnetic fields on sprouting and early growth of *Raphanus sativus*. *Bioelectrochemistry and Bioenergetic* 32:67–76.
Takahashi F, Kamezaki T. 1985. Effect of magnetism of growth of *Chlorella. Hakkokogaku* 63:71-74.
Todaka D, Matsushima H, Morohashi Y. 2000. Water stress enhances β–amylase activity in cucumber cotyledons. *Journal of Experimental Botany* 51:739-745.
Wada H, Koshiba T, Matsui T, Sato M. 1998. Involvement of peroxidase in differential sensitivity to γ - radiation in seedlings of two Nicotiana species. *Plant Science* 132:109- 119.
Zhang J, Kirkham M B. 1994. Drought-stress induced changes in activities of superoxide dismutase, catalase and peroxidase in wheat species. *Plant and Cell Physiology* 35:785- 791.

DISCUSSION ON THE INFLUENCE OF THE ELECTRIC CHARGE OF AEROSOL PARTICLES ON THEIR DEPOSITION IN HUMAN RESPIRATORY SYSTEM

ZYGMUNT J. GRABARCZYK

CENTRAL INSTITUTE FOR LABOUR PROTECTION – NATIONAL RESEARCH INSTITUTE, ul. Czerniakowska 16, 00-701 Warszawa, POLAND

Abstract

Aerosol particle deposition in human respiratory system is a complex function of the size and geometry of the particles. There are distinguished three main mechanisms of the deposition of the particles during the breathing – inertial force, Brownian motion and gravitational force. Depending on the size, the significance of that mechanisms and the region of respiratory system the efficiency of them is different. The fourth mechanism – electrostatic forces – because of the theoretical predictions (mainly the works of Yu) is neglected usually. The theoretical analysis of the electric forces is limited to passive mechanisms of electrostatic dispersion and the image force in tubes and bulbs of smooth, grounded surfaces and the viscous gas medium. The experimental work of Cohen made with the cast of human air ducts shows that deposition can be significantly higher than that theoretically predicted. The analysis of the influence of the image forces acting at the distance lower than free length and hypothetical non-zero potential of the parts of inner duct surfaces on the particle settlement shows that it can be more efficient for nano-particles than the previous theoretical and experimental works showed.

Key words: aerosol, electric charge, respiratory system, particle deposition, image force

Introduction

The influence of the electric charge on the aerosol particles on the efficiency of their deposition in human airways is usually neglected. A lot of theoretical and experimental work has proved that the deposition of uncharged aerosol particles in airways is governed by following mechanisms:

- diffusion towards the inner surfaces of the respiratory ducts,
- gravitational sedimentation,
- inertial impaction,
- interception.

The deposition efficiency of individual mechanisms depends on particle size and shape and on the considered part of the airways. Diffusion dominates for small particles, especially for nano-particles, and sedimentation dominates in case of coarse particles (larger than 1 μm). The efficiency of deposition in different parts of human respiratory system was shown in Fig. 1. This picture was obtained by NRBP on the basis of calculations using HRTM model (2004). The other authors report the similar deposition curves, so this one can be treated as a representative view. The experimental and analytical research work during the years has shown that the electrical charge of the particle increases its deposition. Those research works could be divided into few groups:

- measurements of the dust retention in exposed animals,
- measurements of the dust retention in exposed humans (very rare),
- measurements and calculations of the deposition in the surrogates of parts of the air ducts,
- measurements of the particle deposition in the hollow airway cast of the human lungs.

The data from the human studies made in *vivo* are rare and difficult to obtain, especially concerning the values of regional depositions. For that very important are studies with hollow casts of human airways, which seem to be the closest to the real conditions and can be useful for verify calculations.

Cohen et al. (1995) gave the detailed review of research results up to 1995. Generally, she contrasted theoretical and experimental results. They showed that the real increase of the deposition of charged particles in airways surrogates or casts (especially in her own experiments) is higher than that predicted theoretically (e.g. *Yu*, *Yu* and *Chandra*). There is general agreement, that the dominating electrical mechanism for the typical particle concentrations is the image force attracting the charge toward the conducting surface.

The new impact to the scientific interest of the share of the image forces in the particle deposition, brought the hypothesis of *Fews, Henshaw et al*. (1999 a, b) for the explanation for the increase number of some cancer cases (especially childhood leukaemia) among the populations living in the vicinity of very high voltage AC powerlines, shown in epidemiological studies. There is a common believe that the very weak AC magnetic fields (about 0.5 to few hundred of nT) could promote the development of some rare kind of cancers, but still the mechanisms of that are not understood. According to *Henshaw, Fews, et al.*, the corona discharge in HV powerlines could charge the particles of aerosol pollutants passing with the wind through the corona region. This could cause the increased deposition of charged pollutants, including cancerigenic substances existing in the air, in human respiratory system, and increase the risk of developing of some pulmonary and cancer diseases. They experimentally confirmed the existence of the cloud of ions on the leeward side of the HV AC powerlines on the basis of measurements of the vertical component of the electrostatic field at the ground level, up and down the wind. In 2005, *Grabarczyk et al*. (2005) confirmed the existence of increase in the concentration of the space charge carried by the particles sized 2 - 22 nm, down the wind of the 110 and 400 kV AC powerlines. This hypothesis was analysed carefully by the *ad hock* group of experts, and the results were published by National Radiological Protection Board (2004). They concluded that the probability of the adverse health effects of pollutants charged by HV AC powerlines is not high, but many questions need the answer before the conclusions.

The main problem, which still is not clear, is the difference between the calculated and measured deposition of charged particles in the respiratory system. It seems that this is important only near processes, which can generate the high fractions of charged nano-particles or charge fine and coarse particles close to their charge saturation.

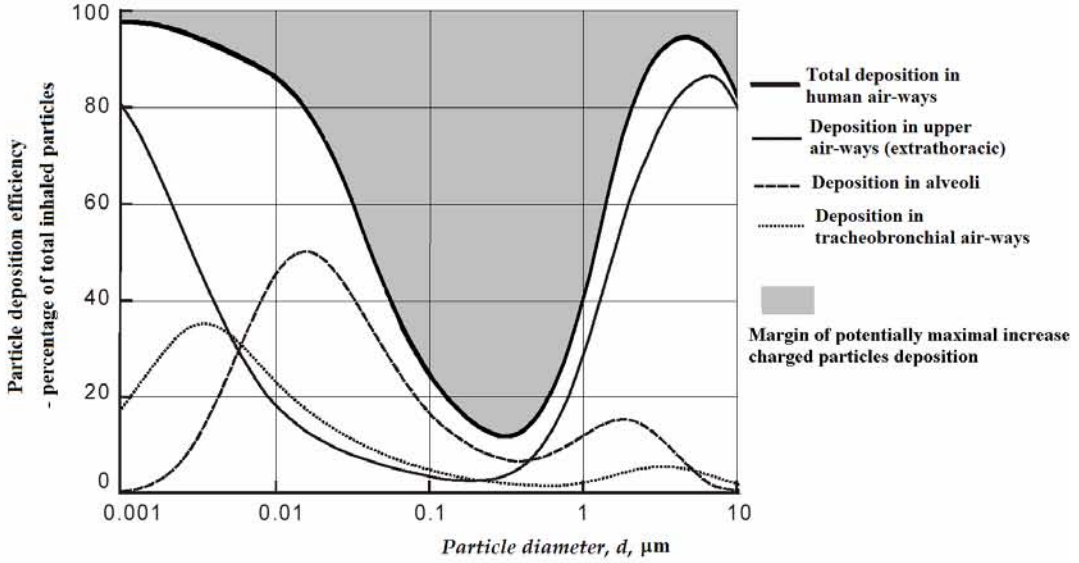


Figure 1. Total and regional deposition efficiency of spherical, uncharged particles in human respiratory system, after NRPB calculations using HRTM model (2004)

Discussion

There are the crucial points of the discussion on the significance for human health of the inhalation of the charged aerosol particles:

1) the potential margin for the possible increase of the deposition by any active factor, other than diffusion, gravitation impaction or interception,
2) the real values of deposition enhancement by the image forces,
3) the influence of image forces on the regional increase of deposition,
4) the health effects of the deposition increased by image forces,
5) the way in which image forces can enhance the efficiency of the other, mentioned above, mechanisms:

Ad 1. The potential, theoretically possible increase of the deposition is shown in Fig 1 (the grey area over the total deposition curve). It can be seen well, that for the particles sized below 10 nm and above 5 μm, the margin is very low, about a few percent. However, in the size range 0.1 – 1 μm the margin is very wide, and at about 0.3 – 0.4 μm ten-fold increase of deposition is theoretically possible. In this range, all the local depositions are low, so they could be potentially increased.

Ad 2. The real values of deposition efficiency can be calculated for all airways generations and then be summed, or total deposition can be measured with hollow cast model. Those data are not complete now and need further studies. Especially the reason for which the experimental exposition is higher than theoretically predicted, should

be explained. *Yu* et al have done most of the theoretical calculations. He derived formulas for calculating the deposition efficiency at different generation of air ducts, for parabolic and for slug airflow, and some calculations for bend pipes and some calculations for simultaneous electric effect and diffusion or gravitation.
Ad 3. As the image forces are "short distant" they can be effective rather in the narrow air tubes (e.g. bronchial region or alveoli). They should be active in similar region as the diffusion deposition dominates.
Ad. 4. The health effects of deposition depend on the kind and amount inhaled material rather than on the mechanism of deposition. So the electrostatic deposition potentially could be biologically active it could significantly increase the amount of deposited pollutants or move the deposition to the more sensitive region. The last one not seems very likely. On the other hand if image forces enhanced the deposition, they should in obvious way to cause earlier deposition, that means in lower (in sense of the number) generations.
Ad. 5. This not clear if the electrical and mechanical forces responsible for deposition can enhance or weak each other. The simplest way is to treat them as the additive factors, but likely they are not. *Chen* and *Yu* (1993) proposed the formula for the combined efficiency $\eta = \mathrm{sqrt}(\eta_1^2 + \eta_2^2 - 2\eta_1\eta_2)$ where η_x - individual efficiencies by factor 1 and factor 2.

This should be noticed that in the atmospheric conditions the aerosol particles are in thermodynamic equilibrium, and the charge carried by particles is rather low (see Fig. 2.), especially in the case of free molecular regime particles (very small particles), so probably the health effect could be small or negligible. However, if compare the atmospheric aerosol to the industrial one, especially to the particles being atomized mechanically or charged electrically (e.g. electrostatic painting), their charge could be closer to the possible maximum (limited by the electric breakdown of the air – about $3 \cdot 10^6$ V/m) and the image effect could be significant.

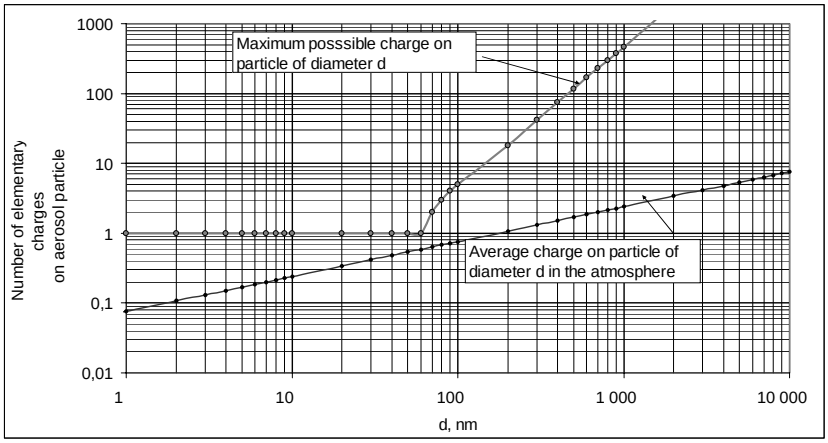


Figure 2. Number of elementary charge carried by aerosol particles seized 1 nm – 10 μm. Grey line – maximum values limited by electric breakdown of the air, black line – the average values typical for the thermodynamic equilibrium in the atmospheric conditions.

The calculations made by *Yu*, were based on the simplifying assumptions of smooth inner surfaces of analysed pipe like surrogates of the airway, the ideal conductivity, and bioelectrical passivity (no biomechanical or bioelectrical activity of epithelial cells was concerned).

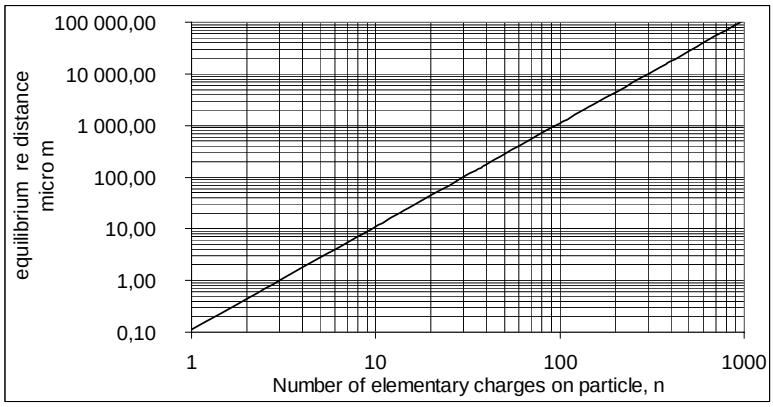


Figure 3. Critical distance from the conducting surface for which the thermal and electric energy (image force energy) are equal, versus number of elementary charge carried by particle.

Diffusion and image force are "short distance" mechanisms of deposition. Potential energy of image force of

charged particle is proportional to the second power of the particle charge. If neglect the other forces acting on the particle, every particle with energy of image force greater than thermal energy, should achieve the conducting surface. The relation between the particle charge and the border distance at which both kinds of energy are equal, is shown in Fig. 3. Particles below the curve in Fig. 3 theoretically, should settle on the conducting surface. However, for the longest distances and coarse particles, this could take a long time, probably longer than sedimentation for large particles. For that, the more effective is to compare the time of flight *T* of the air along the considered airway (e.g. pipe model) with the time τ of the drift of the particle from the point placed at the input cross section to the inner surface of the pipe. Practically the task is to find the minimum radius of the cylinder coaxial with the pipe, above which all the particles carrying charge *q* are deposited, it means for which $T \geq \tau$. The profile of the airflow in the pipe is complex. Usually there have been analysed two modes of the laminar airflow – the mode without the boundary layer at the inner surface of the pipe (air speed is constant at the all cross section area –slug flow), and with boundary layer (parabolic flow). The choice of the model depends on the length of the pipe, sharpness of the surface, and air speed, usually for short airways there is no enough time for developing full parabolic flow. According to the calculations by *Yu* and *Chandra* (1978), the deposition by the image forces is more effective for slug than for parabolic flow.

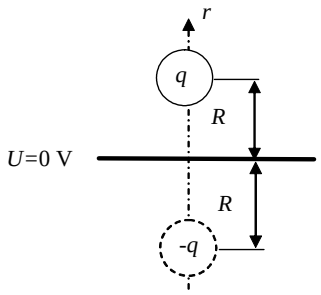


Figure 3. The simplified model of image effect of charge *q* over the conducting plane (*U* = 0V)
R - the distance between the charge and the conducting, grounded plane, (-*q*) – image of the charge (*q*).

For the analysis of the image, force effect there can be used the model shown in Fig. 3. This is the exact model for plane, conducting and grounded material. In case of the respiratory system the cylindrical pipes or spherical conducting cavities are used, where (-*q*) = *K*·*q*, where *K* is a function of the shape of the conducting material and distance of the charge *q* to the conducting surface. In the atmospheric air, there is the most important, and usually correct the common assumption that the charged particle moves along the electric field line, with the average speed:

$$\overline{\mathbf{v}(\mathbf{r})} = \mu\, \mathbf{E}(\mathbf{r}), \tag{1}$$

where, μ is the mobility of the charged particle.

In geometry case shown in Fig. 3, in the atmospheric air, which is viscous, the particle movement forced by the image force can be described by the following differential equation:

$$\frac{dr}{dt} = -\mu E = -\frac{\mu q}{16\pi\varepsilon_0 r^2}, \tag{2}$$

with the initial condition for the particle drift $r(t = 0) = R$.

That relation is only statistically true. If the distance *R* is enough small, comparable with the particle free path, the particle movement can be described by the following equation:

$$m\frac{d^2 r}{dt^2} = qE = \frac{q^2}{16\pi\varepsilon_0 r^2}, \tag{3}$$

and the initial conditions are: $r(t = 0) = R$ and $v(t = 0) = 0$, where *m* is the particle mass.

Solution of the Eq. 2 is:

$$\tau = \left(R^3 - r^3\right)\frac{16\pi\varepsilon_0}{3\mu q}, \qquad \text{or} \qquad r = \sqrt[3]{R^3 - \frac{3\mu q}{16\pi\varepsilon_0}\tau}, \tag{4}$$

and, solution of Eq. 3 is:

$$\tau = \sqrt{\frac{32\pi\varepsilon_0 m}{3q^2}\left(R^3 - r^3\right)}, \qquad \text{or} \qquad r = \sqrt[3]{R^3 - \frac{3q^2}{32\pi\varepsilon_0 m}\tau^2}, \tag{5}$$

where $d/2 \leq r \leq R$, and *d* is the particle diameter.

The ratio of the time of flight τ_2 of the distance *R* in case without collisions (Eq. 5) to the time τ_2 with collisions

(Eq. 4) is:

$$\frac{\tau_2}{\tau_1} = \sqrt{\frac{\gamma\mu^2}{2\varepsilon_0}}, \tag{6}$$

where γ is the particle material density. This ratio is always less then one, and for the fine particles τ_2 is a few orders of magnitude smaller than τ_1.

The free path l of aerosol particle of diameter d and density γ can be calculated from the Eqs 6, 7, after *Friedlaner* (2000):

$$l = \frac{\sqrt{(mkT)}}{3\pi\eta d}\left(1+\frac{2\lambda}{d}\left(A_1 + A_2\exp\left(\frac{-A_3 d}{\lambda}\right)\right)\right), \tag{7}$$

where, A_1=1.257, A_2=0.400, A_3=0.55, η - dynamic viscosity of air, λ - mean free path of the air particles (about 0.065 μm), and

$$m = \frac{4}{3}\pi\left(\frac{d}{2}\right)^3\gamma\,. \tag{8}$$

The relation (Eq. 7) is shown in Fig. 4.

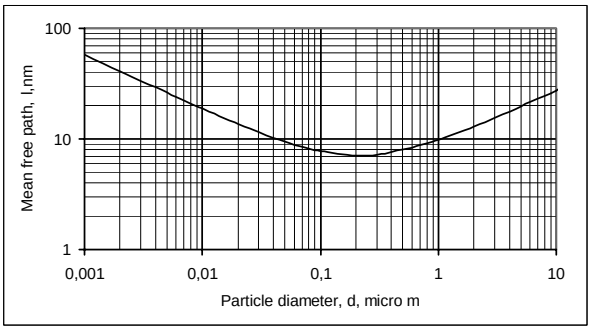


Figure 4. The mean value of the free path l of the aerosol particle of density for $\gamma = 10^3$ kg/m^3 and diameter d

The fraction of the particles for which the ratio (a) of a free path to the mean free path is inside the range $<a_1; a2>$, can be calculated as difference of probabilities $p(a_1)$ - $p(a_2)$. The probability function $p(a) = \exp(-a)$ is shown in Fig.5.

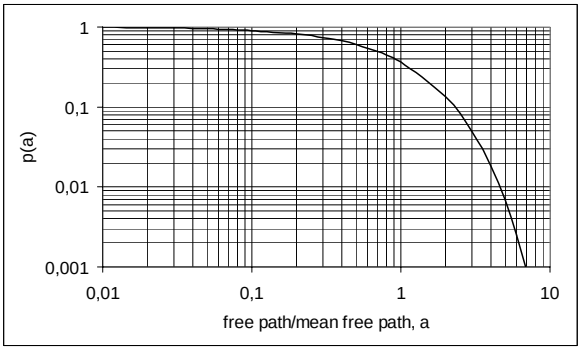


Figure 5. Probability $p(a)$ that the free path of the particle is a – folds of the mean free path.

It can be seen that the free path is larger than mean free path for about 37% of the particle population and larger than twice mean free path for 13,5%. So the image force effect without particle collisions is effective only at a distance from few tenth to few hundred of nanometres, but at such distance it is very strong and all charged particles (even with one elementary charge) would be deposited onto the airway surface. In this case the charged particles which are attracted toward the conducting surface by image force, achieve the surface much sooner than 1 ms if not collide with air particles. This effect can increase the deposition efficiency in smaller airways and if turbulent flow takes place. The effect should by studied more precisely and it seems that it was not concerned before.

Generally, because of *Yu* calculations, there exists general opinion that the image forces do not influence the

deposition in significant level. To verify that opinion the following simple case study, based on the *Yu* and *Chandra* (1978) example of 1 μm charged particles, was carried.

This is put the assumption, that the efficiency of the deposition by image force, in generation number *n* is equal $\eta_{i\,n}$. If the image force would be the only active mechanism in the airway, the deposition in generations from *m*=0 to *m* = *n*≠0 could be expressed as follows:

$$\eta_{i\,0\text{-}n} = \eta_{i\,0} + \sum_{m=1}^{n} \eta_{i\,m}\left(1-\eta_{i\,m-1}\right) \tag{9}$$

That should be noticed that Eq. 9 concerns only the population of the particles of defined diameter and charge, for which the values $\eta_{i\,m}$ were calculated before. As the number of generation is 24, even at the
According to *Yu* and *Chandra*, the deposition efficiency at the chosen generation pipe of the inner radius *R* of inner hole, can be presented for laminar flow, as:

$$P = 1-\left(\frac{r_c}{R}\right)^2, \tag{10}$$

for slug airflow, or:

$$P = \left[1-\left(\frac{r_c}{R}\right)^2\right]^2, \tag{11}$$

for parabolic airflow (with boundary layer), where r_c is the critical radius coaxial with the tested pipe, outside of which all particles are deposited.

The relation between r_c and the characteristics of the particle, pipe and airflow is:

$$\tau = 4\left(\frac{R}{r_c} + 2\ln\frac{r_c}{R} - \frac{r_c}{R}\right) \text{ for slug airflow, and} \tag{12}$$

$$\tau = 4\left(\frac{R}{r_c} + 2\ln\frac{r_c}{R} - \left(\frac{r_c}{R}\right)^2 + \frac{1}{3}\left(\frac{r_c}{R}\right)^3 - \frac{1}{3}\right) \text{ for the parabolic airflow,} \tag{13}$$

where, dimensionless time of residence was defined by *Yu* and *Chandra* (1978) as follows:

$$\tau = \frac{\mu q^2 L}{4\pi\varepsilon_0 R^3 u_0}, \tag{14}$$

where, *L* is the length of the pipe and u_0 the velocity of slug airflow.

On the basis of Eqs. 11-14, *Yu* and *Chandra* (1978) calculated the deposition for each of twenty four generations of the human respiratory system, for the particles of diameter 1 μm and density 1g/cm^3, carrying 100e charge, for breathing at 1000 cm^3 tidal volume, 12 respirations/minute. Those calculations are presented in Figs. 5 and 6 for the parabolic and slug airflows. Additionally, at those Figures, the total efficiencies calculated according to the Eq. 9, are shown also. For chosen particles, the deposition efficiency is between 30% and 70%. To get the more exact results, the airflow profile in specified generation should be known. Theoretically, there is possible to deposit 100% of highly charged particles, including four mentioned before active mechanisms also.

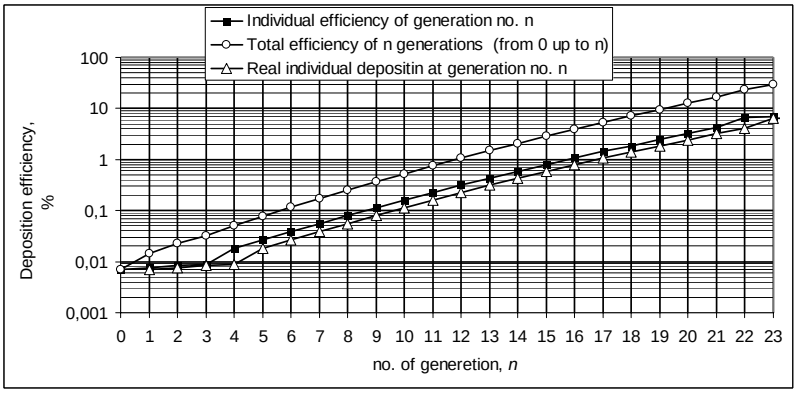


Figure 5. The efficiency of deposition by image forces at the individual generations of human respiratory system, calculated by Yu and Chandra, and ascending cumulative efficiency of the first *n* generations, calculated in this paper, and real cumulative deposition in individual generations. Calculations are made at the parabolic airflow.

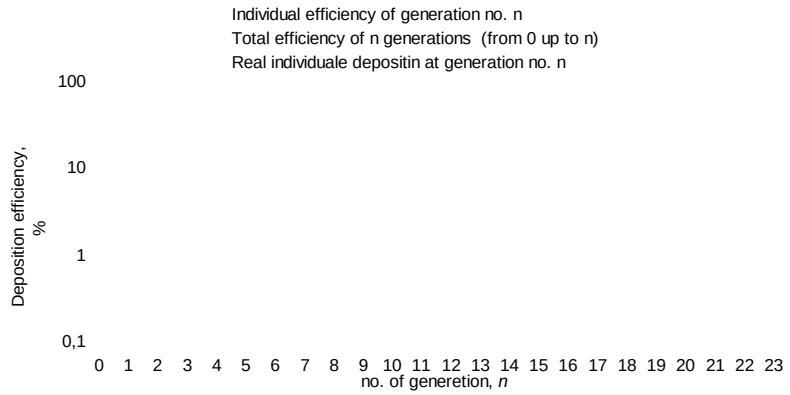


Figure 6. The efficiency of deposition by image forces at the individual generations of human respiratory system, calculated by *Yu* and *Chandra*, and ascending cumulative efficiency of the first *n* generations, calculated in this paper, and real cumulative deposition in individual generations. Calculations are made at the slug airflow.

The experiments of *Cohen et al*. (1995), mentioned before, with the deposition of charged particles in the hollow, conducting cast of human respiratory system showed, that the possible deposition of charged particles can be much higher than theoretically expected. There was measured the deposition of neutral particles, charged with 1e and neutralized particles. The studies with 20 and 125 nm particles were done; their results are shown in the Tab. 1.

Table 1. Deposition efficiency of the charged, neutralized and uncharged fluorescein particles in conducting hollow cast of human airways, at average airflow 5000 ccm/min, measured by *Cohen et al*. (1995)

Electrification of particles	**Particle diameter d = 20 nm**	**Particle diameter d = 125 nm**
	Mean value of deposition, %, ±2σ	Mean value of deposition, %, ±2σ
Single elementary charge (*q*=1e)	6.62±0,70	1.61±0.08
Charge neutralized	1.96±0,29	0.70±0.16
Neutral (*q*=0)	1.24±0,09	0.26±0.06

Those data show that the image force is an important factor enhancing the deposition of charged particles (5.3 folds for 20 nm and 6.2 for 125 nm). The model had to be different from the human respiratory system (e.g. lack of extrathoracic region), so the obtained deposition of neutral particles is significantly lower than that obtained by calculations (see Fig. 1). In case of particles sized above 0.1 μm, which can carry much higher number of elementary charges than only one, there can be expected significantly higher efficiency, which was shown above (see Figs. 5 and 6).

In the cited studies, there were not considered electrical activity of the cells in air ducts. At this moment, there is no data for assessment the significance of bioelectric potentials in deposition of charged particles and the influence of the particles charge on the cilia activity.

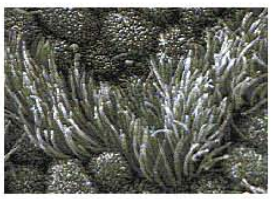


Figure 7. Example of the ciliated cells from the trachea.
Cilia's dimensions are about 10 μm length and 0.3 μm diameter.
After*: Kenneth S. Saladin, Anatomy and Physiology, the Unit of Form and Function,* WBC/McGraw Hill, 1998, p. 116.

The cilia on epithelial cells (see Fig. 7) move the mucus along a surface layer of saline. This is very likely that the cilia, beating with the frequency about few tenth of Hertz, generate some evoke potentials which should be different during power and recovery strokes. Mucus and saline layers separate the inner space of the airway duct from them, but those layers are not ideal conductors and are not continuous, so there is possible the penetration of electrostatic field of them into the airway duct space. If consider the sizes of cilia and surrounding cells and typical bioelectrical potential, it can be expected the electric field strength of order several to few tenths of kV/m. Such potentials can be compared with electrostatic potentials induced by charged particles between them and the mucus layer or cilia. The potential distribution between the charged particle and conducting surface (as in the Fig. 3) can be expressed as:

$$U(r) = \frac{q}{2\pi\varepsilon_0 R}\left(\frac{r}{R^2 - r^2}\right), \tag{15}$$

and is illustrated for q = 1e at the Fig. 8. The change of the potential conducting surface from zero up to U, in rough modelling, can be concern as a virtual change of the distance R. The result of approximate calculations of this change dr related to the distance R, are shown in Fig. 8. This is the case of the particle charge q = 1e, for which the sensitivity of the particle to the changes of the conducting surface potential is the highest. The sign of virtual dr is positive if the signs of the surface and particle are opposite, and negative if both signs are the same, respectively. For typical membrane potential about 20 mV, the influence of bioelectric potential is very effective compare to the image forces if R>1 μm (dr/R > 0.9).

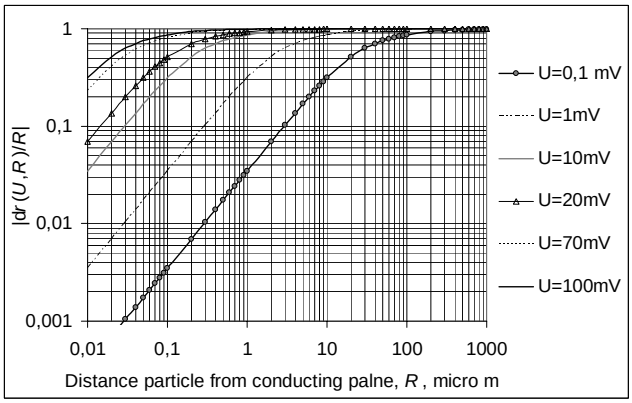


Figure 8. The virtual change |dr/R| of the distance R between the conducting plane and charge particle (q=1e), when change the conducting plane potential from zero to U.

Summary

The efficiency of charged particles deposition in human airways can significant, especially for highly charged aerosol particles. The above analysis made on the example of individual deposition efficiency of 24 generations of airway ducts, using calculation by *Yu* and *Chandra*, has shown that image forces acting alone are able to deposit up to 30-70% of highly charged particles. If include mechanical deposition factors, that efficiency could arise even more. Especially important can be increase of the deposition particles sized 0.1 - 1μm, where the deposition spare margin is very large, up to ten folds. As the experiments of *Cohen et al*. showed, the deposition of charge 125 nm particles, can be about six folds higher than those of zero charged, potentially this margin can be filled. The analysis of the example of 1 μm and 100e charged particles showed that not only the total deposition increase, but the individual deposition in all generation also. So it seems unlikely, that charging of aerosol particles could cause stopping them in upper parts of airways and significantly prevent the deposition in bronchioli and alveoli, which could positive health effect.

The significant increase of charged particle deposition, on the theoretical basis seems to be very probable if the particles charge is close to their saturation charge, and the most of the particle population is highly charged. Such cases are very rare in practice, excluding some very special conditions like particles charge in electrostatic precipitators or portable electrostatic air cleaners, paint powder particles at the electrostatic painting, and some other technologies. In the processes of particle atomization, young particles which did not achieve the state of thermodynamic equilibrium, could be electrified highly also, and the almost whole population of them can be charged.

The attention should paid to bacteria, especially water born, which charge can be very high, in some cases even up to 10^4e (*Mainelis*, 2001), but always much higher than that of the non-biological particles in the same environment. For such biological objects, the deposition in human airways can be very effective.

Real efficiency of the image forces can be enhanced also, as it was shown above, by very fast non-collision drift of the particles to the duct surface from the distance close to the free path of the particles. In this case the most effective could be attracting of nano-particles (see Fig. 4) and the least effective of 0,3-0,4 μm particles. This hypothetical effect could enhance the deposition during turbulent airflow much more than during laminar flow.

Other proposed hypothesis is that the deposition of charged particles can be enhanced if some bioelectric potential differences occur on the inner surface of the air-ducts. This effect could modulate the virtual distance of the particles to the inner surface of air duct and could be significantly stronger, especially for small charge on the particles, than the image force effect. These hypotheses should be tested experimentally, but it seems very difficult in the latest case.

Acknowledgements

This paper has been prepared on the basis of the results of a task carried out within the scope the second stage of the National Programme "Adaptation of Working Conditions in Poland to European Union Standards", partly supported - within the scope of research - in 2005–2005 by the Ministry of Science and Higher Education. The

Central Institute for Labour Protection – National Research Institute has been the Programme's main co-ordinator.

References

1. Chen, Y.K., Yu, C.P. (1993), Particle deposition from duct flows by combined mechanisms, *Aerosol Sci. Technol.,* 19, 389-395
2. Cohen, B.S., Xiong, J.Q., Fang Ching-Ping, Li, W., (1998), Deposition of charged particles on lung airways, *Health Physics*, vol. 74, no. 5, 554-560
3. Cohen, B.S., Xiong, J.Q., Li, W. (1995). The influence of charge on the deposition behavior of aerosol particles with emphasis on singly charged nanometer sized particles. 153-164 w: Ed. Marijnissen, J.C.M., Gradoń, L. *Aerosol inhalation: Recent research frontiers*. Kluwer Academic Publishers
4. Fews, A.P., Henshaw, D.L., Keitch, P.A., Close, J.J., Wilding, R.J (1999a). Increased exposure to pollutant aerosols under high voltage power lines. *Int. J. Radiat. Biology,* vol. 75, no. 12, 1505-1521
5. Fews, A.P., Henshaw, D.L. Wilding, R.J. & Keitch, P.A. (1999b). Corona ions from powerlines and increased exposure to pollutant aerosols. *Int. J. Radiation Biology,* 75(12), 1523–1531
6. Friedlander, S.K., Smoke, Dust and Haze. Fundamentals of Aerosol Dynamics. Oxford University Press
7. Grabarczyk, Z., J., Berliński, J., (2005), Charging of atmosphere aerosols by AC HV power lines, *Journal of Electrostatics*, 63, 755–759
8. Henshaw, D.,I., *et al*. (1996). Enhanced deposition of radon daughter nuclei in the vicinity of power frequency electromagnetic fields. *Int. J. Radiat. Biol.* 69(1), 25-38.
9. Mainelis, G. *et al*., Electrical charges on airborne microorganisms, *Aerosol Science,* 32, 2001, 1087-1110
10. NRPB (2004). Particle deposition in the vicinity of power lines and possible effects on health. Report of an independent Advisory Group on Non-ionising Radiation and its Ad Hoc Group on Corona Ions. National Radiological Protection board. *Documents of NRPB. vol. 15, No. 1. 2004*.
11. Yu, C.P., Chandra, K. (1978). Deposition of charged particles from laminar flows in rectangular and cylindrical channels by image force, *J. Aerosol Sci.* (9), 175-180

EXTREMELY LOW FREQUENCY MAGNETIC FIELD PROMOTES DIFFERENTIATION OF THE EX VIVO EXPANDED HUMAN CARDIAC STEM CELLS

POZZI D.[1], LISI A.[2], MESSINA E.[1], LEDDA M.[2], GAETANI R.[1], D`EMILIO E.[3], GIULIANI L.[3],BERTANI F.[1], CHIMENTI I.[1], ROSOLA E.[2], BARILE L.[1], GIACOMELLO A.[1], GRIMALDI S.[2]

[1]DEPARTMENT OF EXPERIMENTAL MEDICINE AND PATHOLOGY UNIVERSITY OF ROME "LA SAPIENZA", ITALY;
[2] INSTITUT OF NEUROBIOLOGY AND MOLECULAR MEDICINE CNR ROME, ITALY; [3] ISPESL DIPIA ROME, ITALY.

Abstract

Studies for the identification of suitable stem cells culture and differentiating conditions that are devoid of xenogenic growth supplements is actually considered an important issue for the clinical applicability of cell therapy for heart failure. We have recently demonstrated the possibility to obtain Cardiac Stem Cells (CSCs), from human endomyocardial biopsy specimens. CSCs self-assemble into multi-cellular clusters known as cardiospheres (CSps) that engraft and partially regenerate infarcted myocardium.

CSps were exposed for five days in an incubator inside a solenoid system with temperature and humidity and CO_2 regulated. This exposure system were placed in an a-magnetic shielded room in the simultaneous presence of a static MF and a low-alternating-frequency-MF, close to the cyclotron frequency corresponding to the charge/mass ratio of Ca^{++} ion. In this exposure conditions CSps modulate their differentiation turning on cardiogenesis and turning off vasculogenesis. Cardiac markers such as Troponin I (TnI) or Myosin Heavy Chain (MHC) were up-regulated, conversely angiogenic markers such as Vascular Endothelial Growth Factor (VEGF) or Kinase Domain Receptor (KDR) were down-regulated as evidenced by immunocytochemistry. The improvement in the cardiogenic differentiation was confirmed by Real-Time PCR and Western Blotting analysis. Interestingly, an increase in the proliferation was observed and evidenced by Brd-U incorporation (ELISA) and cell counting kit-8 (WST-8) analysis.

Exposure to Extremely Low Frequence Magnetic Field (ELF-*MF)* can modulates the cardiogenic *versus* angiogenic differentiation process of *ex vivo* expanded CSCs.This may pave the way for novel approaches in tissue engineering and cell therapy.

Introduction

In order to increase the reliability and the clinical feasibility of the CSCs employment for cardiac cell therapy we need new methods that allow a modulation of the differentiation process with a minimal cell manipulation.

CSCs can be clonally expanded from myocardial biopsies; these cells are spontaneously shed from human surgical specimens and murine heart samples in primary culture. This heterogeneous population of cells expresses c-kit. These cells are self-renewing, clonogenic and multipotent giving rise spontaneously to cardiomyocytes, smooth muscle cells and endothelial cells. In suspension culture they form multicellular clusters dubbed Cardiospheres (CSps).[1]

Recently spontaneous differentiation of ES cells into cardiac myocytes by exposure to ELF-MF has been reported[2]. We assessed the hypothesis that the exposure of CSps to defined Magnetic Field could modulate the cardiac differentiation process with a minimal cell manipulation.

Methods and results

Human biopsy specimens were obtained from patients undergoing clinically-indicated percutaneous endomyocardial biopsy and processed. Samples were stored on ice in high potassium cardioplegic solution and processed within two hours. Briefly, samples were cut into fragments, washed, partially enzymatically digested, and the single cells discarded. The remaining tissue fragments were cultured as explants on dishes.

A lawn of flat cells spreads from the biopsy and covers the bottom of the dish in 14-20 days. Cells can be seen budding off from the main explant and then seeding the dish, a process which is robust by 12-18 days. The cells surrounding the explant are harvested, initially after 5-7 days, and then every 4-5 days (for a total of 4 harvests). When grown in suspension, the cells form CSps within 12-20 days. On the basis of our previous results obtained with other cellular model (cheratinocytes, neuronal cells) [3-5], CSps were exposed for five days in the a-magnetic room with simultaneous presence of a static Magnetic Field and a ELF-MF, close to the cyclotron frequency corresponding to the charge/mass ratio of Ca^{++} ion.

The equipment for electro-magnetic field (solenoid) production is installed in a-magnetic room. This equipment include cellular incubator made to a-magnetic material were temperature regulation (37± 0.1°C) and atmosphere (5% CO2) and humidity were provided and continuously controlled and recorded by a lab view program embedded computer.

The main body of the solenoid is a cylinder in PVC 5 mm thick and has a diameter of 33 cm and a height of 3 m. It is made of 3,300 turns of 1 mm diameter copper wire. It is driven from three amplifiers and a signal generator that generated static and alternate current for electromagnetic field production. This equipment is able to produce 0.01Hz to 1 KHz frequency and 10 nT to 1mT of electromagnetic field and induction respectively at 33 mV RMS drove.

Under these conditions an increase in cell metabolism was observed and evidenced by cell counting kit-8 (WST-8) analysis (Fig. 1). Moreover, cardiac markers such as Troponin I (TnI) or Myosin Heavy Chain (MHC) were up-regulated. Conversely angiogenic markers such as Vascular Endothelial Growth Factor (VEGF) or Kinase Domain Receptor (KDR) were down-regulated as evidenced by immunocytochemistry (Fig. 2) and by RT-PCR (Fig. 3).

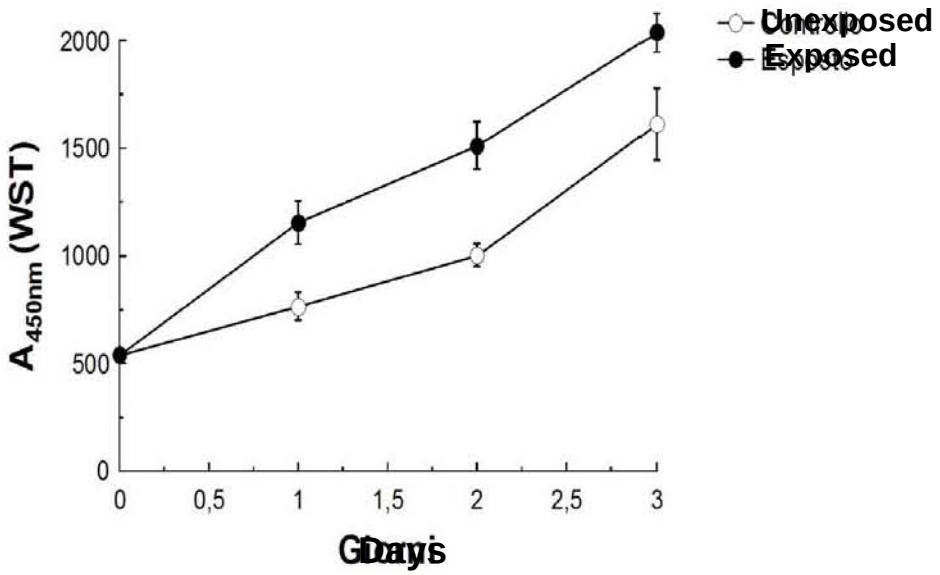


Figure 1: ***Metabolic activity***

Evaluation of cell metabolism by utilizing sensitive colorimetric assays. WST-8 is reduced by dehydrogenases in cells to give a yellow colored product (formazan), which is soluble in the tissue culture medium. The amount of the formazan dye generated by the activity of dehydrogenases in cells is directly proportional to the number of living cells. Figure shows that cells exposed to ELF-MF (●) have higher metabolic activity then the unexposed cells (○).

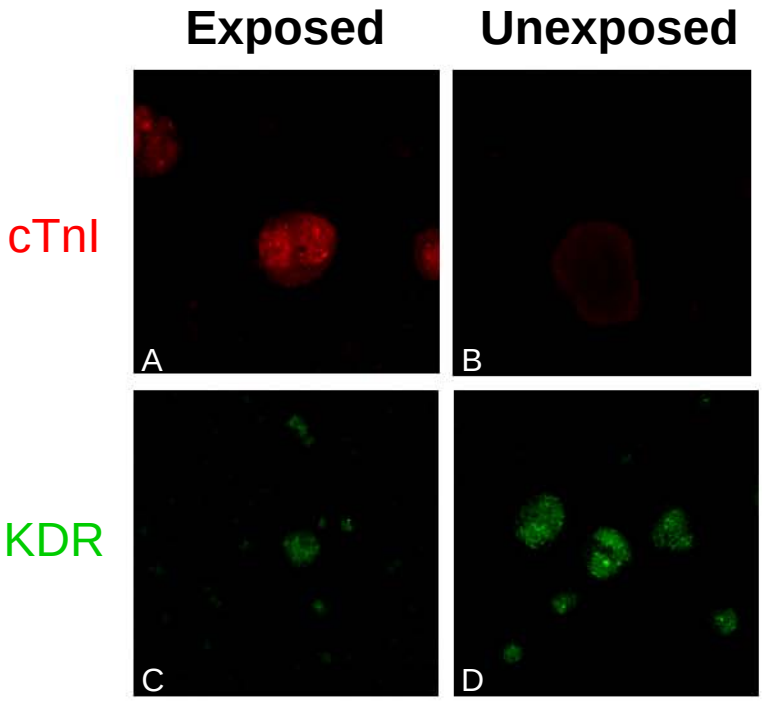


Figure 2: ***Cardiosphere and CDC Phenotypes***

A) Cardiospheres expressing cardiac TnI after exposure to the ELF-MF for 5 days. C-D) The exposure to the magnetic field seems to down-regulate the vasculogenesis

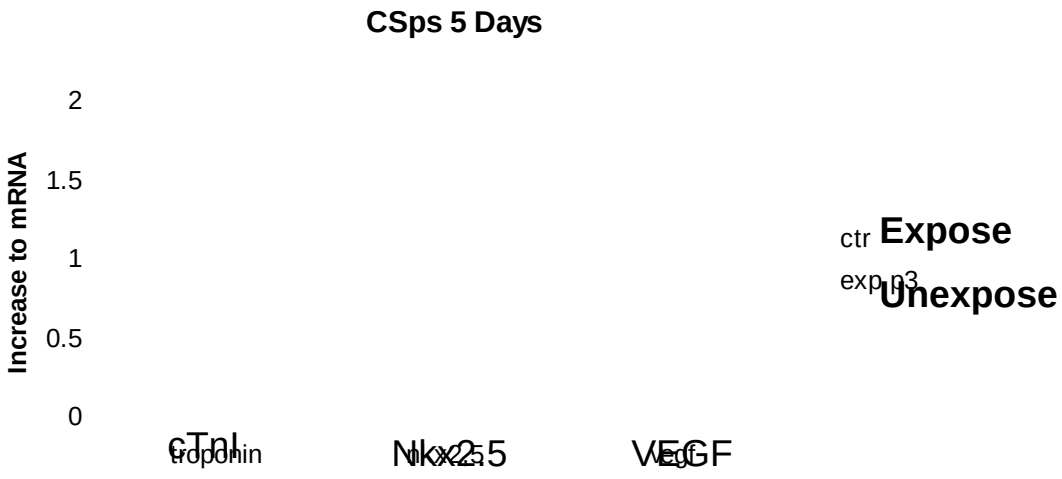


Figure 3: ***Real Time PCR***

Effect of field exposure on expression of cardiac markers such as cTnI,Nkx 2.5 and angiogenic markers such as VEGEF after five days. The column diagram shows the differences in mRNA production of exposed (■) and unexposed (□) CSps.

Discussion

One hundred years ago the humans were exposed only to natural electromagnetic field (EMF). With technical and industrial growth, the EMF generated by human activities became several times higher than the field found in nature.

Because most of the physiological processes of the eukaryotic cell are voltage regulated, in the last 20 years underwent a strong increase of the interest to investigate the effect of extremely low frequency electric and magnetic fields [6-8].

Some of this studies reported changes induced in calcium efflux from chicken brain hemispheres [9], nerve regeneration [10], alteration gene transcription [11], and they may also play a synergic role in cellular processes that are already activated, such as cell proliferation and cell differentiation.

The possible mechanisms of the induced effects are not known, although a number of theoretical models have been proposed) [12-14]. Studies focusing on the role of Calcium signalling in the mechanisms of the ELF-MF-induced differentiation are ongoing in our laboratory.

We have obtained data showing that exposure of the *ex vivo* expanded CSps to ELF-MF modulates their differentiation turning on cardiogenesis and turning off vasculogenesis. Interestingly this effect was accompanied by increase of cellular metabolism and proliferation.

If confirmed, these results should increase the reliability and the clinical feasibility of the CSCs employment for cardiac cell therapy.

References

1. Messina E., et al. (2004) Isolation and expansion of adult cardiac stem cells from human and murine heart. *Circ Res.;95(9):911-21*
2. Ventura C. et al. (2004) Turning on stem cell cardiogenesis with extremely low frequency magnetic fields**.** *The FASEB Journal* 2004 19(1):155-7
3. Lisi A., et al. (2005) Exposure to 50Hz electro-magnetic radiation promote early maturation and differentiation in newborn rat cerebellar granule neurons. *J. Cell. Physiology, 204, 532-538*
4. Manni V., et al. (2002) Effect of extremely low frequency (50 Hz) magnetic field on morphological and biochemical properties of human keratinocytes. *Bioelectromagnetics .23:298–305.*
5. Manni V., (2004) Effect of low frequency (50 Hz) non ionising radiation on primary human oral keratinocytes (HOK). *Bioelectromagnetics 25:118–126.*
6. Blank M., et al. (1987) Mechanistic approaches to interactions of electromagnetic field with living systems. *New York: B. Plenum.*
7. Tenforde TS. (1995) Interaction of extremely low frequency electric and magnetic fields with humans. *In: Polk C, Postow E, editors. Handbook of biological effects of electro-magnetic fields, 2nd edition. Boca Raton: CRC Press, pp 185–230.*
8. Zhadin MN., (2001) Review of Russian literature on biological action of DC and low-frequency AC magnetic fields. *Bioelectromagnetics 22(1):27–45.*
9. Blackman C.F., (1988) Stimulation of brain tissue in vitro by extremely low frequency, low intensity, sinusoidal electromagnetic field. *Prog Clin Biol Res 257: 107-117;*
10. Rusovan A, et al. (1992) Magnetic fields stimulate peripheral nerve regeneration hypophyctiomia rats. *Neuroreport 3(12):1039–1041.*
11. Phillips JL., et al. (1992) Magnetic fieldinduced changes in specific gene transcription. *Biochimica Biophysica Acta1132:140–144.*
12. Glaser R., et al. (1992) Current concepts of the interaction of of weak electro-magnetic fields with cells. *Bioelectrochem Bioener 27:255–268.*
13. Liburdy RP., et al. (1992) Calcium signalling in lymphocytes and ELF fields: Evidence for an electric field metric and a site of interaction involving calcium ion channels. *FEBS Lett 301(1):53–59.*
14. Barnes PS., et al.(1996) Effect of electro-magnetic field on the rate of chemical reactions. *Biophysics 41:801–880.*

OCCUPATIONAL ELECTROMAGNETIC FIELD EXPOSURE AND INDUCED CURRENT'S HAZARDS FROM ELECTROSURGERY DEVICES

KRZYSZTOF GRYZ, JOLANTA KARPOWICZ

CENTRAL INSTITUTE FOR LABOUR PROTECTION – NATIONAL RESEARCH INSTITUTE, WARSZAWA, POLAND, e-mail: krgry@ciop.pl

Abstract

The investigations concerning medical staff exposure to electromagnetic fields and induced currents hazards from electrosurgery devices have been completed. The exposure has been evaluated following the European Directive 2004/40/EC and national occupational safety and health regulations. The main sources of workers exposure are powered electrode and cables. Electromagnetic fields from electrosurgery devices are pulsed modulated and have heterogeneous spatial distribution. It has been found that in the vicinity of electrosurgical devices, the area of electromagnetic fields to which only workers operating the source of field should be exposed can exist up to the distance of tens of centimetres from the active electrode and supplying cables. In the case when the cables are placed directly on the surgeon's body the overexposure of workers can appear. The current flowing through the arm of surgeon keeping the electrode emitting electric field of the maximum strength (app. 1000 V/m or higher) can exceed the permissible value of 40 mA established by the Directive 2004/40/EC for contact current. The obtained results of measurements and suggestions for reduction of the surgeon's exposure are presented.

Keywords: electromagnetic fields, occupational exposure, induced currents, electrosurgery.

Introduction

Electrosurgery is used for various surgical treatments - to cut or to coagulate a patient's tissues. Electromagnetic hazards produced by these apparatus are essential for a big group of medical staff given a common use of electrosurgery devices. Electrosurgery devices consist of a generator (with output power of up to 500 W, but usually the output power used during surgical treatment is of 50-150 W), an active (powered) electrode connected with the generator by long cable and a passive electrode, fixed at a patient's body and connected by long cable with "0" electric potential of the generator.

Controllable surgical effect is a result of the flow of radiofrequency (RF) currents through the tissues of the body and local heating them. This current is the result of capacitive coupling of powered electrode with a patient's body. Current can flow with or without a direct contact between the active electrode and the body of patient if the potential of the electrode is higher than 200 V in the relation to potential of the tissues. Electric arc can be burned under the active electrode in the case of a higher potential of the electrode.

Currents of frequency above 300 kHz (up to approx. MHz) are used to avoid electrical stimulation of tissues. The waveforms of electric potential and current (and in consequences, electromagnetic field (EMF) produced in the vicinity of cables) depend on a type of a device and it's selected mode of a device operation. As a result, the EMF waveform changes from sinusoidal (usually exists during cut mode) to pulsed modulated (during different coagulation modes) – fig. 1, and additionally it is always pulsed modulated by the switch-on and switch-off actions of surgeon which are taking following surgical treatment needs.

The sources of the occupational exposure are mainly [2]:

- the active electrode at a high electric potential from which the RF current penetrates the tissue
- the cables connecting the generator with the active electrode, kept in the hand by a surgeon, and with the passive electrode (grounded plate), mounted to the patient's body.

The additional sources of EMF can be:

- the generator in the case of not leakproof housing (without electromagnetic shield),
- metallic objects located in the vicinity of the electrodes cables (for example, surgical or instrumentation's tables) and which can become secondary sources of EMF.

The EMF is produced from the moment of activation of an electrosurgery device. It may be operated by foot-control or through a button-control on the handle of the active electrode.

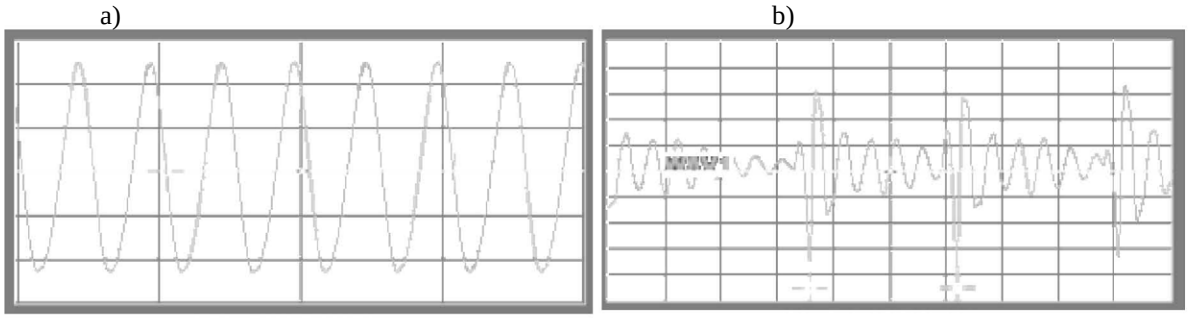


Fig. 1. Examples of EMF waveform registered in the vicinity of electrosurgery devices: a) pure cut mode; b) coagulation “spray” mode.

Electrodes and supplying cables are sources of strong electric field because of radiofrequency (RF) high voltage between electrodes. The exposure to EMF of a surgeon and medical staff depends on the selected mode of device operation, the kind of active electrode used and the location of cables connecting electrodes with generator.

During patient’s treatment, generator and cables can be located in various places against to the surgical table and medical staff bodies. It is crucial for the level of exposure to electric field and capacitive coupling between elements of electrosurgery device and the worker’s body and it determines the level of current flowing through the worker’s body, similarly to currents through the patient’s tissues. If the cables create loops, an increased magnetic field exists also in their vicinity.

The surgeon, who keeps the active electrode in hand, is usually the most exposed person from the team. The hand's exposure always exists, but other parts of the body can be also exposed as a result of the contact with cables, e.g. head's or torso's EMF exposure.

Methods

The EMF measurements have been performed to assess the medical staff exposure to EMF during the use electrosurgery devices [2]. The measurements of RMS electric and magnetic field strength have been conducted according to the Polish Standard PN-T-06580:2002 [6]. Broadband electric and magnetic field strength meter EMR 300 from Wandel & Goltermann with H-field probe type 13 (0.02-250 A/m; 300 kHz – 30 MHz) and E-field probe type 8 (1-800 V/m; 100 kHz – 3 GHz) has been used. The obtained results have been evaluated according to the Polish national regulations concerning the limitation of occupational exposure to EMF of 0 Hz - 300 GHz frequency range [5, 7]. This regulation stated that the worker’s exposure assessment should be performed on the results of the spot measurements of RMS value of unperturbed (it means existing in the workplace during the absence of workers) electric and magnetic field strength (the maximum result of measurements over the worker’s body position in the workplace).

Additionally, the investigated EMF exposure of medical staff has been analysed following the internationally published limitations [5], European Directive 2004/40/EC [1], ICNIRP's guidelines [3] and IEEE standard [4]. According to the European Directive, workers' exposure assessment should be performed on the results of measurements of RMS value of unperturbed (existing in the workplace during the absence of workers) electric and magnetic field strength averaged over the workers body position and averaged for particular time, which depends on the frequency of assessed fields. For example, for the EMF of the frequency 100 kHz - 10 GHz, E and H should be averaged within any 6 minutes of worker's exposure and E^2 and H^2 should be averaged over the worker's body position. Electric field strength (E) and magnetic field strength (H) were included into the set of the Directive’s “action values”, which were defined as the set of external measures, which can be used to describe the EMF exposure for testing and roughly assessing environmental conditions in the workplace. The exposure results inside exposed body, which were taken as “exposure limit values” (internal measures) refer to

the physical quantities as current density (J) and specific energy absorption rate (SAR) should be considered in the case of environmental exposure conditions exceeding above-mentioned "action values". Additionally, Directive's provisions refer to contact current (I_C) and limb induced current (I_L), which can be also used for testing the compliance with "exposure limit values".

Exposure limitation in the frequency range of EMF produced by electrosurgery devices established by Polish national regulations and European Directive is shown in table 1.

Table 1.

Electric and magnetic field strength – exposure limitation established in Poland [6] and by European Directive's "action values" [1].

Frequency range	Exposure limitation in Poland				Directive 2004/40/EC	
	Electric field strength, E [V/m]		Magnetic field strength, H [A/m]		Electric field strength, E	Magnetic field strength, H
	prohibited exposure	8-hours exposure	prohibited exposure	8-hours exposure	[V/m]	[A/m]
300 kHz $< f \leq$ 800 kHz	1000	100	100	10	610	1.6/f
0.8 MHz $< f \leq$ 1 MHz	1000	100	80/f	8/f	610	1.6/f
1 MHz $< f \leq$ 3 MHz	1000	100	80/f	8/f	610/f	1.6/f

f - frequency in MHz

Measurements of RMS current flowing through surgeon's hand (fig. 2) keeping the active electrode (Holaday HI-3702 clamp-on meter) and through feet (Narda 8850 stand-on meter) have been also conducted. These currents are the results of coupling between element with high electric potential (active electrode or cable) and workers body. This current should be considered rather as induced current than contact current.



Fig. 2. The clamp-on meter measurements of the current in surgeon's hand.

The assessment of these quantities may be carried out following the permissible values as specified in Directive 2004/40/EC [1] and in ICNIRP guidelines [3] for contact current or permissible values for induced current in the feet specified in IEEE standard [4]. The Directive's criteria for induced current in limbs are not given for frequency below 10 MHz. Polish regulations don't refer directly to current inside workers body. Exposure limitation of contact and induced current in the frequency range of EMF produced by electrosurgery devices established by European Directive and IEEE standard is shown in table 2.

Table 2.

Contact and induced current – exposure limitation established by European Directive [1] and by IEEE [4].

Frequency range	Directive 2004/40/EC		IEEE			
	Contact current, I_C [mA]	Limb induced current, I_L [mA]	Contact current, I_C [mA]		Induced current in feet, I_L [mA]	
			for touch	for grasp	each foot	both feet
100 kHz $< f \leq$ 10 MHz	40	not specified	50	100	100	200
10 MHz $< f \leq$ 110 MHz	40	100	50	100	100	200

Measurements were performed for more than 30 types of common-used electrosurgery devices: various types of ERBE, Aesculap, Bovie, Valleylab and Olympus operated in the various modes. The output power during investigations (approx. 100-150 W) was a little higher than during normal work to obtain results representing the worst case of workers exposure conditions.

For the technical reasons, measurements have been performed during a simulated operation - absorbent cotton with saline has been used as phantom equivalent to the patient's body.

Results

The results obtained have shown that the surgeon is usually exposed to non-homogenous electric field. Metallic objects, which are in the operating theatre influence on spatial distribution of electric field. The level of exposure of medical staff can be changed by 2-3- fold depending on the location of these objects.

In the worst case implying the use of a monopolar electrode and non-shielded cables surgeon's hand keeping this electrode can be exposed to electric field exceeding 1000 V/m, head and torso up to a few tens V/m (fig. 3). When the cables touch the surgeon's body then the torso exposure is stronger, up to the level of the exposure of hand keeping electrode.

Near electrosurgical devices, the area of electric field strength exceeding 10 V/m can exist up to the distance of 70-100 cm from the active electrode and supplying cables.

Magnetic field in the nearest distance of electrodes and cables (5-10 cm) is usually below 1 A/m.

For the operation with output power less than 50 W or with the use of bipolar electrode, electric field exposing the hand is less than 80 V/m and less than 30 V/m in the case of head and torso exposure.

Electric field around the housing of the generator with effective EMF shielding is below 30 V/m during the use of both kinds of electrodes.

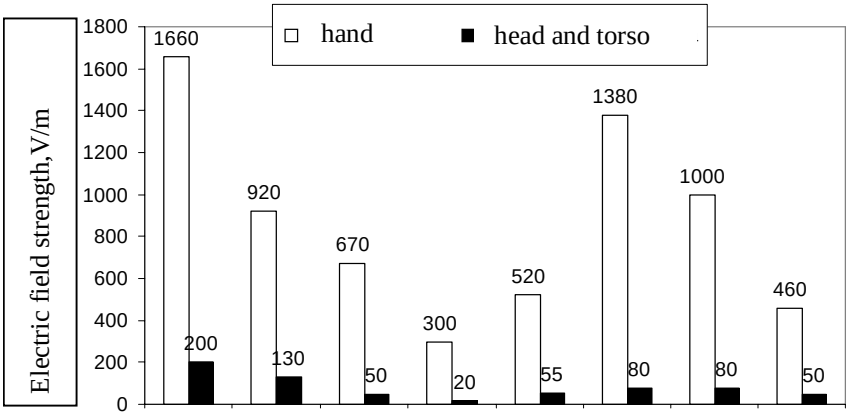


Fig 3. The examples of surgeon's exposure to electric field during the use of various electrosurgery devices (output power 100-150 W, a monopolar active electrode, cables far from the torso and head).

The execution of electrosurgical treatment with an electric arc burned under the active electrode lead to significant increase of electric field affecting on medical staff. The level of exposure during electric arc-surgery can be 4-fold higher in comparison to the operation without arc (fig. 4).

Waveform of EMF as well as the level of exposure in the vicinity of active electrode and supplying cables depend on the mode of electrosurgery devices operation. Figure 5 illustrates how electric field strength from the same electrosurgical device depends on it's selected mode.

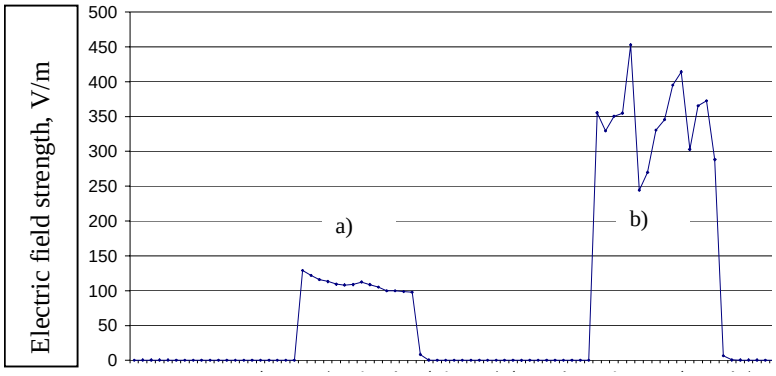


Fig. 4. The examples of registration of electric field strength in the vicinity of active electrode: a) cut mode without burned electric arc; b) cut mode with burned electric arc.

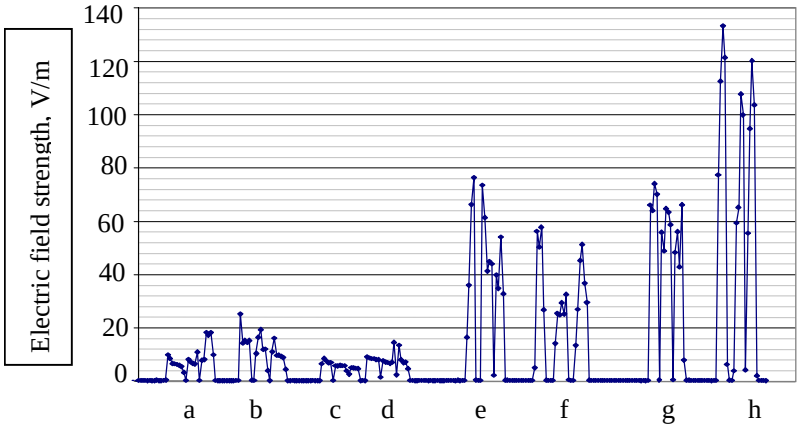


Fig 5. Examples of registration of electric field strength in the vicinity of electrosurgery device - various modes of operation: a) cut ”pure”; b) cut “blend”; c) coagulation „desicate”; d) coagulation „fulgurate”; e) coagulation „spray”; f) cut „pure” with argon; g) cut „blend” with argon; h) coagulation „spray” with argon.

The results presented indicate the possibility of a high exposure of the surgeon’s hand in the case of keeping the active electrode or touching the cable to forearm. Measurements of current in surgeon’s body may be used for additional assessment of exposure conditions and internal results in exposed body. The investigations carried out show, for example, that current in the hand keeping the active electrode can be of order 5 - 18 mA in the case of electric field strength of approx. 70 V/m in the distance of 5-10 cm from a monopolar active electrode (fig. 6), and significantly depends on the location of cable towards the hand.

Current in the feet of surgeon, insulated by shoes from ground and without direct contact with cables, is below 20 mA when electric field strength in the vicinity of monopolar active electrode is approx. 250 V/m. Taking into account the possibility of exposure to a stronger field (app. 1000 V/m or even higher) or a contact of the body with the cables, the current flowing through the arm of surgeon keeping the electrode can exceed the permissible values established in the Directive 2004/40/EC for contact current (40 mA).

The results obtained also indicate that current measured by clamp-on meter in the hand keeping the active electrode is approx. 2-fold higher than current measured by stand-on meter in the feet.

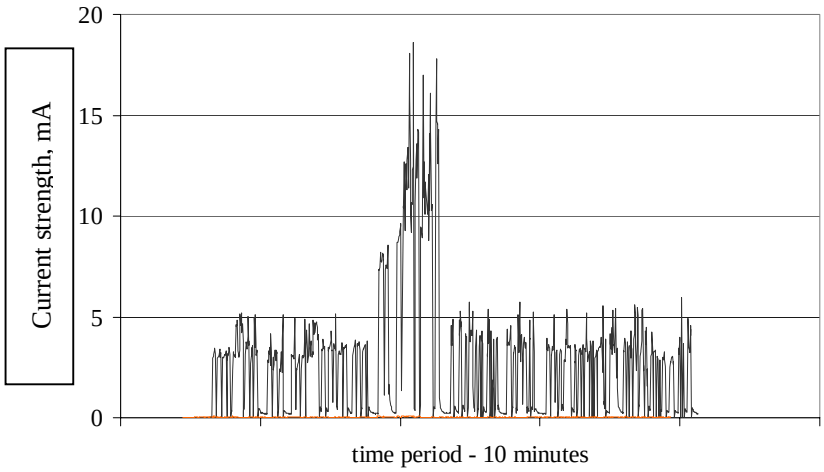


Fig 6. The examples of registration of current in surgeon’s hand exposed to EMF from the electrode's cable.

The conclusive assessment of surgeons exposure to EMF, presenting compliance with European Directive provisions concerning internal measures (“exposure limit values”), will be possible after publishing harmonised European standards. These standards should fixed in details the protocol for measurements or calculations, necessary for such exposure assessment. The numerical simulations for the verification of the compliance of particular EMF exposure scenarios with the Directive provisions need the use of a high resolution of the worker’s body models and an adequate representation of the workplace environment. For the electro-surgeon's EMF exposure, the conditions such as calculations for particular exposure situations need high professional skills, specialised software and they are very often time-consuming. The basic problems identified during pilot calculations are: the representation of the realistic posture of worker's body, the adequate representation of the electrical grounding conditions at the workplace and the adequate representation of realistic impedance of near-field produced by electrosurgery devices, as well as it's dynamic changes in the course of surgery treatment.

The additional problem with assessment of measurements results can appear for highly modulated EMF, when the properties of the used EMF meters calibrated in harmonic field cannot be relevant to such field's measurements and then the use of correction's factors taking into consideration the waveform of incident fields should be recommended. It was analysed for various kinds of modulations of EMF produced by various devices examined that the value of the measurement's uncertainty component coming in consequences of measurements of modulated fields in the case of common electrosurgery devices can be on the level of 50%. It is possible to find both effects, overestimation and underestimation in the EMF strength measurement's results.

Conclusion

In consideration of a necessity to keep the active electrode in the hand, complete elimination of surgeon's exposure to strong electric field is impossible. The reduction of the surgeon's exposure can be reached by the proper positioning of the cables supplying a monopolar electrode. The exposure of others persons from medical staff is relatively weak if they don’t have a direct contact with cables. In the worst case of cable's location and electrosurgery devicee's output power, the EMF overexposure can occur. The surgeon’s EMF exposure assessment for the case of the use of a monopolar electrode should be completed with measurements or calculation of currents flowing through the body.

The results of the investigations presented show that the effective reduction of the surgeon exposure can be obtained by keeping cables between the generator and the surgeon’s hand without a contact with the bodies of workers. Cables located at the surgical table decrease the surgeon’s exposure but increase the influence of electric field on other medical workers (e.g. nurses). A compromise is indispensable in that situation. A radical reduction of the EMF exposure level is possible by the use of the bipolar electrode if a kind of surgical treatment allows for that. Avoiding work with burned electric arc under the electrode reduces the exposure of personnel, too.

If weak electric field near the electrode is found (usually in the case when output power is approx. 50 W or less, the use of bipolar electrodes or shielded cables) measurements of electric field strength can be considered as

sufficient to confirm a low level of exposure there. The measurements uncertainty and the consequences of a high modulation of EMF from electrosurgery devices for the measurement's results should be analysed very carefully in every case when a relatively high level of exposure is found at the workplace.

Acknowledgments

The investigations supported by the State Committee for Scientific Research of Poland and Poland's Ministry of Economy, Labour and Social Policy (grant 1.A.03)

References

1. Directive 2004/40/EC of the European Parliament and of the Council of on the minimum health and safety requirements regarding the exposure of workers to the risks arising from physical agents (electromagnetic fields) (18th individual Directive within the meaning of Article 16(1) of Directive 89/391/EEC), O.J. Nr L-184, 2004.
2. Gryz K. Karpowicz J.; Electromagnetic hazards from electrosurgery – assessment of occupational exposure to electromagnetic field and currents induced in the body, Roczniki PZH, (in Polish)
3. ICNIRP Guidelines for Limiting Exposure to Time-Varying Electric, Magnetic, and Electromagnetic Fields (up to 300 GHz), Health Physics, 1998, 74, 4 (April), 494-522.
4. IEEE Std C95.1, Standard for Safety Levels with Respect to Human Exposure to Radio Frequency Electromagnetic Fields, 3 kHz to 300 GHz. 2005 Edition Published by the Institute of Electrical and Electronics Engineers, New York, USA, 2006.
5. Karpowicz J., Hietanen M., Gryz K. - EU Directive, ICNIRP Guidelines and Polish Legislations on Electromagnetic Fields - International Journal of Occupational Safety and Ergonomics (JOSE), 2006, vol. 12, No. 2, 125-136
6. Polish Standard PN-T-06580:2002. Labour protection in electromagnetic fields and radiation of the frequency range from 0 Hz to 300 GHz. Part 1: Terminology. Part 3. Methods of measurement and evaluation of the field on the work stands (in Polish).
7. Regulation of the Minister of Labour and Social Policy of 29 November 2002 on the maximum admissible concentrations and intensities for agents harmful to health in the working environment. Dz. U. 2002;217(item 1833):13614–60 (In Polish)

-Measurement of Complex Permittivities of Biomedial tissue at Millimeter Wave Band

Masahiro Hanazawa*, Atsuhiro Nishikata* ** and Soichi Watanabe*

****National Institute of Information and Communications Technologies***
*****Tokyo Institute of Technologies***

Abstract

For this paper, we directed our attention to the free-space method using a dielectric lens antenna, using this method to measure the permittivity of a cow's blood in the millimeter-wave band. We confirmed that measurement results under this method were in agreement with measurement results obtained by the coaxial probe method; here we report on the measurement results up to 65 GHz.

Introduction

Recently, utilized frequency band has been extended to higher frequency region including millimeter-wave band. The electromagnetic dosimetory is therefore required in the millimeter-wave band. This area of study deals with a simulation of exposure and a calculation of internal field within an exposed human body. A permittivity of a tissue is required for electromagnetic dosimetry and it well known that the permittivities of the biological tissues have frequency dispersion. Under these backgrounds, a great number of measurement methods of dielectric constants have been studied in various frequency bands [1]-[3]. However, few studies on permittivities of biological tissues have been reported in millimeter-wave band. Therefore strong demands for measurement of the dielectric constants of biological tissues in the millimeter-wave band exist.
In this study, we gave attention to a free space method using a lens antenna [4] and measured dielectric constants of cow's whole-blood samples from 33 GHz to 65 GHz. As a result, these were in good agreement with those measured by an alternative method (coaxial probe method). The result suggests that the proposed method can be used for permittivity measurement of a biological tissue in millimeter-wave band even higher than 65 GHz.

Measurement theory

We used the multi-line model for determining a complex coefficient of a surface of a liquid. We defined a measured cascade matrix of the glass of measured scattering parameter.

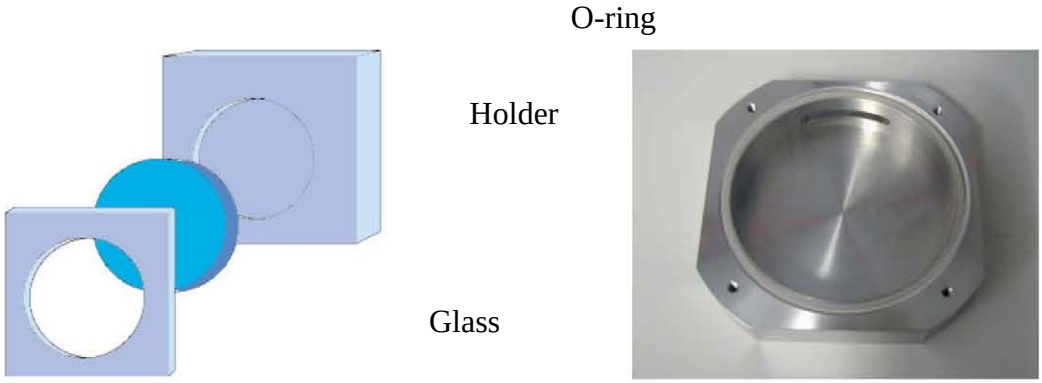
$$[T_g] = \frac{1}{S_{21}} \begin{bmatrix} (S_{21}S_{21} - S_{11}S_{22}) & S_{11} \\ -S_{22} & 1 \end{bmatrix} \qquad (1)$$

The measured cascade matrix can be also be written as

$$[R_T] = [T_g][R_s] \qquad (2)$$

Where cascade matrix $[R_T]$ and $[R_S]$ represent reflection coefficient of the glass and of the sample. If we neglect the reflection wave from the bottom of the holder, we can relate the complex permittivity of a liquid to the complex reflection coefficient. So from scattering parameter measurements, we determine the complex permittivity of the sample within the holder.

Measurement method



(a) Composition (b) picture

Fig.1. Composition and picture of sample holder.

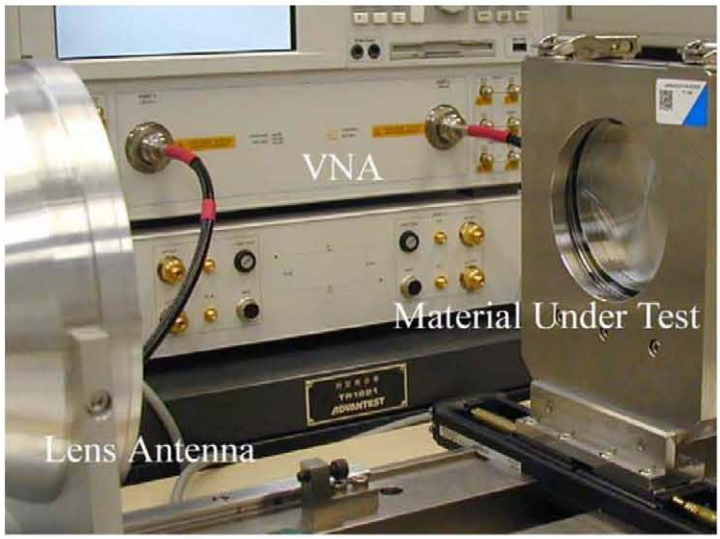


Fig.2. Picture of measurement set-up.

Figures 1 and 2 show a measurement set up and a sample holder, respectively. As shown in Fig.2, a liquid agent is hold with an optical glass and a tank made from a stainless steel. This measurement, as shown in Fig. 1, an electromagnetic wave generated by a VNA (Vector Network Analyser) is transmitted from the lens antenna to a test sample held by the sample holder. The lens antenna then receives a reflected wave (S_{11}) from the sample. These waves and T-parameter of the optical glass are then used to calculate the complex permittivity of the sample. Since in this measurement the metal plate of the holder and deformation of the liquid surface on the top surface of the holder may result in measurement errors, a high-directivity lens antenna [4] was used, as well as a 65-cm^2 holder (sufficiently large for the test irradiation area). Calibration was carried out via TRL (Through-Reflection-Line), which does not require any open and load standards [5]. The room temperature and the temperature of the blood during measurement were approximately 24°C and 22°C, respectively.

Measurement results

The permittivity of the blood of a cow was measured using the sample holder and the measurement set-up mentioned above. Fig. 3 shows the measurement results using the above set-up as well as measurement results using the coaxial probe method. Note that although the lens antenna used in measurement is functional in the frequency range from 18 GHz to 110 GHz, it features a cut-off frequency because it is connected to the VNA through a coaxial waveguide converter. Measurement was therefore performed using two types of waveguide, the WR22 and the WR15.
The measurement results using the WR22 and those using the probe method showed agreement, confirming that the measuring method proposed in this paper enables millimetre-wave band measurement of the permittivity of a biological tissue. Moreover, permittivity in a range from 50 GHz to 65 GHz (difficult to measure with existing coaxial probes) was measured by changing to the WR15 waveguide. As a result, the measurement results agree with those of the above-mentioned WR22 (with a difference of approximately 5%); we thus concluded that the experiment successfully demonstrated the possibility of measuring the permittivity of a biological tissue using a wide range of frequencies. We inferred that the difference noted above was most likely brought about due to factors such as variation in liquid temperature and absorption of water in the liquid agent.

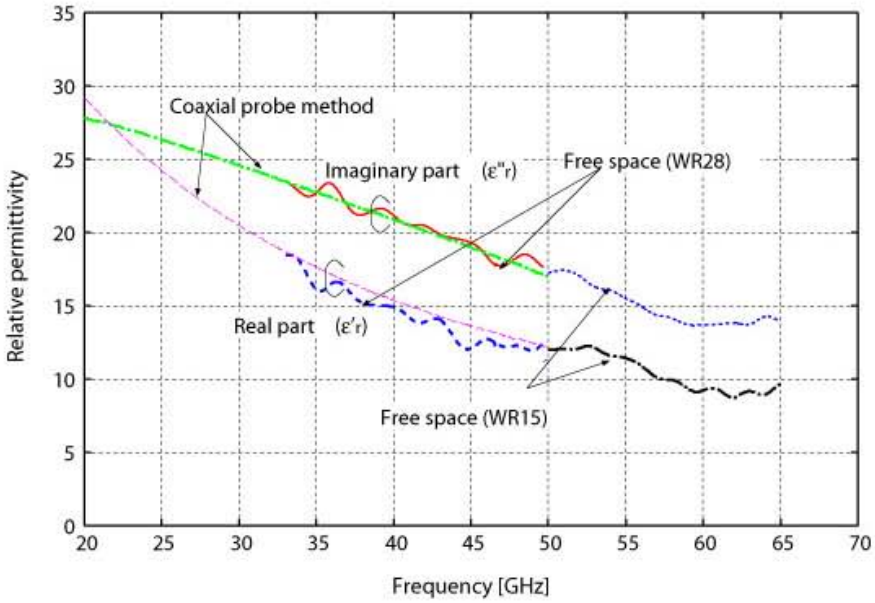


Fig.3. Measurement result (blood).

Conclusion

For this paper, we directed our attention to the free-space method using a dielectric lens antenna, using this method to measure the permittivity of the blood in millimeter-wave band. Based on our results, we confirmed that the measurement values obtained under this method were in agreement with the measured values obtained by the coaxial probe method, demonstrating that this method is appropriate for the measurement of permittivity of a biological tissue in the millimeter-wave band. Investigation of changes in liquid temperature remains as issues to be resolved in the future.

Acknowledgements

We are thankful to Mr. Noda of OSHIMA PROTOTYPE EMGINEERING Co., Ltd, who manufactured the sample holder.

Reference

[1] C Gabriel, R W Lau and C Gabriel "The dielectric properties of biological tissue : II Measurement in the frequency range 10 Hz to 20 GHz," Physics Medicine and Biology Vol.42, pp.2251-2269 (1996).
[2] J M Alison and R J Sheppard "Dielectric properties of human blood at microwave frequencies," Physics Medicine and Biology Vol.38, pp.971-978 (1998).
[3] C.M Alabaster "Permittivity of human skin in millimetre wave band," Electronics letter, Vol.39, No.21 (2003).
[4] K. Ghodgaonker, V. V. Varadan and V. K. Varadan, ``A Free-Space Method for Measurement of Dielectric Constant and Loss Tangents at Microwave Frequencies, `` IEEE Trans. IM-38, pp. 789 -793, (1989).
[5]R.B.Marls "A Multiline Method of Network Analyzer Calibration," IEEE Trans. MTT Vol.39, No.7, pp.1205-1215, (1991).

UMTS MOBILE PHONE BASE STATION AND HEALTH EFFECTS

SABINE HEINRICH[1], SABINE SCHLITTMEIER[2] , JÜRGEN HELLBRÜCK[2]

[1] INSTITUTE FOR OCCUPATIONAL AND ENVIRONMENTAL MEDICINE, UNIT FOR OCCUPATIONAL AND ENVIRONMENTAL EPIDEMIOLOGY & NETTEACHING, ZIEMSSENSTR. 1; 80336 MUNICH, GERMANY

E-MAIL: SABINE.HEINRICH@MED.UNI-MUENCHEN.DE

[2] WORK, ENVIRONMENTAL AND HEALTH PSYCHOLOGY, CATHOLIC UNIVERSITY OF EICHSTÄTT-INGOLSTADT, OSTENSTRAßE 26-28, 85072 EICHSTÄTT, GERMANY

Abstract

The increasing number of mobile phone base stations in Germany is associated with concerns in the population that the electromagnetic fields (EMF) could have adverse effects on health and well-being. The aim of the study was to investigate the association between EMFs of a UMTS-mobile phone base station and health of office workers.
A newly installed UMTS (Universal Mobile Telecommunications System) - base station was in a double blind fashion randomly turned on and off for 24-hours over a period of three months. Using an online questionnaire participants (n = 95) indicated their health at the beginning and the end of each working day. In addition, participants assessed whether the base station was turned on or off.
No evidence for an association between the exposure of the mobile phone base station and health of the participants was found. However, when the participants thought that the base station was turned on they indicated statistically significant more health complaints.
On the basis of the results of the study no association between the exposure to an UMTS base station and health could be shown. A follow-up study with a larger sample of the general population and personal dosimetry would be desirable.

Introduction

Proliferation of mobile phone base stations enables more and more people worldwide to use new telecommunication systems. However, many people are concerned about possible adverse health effects of the electromagnetic fields emitted by cellular phones and mobile phone base stations, even if exposure levels are far below those recommended. (Bavarian State Ministry of the Environment, Public Health and Consumer Protection, 2003). In Germany, introduction of UMTS (Universal Mobile Telecommunications System) requires installation of 15.000 new base stations. One reason for the concern about health effects of mobile phone base stations is the inability of neighbouring residents to regulate the duration and timing of these electromagnetic fields (Revermann 2003).

Despite the concerns, few studies of the effects of exposure to mobile phone base stations have been published. Published studies – e.g. by Santini et al. (2002) and Navarro et al. (2003) - have numerous methodological problems, so that their results are likely to be biased. The main issue is the valid exposure assessment, and it was not fully resolved in the pilot study of Hutter et al. (2002), who measured exposure to the base stations in the participants` bedrooms. Level of electromagnetic emissions of a mobile phone base station varies over time, making it difficult to capture accurately. To date, specific variation of the exposure over time has only been possible in laboratory studies.

Thus, the effects of UMTS exposure on human health and well-being have only been investigated in laboratory settings. Zwamborn et al. (2003) exposed people who reported sensitivity to radio-frequency waves (electrosensitive group) and a control group to a 1 V/m field at 900 MHz and 1800 MHz by replicating GSM fields, and also 2100 MHz UMTS fields. The study found a statistically significant association between the UMTS fields and well-being for both groups. By contrast, no effect was seen for the GSM frequencies at 900 and 1800 MHz. However, a Swiss follow-up study did not confirm these results (Regel et al. 2006). In a double blind provocation study (900 MHZ GSM mobile phone signal), Rubin et al. (2006) tested persons reporting electrosensitivity and controls but found no evidence either for the ability of electrosensitive people to detect such signals or of any increased symptom severity among them.

Within the feasibility study presented here, a newly installed UMTS mobile phone base station could be used for study purposes over a period of three months. The aim of this double-blind experiment was to investigate whether the electromagnetic fields of a UMTS base station influence the well-being of office employees working in its proximity. In addition, it should be taken into consideration in what way psychological factors like causal attribution are involved.

Material and Methods

The study took place from September to December 2003.

Participants

Overall 104 employees of the Bavarian Environmental Agency participated in the study. Of them, 95 participants (67 male and 28 female), age between 26 and 62 years (median = 40), answered the questionnaire in the morning and in the evening on at least 25 percent of the 70 days of the study and could thus be included in the analyses. Of these 95 participants, 71 (75 %) completed the daily questionnaires on at least 42 out of the 70 working days (60 %). Reasons for questionnaire non-completion were holidays, work outside the agency or sickness leaves. Most of the participants had a high level of education (university degree or doctoral level). All subjects gave their written informed consent to the participation.

Study design

The UMTS-mobile phone base station was installed in summer 2003 on the roof of the Bavarian Environmental Protection Agency. The mobile phone base station was switched on or off (control days) for one, two or three consecutive business days. The number of exposure and control days was equal (n = 35 each). We thus created six different exposure conditions, which differed by operating status (on, off) and duration (one to three days). Differing duration of the UMTS-exposure would enable to assess its potential cumulative effects on health.

Double-blinding

Several measures were taken to ensure the double-blind design. The operating status of the base station was chosen randomly from three possible versions. The power of the base station was recorded over the study period, with notebook and record located in a closed room. A modification on the software of the base station guaranteed that the operating status of the base station could not be received by a mobile phone. In addition, the base station had its own electricity.

Exposures

The mobile phone base station manufactured by Kathrein (type K742 212) transmitted the UMTS signal with a mean frequency of 2167,1 MHz, 5 MHz frequency range und a transmitting power of 20 W. With the downward tilt of the antenna of 8° it was possible to achieve maximum exposure level in the office building.

The UMTS exposure of the participants differed by the location of their offices in the building. Exposure measurements were carried out in the empty offices of all participants on weekends with base station turned on. Measurements were done by a physicist of the Bavarian Environmental Agency. The UMTS exposure in the offices ranged from 0.05 V/m (detection limit) to 0.53 V/m. The mean level was 0.10 V/m (standard deviation 0.09 V/m).

Questionnaire

Using an online questionnaire, participants indicated their health condition at the beginning and the end of each working day. The questionnaire contained items on health complaints that were used in connection with electromagnetic fields in several publications (Berg et al. 2004, David et al. 2002, Frick et al. 2002, Hietanen et al. 2002, Hillert et al. 1999, Röösli et al. 2004). A summary of the items is shown in table 1. In addition, participants were asked to guess whether the base station was on or off.

Table 1: Online-questionnaire used to evaluate health symptoms and the mean scores (M) and standard deviations (SD) of the score differences between morning and afternoon score, listed by operating status of the mobile phone base station (on or off)

Question: „How intensively did you experience the following health complaints today since you started working this morning? “

Answer categories: rarely–slightly–somewhat –strong–very strong

	M (SD)		
	MBS switched off	MBS switched on	p
concentration problems	0.090 (0.217)	0.138 (0.211)	0.680
lack of energy	0.037 (0.566)	0.065 (0.230)	0.161
headache	0.128 (0.274)	0.152 (0.214)	0.187
neck and shoulder pain	0.044 (0.194)	0.067 (0.182)	0.219
strong perspiration	0.008 (0.143)	0.029 (0.138)	0.181
dejection	0.002 (0.179)	0.018 (0.129)	0.172
feeling of pressure at the ear	0.010 (0.135)	0.022 (0.134)	0.616
tinnitus	0.020 (0.126)	0.032 (0.151)	0.075
breathing difficulties	-0.004 (0.077)	0.007 (0.039)	0.165
lack of appetite	0.000 (0.084)	0.003 (0.075)	0.563
paraesthesia	0.015 (0.120)	0.017 (0.106)	0.978
dry skin	0.006 (0.143)	0.008 (0.128)	0.685
allergic disorders	-0.005 (0.055)	-0.003 (0.055)	0.782
restlessness	0.020 (0.327)	0.021 (0.143)	0.371
cardiac symptoms	-0.001 (0.056)	0.000 (0.064)	0.699
nervousness	0.020 (0.206)	0.020 (0.129)	0.674
irritability	0.022 (0.245)	0.021 (0.123)	0.448
dizziness	0.018 (0.058)	0.015 (0.066)	0.604
feeling of anxiety	-0.005 (0.220)	-0.009 (0.075)	0.237
limb pain	0.012 (0.101)	0.003 (0.098)	0.202
back pain	0.051 (0.171)	0.042 (0.186)	0.494

Statistical analyses

Complaints were assessed on a five-point Likert scale: “rarely” = 1, “slightly” = 2, “somewhat” = 3, “strong” = 4, “very strong” = 5. In order to assess the change in well-being during the day, the score difference between morning and afternoon was calculated. The overall level of well-being was calculated as the sum of answers to the 21 questionnaire items. Higher score indicated worse well-being. The absolute change in the overall score over the working day was calculated as the difference between morning and afternoon score.

We used two sided t-tests for paired samples and ANOVA to examine the research questions of this study. Statistical analyses were carried out using SPSS 11.5.

Results

On average, the well-being decreased slightly, but not significantly, over the course of the working day. As shown in table 1, the mean symptom score did not differ statistically significantly over the working day between exposure and control days. In order to study a potential accumulation of effects, the mean change in symptom scores over a series of 1, 2 or 3 days with exposure was compared with sham-exposure (table 2). The ANOVA did not indicate statistically significant differences between the exposure conditions. (operating status: $F = 1,36$, $p = 0,35$; duration: $F = 0,66$, $p = 0,52$; interaction: $F = 0,37$, $p = 0,69$).

In contrast, the mean symptom score was significantly higher if the participants considered the base station to be switched on ($M = 1,93$; $SD = 2,49$) than on days they considered unexposed ($M = 0,16$; $SD = 0,95$; $T(77) = -6,66$, $p < 0,01$).

Table 1: Mean scores (M) und standard deviations (SD) of the overall score differences from all participants dependant on the exposure of the mobile phone base station (MBS)

(n = 90 due to missing values)

	MBS switched off			**MBS switched on**		
	1 day	**2 days**	**3 days**	**1 day**	**2 days**	**3 days**
M	0,54	0,47	0,64	0,77	0,56	0,65
SD	(1,48)	(1,19)	(2,14)	(1,26)	(1,37)	(1,63)

Discussion

We aimed to investigate the association between electromagnetic fields of a UMTS mobile phone base station and health complaints reported by office workers. A newly installed base station was in a double blind design randomly turned on and off for 24-hours over a period of three months. 95 office workers participated in this field experiment and reported health status daily using an online questionnaire.

No evidence for an association between UMTS mobile phone base station exposure and self-reported health complaints was found. In general, the reported complaints increased over of the working day. This increase was associated neither with exposure presence nor with its duration. These findings are in agreement with previous provocation studies, which used different frequencies (Andersson et al. 1996, David et al. 2002, Hietanen et al. 2002, Koivisto et al. 2001, Lyskov et al. 2001, Radon and Maschke 1998, Regel et al. 2006, Rubin et al. 2006). As this was a pilot study including a relatively small sample the results can not be generalized.

Only the association of perceived exposure condition with health was statistically significant. This might be interpreted as an incorrect attribution, which strongly emphasises the importance of using (double-) blind designs in corresponding research. This effect has also been shown in studies on EMF and health complaints (Andersson et al. 1996, Bergqvist et al. 1998, Harlacher und Schahn 1998, Hillert und Kolmodin-Hedman 1997).

One advantage of our study was the objective exposure assessment. However, as only exposure in the workplace was taken into account exposure assessment was incomplete. This problem might only be overcome with personal dosimetry (Radon et al. 2006). Overall exposure levels in our study were comparable to those found in other studies (Schüz and Mann 2000, Bernkopf 2004).

The results of this pilot study show feasibility of using online questionnaire. However, an investigation with online questionnaire is only possible in a specific Internet-using population, like office workers. In a follow-up study it could be useful to employ a CAPI (computer assisted personal interview). Also the use of a PDA (Personal Digital Assistant) and Handheld-computer might be feasible as recently shown by Schreckenberg and Guski (2005).

Overall, the results of this study show that the online questionnaire developed is practicable. The questionnaire instrument is capable to register health complaints. No evidence for an association between exposure to mobile phone base station and self-reported health complaints was found. However, well-being depended on the self-reported exposure condition. This might indicate an incorrect attribution, which strongly emphasises the importance of using (double-) blind designs in corresponding research. A follow-up study with a larger sample of the general population and personal dosimetry would be desirable.

Acknowledgements

The study was supported by the Bavarian Environmental Agency.

References

Andersson B, Berg M, Arnetz BB, et al. (1996): A cognitive-behavioral treatment of patients suffering from "Electric Hypersensitivity". Journal of Occupational and Environmental Medicine 38(8), 752-758.

Bavarian State Ministry of the Environment, Public Health and Consumer Protectio (2003). Stichwort Mobilfunk. München

Berg G, Breckenkamp J, Schlehofer B, et al. (2004). Querschnittstudie zur Erfassung und Bewertung möglicher gesundheitlicher Beeinträchtigungen durch die Felder von Mobilfunkbasisstationen - Zwischenbericht zum Abschluss der Pilotphase. Bielefeld, Heidelberg, Mainz, München, http:/www.emf-forschungsprogramm.de/forschung/epidemiologie_verg/epi_020_Zwie_01.pdf.

Bernkopf J (2004). EMF-Monitoring in Bayern - Messungen der elektromagnetischen Felder in Wohngebieten. Augsburg, Bayerisches Landesamt für Umweltschutz (LfU); www.bayern.de/lfu/wir/.

David E, Reißenweber J, Wojtysiak A, Pfotenhauer M (2002): Das Phänomen der Elektrosensibilität. Umweltmedizin in Forschung und Praxis 7(1), 7-16.

Frick U, Rehm J, Eichhammer P (2002): Risk perception, somatization and self report of complaints related to electromagnetic fields - A randomized survey study. International Journal of Hygiene and Environmental Health 205, 353-360.

Hietanen M, Hämäläinen A-M, Husman T (2002): Hypersensitivity symptoms associated with exposure to cellular telephones: no causal link. Bioelectromagnetics 23, 264-270.

Hillert L, Kolmodin-Hedman B, Söderman E, Arnetz BB (1999): Hypersensitivity to electricity: Working definition and additional characterization of the syndrom. Journal of Psychosomatic Research 47(5), 429-438.

Hutter H-P, Moshammer H, Kundi M (2002): Mobilfunk-Basisstationen: Erste Ergebnisse von zwei Feldstudien. Umweltmedizin in Forschung und Praxis 7(4), 213-213.

Koivisto M, Haarala C, Krause CM, et al. (2001): GSM phone signal does not produce subjektive symptoms. Bioelectromagnetics 22(3), 212-215.

Lyskov E, Sandström M, Hansson Mild K (2001): Provocation study of persons with perceived electrical hypersensitivity and controls using magnetic field exposure and recording of electrophysiological characteristics. Bioelectromagnetics 22, 457-462.

Navarro EA, Segura J, Portoles M, Gomez-Perretta C (2003): The microwave syndrom: a preliminary study in spain. Electromagnetic Biology and Medicine 22, 161-169.

Radon K, Maschke C (1998): Gibt es Elektrosensibilität im D-Netzbereich? Umweltmedizin in Forschung und Praxis 3, 125-129.

Radon K, Spegel H, Meyer N, et al. (2006): Personal Dosimetry of Exposure to Mobile Phone Base Stations? An Epidemiologic Feasability Study Comparing the Maschek Dosimeter Prototype and the Antennessa DSP-090 System. Bioelectromagnetics 27, 77-81.

Regel SJ, Negovetic S, Röösli M, et al. (2006): UMTS Base Station-Like Exposure, -Being and Cognitive Performance. Environmental Health Perspectives online: http://dx.doi.org with doi adresse: 10.1289/ehp.8934.

Revermann C (2003). Risiko Mobilfunk. Berlin, edition sigma.

Röösli M, Moser M, Baldinini Y, Braun-Fahrländer C (2004): Symptoms of ill health ascribed to electromagnetic field exposure - a questionnaire survey. International Journal of Hygiene and Environmental Health 207(2), 141-150.

Rubin GJ, Hahn G, Everitt BS, Cleare AJ, Wessely S (2006): Are some people sensitive to mobile phone signals? Within participants double blind randomised provocation study. Britisch medical Journal 332(7546), 886-891

Santini R, Santini P, Danze JM, Le Ruz P, Seigne M (2002): Study of the health of people living in the vicinity of mobile phone base stations: 1. Influences of distance and sex. Pathologie Biologie 50(6), 369-373.

Schreckenberg D, Guski R (2005): Lärmbelästigung
durch Straßen- und Schienenverkehr zu unterschiedlichen Tageszeiten. Umweltmed Forsch Prax 10(2), 67-76.

Schüz J, Mann S (2000): A discussion of potential exposure metrics for use in epidemiological studies on human exposure to radiowaves from mobile phone base stations. Journal of Exposure Analysis and Environmental Epidemiology 10(6), 600-605.

Zwamborn APM, Vossen SHJA, van Leersum BJAM, Ouwens MA, Mäkel WN (2003). Effects of global communication system radio-frequency field on well being and cognitive functions of human subjects with and without subjective complaints, Netherlands Organisation for Applied Scientific Research (TNO).

EXPERIMENTAL INVESTIGATIONS ON THE BIOLOGICAL FREE RADICAL PRODUCTION IN HUMAN BLOOD CELLS DUE TO MICROWAVE EXPOSURE

M. ENDO, T. HIKAGE, T. MANABE AND T. NOJIMA

GRADUATE SCHOOL OF INFORMATION SCIENCE AND TECHNOLOGY,
HOKKAIDO UNIVERSITY
KITA 14, NISHI 9, KITA-KU, SAPPORO, HOKKAIDO, 060-0814 JAPAN
E-MAIL: endo@emwtinfo.ice.eng.hokudai.ac.jp, {hikage, nojima}@wtemc.ist.hokudai.ac.jp

Abstract

The purpose of this study is to investigate the effects of microwave exposure on biological free radical production, focusing especially on mobile radio frequencies. In vitro experiments for the hydroxyl radical production on human white blood cells after exposure to modulated or non-modulated 900 MHz and 2.45 GHz microwave were performed. Several signals were used: continuous-wave (CW), several typical modulations of the GSM, PDC, cdma2000, and non-modulated pulse-wave. Developed 900 MHz ridged-waveguide exposure equipment and 2.45 GHz open-type equipment were used for high intensity irradiation, and the specific absorption rates (SARs) were estimated by numerical simulations. The fluorescence probe method was adopted to estimate the radical production. Furthermore heat (20°C-39°C) was used for the purpose of controlling the hydroxyl radical excitation.

The exposure experiments were carried out by using about six hundred tissues, and the free radical production was estimated with the fluorescence images. Some irradiations produced a difference in free radical production. However, this difference disappeared when data was compared to the heat controls.

As a result, any free radical production due to non-thermal effect of microwave exposure was not detected.

Introduction

It has been already suggested that the microwave EMF interactions with biomolecules, or with portions of biological structure, are unlikely at the frequencies below the high gigahertz spectral regions [1]. However, to the best of the authors' knowledge, there have not been any investigations conducted so far concerning the possibility of biological interactions due to the microwave EMF, which may result in the production of free radicals.

A free radical is an atom or a molecule with an unpaired electron and has a high chemical reactivity. There are various kinds of free radicals. If the radical production occurs in living tissues, it can trigger a chain reaction resulting in various influences on important cellular components such as DNA, or the cell membrane in the worst case [2,3,4]. Thus, in the discussion on the adverse health effect issues due to microwave irradiation, it is very important to obtain reliable experimental evidences revealing the fact that microwave EMF irradiation might not affect free radical production directly.

It is known that white blood cells (WBCs) generate free radicals to destroy bacteria and viruses. In order to investigate the biological free radical production in human WBC, experiments of 900 MHz and 2.45 GHz microwave exposure are conducted in this study.

Materials and Methods

The procedure for preparing the WBC sample is shown Figure 1. Firstly, dextran is added to whole blood taken from a healthy person. After letting it stand for 30 minutes, the supernatant fluid is obtained. Secondly, in order to separate into an upper plasma layer and a lower WBC layer, the blood samples are centrifuged at 400 g for 6 minutes. The plasma layer is removed and then 2 ml calcium, magnesium free phosphate buffered saline (CMF-PBS) is added to the settlement cell. Finally, 1950 μl CMF-PBS and 100 μl 2',7'-dichlorodihydrofluorescein diacetate (DCFH) are added to this 50 μl settlement cell. This WBC sample is used for this experiment.

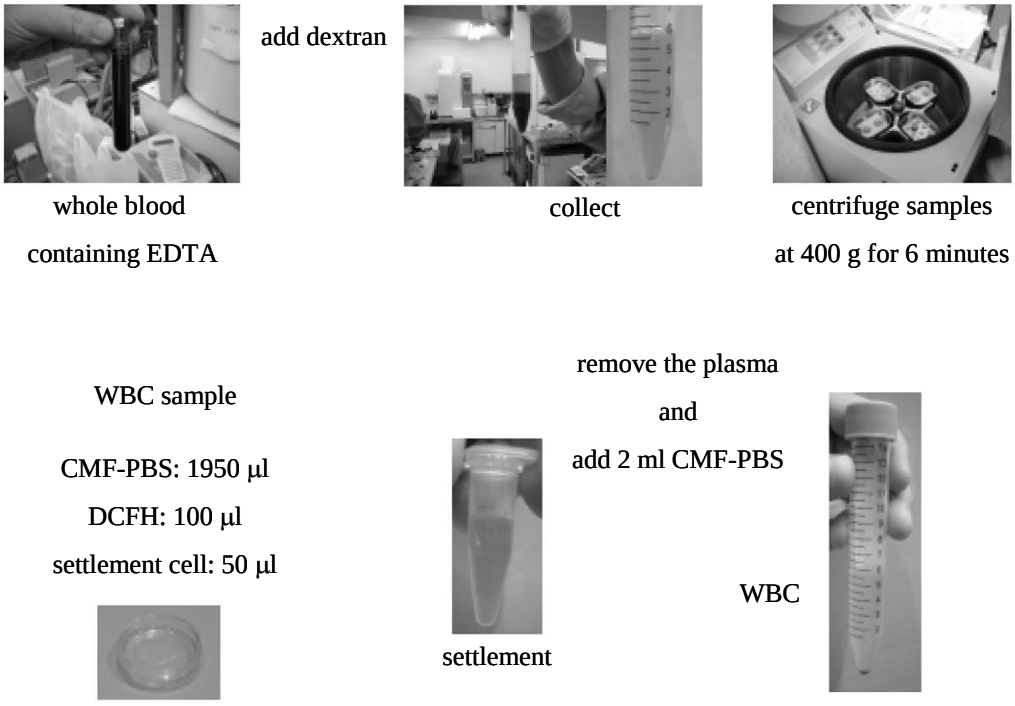


Figure 1. The procedure for preparing WBC sample

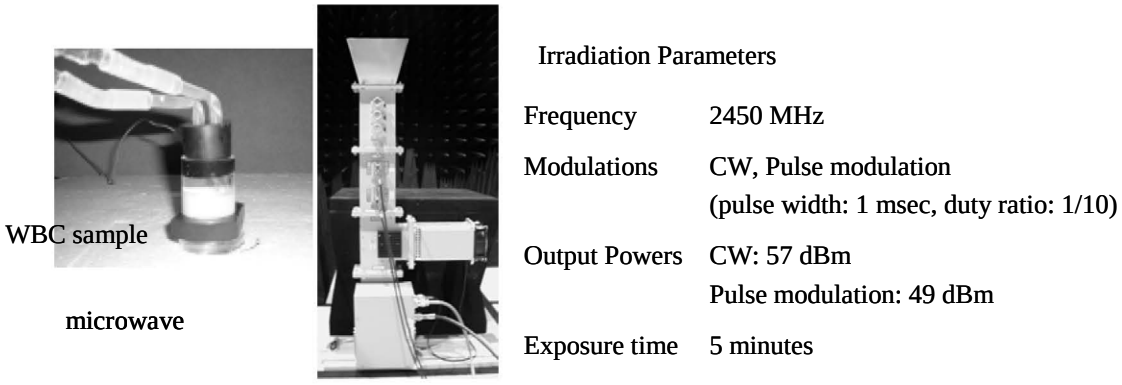


Figure 2. Open-type exposure equipment of 2.45 GHz

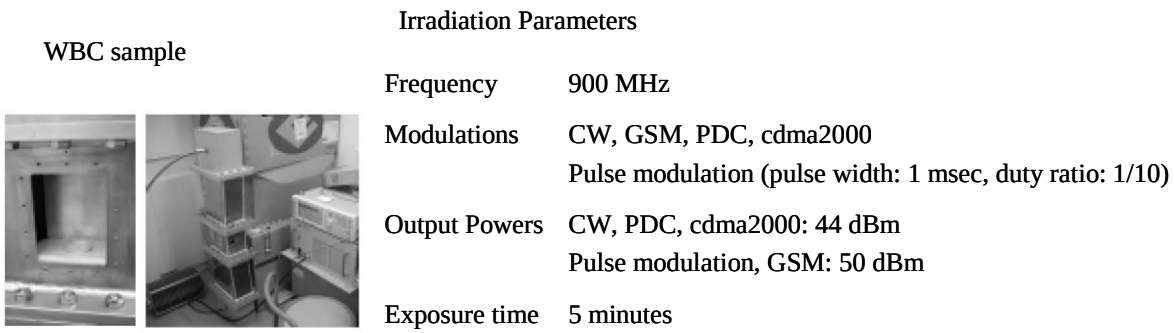


Figure 3. Ridged-waveguide exposure equipment of 900 MHz

Figure 2 and Figure 3 show the developed 2.45 GHz open-type exposure equipment and 900 MHz ridged-waveguide exposure equipment [5,6,7]. These exposure equipments can achieve high intensity and a uniform exposure on the WBC sample and they are available at the same time without special degradation of the impedance matching caused by the scattering waves from the WBC sample.

In the case of exposure to 2.45 GHz microwave, we carry out the irradiations for five minutes with continuous-wave (CW) or high power pulse modulated wave that provided the pulse width and duty ratio of 1 msec and 1/10, respectively. Figure 4 (a) shows the exposure plane on which the WBC sample is located. This plane is positioned at a distance of 205 mm from the centre of the horn antenna. Figure 4 (b) shows the electric field distribution of CW measured in this area. In addition, Figure 4 (c) shows the electric field distribution of CW obtained in this area by using numerical analysis. The FDTD based commercial software, SEMCAD [8] is used for the estimation. From these Figures, the computed result agrees well with measured ones. Furthermore, the thermostatic device shown in Figure 5 is adopted to maintain the temperature of the WBC sample at less than 39 degrees Celsius. The SAR of the WBC sample exposed on the petri dish is obtained by measurement and calculation. The increase in temperature during the exposure is used for estimation of SAR. FDTD analysis is used for SAR calculation as well. When we measure the SAR, the PBS does not touch the thermostatic device. Figure 6 shows the FDTD model. Figure 7 and Table 1 show these results as well.

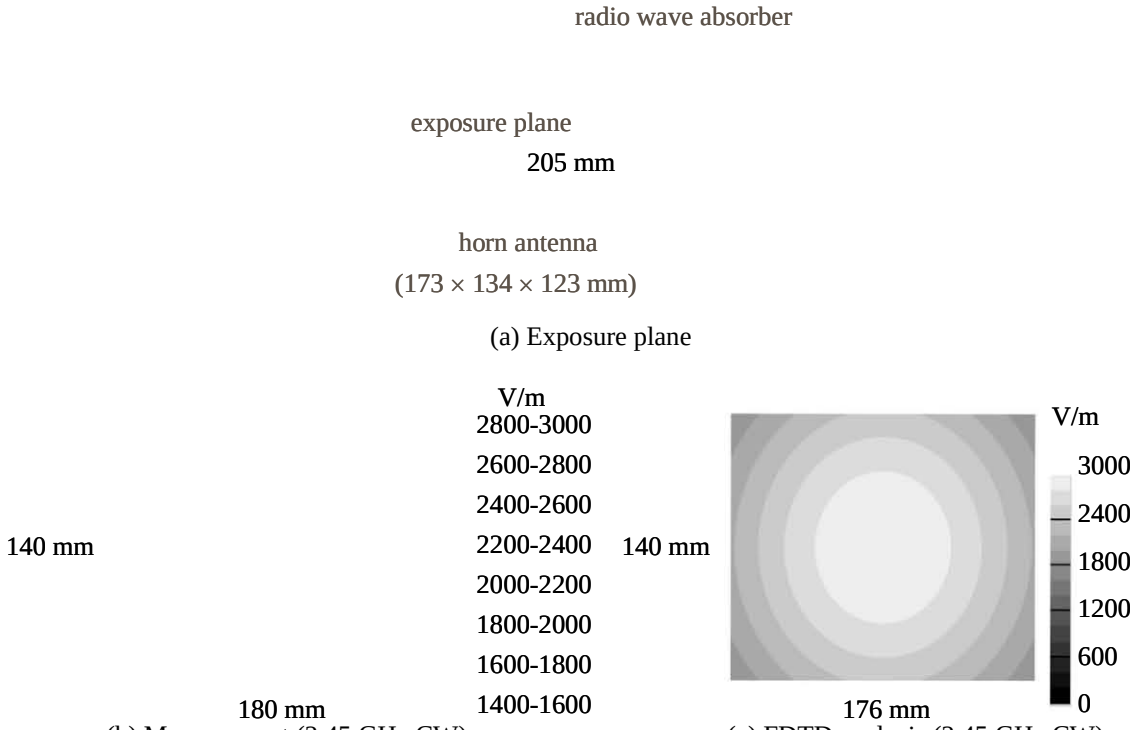


Figure 4. Electric field distributions on exposure plane

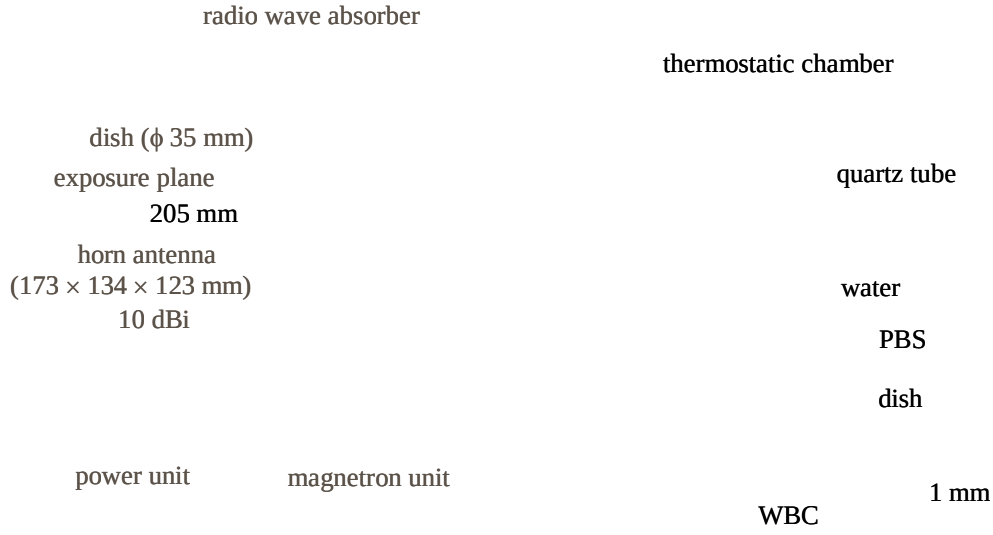


Figure 5. Exposure equipment of 2.45 GHz

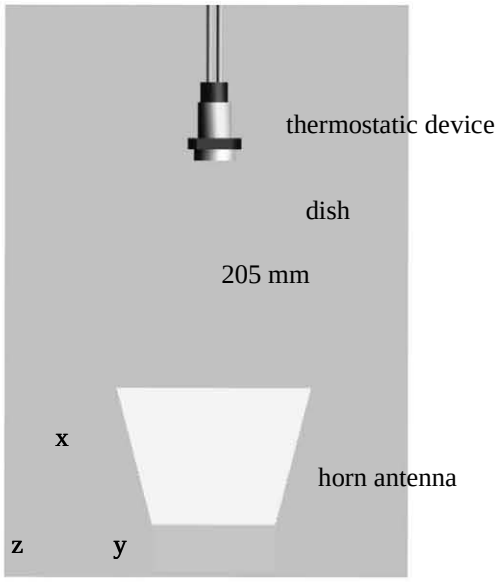


Figure 6. FDTD model (2.45 GHz)

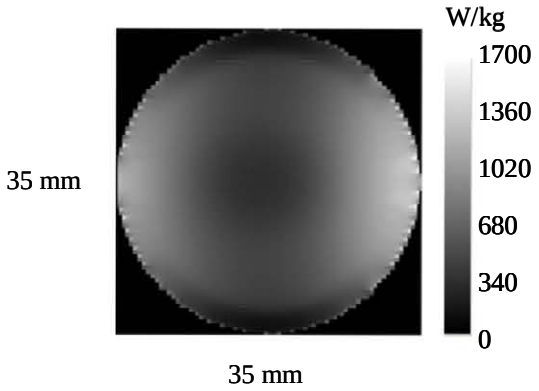


Figure 7. SAR distribution (2.45 GHz)

	measurement	FDTD analysis
Ave. SAR [W/kg]	725	632

Table 1. Measurement and analysis results of SAR (2.45 GHz)

In the case of exposure to 900 MHz microwave, the duration of exposure is 5 minutes. Moreover, several signals are used: CW, GSM, PDC (half rate), cdma2000 and pulse waves. During exposure, the temperature of the cells never exceeded 39 degrees Celsius. Table 2 shows both measured and calculated electric field strengths at the point that the WBC sample is located. In addition, the SAR of the WBC sample exposed on the petri dish is obtained by both measurement and calculation. In order to estimate the SAR of the WBC sample, the waveguide's output powers are measured. Then, the output power with or without the WBC sample in the waveguide are compared to estimate the SAR. Figure 8 shows the FDTD model. Figure 9 and Table 3 show these results.

	measurements					FDTD analysis
Modulations	CW	Pulse	GSM	PDC	cdma2000	CW
E-field strengths [V/m]	1140	615	960	1140	1160	1730

Table 2. E-field strengths central axis of the exposure plane (900 MHz)

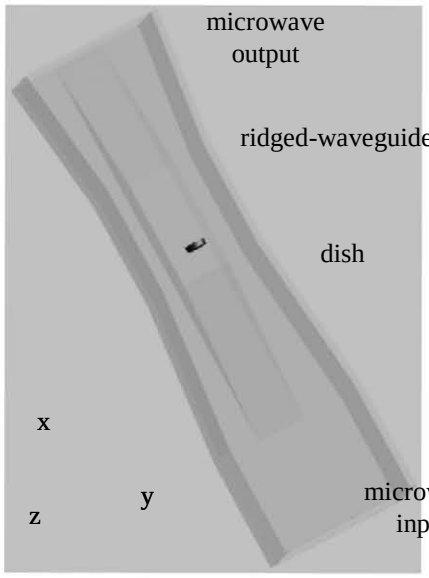


Figure 8. FDTD model (900 MHz)

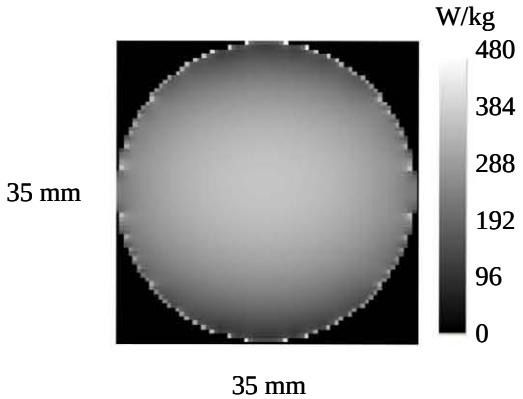


Figure 9. SAR distribution (900 MHz)

	measurement	FDTD analysis
Ave. SAR [W/kg]	150	276

Table 3. Measurements and analysis results of SAR (900 MHz)

The fluorescence probe method is adopted to estimate free radical production. First, DCFH which is used for fluorescence probe of hydroxyl radical production is added to the WBC sample. Secondly, the WBC sample is exposed to RF microwave for 5 minutes. Finally, fluorescence intensity is measured.

Results

Figure 10 and Figure 11 show the fluorescence intensities of WBCs after exposure to 2.45 GHz and 900 MHz microwaves respectively. The control (sham exposure) is defined as the WBC sample that was not exposed to microwaves and increased in temperature by thermostatic device. In the case of 2.45 GHz exposures, there are no obvious differences between the control and the WBC exposed by CW or pulse modulated microwave. In addition, in the case of 900MHz exposures, no significant differences in radical production are detected after any modulated microwave exposures. At both frequencies, no radical excitation is observed in the WBC after irradiation by microwaves, provided that the temperatures of target samples did not exceed 39 degrees Celsius.

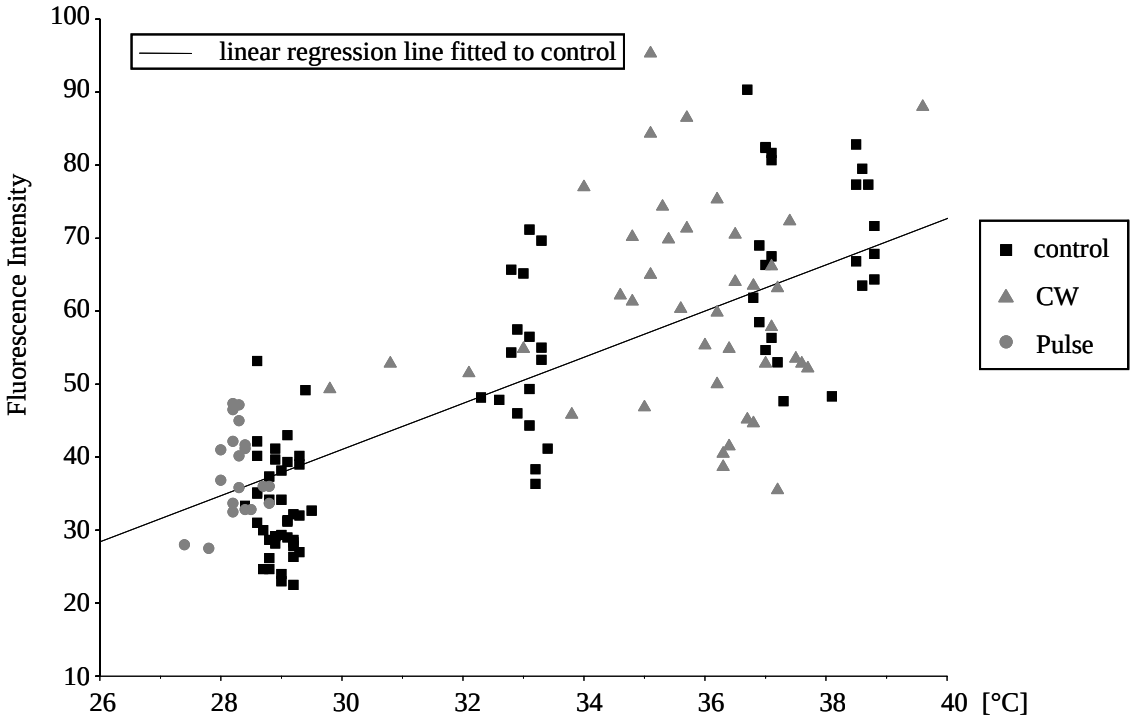


Figure 10. Fluorescence intensities of WBCs after exposure to 2.45 GHz microwave

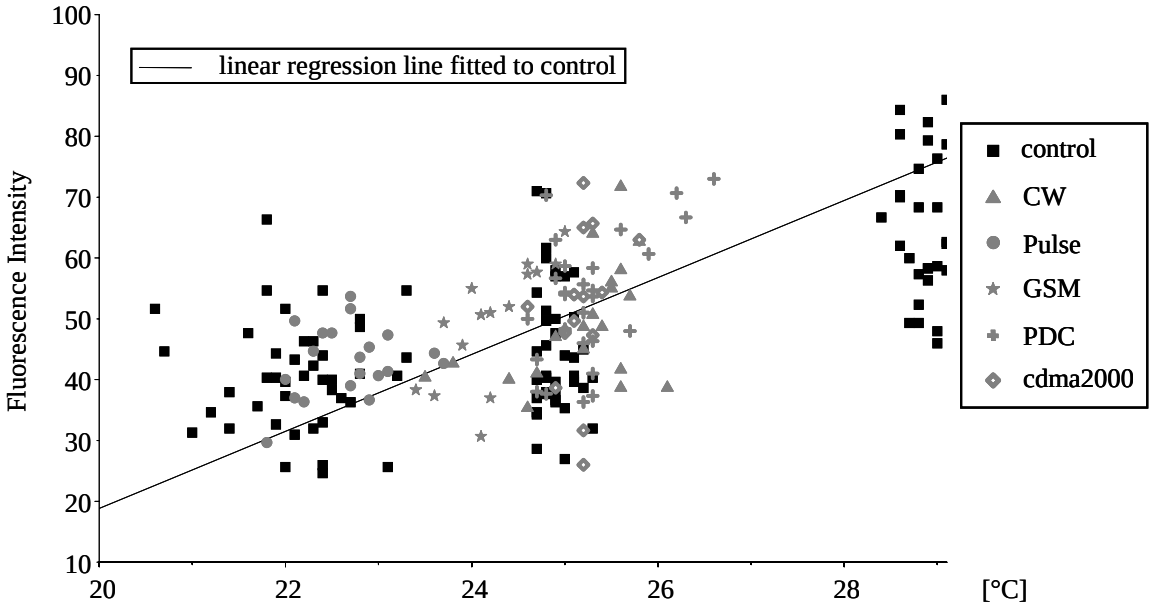


Figure 11. Fluorescence intensities of WBCs after exposure to 900 MHz microwave

Summary
Experiments for the biological free radical that treats human WBCs were performed. In the experiments, both modulated and non-modulated 900 MHz and 2.45 GHz microwaves were irradiated. Furthermore, the electric field strengths on the exposure plane and SARs of the WBCs were estimated by using measurement and FDTD simulation. The differences due to biological uncertainty in experimental results obtained under the same conditions (cell temperature, exposure condition) could not be negligible, and therefore, our experiments were carried out by using many WBC samples.
From our experiments, there was no difference in fluorescence intensities estimated by the fluorescence images of between the control (sham exposure) and the exposed samples. In addition, the intensities of the samples after exposure to modulated microwaves agreed with those after exposure to non-modulated microwaves. The fluorescence intensities which are proportional to radical production in WBCs depended on the temperatures of the samples. As a result, any free radical production due to non-thermal effects of 2.45 GHz or 900 MHz microwave exposure was not detected.
More precise SARs calculations and a statistical analysis of the fluorescence intensities data obtained by many of our experiments will be conducted.

Acknowledgements
This work is supported by Grant-in-Aid from the Ministry of Internal Affairs and Communications (MIC) of Japan.

References
[1] R.K. Adair, “Biophysical limits on A thermal effects of RF and microwave radiation”, Bioelectromagnetics Vol24, No.1, pp.39-48, (2003)
[2] W.Ross Adey, “Potential Therapeutic Applications of Nonthermal Electromagnetic Fields: Ensemble Organization of Cells in Tissue as a Factor in Biological Field Sensing”, Bioelectromagnetic Medicine, New York:Mercel Dekker Inc. (2004)
[3] M.H. Repacholi and B. Greenebaum, “Interaction of Static and Extremely Low Frequency Electric and Mgnetic Fields With Living Systems: Health Effects and Research Needs”, Bioelectromagnetics, 20, pp.133-160 (1999)
[4] H. Kamada and H. Ohya, “Overview of Laboratory Technology on Bioradicals”, Journal of IEICE, vol.81, No.2, pp.146-153
[5] T. Hikage, T. Manabe, and T. Nojima, “Microwave Exposure Effects on the Biological Free Radical Production –2.45 GHz exposure system desigh and estimation with ESR –”, BIOLOGICAL EFFECTS of EMFs 3rd International Workshop, pp. 82-86, (2004).
[6] T. Manabe, T. Hikage and T. Nojima, “Experimental investigations on the Biological Free Radical Production – 2.45 GHz & 900 MHz exposure systems design and estimation with ESR –”, XXVIIIth URSI General Assembly at New Delhi, India on October 23-29, (2005)
[7] T. Hikage, T. Manabe, M Endo and T. Nojima, “EXPERIMENTAL INVESTIGATIONS ON THE BIOLOGICAL FREE RADICAL PRODUCTION IN HUMAN FIBROBLASTS DUE TO MICROWAVE EXPOSURE”, The Bioelectromagnetics Society the 28th Annual Meeting at Cancun, Mexico on June 11-15, P-B-78, (2006)
[8] SEMCAD: Schmid & Partner Engineering AG, Zurich, Switzerland

Mobile radio base station-emitted radiation does not induce phosphorylation of hsp27 or cellular stress response.

M. Sekijima[1], H. Hirose[1], N. Sakuma[1], N. Kaji[1], K. Nakayama[1], T. Nojima[2], J. Miyakoshi[3]

[1]Research division for advanced technology, Kashima Laboratory, Mitsubishi Chemical Safety Institute Ltd., 14 Sunayama, Kamisu 314-0255, Japan. [2]Division of Electronics and Information Engineering, Graduate School of Hokkaido University, N-13, W-8, Kita-ku, Sapporo 060-8628, Japan. [3]Department of Radiological Technology School of Health Sciences, Faculty of Medicine, Hirosaki University, 66-1 Hon-cho, Hirosaki 036-8564, Japan.

ABSTRACT

The objective was to assess any signs of stress or apoptosis induced by radiofrequency (RF) fields, which corresponds to the limit of the average whole body SAR for general public exposure defined as a basic restriction in the ICNIRP guidelines. We investigated if continuous wave (CW) and Wide band Code Division Multiple Access (W-CDMA) RF fields at 2.1425 GHz, which corresponded to the middle frequency allocated to the downlink band of the IMT-2000 from mobile radio base stations, induce activation of hsp27 and p53. All levels and types of the investigated RF fields did not result in a statistically significant increase or decrease in hsp27[pS82] protein or p53[pS15] protein of each sample. No noticeable differences were observed between any of the RF field exposure groups and the sham exposed controls in the gene expression profile, including hsp or p53 related genes, in either the RF field experiments. These results confirm that RF exposure to W-CDMA and CW at 2.1425 GHz cannot be associated with apoptosis or cancer via induction of the p53 pathway or hsp response at the limit of the average whole-body SAR level (80 mW/kg) as defined by the ICNIRP guidelines.

INTRODUCTION

The rapid introduction of mobile telecommunication services over the last decade has drastically increased the amount of radiofrequency (RF) field irradiation frequencies and energies in our living environment. In order to continue stable growth and expansion of RF utilizations, it is necessary to investigate the possibility of any biological health effects of RF fields and to obtain reliable confirmation data with respect to safety. It is important to examine the possible biological effects and to obtain reliable data for 2-GHz band RF irradiation to facilitate the smooth deployment of the International Mobile Telecommunication 2000 (IMT-2000) cellular system. We conducted a study focusing on the effects of a practical modulated signal for Wideband Code Division Multiple Access (W-CDMA) as well as a continuous wave (CW) at 2.1425 GHz, which corresponds to the middle frequency allocated to the downlink band of IMT-2000 from mobile radio base stations.

French et al [2001] proposed that repeated exposure to mobile phone radiation acts as a repetitive stress leading to continuous expression of hsps in exposed cells and tissues, which in turn affects their normal regulation, and cancer results. Hsp27 phosphorylation in the human endothelial cell line EA.hy926 showed a transient increase by 1 h of non-thermal exposure to 900 MHz GSM mobile phone radiations [Leszczynski et al., 2002]. They proposed a hypothetical mechanism whereby RF exposure could be associated with cancer. We examined the induction of hsp27 phosphorylation and other cellular stress response that activate the p53 or the p53 signaling pathway using cultures of the human tumor A172 cells and untransformed IMR-90 cells. The results suggest that RF radiation at a SAR of the mobile radio base station level does not affect the stress response pathways following hsp27 phosphorylation.

METHODS

Exposure System

A detailed description of the exposure system has been published by Iyama et al. [2004]. Briefly, two identical RF field exposure incubators, one for RF field exposure and the other for sham exposure, were established in separate anechoic chambers, and a mechanical switch in a dummy box allows the selection of RF field exposure or sham exposure (Fig.1). This system allowed simultaneous exposure of 49 (7 x 7 array), 35 mm culture dishes to a 2.1425 GHz RF electromagnetic field, which corresponds to the center frequency of the IMT-2000 down link band, with a uniform SAR distribution in the medium of all 49 culture dishes. The main unit for the cell exposure provides identical air to the two culture units through sealed ducts at the appropriate temperature (37.0°C), CO_2 (5.0 %), and humidity (>90 %). The mean SAR of the culture fluid at the bottom of the inner 25 culture dishes (5 x 5 array) used in the in vitro experiments was 139 mW/kg for an antenna input power of 1 W, and the standard deviation of the SAR distribution was 47%. The W-CDMA cellular system is one of the component systems of the IMT-2000 cellular system, and its frequency spectrum is shown in Figure 2. W-CDMA adopts Direct Sequence CDMA (DS-CDMA) and Frequency Division Duplex (FDD) as a multiple access and duplex scheme, respectively. The chip rate of the spread code of this system is 3.84 Mcps. A beam-formed RF exposure incubator employing a horn antenna, a dielectric lens, and a culture case in an anechoic chamber was developed for large-scale *in vitro* studies.

Cells

Human glioblastoma A172 cells and human IMR-90 fibroblasts from fetal lungs were obtained from the American Type Culture Collection (ATCC, Rockville, MD). A172 cells were cultured in Dulbecco's Modified Eagle Medium (Invitrogen, Tokyo, Japan) supplemented with 10% heat-inactivated fetal calf serum (FCS; Invitrogen), 100 U/ml penicillin and 100 μg/ml streptomycin, and IMR-90 fibroblasts were grown in Eagle's minimal essential medium with Earle's balanced salts (Invitrogen) supplemented with 0.1 mM non-essential amino acids, 1.0 mM sodium pyruvate, 10% heat-inactivated FCS, 100 U/ml penicillin, and 100 μg/ml streptomycin. The both cells have been previously used in RF field research [Sakuma et al., 2006].

Experimental Design

The experimental design has been described by Hirose et al. [2006a,b]. A172 cells were exposed to W-CDMA radiation at SARs of 80, 250, and 800 mW/kg, and to CW radiation at 80 mW/kg for 24 or 48 h, which equates to one or two doubling times of the cell. IMR-90 cells were exposed to W-CDMA at 80 and 800 mW/kg, and CW at 80 mW/kg for 28 h, which is one doubling time of the cell. The cells were also exposed to W-CDMA radiation at SARs of 80 and 800 mW/kg for 2 h. The RF field exposure was processed in a blind manner. Exposure to W-CDMA signals in the study was 80 mW/kg, which corresponds to the limit of the average whole-body SAR for general public exposure defined as a basic restriction by the ICNIRP guidelines [1998]. The air temperature was monitored for all cultures during the course of the sham and RF field exposure, resulting in 37.0±0.3°C, 37.0±0.1°C, and 37.0±0.1°C at SARs of 800, 250 and 80 mW/kg for W-CDMA radiation, respectively.

Detection of Hsp27 and p53 Phosphorylation

To determine changes in hsp27[pS82] or p53[pS15], HSP27[pS82] and Total HSP27 or p53[pS15] and Total p53 Antibody Bead Kits (BioSource, Camarillo, CA) were used according to the manufacturer's instruction. The specific proteins were detected using the bead-based multiplex assay [Carson and Vignali, 1999], which is similar to a capture sandwich immunoassay.

Microarray hybridization

Human genome HG-U133 Plus2.0 (Affymetrix, Santa Clara, CA) was used for the analysis of heat shock and p53 related gene expressions in cells exposed to RF fields. Data were analyzed using Affymetrix®

Microarray Suite 5.0 software.

RT-PCR analysis

The pairs of primers and the TaqMan probes [tumor protein 53 (TP53), TP53 binding protein 2 (TP53BP2), apoptotic protease activating factor (APAF1), and caspase 9 (CASP9)] for the target mRNAs were purchased from Applied Biosystems (Foster City, CA). The TaqMan OneStep RT-PCR Master Mix Reagents Kit (Applied Biosystems) was used for the RT-PCR reaction. Amplification and detection were performed using the ABI PRISM 7700 Sequence Detector System (Applied Biosystems).

Indirect Immunofluorescence Analysis

For visualization, cells were incubated with anti-hsp27 (diluted at 10 μg/ml) or anti-hsp70 (diluted at 5 μg/ml) antibodies (Stressgen, BC, Canada) for 1 h, and then incubated with Alexa Fluor 488-labeled goat anti-mouse IgG antibody (Molecular Probes, Eugene, OR) diluted at 10 μg/ml for 30 min.

Detection of Apoptosis

Apoptosis was evaluated using the annexin V affinity assay [Koopman et al., 1994]. The procedure using the fluorescein-conjugated annexin V (annexin V-FITC; BD Biosciences, Franklin Lakes, NJ) was carried out according to the manufacturer's technical protocol. The cell samples were analyzed by flow cytometry (EPICS ALTRA, Beckman Coulter, Tokyo, Japan).

Statistical Analysis

The gene expression levels obtained with GeneChip expression analysis were analyzed by Welch's t-test using the data for the sham-exposed samples and the RF field-exposed samples in either the 2.1425 GHz W-CDMA at a SAR of 80, 250 or 800 mW/kg or CW at 80 mW/kg RF field experiments. The multiplicity problem was controlled by the Benjamini and Hochberg false discovery rate [Benjamini and Hochberg, 1995]. A p-value of less than 0.05 was considered statistically significant.

RESULTS

Expression of phosphorylated hsp27 at serine 82

As shown in Figures 3-1 and -2, the exposure to W-CDMA or CW radiations at a SAR of 80, 250 or 800 mW/kg for 2-48 h resulted in similar measurements of hsp27[pS82] compared to sham exposed controls. The exposure to all of the presented RF fields did not result in a statistically significant change in hsp27[pS82]. The exposure to W-CDMA at a SAR of 80 or 800 mW/kg for 2-48 h did not noticeably change the total hsp27 level in either cell. Moreover, there were no significant changes in total hsp27 expression levels in the cells exposed to W-CDMA signal at 250 mW/kg or CW signal at 80 mW/kg.

Heat shock gene expression

In the RF field exposure experiments, 18,041-24,119 and 18,971-23,180 genes were "present" or "marginal" in A172 and IMR-90 cells, respectively, of 54,675 gene probe sets. We evaluated the changes in gene expression by RF field exposure on their genes that were "present" or "marginal" in A172 or IMR-90 cells. No significant differences were observed between any of the RF field exposure groups and the sham-exposed controls in the gene expression profile, including hsp related genes in either experiments of exposure to W-CDMA or CW signal for 2-48 h.

Cellular localization of hsp27 and hsp70

There was no remarkable effect on the induction of translocation or expression of hsp27 or hsp70 after exposure to W-CDMA or CW signal at a SAR of 80, 250 or 800 mW/kg for 2-48 h. Immunofluorescence staining revealed that some of A172 cells in sham culture expressed a high level of hsp27 and some of IMR-90 cells in sham culture expressed a low level of hsp27. It was found that some of A172 and IMR-90 cells in sham cultures expressed a very low level of hsp70.

Expression of phosphorylated p53 at serine 15

The exposure to W-CDMA or CW radiations resulted in similar measurements of p53[pS15] compared to sham-exposed controls, and resulted in similar values of total p53 compared with sham-exposed controls. The exposure to all of the presented RF fields did not result in statistically significant changes in p53[pS15] (Fig. 4), or the total p53 in each sample. All of the measurements of p53[pS15] protein in the RF field exposure samples were close to the lower limit of the analytical sensitivity of the assay, and almost equal to those in sham-exposed and non-treated samples, or could not be detected with the used p53[pS15] Antibody Bead Kit.

p53-related Gene Expression

There were no noticeable changes of p53 related gene expression levels in A172 or IMR-90 cells exposed to W-CDMA radiation (SARs of 80, 250 or 800 mW/kg) or CW radiation (80 mW/kg). We analyzed the gene expression of TP53, TP53BP2, APAF1, and CASP9 to reconfirm the change of the p53-dependent apoptosis signal cascade on a molecular level by the exposure to RF signals, using a real-time RT-PCR analysis. Relative gene expression was determined based on the threshold cycles of the RF field or sham exposed samples. No noticeable effect on TP53, TP53BP2, APAF1, and CASP9 gene expression was observed after exposure to W-CDMA or CW radiation, as expression ratios were below 2-fold and over 0.5-fold in two independent experiments performed with triplicate RNA samples.

Induction of Apoptosis

The exposure to W-CDMA or CW radiations resulted in a similar percentage of apoptotic cells compared to sham-exposed controls (1.1-3.7 % compared to 1.2-3.0 % in the case of A172 cells, and 2.4 or 4.1 % to 2.4 or 4.7 % in the case of IMR-90 cells). No statistically significant differences were observed between any of the RF field exposure groups and the sham-exposed controls in percentage of apoptotic cells, in either the 2.1425 GHz W-CDMA or CW radiation exposure experiments.

CONCLUSION

Hsp27 and p53 phosphorylation in A172 cells and IMR-90 fibroblasts are not induced by exposure to W-CDMA or CW RF radiation. Furthermore, changes in gene expression levels of hsp family and p53-related genes, and the frequency of apoptotic cell death were not induced by any of the RF exposure.

The results confirm that RF exposure to W-CDMA and CW at 2.1425 GHz cannot be associated with apoptosis or cancer via induction of the p53 pathway or hsp response at the limit of the average whole-body SAR level (80 mW/kg) as defined by the ICNIRP guidelines.

ACKNOWLEDGEMENT

This work was supported by NTT DoCoMo Inc., Japan.

REFERENCES

Benjamini, Hochberg, 1995. Controlling the false discovery rate: a practical and powerful approach to multiple testing. J R Statist Soc B 57, 289-300.

Carson R, Vignali D. 1999. Simultaneous question of fifteen cytokines using a multiplexed flow cytometric assay. J Immunol Meth 227, 41-52.

French PW, Penny R, Laurence JA, McKenzie DR. 2001. Mobile phones, heat shock proteins and cancer. Differentiation 67: 93-97.

Hirose H., Sakuma N., Kaji N., Suhara T., Sekijima M., Nojima T., Miyakoshi J. 2006a. Phosphorylation and gene expression of p53 are not affected in human cells exposed to 2.1425 GHz band CW or W-CDMA modulated radiation allocated to mobile radio base stations. Bioelectromagnetics 27: in press.

Hirose H., Sakuma N., Kaji N., Nakayama K., Inoue K., Sekijima M., Nojima T., Miyakoshi J. 2006b. Mobile Phone Base Station-Emitted Radiation Does Not Induce Phosphorylation of Hsp27. Bioelectromagnetics: accepted.

ICNIRP. 1998. Guidelines for limiting exposure to time varying electric, magnetic and electromagnetic fields (up to 300 GHz). Health Phys 74: 494-522.

Iyama T, Ebara H, Tarusawa Y, Uebayashi S, Sekijima M, Nojima T, Miyakoshi J. 2004. Large-scale i*n vitro e*xperiment system for 2 GHz-exposure. Bioelectromagnetics 25: 599-606.

Koopman G, Reutelingsperger CP, Kuijten GA, Keehnen RM, Pals ST, van Oers MH. 1994. Annexin V for flow cytometric detection of phosphatidylserine expression on B cells undergoing apoptosis. Blood 84: 1415-1420.

Leszczynski D, Joenvaara S, Reivinen J, Kuokka R. 2002. Non-thermal activation of the hsp27/p38MAPK stress pathway by mobile phone radiation in human endothelial cells: Molecular mechanism for cancer- and blood-brain barrier-related effects. Differentiation 70: 120-129.

Sakuma N, Komatsubara Y, Takeda H, Hirose H, Sekijima M, Nojima T, Miyakoshi J. 2006. DNA strand breaks are not induced in human cells exposed to 2.1425 GHz band CW and W-CDMA modulated radiofrequency fields allocated to mobile radio base stations. Bioelectromagnetics 27: 51-57.

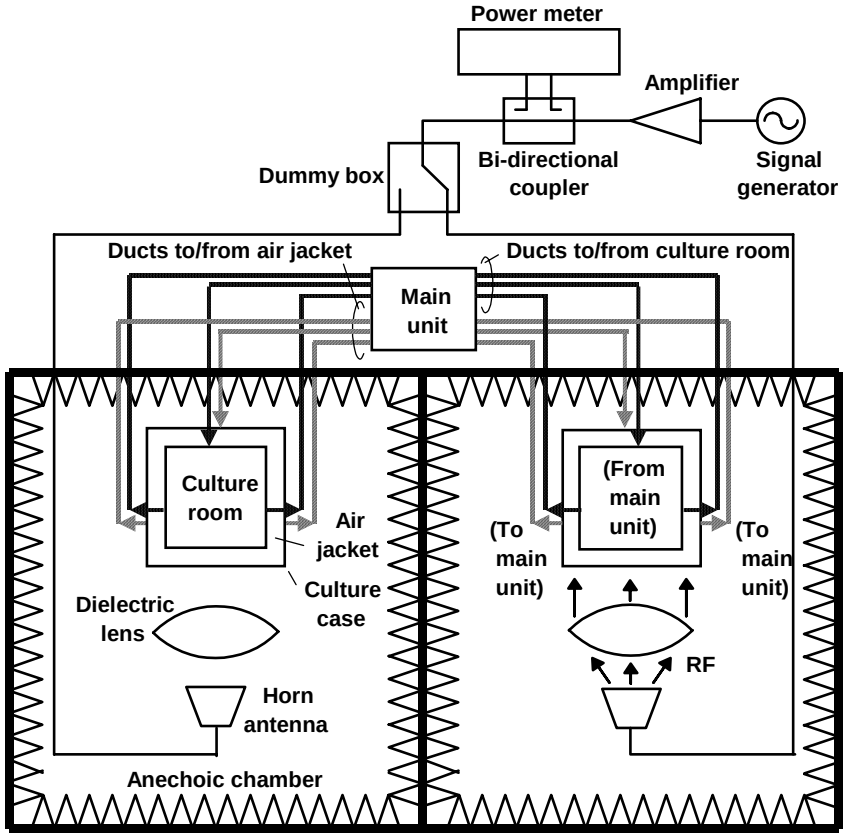


Figure 1. RF exposure system for *in vitro* experiments [Iyama et al., 2004]. Arrows from the horn antenna indicate the direction in which the RF travels. Schematic diagram of the electrical design and the air circulation in the RF exposure system. In this figure, the system on the right is for RF exposure and that on the left is for sham exposure.

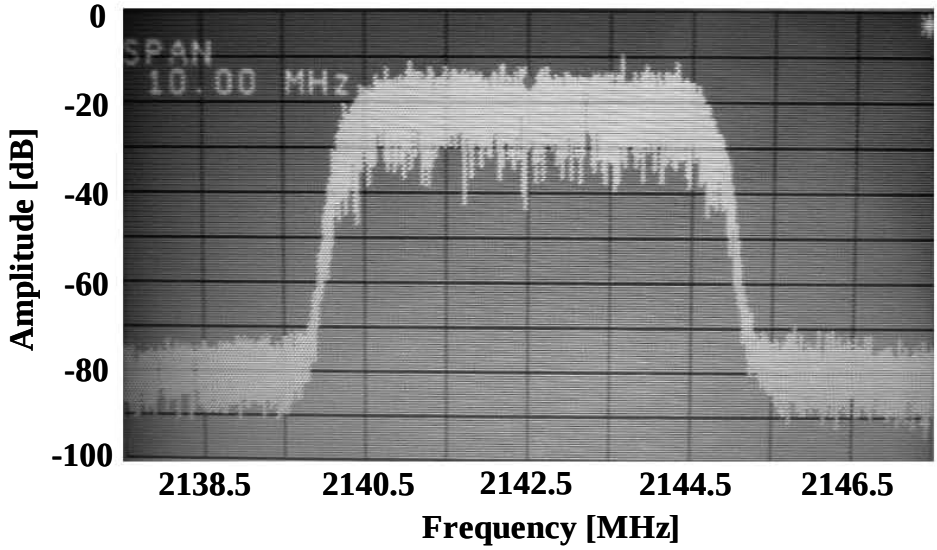


Figure 2. W-CDMA frequency spectrum.

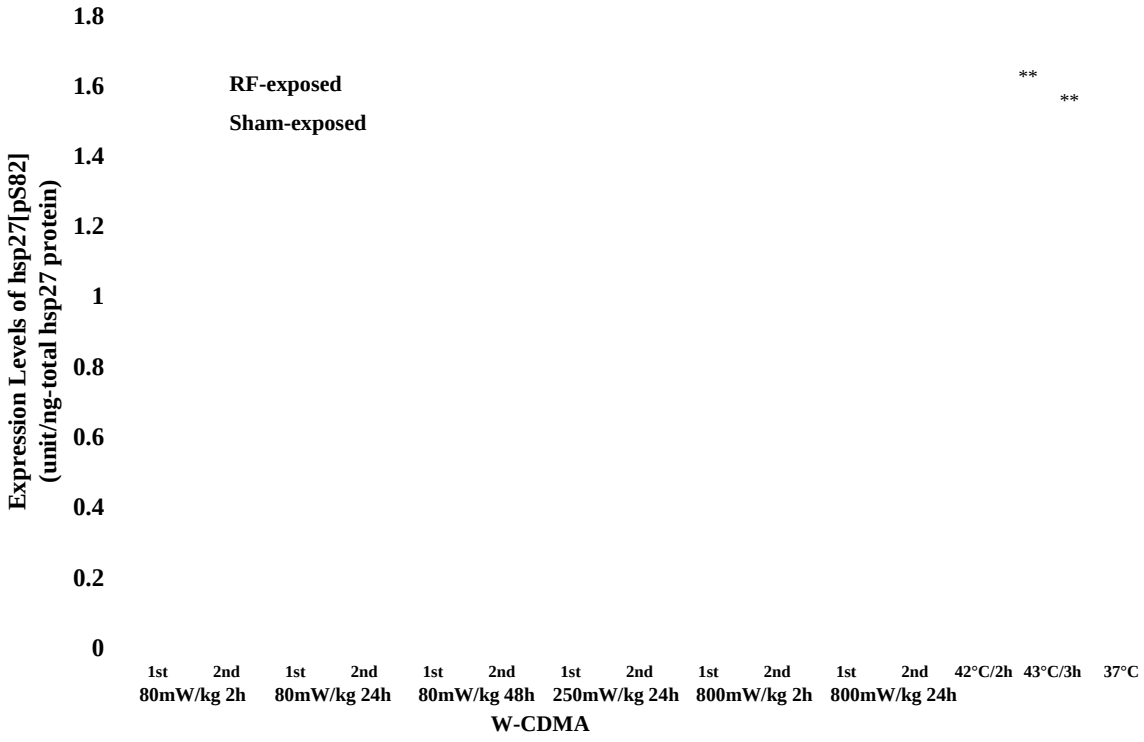


Figure 3-1. Expression levels of phosphorylated hsp27 in A172 cells exposed to W-CDMA RF field. Experiments under the same RF field exposure conditions were repeat twice, and 3 different cultures were used in each experiment. No statistically significant differences were observed between any of the RF field exposure groups and the sham-exposed controls in either the 2.1425 GHz W-CDMA RF field experiments. Other cultures were treated with heat at 42 or 43°C in a temperature-controlled water bath and at 37°C in a conventional incubator. **; $p<0.01$

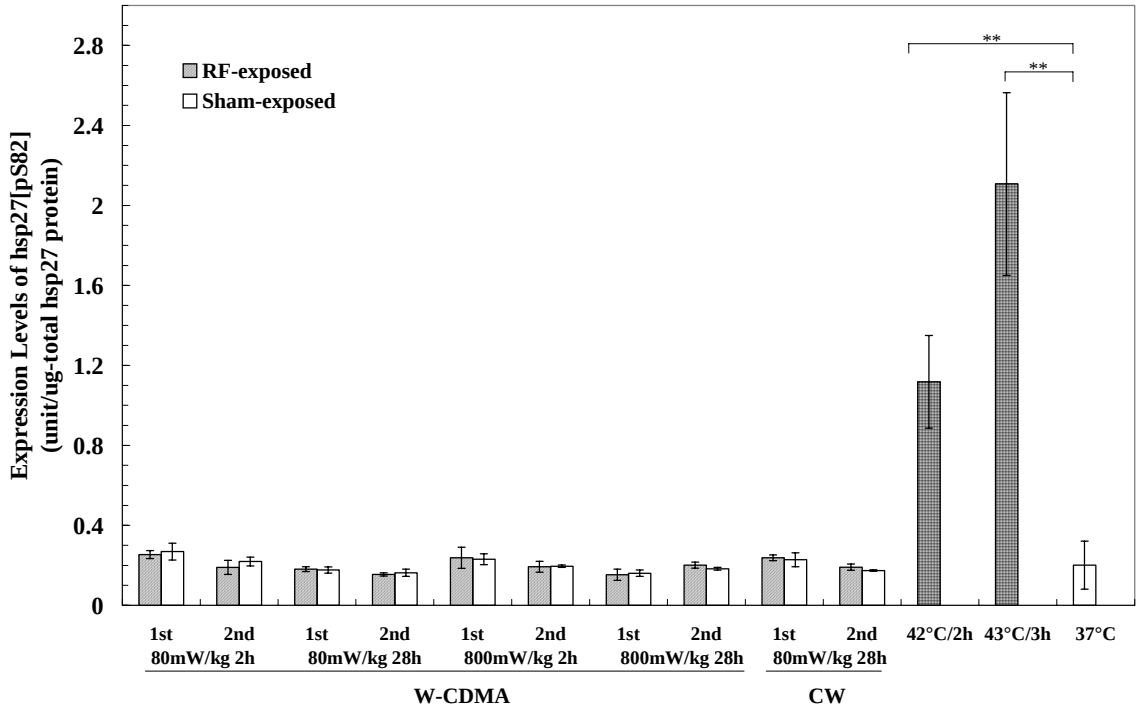


Figure 3-2. Expression levels of phosphorylated hsp27 in IMR-90 cells exposed to W-CDMA and CW RF fields. Experiments under the same RF field exposure conditions were repeat twice, and 3 different cultures were used in each experiment. No statistically significant differences were observed between any of the RF field exposure groups and the sham-exposed controls in either the 2.1425 GHz W-CDMA or CW RF field experiments. Other cultures were treated with heat at 42 or 43°C in a temperature-controlled water bath and at 37°C in a conventional incubator. **; $p<0.01$

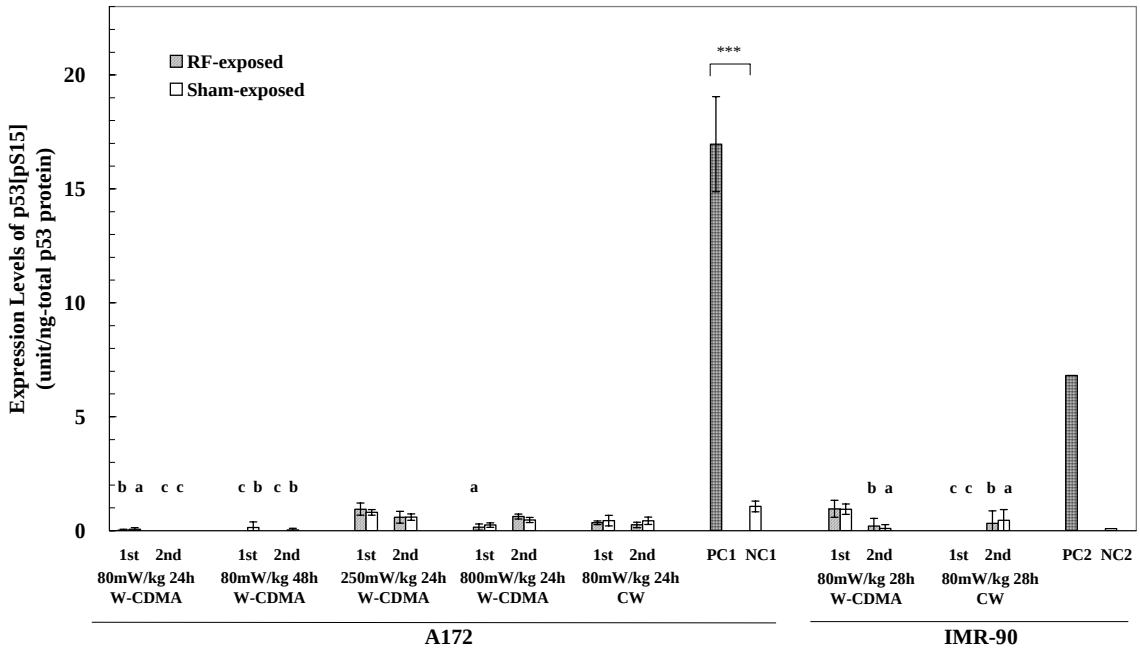


Figure 4. Expression levels of phosphorylated p53 at serine 15. Experiments under the same RF field exposure conditions were repeated twice, and 3 different cultures were used in each experiment. Undetectable samples (presented to zero) were one (a), two (b) or three (c) in 3 different culture samples. Treatment of A172 cells with 1.7 μmol/l (1.0 μg/ml) Dox (positive control; PC1) resulted in a statistically significant increase ($^{***}p<0.001$, n=5) compared to RF field- and sham-exposed samples, and non-treated samples (negative control; NC1). Treatment of IMR-90 fibroblasts to heat shock at 42°C (positive control; PC2) resulted in a remarkable increase (n=2) compared to RF field- and sham-exposed samples, and the non-treated samples (negative control; NC2).

REAL-TIME MEASUREMENT OF BRAIN MICROCIRCULATION DURING RF-EMF EXPOSURE USING AN "8"-SHAPED LOOP ANTENNA.

HIROTA S.[1], MASUDA H. [1], USHIYAMA A. [1], TAKAHASHI M. [1], TANAKA S. [2], KAWAI H. [2], WAKE K. [2], WATANABE S. [2], TAKI M. [3] and OHKUBO C. [4]

[1]Dept. of Environmental Health, National Institute of Public Health, 2-3-6 Minimi, Wako-shi, Saitama 351-0197, JAPAN. [2] Electromagnetic compatibility group, applied electromagnetic research center, National Institute of Information and Communications Technology, 4-2-1 nukui-kitamachi, koganei, Tokyo 184-8795, Japan. [3]Dept. of Electrical and electronic Engineering, Tokyo Metropolitan University, 1-1 minami-osawa, hachioji, Tokyo 192-0397, Japan. [4]RAD, World Health Organization, Geneva CH1211, Switzerland.

Abstract

Few studies have directly observed brain microcirculation during exposure to radio frequency electromagnetic fields (RF-EMF). The aim of present study was to investigate whether RF-EMF exposure induces acute effects on brain microcirculation being transiently observed only during RF-EMF radiation period. Male Sprague-Dawley rats (8 weeks old) were subjected to cranial window implantation prior to the exposure experiments and fluorescent intravital-microscopic observation under anesthesia. To simultaneously perform a microcirculatory observation and RF-EMF exposure, we developed and used an ''8''-shaped loop antenna. Rat's head was locally exposed to 1,457MHz electromagnetic near-field TDMA signal for PDC systems by the ''8''-shaped loop antenna. RF-EMF exposure intensity was maintained at 2.0 W/kg of the averaged SAR in parietal targeted area. During experimental period including RF-EMF exposure, four microcirculatory parameters (BBB-function, plasma velocities, leukocyte behaviours, and arterial vasomotion) were measured. No changes in any of the four microcirculatory parameters were elicited by RF-EMF exposure. The results revealed that there were no RF-EMF exposure effects on brain microcirculatory parameters, at least on BBB-function, plasma velocities, leukocyte behaviours, or arteriolar vasomotion under the present exposure conditions.

Introduction

Few studies have directly observed brain microcirculation during exposure to radio frequency electromagnetic fields (RF-EMF). Our previous study showed no effects of RF-EMF exposure on blood-brain barrier (BBB), plasma velocity or vessel diameter, as microcirculatory parameters in rat brain using a cranial window method [1]. However, the changes in these parameters were measured just after RF-EMF exposure, but not during exposure. To simultaneously perform measurements of rat brain microcirculation and RF-EMF exposure to a local cerebral region just under the cranial window, we developed a new type of antenna, ''8''-shaped loop antenna [2]. The aim of present study was to investigate whether RF-EMF exposure induces acute effects on brain microcirculation being transiently observed only during RF-EMF radiation period.

Male Sprague-Dawley rats (8 weeks old) were used. The rats were divided into two groups: RF group was exposed to RF-EMF and Sham group was not exposed to any RF-EMF. All rats were subjected to cranial window implantation and intravital-microscopic observation under pentobarbital anesthesia with a cocktail of ketamine and xylazine. The pial microcirculation within cranial windows was observed using a fluorescent microscope equipped with an EBCCD camera. In order to measure four microcirculatory parameters, BBB function, plasma velocities, leukocyte behaviours, and arteriole vasomotion, we used rhodamine 6G for leukocyte behaviours and FITC-Dx (70k or 2000k) for the other three parameters.

Rat heads were locally exposed to 1,457MHz electromagnetic near-field TDMA (time division multiple access) signal for PDC (Personal Digital Cellular, Japanese cellular telephone standard) systems by the ''8''-shaped loop antenna placed 4 mm upward to the cranial window. RF-EMF exposure was maintained at 2.0 W/kg of the averaged SAR in parietal targeted area.

Arteriolar vasomotion was observed during 12 min experimental period including 3 min RF-EMF exposure. The other three microcirculatory parameters, BBB-function, plasma velocity, and leukocyte behaviour in pial venules were measured every 10 min during 80 min experimental period including 50 min RF-EMF exposure. The results were compared between RF and Sham group. The statistical analysis was performed by Student's t-test or ANOVA.

Using an intravital fluorescence microscopy and the ''8''-shaped loop antenna enable us to observe rat pial microcirculation directly, and expose RF-EMF to rat, simultaneously (Fig. 1). Plasma image flowing in microvessels of the pia mater was visualized by FITC-Dx injected into vein.

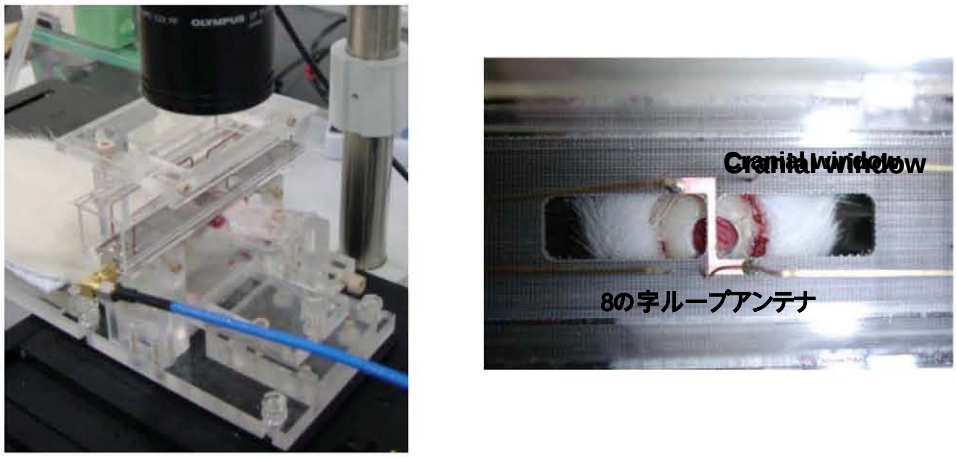


Fig. 1. Real-time measurement system

Blood-brain barrier permeability was evaluated by extravasation of FITC-Dx (70k) molecules injected into a rat venule. Although fluorescence intensity of pia mater area decreased through an experimental period, there were no significant difference in the fluorescence intensity between sham and RF group.

Velocities of plasma flowing in pial venules were measured by a dual-slit method and indicated as a relative (%) velocity of initial value. No significant difference in the percent velocities between two groups were showed until the end of experiment.

Leukocyte behaviours were evaluated by the numbers of rolling and sticking leukocytes stained with rhodamine 6G at 0, 10, 20, 40 min after beginning of the exposure. No significant difference in these numbers was found between two groups.

The arteriole vasomotions were monitored pre-, during, and post- RF exposure (Fig. 2). As an index for dynamic changes in the vasomotion, we calculated the mean value of arteriolar diameter for each experimental period and showed them as a relative (%) diameter of pre-exposure. As a result, no significant difference in the arteriolar diameter was found between two groups.

Summary

Our developed new type of loop antenna, the ''8''-shamped loop antenna succeeded to concentrate SAR distribution into the target area just under the cranial window. This was convenience to evaluate dynamic changes in microcirculatory parameters in the target area during RF-EMF exposure. In present experiment, we focused on four microcirculatory parameters, BBB-function, plasma velocities, leukocyte behaviours, and arterial vasomotion. However, no significant differences of these parameters were recognized between sham and exposed group even in during exposure period. The results revealed that there were no RF-EMF exposure effects on brain microcirculatory parameters, at least on BBB-function, plasma velocities, leukocyte behaviours, or arterial vasomotion under the present exposure conditions.

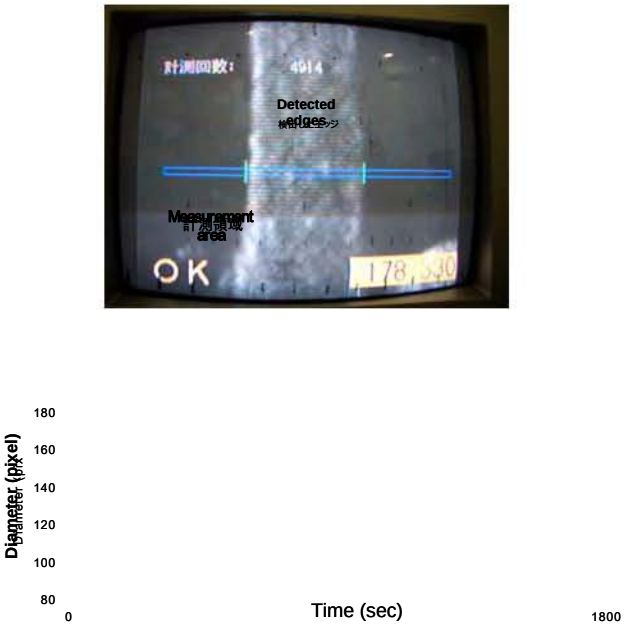


Fig. 2. The changes in pial ateriole diameter were measured using an automatically edge detection camera.

Acknowledgments

This study was financially supported by The Committee to Promote Research on the Possible Biological Effects of Electromagnetic Fields, Ministry of Internal Affairs and Communications, Japan.

References

[1] H. Masuda, K. Wake, S. Watanabe, M. Taki, and C. Ohkubo, “Acute effects of local exposure to radio-frequency electromagnetic fields on the cerebral microcirculation in rats,” BEMS 2001 Abstract book, pp.139-140, June 2001.

[2] H. Watanabe, K. Wake, M. Hanazawa, S. Watanabe, H. Masuda, C. Ohkubo, M. Taki, Y. Yamanaka, and T. Uno. “Dosimetry of rat-head SAR caused by a high-performance ‘‘8’’-shaped loop antenna.” BEMS 2004 Abstract book, pp.52-53, June 2004.

DEVELOPMENT OF CALCULATION PROGRAM 16MAGEXPO ON 24-HOUR PERSONAL MAGNETIC FIELD EXPOSURE UNDER HIGH SCHOOL STUDENTS

MUNNO JU[1], KWANGHO YANG[1], SUNGHO MYUNG[1], GIHYUN HWANG[2], JAEJOON KIM[3], SEUNGDO BAIK[3]

1. KOREA ELECTROTECHNOLOGY RESEARCH INS., CHANGWON, KOREA
2. DONGSEO UNIVERSITY, BUSAN, KOREA
3. KOREA ELECTRIC POWER CO., SEOUL, KOREA

Abstract

Currently, a number of scientific researches are conducted on potential health hazards of electric and magnetic fields. There is a non-objective and psychological belief that they are harmful. However, no scientific and objective proof exists. The ELF magnetic field (MF) has become one of the Korea's social issues due to MF's possible harmful health effect, especially for children under 17 years of age. Therefore, in order to evaluate the magnetic field exposure levels of those children in their general living environment, personal MF exposures of 347 subjects were measured in 2005 with government funding. This study developed the calculation program 16MAGEXPO based on the above measured database to predict personal MF exposure. This program can serve as a valuable tool in estimating 24-hour personal MF exposure without directly measuring the exposure. Three types of personal MF exposure estimation formulas - a formula for infants and preschool children from 1 to 7 years of age, a formula for elementary school children from 8 to 13 years of age and a formula for junior high school students from 14 to 16 years of age - were developed by applying evolutionary computation method to the measured database. Genetic algorithm (GA) and genetic programming (GP) were used among evolutionary computations. After tuning the database with the above methods, final three formulas with the smallest estimation error were selected. The target estimation error was approximately 0.3 mG. The seven parameters of each formula included gender (G), age (A), house type (H), house size (HS), distance between residence and power line (RD), power line voltage class (KV) and the usage and condition of electrical appliances (RULE).

I. Introduction

There is an increasing concern on possible health hazard caused by exposure to power frequency EMF, a part of electro-magnetic interference that is considered the 4th environmental pollution. The concerns over potentially negative biological effects produced by power lines and other sources began in 1979 when Wertheimer and Leeper reported that children living in the vicinity of high-voltage transmission lines had an increasing risk for developing cancer than other children. Although a number of researches were conducted on this subject, biological effects of EMF still remain a heated technological and medical controversy.[1, 2, 3] Therefore, this research developed a method to indirectly estimate the EMF level generated by using electrical energy for participants under 17 years of age. Exposure estimation formulas and calculation program (16MAGEXPO) will provide a method of epidemiological survey for the EMF's biological effects. The 347 participants, ranging from infants to junior high students, were divided into three age brackets to establish EMF exposure estimation formulas. The evolutionary computation was used as an optimization method.

II. Participant Database

The measured personal MF exposure database could be secured by participants who resided near transmission lines up to 345kV. These participants were categorized by the radial distance from the power line and age groups. The subjects included 62 infants to preschool children (1-7 years old), 261 elementary school children (8-13 years old) and 24 junior high students (14-16 years old). In Figure 1, junior high students and preschool children wore a MF measurement meter (Model EMDEX-Lite, Enertech, USA).



Fig. 1 Surveying personal MF exposure for junior high students and preschool children

III. Evolutionary Computations as Optimization Method

A. Evolutionary Computations

Evolutionary computations (ECs) have received significant attention during the last decade, although ECs were originally introduced in the late 1950's [4, 5]. ECs are search algorithms based on the mechanics of genetics and natural selection. ECs combine the survival of the fittest mechanism among string structures with a structured, yet randomized, information exchange to form a search algorithm. ECs efficiently exploit historical information to speculate on new search points with improved performance. In another words, ECs are search methods combining elements of directed and stochastic search, which can strike a remarkable balance between exploration and exploitation of global and local search capability. This research describes the GA and GP application procedures in developing personal MF exposure estimation formulas. The GA was developed by John Holland in the early 1970's. It finds the best solution for the environment by searching the solution space with a probability method and a hierarchical exchange of information between each individual (string or chromosome). GA does not use real parameters but uses chromosomes composed of string coded genotype. GA simulates crossover and mutation of natural systems, thus giving it a global searching capability. GP follows the trend of the GA paradigm but uses trees to represent genotypes. Trees provide a flexible representation for creating and manipulating programs. GP starts with an initial population of randomly generated computer programs (S-expressions) composed of functions and terminals appropriate to the problem domain. Each individual computer program in the population is measured in terms of how well it performs in the particular problem environment. This measure is called the fitness measure. [5, 6]

B. Applications to Develope Formulas

The ECs optimization method was applied to the measured database to develop personal MF exposure estimation formulas. During the development, the following key techniques were employed

1) Types and characteristics of parameters

The 6 main parameters included Gender (G), Age (A), House Type (H), House Size (HS), Radial Distance (RD), and Power Line Voltage (KV). However, occupation was excluded from the parameter. We also added a supplemental parameter called the 'RULE' to increase the estimation accuracy. This RULE represents the length and pattern of electrical appliances usage such as PC and electric heat mat. On the other hand, variables with negligible effects such as sleep, school, commute to and from school and TV watching have not been included in the rules.

2) Radial distance

In order to measure the distance between the power line and the residence, Radial Distance (RD-1), which is considered the real distance, was used instead of Lateral Distance (LD). A digital laser distance meter was used to measure the distance. If distance is difficult to measure, distance RD-2 between tower and the residence was applied.

3) Power line voltage

This research used transmission and distribution line voltage as a parameter instead of load current that directly decides MF level of the power line. The voltage was chosen because the load current fluctuates tremendously by day and season. This research also revealed that there is a significant similarity between increase in transmission line voltage and increase in average MF.

4) Code table of main parameters

Table 1 outlines the main parameter codes and input values during database (DB) tuning.

Table 1. Codes and input values of main parameters

Gender **(G)**	Age **(A)**	House Type **(H)**	House Size **(HS)**	Radial Distance **(RD)**	Power Line Voltage **(KV)**
·Male: 10 ·Female: 20	·1~16	·Apt.: 10 ·Etc.: 20	·the square footage of the unit	·0~30m: 10 ·31~50m: 20 ·51m or more: 30	·Line Voltage

5) Applications of ECs

Table 2 describes the DB tuning parameters of each method based on ECs. Equation 1 illustrates the general objective function for genetic algorithm.

Table 2. Tuning parameters of genetic optimizations

ECs	Generations	Population Size	Crossover Probability	Mutation Probability
GA	2,000	100	0.95	0.05
GP	200,000	1,000	0.8	0.08

$$MFExposure = k1\log(G) + k2\log(A) + k3\log(H) + k4\log(HS) + k5\log(RD) + k6\log(KV) + Rule \quad (1)$$

IV. The Results of Formulas Development

A. Development Conditions

The conditional criteria and functional evaluation characteristics for developing MF exposure estimation formula are as follows:

1) Six parameters: G, A, H, HS, RD and KV
2) Supplementary rules were applied to reduce estimation error.
3) Target error value: mean absolute estimation error below 0.3mG, or tuning and verification errors below 30%.
4) KV: Actual power line voltage. However, if RD is over 100m, '1' is inputted to bring KV term to '0'.
5) Database was tuned with GA and GP first. Then, formulas with the smallest estimation error or ones that incorporated the most parameters were chosen for each case.
6) When the formula produced a negative value due to a peculiar problem between the formula parameters under normal condition, a penalty was issued to the fitness of string (chromosome) during DB tuning.
7) HS: For apartments, the square footage of the unit was used. For houses and villas, the square footage of the floor which the participants live was used.

B. Resulting Formulas and Their Applicable Conditions

1) Types of formulas

This research developed six types of formulas as below.

◦ Formula for infants and preschool children: 1 type (Equation 2)
◦ Formula for elementary school children: 1 type
◦ Formulas for junior high school students: 2 types
◦ Supplementary formulas for elementary school children and junior high school students : 2 types

2) Sample result of personal MF exposure estimation formula for infants and preschool children and their applicable conditions

$$\#1MFExp = -0.002\log(G) + 0.003\log(A) + 0.94\log(H) - 0.24\log(HS) - 1.22\log(RD) + 1.09\log(KV) + Rule \quad (2)$$

• Applicable condition
- A: Ages between 1 and 7
- KV: 22.9~345 kV

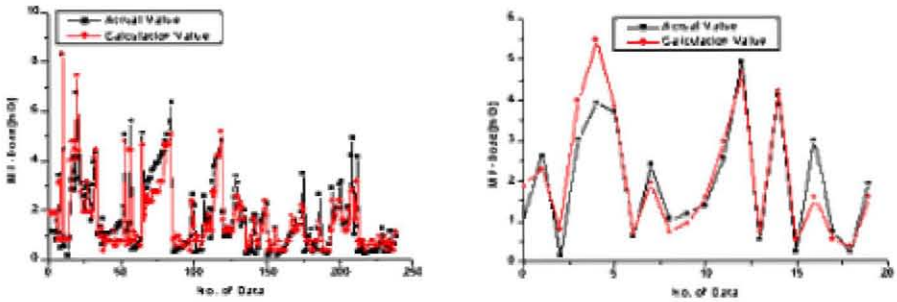
C. Estimation Error

Table 3 combined the estimation errors of each formula; thus, displaying the reliability of each formula. Most estimation errors satisfy the target error of approximately 0.3mG (~30%). Yet, supplementary formulas exceeded

the target error due to their DB characteristics. The supplementary formulas are applicable only if participants' powre line voltage (KV) does not meet the criteria. Figure 2 is the graphic representation of the DB tuning and verification trend in case of elementary school children.

Table 3. Collection of MF exposure estimation formula errors

Formula type	Tuning percentage error (Tuning error/ average measurement value)	Verification percentage error (Validation error/ average measurement value		
Formula for infants & preschool children	32.1 % (0.36/1.12 mG)	29.6 % (0.37/1.25 mG)		
Formula for elementary school children	26.2 % (0.43/1.64 mG)	22.8 % (0.45/1.97 mG)		
Formulas for junior high school student	25.0 % (0.28/1.12 mG)	27.9 % (0.29/1.04 mG)		
Supplementary formulas for elementary school children & junior high school student	41.3 % (0.66/1.60 mG)	Elementary school children & junior high school students 39.7 % (0.71/1.79 mG)	Elementary school children 40.6 % (0.8/1.97 mG)	Junior high school students 33.7 % (0.35/1.04 mG)



(a) DB tuning trend (b) DB verification trend

Fig. 2 Example of DB tuning and verification trends in elementary student database

V. MF Exposure Calculation Program 16MAGEXPO

A. 16MAGEXPO Features

The measurement of MF exposure is rather complicated, and it may be impossible according to circumstances,. 16MAGEXPO allows accurate estimation of the personal MF exposure level without directly measuring. The following is the main features of 16MAGEXPO.

1) Calculates personal MF exposure level by incorporating all MF sources commonly found in daily living environment.
2) Applies to children younger than 17 years old, including infants.
3) Any person, including non-experts, can predict personal MF exposure level if six personal parameters such as gender, age, house type, house size, distance between the residence and power line, and power line voltage and daily lifestyle of rules are known.
4) Rules are variables decided by electrical appliances usage such as PC and electric heat mat. Rules are introduced to enhance the prediction accuracy.
5) This program contains 6 types of personal MF exposure estimation formulas, and the prediction can be made as accurate as mean absolute error below 0.4mG.
6) This program will serve as a valuable tool in surveying and evaluating ELF MF's epidemiological effects.

B. Calculation Modules of 16MAGEXPO

16MAGEXPO has three calculation modules, infants and preschool children, elementary school children and junior high school students as shown in Figure 3. Figure 4 is the screen shot of the main menu. When you select a module button (for example: Infant and preschool child), a detailed calculation screen appears as shown in Figure 5. In the calculation screen, enter the calculation condition first and execute to display the 24-hour personal MF exposure result. If calculating multiple computation cases, use the output files as described in Table 4.

C. Main Calculation Functions of 16MAGEXPO

The following is the main calculation functions of 16MAGEXPO.

1) Calculates personal MF exposure level based on personal traits such as gender and age and living environment conditions such as house size, residence condition, and power line voltage.
2) Enhances the estimation accuracy by integrating daily usage pattern of electrical appliances such as electric heat mat that generate high magnetic field.
3) The user maintains the input file by entering above parameters in a menu-driven method.
4) Personal traits, rules, and calculation results are stored and maintained as an output file of Table 4.

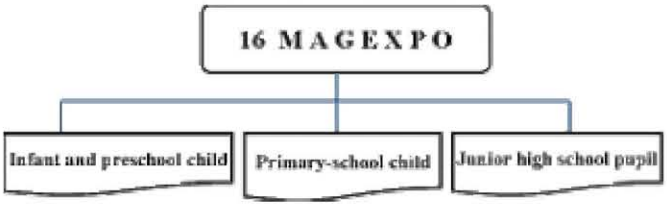


Fig. 3 Diagram of 16MAGEXPO calculation module

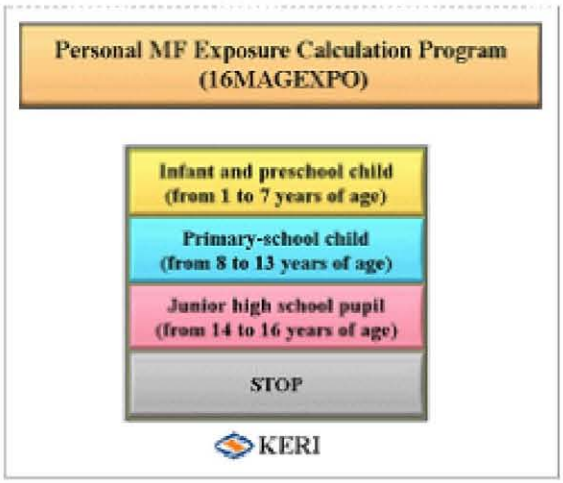


Fig. 4 Main menu of 16MAGEXPO

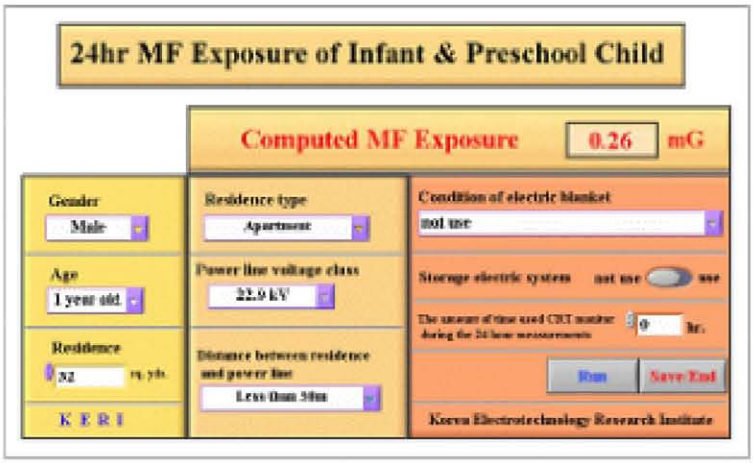


Fig. 5 A 24-hour personal MF exposure calculation sample for infants and preschool children

Table 4. A sample of output file about 24-hour personal MF exposure

G	A	HS [yard^2]	H	RD [m]	KV [kV]	k1	k2	k3 [hr]	MF [mG]
20.00	11.0	142.3	20.00	30.00	345.0	0.00	0.00	0.00	1.33
10.00	13.0	142.3	20.00	30.00	345.0	0.00	0.00	0.00	1.33
10.00	8.00	87.00	20.00	30.00	345.0	0.00	0.00	0.00	1.33
10.00	8.00	261.0	10.00	30.00	345.0	0.00	0.00	0.00	1.17
10.00	8.00	261.0	10.00	10.00	345.0	0.00	0.00	0.00	3.82
10.00	8.00	261.0	10.00	30.01	345.0	0.00	0.00	0.00	1.17
10.00	8.00	261.0	10.00	20.00	345.0	0.00	0.00	0.00	1.93
10.00	8.00	261.0	10.00	20.00	22.90	0.00	0.00	0.00	1.16
10.00	8.00	261.0	10.00	20.00	22.90	1.00	1.00	0.00	3.66
10.00	8.00	261.0	10.00	20.00	22.90	2.00	1.00	0.00	7.66
10.00	8.00	261.0	10.00	20.00	22.90	3.00	1.00	0.00	4.16
10.00	8.00	261.0	10.00	20.00	22.90	3.00	1.00	1.00	4.56
10.00	8.00	261.0	10.00	20.00	22.90	3.00	0.00	1.00	3.56

VI. Conclusions

The human health problem caused by ELF magnetic field has become one of Korea's most debated social issues. The possible health effect on children less than 17 years of age is especially a matter of primary concern. Therefore, this paper proposed the 16MAGEXPO software that can estimate personal MF exposure levels of the above children in their general living environment. The key features and significance of this software development are as follows:

1) The data used to develop estimation formulas were collected from 347 participants.
2) Since the program was designed to estimate the effects of MF near power lines, participants living close to power lines were selected. As a result, as much as 24% of the participants lived within 50m from power lines.
3) Total of six formulas was developed, including a formula for infants and preschool children.
4) The program chose gender, age, house type, house size (square footage), radial distance between residence and power lines and line voltage as parameters. This research revealed that the voltage, distance, and age parameters are highly relative to the MF exposure level.
5) First time in the world, the evolutionary computation suitable for this problem was used as an optimization method. This computation showed that these estimation formulas yielded approximately 0.4mG mean average errors. However, the supplementary formulas, which have limited use, resulted in higher estimation errors. The target estimation error was approximately 0.3 mG.
6) This research developed the personal MF exposure estimation program, 16MAGEXPO, by utilizing the previously mentioned estimation formulas and daily living patterns (rules). The program based on LabView can be used to calculate personal MF exposure for children less than 17 years of age.
7) 16MAGEXPO can serve as a valuable tool in estimating 24-hour personal MF exposure in children without directly measuring.
8) This software marks the suggestion of a new MF exposure estimation method since the introduction of the wire code in late 1970's. In addition, this software will provide an effective and practical means to study MF's effects on human health, especially the epidemiological study on correlation between magnetic field and childhood cancer.

REFERENCES

[1] Zaffanella L.E., Kalton, G.W., “Survey of Personal Magnetic Field Exposure, Phase Ⅱ: 1000-Person Survey”. EMF RAPID Engineering Project #6, Enertech Consultant, 1998

[2] ICNIRP Guidelines, “ICNIRP (International Commission on Non-Ionizing Radiation Protection), Guidelines for Limiting Exposure to Time-Varying Electric Magnetic, and Electromagnetic Fields (up to 300GHz), Preprint scheduled to appear in Health Physics”, Vol. 74, No. 4, 1998, pp. 494-522

[3] Christopher J. Portier, Mary S. Wolfe, "Assessment of Health Effects from Exposure to Power-Line Frequency Electric and Magnetic Fields", NIEHS Working Group Report, June 1998

[4] D. E. Goldberg, *Genetic Algorithms in Search, Optimization, and Machine Learning*, Reading, MA: Addison-Wesley, 1989.

[5] J. R. Koza, *Genetic Programming*, MIT, London, England, 1993, pp. 162-169.

[6] J. A. Miller, W. D. Potter, et al., "An Evaluation of Local Improvement Operators for Genetic Algorithms", *IEEE Transactions on Systems, Man, and Cybernetics*, Vol. 23, No. 5, Sep./Oct. 1993, pp. 1340-1351.

Calculation of Induced Current Inside a Human Body near an IH Cooker by SPFD Method

Yoshitsugu KAMIMURA, Kunihiko ITO and Yoshifumi YAMADA

Utsunomiya University, 7-1-2 Yoto, Utsunomiya 321-8585 Japan
(*gami@is.utsunomiya-u.ac.jp*)

Abstract

In this study, magnetic field exposure of human body near an induction heating (IH) cooker is numerically evaluated using Scalar Potential Finite Difference (SPFD) method. The maximum induced current densities are compared among three kinds of anatomical human body models of the Japanese adult male/female and the American adult male. The induced current densities are averaged over one square centimeter in the area, and they are compared with the guideline of International Commission on Non-Ionized Radiation Protection (ICNIRP). As a result, it is found that the maximum induced current densities are considerably different among these three models of the human body, and the induced current exceeding the guideline of ICNIRP may not flow inside human body in the case with a portable type IH cooker and a pan designed for the IH cooker. In addition, reducing the computation load and the computer resource by dividing the model is considered. As a result, the difference of calculation result by dividing the model is almost negligible, and computation load is decreased.

Introduction

Recently, people have been concerned about the effect of the electromagnetic field on the human body. Because the IH cooker is widespread in Japan, the Japanese especially has the interest of influence on health by the leakage magnetic field. The basic restrictions for exposure to electromagnetic fields in each frequency band are determined by ICNIRP. At the frequency of 20 kHz (internal frequency of the IH cooker used in this study), the basic restriction for the exposure to the induced current density is 40 mA/m^2 (for the general public exposure) and 200 mA/m^2 (for the occupational exposure)[1].

In this study, we use the small loop as a magnetic source equivalent to the IH cooker. We calculate the potential and the induced current density inside the body by SPFD method which is useful for the low frequency magnetic field exposure problem. We use the male and the female models of National Institute of Information and Communications Technology (NICT) as Japanese standard human models[2], and the male model of the Air Force Research Laboratory (AFRL) of Brooks City-Base as a reference[3]. We calculate the induced current density distribution for these models, average them over a cross-section of 1 cm^2 perpendicular to the each direction of axes, and compare those magnitude with the guideline of ICNIRP.

Methods

SPFD method:

The SPFD method is a numerical technique used for calculating potential and the induced current inside conductor under the low frequency magnetic field[4]. At first, we digitize the subject to three dimension cells. The edge conductance s is posited to the each edge of the cell. The scalar potential Ψ is assumed to each node. A simple finite difference equation is given as

$$\left(\sum_{r=1}^{6} s_r\right)\psi_0 - \sum_{r=1}^{6} s_r\psi_r = i\omega\sum_{r=1}^{6}(-1)^{r+1} s_r l\vec{A}_r \,, \qquad (1)$$

where r is the local node index (1~6) and target node is labeled 0. The symbol l denotes the length of the edge, and A_r is the magnetic vector potential tangent to the r-th edge. The set of equations are arranged to the simultaneous equations of unknown Ψ, and solved by SOR method or conjugate gradient method.

Numerical models and source:

In this study, we use three kinds of anatomical human models (Figs.1-3). Figs.1 and 2 are the Japanese male and female models, respectively, developed by NICT. The cell size is 2 mm. Fig.3 shows the male model developed by AFRL. The cell size of the model which we used is 3 mm. The conductivities of the tissues in all models are obtained from Gabriel's report[4].

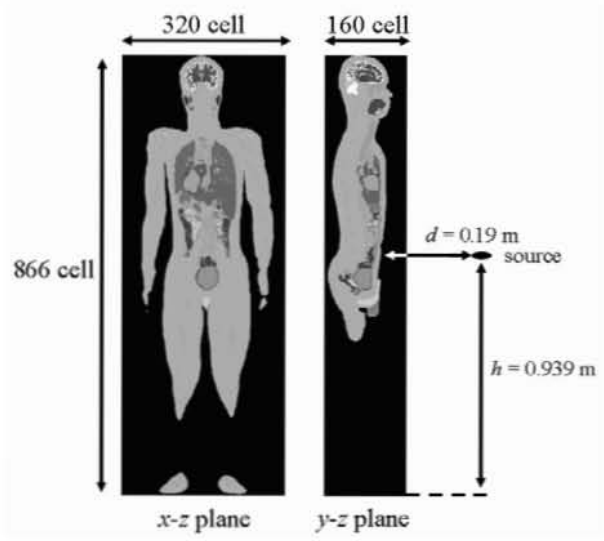


Fig.1 NICT male model and magnetic source.

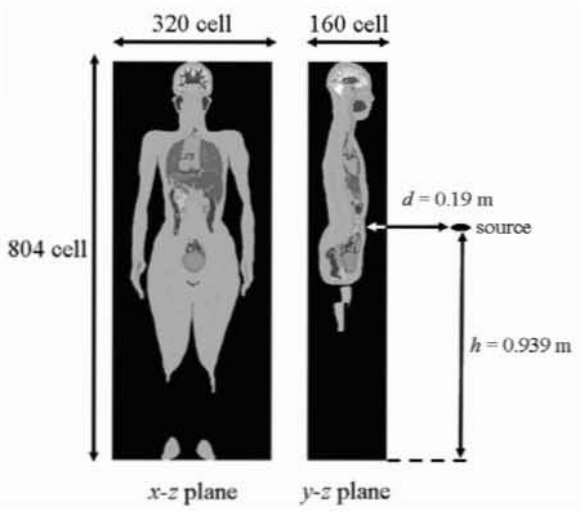


Fig.2 NICT female model and magnetic source.

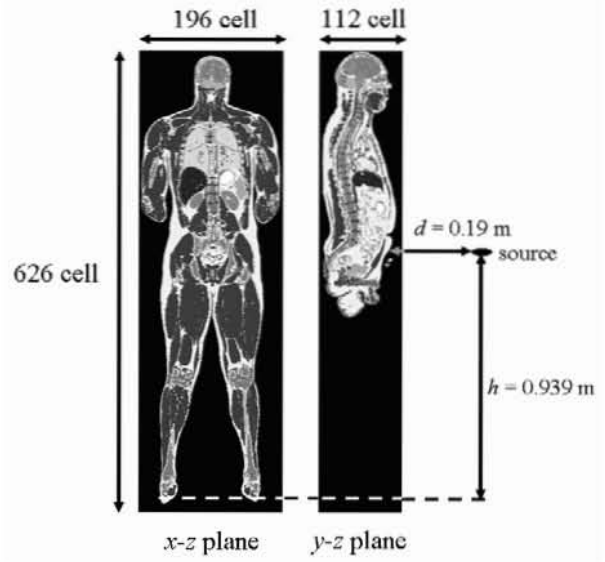


Fig.3 AFRL male model and magnetic source.

A small loop is posited to 0.939 m in height and the distance 0.19 m as a magnetic source equivalent to the IH cooker. The axis of the loop is *z*-direction. The magnetic moment is 1.07×10^6 wbm when we use a portable IH cooker and a pan designed for the IH cooker, and the frequency is 20 kHz.

Averaging filter:

According to the guideline of ICNIRP, the current densities should be averaged over a cross-section of 1 cm^2 perpendicular to the current direction[1]. We calculate the running average using 2D filter like Fig. 4 in the perpendicular plane for each component of current. The cell at the center of the filter represents the tissue after averaging. When the cell size of the model is 3 mm, an equivalent area is adjusted to 1 cm^2 by weighting as shown in Fig. 5.

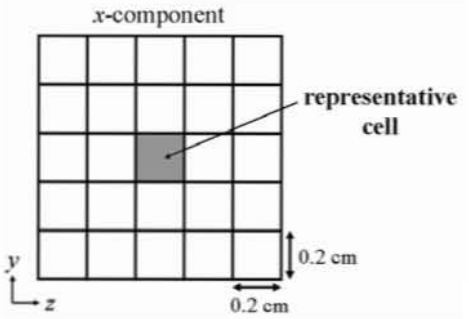


Fig.4 Averaging filter for 2 mm model.

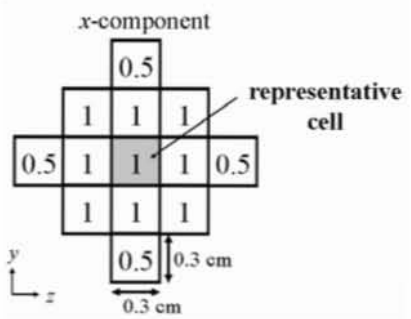


Fig.5 Averaging filter for 3 mm model.

Dividing of models:

When a magnetic source is replaced with small dipole, the current doesn't have *z* component in the *x*-*y* plane including the source since the external magnetic field has only *z* component in that plane. Therefore, we can calculate the induced current density independently by dividing the body into the upper and the lower half by that plane. The saving of the computer resource is expected by dividing the models. We investigate whether the computation load can be reduced by dividing as shown in Fig. 6.

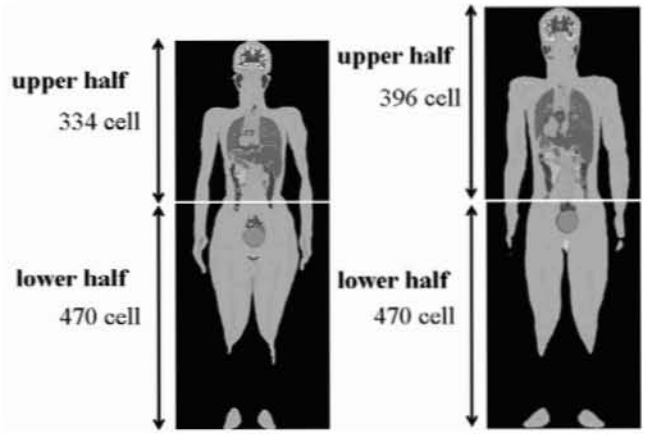


Fig.6 Dividing of the models of NICT.

Results

NICT male model:

Figure 7 shows the comparison between the raw value and averaged value, concerning the maxumum induced current density in each tissue for NICT male model. Figure 8 shows the distribution of averaged current densities in the cross section of the same height as the source.

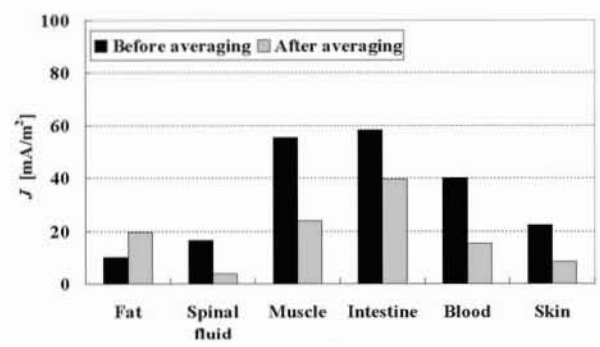


Fig.7 Comparison of induced current density for NICT male model.

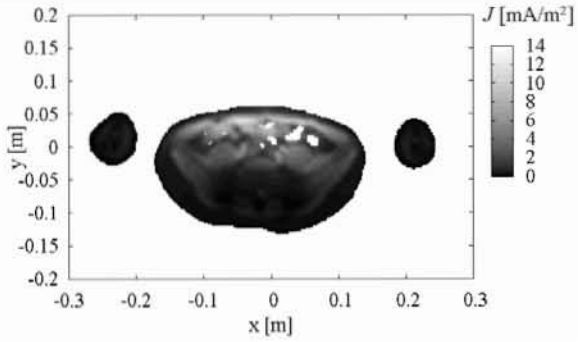


Fig.8 The distribution of averaged current density for NICT male model.

NICT female model:

Figure 9 shows the comparison between the raw value and averaged value, concerning the maxumum induced current density in each tissue for NICT female model. Figure 10 shows the distribution of averaged current densities in the cross section of the same height as the source.

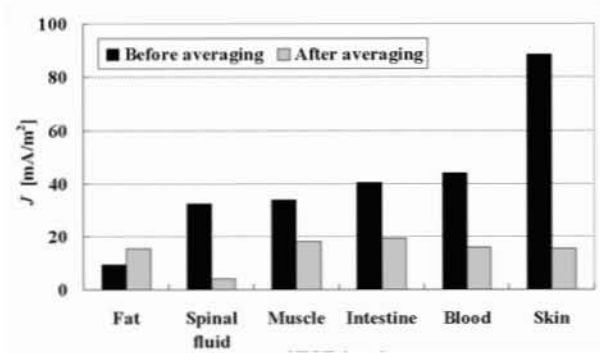


Fig.9 Comparison of induced current density for NICT female model.

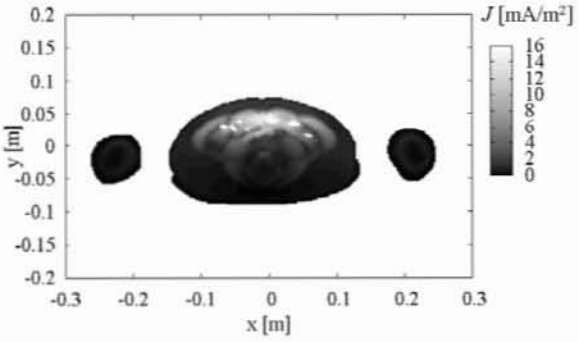


Fig.10 The distribution of averaged current density for NICT female model.

AFRL male model:

Figure 11 shows the comparison between the raw value and averaged value, concerning the maximum induced current density in each tissue for AFRL male model. Figure 12 shows the distribution of averaged current densities in the cross section of the same height as the source.

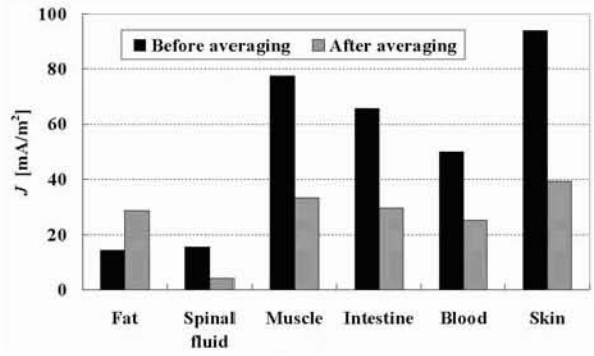


Fig.11 Comparison of induced current density for AFRL male model.

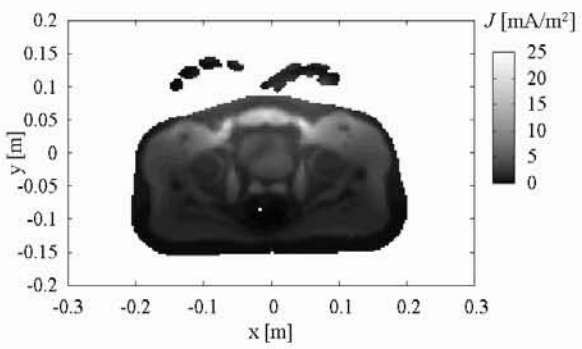


Fig.12 The distribution of averaged current density for AFRL male model.

According to Figs. 7, 9, and 11, the averaged current densities do not exceed the basic restriction 40 mA/m^2 of ICNIRP for the general public. Generally, the model with a fat body has the trend with large averaged current density.

Reduction of computation load by dividing of models:

Comparing the maximum value of the division model with the value of the whole body model, they are almost corresponding (Figs. 13, 14). Tables 1 and 2 show the required computer resource in our computation of the induced current densities. The computing time is proportional to the multiplication of the memory usage with the number of repetitions. Convergence in the upper half model has quickened due to dividing of the model, and the computing time could be saved

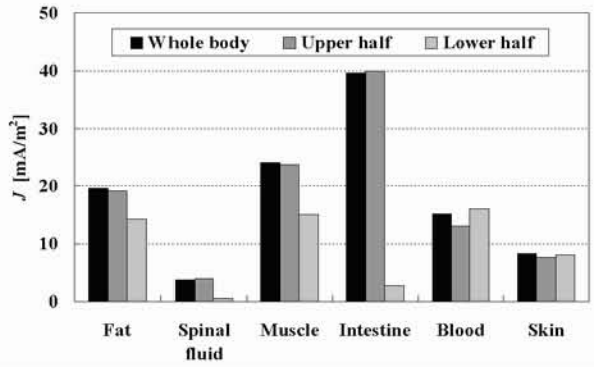


Fig.13 Maximum of averaged current density for divided NICT male model.

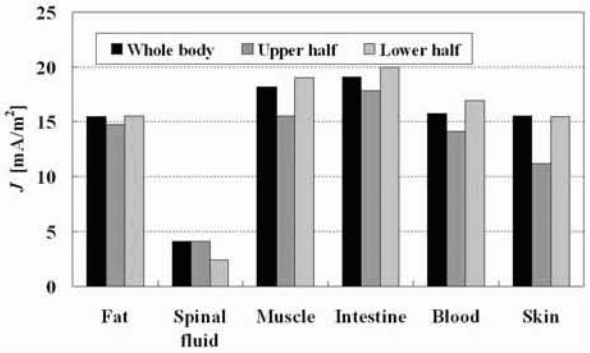


Fig. 14 Maximum of averaged current density for divided NICT female model.

Table 1 Reduction of computor load by dividing of the NICT male model.

	No. of reputation N	Memory usage M (MB)	Load ratio of N*M (%)
Whole body	24466	1532	100
Upper half	9311	707	17.6
Lower half	21664	837	48.4
Division model			66.0

Table 2 Reduction of computor load by dividing of the NICT female model.

	No. of reputation N	Memory usage M (MB)	Load ratio of N*M (%)
Whole body	17797	1423	100
Upper half	6812	598	16.1
Lower half	17727	836	58.5
Division model			74.6

Summary

We have replaced the IH cooker by the small loop, and provided the magnetic vector potential required by the SPFD method theoretically. The induced current densities have been obtained using Japanese anatomically models and the SPFD methods. As a result, it is found that the averaged current densities of them is lower than that of the American male model. The induced current exceeding the guideline of ICNIRP may not flow inside human body in the case with a portable type IH cooker and a pan designed for the IH cooker.

Acknowledgments

This study has been sponsored by Grants-in-Aid for Scientific Research (C) No.17560246 of JSPS.

References

[1] ICNIRP, "Guidelines for limiting exposure to time-varying electric, magnetic and electromagnetic fields (up to 300 GHz)," Health Physics, vol.41, no.4, pp.449-522 (1998).

[2] T. Nagaoka, et al., "Development of realistic high-resolution whole-body voxel models of Japanese adult males and females of average height and weight, and application of models to radio-frequency electromagnetic-field dosimetry," Phisics in Medicine and Biology, 49, pp.1-15 (2004).

[3] Air Force Research Laboratory/ The Human Effectiveness Directorate/ Directed Energy Bioeffects Division, "Dosimetry Models," http://www.brooks.af.mil/AFRL/hed/hedr/HEDR_modeling_irt-temp.htm

[4] T. W. Dawson, J. D. Moerloose and M. A. Stuchly, "Comparison of magnetically induced ELF fields in humans computed by FDTD and scalar potential FD codes," ACES Journal, 11(3), pp.63-71 (1996).

[5] C. Gabriel, "Compilation of the Dielectric Properties of Body Tissues at RF and Microwave Frequencies," Brooks Air Force Base, Report No.AL/ OE-TR-1996-0037, 1996.

SOURCES AND LEVELS OF ELF ELECTRIC AND MAGNETIC FIELDS IN GREECE

E. KARABETSOS G. FILIPPOPOULOS D. KOUTOUNIDIS CH. GOVARI N. SKAMNAKIS

NON IONIZING RADIATION OFFICE
GREEK ATOMIC ENERGY COMMISSION
P. O. BOX 60092, 15310 AGIA PARASKEVI, GREECE

Abstract
The Greek Atomic Energy Commission (EEAE) is the competent national authority for the protection of the general public and the environment from artificially produced non-ionizing radiation. To this end, EEAE carries out measurements in the vicinity of all kinds of sources emitting ELF electric and magnetic fields (e.g. power lines and substations), in order to monitor whether the general public exposure limits are being adhered to. The limit values for the ELF fields in Greece are set exactly the same as those in ICNIRP's guidelines. EEAE has conducted many measurements regarding the levels of ELF electric and magnetic fields in Greece around the elements of the electric power grid where the main interest of the public is focused. Theoretical estimations and typical values based on actual measurements of the fields in the vicinity of all the power lines used in Greece are presented. Measurement results in the vicinity of substations are also presented. In general, the levels of the magnetic field in the vicinity of the power grid elements are well below the established limits; whereas the levels of the electric field may reach values comparable to the safety limits very close to extremely high voltage lines. However, there is no case where the measured values of electric or magnetic fields were higher than the safety limits.

Introduction
Extremely low frequency or ELF electric and magnetic fields are omnipresent in modern societies. The possibility that long-term exposure to these fields might cause adverse health effects is a source for concern, especially for those people residing or working nearby high voltage lines or substations. Competent international scientific committees are watching the scientific developments in order to reach general conclusions about the health effects of these fields, [1].

In 2002, Greece put into force a legislative act, [2], implementing the recommendation, [3], of the Council of the European Union, adopting ICNIRP's limit values, [4], for the protection of the general public. The competent national authority for the protection of the general public and the environment from artificially produced non-ionizing radiation in Greece is the Greek Atomic Energy Commission (EEAE). To this end, the EEAE carries out measurements in the vicinity of all kinds of facilities emitting ELF electric and magnetic fields (e.g. power lines, high voltage substations) in order to monitor whether the general public exposure limits are being adhered to. The EEAE has been accredited in accordance with the requirements of the EN IS0/IEC 17025 standard for performing this kind of measurements. Figure 1 shows the number of annual audits conducted by the Non Ionizing Radiation Office of EEAE in the vicinity of ELF sources. There is an incremental tendency in these measurements reflecting the increasing interest for them.

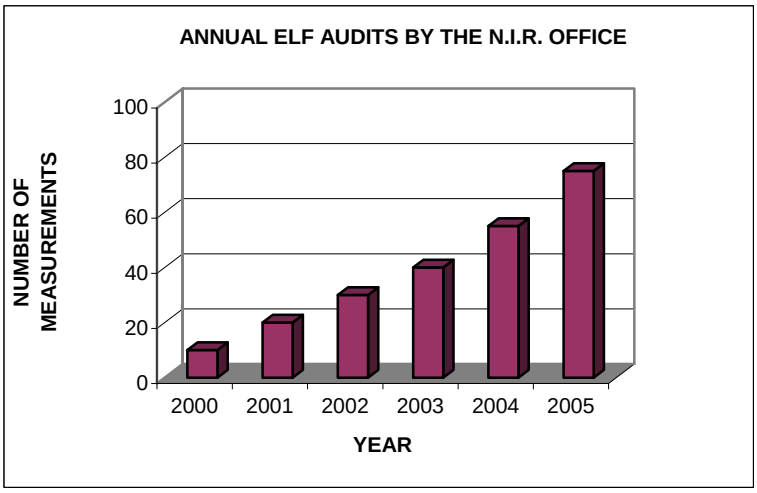


Fig. 1. Annual audits conducted by the Non Ionizing Radiation office of EEAE concerning ELF sources.

In the next paragraphs the main sources of ELF electric and magnetic field exposure of the general public are presented. Domestic sources as the electrical appliances, internal wiring and currents on large grounded metallic objects as water pipes, drains and rails are presented. Also, the exposure resulted from the electric power transmission and distribution system is examined. Special emphasis is given to the situation in Greece and its particularities in relation to other parts of the world. That is because the levels of the electric and magnetic fields are to an important extent depending on the practices applied at electrical installations and on the electric power grid construction and operation, which might be quite different from country to country, [5].

Domestic Sources

In domestic environments the most common sources of ELF fields are the electric appliances, the internal wiring as well as the currents in large grounded objects as water pipes, drains and rails. These sources mainly create magnetic fields in their vicinity, because the created electric field is small due to the low voltage and is further attenuated by closures, walls etc.

The magnetic fields produced by appliances are rapidly attenuated with increasing distance from them and are noteworthy at distances much lower than 1 meter. The field at the surface of the appliance might be very strong, reaching values of hundreds μT. However, in most practical cases the human exposure takes place at much greater distances. Exceptions to this are devices that require their operator to be in close vicinity as electric shavers and hair driers. However, these devises are usually used for short time-periods each day and so the exposure of their operators is limited. Furthermore, exposure from these devises is locally focused in a small area of the body and the coupling of the field with the human body is weak. Taking into account these special exposure situations it is rather impossible that exposure from these sources might be capable to stimulate the neural or muscle cells.

The internal electrical wiring usually does not create important magnetic field levels in its vicinity. The involved practices applied at the construction of these installations are described in the electrical safety codes for the avoidance of the electrocution and other dangers. According to the safety code in Greece, [6], but also in many other parts of the world, the currents at the internal wirings create magnetic fields that at a great extent cancel each other. However, in the rare cases of installations not complying with the terms of the safety code, it is possible to find unusually strong magnetic fields, due to faulty connections or leakage currents. The existence of strong magnetic fields from the internal wiring might be an indication of an installation not complying with electrical safety codes and even hiding risks for electrocution or other dangers (as initiation of a fire).

It is noteworthy that in Greece the main supply is 50Hz and 220V ac voltage (as in the rest of Europe). That means that the currents used in electric appliances and the magnetic fields associated with them are roughly half of those that are used in other parts of the world (as the North America) where 110V are used. Furthermore the 50Hz magnetic fields in Europe induce 20% less internal fields and currents in the body of an exposed individual in relation to the 60Hz used in North America.

Another important source of domestic ELF magnetic fields might be the existence of ground currents at large grounded objects as water pipes, drains and rails. These currents create elevated levels of background magnetic

fields, i.e. fields that decay relatively slowly with the distance from their source. These currents are actually a portion of the returning currents normally located at the neutral conductor. However, the multiple ground connections of the neutral conductor allow alternative paths for the flow of the returning currents back to the power grid through large grounded metallic objects as water pipes, figure 2. Ground currents typically flow if there is a fault on the power system or they can be a normal condition, if there are many connections of the neutral conductor to the ground. However, the use of non-conductive parts at the water supply system significantly reduces the levels of the return currents.

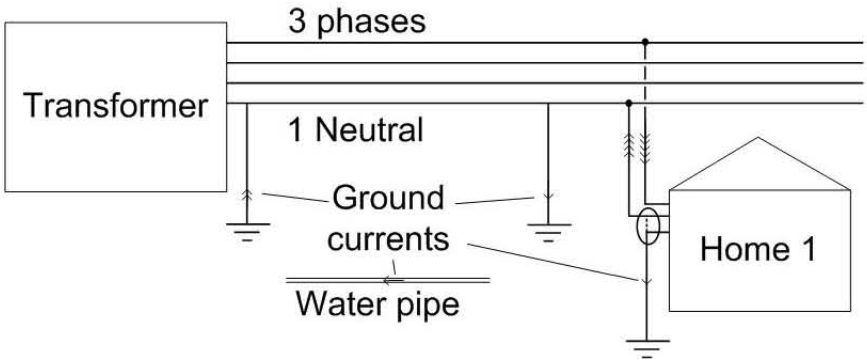


Fig. 2. Mechanisms for the creation of ground return currents. The connection of the neutral conductor with the protective earth (ground) at the beginning of each consumer installation is either prohibited or imperative in Greece, depending on the geographic area.

Electric power distribution

The electric power distribution network is consisted of the low and medium voltage network used for the delivery of the electric power as well as the medium to low voltage substations. In Greece the low voltage is at the nominal level of 220/380V. The medium voltage is at various nominal levels but the last years it is being standardized to 20kV.

The low voltage network is the final piece of the electric network used for the delivery of the electric power at home level. This network consists of overhead and underground lines. These lines create mainly magnetic fields in their vicinity. The created magnetic fields may reach values up to a few μT close to the conductors and attenuate at much lower levels a few meters away from the lines. However, the low voltage loads are usually not well balanced on the three phases of the system and that causes the appearance of currents on the line neutral conductor. A portion of this current might flow on large grounded metallic objects in the vicinity of the line but in special circumstances also far from it, with the results described in the previous paragraph. That also means that there is a net current on the line producing magnetic fields that decay relatively slow with the distance from it.

The medium voltage network is used for the power supply of the substations feeding the low voltage network as well as for the immediate supply of large consumers. The voltage in this network is many times higher than that in low voltage network and so the currents are many times lower for the same amount of transferred power. Table 1 includes typical EMF values found in the vicinity of medium voltage lines in Greece. It is noteworthy that the medium voltage lines do not suffer from the unbalances mentioned for low voltage lines, because the medium voltage loads are usually well balanced and the medium to low voltage substations act as barriers not allowing the low voltage unbalance to pass on the medium voltage side.

The medium to low voltage substations are usually sources of public concern. The attention is mistakenly focused on the transformer, which is used for power transmission from one voltage level to another. However, the transformer itself is not producing any significant levels of electric and magnetic fields in its vicinity. It is the medium and low voltage conductors connected to the transformer that create the electric and magnetic fields. Typically, the medium voltage equipment is the dominant source of the electric fields and the low voltage one is the dominant source for the magnetic fields close to a substation. The electric and magnetic fields produced by these substations does not extent further than a few meters from it. However, the current on the low voltage lines, which are fed by the substation, is higher close to the substation than far from it, as the electric power is dispatched to the various consumers along the line's way.

Electric power transmission

High and extremely high voltage lines are used to carry vast amounts of electric power. In Greece the main centers for electric power generation are located at the north part of the country; whereas the main consumption is occurring at the south part nearby Athens metropolitan area. Three double circuit 400kV (extremely high voltage) power lines are used to carry the electric power from the north to the south. Also, 400kV power lines are used for the interconnections with the neighbour countries at the north. The rest of the transmission is mainly accomplished with 150kV (high voltage) single or double circuit power lines.

Figure 3 shows typical levels of the electric and magnetic fields in the vicinity of the 150kV overhead power lines used in Greece. The magnetic field calculations refer to 50MVA apparent transferred power, which is considered typical for this level of voltage. The capacity for power transmission of these lines reaches 202MVA per three-phase circuit. In the 3rd row of this figure the fields in the vicinity of compact single circuit line are shown. This line creates the least field levels in its vicinity as it was also shown in [7].

Similarly, figure 4 shows typical levels of the electric and magnetic fields in the vicinity of 400kV power lines used in Greece. For these lines the magnetic field calculations refer to a typical level of apparent transferred power of 350MVA (typical capacity is 1400MVA per three-phase circuit). In the 2nd and 3rd row of this figure the fields in the vicinity of a double circuit line with different phase arrangements are shown. The double circuit 400kV power lines in Greece used to be constructed with the symmetrical phase arrangement on the two circuits (2nd row). However, for the barrel type double circuit lines used in Greece, this phase arrangement is not the optimum for the reduction of the produced electric and magnetic fields (actually for the parallel operation of the two circuits this phase arrangement is the worst one) and this led to elevated levels of electric and magnetic fields. The new 400kV double circuit lines are now constructed with opposite phase sequence on the two circuits, which is the optimum phase arrangement (3rd row) for this type of lines and leads to reduced electric and magnetic fields, [7]. Also, the phase sequence on the existing power lines of this kind were switched to the optimum one causing significant reduction of the produced fields,[8].

In Greece there are about 10000km of overhead high voltage power lines (400kV and 150kV) as well as 200km of underground high voltage power lines (150kV). The later are used for transferring high voltage power in the dense populated urban areas. Underground cables do not produce any electric field above the ground. Comparing the magnetic fields produced by an overhead and an underground high voltage line, carrying the same power, the underground cable produces a higher magnetic field value in a narrow area right above it (figure 5).

Table 2 shows worst-case values (based on theoretical estimations) and typical values (based on actual measurements) of electric and magnetic fields in the vicinity of the power lines used in Greece. The levels of the magnetic field are, as a rule, much lower than ICNIRP's reference level for general public exposure to 50Hz magnetic fields (100μT), [4]. The levels of the electric field can reach values close to 5kV/m (ICNIRP's reference level for general public exposure to 50Hz electric fields) under 400kV lines and under worst-case considerations. However, in no case the measured values for the electric field were higher than ICNIRP's reference level.

High Voltage Substations

Regarding the electric and magnetic fields produced in the vicinity of high voltage substations the measurements conducted by EEAE have shown that the equipment installed into the substation does not produce any significant values of electric and magnetic fields outside the substation. It is the power lines connected to it, that produce the levels of electric and magnetic fields measured in the vicinity of the substations. Figure 6 shows a satellite photo of Agios Stefanos 400kV substation of the Greek power transmission system. EEAE was called upon to examine the levels of the produced fields outside this substation and performed measurements around the perimeter of it. The routes of the power lines connected to the substation as well as the measurement points are indicated in figure 6. These measurements verified that far from the power lines there are insignificant levels of fields, whereas close to the power lines the typical electric and magnetic field levels in the vicinity of the corresponding lines are found.

Table 1. Electric and magnetic field levels at the vicinity of the power lines used in Greece. The values refer at a distance of 2m above ground level in the vicinity of overhead lines and at ground surface in the vicinity of underground cables.

Arrangement		**Magnetic field (μT)**	**Electric field (V/m)**
400 kV lines	Worst-case scenario	25	5000
	Typical (underneath the conductors)	1 – 4	2000 – 4000
	Typical (25m aside from line)	0.5 – 2	200 – 500
150 kV lines with lattice towers	Worst case scenario	15	2000
	Typical (underneath the conductors)	0.5 – 2	1000 – 2000
	Typical (25m aside from line)	0.1 – 0.2	100 – 300
150 kV compact lines on poles	Worst case scenario	10	1200
	Typical (underneath the conductors)	0.3 – 1.5	500 – 1000
	Typical (25m aside from line)	0.05 – 0.2	50 – 100
150 kV underground cables	Worst case scenario	20	
	Typical (above the cable)	3 – 6	-
	Typical (25m aside from cable)	< 0,01	
20 kV overhead lines (medium voltage network)	Worst case scenario	5	700
	Typical (underneath the conductors)	0.2 – 0.5	50 – 200
	Typical (25m aside from line)	0.01 – 0.05	10 – 20

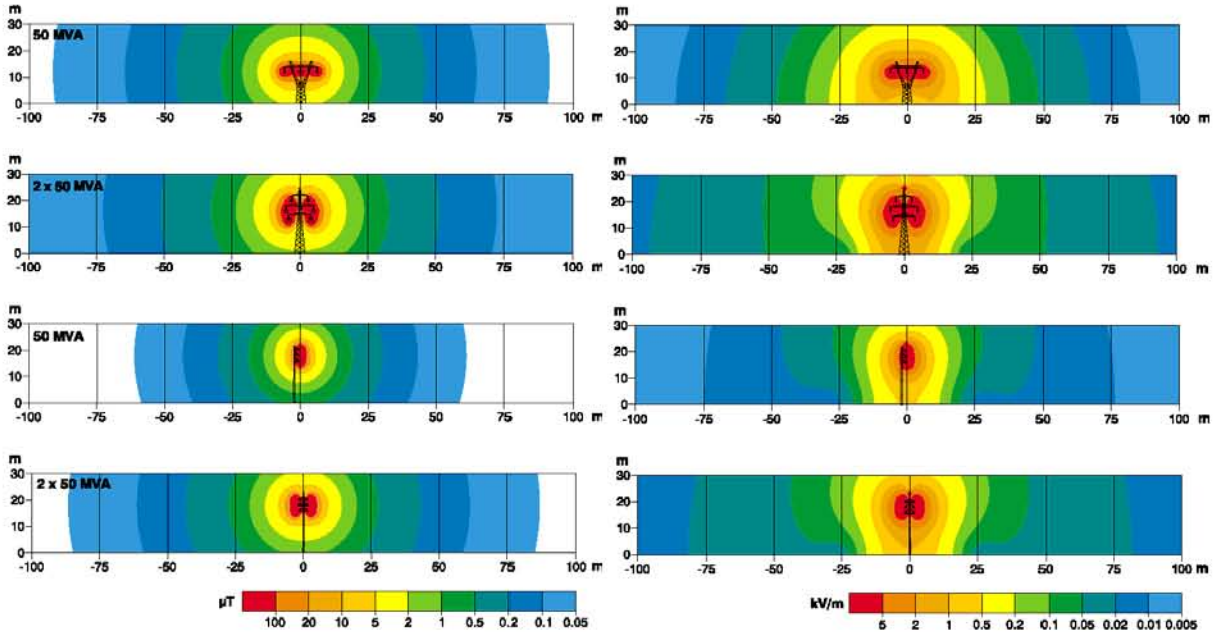


Fig 3. Typical levels for the magnetic field (on the left) and electric field (on the right) in the vicinity of the 150kV overhead power lines used in Greece. The considered clearance of the conductors to the ground was 12m and the indicated power line types are:
1st row: single circuit line on steel lattice towers
2nd row: double circuit line on steel lattice towers
3rd row: compact single circuit line on poles
4th row: compact double circuit line on poles

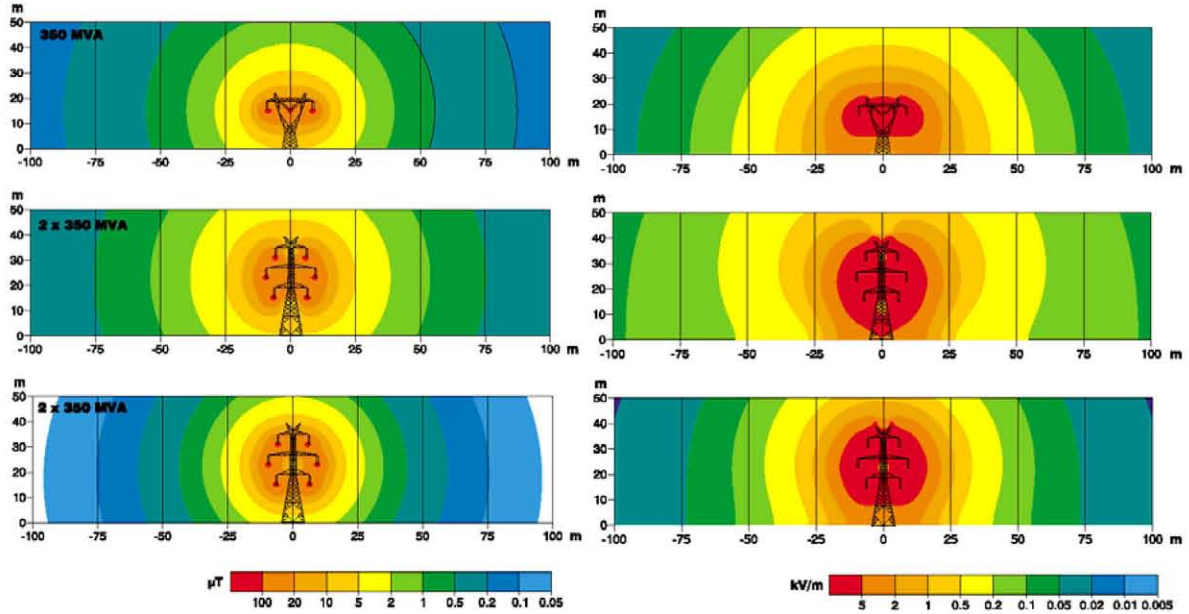


Fig 4. Magnetic field (on the left) and electric field (on the right) in the vicinity of the 400kV overhead power lines used in Greece. The considered clearance of the conductors to the ground was 15m and the indicated power line types are:
1st row: single circuit line
2nd row: double circuit line with the symmetrical phase arrangement
3rd row: double circuit line with the optimum phase arrangement

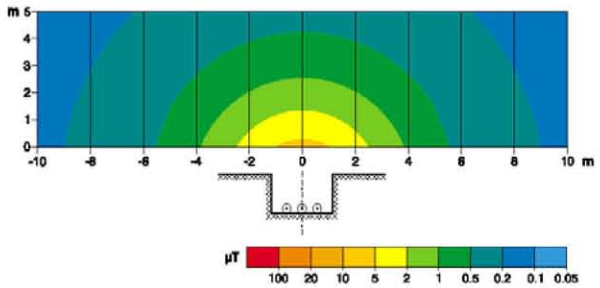


Fig. 5. Magnetic field in the vicinity of a 150kV underground cable carrying 50MVA. The considered cable is buried at 1.5m depth and the distance between the neighbor pole centers is 25cm.

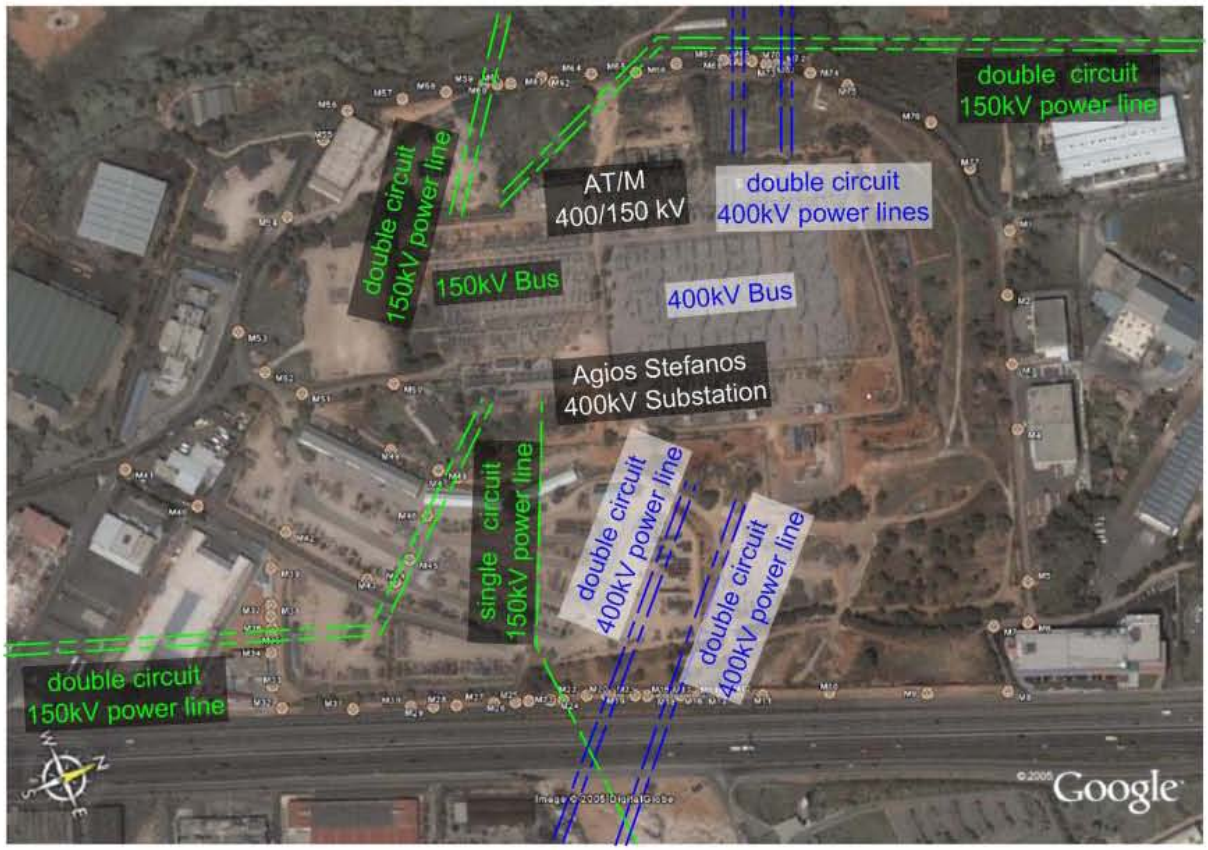


Fig. 6. Satellite photo of Agios Stefanos 400kV substation (Greece) where the routes of 150kV and the 400kV power lines connected to it and the locations where EEAE have conducted measurements outside its perimeter are indicated.

Conclusion

The main sources of ELF magnetic field exposure of the general public in domestic environments are the electrical appliances, the internal wiring and the return currents on large grounded metallic objects as water pipes, drains and rails. The electrical appliances produce fast decreasing fields with distance that typically are considered important only for those devises where the operator must be in the close vicinity of them. The internal wiring normally does not produce any significant levels of magnetic fields, unless there is a faulty connection or a leakage current. The return currents on large grounded metallic objects as water pipes, drains and rails cause elevated levels of background magnetic fields.

Unbalanced loads at low voltage lines might cause net currents on them creating magnetic fields that decay relatively slowly with the distance. The medium voltage network does not suffer from these unbalances. The medium to low voltage transformer does not actually produce any fields in its environment. It is the lines connected to it that produce the electric and magnetic fields in its vicinity.

The electric and magnetic fields in the vicinity of high and extremely high voltage power lines depend on the type of line, its load and the distance from it. In Greece the application of the optimum phase arrangement at double circuit 400kV power lines caused a significant reduction of EMF levels around them. Furthermore, the use of compact lines also reduces the produced fields in relation to lines with normal dimensions. Underground cables create magnetic fields that decay very fast with distance from them. However, the magnetic field might be higher than that of an overhead line in a narrow zone above the cables.

References

[1] G. Filippopoulos, E. Karabetsos, D. Koutounides, Ch. Govari: Health effects of ELF electric and magnetic fields – WHO/IARC evaluation and other recent reviews, Second International Workshop on Biological Effects of Electromagnetic Fields, Rhodes, Greece, October 7-11, 2002.

[2] Greek legislation: Common Ministerial Decision, Protection measures for the exposure of the general public to all low frequency electric and magnetic fields emitting devices, Act No.512/Vol. B/25-4-2002.

[3] European Union Council Recommendation of 12th July 1999 on the limitation of exposure of the general public to electromagnetic fields (0Hz to 300 GHz) (1999/519/EC).
[4] International Commission on Non Ionizing Radiation Protection (ICNIRP), Guidelines for limiting exposure to time – varying electric, magnetic and electromagnetic fields (up to 300 GHz), Health Physics, Vol. 74, No 4, April 1998, pp 494 – 522.
[5] J. Swanson, W.T. Kaune: Comparison of residential power-frequency magnetic fields away from appliances in different countries, Bioelectromagnetics, Vol 20, No 4, pp 244-254, 1999.
[6] Hellenic Organization for Standardization, Requirements for electrical installations, ΕΛΟΤ HD 384, 2004.
[7] D. Tsanakas, G. Filippopoulos, J. Voyazakis, G. Kouvarakis: Compact and optimum phase conductor arrangement for the reduction of electric and magnetic fields, CIGRE Symposium Report 36 – 103, Paris 2000.
[8] E. Mimos, D. Tsanakas, G. Filippopoulos: Measurements of electric and magnetic fields produced by 400kV overhead power lines during the symmetrical and the optimum phase conductor arrangement, 3rd International Workshop on Biological Effects of Electromagnetic Fields, Kos, Greece, October 4-8, 2004.

SOURCES AND LEVELS OF RF ELECTROMAGNETIC FIELDS IN GREECE

E. KARABETSOS G. FILIPPOPOULOS D. KOUTOUNIDIS CH. GOVARI N. SKAMNAKIS

NON IONIZING RADIATION OFFICE
GREEK ATOMIC ENERGY COMMISSION
P. O. BOX 60092, 15310 AGIA PARASKEVI, GREECE

Abstract
The Greek Atomic Energy Commission (EEAE) is the competent national authority for the protection of the general public and the environment from artificially produced non-ionizing radiation. To this end, EEAE carries out measurements in the vicinity of all kinds of sources emitting RF electromagnetic fields (e.g. audio, radio and television antennas, mobile phone base stations, radar and satellite earth stations and other microwave communication systems), in order to monitor whether the general public exposure limits are being adhered to. The safety limits in Greek legislation for the electromagnetic fields emitted by antenna stations, were recently set to 70% of the ICNIRP's values and to 60% of them if the antenna station is closer than 300m from the perimeter of kindergartens, schools, hospitals or eldercare facilities. There are a few exceptional cases where measurements of RF fields conducted by EEAE in the vicinity of radio and TV broadcasting antennas have revealed excess of ICNIRP's reference levels. The results of one such case are presented. About 70% of the RF measurements conducted by EEAE concern cellular phone base stations. EEAE has conducted measurements in the vicinity of 1200 such stations and virtually in all measurements the results are from tens to thousands times below ICNIRP's reference levels for general public protection.

Introduction
The proliferation of wireless communication technologies caused a radical change on the modern society. In Greece the penetration of cell phones is about 80% that is close to the average of the developed world. At the same time there is an increasing concern among people residing nearby cell phone base stations about adverse health effects caused by the presence of the station.

In order to protect against known effects of the exposure to electromagnetic fields, competent committees as ICNIRP have developed exposure guidelines, [1]. In the recommendation, [2], issued in 1999, the EU Council adopted ICNIRP's guidelines for the protection of the general public. Implementing this recommendation, Greece put into force a national legislative act concerning the protection of the public from exposure to electromagnetic fields emitted by all kinds of land-based antenna stations, [3] in 2000. The limits in Greek legislation were set to 80% of the European Recommendation values. Recently, however, the Greek Parliament has voted the Law [4] setting the Greek limit values at 70% of the European Recommendation values, in general, and 60% of them, if the antenna station is closer than 300m from kindergartens, schools, hospitals or elder-care facilities.

The competent national authority for the protection of the general public and the environment from artificially produced non-ionizing radiation in Greece is the Greek Atomic Energy Commission (EEAE). To this end, the EEAE carries out measurements in the vicinity of all kinds of facilities emitting RF electromagnetic fields (e.g. audio, radio and television antennas, mobile phone base stations, radar and satellite earth stations and other microwave communication systems), in order to monitor whether the general public exposure limits are being adhered to. The EEAE has been accredited in accordance with the requirements of the EN IS0/IEC 17025 standard for performing this kind of measurements. Figure 1 shows the number of annual audits conducted by the Non Ionizing Radiation Office of EEAE regarding RF sources. There is an incremental tendency in these measurements reflecting the increasing interest for them.

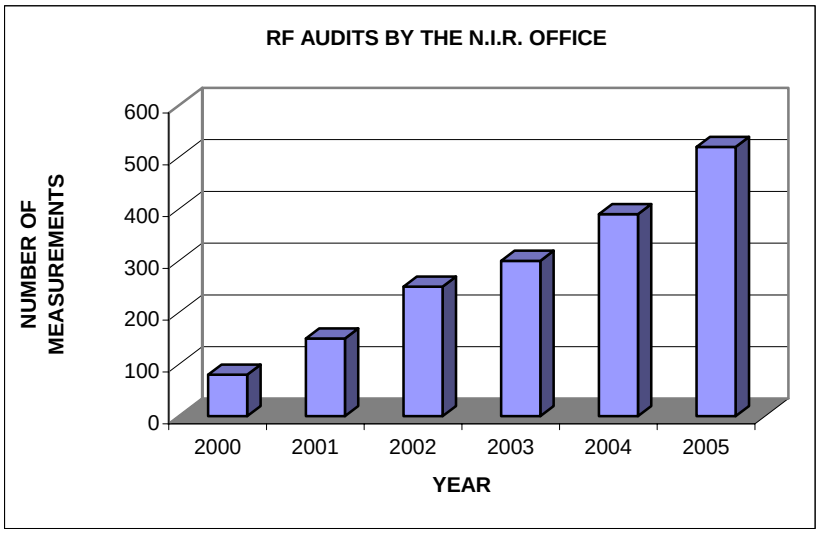


Fig. 1. Annual audits conducted by the Non Ionizing Radiation office of EEAE concerning RF sources.

In the next paragraphs results of measurements conducted by EEAE in the vicinity of the most common types of antenna stations are presented. Though the use of mobile phones is the major source of exposure to RF electromagnetic fields, mobile phones are not treated in this paper. That is because the measurements conducted by EEAE generally concern fixed antenna stations as mobile phone base stations, radio and TV broadcasting stations radar and satellite earth stations and other microwave communication systems. The purpose of these measurements is to check compliance with the limits set in the Greek legislation. Figure 2 shows the percentage of the measurements conducted in the vicinity of mobile phone base stations, radio and TV broadcasting antennas as well as radar facilities. The majority of measurements concern mobile phone base stations. This big ratio is due to the constantly increasing relevant requests from municipal authorities, individual citizens and even the mobile phone network operators.

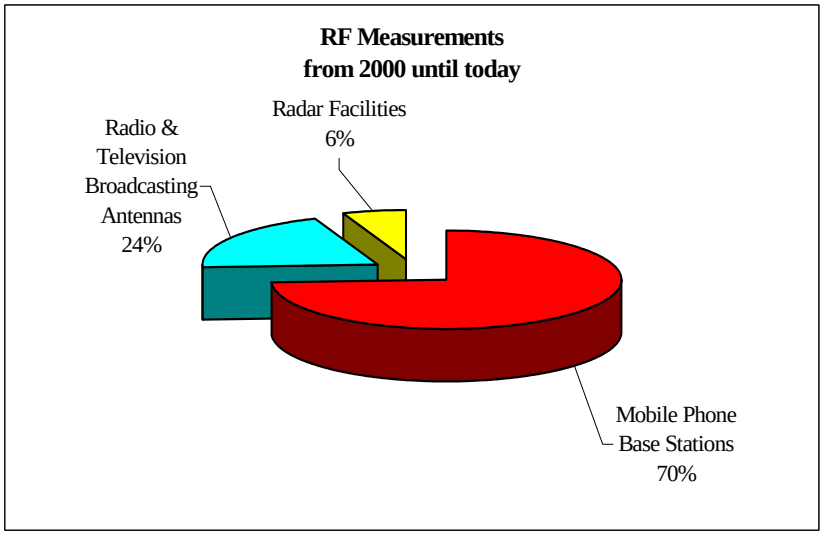


Fig. 2. Percentage of the measurements conducted by EEAE regarding mobile phone base stations, radio and TV broadcasting antennas and radar facilities.

Mobile phone base stations

Mobile phone base station antennas in Greece are, as everywhere else, placed either on top of large metal pylons (in rural places) or on poles on top of buildings (in urban areas). Nowadays, it is also common to find micro antennas in the interior of big buildings such as airports, metro stations, stadiums, etc, where a lot of people are assembled. Throughout the country there are about 6000 base stations installed until now, including the new UMTS stations. The EEAE has conducted measurements in the vicinity of almost 1250 such stations and practically in all cases the results were found to be from tens to thousands times below ICNIRP's reference levels for general public exposure. Table 1 shows typical maximum levels of the electromagnetic fields measured in the vicinity of mobile phone base stations in Greece. It is noted that these values refer to the maximum value at worst-case selected areas in the vicinity of the base station. These areas are usually on the roofs of nearby tall buildings in the main lobe directions of the base station's antennas. The levels of the electromagnetic fields caused by these stations at areas where people normally dwell or work are, as a rule, much lower.

Table 1. Typical maximum values of electromagnetic radiation in the vicinity of mobile phone base stations and the reference levels imposed by the Greek legislation for the frequencies used in mobile phone systems.

		Electric field (V/m)	**Magnetic field (A/m)**	**Equiv. Power Density (W/m^2)**
Typical maximum values		0.25 – 5	0.0005 – 0.01	0.0002 – 0.05
Reference levels for GSM-900*	70%	34.5	0.0929	3.1
	60%	31.9	0.0860	2.7
Reference levels for GSM-1800*	70%	48.8	0.1313	6.3
	60%	45.2	0.1216	5.4
Reference levels for UMTS* (2100MHz)	70%	51	0.1339	7
	60%	47.2	0.1239	6

* The Greek limits are set to 70% of ICNIRP's values for the electromagnetic fields in the vicinity of antenna systems further than 300m from the perimeter of day nurseries, schools, hospitals or elder-care facilities and to 60% of ICNIRP's values closer than 300m from these facilities. The Greek reference levels are calculated from corresponding basic restrictions set to 70% and 60% per case of ICNIRP's basic restrictions.

Radio and TV broadcast stations

In many cases, a great number of powerful radio and TV broadcasting installations have been assembled in one place forming an antenna park. In some of these places, measurements conducted by EEAE have revealed excess of ICNIRP's reference levels. Usually, the excess is limited a few meters away from the antenna installations. In a specific and exceptional case, the side lobe of a powerful installation in an antenna park near Herakleion, Crete Island radiates a nearby, elevated area where an army camp is situated, causing excess of ICNIRP's reference levels in almost half of the camp (see figure 3).

EEAE was called upon to examine the levels of the electromagnetic radiation caused by this antenna park. The measurements performed by EEAE revealed levels of electromagnetic fields much in excess of Greek reference levels (and ICNIRP reference levels as well). After that, the area where the excess occurs was defined and special signs were temporally set in order to warn the personnel of the high EMF levels, until the competent authorities take all the appropriate remedial actions. Figure 3 indicates the area where the electromagnetic fields exceed the Greek reference levels and the points where measurements have been taken. Besides measuring the levels of the electromagnetic fields spectral analyses were also performed in order to specify the contribution of each source to the measured levels. Figures 4 and 5 show the results of spectral analyses per service and per FM radio station, respectively, conducted at point M1 (a typical point). These analyses revealed that the major contribution at the measured fields came from FM radio stations and particularly from a single radio station operating at 97.5MHz.

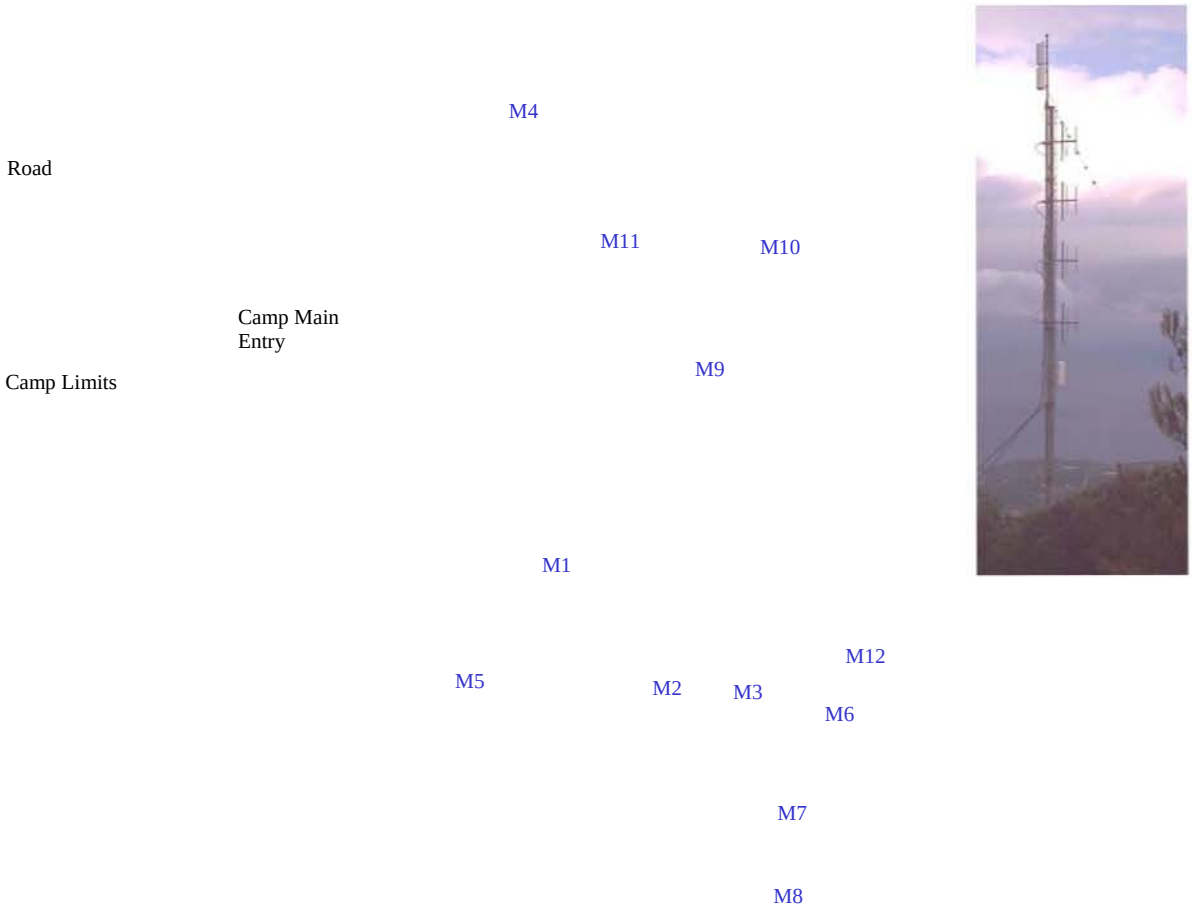


Fig 3. A sketch of the camp and the surrounding area showing the points of measurement (M1- 12) and the area in red where the RF radiation exceeds the Greek reference levels. The photo shows the radio station antenna causing the high radiation levels.

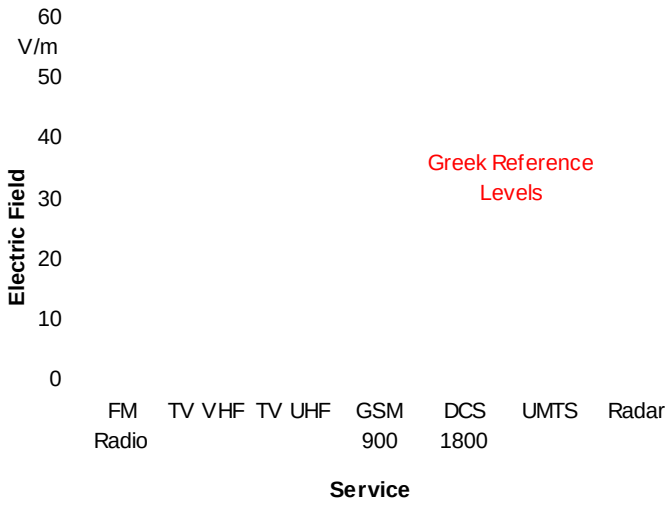


Fig. 4. Spectral analysis per service for the electromagnetic radiation at point M1.

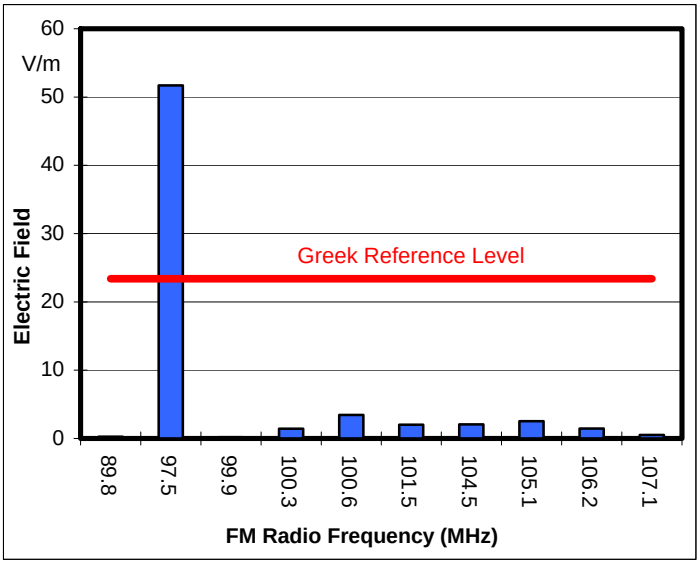


Fig. 5. Spectral analysis per FM radio station for the electromagnetic radiation at point M1.

Radar Stations

EEAE has also conducted measurements in the vicinity of radar installations. Despite the powerful emitted pulses the exposure in the vicinity of these installations is in general some hundreds to thousand times lower than ICNIRP's reference values for general public protection. It is noteworthy that the measurement process in these cases is much more difficult and time requiring because the instrument's response to pulsed modulated fields has to be taken into account and the peak and average exposure has to be calculated.

Conclusions

EEAE carries out measurements in the vicinity of all devices emitting RF electromagnetic fields throughout Greece in order to check compliance with the limits imposed by the Greek Legislation. To that end over one and a half thousand audits have been performed. It is noted that the Greek limits were recently set to 70% of ICNIRP's values in general, and 60% of ICNIRP's values for exposure caused by antenna station at a distance lower than 300m from the perimeter of day nurseries, schools, hospitals or elder-care facilities.

The results of RF electromagnetic field measurements show that there might be cases where powerful radio or TV broadcasting antennas cause levels of these fields greater than the established reference values for human exposure, if proper care were not shown during their design and installation phases. Regarding the electromagnetic field levels in the vicinity of mobile phone base stations, the measurements conducted by EEAE show that the maximum values of electromagnetic fields are typically hundreds to thousand times lower than ICNIRP's reference levels.

References

[1] International Commission on Non Ionizing Radiation Protection (ICNIRP), Guidelines for limiting exposure to time – varying electric, magnetic and electromagnetic fields (up to 300 GHz), Health Physics, Vol. 74, No 4, April 1998, pp 494 – 522.
[2] European Union Council Recommendation of 12th July 1999 on the limitation of exposure of the general public to electromagnetic fields (0Hz to 300 GHz) (1999/519/EC).
[3] Greek legislation: Common Ministerial Decision, Protection measures for the exposure of the general public to all land based antenna stations, Act No.1105/Vol. B/6-9-2000.
[4] Greek legislation: Law No 3431 About electronic communications and other provisions, Act No.13/A/03-02-2006.

DEVELOPMENT OF MOTOR AND PSYCHOLOGICAL FUNCTION ON CHILDREN AND ELECTROMAGNETIC FIELD

ANTON KOLODYNSKI & VALDA KOLODYNSKA

Institute of Biology University of Latvia,

3 Miera str., Salaspils, LV- 2269, Latvia

Email: anton.kolodynski@email.lubi.edu.lv

ABSTRACT

The use of mobile connection that relates to electromagnetic satiation is rapidly increasing during the recent 10 years in Latvia. People who carry mobile phones constantly subject themselves to the action of an electromagnetic field (EMF). And in the process of talking the mobile phone EMF exceeds the standards admissible by a factor of 10 times.

The number of children who always use mobile phones rapidly augments too. According to our data (2005) every tenth pupil of the first form has a mobile phone. Moreover, at the age of the secondary school nearly every pupil has a mobile phone.

The main tasks of the studies were the EMF influence on the development of the children motor and psychological function. The intensity of the EMF influence determined on the children neuropsychic development peculiarities was studied.

A complex of motor and psychological parameters was found.

The studies were performed every year on 112 children in 2 schools of Riga from 1996 and will be finished in 2008. Tests were carried out with every child determining their motor functions (taping-test, reaction time on sound stimuli were given binaurally or bilaterally with stereo earphones and light stimuli presented at the centre of table and on the left or right sides), psychological IQ—by Raven's test, capacity for attention switching was tested according to a modified Shulte's procedure, stability and capacity to focus attention were studied using an "entangled line" test, and memory was tested by the capacity to remember numbers functions.

The paper presents the preliminary results of experiments on a possible interdependence between EMF and children motor and psychological functions development.

Key words: children, development, mobile phone, IQ, attention, reaction time, tapping-test.

INTRODUCTION

Children, like adults, are subjected to the effect of harmful environmental factors, including also those generated by electromagnetic fields (EMF) of modern communication systems. At the same time, recent reviews demonstrate that there has been little research on the EMF effects on children.

The literature data available contain no common opinion on the mechanism of EMF effect on human health. There are studies on the heat effect of high frequency EMF on human health (Maier *et al*., 2000; Kumar, 2001; Liesenkotter, 2002; Lin *et al*., 2002; Walton, 2002; Evans-Pughe, 2003; Hocking, 2003), human body (Schonborn *et al*., 1998; Nesse *et al*., 2001; Lin, 2003; Toropainen, 2003), nervous system (Croft *et al*., 2002; Hamblin and Wood, 2002; Hietanen *et al*., 2002; Hossmann and Hermann, 2003; Huber *et al*., 2003; Salford *et al*., 2003), and psychological function (Lee *et al*., 2001; Edelstyn and Oldershaw, 2002; Haarala *et al*., 2003;); however, the data available are on contradictory. The number of children who persistently use mobile phones has rapidly increased as well. The studies were performed with a psychophysiological diagnostic system "Polytest-8802 (Produced by Engineering Center of Latvian Academy of Science, Latvia). The "Polytest-8802" is a specialized computer that uses psychophysiological reactions to determine human functional state. In total, 11 tests were made for each child. A rest break was included and the test duration was 70 minutes. Each test included twenty measurements that were used to obtain the arithmetical mean, standard deviation, and standard error of the mean (Kolodynski and Kolodynska, 1996, 2006). The studies were performed on 112 children (57 boys and 55 girls) in 2 schools of Riga in 1996–2003 (Table 1).

Tapping-test. To evaluate the functional state of the neuromuscular system, a tapping-test was used. The children examined had to press two keys with their right and left hands at maximum rate for 30 seconds. The rate of key pressing per second was registered for each hand separately.

Reaction time Red light diodes were used to present light stimuli at the centre of the table and on the left and right sides. The visible diameter of the light was 2.5 mm and the stimulus duration was 40 ms. Sound stimuli were given with stereo earphones (intensity, 60 dB; stimulus duration, 100 ms; frequency, 1 kHz). The interval between both light and sound stimuli was randomized (2.5–4 s). Children had to rapidly press and release keys after stimuli. Presentations of stimuli from the table centre or binaurally required the child to press both keys simultaneously. When the stimulus was presented from the side of the table, or in one earphone, the subject had to press the key on the side corresponding to the stimulus. In the cross variant of the test, the subject had press the key at the side opposite that of the stimulus. The response time, duration of press contact, and the number of errors were registered.

Attention. The capacity for attention switching was tested according to a modified Shulte's procedure. The procedure used a double-colored table of 64 squares. Each square consisted of two numbers: large black and small red colors (index), as well as a response button. At the beginning of the test the monitor displayed a number which the child was required to find among the black numbers. When the required black number was found, the child was required to press the appropriate key and memorized the associated red number. This new number was then searched for among the black numbers and the process was repeated 20 times.

The stability and capacity to focus attention were studied with the "entangled lines" test. The test table was covered with entangled lines. Each line began with a number on the left side and finishes with another number on the right side. The child was required to rapidly follow each line visually and press the key at its finish. The time taken to follow every line and the number of errors were registered.

Memory. Memory was tested by the capacity to remember numbers. During the experiment, a series of numbers of increasing complexity was presented, beginning with three digits and ending with nine. White digits of 6 x 10 mm, on a dark-grey background were presented on the computer monitor. During one test, three numbers were displayed on a monitor at 1 second intervals. The child then entered the three numbers on the keyboard. This was repeated seven times, progressively increasing the number of numbers displayed from three to nine. One volume of operative memory was determined according to the formula $V = A + (m/n)$ where A is the largest numbers of digits in the operation which was successfully reproduced by the child in all experiments, n is the number of experiments, m is the number of correctly reproduced number series.

Test of Raven's (Q I). The data obtained were transferred to the Wexler's scale, where the mean parameter value was equated to 100 points and a deviation from the mean value for one standard deviation – to 15 points.

Statistics**. S**tatistically significant differences were evaluated by Student's criteria for quantitative variables and Pearson's coefficient was used for analysis of correlations.

Results. In each age group were tested 55 girls and 57 boys (Table 1). The duration of talks using mobile phone increased with age from 3 min/day (7 years old children's) to 21 min/day (14 years old children's). Mean power of mobile phone 0.6 W (GSM-900).

Table 1

MEAN AGE±STANDARD ERROR (YEARS) IN FEMALE AND MALE CHILDREN

Forms	Sex	Mean age ± SE, years
1st form	Female	7.3±0.04
	Male	7.4±0.03
2nd form	Female	8.2±0.02
	Male	8.5±0.03
3rd form	Female	9.4±0.03
	Male	9.6±0.05
4th form	Female	10.3±0.03
	Male	10.5±0.04
5th form	Female	11.5±0.03
	Male	11.6±0.02
6th form	Female	123±0.04
	Male	12.4±0.03
7th form	Female	13.5±0.05
	Male	13.6±0.03
8th form	Female	14.4±0.03
	Male	14.5±0.03

The rates of all motor reaction (tapping-test end reaction time) tests in boys were better then in girls Table 2 and Table 3).

The rates of all attention (attention switching and attention concentration) tests in girls were better then in boys.

No differences in the volume of operative memory and the time required to fulfil the test for the rate of the attention switching were detected (Table 4).

A weak negative correlation dependence was observed between the duration of daily conversations using MT and intellect $r = 0.37$ ($P < 0.01$) and concentration of attention $r = 0.29$ ($P < 0.05$).

The pupils began to use mobile telephones at different time. Therefore, the analysis of the data obtained was started from the analysis of separated cases. In example, the testing results of one girl aged 7 to 14 (Fiig.1 and Fig.2) during eight years. The start of the persistently MT use – in the 5th form. Figures 1 and 2 demonstrate a worsening of some motor and psychological parameters during the first year of using MT, later these parameters gradually become more equable. On the basis of this observation 2 groups of pupils were chosen for the analysis: those who use MT during the first year and those who use MT during more than one year.

It turned out that the highest worsening of the parameters is observed during the first year of MT use, and the parameters improve more quickly in the children who started to use MT later (Fig.3 and Fig.4.).

Table 2

MEAN±STANDARD ERROR OF THE RESPONS REACTION TIMES USING LEFT HAND TO LATERILIZED LIGHT (RTL) AND MONAAURAL SOUND (RTS) STIMULI AND RETENTION TIME OF KEYS IN THE PRESSED STATE FOR LGHT (RTLP) AND SOUND (RTSP) STIMULI IN FEMALE AND MALE CHILDREN

Forms	Sex	Light stimuli		Sound stimuli	
		RTL, ms	RTLP, ms	RTS, ms	RTSP, ms
1st form	Female	500±12	286±1`1	595±32	279±13
	Male	476±11	295±10	483±27	305±21
2nd form	Female	457±7	269±10	523±21	287±14
	Male	438±10	256±8	518±20	266±11
3rd form	Female	435±9	241±6	558±15	245±7
	Male	401±8	227±7	475±25	234±8
4th form	Female	388±5	230±5	467±11	264±6
	Male	370±5	225±4	432±10	245±5
5th form	Female	373±5	223±5	457±11	259±6
	Male	348±4	231±5	389±9	241±7
6th form	Female	360±5	224±5	451±10	263±7
	Male	323±4	200±5	371±8	228±6
7th form	Female	338±4	211±4	377±8	250±7
	Male	313±5	185±4	343±6	207±5
8th form	Female	330±3	215±4	363±6	235±4
	Male	304±3	178±4	324±5	194±4

Table 3

MEAN±STANDARD ERROR OF THE TAPPING TEST FREQUENCES FOR LEFT (TTL) AND RIGHT (TTR) HANDS AND RETENTION TIME OF KEYS IN THE PRESSED STATE FOR LEFT (TTLP) AND RIGHT (TTRP) HANDS IN FEMALE AND MALE CHILDREN

Forms	Sex	Left hand		Right hand	
		TTL, Hz	TTLP, ms	TTR, Hz	TTRP, ms
1st form	Female	4.02±0.09	125±6	4.21±0.10	105±6
	Male	3.91±0.15	132±7	4.15±0.14	108±6
2nd form	Female	4.14±0.10	118±6	4.23±0.10	108±5
	Male	4.28±0.10	108±6	4.63±0.09	87±5
3rd form	Female	4.39±0.08	108±4	4.68±0.07	88±3
	Male	4.71±0.07	93±3	8.88±0.07	78±2
4th form	Female	4.85±0.07	98±3	5.01±0.06	85±3
	Male	4.90±0.06	91±3	5.17±0.06	76±1
5th form	Female	4.92±0.05	90±2	5.19±0.06	75±2
	Male	5.09±0.05	87±2	5.37±0.06	74±2
6th form	Female	5.15±0.05	88±2	5.38±0.06	75±2
	Male	5.29±0.05	84±2	5.59±0.06	71±2
7th form	Female	5.36±0.05	85±2	5.60±0.05	71±2
	Male	5.45±0.05	81±2	5.72±0.05	68±2
8th form	Female	5.38±0.05	88±2	5.61±0.04	78±2
	Male	5.71±0.06	80±1	5.92±0.06	67±1

Table 4

MEAN±STANDARD ERROR OF THE ATTENTION SWICHING (A1), CAPACITY TO FOCUS ATTENTION (A2) TESTS AND THE CAPACITY OF OPERATVE MEMORY (MEM) IN FEMALE AND MALE CHILDREN

Forms	Sex	A1, s	A2, s	MEM
1st form	Female	19.1±3.0	17.6±3.0	5.5±0.7
	Male	24.8±3.0	16.5±1.0	5.4±0.3
2nd form	Female	21.0±1.1	13.9±0.5	5.9±0.2
	Male	21.5±1.0	14.0±0.7	5.4±0.2
3rd form	Female	16.7±0.6	11.7±0.4	6.2±0.2
	Male	17.4±0.7	12.3±0.4	6.0±0.2
4th form	Female	12.3±0.3	10.0±0.3	7.6±0.2
	Male	14.0±0.4	10.3±0.3	6.8±0.2
5th form	Female	11.2±0.4	9.4±0.2	7.8±0.2
	Male	11.9±0.3	9.1±0.2	7.9±0.2
6th form	Female	10.1±0.3	8.8±0.2	8.6±0.2
	Male	11.3±0.3	8.9±0.2	7.9±0/2
7th form	Female	8.8±0.2	8.4±0.2	9.1±0.2
	Male	10.4±0.2	8.4±0.1	8.8±0.2
8th form	Female	8.6±0.1	8.3±0.1	9.5±0.1
	Male	9.4±0.1	8.1±0.1	9.4±0.1

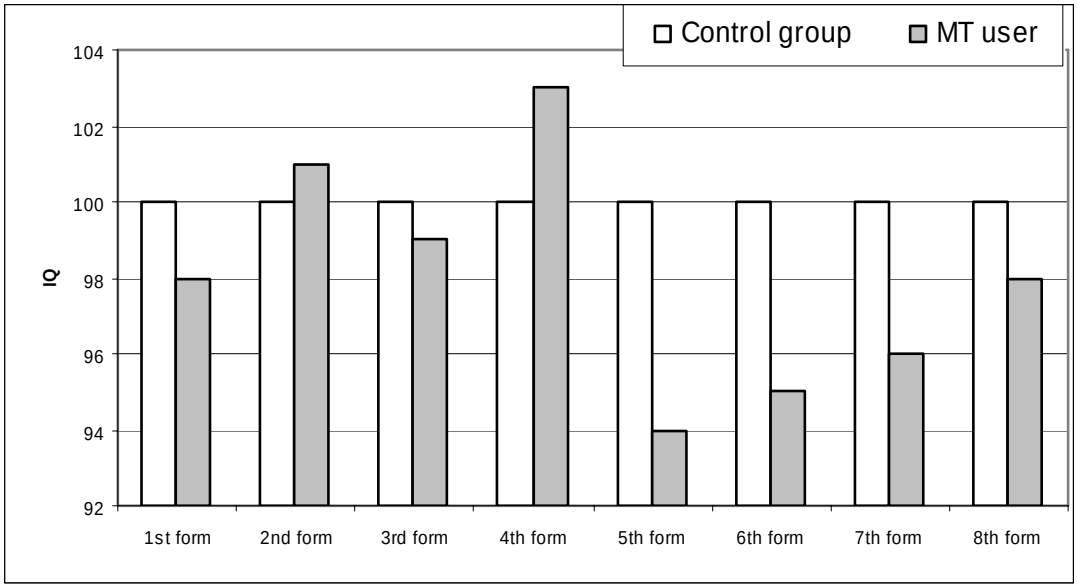


Fig.1. Mean ± SE time to perform the test for IQ. The development of IQ in girl was testing.

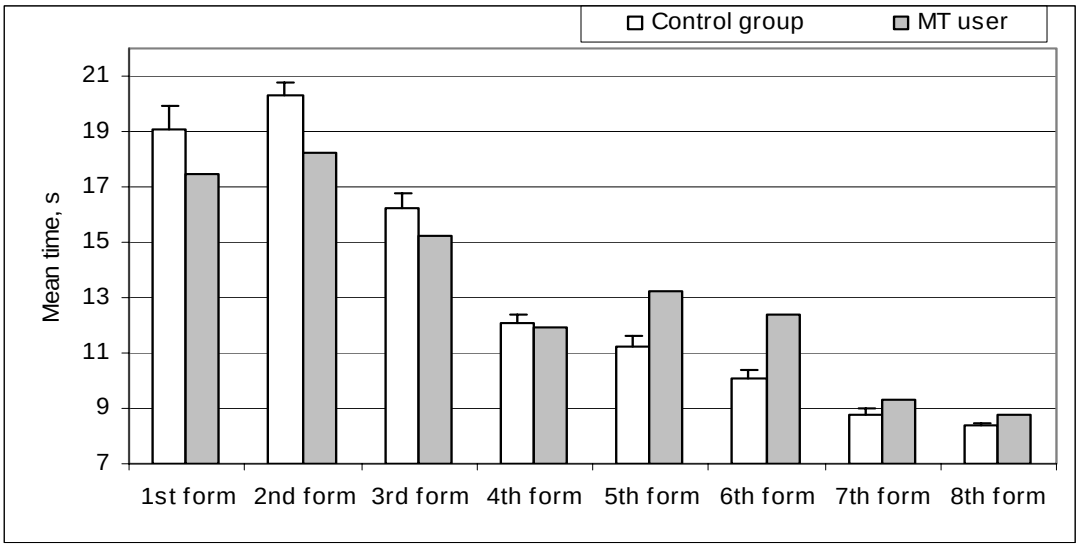


Fig.2. Mean ± SE time to perform the test for attention concentration. The development of attention in girl was testing.

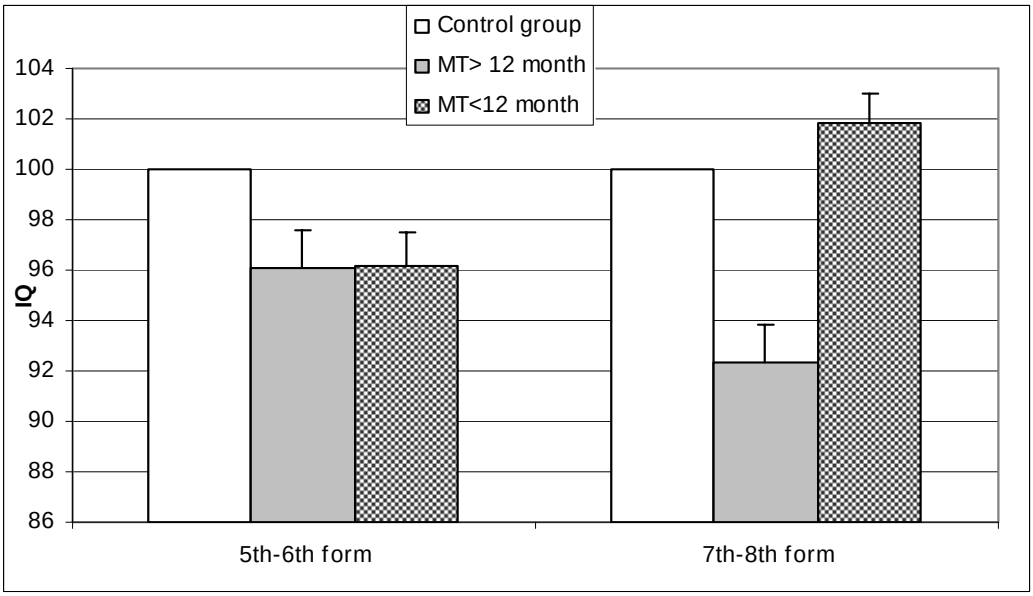


Fig.3. Mean±SE of IQ. The differences are significant ($P < 0.05$) between the mobile phone users and control groups in children of 5th-6th forms and ($P < 0.01$) in children of 7th-8th form for MT >12 month group with control..

Unexpectedly, IQ differences were found between the mobile phone users and control groups in children of 5th-6th forms and in children of 7th-8th form for "MT >12 month" group with control..

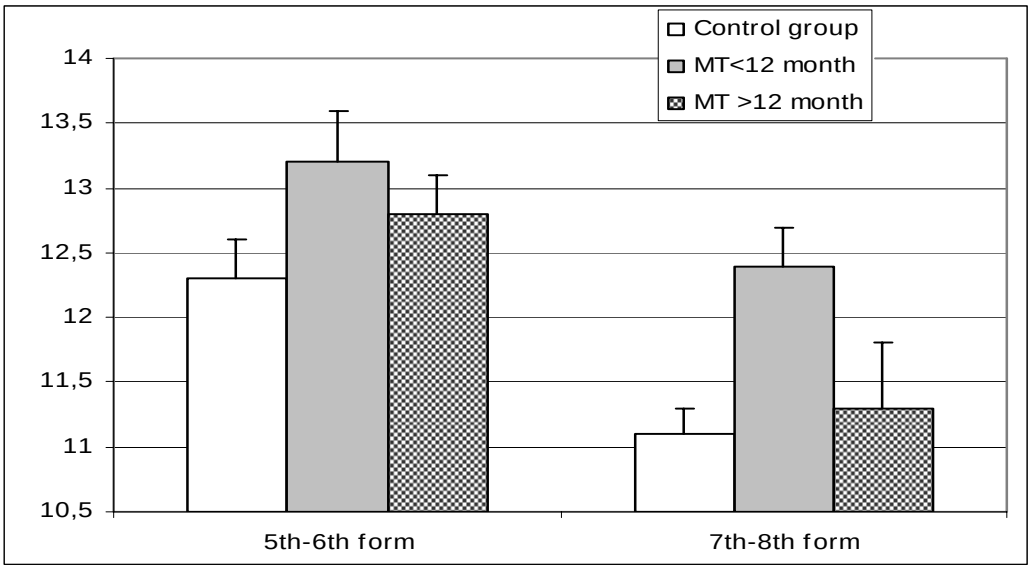


Fig.4. Mean ± SE time (s) to perform the test for attention concentration. The differences are significant ($P < 0.05$) between the mobile phone users of 5th-6th forms and ($P < 0.01$) in children of 7th-8th form for MT >12 month group.

Younger children using mobile phone are more sensitive to the EMF radiation than oldest and have worse results to IQ and attention tests (Fig.3. and Fig.4).

SUMMARY

The highest shifts in motor and psychological parameters are detected during the first year of MT use, and later they gradually improve.

The improvement of parameters proceeds more rapidly in the children who started to constantly use MT at an elder age.

The improvement of parameters proceeds more rapidly in the children who started to constantly use MT at an elder age.

The analysis of the data obtained will be continued basing on the working hypothesis on that the oldest children organism, being adapted to the EMF chronic influence better, responses by the increase in the IQ and attention after 12 month of mobile phone using..

Children are more sensitive to the EMF radiation than adults, and on the basis of the data available, the Independent Expert Group on Mobile Phones (IEGMP) in the United Kingdom came to the conclusion that children may be more vulnerable because they have a developing nervous system, children's brain tissue is more conductive than that of adults since is has a higher water content and ion concentrations, children have a greater absorption of RF energy at mobile telephone frequencies in the tissues of the head, and that children would have a longer lifetime of exposure. The IEGMP also recommended that, as a precautionary approach, mobile phone use by children should be for non-essential calls only, and that the mobile phone industry should refrain from promoting mobile phones to children.

The authors of the paper support the point of view of the IEGMP.

The research should be continued in this direction, including the individual dosimetry and analysis of each separate case.

.

ACKNOWLEDGEMENTS

This study was supported by a grant No 1429 from the Latvian Council of Science

REFERENCES

Croft, R. J., Chandler, J. S., Burgess, A. P., Barry, R. J. (2002) Acute mobile phone operation affects neural function in humans. *Clin. Neurophysiol*., **113** (10), pp. 1623–1632.

Edelstyn, N., Oldershaw, A. (2002) The acute effects of exposure to the electromagnetic field emitted by mobile phones on human attention. *NeuroReport*, **13** (1), pp. 119–121.

Evans-Pughe, C. (2003). Phones and health—the science. *IEE Rev.*, **49** (5), pp. 16–17.

Haarala, C., Bjornberg, L., Ek, M., Laine, M., Revonsuo, A., Koivisto, M., Hamalainen, H. (2003) Effect of a 902 MHz electromagnetic field emitted by mobile phones on human cognitive function: A replication study. *Bioelectromagnetics*, **24** (4), p. 283–288.

Hamblin, D. L., Wood, A. W. (2002) Effects of mobile phone emissions on human brain activity and sleep variables. *Int. J. Radiat. Biol*., **78** (8), pp. 659–669.

Hietanen, M., Hamalainen, A.-M., Husman, T. (2002) Hypersensitivity symptoms associated with exposure to cellular telephones: No causal link. *Bioelectromagnetics*, **23** (4), p. 264–270.

Hocking, B. (2003) Update on mobile phones and health. *Int. Med. J*., **33** (5/6), p. 235.

Hossmann, K.-A., Hermann, D. M. (2003) Effects of electromagnetic radiation of mobile phones on the central nervous system. *Bioelectromagnetics*, **24** (1), pp. 49–62.

Huber, R., Schuderer, J., Graf, T., Jutz, K. (2003) Radio frequency electromagnetic field exposure in humans: Estimation of SAR distribution in the brain, effects on sleep and heart rate. *Bioelectromagnetics*, **24** (4), pp. 262–276.

Kolodynski, A., Kolodynska, V. (1996) Motor and psychological function of school children living in the area of the Skrunda Radio Location Station in Latvia. *Sci. Total Environ*., **180** (1), pp. 87–93.

Kolodynski, A., Kolodynska, V. (2006) Differences between the motor and psychological functions of children who persistently use mobile phone. Proceeding of the Latvian Academy of Science. Section B, Vol. 60,No 1 (642), pp 16-19.

Kumar, A. (2001) Electromagnetic radiation and biological effects. *International Symposium on Electromagnetic Compatibility, Vol. 2, Piscataway, NJ, USA.* Institute of Electrical and Electronical Engineers Inc., **NJ,** pp. 1048–1053.

Lee, T., Ho, S., Tsang, L., Yang, S., Li, L., Chan, C. (2001) Effect on human attention of exposure to the electromagnetic field emitted by mobile phones. *NeuroReport*, 12 (4), pp. 729–31.

Liesenkotter, B. (2002) Analysis of the contended health risks due to digitally modulated mobile phone radiation. *Ztschr. Med. Phys*., **12** (3), p. 198–203.

Lin, J. C. (2002) Health effects: Scientific research and mobile phone testing. *IEEE Microwave Magazine*, **3** (4), pp. 26–30.

Lin, J. C. (2003) Risks to children from cellular telephone radiation. *IEEE Microwave Magazine*, **4** (1), pp. 20–26.

Maier, M., Blakemore, C., Koivisto, M. (2000) The health hazards of mobile phones. *Brit. Med. J*., **320**, Issue 7245, p. 1288-1289.

Maier, R. (2001) Do pulsed electromagnetic fields impair CNS activity? *Biomedizinische Technik*, **46** (1–2), p. 18–23.

Nesse, R., Nikookar, H., Ligthart, L. P. (2001) An overview of the effects of mobile phone radiation on the human body. In: *2001 European Conference on Wireless Technology: Conference Proceedings.* Microwave Engineering European, London, p. 73–76.

Pandere, D., Andaburska, M. (eds.) (2001) *Rīgas pašvaldību izglītības iestāžu audzēkņu veselības stāvoklis laika posmā no 1995. mācību gada līdz 2001. mācību gadam* [Health of Pupils from Rīga Municipal Educational Institutions during 1995–2001 School Years]. Rīga, Rīgas domes Izglītības, jaunatnes un sporta departaments, 177 lpp. (in Latvian).

Salford, L. G., Brun, A. E., Eberhardt, J. L., Malmgren, L., Persson, B. (2003). Nerve cell damage in mammalian brain after exposure to microwaves from GSM mobile phones. *Environ. Health Perspectives*, **III** (7), p. 881-883.

Schonborn, F., Burkhardt, M., Kuster, N. (1998) Differences in energy absorption between heads of adults and children in the near field of sources. *Health Phys*., **74** (2), pp. 160–168.

Toropainen, A. (2003) Human exposure by mobile phones in enclosed areas. *Bioelectromagnetics*, 24 (1), pp. 63–65.

DNA-damaging effects of UMTS electromagnetic fields in human cells *in vitro*

Elisabeth Kratochvil[1], Claudia Schwarz[1], Petra Hartbauer[1], Marietta Weninger[1], Alexander Pilger[1], Franz Adlkofer[2], Hugo W. Rüdiger[1]

[1] Medical University of Vienna, Division of Occupational Medicine, Vienna, Austria
[2] Verum Foundation, Munich, Germany

Our previous research demonstrated that radiofrequency electrsignals have genotoxic properties *in vitro*[1]; there are no corresponding data concerning the recently introduced European mobile communication standard UMTS (Universal Mobile Telecommunication Standard) as yet. A putative genotoxic potential of UMTS signals was investigated in cultured human cells using the alkaline comet assay and the cytokinesis-blocked micronucleus assay.

Materials and Methods

Cultured human fibroblasts (diploid fibroblasts obtained from a male 6 year old healthy donor) were continuously exposed to UMTS test signals (carrier frequency 1950 MHz) in a temperature-controlled exposure setup[2] specially designed for blind *in vitro* exposures of cell monolayers and provided by the IT'IS foundation (Zurich, Switzerland). Various exposure conditions (specific absorption rate SAR: 1 and 2 W/kg; exposure time: 4, 16 and 24 hours) were tested. Each exposure condition was tested in duplicate. Positive (comet assay: 5 min UV light/254 nm, which equals 0,6 kJ/m^2; micronucleus assay: 3 µg Bleomycin/ml - time corresponding to the exposure time) and negative controls were included in each set of experiments to check for effective operation of the method.DNA damage was assessed in terms of DNA strand breaks (alkaline comet assay, evaluated by visual classification[3]) and micronuclei (cytokinesis-blocked micronucleus assay[4]).

Summary

Exposure to UMTS signals resulted in a twofold increase in DNA strand breaks after 16 and 24 hours for both SAR investigated. In addition, a corresponding doubling in micronuclei frequency was detected.
Preliminary experiments using peripheral blood lymphocytes showed no increase in DNA strand breaks after UMTS exposure (not shown).
In conclusion, UMTS signals may have genotoxic effects in certain cell systems *in vitro* below and at the current European safety limit (2 W/kg).

References

[1]Diem, E., Schwarz, C., Adlkofer, F., Jahn, O. & Rüdiger, H. (2005). Non-thermal DNA breakage by mobile phone radiation (1800 MHz) in human fibroblasts and transformed GFSH-R17 rat granulosa cells in vitro. *Mutat Res* **583:** 178-183.

[2]Schonborn, F., Pokovic, K., Burkhard, M. & Kuster, N. (2001). Basis for optimization of in vitro exposure apparatus for health hazard evaluations of mobile communications. *Bioelectromagnetics* **22:** 547-559.

[3]Ivancsits, S., Diem, E., Jahn, O. & Rüdiger, H. (2003). Intermittent extremely low frequency electromagnetic fields cause DNA damage in a dose-dependent way. *Int Arch Occup Environ Health* **76:** 431-436.

[4]Fenech, M. (1993). The cytokinesis-block micronucleus technique: a detailed description of the method and its application to genotoxicity studies in human populations. *Mutat Res* **285:** 35-44.

LOW-FREQUENCY ELECTROMAGNETIC FIELD PROMOTE THE EXPRESSION OF DIFFERENTIATION MARKERS IN PLURIPOTENT HUMAN MESENCHIMAL STEM CELLS (hMSC).

LEDDA M.●., ROSOLA E.●., PATTI A.M.♦., VULCANO A.♦ D' EMILIA E.© GILIBERTI C. ©., GIULIANI L. ©., POZZI D.±., GRIMALDI S.●. and LISI A. ●

●Istituto di Neurobiologia e Medicina Molecolare C.N.R. Rome Italy

♦Dipartimento di Scienze di Sanità Pubblica G. Sanarelli Università "La Sapienza" Rome Italy

© ISPESL-DIPIA Rome Italy

± Dipartimento di medicina sperimentale e patologia Università La Sapienza Roma Italy

ABSTRACT

Reports of biological effects of low-energy electromagnetic field (EMF) have increased in recent years. Particularly debated is the question of the epidemiological evidence of adverse effects of an extremely low frequency magnetic field (ELF-MF) generated by 50-60 Hz high voltage power transmission lines, video display terminals, electric blankets and other home appliances, which raise the possibility of deleterious health effects from exposure to radio frequency or low frequency fields. A valid objection is that field intensity is many orders of magnitude below the noise threshold so that selective, cooperative, or amplifying mechanisms must be postulated. The therapeutic potential of magnetic field can be seen in the proven efficacy of low-energy, pulsed magnetic fields in non-union bone fracture healing (Bassett, 1993), confirming that under certain conditions non-ionizing electromagnetic energy can influence physiological processes in organisms. Low frequency magnetic fields at 50 or 60 Hz are also reported to stimulate nerve regeneration (Rusovan and Kanje, 1992) alteration gene transcription (Phillips et al., 1992), and they may also play a synergic role in cellular processes that are already activated, such as cell proliferation and cell differentiation (Walleczeck, 1992; Manni et al., 2002., Lisi et al 2005).
The possible mechanisms of the induced effects are not known, although a number of theoretical models have been proposed (Glaser, 1992., Liburdy, 1992., Barnes,1996).
In this work we have studied the effect of EMF radiations on human mesenchymal Stem Cells (hMSC) differentiation
In litterature is well described that this cells are able to differentiate to osteoblast following treatment with chemical agents such as dexamethasone. Regulation of osteoblast differentiation its an important fenomena that must occur to mantain the continuos supply of mature osteoblast needed for bone growth, remodelling, and in particular for bone repair.

INTRODUCTION

Culture and differentiation of mesenchymal stem cells. Height- ten ml of bone marrow, obtained from iliac crest, was mixed with one volume of phosphate-buffered saline and nucleated cell fraction was enriched for mesenchymal stem cells by density-gradient centrifugation over Lympholyte-H cushion. The cells at the medium- Lympholyte-H interface were collected, washed three times with culture medium and seeded into culture flask. Confluent monolayers of adherent cells were obtained about one week after the start of cell division. Subcultivation was performed by replating at $6x10^3$ cells per cm^2 flasks. To promote osteogenic differentiation
cells were stimulated during subpassages by cultivation in standard medium supplemented with 100nM dexamethasone or by exposure to extremely low frequency electromagnetic field (50Hz 1mT)under controlled condition.

Cells were continuously exposed to a sinusoidal 50 Hz magnetic field at a flux density of 1 mT (10 G) (rms) in a temperature regulated solenoid. Temperature regulation (37 ± 0.2 °C) and 5% CO_2 was provided. Temperature was continuously recorded by a Hanna HI 9274 OC printing thermometer, within the centre of the solenoid and was in the 37°C ± 0.2 range. In a control experiment the sample was placed in an identical cell incubator containing the solenoid with no field, in the same conditions as the exposed one. All experiments were under blind conditions. The solenoid manufacture has been published elsewhere (Santoro et al, 1997; Lisi et al, 2000; Manni et al, 2004, Lisi et al, 2005).

The main body of the solenoid is a cylinder in concrete-asbestos 2 cm thick and has a diameter of 20 cm and a height of 40 cm. It is made of 1200 turns of 2 mm diameter copper wire wound in three layers in continuous forward-backward fashion. It is driven from the 50 Hz power mains through a variable autotransformer and generates a flux density of 1 mT (rms) for an applied voltage of 6 Volts (rms).The solenoid is then placed into a cell incubator with its centre ventilated by the fan for appropriate air circulation. The modest heat due to Joule effect is efficiently dispersed by the continuous forced ventilation in the total mass of the CO_2 incubator. Field density measured with a calibrated Hall probe, is within – 5% of centre value inside the cylindrical exposure volume of 11 cm by 17 cm along the solenoid axis. The measured geomagnetic ambient field is 32 μT (vertical component) and 16μ T (horizontal component). Stray ambient ac fields are below 0.1 μT. An often overlooked fact related to solenoids is the presence of an almost homogeneous electric field oriented parallel to the magnetic field (Chute et al., 1981) unless adequate electric shielding is used (Stauffer et al., 1994). An approximate estimate of this field may be obtained from the voltage across the extremes of the inner of the six layers and its length. The corresponding field induced by capacity coupling in the culture medium will be in the order of 0.01 μV/cm (Foster et al., 1995).

SUMMARY

Exposure to low frequency electromagnetic field for 5 days resulted in a change in plasma membrane morphology and this modification were also accompanied by a rearrangement in actin filaments as showed by confocal miscroscopy analysis after cells labeling with FITC-phalloidin.
In particular, mesenchimal cells exposed to the field showed the same actin organization found in cells after treatement with dexamethasone. The differentiating effect of dexamethasone were potentiate by exposure to the field.
After 5 days of exposure, the mRNA expression for osteoblast markers differentiation such as Alkaline Phosfatase (AP), Osteocalcin (OCL) and Osteopontin (OPN) increase (Fig.1) this result were further confirmed by indirect immunofluorescence assay for osteopontin Osteopontin showed an increase in exposed and dexamethasone-esposed cells with respect to control (Fig. 2).
In conclusion our finding demonstrated that exposure to ELF can act as a differentiating agent on mesenchymal human cells outlining the relevance of low frequency electro-magnetic field as a terapeutical agent suggesting a possible use of ELF as support in medicine for different pathologies therapy.

Aknowledgements

This work as been partially supported by grant ISPESL B1/42/DIPIA/04 and B1/45-a/DIPIA/04

REFERENCES

Barnes PS. 1996. Effect of electro-magnetic field on the rate of chemical reactions.Biophysics 41:801–880.

Basset CAL. 1993. Beneficial effects of electro-magnetic fields. J Cell Biochem. 51:387–393.

Foster KR, Schwan H. 1995. Dielectric properties of tissues. In: Polk C, Postow E, editors. Handbook of biological effects of electro-magnetic fields, 2nd edition.Boca Raton, FL: CRC Press, pp 27–96.

Glaser R. 1992. Current concepts of the interaction of of weak electro-magnetic fields with cells. Bioelectrochem Bioener 27:255–268.

Liburdy RP. 1992. Calcium signalling in lymphocytes and ELF fields: Evidence for an electric field metric and a site of interaction involving calcium ion channels. FEBS Lett 301(1):53–59.

Lisi A, Pozzi D, Pasquali E, Rieti S, Girasole M, Cricenti A, Generosi R, Serafino AL, Congiu-Castellano A, Ravagnan G, Grimaldi S. 2000. Three dimensional (3D) analysis of the morphological changes induced by 50 Hz magnetic field exposure on human lymphoblastoid cells (Raji). Bioelectromagnetics 21:46–51.

Lisi, A., Ciotti, M.T., Ledda, M., Pieri, M., Zona, C., Mercanti, D., Rieti, S., Giuliani, L., Grimaldi, S. (2005). Exposure to 50Hz electro-magnetic radiation promote early maturation and differentiation in newborn rat cerebellar granule neurons. J. Cell. Physiology, 204, 532-538

Manni V, Lisi A, Pozzi D, Rieti S, Serafino AL, Ledda M, Giuliani L, Grimaldi S.2002. Effect of extremely low frequency (50 Hz) magnetic field on morphological and biochemical properties of human keratinocytes. Bioelectromagnetics.23:298–305.

Phillips JL, Haggren W, Thomas WJ, Jones TI, Adey W. 1992. Magnetic fieldinduced changes in specific gene transcription. Biochimica Biophysica Acta1132:140–144.

Rusovan A, Kanje M. 1992. Magnetic fields stimulate peripheral nerve regeneration hypophyctiomia rats. Neuroreport 3(12):1039–1041.

Santoro N, Lisi A, Pozzi D, Pasquali E, Serafino A, Grimaldi S. 1997. Effect of extremely low frequency magnetic field exposure on morphological and biophysical properties of human lymphoid cell line (Raji). Biochim Biophys Acta 1357:281–290.

Walleczeck J. 1992. Electro-magnetic field effect on cells of the immune system:The role of calcium signalling. Faseb J 6:3177–3185.